公益財団法人　老年病研究所

業　績　集

第２０集

２０２０

令和２年7月

公益財団法人　老年病研究所

業　績　集

第20集

2020

令和2年7月

ま え が き

公益財団法人老年病研究所業績集第20集（2020年版）をまとめることができました。ご覧いただけると幸いです。

平成31年（2019年）は２月に探査機「はやぶさ２」が小惑星リュウグウへの着地に成功し、石や砂などの試料を採取できた可能性が大きいというニュースがあり、令和１年９月にはラグビーW杯日本大会が開催され、日本チームの活躍に日本中が沸きました。10月には東日本各地で台風の被害が甚大でした。令和２年（2020年）に入ると中国武漢で発生した新型コロナ感染が世界中に広がり、死者も多く世界の市民生活や経済活動にも甚大な悪影響を及ぼしております。東京五輪も１年延長され、医学関連の学会も次々に延期や中止に追い込まれました。４月には全国に非常事態宣言が出され、日常生活や経済活動が制限され、先の見えない状態が続いております。非常事態宣言は解除されましたが、早期に終息に向かうことを期待したいと思います。

最近、本業績集にも載せてあるOkamoto K, Amari M, Fukuda T, Suzuki K, Takatama M:Astrocytic tau pathologies in aged human brain. Neuropathology 39:184-193, 2019.が「Top Downloaded Paper 2018-2019」になったとの認定書を出版社（Wiley）から受け取りました。2018年１月から2019年12月までの間のダウンロード数が多かったようです。当院での多数の剖検脳を用いた私達の論文は、注目され多く読まれているようです。

当院は「基幹型研修病院」として、2019年４月から２名の初期研修医を受け入れ、2020年にはさらに２名の初期研修医を受け入れました。職員が協力して、研修医が満足するような医療や研修を行っていきたいものと思っています。

毎年同じことを述べて恐縮ですが、当院には、内科、脳神経内科、循環器内科、脳神経外科、整形外科、眼科、歯科、病理診断科などがあり、各々の角度から臨床的研究を推進しております。研究成果の発表（学会発表等）の項目を見ていただきますと、医師、薬剤師、看護師、リハビリスタッフなど多くの職員が学会などで発表しているのが分かります。2020年度は新たな優秀なスタッフも加わりましたので診療や研究がさらに充実するものと期待しています。

今後とも、高玉理事長と佐藤病院長を中心に、地域医療の発展のためにさらに職員一同努力する所存ですので、ご支援、ご協力をよろしくお願いします。

令和２年７月

公益財団法人　老年病研究所
所長　岡本　幸市

目　　次

Neuropathology 2019; **39**, 187–193 doi:10.1111/neup.12544

Original Article

Astrocytic tau pathologies in aged human brain

Koichi Okamoto,[1] Masakuni Amari,[1] Toshio Fukuda,[2] Keiji Suzuki[2] and Masamitsu Takatama[3]

Departments of [1]Neurology, [2]Pathology and [3]Internal Medicine, Geriatrics Research Institute and Hospital, Maebashi, Japan

Argyrophilic and tau-positive abnormal structures in astrocytes are frequent in aged brains, with a new nomenclature of aging-related tau astrogliopathy (ARTAG) proposed. The two major cytomorphologies of ARTAG are thorn-shaped astrocytes (TSA) and granular or fuzzy tau immunoreactivity in processes of astrocytes (GFA). We selected 28 cases in which many AT8-identified astrocytic tauopathies were observed in the central nervous system from 330 routine aged autopsied cases, including Alzheimer's disease. AT8-identified and Gallyas silver staining-positive TSA were observed in subpial, subependymal, perivascular areas as well as white matter. These TSA were 4-repeat (4R) tau-positive. In contrast, 3-repeat (3R)-tau was negative in TSA, but positive in short thick cell processes, likely neuropil threads, in subpial and subependymal areas. The frequency of 3R-tau-positive processes was variable. Small dot-like AT8-identified astrocytic processes surrounding vessels in the neuropil were also positive for 4R-tau, but negative for 3R-tau. GFA in cerebral gray matter were AT8-identified and Gallyas-positive, and positive for 4R-tau but negative for 3R-tau. In this study, we did not identify 3R-tau+/4R-tau+ or 3R-tau+/4R-tau− astrocytes. Further studies are needed to clarify the nature and progression of glial tau-positive structures in ARTAG.

Key words: 4-repeat tau, ARTAG, astrocyte, pathology, tau.

INTRODUCTION

Tau is a microtubule-associated protein that binds to tubulin and promotes its polymerization and stabilization into microtubules.[1–3] Tau plays an important role in maintaining axonal transport and neuronal integrity, but is expressed at low levels in glial cells.[2] In the adult human brain, six tau isoforms are expressed as a result of messenger RNA (mRNA) splicing. They are divided into two groups, 3-repeat (3R)-tau and 4-repeat (4R)-tau isoforms, depending on exon 10 expression.[1–3] Isoform-specific tau antibodies are useful tools, and anti-3R-tau and anti-4R-tau antibodies have been widely used to investigate tau pathologies.[2,4–7]

Tauopathies are defined as neurodegenerative diseases with prominent tau pathology in neurons and glial cells of the central nervous system (CNS), and are classified as predominant 3R-tau pathology, mixed 3R/4R-tau pathology, or 4R-tau pathology.[2,7] Nonetheless, it remains unclear why different tau isoforms accumulate in different diseases, and how they lead to the formation of abnormal filamentous structures and pathologies.[8] In Alzheimer's disease (AD), transition from 4R-tau to 3R-tau was proposed based on immunohistochemical studies.[4,9]

Recently, brains with many Alzheimer neurofibrillary tangles (NFTs), which were indistinguishable from those of AD but lacked amyloid-β (Aβ) plaques, were named primary age-related tauopathy (PART).[10] Argyrophilic and tau-positive abnormal structures in astrocytes are frequent in the aged brain, and a new nomenclature was proposed of aging-related tau astrogliopathy (ARTAG).[11] ARTAG occurs mainly, but not exclusively, in individuals over 60 years of age.[11] The two major cytomorphologies of ARTAG are thorn-shaped astrocytes (TSA) and granular or fuzzy tau immunoreactivity in processes of astrocytes (GFA).[11,12] TSA are observed in subpial, subependymal, or perivascular areas, as well as white matter. GFA are found mainly in gray matter[11] TSA are recognized using AT8 and 4R-tau immunostaining, but are negative with anti-3R-tau antibody.[11–13] In contrast, GFA immunostaining has not been clearly reported. Meanwhile, formation of primary or secondary glial tau-positive structures by neuronal degeneration is not well known. The ratio of 3R to 4R isoforms in adult human brain is approximately one.[2,3] Immunoreactivities of 3R-tau and 4R-tau are grossly homogeneous among

Correspondence: Koichi Okamoto, MD, PhD, Department of Neurology, Geriatrics Research Institute and Hospital, 3-26-8 Otomo-machi, Maebashi, Gunma 371-0847, Japan. Email: okamotok@ronenbyo.or.jp

Received 05 December 2018; revised and accepted 01 February 2019; published online 01 April 2019.

neurons and glia in sporadic tauopathies.[5] Further, glial tangles are suggested to resemble the pretangles that occur in neurons and thought to represent an early stage of NFTs.[14] Regardless of tauopathy, astroglial tau inclusions are mostly 4R-tau immunoreactive.[11] Thus, we wanted to determine if ARTAG is truly negative for anti-3R-tau antibody. Consequently, we examined ARTAG in aged brains using Gallyas methods, and AT8, 3R-tau, and 4R-tau immunostaining.

MATERIALS AND METHODS

We examined senile changes in aged autopsied brains at our institute. Autopsies were performed in accordance with established procedures. The majority of patients were autopsied within 4–5 h after death. Samples were used in this study after obtaining informed consent from the family of each patient. Brains were fixed in phosphate-buffered formalin and embedded in paraffin. In total, we selected 28 cases in which many AT8-positve astrocytic tauopathies were detected in the CNS from 330 routine aged autopsied cases, including AD.[15] The cases comprised 18 men and 10 women, with an average age at death of 84.7 years (70–79 years, six cases; 80–89 years, 14 cases; 90–99 years, six cases; 100–104 years, two cases). The primary causes of death were AD (seven cases), cerebrovascular disease (seven cases), pneumonia (five cases), malignancies (four cases), frontotemporal dementia (one case), amyotrophic lateral sclerosis (one case), and others (three cases). In this study, the brain stem, temporal cortex (including hippocampus), and basal ganglia were mainly examined. Tissues were fixed with 4% paraformaldehyde in phosphate-buffered saline (PBS), pH 7.4, and embedded in paraffin. Five-micrometer-thick serial sections of the brain were stained with hematoxylin and eosin (HE), Klüver–Barrera, Gallyas–Braak (Gallyas) methods and immunostained with several antibodies as follows. Deparaffinized sections were incubated with 1% H_2O_2 in methanol for 30 min to eliminate endogenous peroxidase activity in the tissue. Nonspecific binding sites on sections were blocked with normal serum, and the sections then incubated overnight at 4°C with the following antibodies for immunostaining: monoclonal anti-phosphorylated tau antibody (AT8) (1:200; Innogenetics, Gent, Belgium), monoclonal anti-Aβ-17-24 (4G8) antibody (1:20000; Covance, Princeton, NJ, USA), monoclonal anti-glial fibrillary acidic protein (GFAP) antibody (1:10000; Dako, Glostrup, Denmark), polyclonal anti-ubiquitin antibody (1:2000; Dako), monoclonal anti-3R-tau antibody (1:500; Millipore, Burlington, MA, USA), and monoclonal anti-4R-tau antibody (1:750; Millipore). Sections were washed in PBS for 30 min, and incubated with Histofine simple stain MAX-PO (Nichirei, Tokyo, Japan). For 3R-tau immunostaining, sections were additionally pretreated with 0.25% $KMnO_4$ for 15 min followed by 2% oxalic acid for 3 min at room temperature.[16]

RESULTS

Anti-3R-tau and anti-4R-tau antibodies clearly immunostained NFTs in the CA1 region of aged and AD brains (Fig. 1A, B). Neuropil threads were predominantly immunostained by anti-3R-tau antibody (Fig. 1B). In many ghost tangles (Fig. 1C) in the CA1 region of the hippocampus, a few fine filaments were observed by anti-4R-tau antibody in AD brains (Fig. 1D). Meanwhile, ghost tangles were clearly identified by anti-3R-tau antibody (Fig. 1E).

Pathological accumulation of abnormal AT8-identified phosphorylated tau protein was frequently detected in astrocytes in the examined brains, especially AD brains. TSA were observed in subpial, subependymal, and perivascular areas, as well as cerebral white matter. TSA and small dot-like structures in subpial regions of the temporal cortex were identified by AT8 (Fig. 2A), Gallyas methods (Fig. 2B), and anti-4R-tau antibody (Fig. 2C). In contrast, 3R-tau staining was negative for TSA (Fig. 2D), but positive for short thick cell processes, probably neuropil threads. The frequency of short thick cell processes was variable.

AT8-identified endfeet of astrocytic processes surrounding small vessels in the neuropil and a few TSA (Fig. 3A) were also positive for Gallyas methods (Fig. 3B) and 4R-tau immunostaining (Fig. 3C), but negative for 3R-tau immunostaining (Fig. 3D).

The subependymal region around the cerebral aqueduct and lateral ventricles showed AT8-identified fibrils and scattered TSA (Fig. 4A), which were similarly stained by Gallyas methods (Fig. 4B) and 4R-tau immunostaining (Fig. 4C). 3R-tau positive cell processes were relatively frequently observed, but TSA themselves were negative for 3R-tau (Fig. 4D).

Many TSA in the white matter of the temporal cortex showed AT8-identified (Fig. 5A), Gallyas-positive (Fig. 5B), and 4R-tau positive (Fig. 5C) staining, but were negative for 3R-tau (Fig. 5D).

GFA in the gray matter of the temporal cortex showed AT8-identified (Fig. 6A) and Gallyas-positive (Fig. 6B) staining. This mostly occupied astrocytic perikarya and ramified into cell processes in the cerebral gray matter, and was positive for 4R-tau (Fig. 6C) but negative for 3R-tau immunostaining (Fig. 6D).

TSA and GFA were negative for ubiquitin immunostaining (data not shown).

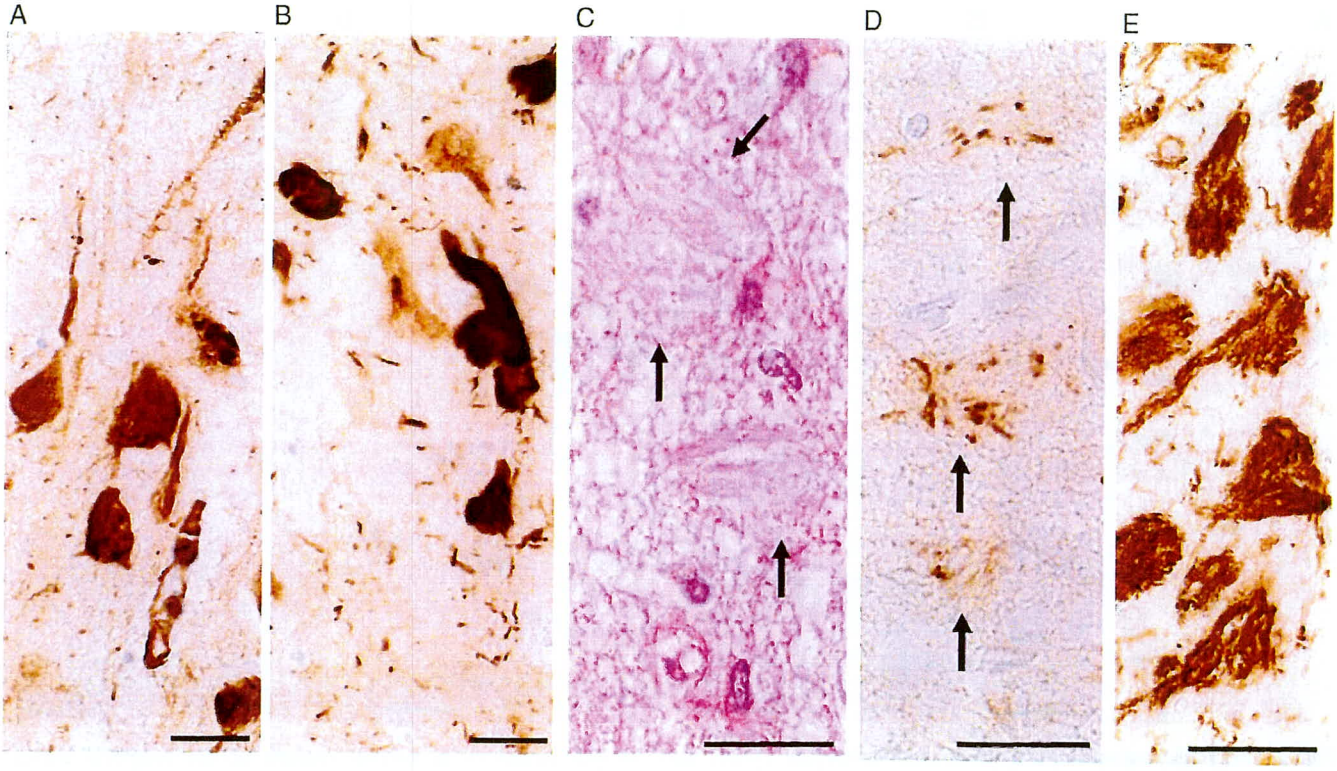

Fig. 1 Microphotographs of sections from the hippocampal CA1 region of an aged brain (A, B) and Alzheimer's disease brains (C-E). In the aged brain, neurofibrillary tangles are clearly immunoreactive for 4R-tau (A) and 3R-tau (B), equally, while neuropil threads are predominantly immunoreactive for 3R-tau as compared to 4R-tau. In the Alzheimer's disease brains, many ghost tangles with a few fine filaments (arrows) are seen on an HE-stained section (C) and are immunoreactive for 4R-tau (D) and well immunoreactive for 3R-tau (E). Scale bars: 25 μm (A–E).

DISCUSSION

The 3R-tau and 4R-tau antibodies used in this study were sufficient to examine tauopathies. Namely, as previously noted, NFTs were clearly immunostained with both antibodies, while neuropil threads were predominantly immunostained with anti-3R-tau antibody. Ghost tangles were clearly identified by 3R-tau and poorly immunostained by 4R-tau.[4,5]

Tauopathies are clinically, morphologically, and biochemically heterogeneous neurodegenerative diseases characterized by accumulation of phosphorylated tau in neurons and glial cells.[2] Recently, argyrophilic and tau-positive abnormal structures in astrocytes were frequently noted in aged brains, with the new nomenclature of ARTAG proposed.[11] Reports on tau astrogliopathies are increasing.[17–22] Ferrer *et al.*, found that tau pathology in glial cells largely parallels, but is not identical to, that in neurons in many tauopathies.[7] Hyperphosphorylated tau accumulation in glial cells often produces disease-specific astroglial phenotypes, such as tufted astrocytes in progressive supranuclear palsy (PSP), astrocytic plaques in corticobasal degeneration (CBD), ramified astrocytes in Pick's disease (PiD), or globular astroglial inclusions in globular glial tauopathies.[2,5–7] Astroglial deposition was 4R-tau-positive in AD, aged brain, PSP, CBD, and argyrophilic grain disease, whereas astrocyte inclusions were 3R-tau-positive in PiD. A few protoplasmic astrocytes in PSP contained 3R-tau, and a few reactive astrocytes in PiD contained 4R-tau.[7]

ARTAG is defined by the presence of two types of tau-bearing astrocytes: TSA and GFA.[11] Ikeda *et al.*[23] were the first to describe tau-positive TSAs, which are similar in morphology to the tau-positive astrocytes described by Nishimura *et al.* for PSP.[24] In TSA, tau immunoreactivity is localized in astrocytic perikarya with extensions into proximal parts of astrocytic processes. Inclusions are also found in astrocytic endfeet at the glia limitans surrounding blood vessels and the pial surface.[11] These are preferentially found at subpial and perivascular locations and white matter, and less often as clusters in gray matter. TSA are composed of hyperphosphorylated 4R-tau with features of pretangles lacking tau truncation of terminal regions,[12] and are considered to be putative glial counterparts of neuronal pretangles.[13] In this study, TSA were positive for 4R-tau but negative for 3R-tau, as previously reported. Variable frequent short thick cell processes in subpial and subependymal areas were positive for 3R-tau. As these processes are wider in diameter than astrocytic processes

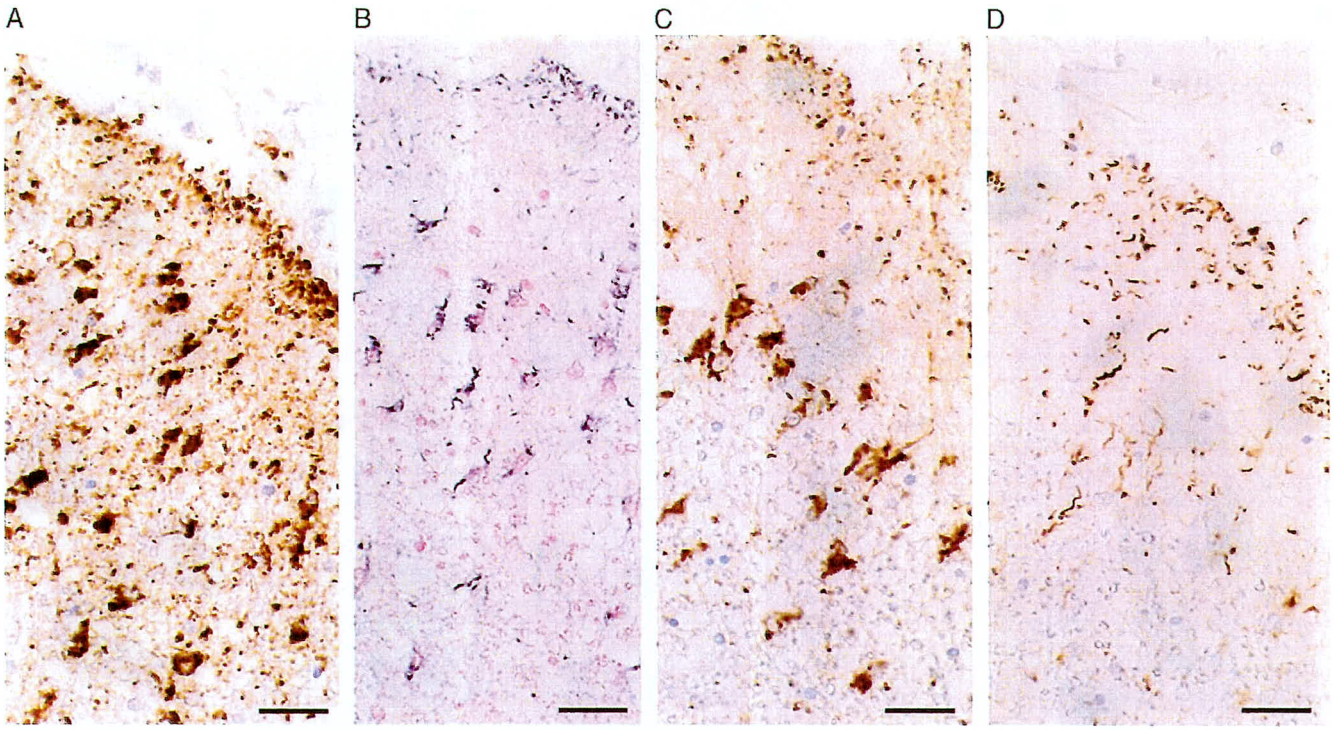

Fig. 2 Microphotographs of thorn-shaped astrocytes (TSA) and dot-like structures in subpial regions of the temporal cortex. AT8-identified structures (A) are similar to those detected by Gallyas methods (B) and 4R-tau immunohistochemistry (C), particularly in TSA and small dot-like structures. In contrast, 3R-tau immunoreactivity is absent in TSA, but present in short thick cell processes, which are likely neuropil threads (D). The frequency of short thick cell processes is variable. Scale bars: 25 μm (A–D).

4

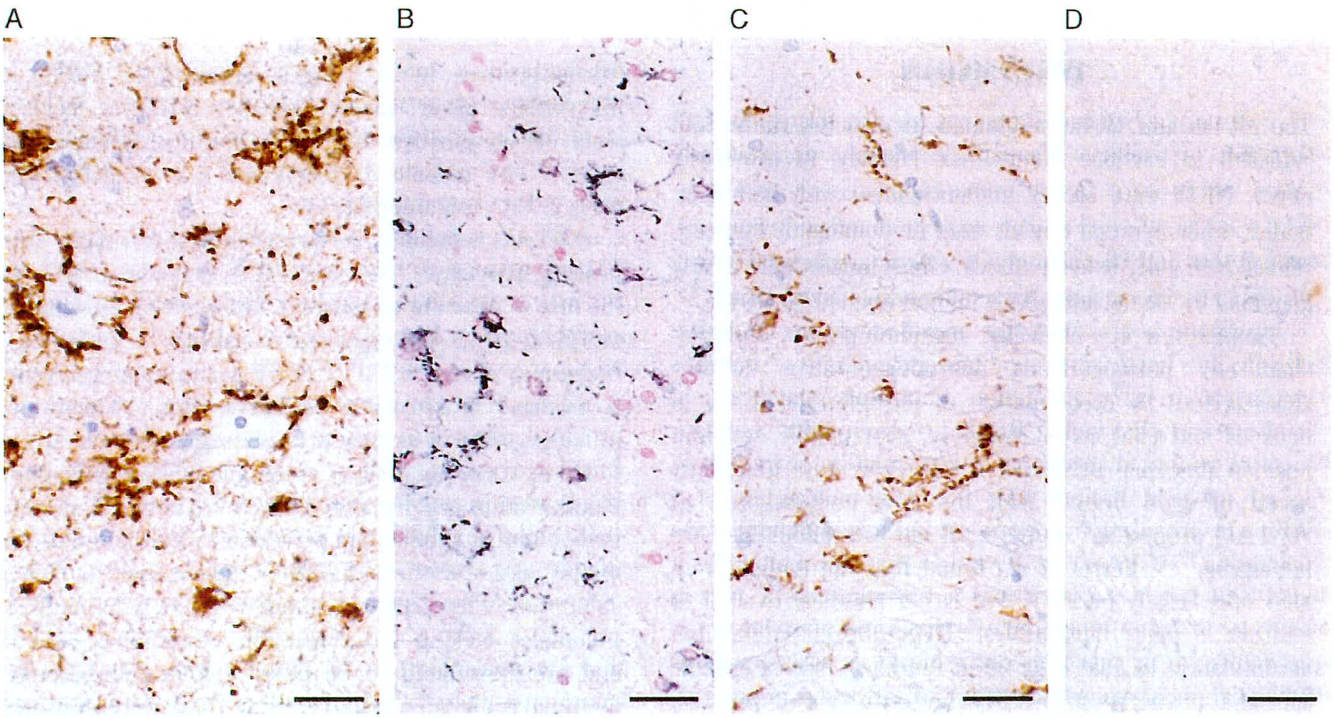

Fig. 3 Microphotographs of astrocytes surrounding small vessels in the basal ganglia. Astrocytic endfeet processes surrounding small vessels, small dot-like structures, and thorn-shaped astrocytes (TSA) in the neuropil are identified by AT8 (B) and positive for 4R-tau (C) but negative for 3R-tau (D). Scale bars: 25 μm (A–D).

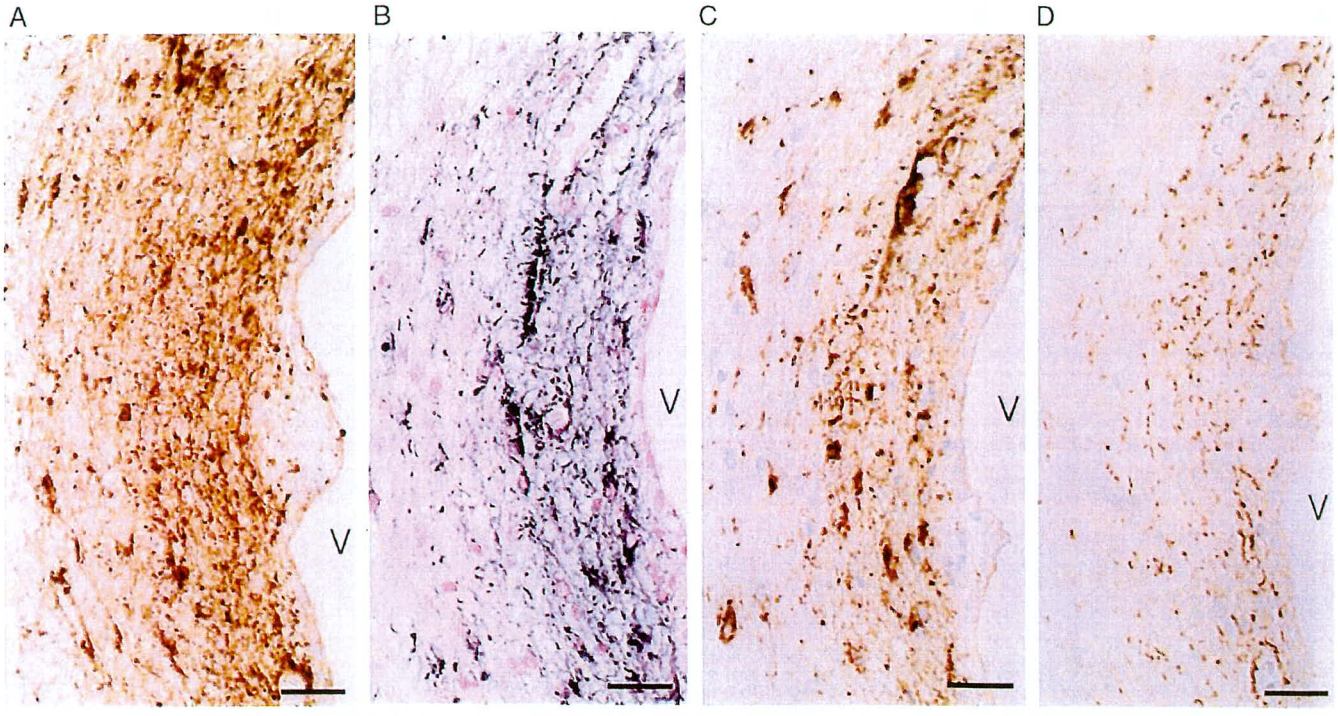

Fig. 4 Microphotographs of subependymal regions around the cerebral aqueduct. AT8-identified fibrils and thorn-shaped astrocytes (TSA) (A) are similar as detected by Gallyas methods (B) and 4R-tau immunostaining (C). 3R-tau-positive cell processes are frequently observed, while TSA are negative for 3R-tau (D). V: ventricle. Scale bars: 25 μm (A–D).

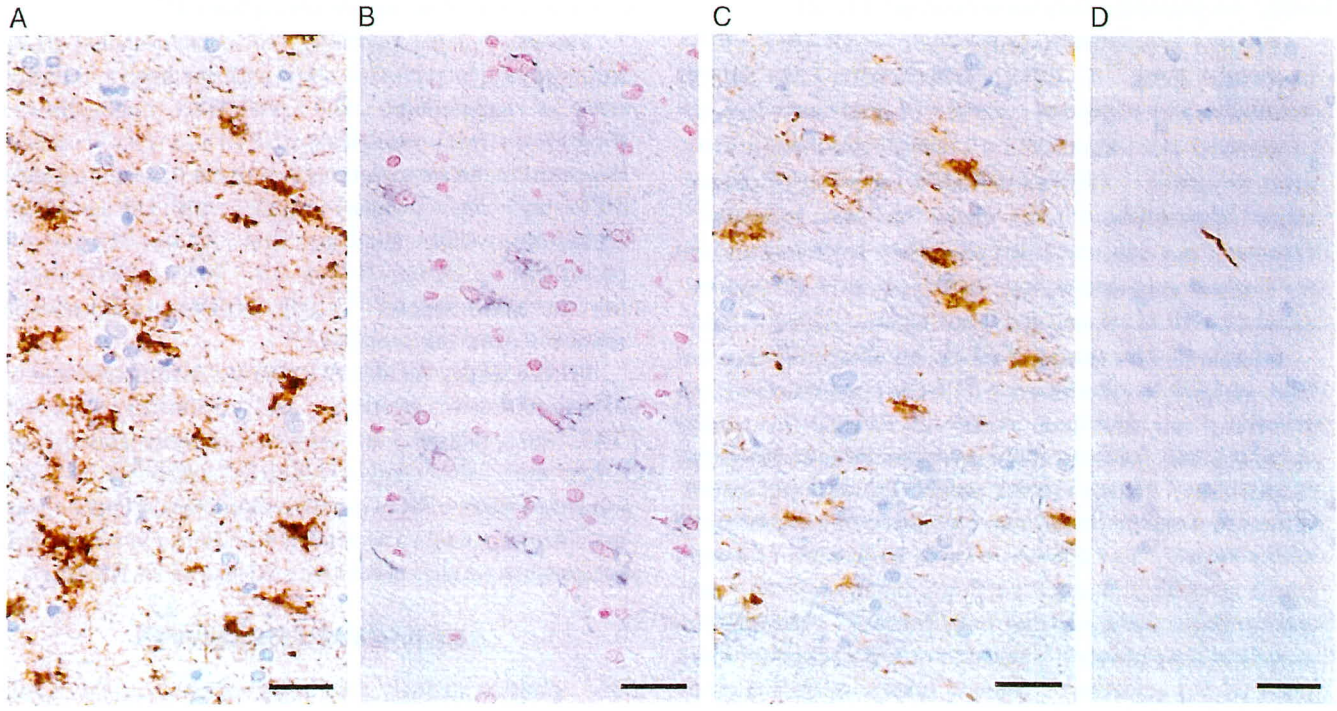

Fig. 5 Astrocytes in the white matter of the temporal cortex. Many thorn-shaped astrocytes (TSA) are AT8-identified (A), Gallyas-positive (B) and 4R-tau-positive (C), while the cells are negative for 3R-tau (D). Scale bars: 25 μm (A–D).

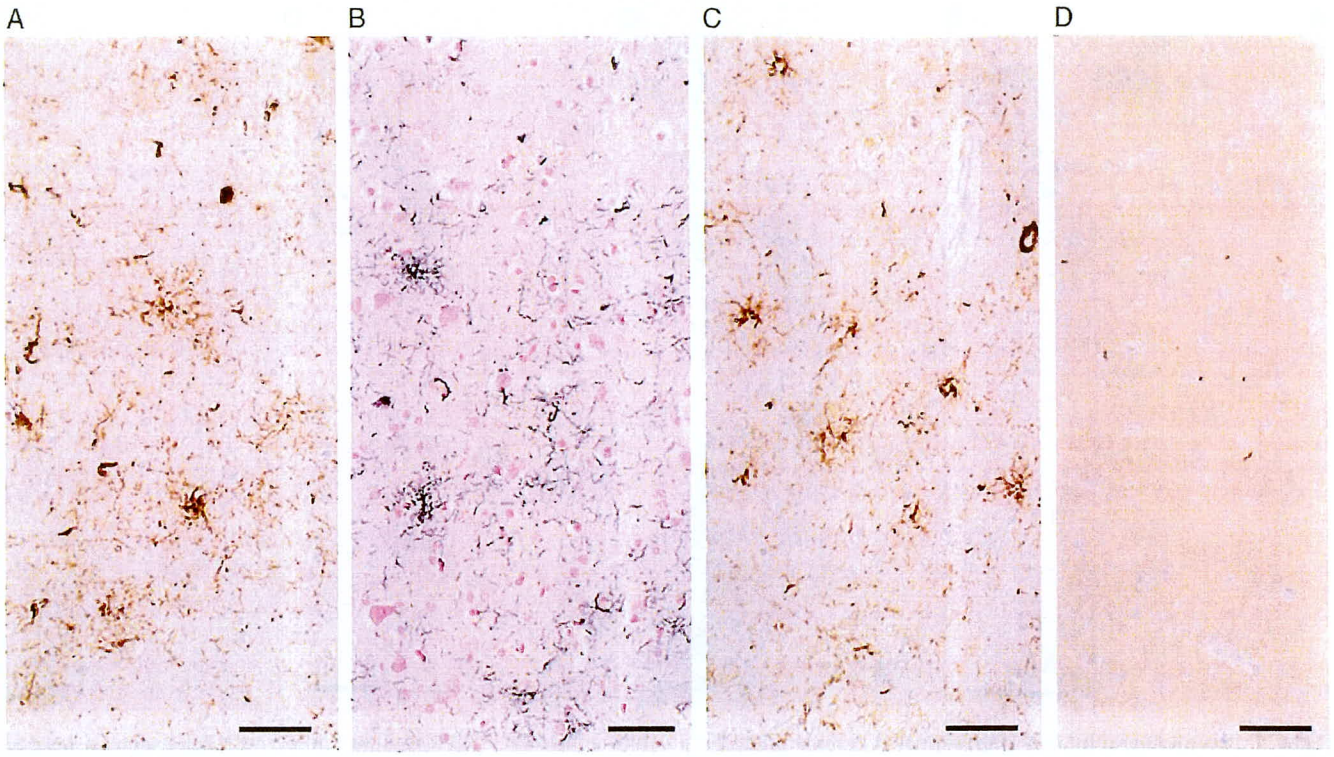

Fig. 6 Granular or fuzzy tau immunoreactivity in processes of astrocytes (GFA) in the gray matter of the temporal cortex. AT8-identified (A) and Gallyas-positive (B) structures occupying mostly astrocytic perikaryal and ramifying into the cell processes in the cerebral gray matter are positive for 4R-tau (C) but negative for 3R-tau (D). Scale bars: 50 μm (A–D).

but similar to neuropil threads in CA1 areas of AD brains,[5] we presumed they were neuropil threads.

Another predominant morphology of ARTAG is GFA in cortical areas.[11] In GFA, phosphorylated tau densely accumulates in perinuclear regions of astrocytes, and fine or granular tau accumulates on radially distributed astrocytic processes.[11] Gallyas methods occasionally demonstrate argyrophilia in the soma but not processes.[11] However, the soma and cell processes were well stained by Gallyas methods in our study, as well as immunostained by 4R-tau but negative for 3R-tau, similar to TSA.

Compared with neuronal NFTs, the major difference of TSA and GFA is the absence of 3R-tau immunoreactivity. Abnormal tau deposition occurs in neurons by specific steps, but little is known about progression of tau pathology in glial cells.[7] Changes in tau phosphorylation and conformation are similar in neurons and astrocytes in tauopathy of the elderly.[7] Tau mRNA is found in neurons in human brains suggesting that astrocytic tau immunoreactivity may purely reflect uptake of tau from neurons.[17] Nonetheless, astrocytic tau pathology is detected in regions without other types of tau pathology.[17] Recent studies suggest that the first step of astrocytic pathology might be fine granular accumulation in astrocytic processes.[17] These tau deposits are then transported from distal to proximal segments of the astrocytic cytoskeleton and eventually aggregate, becoming argyrophilic and/or ubiquitinated.[17]

Variation in the morphology of immunolabeled structures may be interpreted as representing stages in the process of aggregation and fibrillation, analogous to progression from pretangles to NFTs in AD.[4,9] Namely, tau-positive neurons undergo evolution from pretangles to NFTs and then to ghost tangles, with the associated expression profile changing from 3R-tau–/4R-tau+ for pretangles to 3R-tau+/4R-tau+ for NFTs to 3R-tau+/4R-tau– for ghost tangles.[14,25] Glial tangles are suggested to resemble neuronal pretangles.[14]

In this study, we did not identify 3R-tau+/4R-tau+ or 3R-tau+/4R-tau– astrocytes. As previously reported,[23] TSA were negative for ubiquitin immunostaining, and GFA were also negative for this antibody. In more advanced stages, 3R-tau positive astrocytes might be present. Further studies are needed to clarify the nature and progression of glial tau-positive structures in ARTAG.

ACKNOWLEDGMENTS

The authors express their appreciation to Ms. Kunie Watanabe for her excellent technical assistance. We thank Rachel James, PhD, from Edanz Group (www.Edanzediting.com/ac) for editing a draft of this manuscript.

DISCLOSURE

Authors declare no conflicts of interest for this article.

REFERENCES

1. Avila J, Lucas JJ, Pérez M, Hernández F. Role of tau protein in both physiological and pathological conditions. *Physiol Rev* 2004; **84**: 361–384.
2. Kovacs GG. Invited review: Neuropathology of tauopathies: Principles and practice. *Neuropathol Appl Neurobiol* 2015; **41**: 3–23.
3. Hasegawa M. Molecular mechanisms in the pathogenesis of Alzheimer's disease and tauopathies-prion-like seeded aggregation and phosphorylation. *Biomolecules* 2016; **6**(). pii:: E24. https://doi.org/10.3390/biom6020024
4. Hasegawa M, Watanabe S, Kondo H *et al.* 3R and 4R tau isoforms in paired helical filaments in Alzheimer's disease. *Acta Neuropathol* 2014; **127**: 303–305.
5. Yoshida M. Cellular tau pathology and immunohistochemical study of tau isoforms in sporadic tauopathies. *Neuropathology* 2006; **26**: 457–470.
6. Kovacs GG, Molnár K, László L *et al.* A peculiar constellation of tau pathology defines a subset of dementia in the elderly. *Acta Neuropathol* 2011; **122**: 205–222.
7. Ferrer I, López-González I, Carmona M *et al.* Glial and neuronal tau pathology in tauopathies: characterization of disease-specific phenotypes and tau pathology progression. *J Neuropathol Exp Neurol* 2014; **73**: 81–97.
8. Dan A, Takahashi M, Masuda-Suzukake M *et al.* Extensive deamidation at asparagine reside 279 accounts for weak immunoreactivity of tau with RD4 antibody in Alzheimer's disease brain. *Acta Neuropathol Commun* 2013; **1**: 54. https://doi.org/10.1186/2051-5960-1-54
9. Hara M, Hirokawa K, Kamei S, Uchihara T. Isoform transition from four-repeat to three-repeat tau underlies dendrosomatic and regional progression of neurofibrillary pathology. *Acta Neuropathol* 2013; **125**: 565–579.
10. Crary JF, Trojanowski JQ, Schneider JA *et al.* Primary age-related tauopathy (PART): A common pathology associated with human aging. *Acta Neuropathol* 2014; **128**: 755–766.
11. Kovacs GG, Ferrer I, Grinberg LT *et al.* Aging-related tau astrogliopathy (ARTAG): Harmonized evaluation strategy. *Acta Neuropathol* 2016; **131**: 87–102.
12. Ferrer I, Garcia MA, González IL *et al.* Aging-related tau astrogliopathy (ARTAG): Not only tau phosphorylation in astrocytes. *Brain Pathol* 2018 (Feb 3); **28**(6): 965–985. https://doi.org/10.1111/bpa.12593 [Epub ahead of print]
13. López-González I, Carmona M, Blanco R *et al.* Characterization of thorn-shaped astrocytes in white matter of temporal lobe in Alzheimer's disease brains. *Brain Pathol* 2013; **23**: 144–153.
14. Ikeda K, Akiyama H, Arai T, Nishimura T. Glial tau pathology in neurodegenerative diseases: their nature and comparison with neuronal tangles. *Neurobiol Aging* 1998; **19**: S85–S91.
15. Okamoto K, Amari M, Fukuda T, Suzuki TM. Comparison of AT8 immunoreactivity in the locus ceruleus and hippocampus of 154 brains from routine autopsies. *Neuropathology* 2017; **37**: 306–310.
16. Uchihara T, Nakamura A, Shibuya K, Yagishita S. Specific detection of pathological three-repeat tau after pretreatment with potassium permanganate and oxalic acid on PSP/CBD brains. *Brain Pathlol* 2011; **21**: 180–188.
17. Kovacs GG, Lee VM, Trojanowski JQ. Protein astrogliopathies in human neurodegenerative diseases and aging. *Brain Pathol* 2017; **27**: 675–690.
18. Ahmed Z, Bigio EH, Budka H *et al.* Globular glial tauopathy (GGT): Consensus recommendation. *Acta Neuropathol* 2013; **126**: 537–544.
19. Ikeda C, Yokota O, Nagao S *et al.* The relationship between development of neuronal and astrocytic tau pathologies in subcortical nuclei and progression of argyrophilic grain disease. *Brain Pathol* 2016; **26**: 488–505.
20. Kovacs GG, Xie SX, Lee EB *et al.* Multisite assessment of aging-related tau astrogliopathy. *J Neuropathol Exp Neurol* 2017; **76**: 605–619.
21. Kovacs GG, Xie SX, Robinson JL *et al.* Sequential stages and distribution patterns of aging-related tau astroglipathy (ARTAG) in the human brain. *Acta Neuropathol Commun* 2018; **6**: 50. https://doi.org/10.1186/s40478-018-0552-y.
22. Ikeda C, Yokota O, Miki T *et al.* Astrocytic tau pathology in argyrophilic grain disease and related four-repeat tauopathies. *Acta Med Okayama* 2018; **72**: 211–221.
23. Ikeda K, Akiyama H, Kondo H *et al.* Thorn-shaped astrocytes: Possibly secondarily induced tau-positive glial fibrillary tangles. *Acta Neuropathol* 1995; **90**: 620–625.
24. Nishimura T, Ikeda K, Akiyama H *et al.* Immunohistochemical investigation of tau-positive structures in the cerebral cortex of patients with progressive supranuclear palsy. *Neurosci Lett* 1995; **201**: 123–126.
25. Uchihara T. Pretangles and neurofibrillary changes: Similarities and differences between AD and CBD based on molecular evolution. *Neuropathology* 2014; **34**: 571–577.

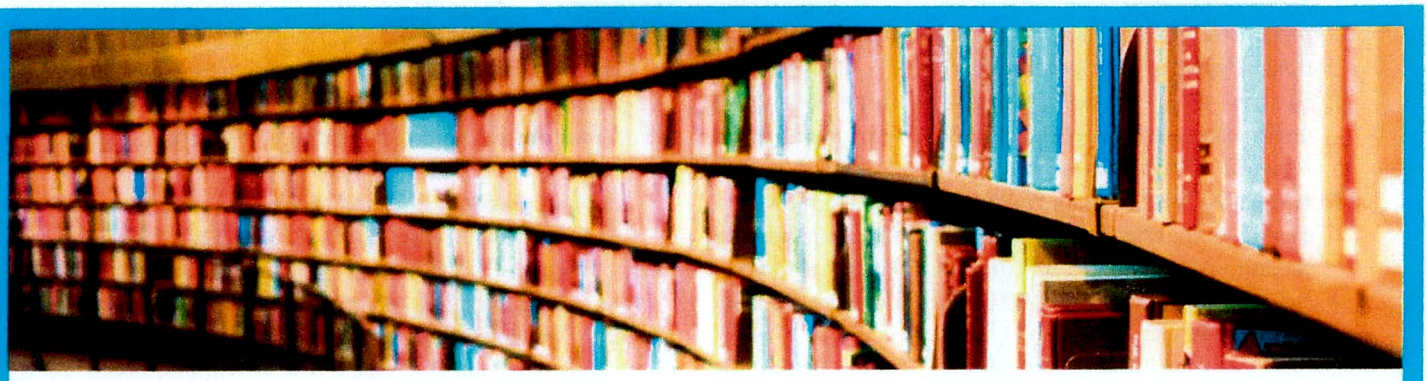

TOP DOWNLOADED PAPER 2018-2019

CONGRATULATIONS TO

Koichi Okamoto

whose paper has been recognized as
one of the most read in

WILEY

Clinical & Experimental
Neuroimmunology

Clinical and Experimental Neuroimmunology **10** (2019) 57–60

CASE REPORT

Case of white-eyed shunt carotid-cavernous sinus fistula mimicking optic neuritis

Shintaro Hayashi,[1,2] Kiyoshi Mashio[1] and Koichi Okamoto[3]

[1]Department of Neurology, Gunma Rehabilitation Hospital, Nakanjo, Agatsuma, Gunma, Japan, [2]Department of Neurology, Gunma University Graduate School of Medicine, Maebashi-city, Gunma, Japan, [3]Geriatrics Research Institute and Hospital, Maebashi-city, Gunma, Japan

Keywords
angiography; carotid-cavernous sinus fistula; optic neuritis; posterior draining; white-eyed shunt

Correspondence
Shintaro Hayashi, MD, PhD, Department of Neurology, Gunma Rehabilitation Hospital, 2136 Kami-Sawatari, Nakanojo, Agatsuma, Gunma 377-0541, Japan.
Tel: +81-279-66-2121
Fax: +81-279-66-2900
Email: cho7pa2_0529@yahoo.co.jp

Received: 23 July 2018; revised: 9 September 2018; accepted: 28 September 2018.

Abstract

Background The typical orbito-ocular manifestations of carotid-cavernous sinus fistulas are conjunctival hyperemia, chemosis and exophthalmos as a result of increased fistular flow directed anteriorly in the ophthalmic veins. These congestive features are absent if the flow is directed posteriorly, resulting in "white-eyed shunts." We describe a rare carotid-cavernous sinus fistula case presenting with optic neuritis-like manifestations.

Case presentation A 71-year-old Japanese woman developed periorbital pain, impaired visual acuity with an upper horizontal visual field defect, diminished light reflexes and a relative afferent pupillary defect in her right eye. There were no congestive features in her eyes. Intraocular pressure was normal in both eyes, but fundoscopy revealed a pale optic disc in the right eye. Serum anti-aquaporin-4 antibodies were negative. Although optic neuritis was suspected, high-dose corticosteroid administration did not result in improvement. When referred to Department of Neurology, Gunma University Hospital, she showed a subtle, incomplete oculomotor nerve palsy in the right eye. Magnetic resonance angiography suggested carotid-cavernous sinus fistula (CCF), and cerebral angiography showed fistulous drainage into the cavernous sinus and inferior petrosal sinus, and a delayed opacification of the superior orbital and angular facial veins on the right side. A diagnosis of white-eyed shunt CCF was made, and a coil embolization procedure was carried out. However, there was no symptom improvement.

Conclusions It is difficult to diagnose white-eyed shunt CCF based only on physical findings, especially when there is an absence of ocular congestive features. We discuss the possible mechanisms underlying the optic neuritis-like symptoms of CCF.

Introduction

Carotid-cavernous sinus fistulas (CCF) typically cause conjunctival hyperemia, chemosis, orbital soft-tissue swelling, exophthalmos and ptosis as a result of increased fistular flow directed anteriorly in the ophthalmic veins.[1–4] However, it is less well-recognized that these congestive features will be absent if the fistular flow is directed posteriorly, resulting in "white-eyed shunts" (WES), as previously described in some reports.[3–9] A case of CCF presenting with WES (CCF/WES) might be difficult to diagnose based only on physical findings, and might be missed unless cerebral angiography is carried out. We present the first report of a patient with CCF/WES mimicking optic neuritis.

Case report

A previously healthy 71-year-old Japanese woman experienced acute pain in the right periorbital region and presented with an upper horizontal visual field defect in her right eye. The pain worsened over the next few days, and her visual field defect enlarged. She was admitted to the Ophthalmology Department at Gunma University Hospital. Examination of her

right eye revealed mydriasis (6.0 mm in diameter), an absence of direct and indirect light reflexes, and a relative afferent pupillary defect. No extraocular movement disturbances were noted by the treating ophthalmologist, and there were no signs of exophthalmos, conjunctival hyperemia or audible bruit over the eyes or the temples. Funduscopy showed no abnormalities, except for a pale optic disc in her right eye, and retinal fluorescein angiography was not carried out. Her intraocular pressures were 18.3 (right)/12.7 (left) mmHg, and her visual acuity was "hand motion" (not correctable) in the right eye, and 120/100 in the left; her vision was restricted to the nasal lower quadrant. Serum anti-aquaporin-4 antibodies were negative. Right optic neuritis was initially suspected, and the patient was administered one course of intravenous methylprednisolone pulse therapy (1 g/day for 3 days). Although the visual field defect did not improve, there was a reduction of pain. It was at this time that she was referred to Department of Neurology. Neurological examinations revealed mild ptosis (Fig. 1a), a slight abduction of the right eye (Fig. 1a) and subtle restriction of adduction in the right extraocular movement (Fig. 1b). Cranial magnetic resonance images showed marked dilatation of the superior orbital vein (SOV) bilaterally and thrombus inside the venous lumen (Fig. 1f, g). Three-dimensional time-

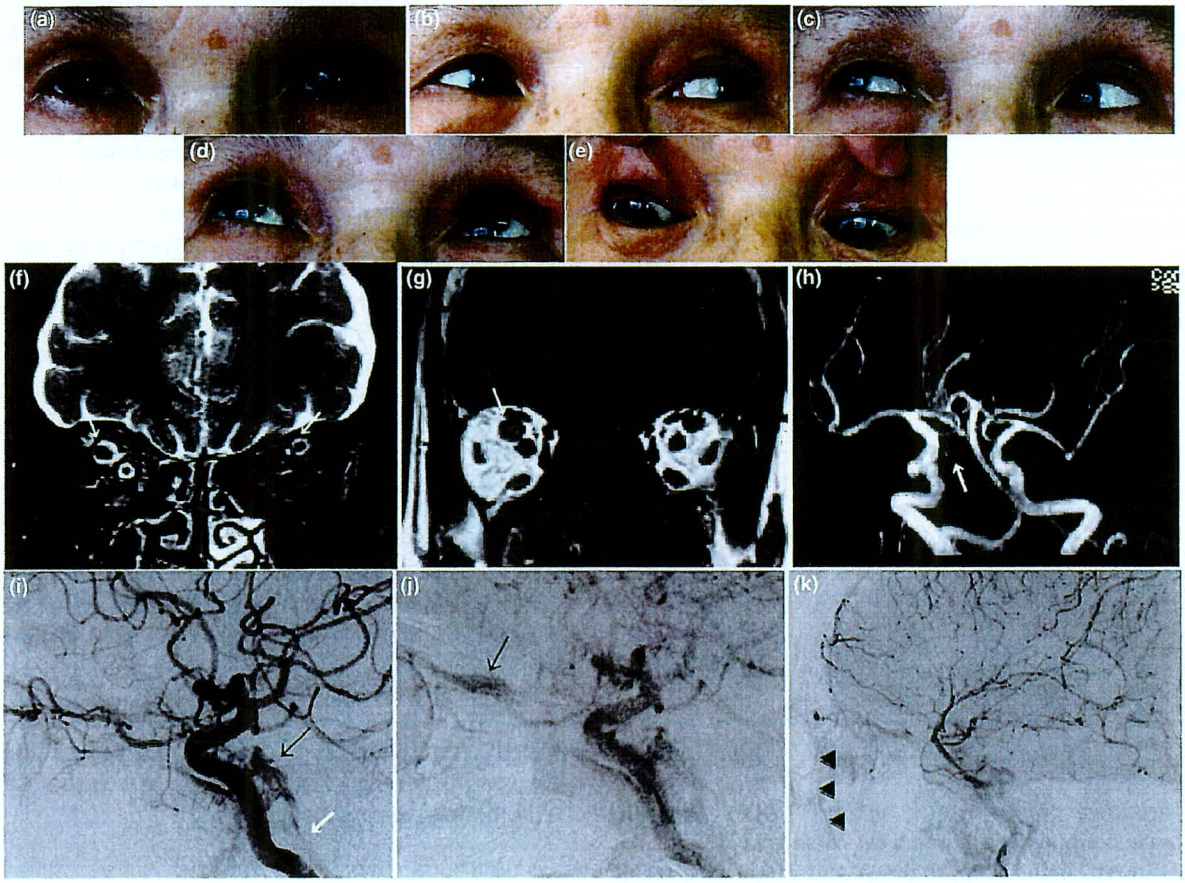

Figure 1 (a–e) Patient's ocular appearance. (a) Mild ptosis of the right eye was present, and (a) a slight adduction of the right eye and (b) a subtle restriction of adduction in the right extraocular movement could be seen, (a–e) but there were no signs of exophthalmos or conjunctival hyperemia. (f–h) Magnetic resonance images. (f) Coronal fat-suppressed T2-weighted images show dilated bilateral superior orbital veins with right-side predominance (arrows). (g) T1-weighted image shows the disappearance of flow void signal in the right superior orbital veins, indicating a thrombus formation in the venous lumen (arrow). (g) There are no enlarged, engorged extraocular muscles. (h) Three-dimensional time-of-flight magnetic resonance angiography shows a crepe-like profile extending from the posterior aspect of the cavernous portion of the internal carotid artery (arrow), indicating shunt flow into the inferior petrosal sinus from the fistula. (i–k) Cerebral angiography. Illustrated here is a selected right internal carotid arteriogram (lateral view). (i) The arterial phase shows fistulous drainage into the cavernous sinus (black arrow) and inferior petrosal sinus (white arrow). (j) Delayed opacification of the superior orbital veins is also observed (arrow). (k) The right angular facial vein appears to be recognizable (arrowheads).

of-flight magnetic resonance angiography showed a crepe-like profile extending from the posterior aspect of the cavernous portion of the internal carotid artery (Fig. 1h), indicating shunt flow into the inferior petrosal sinus from the fistula. No other abnormalities, including periventricular ovoid lesions, which would have been indicative of multiple sclerosis, were observed. Cerebral angiography (Fig. 1i–k) showed that the CCF was supplied by the meningohypophyseal trunk of the internal carotid artery with drainage into the inferior petrosal sinus, and also showed a delayed opacification of the SOV. The outflow from the right cavernous sinus into the intercavernous sinus was abnormal, and there were well-developed anastomoses between the SOV and the angular facial vein. Coil embolization was carried out 7 weeks after the onset of symptoms, with no visible improvement.

Discussion

The visual symptoms of the current patient occurred with a sudden onset, which was consistent with diagnoses of both CCF and optic neuritis. However, it is noteworthy that the optic disc was initially found to already be pale. Given that such a change usually takes several weeks, there might have been preceding pathological events, such as a subclinical optic nerve ischemia. Dural CCF occasionally produces aseptic cavernous sinus thrombosis.[10,11] Grove found that a majority of patients with these fistulas were middle-aged or elderly woman.[10] In the present patient, fat-suppressed T2-weighted images of magnetic resonance images and cerebral angiography disclosed slow flow in the right SOV, and T1-weighted images suggested a thrombus formation in the venous lumen. These findings suggest that the outflow from the CCF gradually shifted from an anterior (orbital) direction to a posterior (intracranial) direction, because of SOV thrombosis. That might explain the gradual manner of our patient's CCF development. Although the precise cause of the ischemic insult to the retrobulbar optic nerve was unknown, cerebral angiography showed that it occurred in the setting of an ipsilateral dural CCF. The patient had anterior (SOV), posterior (meningohypophyseal trunk, inferior petrosal sinus) and lateral (intercavernous sinus) drainage, suggesting that the optic nerve was being deprived of its normal arterial supply, which eventually caused acute posterior ischemic optic neuropathy.[1] The detection of a reduced choroidal blush in the acute phase with retinal fluorescein angiography would have supported this view, but this test was unfortunately not carried out, because optic neuritis was initially considered as the diagnosis by the treating ophthalmologist. Although cerebral angiography revealed anterior draining (SOV), the classic external ocular signs, such as exophthalmos with conjunctival hyperemia and edema, were absent in the present patient. The extent of these orbito-ocular manifestations in CCF depends primarily on an increase of venous pressure in the SOV, due to either a stenosis of the anterior aspect of the orbital veins, hypoplasticity or an occlusion of the petrosal pathways.[2] The dispersion of the shunt flow associated with multiple venous drainages and the well-developed anastomoses observed between the SOV and the angular facial vein might have contributed to the absence of classical orbito-ocular signs in the present patient by relieving the venous hypertension of the SOV. This hypothesis is supported by the observation that the patient's intraocular pressure, which is affected by the venous pressure of the SOV, remained normal. Furthermore, there was no sign of engorged extraocular muscles.

To the best of our knowledge, only 50 CCF/WES cases have been reported to date: 34 with abducens nerve palsies,[3–8] 14 with oculomotor nerve palsies[4,6,8,9] and two with trochlear nerve palsies.[5,8] Although the disturbance of the patient's right eye adduction was quite subtle in the present patient (Fig. 1a, b), the finding that the right eye also had mild ptosis and an abnormal pupillary light reflex led us to conclude that there was an incomplete paralysis of the right oculomotor nerve. The patient never complained of diplopia, and this might be because the right eye had a manual valve from the onset. If the CCF shunt drains posteriorly into the inferior petrosal sinus, an isolated oculomotor,[9,12] trochlear or abducens nerve palsy[13,14] might develop; however, why these nerves were only partially disturbed in the present patient is yet unknown.

The findings presented here strongly suggest that we should be aware that CCF/WES could masquerade as optic neuritis when ophthalmoplegia is subtle, and that magnetic resonance angiography and coronal orbital fat-suppressed magnetic resonance images might be necessary to establish the correct diagnosis.

Acknowledgments

We thank Patrice Voss PhD and Claire Barnes PhD from Edanz Group (www.edanzediting.com/ac) for editing a draft of this manuscript.

This work was supported by a Grant-in-Aid for Scientific Research (C) (No. 16K09721) from the

Ministry of Education, Science, Sports, Culture and Technology of Japan to S. Hayashi.

Conflict of interest

None declared.

Disclosure of ethical statement

All informed consent was obtained from the subject.

References

1. Hashimoto M, Ohtsuka K, Suzuki Y, et al. A case of posterior ischemic optic neuropathy in a posterior-draining dural cavernous sinus fistula. *J Neuroophthalmol.* 2005; **25**: 176–9.
2. Barrow DL, Spector RH, Braun IF, et al. Classification and treatment of spontaneous carotid-cavernous sinus fistulas. *J Neurosurg.* 1985; **62**: 248–56.
3. Kim JW, Kim SJ, Kim MR. Traumatic carotid-cavernou sinus fistula accompanying abducens nerve (VI) palsy in blowout fractures: missed diagnosis of 'white-eyed shunt'. *Int J Oral Maxillofac Surg.* 2013; **42**: 470–3.
4. Acierno MD, Trobe JD, Cornblath WT, et al. Painful oculomotor palsy caused by posterior-draining dural carotid cavernous fistulas. *Arch Ophthalmol.* 1995; **113**: 1045–9.
5. Ogawa G, Tanabe H, Kanzaki M, et al. Two cases of idiopathic carotid-cavernous fistula with headache and ophthalmoplegia. *Rinsho Shinkeigaku (Clin Neurol).* 2007; **47**: 516–8.
6. Uehara T, Tabuchi M, Kawaguchi T, Mori E. Spontaneous dural carotid cavernous sinus fistula presenting isolated ophthalmoplegia. Evaluation with MR angiography. *Neurology.* 1998; **50**: 814–6.
7. Ikeda K, Deguchi K, Tsukaguchi M, Sasaki I, Shimamura M, Urai Y. Absence of orbito-ocular signs in dural carotid-cavernous sinus fistula with a prominent anterior venous drainage. *J Neurol Sci.* 2005; **236**: 81–4.
8. Wu HC, Ro LS, Chen CJ, Chen ST, Lee TH, Chen YC. Isolated ocular motor nerve palsy in dural carotid-cavernous sinus fistula. *Eur J Neurol.* 2006; **13**: 1221–5.
9. Hawke SH, Mullie MA, Hoyt WF, Hallinan JM, Halmagyi GM. Painful oculomotor nerve palsy due to dural-cavernous sinus shunt. *Arch Neurol.* 1989; **46**: 1252–5.
10. Grove AS Jr. The dural shunt syndrome. Pathophysiology and clinical course. *Ophthalmology.* 1984; **91**: 31–44.
11. Seeger JF, Gabrielsen TO, Giannotta SL, Lotz PR. Carotid-cavernous sinus fistulas and venous thrombosis. *AJNR Am J Neuroradiol.* 1980; **1**: 141–8.
12. Sempere AP, Menendez BM, Alvarez CC, hallinan JM, Halmagyi GM. Painful oculomotor nerve palsy due to dural-cavernous sinus fustula. *Eur Neurol.* 1991; **31**: 186–7.
13. Newton TH, Hoyt WF. Dural arteriovenous shunts in the region of the cavernous sinus. *Neuroradiology.* 1970; **1**: 71–81.
14. Leonard TJK, Moseley IF, Sanders MD. Ophthalmoplegia in carotid cavernous sinus fistula. *Br J Ophthalmol.* 1984; **68**: 128–34.

OPEN ACCESS

RESEARCH PAPER

Ultra-high-dose methylcobalamin in amyotrophic lateral sclerosis: a long-term phase II/III randomised controlled study

Ryuji Kaji,[1] Takashi Imai,[2,3] Yasuo Iwasaki,[4] Koichi Okamoto,[5] Masanori Nakagawa,[6] Yasuo Ohashi,[7] Takao Takase,[8] Takahisa Hanada,[8] Hiroki Shimizu,[8] Kunio Tashiro,[9] Shigeki Kuzuhara[10]

► Additional material is published online only. To view please visit the journal online (http://dx.doi.org/10.1136/jnnp-2018-319294).

For numbered affiliations see end of article.

Correspondence to
Professor Ryuji Kaji, Department of Neurology, Tokushima University School of Medicine, Tokushima 770-8503, Japan; rkaji@tokushima-u.ac.jp

Received 24 July 2018
Revised 20 November 2018
Accepted 27 November 2018
Published Online First 13 January 2019

ABSTRACT

Objective To evaluate the efficacy and safety of intramuscular ultra-high-dose methylcobalamin in patients with amyotrophic lateral sclerosis (ALS).

Methods 373 patients with ALS (El Escorial definite or probable; laboratory-supported probable; duration ≤36 months) were randomly assigned to placebo, 25 mg or 50 mg of methylcobalamin groups. The primary endpoints were the time interval to primary events (death or full ventilation support) and changes in the Revised ALS Functional Rating Scale (ALSFRS-R) score from baseline to week 182. Efficacy was also evaluated using post-hoc analyses in patients diagnosed early (entered ≤12 months after symptom onset).

Results No significant differences were detected in either primary endpoint (minimal p value=0.087). However, post-hoc analyses of methylcobalamin-treated patients diagnosed and entered early (≤12 months' duration) showed longer time intervals to the primary event ($p<0.025$) and less decreases in the ALSFRS-R score ($p<0.025$) than the placebo group. The incidence of treatment-related adverse events was similar and low in all groups.

Conclusion Although ultra-high-dose methylcobalamin did not show significant efficacy in the whole cohort, this treatment may prolong survival and retard symptomatic progression without major side effects if started early.

Trial registration number NCT00444613.

INTRODUCTION

Amyotrophic lateral sclerosis (ALS) is an intractable neurodegenerative disease characterised by motor neuron degeneration typically presenting with muscle weakness and atrophy.[1] Respiratory failure due to muscle weakness is the major cause of death. Without mechanical ventilation support, patients succumb to this disease within 3–6 years from its onset.

The widely used drug for ALS, riluzole, provides modest prolongation of survival (2–3 months), but no beneficial effects were shown on muscle strength and little on bulbar function.[2] Moreover, safety concerns, such as liver dysfunction, exist.[2] Edaravone has been approved for retarding the clinical deterioration of ALS, but its effect on the survival is unknown.[3]

The deficiency in vitamin B_{12} is associated with central nervous system lesions including subacute combined degeneration of the cord, indicating an important function of B_{12} in the spinal cord and the brain. Methylcobalamin, an active vitamin B_{12}, used in Japan to treat peripheral neuropathy and megaloblastic anaemia, is a potential candidate for ALS treatment. It functions as a coenzyme for homocysteine remethylation as a methyl donor, and inhibits neuronal degeneration by decreasing levels of homocysteine, the accumulation of which contributes to neuronal degeneration in patients with ALS.[4 5] It also activates extracellular signal-regulated kinases 1 and 2 and Akt to induce neurite outgrowth and prolong neuronal survival.[6] Cyanates/cyanide conjugates of B_{12} are not acting as methyl donor and have not been proven to show these effects.

Preclinical studies have reported that methylcobalamin protects neurons against glutamate neurotoxicity[7 8] and promotes nerve regeneration.[9] It has also been shown that intraperitoneal ultra-high dosage inhibits disease progression in a wobbler mouse.[10] Oral administration in high dose would be ineffective because of the limited availability of the gastric intrinsic factor for its absorption. Clinical studies have demonstrated the efficacy of intramuscular ultra-high-dose methylcobalamin on compound muscle action potentials.[11] Moreover, a small-sized study has demonstrated that, if started early in the disease course, ultra-high-dose methylcobalamin prolongs ventilation-free survival.[12]

Based on these results, we conducted a long-term phase II/III clinical trial to evaluate the efficacy and safety of intramuscular ultra-high-dose methylcobalamin in Japanese patients with ALS.

METHODS

This multicentre, randomised, double-blind, placebo-controlled clinical trial was conducted from December 2006 to March 2014 at 51 sites in Japan.

Patients

Patients satisfying the following inclusion criteria were eligible: outpatients aged 20 years or older; clinically definite, clinically probable, or clinically probable, laboratory-supported ALS diagnosis according to the revised El Escorial criteria (Airlie House criteria)[13]; duration from the symptom onset

To cite: Kaji R, Imai T, Iwasaki Y, *et al*. *J Neurol Neurosurg Psychiatry* 2019;**90**:451–457.

≤3 years; stage 1 or 2 of the Japanese ALS severity classification[14] (scores range from 1 to 5: 1 denotes no difficulty in daily living and working; 2, ability to live or work unaided; 3, requirement of assistance in daily living due to incapability of managing social life; 4, requirement of constant assistance in all aspects of daily living; and 5, bedridden status requiring a life support system); and Revised ALS Functional Rating Scale (ALSFRS-R) score[15] decrease by 1–3 points during the 12-week observation period. The definition of onset was the initial time that the patient recognised weakness or any other motor symptoms other than twitching or cramping of muscles. The key exclusion criteria were tracheostomy or previous use of non-invasive ventilation, per cent-predicted forced vital capacity (%FVC) ≤60%, multiple conduction blocks, new start or change in the dose or administration of riluzole after the observation period began, or serious cardiovascular, renal, hepatic disease or any haematological changes suggestive of B_{12} deficiency.

This report follows the Consolidated Standards of Reporting Trials guidelines.

Randomisation and treatment

The patients were centrally randomised to the placebo or 25 mg or 50 mg methylcobalamin groups using the order of registration with a minimisation algorithm to balance the following factors: onset type (bulbar or upper or lower motor neuron onset), riluzole coadministration, ALSFRS-R score before study enrolment, and the change in this score during the observation period.

Allocated drugs were intramuscularly administered twice per week starting from the end of the observation period (12 weeks) and continued for 182 weeks in a manner that the patients and their caregivers could not see the formulation colour (the active ingredients in methylcobalamin colour the formulation red). Changes in riluzole administration were not allowed. Edaravone was not used in any of the subjects.

Outcome measures

The primary endpoints were the time to primary events and the change in ALSFRS-R score from baseline to week 182. The primary events were defined as death by any cause or invasive or non-invasive ventilation support ≥22 hours per day due to ALS progression. On the occurrence of a primary event, treatment was discontinued. ALSFRS-R quantitatively evaluates the progression of disability by measuring respiratory function and physical ability in daily living.

The secondary endpoints included muscle strength assessed using the manual muscle test (Medical Research Council Scale), physical functional status measured with the Norris Scale,[16] respiratory function assessed using %FVC, grip strength, and the quality of life evaluated using the ALS Assessment Questionnaire-40.[17]

The primary and secondary efficacy endpoints were evaluated using post-hoc analyses in a subgroup of patients diagnosed early (at screening ≤12 months after symptom onset) based on previous studies.[11 12]

Drug safety was evaluated on the incidence of adverse events and the results of laboratory tests, vital signs and an ECG. Events due to the progression of ALS were not counted as adverse events; however, all deaths were counted as adverse events regardless of cause.

All assessments, except for ECG, were conducted on weeks 0, 4 and 16, and at 12-week intervals thereafter to week 172, and on week 182. For patients who discontinued therapy due to the primary event, the last assessment was conducted within 4 weeks of the day the event occurred. Different investigators were responsible for drug administration, as well as efficacy, ALSFRS-R and safety assessments, to maintain blindness throughout the study, because the active ingredients in methylcobalamin colour urine red.

Statistical analysis

The sample size was originally set at 200 primary events in 300 patients (100 per group) for 130 weeks to detect a significant difference in the HR for the time to primary event between the groups at a one-sided significance level of 1%, with a power of 90%, based on an estimated HR of the primary events of 0.5–0.6 and effect size in the ALSFRS-R analysis of 0.3–0.4. However, the sample size and study duration were revised while maintaining blindness to 360 patients (120 per group) and 182 weeks because of a low rate of primary events.

Two interim analyses by an independent data monitoring committee were performed to assess safety and futility.

The efficacy analyses were conducted using a population analysis for those patients who received methylcobalamin and had evaluable primary endpoint data based on the intention-to-treat principle. This was called the full analysis set. The safety analyses were made on a safety data set composed of those patients who were evaluated for safety. Missing data from patients who discontinued methylcobalamin after a primary event were imputed with the final evaluation data after discontinuation.

Methylcobalamin efficacy and dose–response relationships were simultaneously evaluated using contrast coefficients to compare placebo with 50 mg and placebo with all methylcobalamin groups combined, respectively. The time interval to the primary event was compared among groups using log-rank scores, and the changes in the ALSFRS-R score and secondary endpoint measures were evaluated using the Wilcoxon score (patients who died or whose data after a primary event were not collected within 28 days from the event were ranked worst). The p values for the primary test were adjusted for multiplicity, with the statistical analysis plan described in online supplementary e-appendix. In addition, the Cox proportional hazards model with backward elimination for the placebo group was used with variables including the interval between symptom onset and diagnosis (≤12 months, >12 months), gender, %FVC (<90%, ≥90%) and several other variables to explore prognostic factors for events post hoc. Analyses were performed using SAS V.9.3 software.

RESULTS

A total of 373 patients were enrolled and randomly assigned to placebo or 25 mg or 50 mg methylcobalamin groups (124, 124 and 125 patients, respectively; figure 1). Exclusion of 3 patients (1 and 2 patients in the placebo and 50 mg groups, respectively) for not satisfying the diagnostic criteria yielded 370 patients. The study was completed by 260 patients, with 113 patients withdrawn because they declined to participate.

The baseline demographic and disease characteristics were similar among the groups, without significant differences (table 1). Approximately half the patients were diagnosed as having clinically probable ALS (46.2%) and had upper motor neuron-onset ALS (49.5%). Most of the patients (89.7%) were being treated with riluzole at the screening. The number of patients with diabetes was 53 (16 in placebo, 18 in 25 mg and 19 in 50 mg groups), 6 of whom received metformin, which could potentially affect B_{12} levels. There were however no changes in haematological data in this study.

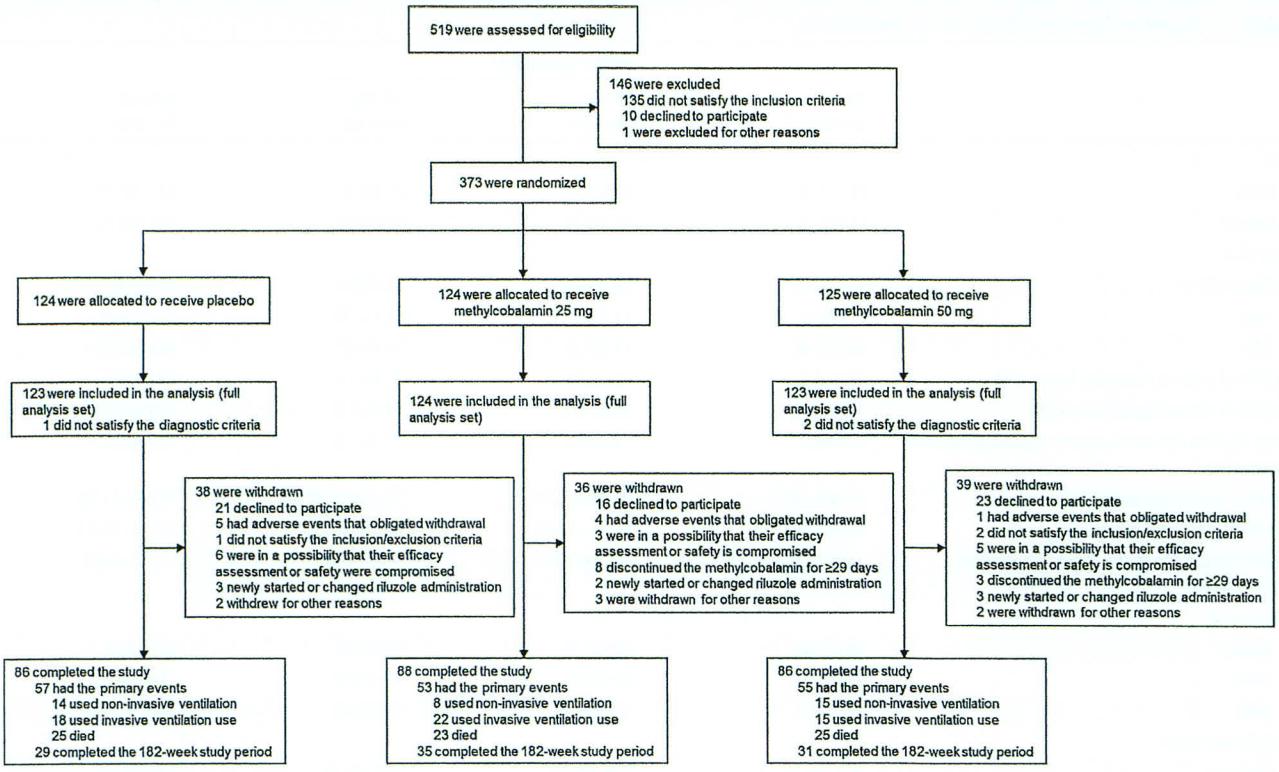

Figure 1 Patient flow.

Efficacy

Significant differences were not detected for either primary endpoint; the minimal crude p value was 0.09 for the change in the ALSFRS-R score, and its adjusted value was 0.19 (table 2). The time to the primary event was slightly prolonged in the active treatment groups (HR [95% CI]: 0.83 [0.58 to 1.20] for 25 mg and 0.92 [0.65 to 1.32] for 50 mg methylcobalamin groups). The median time to the primary event was 880 for placebo, 1147 for 25 mg and 954 days for 50 mg methylcobalamin groups (figure 2A). The median change in the ALSFRS-R score from baseline to week 182 decreased in relation to the allocated dose: −24.0 for placebo, −22.0 for 25 mg and −21.0 for 50 mg methylcobalamin groups (figure 2B).

For the secondary endpoints, the median change in manual muscle test and the Norris Scale scores from baseline to week 182 decreased in a dose-dependent manner, although this decrease was not significantly different among the groups (online supplementary table e-1).

Patients diagnosed early (duration ≤12 months)

The post-hoc analysis of the subgroup of patients diagnosed early (diagnosed with ALS ≤12 months after symptom onset) demonstrated a significant dose–response-dependent prolongation in time to the primary event (HR [95% CI]: 0.64 [0.38 to 1.09] for 25 mg [p=0.01] and 0.50 [0.27 to 0.93] for 50 mg [p=0.01] methylcobalamin groups). The median time to the primary event (95% CI) was 570 (465 to 720) days for placebo, 1087 (564 to –) days for 25 mg, and 1197 (609 to –) days for 50 mg methylcobalamin groups (table 2, figure 2C).

The change in the ALSFRS-R score also decreased in a dose-dependent manner (the p value for 25 mg was 0.01 and was 0.003 for 50 mg methylcobalamin compared with placebo; figure 2D). To confirm the validity of the results, the time-related changes in the efficacies on the primary event and on ALSFRS-R scores were analysed; methylcobalamin exhibited efficacy or a trend towards efficacy on primary events in patients diagnosed ≤12 months after symptom onset. Additionally, efficacy or a trend towards efficacy on ALSFRS-R scores was frequently observed in the first 24 months after symptom onset (online supplementary tables e-2 and e-3).

Among the secondary endpoints, a dose–response inhibition in worsening was shown in the Norris Scale score (p values: 0.008 for 25 mg and 0.005 for 50 mg) and %FVC (p values of 0.004 for 25 mg and <0.001 for 50 mg) (online supplementary table e-4).

Patients with other poor prognostic factors

Applying the Cox proportional hazards model with backward elimination to data in the placebo group determined the following poor prognostic factors: diagnostic interval >12 months, being male, %FVC being <90% and being without riluzole (online supplementary table e-5). Methylcobalamin at both 25 mg and 50 mg tended to reduce the HR in men and %FVC <90% (HR, 0.76–0.77; online supplementary table e-6). The decreased ALSFRS-R score (95% CI) in the 50 mg group was 4.3 (0.7 to 7.9; p=0.095) for men and 4.5 (0.9 to 8.1; p=0.020) for %FVC <90% (online supplementary table e-7).

Safety

Adverse events were reported by more than 97% of patients in each group. Treatment-related adverse events were reported with a similar incidence of 4.1% (5/123), 7.3% (9/124) and 5.7% (7/123) in the placebo, 25 mg and 50 mg methylcobalamin groups, respectively. The incidence of serious adverse events was also similar in the placebo, 25 mg and 50 mg methylcobalamin groups: 64.2%, 62.1% and 65.0%, respectively. Of the six patients who died of causes other than ALS progression, the cause of one death in the 50 mg methylcobalamin group was due to cardiac arrest following myocardial infarction or arrhythmia,

Table 1 Baseline characteristics of study participants

	Placebo (n=123)	Methylcobalamin 25 mg (n=124)	Methylcobalamin 50 mg (n=123)	Overall (n=370)
Sex				
Male	71 (57.7)	81 (65.3)	71 (57.7)	223 (60.3)
Female	52 (42.3)	43 (34.7)	52 (42.3)	147 (39.7)
Age, years				
Mean±SD	62.2±10.7	60.8±10.1	62.4±9.6	61.8±10.1
<65	61 (49.6)	77 (62.1)	65 (52.8)	203 (54.9)
≥65	62 (50.4)	47 (37.9)	58 (47.2)	167 (45.1)
ALSFRS-R score at screening (mean±SD)	42.1±3.5	41.7±3.8	41.9±3.8	41.9±3.7
ALSFRS-R at enrolment (mean±SD)	40.1±3.5	39.8±4.0	39.9±4.0	40.0±3.8
Time lag from symptom onset to diagnosis, months (mean±SD)	19.6±8.1	19.2±8.2	19.7±7.8	19.5±8.0
%FVC at screening (mean±SD)	97.40±18.22	93.75±17.26	93.99±15.97	95.04±17.21
%FVC at enrolment (mean±SD)	92.83±20.07	89.98±17.45	89.39±17.55	90.74±18.41
%FVC change during the observation period (mean±SD)	−4.57±10.63	−3.76±9.36	−4.59±8.77	−4.31±9.60
Onset type				
Bulbar	30 (24.4)	29 (23.4)	28 (22.8)	87 (23.5)
UMN	60 (48.8)	62 (50.0)	61 (49.6)	183 (49.5)
LMN	33 (26.8)	33 (26.6)	34 (27.6)	100 (27.0)
ALS disease type				
Sporadic	117 (95.1)	122 (98.4)	118 (95.9)	357 (96.5)
Familial	6 (4.9)	2 (1.6)	5 (4.1)	13 (3.5)
Riluzole coadministration during the observation period	110 (89.4)	112 (90.3)	110 (89.4)	332 (89.7)
Diagnosis*				
Clinically definite ALS	33 (26.8)	43 (34.7)	49 (39.8)	125 (33.8)
Clinically probable ALS	62 (50.4)	60 (48.4)	49 (39.8)	171 (46.2)
Clinically probable, laboratory-supported ALS	28 (22.8)	21 (16.9)	25 (20.3)	74 (20.0)
ALS severity at enrolment				
Stage I	14 (11.4)	20 (16.1)	17 (13.8)	51 (13.8)
Stage II	109 (88.6)	104 (83.9)	106 (86.2)	319 (86.2)
ALSFRS-R score change during the observation period				
−1	42 (34.1)	45 (36.3)	42 (34.1)	129 (34.9)
−2	46 (37.4)	41 (33.1)	45 (36.6)	132 (35.7)
−3	35 (28.5)	38 (30.6)	36 (29.3)	109 (29.5)

Data were compared among groups using one-way analysis of variance for continuous, χ^2 test for nominal and Kruskal-Wallis test for ordinal variables. Unless otherwise stated, values represent the number followed by the percentage of participants.

*Diagnoses were made according to the revised El Escorial criteria (Airlie House criteria).

ALS, amyotrophic lateral sclerosis; ALSFRS-R, Revised ALS Functional Rating Scale; %FVC, per cent-predicted forced vital capacity; LMN, lower motor neuron; UMN, upper motor neuron.

and was considered unrelated to the medication based on the patient's history. There were no clinically significant changes in the results of laboratory tests, vital signs or ECGs among groups. Statistical details are available on request.

Classification of evidence

The research aims of this study were to evaluate the efficacy and safety of long-term ultra-high-dose methylcobalamin (25 mg and 50 mg) in Japanese patients with ALS and the efficacy in patients whose ALS was diagnosed early. Methylcobalamin was not found to be significantly superior to placebo in the whole cohort. However, in patients diagnosed early (≤12 months after symptom onset), this study provides post-hoc class II evidence that ultra-high-dose methylcobalamin prolongs time to death or ventilation support (HR [95% CI]: 0.64 [0.38 to 1.09] for 25 mg group and 0.50 [0.27 to 0.93] for 50 mg group; p=0.01 for placebo vs both methylcobalamin groups combined) and decreased ALSFRS-R scores (p=0.003 for 50 mg and p=0.01 for all methylcobalamin groups) in a dose-responsive manner. The incidence of treatment-related adverse events was similar and low in all groups.

DISCUSSION

This long-term study evaluated the efficacy and safety of high-dose methylcobalamin (25 mg and 50 mg administered intramuscularly twice per week) in patients with ALS using the survival (or being fully bound to respirator) as the primary event. Because of the time and expenses incurred, it is becoming more and more difficult to conduct large-scale, long-term studies assessing the survival such as in the present study.

Although the superiority of methylcobalamin over placebo in terms of either the time to primary events or the change in ALSFRS-R score was not confirmed when data from all

Table 2 Primary efficacy endpoints analysed in two patient populations

(A) Analysis conducted using data from all participants

Primary efficacy endpoints	Placebo (n=123)	Methylcobalamin 25 mg (n=124)	Methylcobalamin 50 mg (n=123)	Crude p value (comparison with placebo) 50 mg	Crude p value (comparison with placebo) Methylcobalamin	Adjusted p value (comparison with placebo) 50 mg	Adjusted p value (comparison with placebo) Methylcobalamin
Time to the primary event*, day							
Median (95% CI)	880 (678 to 1217	1147 (819 to –)	954 (777 to –)	0.33†	0.20†	0.15†	0.13†
First quartile (25%) (95% CI)	465 (363 to 538)	499 (392 to 610)	503 (377 to 627)				
Third quartile (75%) (95% CI)	–‡	‡	–‡				
HR vs the placebo group in each active group (95% CI)	–	0.83 (0.58 to 1.20)	0.92 (0.65 to 1.32)				
HR vs the placebo group in total active group (95% CI)	–	0.88 (0.64 to 1.20)					
Change in ALSFRS-R score							
Patients, n	123	124	122				
Median (min, max)	–24.0 (–42, –1)	–22.0 (–42, 2)	–21.0 (–39, 1)	0.15§	0.09§	0.18§	0.19§
First quartile (25%)	–30.0	–30.5	–27.0				
Third quartile (75%)	–16.0	–12.5	–10.0				

(B) Analysis conducted using data from the subgroup of patients diagnosed early (≤12 months after symptom onset)

Primary efficacy endpoints	Placebo	Methylcobalamin 25 mg	Methylcobalamin 50 mg	P value (comparison with placebo) 50 mg	P value (comparison with placebo) Methylcobalamin
Time to primary event*, day					
Median (95% CI)	570 (465 to 720)	1087 (564 to –)	1197 (609 to –)	0.01†	0.01†
First quartile (25%) (95% CI)	363 (201 to 491)	410 (304 to 594)	448 (337 to 1062)		
Third quartile (75%) (95% CI)	925 (709 to –)	– (1186)	– (–, –)¶		
HR vs the placebo group in each active group (95% CI)		0.64 (0.38 to 1.09)	0.50 (0.27 to 0.93)		
HR vs the placebo group in total active group (95% CI)		0.57 (0.35 to 0.92)			
Change in ALSFRS-R score					
Patients, n	48	54	41		
Median (min, max)	–26.5 (–40, –3)	–26.5 (–40, 0)	–22.0 (–38, 1)	0.003§	0.01§
First quartile (25%)	–32.5	–32.0	–27.0		
Third quartile (75%)	–20.0	–19.0	–9.0		

*Primary events defined as death for any cause or invasive or non-invasive ventilation support for ≥22 hours due to ALS progression.
†Intergroup difference analysed using log-rank score.
‡Third quartile of the primary event-free survival was not calculable in any of the groups.
§Intergroup difference analysed using Wilcoxon score.
¶Third quartile of time to the primary event was not calculable in the 50 mg methylcobalamin group.
ALS, amyotrophic lateral sclerosis; ALSFRS-R, Revised ALS Functional Rating Scale.

participants were analysed, a post-hoc analysis using only the subgroup of patients diagnosed early (diagnosed ≤12 months after symptom onset) demonstrated the efficacy of methylcobalamin. This subgroup suggested dose–response relationships for both survival prolongation and functional measures.

Despite the lack of a statistically significant difference compared with placebo as a whole, deterioration in ALSFRS-R, Manual Muscle Testing (MMT) and Norris scales scores tended to be less pronounced with the higher dose of methylcobalamin. These findings warrant a pivotal phase III clinical trial of ultra-high-dose methylcobalamin exploring its effect on ALSFRS-R for a shorter period (16 weeks), recruiting patients with less than 12 months' duration after onset (Clinical Trial of Ultra-high Dose Methylcobalamin for ALS (JETALS), ClinicalTrials.gov NCT03548311).

The length of time between the first ALS symptom and the initial clinic visit correlated with patient survival, likely because those with rapid progression tend to be captured early by the current diagnostic criteria.[18] Those participants with less time between symptom onset and initial clinical visit exhibited shorter survival times. In the present study, the percentage of patients in the placebo group who experienced a primary event (95% CI) was 75.6% (60.1% to 90.1%) for those with a duration of ALS ≤12 months and 51.8% (38.8% to 64.7%) for those >12 months. The median change in the ALSFRS-R scores from baseline to week 182 was −26.5 for those ≤12 months and −21.0 for those >12 months after symptom onset.

Besides those with early diagnosis (ie, rapid disease progression), a similar trend towards poor prognosis regarding time to primary events (or survival) was found in the other two subgroups: being male and having %FVC <90% (online supplementary table e-6). Interestingly, in these three subgroups, methylcobalamin also tended to show a positive influence in the survival and in other endpoints (ALSFRS-R, Norris Scale score and %FVC; online supplementary table e-7). These results could reinforce the efficacy of methylcobalamin in ALS. Provided that findings in favour of methylcobalamin were obtained only in these subgroups and not in the whole cohort, it may be difficult to evaluate the efficacy of a therapeutic drug in patients with slow and variable progression of the disease.

Alternatively, methylcobalamin may be more efficacious when treatment is started at an early stage of ALS. A recent

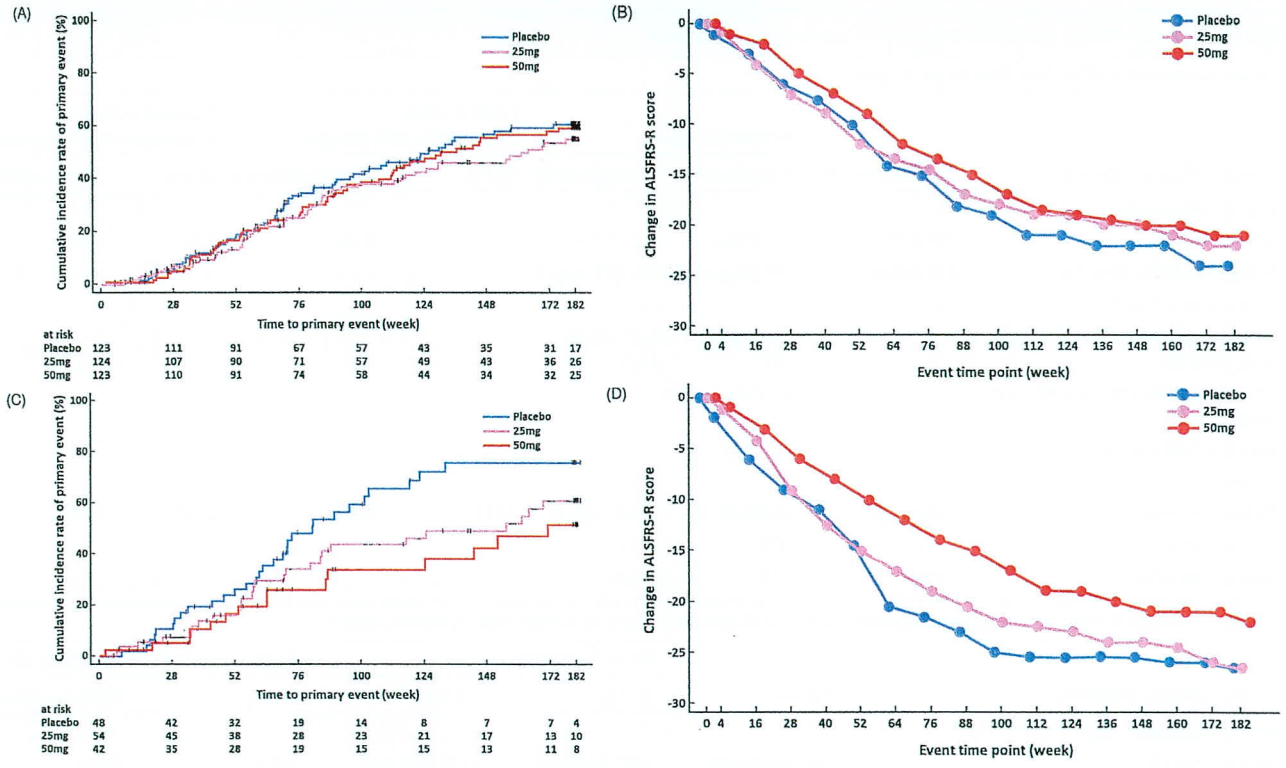

Figure 2 Primary efficacy endpoints in all patients (A, B) and the subgroup of patients diagnosed early (≤12 months after symptom onset) (C, D). ALSFRS-R, Revised Amyotrophic Lateral Sclerosis Functional Rating Scale.

clinical trial of erythropoietin recruiting patients up to 18 months after onset showed a tendency for longer survival and less decrease of ALSFRS-R score up to 6 months.[19] Baumann and colleagues[20] demonstrated that the half-life of lower motor neurons is approximately 1 year and that these motor neurons decay exponentially in ALS. This means that the number of lower motor neurons is already halved at 1 year after symptom onset. Therefore, in modifying the progression of ALS, a therapeutic agent started late in the progression has only a fraction of the normal lower motor neuron population remaining, with a small number of lower motor neurons sustaining a large number of muscle fibres.

As previously suggested[21] the reason so many clinical trials may fail despite the promising results of animal studies is partly due to the late treatment start in humans compared with that in animal models. The El Escorial criteria up to the clinically probable, laboratory-supported level may not be sensitive enough to detect patients with ALS in the early stage of the disease for participation in clinical trials, in contrast to the detection criteria used in animal studies.

In clinical settings, the average delay from symptom onset to an ALS diagnosis is approximately 1 year, and a delay of ≤12 months accounts for about 40% of patients.[21–23] The newly developed Awaji criteria,[24] incorporated into the El Escorial criteria, may shorten the delay to 9 months.[25–28] In this study, methylcobalamin showed prominent prolongation of survival with slower functional decline in patients diagnosed early (≤12 months after symptom onset). Currently, approximately half of the ALS population could benefit from methylcobalamin treatment using the revised El Escorial diagnostic criteria; however, if the use of the Awaji criteria becomes the standard practice, most patients could benefit from this therapy, if the promise is fulfilled in the currently ongoing JETALS study, which uses the Awaji criteria for entry for the first time. The inconvenience of intramuscular injections may be overcome by allowing injections by patients or their caregivers, which is currently employed in the JETALS study.

Further limitations of this trial should be noted. First, the strict criteria for study inclusion may have excluded some patients with ALS, which has heterogeneous pathogeneses. Second, although post-hoc analysis identified only one subgroup of patients, additional factors may influence the efficacy and safety profile of methylcobalamin. Third, we did not examine higher doses (>50 mg) for dose finding, and it is possible that these mega-doses might have even better outcome. These potential factors may warrant future analyses in other study cohorts such as JETALS.

In conclusion, ultra-high-dose methylcobalamin was not found to be significantly superior to placebo. However, ultra-high-dose methylcobalamin therapy may improve the prognosis of patients with ALS if administered early in the disease course. Therapeutic agents that failed in the previous clinical trials could be reanalysed for potential efficacy in ALS, taking into account the duration of the disease at the start of therapy. Criteria enabling earlier diagnosis and a change in the physician's attitude towards offering an early diagnosis and treatment should yield better future outcomes for the patients than ever.

Author affiliations
[1]Department of Neurology, Tokushima University Hospital, Tokushima, Japan
[2]National Hospital Organization Miyagi National Hospital, Sendai, Japan
[3]Tokushukai ALS Care Center, Tokushukai, Japan
[4]Department of Neurology, Toho University Omori Medical Center, Tokyo, Japan
[5]Department of Neurology, Geriatrics Research Institute and Hospital, Maebashi, Gunma, Japan
[6]North Medical Center, Kyoto Prefectural University of Medicine, Kyoto, Japan
[7]Department of Integrated Science and Engineering for Sustainable Society, Chuo University, Hachioji, Japan
[8]Eisai, Tokyo, Japan
[9]Department of Neurology, Hokuyukai Neurological Hospital, Sapporo, Japan
[10]School of Nursing, Suzuka University of Medical Science, Suzuka, Japan

Acknowledgements We thank all patients for their participation and the site staff for their contributions. Contributors (trial conduct supervision by site): Ichiro Yabe (Hokkaido University Hospital), Jun Kawamata (Sapporo Medical University Hospital), Hiroto Takada (National Hospital Organization Aomori Hospital), Keiji Chida (National Hospital Organization Iwate Hospital), Masashi Aoki (Tohoku University Hospital), Hiroaki Ito (National Hospital Organization Miyagi Hospital), Masashiro Sugawara (Akita University Hospital), Muneshige Tobita (National Hospital Organization Yonezawa Hospital), Yoshihiro Sugiura (Fukushima Medical University Hospital), Mitsuya Morita (Jichi Medical University Hospital), Yukio Fujita (Gunma University Hospital), Yuichi Maruki (Saitama Neuropsychiatric Institute), Katsuhisa Ogata (National Hospital Organization Higashi Saitama Hospital), Kimihito Arai (National Hospital Organization Chiba-East-Hospital), Hidehiro Mizusawa (Tokyo Medical and Dental University Hospital), Masashi Takanashi (Juntendo University Hospital), Yasuo Iwasaki (Toho University Omori Medical Center), Takashi Sakamoto (National Center Hospital, National Center of Neurology and Psychiatry), Mieko Ogino (The Kitasato Institute, Kitasato University East Hospital), Kazuko Hasegawa (National Hospital Organization Sagamihara Hospital), Ichiro Imafuku (Japan Labour Health and Welfare Organization, Yokohama Rosai Hospital), Kazuhiro Muramatsu (Saiseikai Yokohama-shi Tobu Hospital), Ryoko Koike (National Hospital Organization Nishi-Niigata Chuo Hospital), Yousuke Yonemochi (National Hospital Organization Niigata Hospital), Kiyonobu Komai (National Hospital Organization Iou Hospital), Hiroyuki Yahikozawa (Nagano Red Cross Hospital), Koichi Mizoguchi (National Hospital Organization, National Epilepsy Center, Shizuoka Institute of Epilepsy and Neurological Disorders), Tsuyoshi Uchiyama (Seirei Social Welfare Community, Seirei Hamamatsu General Hospital), Naoki Atsuta (Nagoya University Hospital), Kazuya Nokura (Fujita Health University Banbuntane Hotokukai Hospital), Akira Taniguchi (Mie University Hospital), Kengo Maeda (Shiga University of Medical Science Hospital), Hideyuki Sawada (National Hospital Organization Utano Hospital), Toshiki Mizuno (University Hospital Kyoto Prefectural, University of Medicine), Harutoshi Fujimura (National Hospital Organization Toneyama Hospital), Kenya Murata (Wakayama Medical University Hospital), Yuetsu Ihara (National Hospital Organization Minami-Okayama Medical Center), Kouichi Noda (National Hospital Organization Higashihiroshima Medical Center), Masanori Hiji (Mifukai Vihara Hananosato Hospital), Chigusa Watanabe (National Hospital Organization Hiroshima-Nishi Medical Center), Takeo Yoshimura (Shakaihoken Shimonoseki Kohsei Hospital), Hiromasa Fukuba (National Hospital Organization Yanai Medical Center), Ryuji Kaji (Tokushima University Hospital), Shuji Hashiguchi (National Hospital Organization Tokushima Hospital), Masahiro Nomoto (Ehime University Hospital), Yasushi Osaki (Kochi Medical School Hospital), Hiroyuki Nakazawa (Nankoku Hospital), Hitoshi Kikuchi (Murakami Karindoh Hospital), Tomoaki Yuhi (Hospital of University of Occupational and Environmental Health, Japan), Tomoko Narita (National Hospital Organization Nagasaki Kawatana Medical Center) and Masahito Suehara (National Hospital Organization Okinawa Hospital). Draft manuscript editing was provided by Clinical Study Support (Nagoya, Japan) under contract with Eisai. Statistical analysis was conducted by Yasuo Ohashi, PhD, Chuo University, Department of Integrated Science and Engineering for Sustainable Society, and Takao Takase, MSc, Eisai.

Contributions RK designed the study, interpreted the data and drafted the manuscript. TI designed the study. YI designed the study. KO designed the study. MN designed the study. YO designed the study and performed the statistical analysis. TT designed the study, performed the statistical analysis, interpreted the data and drafted the manuscript. TH interpreted the data and drafted the manuscript. HS designed the study, interpreted the data and drafted the manuscript. KT designed the study and interpreted the data. SK designed the study and interpreted the data.

Funding This study was funded by Eisai.

Competing interests RK received grants from Eisai during the conduct of the study and has a patent on the Method of treating amyotrophic lateral sclerosis (US 20130344081 A1 licensed). TI received grants from Eisai during the conduct of the study. YI reports no disclosures. KO reports no disclosures. MN reports no disclosures. YO received personal fees from Statcom, Sanofi, Eisai, Chugai, Taiho, Shionogi and Kowa, and non-financial support from Yakult Honsha and Takeda outside the submitted work. TT is employed by Eisai. TH is employed by Eisai. HS is employed by Eisai. KT received grants from Eisai during the conduct of the study. SK received grants from Eisai during the conduct of the study.

Patient consent for publication Not required.

Ethics approval This study is conducted in accordance with the principles of the Declaration of Helsinki. The protocol was approved by the institutional review board at each centre. All eligible patients provided written informed consent.

Provenance and peer review Not commissioned; externally peer reviewed.

REFERENCES

1 Kiernan MC, Vucic S, Cheah BC, *et al*. Amyotrophic lateral sclerosis. *Lancet* 2011;377:942–55.
2 Miller RG, Mitchell JD, Moore DH. Riluzole for amyotrophic lateral sclerosis (ALS)/motor neuron disease (MND). *Cochrane Database Syst Rev* 2012;3:CD001447.
3 Writing Group, Edaravone (MCI-186) ALS 19 Study Group. Safety and efficacy of edaravone in well defined patients with amyotrophic lateral sclerosis: a randomised, double-blind, placebo-controlled trial. *Lancet Neurol* 2017;16:505–12.
4 Zoccolella S, Simone IL, Lamberti P, *et al*. Elevated plasma homocysteine levels in patients with amyotrophic lateral sclerosis. *Neurology* 2008;70:222–5.
5 Zoccolella S, Bendotti C, Beghi E, *et al*. Homocysteine levels and amyotrophic lateral sclerosis: A possible link. *Amyotroph Lateral Scler* 2010;11(1-2):140–7.
6 Okada K, Tanaka H, Temporin K, *et al*. Methylcobalamin increases Erk1/2 and Akt activities through the methylation cycle and promotes nerve regeneration in a rat sciatic nerve injury model. *Exp Neurol* 2010;222:191–203.
7 Akaike A, Tamura Y, Sato Y, *et al*. Protective effects of a vitamin B12 analog, methylcobalamin, against glutamate cytotoxicity in cultured cortical neurons. *Eur J Pharmacol* 1993;241:1–6.
8 Kikuchi M, Kashii S, Honda Y, *et al*. Protective effects of methylcobalamin, a vitamin B12 analog, against glutamate-induced neurotoxicity in retinal cell culture. *Invest Ophthalmol Vis Sci* 1997;38:848–54.
9 Watanabe T, Kaji R, Oka N, *et al*. Ultra-high dose methylcobalamin promotes nerve regeneration in experimental acrylamide neuropathy. *J Neurol Sci* 1994;122:140–3.
10 Ikeda K, Iwasaki Y, Kaji R. Neuroprotective effect of ultra-high dose methylcobalamin in wobbler mouse model of amyotrophic lateral sclerosis. *J Neurol Sci* 2015;354(1-2):70–4.
11 Kaji R, Kodama M, Imamura A, *et al*. Effect of ultrahigh-dose methylcobalamin on compound muscle action potentials in amyotrophic lateral sclerosis: a double-blind controlled study. *Muscle Nerve* 1998;21:1775–8.
12 Izumi Y, Kaji R. [Clinical trials of ultra-high-dose methylcobalamin in ALS]. *Brain Nerve* 2007;59:1141–7.
13 Brooks BR, Miller RG, Swash M, *et al*. El Escorial revisited: revised criteria for the diagnosis of amyotrophic lateral sclerosis. *Amyotroph Lateral Scler Other Motor Neuron Disord* 2000;1:293–9.
14 Moriwaka F. Criteria for disease stage and severity in amyotrophic lateral sclerosis [in Japanese]. *Naika* 2005;95:1551–5.
15 Cedarbaum JM, Stambler N, Malta E, *et al*. The ALSFRS-R: a revised ALS functional rating scale that incorporates assessments of respiratory function. *J Neurol Sci* 1999;169(1-2):13–21.
16 Hillel AD, Miller RM, Yorkston K, *et al*. Amyotrophic lateral sclerosis severity scale. *Neuroepidemiology* 1989;8:142–50.
17 Jenkinson C, Fitzpatrick R, Brennan C, *et al*. Development and validation of a short measure of health status for individuals with amyotrophic lateral sclerosis/motor neurone disease: the ALSAQ-40. *J Neurol* 1999;246(Suppl 3):III16–III21.
18 Traxinger K, Kelly C, Johnson BA, *et al*. Prognosis and epidemiology of amyotrophic lateral sclerosis: Analysis of a clinic population, 1997-2011. *Neurol Clin Pract* 2013;3:313–20.
19 Lauria G, Dalla Bella E, Antonini G, *et al*. Erythropoietin in amyotrophic lateral sclerosis: a multicentre, randomised, double blind, placebo controlled, phase III study. *J Neurol Neurosurg Psychiatry* 2015;86:879–86.
20 Baumann F, Henderson RD, Gareth Ridall P, *et al*. Quantitative studies of lower motor neuron degeneration in amyotrophic lateral sclerosis: evidence for exponential decay of motor unit numbers and greatest rate of loss at the site of onset. *Clin Neurophysiol* 2012;123:2092–8.
21 Mitsumoto H, Brooks BR, Silani V. Clinical trials in amyotrophic lateral sclerosis: why so many negative trials and how can trials be improved? *Lancet Neurol* 2014;13:1127–38.
22 Iwasaki Y, Ikeda K, Ichikawa Y, *et al*. The diagnostic interval in amyotrophic lateral sclerosis. *Clin Neurol Neurosurg* 2002;104:87–9.
23 Paganoni S, Macklin EA, Lee A, *et al*. Diagnostic timelines and delays in diagnosing amyotrophic lateral sclerosis (ALS). *Amyotroph Lateral Scler Frontotemporal Degener* 2014;15(5-6):453–6.
24 de Carvalho M, Dengler R, Eisen A, *et al*. Electrodiagnostic criteria for diagnosis of ALS. *Clin Neurophysiol* 2008;119:497–503.
25 Okita T, Nodera H, Shibuta Y, *et al*. Can Awaji ALS criteria provide earlier diagnosis than the revised El Escorial criteria? *J Neurol Sci* 2011;302(1-2):29–32.
26 Costa J, Swash M, de Carvalho M. Awaji criteria for the diagnosis of amyotrophic lateral sclerosis:a systematic review. *Arch Neurol* 2012;69:1410–6.
27 Geevasinga N, Menon P, Scherman DB, *et al*. Diagnostic criteria in amyotrophic lateral sclerosis: A multicenter prospective study. *Neurology* 2016;87:684–90.
28 Geevasinga N, Loy CT, Menon P, *et al*. Awaji criteria improves the diagnostic sensitivity in amyotrophic lateral sclerosis: A systematic review using individual patient data. *Clin Neurophysiol* 2016;127:2684–91.

Treatment of a Scalp Arteriovenous Malformation by a Combination of Embolization and Surgical Removal

Atsushi Kuwano[1,2], Isao Naitou[3], Naoko Miyamoto[3], Koji Arai[1,2], Takakazu Kawamata[2]

Key words
- Cerebral blood flow
- Onyx
- Scalp arteriovenous malformation

Abbreviations and Acronyms
CT: Computed tomography

From the [1]Department of Neurosurgery, Isesaki-Sawa Medical Association Hospital, Isesaki, Gunnma; [2]Department of Neurosurgery, Tokyo Women's Medical University, Shinjuku, Tokyo; and [3]Department of Neurosurgery, Geriatrics Research Institute and Hospital, Maebashi, Gunnma, Japan

To whom correspondence should be addressed: Atsushi Kuwano, M.D. [E-mail: kuwano.atsushi@twmu.ac.jp]

Citation: World Neurosurg. (2020) 138:93-97. https://doi.org/10.1016/j.wneu.2020.02.138

Journal homepage: www.journals.elsevier.com/world-neurosurgery

Available online: www.sciencedirect.com

1878-8750/$ - see front matter

BACKGROUND: **Scalp arteriovenous malformation is a rare disease. In terms of treatment, surgical removal is often effective and performed. With the development of endovascular treatments, a combination of surgical removal and embolization is now often performed.**

CASE DESCRIPTION: **A 44-year-old man presented with a mass in his left occipital region. Cerebral angiography led to a diagnosis of scalp arteriovenous malformation. Although he had no neurologic deficits, perfusion computed tomography (CT) scan showed a slight decrease in blood flow in the left cerebral hemisphere, which was presumed to have been caused by the scalp arteriovenous malformation. He suffered from a sleep disorder caused by tinnitus, and a discomfort with the lesion itself; therefore, we decided to surgically remove the lesion. To suppress intraoperative bleeding and safely perform the surgery, preoperative embolization was also planned. After treatment, he had no neurologic deficits and the sleep disorder improved. Perfusion CT scan performed after the surgery showed an improvement in cerebral blood flow in the left cerebral hemisphere.**

CONCLUSIONS: **Because cerebral blood flow may decrease depending on the progression of the lesion, the cerebral blood flow should be evaluated. Considering the treatment modalities depending on the lesion can provide treatment with less recurrence and higher patient satisfaction.**

20

INTRODUCTION

Scalp arteriovenous malformation is a rare disease that can interfere with daily life.[1,2] The underlying cause could be trauma, congenital, or idiopathic.[3,4] Clinical symptoms include headache, local pain, bruits, tinnitus, and larger lesions that can result in skin necrosis.[2,5,6] In addition, epilepsy and cerebral ischemia may be caused by extracranial shunting of common carotid blood flow.[7,8] In terms of treatment, surgical removal is often effective and performed.[5,6,9] With the development of endovascular treatments, a combination of surgical removal and embolization is now often performed.

Here, we report a case of scalp arteriovenous malformation that was treated with a combination of embolization and surgical removal.

CASE REPORT

A 44-year-old man presented with a mass in his left occipital region 6 months before visiting our department. The mass lesion gradually increased with pulsation. As the mass lesion grew, tinnitus began to appear. As the symptoms worsened, he suffered from a sleep disorder caused by tinnitus, and felt uncomfortable with the lesion when he was in the supine position, which prompted him to visit our department. During the visit, no neurologic deficits were observed, and a mass of approximately 30 mm was found in his left occipital region. Magnetic resonance angiography revealed an abnormal blood vessel mass consistent with the lesion (**Figure 1**). Cerebral angiography showed that the occipital and posterior auricular arteries were acting as feeders, whereas the superficial vein was acting as a drainer, which subsequently led to the formation of the abnormal blood vessel mass (**Figure 2**). These arteries and veins did not interact in the intracranial area, leading to a diagnosis of scalp arteriovenous malformation. Perfusion computed tomography (CT) scan was performed to evaluate cerebral blood flow, therefore revealing a slight decrease in flow in the left cerebral hemisphere (**Figure 1**). Because the patient suffered from tinnitus and had trouble sleeping because of discomfort from the lesion, we decided to perform surgery to remove the lesion.

To reduce the amount of bleeding and safely remove the lesion, we decided to perform embolization in advance. During embolization, we injected Onyx through the occipital artery branch to embolize the nidus. Finally, the feeder, nidus, and drainer were embolized. Tinnitus disappeared immediately after embolization, but the discomfort caused by the lesion remained. Next, we removed the lesion. To preserve the blood flow in skin, a skin incision was performed from the cranial side to caudal side on the lesion such that the occipital and posterior auricular arteries were not cut (**Figure 3**). The nidus was subsequently submitted to pathology for analysis. The

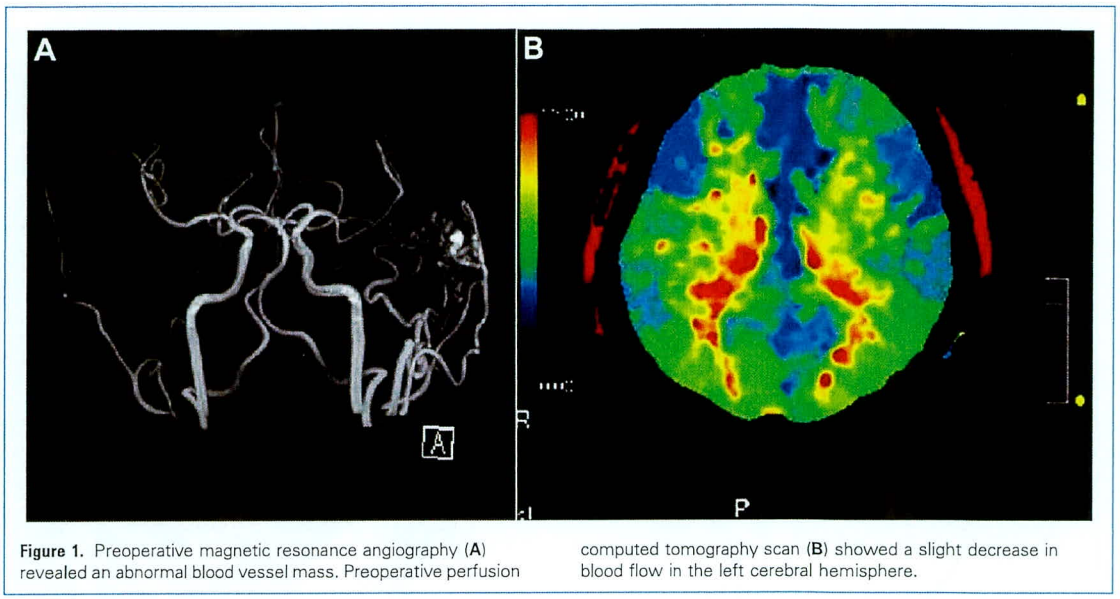

Figure 1. Preoperative magnetic resonance angiography (**A**) revealed an abnormal blood vessel mass. Preoperative perfusion computed tomography scan (**B**) showed a slight decrease in blood flow in the left cerebral hemisphere.

discomfort caused by the lesion disappeared after removal of the lesion. Postoperatively, the patient had no neurologic deficits, the nidus was no longer observed in the magnetic resonance angiography, and perfusion CT scan showed improved cerebral blood flow in the left cerebral hemisphere (**Figure 4**). The pathology results of the resected lesion revealed an abnormal blood vessel mass with mixed arteries and veins of various sizes, and the findings were consistent with arteriovenous malformations. Furthermore, Onyx and thrombus were confirmed in the lumen of the blood vessels (**Figure 5**).

DISCUSSION

Scalp arteriovenous malformation is an abnormal blood vessel mass between the feeding arteries and draining veins, without an intervening capillary bed within the subcutaneous layer.[1,2] Clinical symptoms include headache, local pain, bruits, tinnitus, and larger lesions that can result in skin necrosis.[2,5,6] Additionally, epilepsy and cerebral ischemia may be caused by extracranial shunting of common carotid blood flow.[7,8] In terms of treatment, surgical removal is effective and most widely performed.[5,6,9] With the development of endovascular treatments, a combination

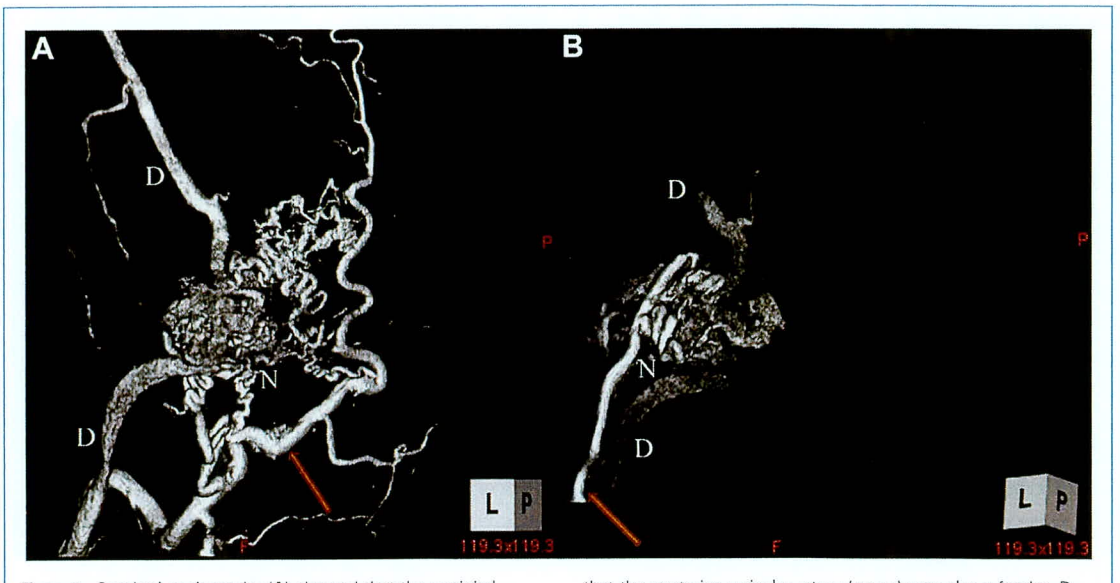

Figure 2. Cerebral angiography (**A**) showed that the occipital artery (*arrow*) was a feeder. Cerebral angiography (**B**) showed that the posterior auricular artery (*arrow*) was also a feeder. D, drainer; N, nidus.

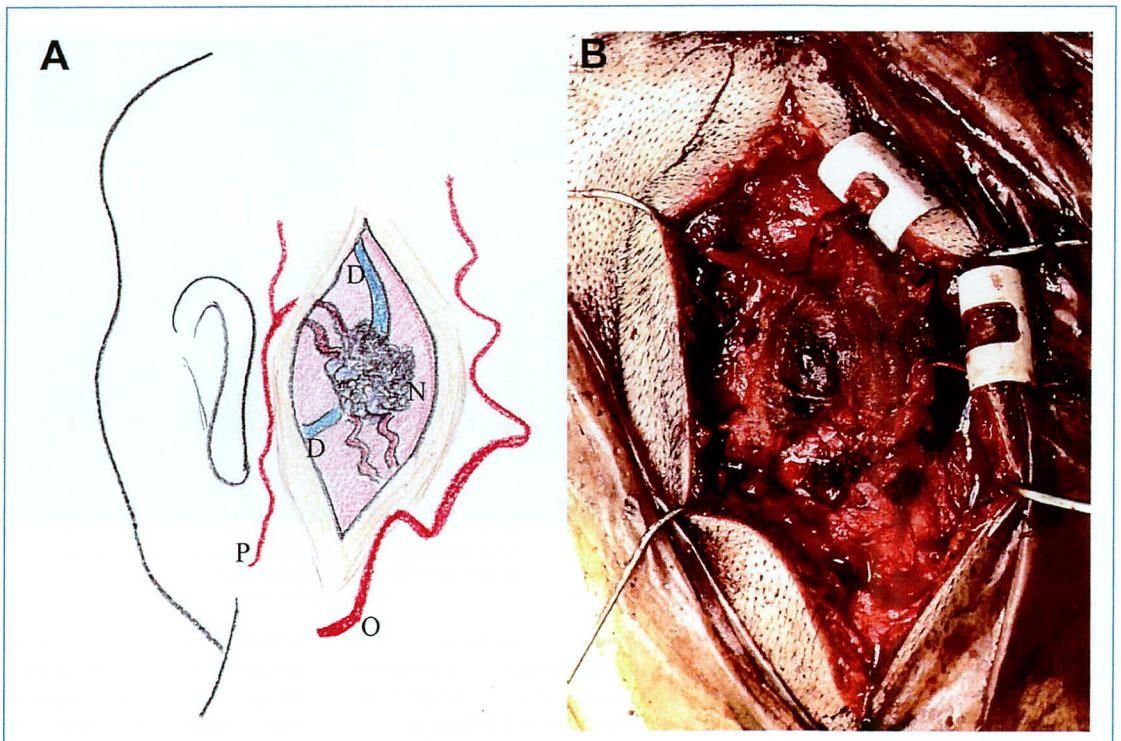

Figure 3. Intraoperative images of nidus removal. To preserve the blood flow in skin, a skin incision was performed from the cranial side to caudal side on the lesion such that the occipital and posterior auricular arteries were not cut (**A**). The nidus was dyed black with Onyx (**B**). D, drainer; N, nidus; O, occipital artery; P, posterior auricular artery.

22

of surgical removal and embolization is now often performed.

In the presented case, the patient visited our department because of the lesion, which caused sleep disturbance because of tinnitus and discomfort with the lesion itself. Furthermore, the patient was diagnosed with a scalp arteriovenous malformation via cerebral angiography. Therefore, surgical resection of the mass was recommended. Although he had no neurologic deficits, perfusion CT scan

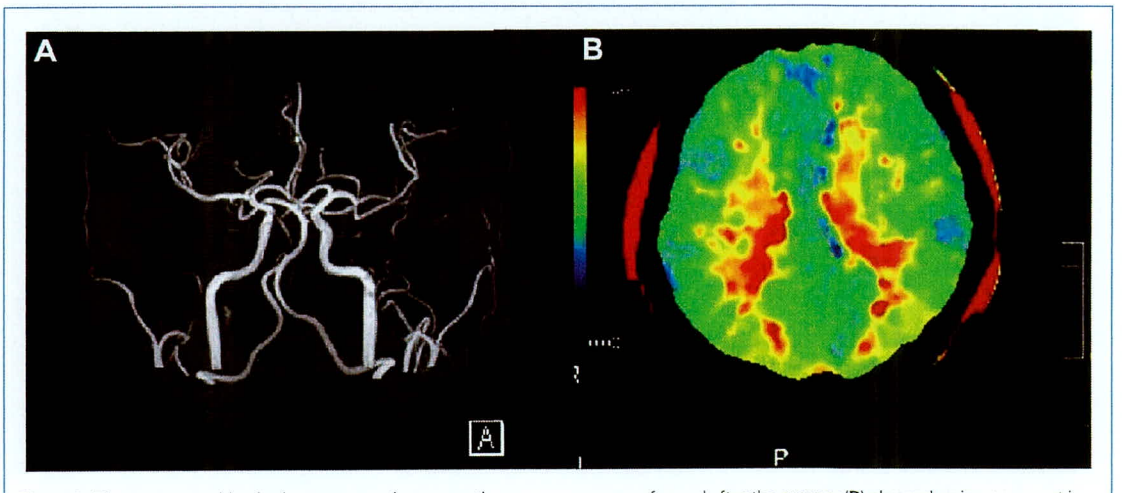

Figure 4. There was no nidus in the postoperative magnetic resonance angiography (**A**). Perfusion computed tomography scan performed after the surgery (**B**) showed an improvement in cerebral blood flow in the left cerebral hemisphere.

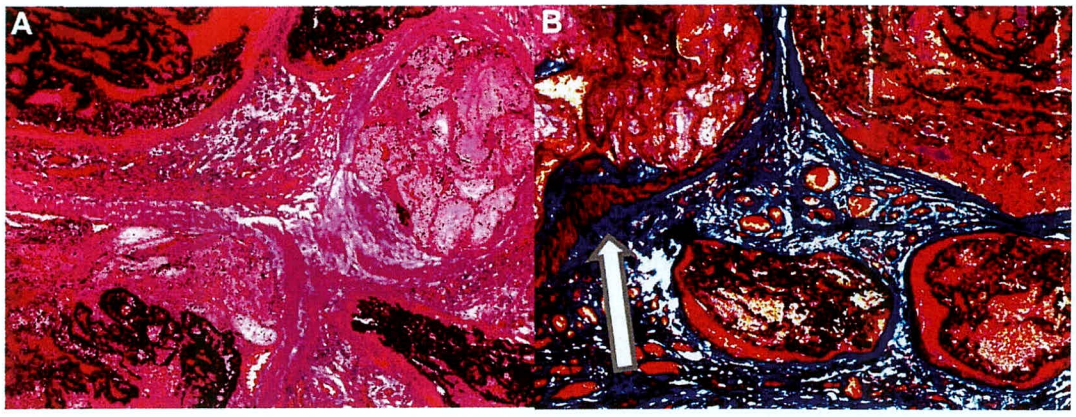

Figure 5. Pathologic images of nidus. (**A**) Hematoxylin and eosin stain (original magnification ×50) showed that Onyx and thrombus were confirmed in the lumen of the blood vessels. (**B**) Azan stain (original magnification ×50) showed discrimination between arteries and veins. Arteries (*arrow*) had smooth muscles and thick walls. The pathologic findings were consistent with arteriovenous malformation, with mixed arteries and veins.

showed a slight decrease in blood flow in the left cerebral hemisphere, which was presumed to have been caused by the scalp arteriovenous malformation.

This case was diagnosed with scalp arteriovenous malformation, which is sometimes referred to scalp arteriovenous fistula.[10] Although these terms are used interchangeably, they should be distinguished from each other because both have different pathologies.[10] The characteristics of cerebral angiography for scalp arteriovenous malformation include the formation of an abnormal blood vessel mass, whereas scalp arteriovenous fistula results in directly anastomoses arteries and veins that do not go through an abnormal vessel mass.[10,11] Because this case presented with an abnormal blood vessel mass, a diagnosis of scalp arteriovenous malformation was made. In both cases, endovascular treatment and removal are typically recommended. Some complications of surgical removal include skin necrosis and intra- and postoperative massive bleeding from the scalp, whereas complications of embolization include neurologic deficits via dangerous anastomosis.[5,9,12,13] Moreover, we observed skin necrosis during the time at which Onyx was used as an embolic substance.[14] In cases of scalp arteriovenous malformation, the patient should be carefully monitored for postoperative recurrence. There have been several studies comparing surgical removal, embolization, and a combination of both for postoperative recurrence.[12,15] These studies reported that embolization alone resulted in potential recurrence, but there was no recurrence with surgical removal or a combination of both.[12,15] We need to understand the characteristics of treatment modalities (Table 1). In cases of recurrence caused by endovascular treatment alone, it has been reported that large lesions or complicated vascular structures are the causes.[2,15,16] If the lesion is large, or the vascular architecture is complex, endovascular treatment alone may be inadequate; therefore, we should make plans that include surgical removal. Understanding the anatomic features of the lesion and considering treatment modalities can provide treatment with less recurrence and higher patient satisfaction.[17]

In this patient, the occipital and posterior auricular arteries were observed as feeders, forming complex nidus, and the vascular architecture was complicated; therefore, endovascular treatment alone was considered to be a high risk of recurrence. In addition to that, a sleep disorder was caused by the discomfort with the lesion itself; therefore, we decided to surgically remove the lesion. Because of the anatomic features of the lesion and sleep disorder caused by it, we decided to treat by a combination of endovascular treatment and surgical removal. To suppress intraoperative bleeding and safely perform the surgery, preoperative embolization was planned. The surgical goal was achieved by embolizing the proximal region of the feeder, but if the entire occipital artery is embolized, skin perfusion of the occipital region would decrease, which was a concern because the patient was judged to have a

Table 1. Advantages and Disadvantages of Treatment Modalities

Treatment Modality	Advantages	Disadvantages
Embolization	Small scar	Neurologic deficits via dangerous anastomosis/recurrence/skin necrosis
Surgical removal	Less recurrence	Intra- and postoperative hemorrhage
Combined treatment	Less recurrence/less hemorrhage	Neurologic deficits via dangerous anastomosis/skin necrosis

risk of skin necrosis after the operation. In this case, to preserve the main trunk of the occipital artery, we decided to perform the embolization starting from the branch of the occipital artery feeder. We were careful not to disrupt the anastomosis between the occipital and vertebral arteries at the cervical vertebrae C1 and C2; therefore, the vertebral artery was imaged from the occipital artery.[18] Because embolization was performed from the distal part of the anastomosis, we were able to perform the embolization safely. Subsequently, embolization was performed from the branch of the occipital artery using Onyx such that the nidus and drainer could be embolized, before finally embolizing the feeder, nidus, and drainer. The patient had no neurologic deficits after the embolization. Thereafter, the lesion was surgically removed. To preserve skin perfusion, the incision was designed with a straight incision just above the lesion such that the occipital and posterior auricular arteries were not damaged. The nidus was hardened by Onyx and turned black, and the amount of intraoperative bleeding was minimal.

Perfusion CT scan performed after the surgery showed an improvement in cerebral blood flow in the left cerebral hemisphere. Some studies have reported epilepsy and ischemic symptoms because of extracranial shunting of common carotid blood flow of the scalp arteriovenous malformation.[7,8] In the presented case, although the patient had no neurologic deficits, the cerebral blood flow was decreased in the left cerebral hemisphere before the surgery, and improved after the surgery. To our knowledge, this is the first case where cerebral blood flow was evaluated for scalp arteriovenous malformation both pre- and postsurgery. In this case, as the lesion increased, there was a risk of symptoms occurring because of extracranial shunting of common carotid blood flow. Therefore, an evaluation of the cerebral blood flow should be performed for cases of scalp arteriovenous malformation.

The pathologic diagnosis was scalp arteriovenous malformation. Onyx and thrombus were confirmed in the lumen of the blood vessels, and the abnormal blood vessel mass had mixed arteries and veins. There was no contradiction between the clinical and pathologic diagnoses.

CONCLUSIONS

We experienced a rare case of scalp arteriovenous malformation treated with a combination of embolization and surgical removal. Because cerebral blood flow may decrease depending on the progression of the lesion, the cerebral blood flow should be evaluated. Considering the treatment modalities depending on the lesion can provide treatment with less recurrence and higher patient satisfaction.

REFERENCES

1. Fard MO, Yousofnejad O, Heydari M. Traumatic arteriovenous malformation of the superficial temporal artery. *Adv Biomed Res.* 2017;6:82.

2. Hasturk AE, Erten F, Ayata T. Giant non-traumatic arteriovenous malformation of the scalp. *Asian J Neurosurg.* 2012;7:39.

3. Kannath SK, Rajan JE. Percutaneous embolization of scalp arteriovenous malformation using new liquid embolic agent, SQUID: a technical report. *J Clin Interv Radiol.* 2017;1:171-174.

4. Oishi H, Yoshida K, Tange Y, Tsuji O, Sonobe M. Treatment of a scalp arteriovenous malformation by a combination of embolization and surgical removal. *Interv Neuroradiol.* 2002;8:293-297.

5. Worm PV, Ruschel LG, Roxo MR, Camelo R. Giant scalp arteriovenous malformation. *Rev Assoc Med Bras (1992).* 2016;62:828-830.

6. Nishijima I, Ikemura R, Gushiken M, Miyagi K, Iha K. Nonsurgical treatment of scalp arteriovenous malformation using a combination of ultrasound-guided thrombin injection and transarterial coil embolization. *J Vasc Surg.* 2012;55:833-836.

7. Mohanty S, Rao C. A large cirsoid aneurysm of the scalp associated with epilepsy. *J Neurol Neurosurg Psychiatry.* 1976;39:835-836.

8. Ohno K, Tone O, Inaba Y, Terasaki T. [Coexistent congenital arteriovenous malformation an aneurysms of the scalp (author's transl)]. *No Shinkei Geka.* 1981;9:1187-1191 (in Japanese).

9. Sugiu K, Hishikawa T, Hiramatsu M, et al. Endovascular treatment for craniofacial arteriovenous fistula/malformation. *J Neuroendovasc Ther.* 2019;13:206-215.

10. Komatsu Y, Narushima K, Kobayashi E, Nose T, Maki Y. Congenital arteriovenous malformation of the scalp–case report. *Neurol Med Chir (Tokyo).* 1989;29:230-234.

11. Matsumaru Y. Endovascular treatment for brain arteriovenous malformation and dural arteriovenous fistula. *Jpn J Neurosurg.* 2013;22:911-916.

12. Xue B, Yi L, Chao Y. Surgical resection of a complex multiple scalp AVF without preoperative embolization: a case report. *Turk Neurosurg.* 2015;25:638-642.

13. Kuwajima A, Chokyu K, Kashimura Y, et al. Two cases of arteriovenous fistula of the scalp in which the pressure cooker technique was useful. *J Neuroendovasc Ther.* 2018;12:416-422.

14. Singla A, Fargen KM, Hoh B. Onyx extrusion through the scalp after embolization of dural arteriovenous fistula. *BMJ Case Rep.* 2015;2015. bcr2015011879.

15. Zheng J, Guo Z, Zhang X, Sun X. Intravascular embolization versus surgical resection for patients with scalp arteriovenous fistula. *Chin Neurosurg J.* 2019;5:3.

16. Corr PD. Cirsoid aneurysm of the scalp. *Singapore Med J.* 2007;48:e268-e269.

17. Hage ZA, Few JW, Surdell DL, Adel JG, Batjer HH, Bendok BR. Modern endovascular and aesthetic surgery techniques to treat arteriovenous malformations of the scalp: case illustration. *Surg Neurol.* 2008;70:198-203 [discussion: 203].

18. Komiyama M. Essential anatomical knowledge for neurointervention: functional neurovascular anatomy. *Jpn J Neurosurg (Tokyo).* 2004;13:116-125.

Conflict of interest statement: The authors declare that the article content was composed in the absence of any commercial or financial relationships that could be construed as a potential conflict of interest.

Received 5 February 2020; accepted 23 February 2020

Citation: World Neurosurg. (2020) 138:93-97.
https://doi.org/10.1016/j.wneu.2020.02.138

*Journal homepage: **www.journals.elsevier.com/world-neurosurgery***

*Available online: **www.sciencedirect.com***

1878-8750/$ - see front matter

Journal of Alzheimer's Disease 73 (2020) 217–227
DOI 10.3233/JAD-191016
IOS Press

A New Serum Biomarker Set to Detect Mild Cognitive Impairment and Alzheimer's Disease by Peptidome Technology

Koji Abe[a,*], Jingwei Shang[a], Xiaowen Shi[a], Toru Yamashita[a], Nozomi Hishikawa[a], Mami Takemoto[a], Ryuta Morihara[a], Yumiko Nakano[a], Yasuyuki Ohta[a], Kentaro Deguchi[b], Masaki Ikeda[c], Yoshio Ikeda[c], Koichi Okamoto[d], Mikio Shoji[d], Masamitsu Takatama[d], Motohisa Kojo[e], Takeshi Kuroda[f], Kenjiro Ono[f], Noriyuki Kimura[g], Etsuro Matsubara[g], Yosuke Osakada[h], Yosuke Wakutani[h], Yoshiki Takao[h], Yasuto Higashi[i], Kyoichi Asada[j], Takehito Senga[j], Lyang-Ja Lee[j] and Kenji Tanaka[j]

[a]*Department of Neurology, Okayama University, Okayama, Japan*
[b]*Department of Neurology, Okayama City Hospital, Okayama, Japan*
[c]*Department of Neurology, Gunma University, Graduate School of Medicine, Maebashi, Japan*
[d]*Department of Neurology, Geriatrics Research Institute and Hospital, Maebashi, Japan*
[e]*Department of Neurology, Ako Chuo Hospital, Ako, Japan*
[f]*Division of Neurology, Department of Medicine, Showa University, School of Medicine, Tokyo, Japan*
[g]*Department of Neurology, Faculty of Medicine, Oita University, Oita, Japan*
[h]*Department of Neurology, Kurashiki Heisei Hospital, Kurashiki, Japan*
[i]*Department of Neurology, Himeji Central Hospital, Himeji, Japan*
[j]*Membrane Protein and Ligand Analysis Center, Protosera Inc., Osaka, Japan*

25

Accepted 17 October 2019

Abstract.

Background: Because dementia is an emerging problem in the world, biochemical markers of cerebrospinal fluid (CSF) and radio-isotopic analyses are helpful for diagnosing Alzheimer's disease (AD). Although blood sample is more feasible and plausible than CSF or radiological biomarkers for screening potential AD, measurements of serum amyloid- β (Aβ), plasma tau, and serum antibodies for $A\beta_{1-42}$ are not yet well established.

Objective: We aimed to identify a new serum biomarker to detect mild cognitive impairment (MCI) and AD in comparison to cognitively healthy control by a new peptidome technology.

Methods: With only 1.5 μl of serum, we examined a new target plate "BLOTCHIP®" plus a matrix-assisted laser desorption/ionization time-of-flight mass spectrometry (MALDI-TOF/MS) to discriminate control ($n = 100$), MCI ($n = 60$), and AD ($n = 99$). In some subjects, cognitive Mini-Mental State Examination (MMSE) were compared to positron emission tomography (PET) with Pittsburgh compound B (PiB) and the serum probability of dementia (SPD). The mother proteins of candidate serum peptides were examined in autopsied AD brains.

Results: Apart from Aβ or tau, the present study discovered a new diagnostic 4-peptides-set biomarker for discriminating control, MCI, and AD with 87% of sensitivity and 65% of specificity between control and AD (***$p < 0.001$). MMSE score was well correlated to brain Aβ deposition and to SPD of AD. The mother proteins of the four peptides were upregulated for coagulation, complement, and plasticity (three proteins), and was downregulated for anti-inflammation (one protein) in AD brains.

*Correspondence to: Professor Koji Abe, 2-5-1 Shikatacho, Okayama 700-8558, Japan. E-mail: abekabek@cc.okayama-u.ac.jp.

ISSN 1387-2877/20/$35.00

Conclusion: The present serum biomarker set provides a new, rapid, non-invasive, highly quantitative and low-cost clinical application for dementia screening, and also suggests an alternative pathomechanism of AD for neuroinflammation and neurovascular unit damage.

Keywords: Alzheimer's disease, biomarker, coagulation, complement, MALDI-TOF, mild cognitive impairment, neuroinflammation, peptidome, plasticity

INTRODUCTION

Dementia is an emerging problem in the world [1], where Alzheimer's disease (AD) occupies more than 65% of dementia in the developed countries, followed by mild cognitive impairment (MCI), vascular dementia (VaD), and other types of dementia [2]. Diagnosis of AD is usually based on clinical criteria, but may be supported by biochemical markers such as a decreased amyloid-β (Aβ) 42 [3], and increased Aβ oligomer [4, 5] and tau protein in cerebrospinal fluid (CSF) [3]. Radiological analyses are also sometimes undertaken as supportive biomarkers of AD with single photon emission computed tomography (SPECT) for evaluating cerebral blood flow [6, 7] and positron emission tomography (PET) for Aβ using Pittsburgh compound B (PiB) [8–10] and tau [11–13]. However, blood samples are more feasible and plausible than CSF or radiological biomarkers for screening emerging number of potential AD and other dementias [14–16]. Several approaches have been reported for measuring serum Aβ [17, 18], plasma phosphorylated-tau [19], and serum miRNA-455-3p [20]. Serum levels of specific antibodies for $A\beta_{1-42}$ monomer and soluble oligomer were not different among normal control, MCI, and AD [21].

Matrix-assisted laser desorption/ionization time-of-flight mass spectrometry (MALDI-TOF/MS) technology can detect small- to medium-sized peptides (1,000–10,000 Da or 10–100 amino acids) in the serum. However, most previous peptidomic analyses required the removal of large amounts of plasma proteins with variable methods before the step of MS analysis, which overlooked hundreds of potentially important endogenous peptides that bind the plasma proteins [22, 23]. In order to compensate such drawbacks of previous peptidomic methodologies, we successfully developed a one-step direct transfer technology using a new target plate "BLOTCHIP®" before MALDI-TOF/MS analysis [24]. Furthermore, this new BLOTCHIP®-MS technology enabled the comprehensive investigation of serum peptides without missing protein-binding peptides, and thus provided a high throughput capacity for discovery of new peptide biomarkers [24]. The aim of the present study was, therefore, to newly discover and validate serum biomarker peptides and to demonstrate the potential usefulness of these candidate peptides for dementia diagnosis.

MATERIALS AND METHODS

Participants and serum

In the present study, participants were prospectively collected at the multicenter, and divided into three groups of cognitively normal control, MCI subject due to AD, and AD patients depending on cognitive function with respect to gender- and age-matching. Cognitive function was examined with Clinical Dementia Rating (CDR) [25, 26] and Mini-Mental State Examination (MMSE) [27]. The participants were clinically evaluated to be cognitively normal, MCI, or AD based on the NINDS-ADRDA criteria [28] or a diagnostic MCI entity [29]. From these participants, 8 ml of blood were collected into a glass test tube (Venoject II, Termo, Japan), which was placed for 1 h at room temperature (RT), and was centrifuged at 1,000 g for 10 min at RT. Resultant supernatant (serum) was divided into 4 Eppendorf tubes (1 ml each) and temporarily stored at –80°C until examination.

BLOTCHIP®-MS analysis

Serum peptidomic analysis was conducted by newly established one-step direct transfer technology "BLOTCHIP®-MS analysis", a rapid quantitative technology for peptidomic analysis [24]. Serum samples (each 1.5 μl) were subjected to 4–12% gradient sodium dodecyl sulfate (SDS)-polyacrylamide gel electrophoresis to separate peptides far from proteins. Next, peptides in the gel were electroblotted onto BLOTCHIP® (Protosera Inc., Osaka, Japan). MALDI matrix, α-cyano-4-hydroxycinnamic acid (CHCA) (Sigma-Aldrich Co., MO, USA), was applied directly onto BLOTCHIP®, and peptidome profiles were obtained in a linear mode of ultrafleX-

treme TOF/TOF (Bruker Daltonics Inc. MA, USA), as previously described in detail [30]. All sample measurements were repeated 4 times.

All statistical analyses of MS spectral data were conducted using ClinProTools version 3.0 (Bruker Daltonics). MS spectra obtained were baseline-subtracted, normalized, recalibrated, and peak-picked within the software. Peak heights, which showed significant statistical differences between 2 groups (control subjects versus AD patients), were analyzed using the Wilcoxon test, a nonparametric test for 2-group comparisons. A probability of $p < 0.05$ was considered statistically significant.

Identification of candidate peptides

Several sera (each 500 μl) containing high amount of each peptide were mixed for candidate peptide identification. Peptides were extracted using a Sep-Pak C18 solid-phase extraction cartridge (Waters Corporation, Milford, MA, USA) with 80% (v/v) acetonitrile (ACN) in water containing 0.1% trifluoroacetic acid (TFA), and the eluent was concentrated up to 100 μL using a CC-105 centrifugal concentrator (TOMY SEIKO Co, Ltd., Tokyo, Japan). Next, the solution was diluted with 400 μL of 2% (v/v) ACN in water containing 0.065% TFA (eluent A) and applied to an ÄKTA purifier (GE Healthcare UK Ltd, Buckinghamshire, England) equipped with a C18 silica-based column (XBridge Shield RP18 2.5 mL, 4.6 mmI.D.*150 mm, Waters Corporation). The eluate was fractionated into 20 fractions (1 mL each) by a liner gradient of 0–100% of 80% (v/v) ACN in water containing 0.05% TFA against eluent A at a flow rate of 1.0 mL/min. Each fraction was concentrated using a CC-105 centrifugal concentrator up to 10 μL.

Then the peptide sequences were analyzed using MALDI-TOF/TOF (ultrafleXtreme TOF/TOF) and LC-MS/MS (Fusion; Thermo Fisher Scientific Inc., Waltham, MA, USA). MALDI-TOF/MS was used for smaller peptide with molecular weight (MW) less than 3,500 Da, and LC-MS/MS for larger peptide with MW of 3,500 Da or more. In search of MALDI-TOF/MS data, MASCOT software was used for a "MS/MS ions search". Parent peptide and MS/MS ions tolerance parameters were set at ± 100 ppm and ± 0.7 Da, respectively. In search of LC-MS/MS data, MASCOT program was used (Matrix Science Inc., Boston, USA). Parent peptide and MS/MS tolerance parameters were set at ± 0.02–0.1 Da and ± 0.1–0.6 Da. Since relatively large peptides were analyzed with LC-MS/MS, the value of the parent peptide tolerance (±0.02–0.1 Da) was set to allow unanticipated modifications in the sequence. Swiss-Prot sequence database, of which taxonomy was limited to "human", was selected for the searches. "oxidation", "phosphorylation", "N-acetylation", and "C-cysteinylation" were selected as variable modifications.

PET imaging

Separately from the above serum analysis, 11 subjects (1 control, 3 MCI, and 7 AD) participated Aβ imaging with Pittsburgh compound B (PiB) detected by positron emission tomography (PET). ^{18}F-labeled PiB (Florbetapir) was synthesized with NEPTIS® plug-01, intravenously injected for 9 participants at an Okayama University-affiliated hospital, and 60–90 min later PET images were detected for 30 min. For two AD patients at Oita University, ^{11}C-PiB was injected to take PET images [9, 10]. As the whole cerebellar region of interest (ROI) for reference, an average of standard uptake value (SUV) from 6 cerebral cortical areas were calculated in order to analyze positive or negative for PiB-PET (positive for more than 1, negative for 1 or less). The sera of these 11 subjects were also measured for BLOTCHIP®-MS analysis.

Immunohistochemistry for human brain

After candidate serum peptides were detected, corresponding protein expressions were examined in AD brain sections. Five cases of pathologically-proven AD brains and 6 cases of control brains were fixed with formalin, embedded in paraffin, and cut on microtome in 5 μm thickness. For Nissl staining, the sections were incubated in 0.1% cresyl violet for 5 min at room temperature, dehydrated gradually in ethanol, and coverslipped with micro cover glass. For single immunohistochemistry, brain sections were dewaxed in xylene and were hydrated in graded ethyl alcohol (100%, 95%, 80%, 70%, 50%) and then distilled water. For antigen retrieval, sections were microwaved in boiling 10 mM citric acid buffers of pH 6. After boiling again, sections were cooled at room temperature for 20 min prior to processing for immunohistochemistry. After incubation in 0.3% hydrogen peroxide/methanol followed by bovine serum albumin, the sections were stained overnight at 4°C with the following primary antibodies: rabbit anti-fibrinogen β chain (FBC)

antibody (1:2500, Sigma, St. Louis, MO); rabbit anti-alpha-2-HS-glycoprotein (AHSG) antibody (1:50, Cloud-Clone Corp, Houston, TX, USA); rabbit anti-fibrinogen α chain (FAC) antibody (1:125, Sigma, St. Louis, MO); rabbit anti-plasma protease C1 Inhibitor (PPC1I) antibody (1:50, Proteintech Group, Chicago, IL). Brain sections were then washed with PBS and treated with suitable biotinylated secondary antibodies (1:500; Vector Laboratories, Burlingame, CA) for 2 h at room temperature. The slides were then treated with avidin-biotin-peroxidase complex (Vectastain ABC Kit; Vector) for 30 min and incubated with diaminobenzidine tetrahydrochloride (DAB). As for the negative control, we stained a set of brain sections in the same manner without the primary antibody. A light microscope (Olympus BX-51, Tokyo, Japan) was used to examine the sections.

For each measurement, we analyzed four randomly selected regions in each section. For the semiquantitative analysis, the number of FBC, AHSG, FAC, and PPC1I-positive cells were calculated in the cerebral cortex and hippocampus (HI).

Statistical analysis

28 Diagnostic performance of the peptides was evaluated using R statistical computing environment software [31]. Receiver operating characteristic (ROC) analysis was performed with package 'Epi' [32] within R software. Areas under the curve (AUC) values were calculated from ROC curve as an indicator of the diagnostic value. The optimal cutoff thresholds for diagnosis were determined according to Youden's index [33]. Multiple binomial logistic regression analysis of peptides was conducted for detection of the best combination of peptides discriminating the two groups using R package 'Aod'. Relative PET value was calculated to be positive as above 1, and negative as 1 or less. Correlation coefficient was also calculated by Pearson product-moment correlation coefficient between MMSE and relative PET value or serum probability of dementia (SPD). Immunohistochemical data were analyzed in GraphPad Prism (version 7.0, GraphPad Software Inc., San Diego, CA, SCR_002798) and presented as mean ± SD. Two-way analysis of ANOVA was used to examine the differences in the expression of immunohistochemistry analysis between groups and brain areas followed by Sidak's multiple comparisons test. In all statistical analyses, data with $p < 0.05$ were considered to be significant.

Table 1
Participants summary of the present study

	Normal control	MCI due to AD	AD patients
No. of subjects	$n = 100$	$n = 60$	$n = 99$
Female gender	60%	43%	56%
Age (y)	80.0 ± 3.9	80.9 ± 3.7	81.9 ± 3.9
MMSE	28.6 ± 1.5	26.0 ± 2.5**	18.4 ± 4.9**,##

Data are expressed mean ± SD. **$p < 0.01$ versus control, ##$p < 0.01$ versus MCI.

The present study was approved by the Ethical Committee of Graduate School of Medicine, Dentistry and Pharmaceutical Science, Okayama University (#OKU-1603-031 = peptidome, #OKU-1709-004 = PET, #OKU-1904-019 = pathology), Gunma University (CIRU-1665), and Oita University (B12-013).

RESULTS

Participants and candidate peptides

Totally 259 participants were collected for the present study, consisted of 100 normal control subjects, 60 MCI due to AD, and 99 AD patients (Table 1). Mean ages of these three groups were 80.0–81.9 years old, that were not significantly different. Mean MMSE were 28.6 ± 1.5, 26.0 ± 2.5 (**$p < 0.01$ versus control), and 18.4 ± 4.9 (**$p < 0.01$ versus control, ##$p < 0.01$ versus MCI) in control, MCI and AD, respectively. Among these three groups, four peptides were identified to show significantly different between control versus MCI, MCI versus AD, and control versus AD (Table 2). The four peptides were 27 amino acid fragment (Peptide #1) of fibrinogen β chain (FBC), 27 amino acid fragment (Peptide #2) of α2-HS-glycoprotein (AHSG), 47 amino acid fragment (Peptide #3) of fibrinogen α chain (FAC), and 34 amino acid fragment (Peptide #4) of plasma protease C1 inhibitor (PPC1I) (details in Table 2).

Diagnostic performances of four peptides

Diagnostic performance of single marker peptide is summarized in Table 3, in which AUC was 0.710 for Peptide #1, 0.615 for Peptide #2, 0.616 for Peptide #3, and 0.594 for Peptide #4, respectively, with variable sensitivity (37–83%) and specificity (36–87%). Some of them showed a low sensitivity but high specificity (Peptide #3), and a high sensitivity but

Table 2
List of 4 identified peptides

Peptide #	Mother protein (abbreviation)	Calculated monoisotopic mass $[M+H]^+$	Amino acid number (N-/C- terminus)	Swiss-Prot accession number	Peptide sequence
1	Fibrinogen β chain (FBC)	2882.54	27 (45–71)	P02675	GHRPLDKKREEAPSLRPAPPPISGGGY
2	α2-HS-glycoprotein (AHSG)	2858.53	27 (341–367)	P02765	TVVQPSVGAAAGPVVPP**C**PGRIRHFKV (C18 = cysteinylation)
3	Fibrinogen α chain (FAC)	5078.35	47 (528–574)	P02671	TF**P**GFFSPMLGEFVSETESRGSESGIFTNTK ESSSHHPGIAEFPSRG (P3 = oxidation)
4	Plasma protease C1 inhibitor (PPC1I)	4151.17	34 (467–500)	P05155	TLLVFEVQQPFLFVLWDQQHKF PVFMGRVYDPRA

Table 3
Diagnostic performance of single marker peptide

Peptide #	Mother protein (abbreviation)	AUC	Sensitivity (%)	Specificity (%)	Elecro- signal cut off	Fold change (AD/Control)	p (Mann-Whitney's U test)
1	Fibrinogen β chain (FBC)	0.710	76	58	3,550	1.44	$^{***}p < 0.001$ (3.1×10^{-7})
2	α2-HS-glycoprotein (AHSG)	0.615	62	59	28,274	0.84	$^{**}p < 0.01$ (0.005)
3	Fibrinogen α chain (FAC)	0.616	37	87	7,995	1.16	$^{**}p < 0.01$ (0.005)
4	Plasma protease C1 inhibitor (PPC1I)	0.594	83	36	1,886	1.60	$^{*}p < 0.05$ (0.021)

Table 4
Diagnostic performance of the four-peptide multi-marker set

Sample data	AUC	Sensitivity (%)	Specificity (%)	Probability cut off	Fold change	p (Mann-Whitney's U test)
Control versus MCI	0.662	72	59	0.357	MCI/Control = 1.39	$^{***}p < 0.001$ (6.2×10^{-4})
MCI versus AD	0.672	77	62	0.477	AD/MCI = 1.37	$^{***}p < 0.001$ (2.8×10^{-4})
Control versus AD	0.804	87	65	0.385	AD/Control = 1.90	$^{***}p < 0.001$ (1.3×10^{-13})

low specificity (Peptide #4). Peptide #2 showed a significantly lower fold change (0.84) compared to the three other increases of Peptide #1, #3, and #4 (Table 3). A multiple binomial logistic regression model was constructed by using the four peptides. After the examination of samples of a training data set (100 control subjects and 99 AD patients), an optimized model with the highest diagnostic performance was obtained as follows: Probability = $1/(1+e\wedge(-(-0.5473 + 3.719E\text{-}04$ [Peptide #1] - 7.584E-05 [Peptide #2] + 1.302E-04 [Peptide #3] + 4.411E-05 [Peptide #4]))) (Equation 1).

With this 4-peptide multi-marker set (Table 4), AUC of control versus MCI was 0.662, of MCI versus AD 0.672, and of control versus AD 0.804 with providing high sensitivity (72–87%) and high specificity (59–65%). To assess validity of the logistic model, k-fold cross validation was conducted. In k-fold cross-validation, the dataset was randomly divided into k subsets with equal size for each group. In this study, k = 5 was chosen. Logistic model using multiple peptides was trained for 5 times with each time leaving out one of the subsets from training. The omitted subset was applied for calculation of the diagnostic values, e.g., AUC. These values were compared with the diagnostic performance of the logistic regression model. By using 5-fold cross validation, AUC of control versus AD was estimated to be 0.796, which was close to the value without cross-validation, 0.804. Fold changes of MCI/control, AD/MCI, and AD/control were 1.39, 1.37, and 1.90, respectively (Table 4).

Figure 1 shows SPD depending on the peptide data among the three groups, which is overlaid by 259 cases of MMSE. These three groups show significantly different SPD between control versus MCI, MCI versus AD, and control versus AD ($^{***}p < 0.001$). A good correlation was found in the increase of SPD and the decrease of MMSE among clinically diagnosed three groups (Fig. 1).

Amyloid PET and brain pathology

Table 5 summarizes SPD data of 11 amyloid PET subjects. One control subject (female) was Aβ-PiB negative, who showed 0.33 SPD. Among three MCI subject (1 male and 2 females), two were Aβ-PiB negative (0.82 and 0.48 SPD) and one was Aβ-PiB

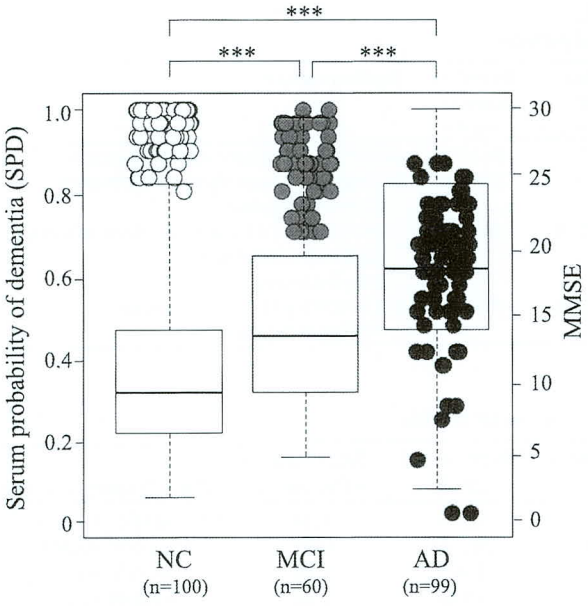

Fig. 1. Serum probability of dementia (SPD, boxes) and MMSE (circles) in 100 normal control (NC) subjects, 60 MCI due to AD subjects, and 99 AD patients. Note serial increase of SPD and decrease of MMSE from NC, MCI to AD. Open circle represent NC, grey MCI, and black AD.

positive with 0.55 SPD. Seven AD patients (5 males and 2 females) were all Aβ-PiB positive with SPD of 0.19–0.57. Of note was a case of MCI with high SPD (0.82), who was Aβ-PiB negative MCI with MMSE of 29, but converted into AD with MMSE of 23 in 2 years. Two other MCI cases with moderate SPD of 0.48 (Aβ-PiB negative) and 0.55 (Aβ-PiB positive) kept stable MMSEs for subsequent 3 and 18 months, respectively, until expiring the visit to our hospital. Figure 2 depicts Aβ-PiB PET negative (Fig. 2A) or positive (Fig. 2B) examples, and correlation coefficients of MMSE versus PET data (Fig. 2C) and MMSE versus SPD data (Fig. 2D) of these 11 subjects, showing a strong correlation of MMSE versus PET ($r=-0.75$, $p=0.0070$) among all 11 subjects (Fig. 2C, oblique dotted line) and a correlation of MMSE versus SPD ($r=-0.67$, $p=0.0908$) in 7 AD patients (Fig. 2D, oblique solid line). Correlation coefficient of MMSE versus SPD was $r=-0.03$ for all 11 subjects (Fig. 2D, dotted line).

Figure 3 shows histochemical analysis of human brain sections in the cerebral cortex (mainly frontal lobe) and HI. Both FBC and FAC were weakly stained in neurons of cortex and HI of control brains, but were strongly induced in AD brain. AHSG was obviously stained in neurons of cortex and HI of control brains, but was weaker in AD brains. PPC1I was clearly stained in neurons of control brains, which enhanced in AD brains. Quantitative analysis showed significant increases of positive cell numbers in the AD than control brains for FBC, FAC, and PPC1I, but a significant decrease for AHSG (Fig. 3, $^{*}p<0.05$ and $^{**}p<0.01$ versus Control).

DISCUSSION

The present study discovered a new serum biomarker with a new peptidome technology. The 4-peptide biomarker set presented a significant difference among age- and gender-matched normal control, MCI, and AD groups with high sensitivity and specificity (Tables 1–4, Fig. 1). Cognitive MMSE score was well correlated to brain Aβ deposition (Fig. 2C) and to SPD of AD (Figs. 1 and 2D), and thus provides a new screening for dementia with a quick, a small amount of serum (1.5 μl), a very low invasive, and a low-cost test. The diagnostic performance of each peptide showed a characteristic balance of sensitivity and specificity to discriminate three subject groups (Table 3), each of which mutually compensated to enable a high sensitivity/specificity with high AUC as the set diagnosis (Table 4).

The present new peptidome technology took BLOTCHIP®-MS method which omits deproteination step, allowing a quick and whole peptides analysis not only for free peptides but also protein-binding peptides in the serum. This method can pick comprehensive serum peptides without missing protein-binding peptides, that were previously lost after deproteination step. Furthermore, such whole

Table 5
Relative Aβ-PET value and serum probability of dementia (SPD) in 11 subjects

	Normal control	MCI			AD						
		1	2	3	1	2	3	4	5	6	7
Age (y)	77	78	85	86	68	71	67	78	71	67	56
MMSE (/30)	30	29	29	27	27	20	18	26	20	24	17
PET result	–	–	–	+	+	+	+	+	+	+	+
Relative PET value	0.94	0.94	0.95	1.42	1.06	1.45	1.47	1.53	1.54	1.96	2.53
SPD	0.33	0.82	0.48	0.55	0.19	0.54	0.57	0.24	0.24	0.50	0.49

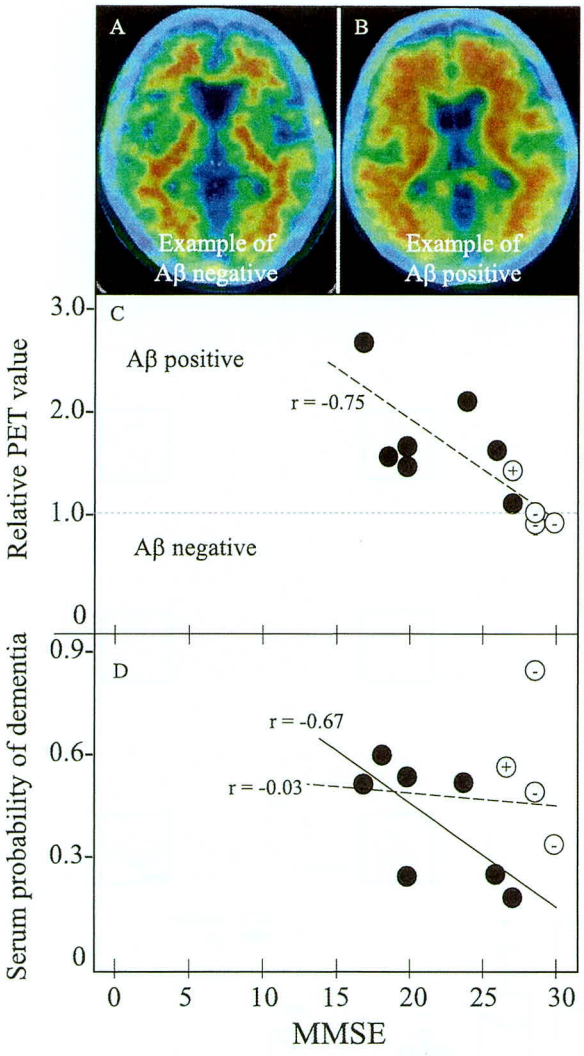

Fig. 2. Amyloid PET and SPD with MMSE in 11 PET subjects for 1 NC, 3 MCI, and 7 AD. Panels A and B shows Aβ negative- and positive-example, (C) MMSE versus relative PET value of negative with 1 or less and positive with more than 1, and (D) MMSE versus SPD. Note the cortical Aβ deposit in PET-positive example (B), the strong correlation of relative PET value with MMSE in all 11 subjects ($r=-0.75$, $p=0.0070$, panel C, oblique dotted line), and a significant correlation of SPD with MMSE in 7 AD patients ($r=-0.67$, $p=0.0908$, panel D, oblique dotted line). Correlation coefficient of SPD versus MMSE was $r=-0.03$, $p=0.9198$ for all 11 subjects (D, dotted line). Open circle represents NC, grey MCI, and black AD. + or – of grey MCI and control are Aβ-PET positive or negative, respectively.

peptides were separated by a simple electrophoresis, and then on-step directly transferred to the high throughput MS analysis. Selection of test tube for blood collection was also very important in the present study. Many hospitals commonly use test tubes which are coated by thrombin to facilitate coagulation and getting serum in a short time. However, our pilot study proved the use of thrombin-coated test tube greatly interfered with the analysis data. Thus, the present study chose a test tube for blood collection that is simply coated by silica (Venoject II), also commonly available in most clinics.

Surprisingly, these peptides were not fragments of Aβ or tau, but were related to coagulation and complement/inflammation systems. The mother protein levels (FBC, FAC, PPC1I) of these three peptides (Peptides #1,3,4) were upregulated and AHSG was downregulated in the human AD patients (Fig. 3). Because frequencies of atrial fibrillation (Af) and the use of anti-coagulative drugs were only between 0 and 4.0% in the control, MCI, and AD groups, the present result is not simply due to the secondary effect of having Af nor the anti-coagulative drug use. FBC and FAC are essential coagulation materials and key contributor of AD pathology [34, 35]. PPC1I is a serpin superfamily, which regulates a pivotal coagulation/neuroinflammation in damaged brain [36, 37], and anti-inflammatory AHSG is regulated under control of pro-inflammatory tumor necrosis factor-α [38, 39]. Thus, the present data strongly suggest a new pathomechanism of AD, that is not simple Aβ and tau hypotheses but are in good accordance to our recent reports that suggested a neurovascular unit (NVU) damage and a neuroinflammation/plasticity of AD brain [40–43].

In fact, a recent report suggested an important role of pericyte for maintaining cerebral circulation and pleiotrophin secretion at NVU [44]. Our previous studies also reported that the mother proteins of these peptides (FAC and PPC1I) were upregulated and AHSG was downregulated in AD model mice, which were enhanced by chronic hypoperfusion [38, 45]. These previous mice reports were confirmed in human AD brain samples in the present study (Fig. 3), suggesting the constant activation of coagulation/plasticity and neuroinflammation process both in simple AD and AD plus hypoperfusion brains. In fact, our recent report showed that PiB-PET positive MCI showed elevations of inflammatory cytokines macrophage inflammatory protein-1β and stem cell growth factor-β in CSF [46]. Furthermore, matrix metalloproteinases involve multiple roles as inflammatory components of AD brain [47], which may be detected by a new PET tracer for microglial activation [48]. A recent report showed that Aβ interacted with fibrinogen and induced its oligomerization [49], which may well support the present data.

Increasing numbers of dementia patients demand a simple and quick screening test for early diagnosis. A recent report to detect serum Aβ showed

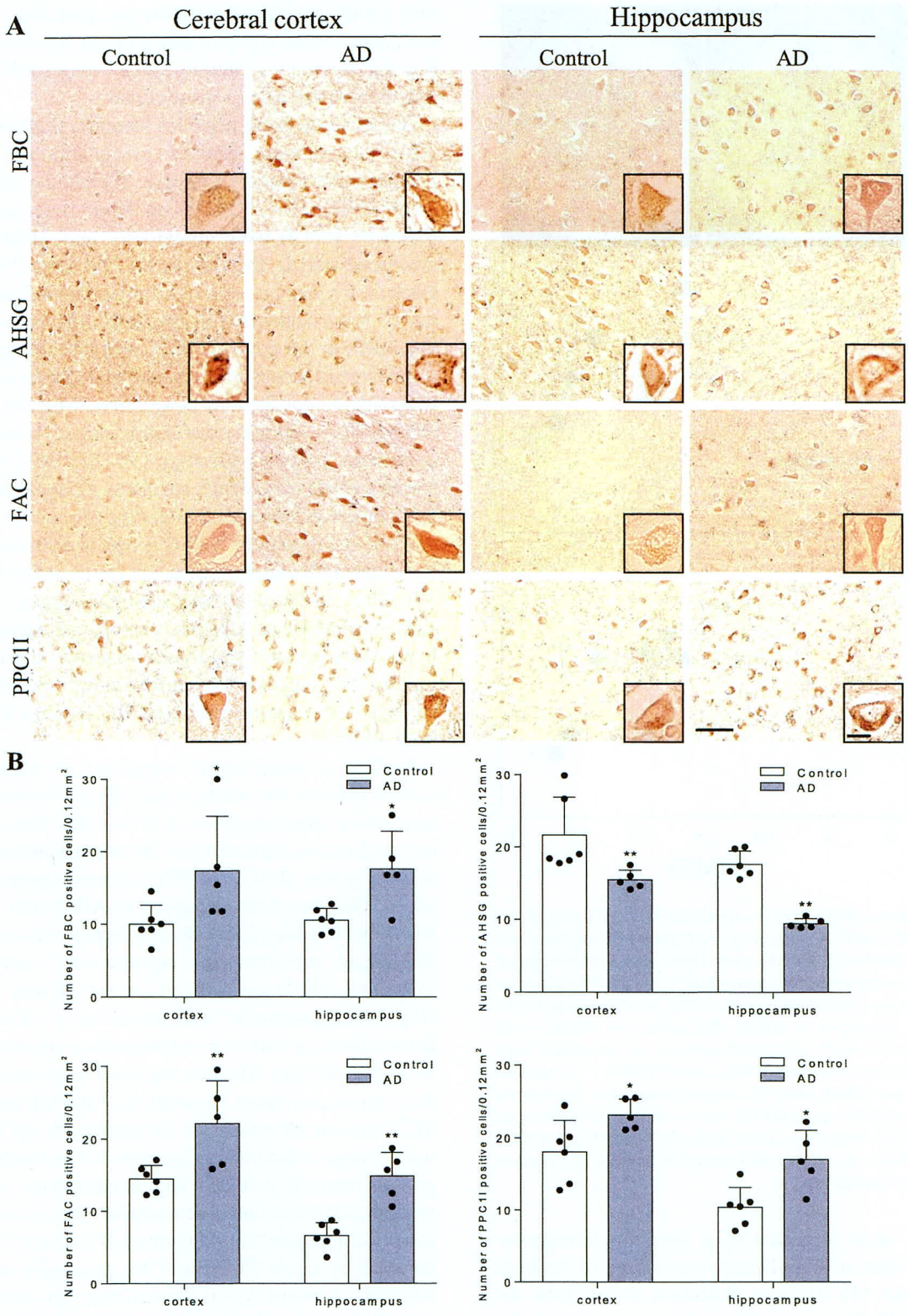

Fig. 3. Immunohistochemical pathology of four mother proteins in AD brain. In comparison to control brains, note significant increases of three proteins (FBC, FAC, and PPC11) and a decrease of AHSG in AD brain. Scale bar = 50 μm (*$p < 0.05$ and **$p < 0.01$ versus Control).

a good correlation to brain Aβ deposition detected by PiB with a combination of immunoprecipitation (IP) plus MALDI-TOF/MS [50]. However, the IP-MS is limited to the measurement of known peptides and is not a popular diagnostic method due to enormous expense and equipment to generate and maintain antibodies. On the other hand, the present BLOTCHIP®-MS analysis requires no pretreatment of blood samples, because whole peptides are effectively dissociated from major blood proteins during one-dimensional polyacrylamide gel electrophoresis process. Thus, the present one dimension/MALDI-TOF (1-DE/MS) system eliminates staining, extracting, loading and many other time-consuming steps taken in 2-DE/MS, thereby greatly reducing analysis time while providing high throughput peptidomic analysis.

The present study provides a new diagnostic biomarker set for MCI and AD by a new peptidome technology, but also suggests an important pathomechanism of AD for neuroinflammation and NVU damage relating to coagulation/plasticity, that could develop a new approach for a disease modifying therapy or to prevent a conversion from MCI to AD. A standardized kit for automated quantitative assessment with ProtoKey® assay [51–54] with this 4-peptides set will enable a rapid, non-invasive, highly quantitative and low-cost clinical application in the near future.

The authors thank all the participants of the present study and Ms. Kadota A. for her enormous contribution of serum preparations. The present study was partly supported by a Grant-in-Aid for Scientific Research (B) 17H0419619, (C) 15K0931607, and 17K1082709, and by Grants-in-Aid from the Research Committees (Kaji R, Toda K, and Tsuji S) from the Japan Agency for Medical Research and Development 7211700176, 7211700180, and 7211700095.

Asada K, Senga T, Lee LJ, and Tanaka K provided BLOTCHIP®-MALDI-TOF/MS analysis at The Membrane Protein and Ligand Analysis Center, Protosera Inc., Osaka, Japan.

Authors' disclosures available online (https://www.j-alz.com/manuscript-disclosures/19-1016r1).

REFERENCES

[1] Abbott A (2011) Dementia: A problem for our age. *Nature* **475**, S2-S4.

[2] Hishikawa N, Fukui Y, Sato K, Kono S, Yamashita T, Ohta Y, Deguchi K, Abe K (2016) Characteristic features of cognitive, affective and daily living functions of late-elderly dementia. *Geriatr Gerontol Int* **16**, 458-465.

[3] Kanai M, Matsubara E, Isoe K, Urakami K, Nakashima K, Arai H, Sasaki H, Abe K, Iwatsubo T, Kosaka T, Watanabe M, Tomidokoro Y, Shizuka M, Mizushima K, Nakamura T, Igeta Y, Ikeda Y, Amari M, Kawarabayashi T, Ishiguro K, Harigaya Y, Wakabayashi K, Okamoto K, Hirai S, Shoji M (1998) Longitudinal study of cerebrospinal fluid levels of tau, A beta1-40, and A beta1-42(43) in Alzheimer's disease: A study in Japan. *Ann Neurol* **44**, 17-26.

[4] Takamura A, Okamoto Y, Kawarabayashi T, Yokoseki T, Shibata M, Mouri A, Nabeshima T, Sun H, Abe K, Urisu T, Yamamoto N, Shoji M, Yanagisawa K, Michikawa M, Matsubara E (2011) Extracellular and intraneuronal HMW-AbetaOs represent a molecular basis of memory loss in Alzheimer's disease model mouse. *Mol Neurodegener* **6**, 20.

[5] Takamura A, Kawarabayashi T, Yokoseki T, Shibata M, Morishima-Kawashima M, Saito Y, Murayama S, Ihara Y, Abe K, Shoji M, Michikawa M, Matsubara E (2011) Dissociation of β-amyloid from lipoprotein in cerebrospinal fluid from Alzheimer's disease accelerates β-amyloid-42 assembly. *J Neurosci Res* **89**, 815-821.

[6] Iizuka T and Kameyama M (2017) Cholinergic enhancement increases regional cerebral blood flow to the posterior cingulate cortex in mild Alzheimer's disease. *Geriatr Gerontol Int* **17**, 951-958.

[7] Yoshii F, Kawaguchi C, Kohara S, Shimizu M, Onaka H, Ryo M, Takahashi W (2018) Characteristic deterioration of ADAS-Jcog subscale scores and correlations with regional cerebral blood flow reductions in Alzheimer's disease. *Neurol Sci* **39**, 909-918.

[8] Cohen AD and Klunk WE (2014) Early detection of Alzheimer's disease using PiB and FDG PET. *Neurobiol Dis* **72**, 117-122.

[9] Yamane T, Ishii K, Sakata M, Ikari Y, Nishio T, Ishii K, Kato T, Ito K, Senda M; J-ADNI Study Group (2017) Inter-rater variability of visual interpretation and comparison with quantitative evaluation of ^{11}C-PiB PET amyloid images of the Japanese Alzheimer's Disease Neuroimaging Initiative (J-ADNI) multicenter study. *Eur J Nucl Med Mol Imaging* **44**, 850-857.

[10] Takemaru M, Kimura N, Abe Y, Goto M, Matsubara E (2017) The evaluation of brain perfusion SPECT using an easy Z-score imaging system in MCI subjects with brain amyloid-β deposition. *Clin Neurol Neurosurg* **160**, 111-115.

[11] Ishiki A, Okamura N, Furukawa K, Furumoto S, Harada R, Tomita N, Hiraoka K, Watanuki S, Ishikawa Y, Tago T, Funaki Y, Iwata R, Tashiro M, Yanai K, Kudo Y, Arai H (2015) Longitudinal assessment of tau pathology in patients with Alzheimer's disease using ^{18}F-THK-5117 positron emission tomography. *PLoS One* **10**, e0140311.

[12] Shimada H, Kitamura S, Shinotoh H, Endo H, Niwa F, Hirano S, Kimura Y, Zhang MR, Kuwabara S, Suhara T, Higuchi M (2016) Association between Aβ and tau accumulations and their influence on clinical features in aging and Alzheimer's disease spectrum brains: A ^{11}C-PBB3-PET study. *Alzheimers Dement (Amst)* **6**, 11-20.

[13] Lemoine L, Gillberg PG, Svedberg M, Stepanov V, Jia Z, Huang J, Nag S, Tian H, Ghetti B, Okamura N, Higuchi M, Halldin C, Nordberg A (2017) Comparative binding properties of the tau PET tracers THK5117, THK5351, PBB3, and T807 in postmortem Alzheimer brains. *Alzheimers Res Ther* **9**, 96.

[14] Van Giau V, An SS (2016) Emergence of exosomal miRNAs as a diagnostic biomarker for Alzheimer's disease. *J Neurol Sci* **360**, 141-152.
[15] Chouraki V, Preis SR, Yang Q, Beiser A, Li S, Larson MG, Weinstein G, Wang TJ, Gerszten RE, Vasan RS, Seshadri S (2017) Association of amine biomarkers with incident dementia and Alzheimer's disease in the Framingham Study. *Alzheimers Dement* **13**, 1327-1336.
[16] Schipke CG, Günter O, Weinert C, Scotton P, Sigle JP, Kallarackal J, Kabelitz D, Finzen A, Feuerhelm-Heidl A (2019) Definition and quantification of six immune- and neuroregulatory serum proteins in healthy and demented elderly. *Neurodegener Dis Manag* **9**, 193-203.
[17] Wang D, Di X, Fu L, Li Y, Han X, Wu H, Cai L, Meng X, Jiang C, Kong W, Su W (2016) Analysis of serum β-amyloid peptides, α2-macroglobulin, complement factor H, and clusterin levels in APP/PS1 transgenic mice during progression of Alzheimer's disease. *Neuroreport* **27**, 1114-1119.
[18] Williams SM, Schulz P, Sierks MR (2016) Oligomeric α-synuclein and β-amyloid variants as potential biomarkers for Parkinson's and Alzheimer's diseases. *Eur J Neurosci* **43**, 3-16.
[19] Tatebe H, Kasai T, Ohmichi T, Kishi Y, Kakeya T, Waragai M, Kondo M, Allsop D, Tokuda T (2017) Quantification of plasma phosphorylated tau to use as a biomarker for brain Alzheimer pathology: Pilot case-control studies including patients with Alzheimer's disease and down syndrome. *Mol Neurodegener* **12**, 63.
[20] Kumar S, Vijayan M, Reddy PH (2017) MicroRNA-455-3p as a potential peripheral biomarker for Alzheimer's disease. *Hum Mol Genet* **26**, 3808-3822.
[21] Klaver AC, Coffey MP, Smith LM, Bennett DA, Finke JM, Dang L, Loeffler DA (2011) ELISA measurement of specific non-antigen-bound antibodies to Aβ1-42 monomer and soluble oligomers in sera from Alzheimer's disease, mild cognitive impaired, and noncognitively impaired subjects. *J Neuroinflammation* **8**, 93.
[22] Lowenthal MS, Mehta AI, Frogale K, Bandle RW, Araujo RP, Hood BL, Veenstra TD, Conrads TP, Goldsmith P, Fishman D, Petricoin EF 3rd, Liotta LA (2005) Analysis of albumin-associated peptides and proteins from ovarian cancer patients. *Clin Chem* **51**, 1933-1945.
[23] Granger J, Siddiqui J, Copeland S, Remick D (2005) Albumin depletion of human plasma also removes low abundance proteins including the cytokines. *Proteomics* **5**, 4713-4718.
[24] Tanaka K, Tsugawa N, Kim YO, Sanuki N, Takeda U, Lee LJ (2009) A new rapid and comprehensive peptidome analysis by one-step direct transfer technology for 1-D electrophoresis/MALDI mass spectrometry. *Biochem Biophys Res Commun* **379**, 110-114.
[25] Hughes CP, Berg L, Danziger WL, Coben LA, Martin RL (1982) A new clinical scale for the staging of dementia. *Br J Psychiatry* **140**, 566-572.
[26] Morris JC (1993) The Clinical Dementia Rating (CDR): Current version and scoring rules. *Neurology* **43**, 2412-2414.
[27] Folstein MF, Folstein SE, McHugh PR (1975) "Mini-mental state". A practical method for grading the cognitive state of patients for the clinician. *J Psychiatr Res* **12**, 189-198.
[28] Mchann G, Drachman D, Folstein M, Katzman R, Price D, Stadlan EM (1984) Clinical diagnosis of Alzheimer's disease: Report of the NINCDS-ADRDA Work Group under the auspices of Department of Health and Human Services Task Force on Alzheimer's Disease. *Neurology* **34**, 939-944.
[29] Petersen RC (2004) Mild cognitive impairment as a diagnostic entity. *J Intern Med* **256**, 183-194.
[30] Araki Y, Nonaka D, Tajima A, Maruyama M, Nitto T, Ishikawa H, Yoshitake H, Yoshida E, Kuronaka N, Asada K, Yanagida M, Nojima M, Yoshida K, Takamori K, Hashiguchi T, Maruyama I, Lee LJ, Tanaka K (2011) Quantitative peptidomic analysis by a newly developed one-step direct transfer technology without depletion of major blood proteins: Its potential utility for monitoring of pathophysiological status in pregnancy-induced hypertension. *Proteomics* **11**, 2727-2737.
[31] Dean CB, Nielsen JD (2007) Generalized linear mixed models: A review and some extensions. *Lifetime Data Anal* **13**, 497-512.
[32] Carstensen BMP, Laara E, Hills M (2013) Epi: A package for statistical analysis in epidemiology. *R package* Version 1.1.49.
[33] Youden WJ (1950) Index for rating diagnostic tests. *Cancer* **3**, 32-35.
[34] Hattori K, Ota M, Sasayama D, Yoshida S, Matsumura R, Miyakawa T, Yokota Y, Yamaguchi S, Noda T, Teraishi T, Hori H, Higuchi T, Kohsaka S, Goto Y, Kunugi H (2015) Increased cerebrospinal fluid fibrinogen in major depressive disorder. *Sci Rep* **5**, 11412.
[35] Cortes-Canteli M, Strickland S (2009) Fibrinogen, a possible key player in Alzheimer's disease. *J Thromb Haemost* **7** Suppl 1, 146-150.
[36] Walker DG, Yasuhara O, Patston PA, Mcgeer EG, Mcgeer PL (1995) Complement C1 inhibitor is produced by brain tissue and is cleaved in Alzheimer disease. *Brain Res* **675**, 75-82.
[37] Timmer NM, Kuiperij HB, de Waal RMW, Verbeek MM (2010) Do amyloid beta-associated factors co-deposit with Abeta in mouse models for Alzheimer's disease? *J Alzheimers Dis* **22**, 345-355.
[38] Shi X, Ohta Y, Liu X, Shang J, Morihara R, Nakano Y, Feng T, Huang Y, Sato K, Takemoto M, Hishikawa N, Yamashita T, Abe K (2019) Acute anti-inflammatory markers ITIH4 and AHSG in mice brain of a novel Alzheimer's disease model. *J Alzheimers Dis* **68**, 1667-1675.
[39] Smith ER, Nilforooshan R, Weaving G, Tabet N (2011) Plasma fetuin-A is associated with the severity of cognitive impairment in mild-to-moderate Alzheimer's disease. *J Alzheimers Dis* **24**, 327-333.
[40] Zhai Y, Yamashita T, Nakano Y, Sun Z, Morihara R, Fukui Y, Ohta Y, Hishikawa N, Abe K (2016) Disruption of white matter integrity by chronic cerebral hypoperfusion in Alzheimer's disease mouse model. *J Alzheimers Dis* **52**, 1311-1319.
[41] Zhai Y, Yamashita T, Nakano Y, Sun Z, Shang J, Feng T, Morihara R, Fukui Y, Ohta Y, Hishikawa N, Abe K (2016) Chronic cerebral hypoperfusion accelerates Alzheimer's disease pathology with cerebrovascular remodeling in a novel mouse model. *J Alzheimers Dis* **53**, 893-905.
[42] Shang J, Yamashita T, Zhai Y, Nakano Y, Morihara R, Fukui Y, Hishikawa N, Ohta Y, Abe K (2016) Strong impact of chronic cerebral hypoperfusion on neurovascular unit, cerebrovascular remodeling, and neurovascular trophic coupling in Alzheimer's disease model mouse. *J Alzheimers Dis* **52**, 113-126.
[43] Shang J, Yamashita T, Zhai Y, Nakano Y, Morihara R, Li X, Tian F, Liu X, Huang Y, Shi X, Sato K, Takemoto M, Hishikawa N, Ohta Y, Abe K (2019) Acceleration of NLRP3 inflammasome by chronic cerebral hypoperfusion

in Alzheimer's disease model mouse. *Neurosci Res* **143**, 61-70.

[44] Nikolakopoulou AM, Montagne A, Kisler K, Dai Z, Wang Y, Huuskonen MT, Sagare AP, Lazic D, Sweeney MD, Kong P, Wang M, Owens NC, Lawson EJ, Xie X, Zhao Z, Zlokovic BV (2019) Pericyte loss leads to circulatory failure and pleiotrophin depletion causing neuron loss. *Nat Neurosci* **22**, 1089-1098.

[45] Shi X, Ohta Y, Liu X, Shang J, Morihara R, Nakano Y, Feng T, Huang Y, Sato K, Takemoto M, Hishikawa N, Yamashita T, Abe K (2019) Chronic cerebral hypoperfusion activates the coagulation and complement cascades in Alzheimer's disease mice. *Neuroscience* **416**, 126-136.

[46] Abe Y, Kimura N, Takahashi R, Gotou M, Mizukami K, Uchida H, Matsubara E (2017) Relationship between cytokine levels in the cerebrospinal fluid and ^{11}C-Pittsburgh compound B retention in patients with mild cognitive impairment. *Geriatr Gerontol Int* **17**, 1907-1913.

[47] Wang XX, Tan MS, Yu JT, Tan L (2014) Matrix metalloproteinases and their multiple roles in Alzheimer's disease. *Biomed Res Int* **2014**, 908636.

[48] Yokokura M, Terada T, Bunai T, Nakaizumi K, Takebayashi K, Iwata Y, Yoshikawa E, Futatsubashi M, Suzuki K, Mori N, Ouchi Y (2017) Depiction of microglial activation in aging and dementia: Positron emission tomography with [(11)C]DPA713 versus [(11)C](R)PK11195. *J Cereb Blood Flow Metab* **37**, 877-889.

[49] Ahn HJ, Zamolodchikov D, Cortes-Canteli M, Norris EH, Glickman JF, Strickland S (2010) Alzheimer's disease peptide beta-amyloid interacts with fibrinogen and induces its oligomerization. *Proc Natl Acad Sci U S A* **107**, 21812-21817.

[50] Nakamura A, Kaneko N, Villemagne VL, Kato T, Doecke J, Dore V, Fowler C, Li QX, Martins R, Rowe C, Tomita T, Matsuzaki K, Ishii K, Ishii K, Arahata Y, Iwamoto S, Ito K, Tanaka K, Masters CL, Yanagisawa K (2018) High performance plasma amyloid-b biomarkers for Alzheimer's disease. *Nature* **554**, 249-254.

[51] Addona TA, Abbatiello SE, Schilling B, Skates SJ, Mani DR, Bunk DM, Spiegelman CH, Zimmerman LJ, Ham AJ, Keshishian H, Hall SC, Allen S, Blackman RK, Borchers CH, Buck C, Cardasis HL, Cusack MP, Dodder NG, Gibson BW, Held JM, Hiltke T, Jackson A, Johansen EB, Kinsinger CR, Li J, Mesri M, Neubert TA, Niles RK, Pulsipher TC, Ransohoff D, Rodriguez H, Rudnick PA, Smith D, Tabb DL, Tegeler TJ, Variyath AM, Vega-Montoto LJ, Wahlander A, Waldemarson S, Wang M, Whiteaker JR, Zhao L, Anderson NL, Fisher SJ, Liebler DC, Paulovich AG, Regnier FE, Tempst P, Carr SA (2009) Multi-site assessment of the precision and reproducibility of multiple reaction monitoring-based measurements of proteins in plasma. *Nat Biotechnol* **27**, 633-641.

[52] Percy AJ, Mohammed Y, Yang J, Borchers CH (2015) A standardized kit for automated quantitative assessment of candidate protein biomarkers in human plasma. *Bioanalysis* **7**, 2991-3004.

[53] Uchiyama K, Naito Y, Yagi N, Mizushima K, Higashimura Y, Hirai Y, Okayama T, Yoshida N, Katada K, Kamada K, Handa O, Ishikawa T, Takagi T, Konishi H, Nonaka D, Asada K, Lee LJ, Tanaka K, Kuriu Y, Nakanishi M, Otsuji E, Itoh Y (2015) Peptidomic analysis via one-step direct transfer technology for colorectal cancer biomarker discovery. *J Proteomics Bioinfom* **S5**, 005.

[54] Uchiyama K, Naito Y, Yagi N, Mizushima K, Higashimura Y, Hirai Y, Dohi O, Okayama T, Yoshida N, Katada K, Kamada K, Handa O, Ishikawa T, Takagi T, Konishi H, Nonaka D, Asada K, Lee LJ, Tanaka K, Kuriu Y, Nakanishi M, Otsuji E, Itoh Y (2018) Selected reaction monitoring for colorectal cancer diagnosis using a set of five serum peptides identified by BLOTCHIP®-MS analysis. *J Gastroenterol* **53**, 1179-1185.

35

29 Cerebrospinal Fluid and Plasma Tau as a Biomarker for Brain Tauopathy

Mikio Shoji

Introduction

Presence of tau in cerebrospinal fluid (CSF) was first discovered by Vandermeeren in 1993 [1]. They developed specific monoclonal antibodies against human tau, and phosphorylated tau (ptau) [2, 3], and set up specific ELISA consisted of AT120 antibody and rabbit anti-human tau antiserum. Quantitation of total 190 CSF samples from Alzheimer's disease, controls and other neurological disease showed assay detection limit of CSF tau was less than 5 pg/ml and increased tau levels in AD compared to those of controls. However, marked overlap value between AD and other neurological diseases was observed in this initial report. In 1995, 5 assay results of CSF tau were published at once. Vigo-Pelfrey group measured CSF tau from 181 patients using ELISA using 16G7 and 16B5 antibody to tau [4]. We also developed different ELISA system using anti-Ht-2 and F-F11 antibodies and confirmed increased CSF tau in AD patients [5]. Data using present common ELISA system for tau and ptau provided Innogenetics N.V. in Belgium (now Fujirebio Europe N.V.) published from this year. Hock reported that CSF tau levels are increased in AD, preclinical stage of AD, familial AD cases, and correlated with severity of dementia. In this assay, AT120 was adopted for captured antibody and combination with HT7 and BT2 was used for reporter antibodies [6]. Blennow first reported the presence of phosphorylated tau at threonine 181 (p181tau) and threonine 231 (ptau231) by ELISA using AT180 for ptau231 and AT270 for ptau181 as captured antibodies and combination of HT7 and AT120 for reporter antibodies. Although tau and ptau levels were significantly increased compared with controls, overlap of assay values were observed also between AD and other neurological diseases [7]. Presently, this p181tau assay system is altered to use HT7 for capture and AT270 for detection antibodies [8]. Arai showed significant increase of CSF tau and presence 50~65 kd tau bands in CSF samples by western blot suggesting that CSF tau might reflect the progressive accumulation of altered tau due to progressive death of neurons in the AD brain [9]. This is short history of developing of CSF tau and ptau assay. Afterward these basic findings, huge number of studies of CSF tau and ptau open up doors to the definite biomarkers for diagnosis and prediction of AD, and the clarification of tauopathy mechanisms, establishment for global standardization, and finally valuable tools for development of essential therapy for AD.

Major papers about CSF tau studies are reviewed and summarized here, and the vison of future is commented.

M. Shoji (✉)
Department of Neurology, Geriatrics Research Institute and Hospital, Maebashi, Japan
e-mail: m-shoji@ronenbyo.or.jp

A. Takashima et al. (eds.), *Tau Biology*, Advances in Experimental Medicine and Biology 1184,
https://doi.org/10.1007/978-981-32-9358-8_29

Definite Biomarker for AD

In the same 1995, another way of AD biomarker had initiated. Motter first reported that CSF Aß42 levels were decreased in spite of increased levels of CSF tau in AD patient [10]. CSF samples from 37 AD, 32 neurological disease and 20 nondemented controls were evaluated by ELISA using 266/277-2 antibodies for Aß42 and 16B5/16G7 antibodies for tau. In 1998, Kanai published the first longitudinal and multicenter study of CSF Aß40, Aß42 and tau. The study consisted of 93 AD, 33 non-AD dementia, 56 other neurological disease CSF samples were evaluated by Innogenetics tau assay and common Aß ELISAs of BAN-50 for capture and BA-27/BC-05 for detecting Aß40/Aß42, respectively. A significant elevation of tau and correlation between the tau levels and the clinical progression were observed in AD. A significant decrease of the Aß42 levels and a significant increase of Aß40/42 ratio were observed in AD suggesting that CSF tau increases with clinical progression of dementia and alteration of Aß42 and Aß40/42 ratio starts at early stages in AD. Efficient diagnostic sensitivity (71%) and specificity (83%) were revealed by using combination of tau and Aß40/42 ratio values. Improvement in sensitivity up to 91% was obtained in longitudinal evaluation [11]. Additional reports by different assay systems supported these findings [12, 13].

Different assay methods of ptau also reported. Increased level of ptau at serine 199 using ELISA with HT-7 and Anti-PS199 was published by Ito in a large scale multicenter study consisted of 570 CSF samples, in 2001 [14]. However, in global standardization study in comparative CSF study among ptau231, ptau181, and ptau199 showed that ptau181 assay reached specificity levels greater than 75% when sensitivity was set at 85% or greater [15].

For clinical application in differential diagnosis of AD, another large-scale multicenter study by Shoji analyzing total 1,031 samples from 366 AD and 168 non-Alzheimer dementia, 316 non-demented neurological disease and 181 normal controls showed the cut-off value of CSF tau was 375 pg/ml, 59% sensitivity and 90% specificity for diagnosis AD compared to other groups. Simultaneously, elevation of CSF tau level was observed in other chronic and acute brain damage disease suggesting required attention for clinical practice [16]. Andreasen also showed sensitivity, specificity and stability of CSF tau in AD in a community-based patient samples showed the cut-off value of CSF tau was 302 pg/ml, 93% sensitivity and 86% specificity for diagnosis AD compared with controls and suggested some neurological conditions (e.g., stroke) increases CSF tau [17]. Finally, these findings were validated by prospective comparisons between antemortem CSF tau and Aß and autopsy-confirmed dementia diagnosis [18].

Systemic Review and Meta-Analysis

From these basic findings era, CSF biomarker study expanded to clarify the diagnostic efficacy of CSF tau and ptau in huge number of cohort studies including AD dementia, mild cognitive impairment (MCI) due to AD, cognitively unimpaired (CU) state in AD and other neurological diseases. According to recent systemic review by Olsson, 231 articles comprising 15,699 AD and 13,018 controls were analyzed and showed CSF tau, ptau and Aß42 strongly differentiated AD form controls, and MCI due to AD from stable MCI. Total 164 cohorts with AD and 153 control cohorts representing 11,341 AD and 7,086 controls showed that average tau concentration ratio between AD and controls are 2.54. In CSF ptau, 98 studies comprising 7,498 AD from 96 cohorts and 5,126 controls from 91 cohorts showed the ptau concentration ratio is 1.88. Comparison between 12 cohorts with 307 MCI and 570 stable MCI showed that average concentration ratio of CSF tau is 1.76 and those analysis with 9 cohorts comprising 251 MCI due to AD and 501 stable MCI of CSF ptau is 1.72 [19].

Differential Diagnosis and Prediction for Onset of AD

During these 20 years, based on development of basic research and neuroimaging tools, clinical classification and diagnosis criteria of neurogenerative dementia have been refined and subdivided in detail. These developments facilitate rigorous evaluation of CSF biomarkers in newly identified neurogenerative diseases. Toledo examined pathology confirmed neurodegenerative dementia patients and showed 26.8% of AD combines another pathology and 14~17% underestimation of biomarker accuracy. CSF tau and ptau are increased in AD and AD-Dementia with Lewy bodies (DLB) [20]. Both tau and ptau values themselves did not discriminate behavior variant frontotemporal lobar degeneration (bvFTLD) and frontotemporal dementia (FTD) without combination of Aß42 values [21, 22]. The systemic review and meta-analysis of idiopathic normal-pressure hydrocephalus indicated significantly reduced levels of tau, ptau and Aß42 compared to healthy normal state [23]. In Creutzfeldt-Jakob disease (CJD), highly elevated CSF levels of tau and 14-3-3 protein are established biomarkers. Rumeileh showed tau yielded 80.6% sensitivity and 75.3% specificity in distinguishing AD from CJD. However, ptau alone showed no eligible significance. Cut-off value was proposed to be >1200 mg in tau and >16.4 in tau/ptau ratio [24]. Ewers studied diagnostic value of CSF Aß42, tau and ptau in 675 CSF samples from controls, AD dementia, subjective memory impairment, vascular dementia, LBD, and FTD, depression, and other neurological disease. As the results, Aß42 showed the best diagnostic accuracy among them. At a sensitivity of 85%, the specificity to differentiate AD dementia against other diagnosis ranged from 42% for DLB, 77% for FTD. However, significant overlap with other non-AD dementia, possibly reflected the underlying mixed pathology [25].

Recently, we have independently reexamined CSF tau and ptau in a total of 213 CSF samples from various neurological diseases and CU subjects [26]. Tau levels were 259.3 ± 162.8 pg/ml in CU, and were significantly higher at 738.4 ± 290.6 pg/ml in AD dementia/MCI ($p < 0.0001$), 1,337 ± 1554 pg/ml in encephalopathy (ENC) ($p = 0.036$), and 415.7 ± 158.2 pg/ml in multiple system atrophy (MSA) ($p = 0.0164$) than in CU. One patient with CJD had a CSF tau level of 1,554 pg/ml (Fig. 29.1a). P181tau levels were 41.69 pg/ml in CU and significantly increased to 88.62 ± 29.69 pg/ml in AD dementia/MCI ($p < 0.0001$). No significant changes were observed in other diseases. The CSF tau/p181 tau ratio was 6.0 ± 1.8 in CU, and increased to 8.2 ± 1.2 in AD dementia/MCI ($p = 0.0038$), 38.8 ± 55.6 in ENC ($p = 0.013$), and 10.2 ± 3.1 in MSA ($P < 0.0001$). In CJD, this ratio was 25.9. Specific changes due to AD processes were recognized in P181tau levels. This study corresponded of previous 1,031 subjects multicenter study showing overlap values in the tauopathy and other neurological disease groups, with moderate measurement sensitivity and specificity as a biomarker using mean ± 2 SD as a cutoff value [16]. Total tau was increased in some diseases because of different pathological processes, including tauopathy due to AD, acute brain injury by ENC and CJD, and axonal degeneration in MSA. No significant changes were detected in total tau, p181tau, or their ratio in CBD, PSP, or FTD. The present results on the CSF tau/p181tau ratio suggest that it was 6:1 and that the phosphorylated-tau tangle pathology increased p181tau and secondarily induced brain injury due to increased total tau levels (8:1), even in AD.

ADNI and DIAN Study Demonstrated Signature of AD

Then, epochal 2 global studies initiated; One is Alzheimer's Disease Neuroimaging Initiative (ADNI) from 2003, which demonstrated natural course of cognitive function, neuroimaging and CSF biomarkers in cognitively unimpaired (CU), MCI and dementia stage of pure sporadic AD. Another is further convincing study of signature of biomarkers in dominantly inherited AD, Dominantly Inherited Alzheimer's Disease (DIAN) from 2008.

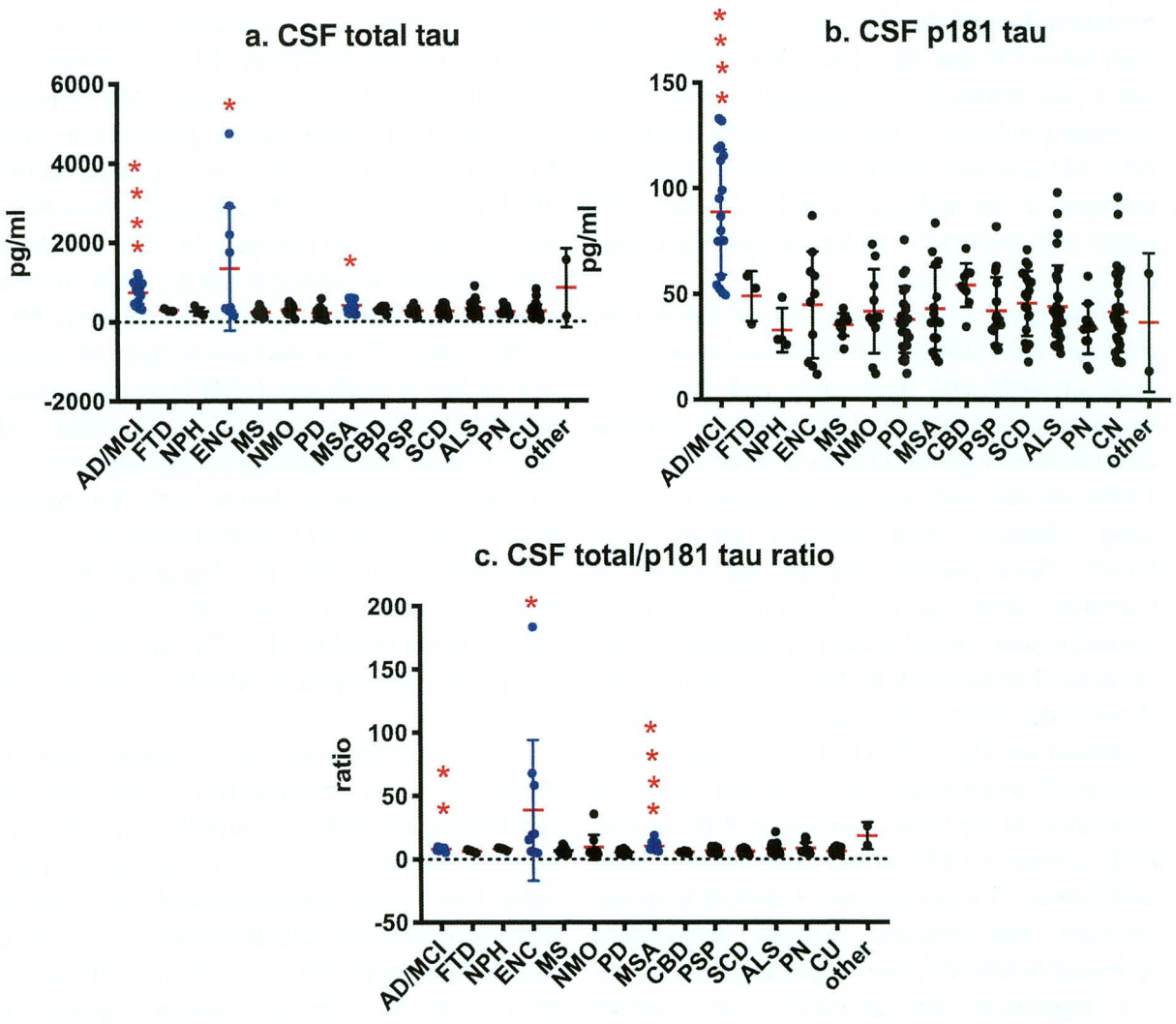

Fig. 29.1 Total tau, phosphorylated-tau in CSF from 231 neurological diseases
*: $p < 0.05$; **: $p < 0.005$; ***: $p < 0.0001$
Abbreviations: *ADD* Alzheimer dementia, *MCI* mild cognitive impairment, *FTD* frontotemporal dementia, *NPH* normal pressure hydrocephalus, *ENC* meningoencephalitis, *MS* multiple sclerosis, *NMO* neuromyelitis optica, *PD* Parkinson's disease, *MSA* multiple system atrophy, *CBD* corticobasal degeneration, *PSP* progressive supranuclear palsy, *SCD* spinocerebellar degeneration, *ALS* amyotrophic lateral sclerosis, *PN* polyneuropathy, *CU* cognitively unimpaired control subjects. Units of CSF total tau and phosphorylated-tau were pg/mL

Shaw showed that CSF Aß42 was the most sensitive biomarker for AD in ADNI cohort and autopsy-confirmed subjects. Cut-offs, sensitivity and specificity discriminating between AD and CU subjects were 93 pg/ml, 69.6% and 92.3% in tau, 23 pg/ml, 67.9%, and 73.1% in ptau 181, 192 pg/ml, 96.4% and 76.9% in Aß42, and 0.39, 85.7% and 84.6% in tau/Aß42 [27]. Multicenter quality control study of ADNI samples using INNO-BIA AlzBIo3, xMAP technology showed intra center assay CV% was 5.3% in Aß42, 6.7% in tau and 10.8% in ptau181. Those of inter-center CV% was 17.9% in Aß42, 13.1% in tau and 14.6% in ptau181 [28]. Follow-up during 48 months in ADNI cohort showed that low Aß42 values were associated longitudinal increase in ptau181, and high baseline ptau181 values were conversely not associated win changes of Aß42 levels [29]. Recent report from ADNI consisted of 56 CU, 73 MCI and 17 AD over 1~7 years follow-up divided by Aß+ and Aß− groups depend on Aß42 cut-offs 192 pg/ml, showed significantly increased baseline levels of CSF tau and ptau in Aß + CU, Aß + MCI and Aß + AD

dementia. Longitudinally, tau levels increased in both Aß + CU and Aß + MCI, but, decreased in Aß + AD dementia. Longitudinally, ptau levels increased in Aß + CU and significantly decline in Aß + AD dementia. Both follow-up study showed increase of tau and ptau mainly increase MCI stage, and conversely decline in dementia stage [30].

DIAN study is the unique study of dominantly inherited AD (DIAD). DIAD is caused by mutations of *APP, APP* duplication and *PSEN-1/-2* mutations. Although the onset age is variable depend on each gene mutation type, penetrance is 100% and the onset age and prognosis is essentially identical with carrier's parent with DIAD. These findings indicate that survey of mutation carrier can reveal definite preclinical alteration and natural course of biomarkers and cognition before onset. In 2012, Bateman clearly showed the order and magnitude of pathologic processes in AD. CSF Aß42 levels appeared to decline 25 years before the symptom onset. Aß deposition in the brain detected by PiB amyloid PET, increased CSF tau and brain atrophy initiated before 15 years of onset. Cerebral hypometabolism and episodic memory disturbance appeared before 10 years. Finally, global cognitive impairment was detected 5 years before onset. Then, 3 years after onset, patients met diagnostic criteria for dementia [31, 32]. Thus, DIAN study conclusively established big data of all alterations of biomarkers and cognitive functions which gradually progress during 25 years and confirmed these orders speculated by ADNI study. Both results by ADNI and DIAN study provide us extremely useful tool to open interventions for prevention of AD.

Prospective Study for Prediction of MCI and Dementia Due to AD

Natural course of CSF biomarkers of incipient AD from CU to MCI was also studied. Hansson examined 137 MCI during 5.2 years follow up and showed 42% developed AD dementia and 15% develop other form of dementia. CSF biomarkers at baseline yielded sensitivity 95% and specificity 83% in combination with tau and Aß42, and those of 95% and 87% in combination ptau181 and Aß42 for detection AD dementia converter [33]. DESCRIPIA prospective study from 20 memory clinic across Europe during 2003–2005 showed CSF AD profile (low Aß42/high tau value) was common in 52% of subjective cognitive impairment (SCI), 68% of non-amnestic MCI (naMCI), 79% of amnestic MCI (aMCI) and 31% CU and associated with cognitive decline in naMCI and aMCI [34]. In subjects with MCI and abnormal CSF Aß42 profile, CSF tau and ptau and hippocampal atrophy can predict further cognitive decline [35]. Prospective 9-year study of 44 CU showed that 6 of 12 with low baseline CSF Aß42 developed AD, but other 6 subjects with low Aß42 and 32 with normal Aß42 did not develop AD. CSF tau and ptau did not predict development AD/DLB over 9 years [36].

Adult Children Study of 169 middle-aged CU during 6 years prospectively also revealed that longitudinal reduction in Aß42 were observed in some individuals as early middle age and low Aß42 levels were associated with the development of cortical amyloid deposition, especially in mid middle age during 55–64 years. CSF tau and ptau as neuronal injury markers dramatically increased in some individuals in mid and late middle aged during 55–74 years [37]. CSF Aß42 was correlated only with PiB binding, but, CSF tau, ptau and hippocampal volume were correlated with the longitudinal alteration in global cognition [38, 39]. Toledo recently reported a global large multicenter study of CSF samples from 1,233 healthy cohort subjects, 40–84 years, from 15 cohorts from 12 different centers by Luminex® assay of Aß42, tau and ptau in Gothenburg Laboratory. At 40 years of age, 76% of subjects were classified normal Aß42, tau and ptau and their frequency decreased to 32% at 85 years. Normal Aß42 and increased tau/ptau group frequency increased slowly from 1% at 44 years to 16% at 85 years. Low Aß42 with high tau/ptau frequency increased from 1% at 53 years to 28% at 85 years. Abnormal low Aß42 were already frequent in middle-life and APOE genotype strongly affects the Aß42, tau and ptau in

Swedish BioFINDER (n = 277) and ADNI (n = 646) [40].

Standardization and Newly Developed Assay Technology

To assay AD biomarkers simultaneously and automatically, the flow cytometric-based Luminex xMAP® technology involves coupling of specific monoclonal antibody sets to the surface of microbeads uniquely identified with a combination of fluorescence dyes in a single sample assuming no cross-reactivity of particular antibodies. The standard assay system named The INNO-BIA AlzBio3 is commonly used to measure Aß42, tau and ptau181 consisted of corresponding capturing antibodies (tau: AT120, ptau181: AT270, Aß42:4D7A3) and biotinylated detection antibodies (HT7 and 3D6). Intra-and interassay CVs were less than 10% for all analytes [41]. Multiplexed quantification correlated with results by usual ELISA assay and improved sample management and quality control of assay [42]. Recently, Roche Diagnostics developed Elecsys assays that utilize the automated cobas 601 analyzer exhibited further precision accuracy, reliability, reproducibility with between-laboratory CV of approximately 4% [43, 44]. Large concordant study between cut-offs for Elecsys assay and amyloid PET using Swedish BioFINDER (n = 277), ADNI (n = 646) and clinical progression in MCI (n = 619) showed tau/Aß42 and ptau/Aß42 ratios were highly concordant with PET classification in BioFINDER (overall agreement: 90%) and ADNI classification (overall agreement: 89–90%) and predicted greater 2-year clinical decline in MCI [44]. The Alzheimer's Association quality control program participated by 40 laboratories in 2011 showed total CVs among centers were 16–28% for ELISA,13–36% for xMAP, and 16–36% for Meso Scale Discovery [45]. Extended quality control program participated 84 laboratories reported that CVs between laboratories were around 20–30%; within-run CVs, less than 5–10%; and longitudinal with-in laboratory CVs were 5–19%. For tau and ptau, between-kit lot effects were less than between-laboratory effects [46]. Temperature at stored, non-frozen time, contamination such as detergent and blood, centrifugation and tube materials have a significant effect on assay variability [47].

Origin of CSF Tau and pTau

During these 25 years, no one believed tau is normally secreted into CSF. Everyone also tried to clarify the missing link between Aß amyloidosis and tauopathy in AD pathological processes. Sato illuminated these issues using kinetic study of stable isotope labelling tau and mass spectrometry in the human central nervous system and iPSC-derived neurons. Brain full length tau is C-terminally truncated at residues 210–230 and released from human neurons in 3 days and ~14 days into CSF. Average half-life of CSF tau is 23 days and its production rates are 26.3 ± 9.2 pg/ml/day. Increase in CSF tau in AD is due to an increase in synthesis and release and positively correlated with amyloidosis. There was no correlation between tau fraction turnover rate and tau PET imaging. Increased tau production and soluble tau secretion are initiated by amyloid toxicity in very early MCI. Then, increased aggregated tau and decreasing elevated CSF tau appear and induce trans-synaptic spreading of aggregated tau, causing cortical cognitive function deficits in early to mild AD dementia stage [48]. He reported that Aß plaque facilitates the rapid amplification of aggregated tau seeds into large tau aggregates in dystrophic neurites of senile plaques, induces formation and spread of neurofibrillary tangles and neuropil threads as secondary seeding events [49].

Association Between CSF Biomarkers and Newly Developing Tau Neuroimaging

Tau PET ligand [^{18}F] flortaucipir have been developed to detect in vivo tau accumulation in AD. Brain tau accumulation initiated from temporal lobe at early MCI stage, progressively

extended to parietofrontal lobes and closely associated with cortical cognitive functions and severity of dementia. Comparison between postmortem brain pathology and regional in vivo uptake of [^{18}F] flortaucipir showed close correlation with density of tau-positive neurites, intrasomal neurofibrillary tangles and total tau burden. No correlations between [^{18}F] flortaucipir and Aß pathology were found [50]. CSF tau and ptau increase from preclinical AD, despite normal [^{18}F] flortaucipir retention, suggesting that appearance of positive tau PET findings initiates later stage of MCI than those of CSF tau and ptau [51, 52].

Plasma Phosphorylated Tau as Possible Biomarker for AD

Recent studies have clarified that the plasma Aß42/40 ratio is inversely correlated with cortical amyloid burden in AD, which can be converted to MCI, and that the plasma Aß42/40 ratio is a useful screening marker for brain Aß amyloidosis in normal individuals [53, 54]. In a similar way, quantitation of plasma tau and ptau as a screening biomarkers for brain tauopathy are developing. Mattsson studied of plasma tau levels using total of 1,284 participants from ADNI and BioFINDER cohorts. Plasma tau partially reflects AD pathology, but the overlap between normal aging and AD is large, especially in patients without dementia [55]. Tatebe tried to quantitate plasma ptau181 using modified Simoa™ Tau 2.0 kit on Simoa HD-1 analyzer (Quantrex). Plasma ptau181 levels were significantly increased in AD and Down syndrome patients compared to controls [56]. Mielke measured plasma ptau 182 using the Meso Scale Discovery platform with antibody AT270 for capture ptau181 and antibody SULFO-TAG-LRL for detection tau from 172 CU, 57 MCI, 40 AD dementia with concurrent Aß and tau PET. Plasma tau and ptau181 levels were higher in AD dementia than those in CU. Plasma ptau181 was more strongly associated with Aß and tau PET [57]. The values of ptau181 measured Simoa or Meso Scale Discovery are very small but totally different. In former report, plasma ptau181 levels are 0.171~0.045 pg/ml. In the later report, those are 6.4~11.6 pg/ml. There are 100 times differences between recent reports. Basic studies such as plasma Aß kinetics from brain to CSF, plasma and mass spectrographic identification studies have not yet performed. Presence of big tau, a close homologues with brain tau presented in human body organs and peripheral nerve systems, has not been clarified yet [58, 59]. Based on these issues, further developing basic study and large scale confirmation studies are expected.

Recommendation in the Diagnostic Evaluation of MCI and Dementia

In 2017, evidence-based guidelines in the diagnostic evaluation of MCI and dementia due to AD were proposed based on systematic reviews using Grading of Recommendations, Assessment, Development, and Evaluation (GRADE) methods by working group comprised 28 international members [60, 61]. The former report recommends the use of CSF markers in predicting the functional or cognitive decline or conversion to AD dementia within 3 years and counseling both before and after the biomarker evaluation. The later report recommends the use of CSF AD biomarkers as a supplement to clinical evaluation, to identify or exclude AD as the cause of dementia, for prognostic evaluation, and for guiding management of patients, particularly in atypical and uncertain cases. As summarized here, huge numbers of basic and clinical dedications during these 25 years for CSF biomarkers revealed the total figures occurred in person due to AD. However, essential aim of CSF biomarkers for contribution of developing disease modifying therapy and intervention in AD pathological processes are still ongoing. In 2018, National Institute on Aging -Alzheimer's Association (NIA-AA) has proposed research framework using ATN classification system of biomarkers toward a biological definition of AD. In this criteria, AD is considered as a continuum, and cognitive staging is

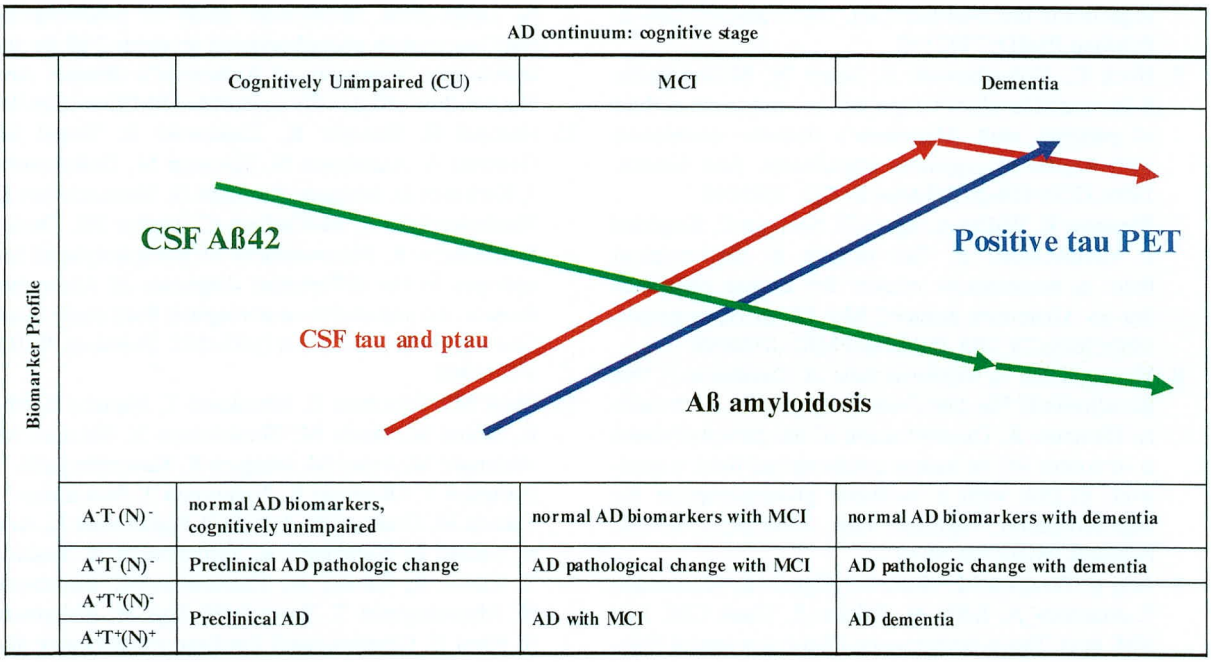

Fig. 29.2 NIA-AA Research Framework and natural course of CSF biomarkers

classified into cognitively unimpaired (CU), MCI and dementia. Biomarker profile is classified in to 3 groups; A: Aggregated Aß or associated pathologic state including CSF Aß42, or Aß42/Aß42 ratio, amyloid PET; T: Aggregated tau (neurofibrillary tangles) or associated pathologic state including CSF ptau and tau PET; (N): neurodegeneration or neuronal injury including Anatomical MRI, FDG PET and CSF tau (Fig. 29.2). Based on this novel NIA-AA research framework criteria, AD process in human brain will be biologically defined further and essential therapy of next generation will be evaluated hopefully [62].

Acknowledgments This study was supported by the Amyloidosis Research Committee Surveys and Research on Special Diseases, the Longevity Science Committee of the Ministry of Health and Welfare of Japan; Scientific Research (C) (18K07385 MS) from the Ministry of Education, Science, and Culture of Japan; the Hirosaki University Institutional Research Grant, and the Center of Innovation Science and Technology-based Radical Innovation and Entrepreneurship Program from the Japan Science and Technology Agency.

Potential Conflicts of Interest The authors have no conflict of interest to report.

References

1. Vandermeeren M, Mercken M, Vanmechelen E, Six J, van de Voorde A, Martin JJ, Cras P. Detection of tau proteins in normal and Alzheimer's disease cerebrospinal fluid with a sensitive sandwich enzyme-linked immunosorbent assay. J Neurochem. 1993;61(5):1828–34. PubMed PMID: 8228996
2. Mercken M, Vandermeeren M, Lübke U, Six J, Boons J, Vanmechelen E, Van de Voorde A, Gheuens J. Affinity purification of human tau proteins and the construction of a sensitive sandwich enzyme-linked immunosorbent assay for human tau detection. J Neurochem. 1992;58(2):548–53. PubMed PMID: 1729400
3. Goedert M, Jakes R, Crowther RA, Cohen P, Vanmechelen E, Vandermeeren M, Cras P. Epitope mapping of monoclonal antibodies to the paired helical filaments of Alzheimer's disease: identification of phosphorylation sites in tau protein. Biochem J 1994;301 (Pt 3):871–877. PubMed PMID: 7519852; PubMed Central PMCID: PMC1137067.
4. Vigo-Pelfrey C, Seubert P, Barbour R, Blomquist C, Lee M, Lee D, Coria F, Chang L, Miller B, Lieberburg I, et al. Elevation of microtubule-associated protein tau in the cerebrospinal fluid of patients with Alzheimer's disease. Neurology. 1995;45(4):788–93. PubMed PMID: 7723971
5. Mori H, Hosoda K, Matsubara E, Nakamoto T, Furiya Y, Endoh R, Usami M, Shoji M, Maruyama S, Hirai S. Tau in cerebrospinal fluids: establishment of the sandwich ELISA with antibody specific to the repeat

sequence in tau. Neurosci Lett. 1995;186(2–3):181–3. PubMed PMID: 7777192
6. Hock C, Golombowski S, Naser W, Müller-Spahn F. Increased levels of tau protein in cerebrospinal fluid of patients with Alzheimer's disease—correlation with degree of cognitive impairment. Ann Neurol. 1995;37(3):414–5. PubMed PMID: 7695246
7. Blennow K, Wallin A, Agren H, Spenger C, Siegfried J, Vanmechelen E. Tau protein in cerebrospinal fluid: a biochemical marker for axonal degeneration in Alzheimer disease? Mol Chem Neuropathol. 1995;26(3):231–45. PubMed PMID: 8748926
8. Vanmechelen E, Vanderstichele H, Davidsson P, Van Kerschaver E, Van Der Perre B, Sjögren M, Andreasen N, Blennow K. Quantification of tau phosphorylated at threonine 181 in human cerebrospinal fluid: a sandwich ELISA with a synthetic phosphopeptide for standardization. Neurosci Lett. 2000;285(1):49–52. PubMed PMID: 1078870
9. Arai H, Terajima M, Miura M, Higuchi S, Muramatsu T, Machida N, Seiki H, Takase S, Clark CM, Lee VM, et al. Tau in cerebrospinal fluid: a potential diagnostic marker in Alzheimer's disease. Ann Neurol. 1995;38(4):649–52. PubMed PMID: 7574462
10. Motter R, Vigo-Pelfrey C, Kholodenko D, Barbour R, Johnson-Wood K, Galasko D, Chang L, Miller B, Clark C, Green R, et al. Reduction of beta-amyloid peptide42 in the cerebrospinal fluid of patients with Alzheimer's disease. Ann Neurol. 1995;38(4):643–8. PubMed PMID: 7574461
11. Kanai M, Matsubara E, Isoe K, Urakami K, Nakashima K, Arai H, Sasaki H, Abe K, Iwatsubo T, Kosaka T, Watanabe M, Tomidokoro Y, Shizuka M, Mizushima K, Nakamura T, Igeta Y, Ikeda Y, Amari M, Kawarabayashi T, Ishiguro K, Harigaya Y, Wakabayashi K, Okamoto K, Hirai S, Shoji M. Longitudinal study of cerebrospinal fluid levels of tau, A beta1-40, and A beta1-42(43) in Alzheimer's disease: a study in Japan. Ann Neurol. 1998;44(1):17–26. PubMed PMID: 9667589
12. Galasko D, Chang L, Motter R, Clark CM, Kaye J, Knopman D, Thomas R, Kholodenko D, Schenk D, Lieberburg I, Miller B, Green R, Basherad R, Kertiles L, Boss MA, Seubert P. High cerebrospinal fluid tau and low amyloid beta42 levels in the clinical diagnosis of Alzheimer disease and relation to apolipoprotein E genotype. Arch Neurol. 1998;55(7):937–45. PubMed PMID: 9678311
13. Hulstaert F, Blennow K, Ivanoiu A, Schoonderwaldt HC, Riemenschneider M, De Deyn PP, Bancher C, Cras P, Wiltfang J, Mehta PD, Iqbal K, Pottel H, Vanmechelen E, Vanderstichele H. Improved discrimination of AD patients using beta-amyloid(1-42) and tau levels in CSF. Neurology. 1999;52(8):1555–62. PubMed PMID: 10331678
14. Itoh N, Arai H, Urakami K, Ishiguro K, Ohno H, Hampel H, Buerger K, Wiltfang J, Otto M, Kretzschmar H, Moeller HJ, Imagawa M, Kohno H, Nakashima K, Kuzuhara S, Sasaki H, Imahori K. Large-scale, multicenter study of cerebrospinal fluid tau protein phosphorylated at serine 199 for the antemortem diagnosis of Alzheimer's disease. Ann Neurol. 2001;50(2):150–6. PubMed PMID: 11506396
15. Hampel H, Buerger K, Zinkowski R, Teipel SJ, Goernitz A, Andreasen N, Sjoegren M, DeBernardis J, Kerkman D, Ishiguro K, Ohno H, Vanmechelen E, Vanderstichele H, McCulloch C, Moller HJ, Davies P, Blennow K. Measurement of phosphorylated tau epitopes in the differential diagnosis of Alzheimer disease: a comparative cerebrospinal fluid study. Arch Gen Psychiatry. 2004;61(1):95–102. PubMed PMID: 14706948
16. Shoji M, Matsubara E, Murakami T, Manabe Y, Abe K, Kanai M, Ikeda M, Tomidokoro Y, Shizuka M, Watanabe M, Amari M, Ishiguro K, Kawarabayashi T, Harigaya Y, Okamoto K, Nishimura T, Nakamura Y, Takeda M, Urakami K, Adachi Y, Nakashima K, Arai H, Sasaki H, Kanemaru K, Yamanouchi H, Yoshida Y, Ichise K, Tanaka K, Hamamoto M, Yamamoto H, Matsubayashi T, Yoshida H, Toji H, Nakamura S, Hirai S. Cerebrospinal fluid tau in dementia disorders: a large scale multicenter study by a Japanese study group. Neurobiol Aging. 2002;23(3):363–70. PubMed PMID: 11959397
17. Andreasen N, Minthon L, Clarberg A, Davidsson P, Gottfries J, Vanmechelen E, Vanderstichele H, Winblad B, Blennow K. Sensitivity, specificity, and stability of CSF-tau in AD in a community-based patient sample. Neurology 1999;53(7):1488–1494. PubMed PMID: 10534256.
18. Clark CM, Xie S, Chittams J, Ewbank D, Peskind E, Galasko D, Morris JC, McKeel DW Jr, Farlow M, Weitlauf SL, Quinn J, Kaye J, Knopman D, Arai H, Doody RS, DeCarli C, Leight S, Lee VM, Trojanowski JQ. Cerebrospinal fluid tau and beta-amyloid: how well do these biomarkers reflect autopsy-confirmed dementia diagnoses? Arch Neurol 2003;60(12):1696–1702. PubMed PMID: 14676043.
19. Olsson B, Lautner R, Andreasson U, Öhrfelt A, Portelius E, Bjerke M, Hölttä M, Rosén C, Olsson C, Strobel G, Wu E, Dakin K, Petzold M, Blennow K, Zetterberg H. CSF and blood biomarkers for the diagnosis of Alzheimer's disease: a systematic review and meta-analysis. Lancet Neurol. 2016;15(7):673–84. https://doi.org/10.1016/S1474-4422(16)00070-3. Epub 2016 Apr 8. Review. PubMed PMID: 27068280
20. Toledo JB, Brettschneider J, Grossman M, Arnold SE, Hu WT, Xie SX, Lee VM, Shaw LM, Trojanowski JQ. CSF biomarkers cutoffs: the importance of coincident neuropathological diseases. Acta Neuropathol. 2012;124(1):23–35. https://doi.org/10.1007/s00401-012-0983-7. Epub 201e2 Apr 22. PubMed PMID: 22526019; PubMed Central PMCID: PMC3551449
21. Marelli C, Gutierrez LA, Menjot de Champfleur N, Charroud C, De Verbizier D, Touchon J, Douillet P, Berr C, Lehmann S, Gabelle A. Late-onset behavioral variant of frontotemporal lobar degeneration versus Alzheimer's disease: interest of cere-

brospinal fluid biomarker ratios. Alzheimers Dement (Amst). 2015;1(3):371–9. https://doi.org/10.1016/j.dadm.2015.06.004. eCollection 2015 Sep. PubMed PMID: 27239517; PubMed Central PMCID: PMC4878372

22. Vergallo A, Carlesi C, Pagni C, Giorgi FS, Baldacci F, Petrozzi L, Ceravolo R, Tognoni G, Siciliano G, Bonuccelli U. A single center study: Aβ42/p-Tau(181) CSF ratio to discriminate AD from FTD in clinical setting. Neurol Sci. 2017;38(10):1791–7. https://doi.org/10.1007/s10072-017-3053-z. Epub 2017 July 19. PubMed PMID: 28726050
23. Chen Z, Liu C, Zhang J, Relkin N, Xing Y, Li Y. Cerebrospinal fluid Aβ42, t-tau, and p-tau levels in the differential diagnosis of idiopathic normal-pressure hydrocephalus: a systematic review and meta-analysis. Fluids Barriers CNS. 2017;14(1):13. https://doi.org/10.1186/s12987-017-0062-5. Review. PubMed PMID: 28486988; PubMed Central PMCID: PMC5424383
24. Abu Rumeileh S, Lattanzio F, Stanzani Maserati M, Rizzi R, Capellari S, Parchi P. Diagnostic accuracy of a combined analysis of cerebrospinal fluid t-PrP, t-tau, p-tau, and Aβ42 in the differential diagnosis of Creutzfeldt-Jakob disease from Alzheimer's disease with emphasis on atypical disease variants. J Alzheimers Dis. 2017;55(4):1471–80. https://doi.org/10.3233/JAD-160740. PubMed PMID: 27886009; PubMed Central PMCID: PMC5181677
25. Ewers M, Mattsson N, Minthon L, Molinuevo JL, Antonell A, Popp J, Jessen F, Herukka SK, Soininen H, Maetzler W, Leyhe T, Bürger K, Taniguchi M, Urakami K, Lista S, Dubois B, Blennow K, Hampel H. CSF biomarkers for the differential diagnosis of Alzheimer's disease: a large-scale international multicenter study. Alzheimers Dement. 2015;11(11):1306–15. https://doi.org/10.1016/j.jalz.2014.12.006. Epub 2015 Mar 21. PubMed PMID: 25804998
26. Seino Y, Nakamura T, Kawarabayashi T, Hirohata M, Narita S, Wakasaya Y, Kaito K, Ueda T, Harigaya Y, Shoji M. CSF and Plasma biomarkers in neurodegenerative diseases. J Alzheimers Dis. 2019;68(1):395–404.
27. Shaw LM, Vanderstichele H, Knapik-Czajka M, Clark CM, Aisen PS, Petersen RC, Blennow K, Soares H, Simon A, Lewczuk P, Dean R, Siemers E, Potter W, Lee VM, Trojanowski JQ, Alzheimer's Disease Neuroimaging Initiative. Cerebrospinal fluid biomarker signature in Alzheimer's disease neuroimaging initiative subjects. Ann Neurol. 2009;65(4):403–13. https://doi.org/10.1002/ana.21610. PubMed PMID: 19296504; PubMed Central PMCID: PMC2696350
28. Shaw LM, Vanderstichele H, Knapik-Czajka M, Figurski M, Coart E, Blennow K, Soares H, Simon AJ, Lewczuk P, Dean RA, Siemers E, Potter W, Lee VM, Trojanowski JQ, Alzheimer's Disease Neuroimaging Initiative. Qualification of the analytical and clinical performance of CSF biomarker analyses in ADNI. Acta Neuropathol. 2011;121(5):597–609. https://doi.org/10.1007/s00401-011-0808-0. Epub 2011 Feb 11. PubMed PMID: 21311900; PubMed Central PMCID: PMC3175107
29. Toledo JB, Xie SX, Trojanowski JQ, Shaw LM. Longitudinal change in CSF Tau and Aβ biomarkers for up to 48 months in ADNI. Acta Neuropathol. 2013;126(5):659–70. https://doi.org/10.1007/s00401-013-1151-4. Epub 2013 Jun 29. PubMed PMID: 23812320; PubMed Central PMCID: PMC3875373
30. Sutphen CL, McCue L, Herries EM, Xiong C, Ladenson JH, Holtzman DM, Fagan AM. ADNI. Longitudinal decreases in multiple cerebrospinal fluid biomarkers of neuronal injury in symptomatic late onset Alzheimer's disease. Alzheimers Dement. 2018;14(7):869–79. https://doi.org/10.1016/j.jalz.2018.01.012. Epub 2018 Mar 23. PubMed PMID: 29580670; PubMed Central PMCID: PMC6110083
31. Bateman RJ, Xiong C, Benzinger TL, Fagan AM, Goate A, Fox NC, Marcus DS, Cairns NJ, Xie X, Blazey TM, Holtzman DM, Santacruz A, Buckles V, Oliver A, Moulder K, Aisen PS, Ghetti B, Klunk WE, McDade E, Martins RN, Masters CL, Mayeux R, Ringman JM, Rossor MN, Schofield PR, Sperling RA, Salloway S, Morris JC, Dominantly Inherited Alzheimer Network. Clinical and biomarker changes in dominantly inherited Alzheimer's disease. N Engl J Med. 2012;367(9):795–804. https://doi.org/10.1056/NEJMoa1202753. Epub 2012 July 11. Erratum in: N Engl J Med. 2012 Aug 23;367(8):780. PubMed PMID: 22784036; PubMed Central PMCID: PMC3474597
32. Fagan AM, Xiong C, Jasielec MS, Bateman RJ, Goate AM, Benzinger TL, Ghetti B, Martins RN, Masters CL, Mayeux R, Ringman JM, Rossor MN, Salloway S, Schofield PR, Sperling RA, Marcus D, Cairns NJ, Buckles VD, Ladenson JH, Morris JC, Holtzman DM, Dominantly Inherited Alzheimer Network. Longitudinal change in CSF biomarkers in autosomal-dominant Alzheimer's disease. Sci Transl Med. 2014;6(226):226ra30. https://doi.org/10.1126/scitranslmed.3007901. PubMed PMID: 24598588; PubMed Central PMCID: PMC4038930
33. Hansson O, Zetterberg H, Buchhave P, Londos E, Blennow K, Minthon L. Association between CSF biomarkers and incipient Alzheimer's disease in patients with mild cognitive impairment: a follow-up study. Lancet Neurol. 2006;5(3):228–34. Erratum in: Lancet Neurol. 2006 Apr;5(4):293. PubMed PMID: 16488378
34. Visser PJ, Verhey F, Knol DL, Scheltens P, Wahlund LO, Freund-Levi Y, Tsolaki M, Minthon L, Wallin AK, Hampel H, Bürger K, Pirttila T, Soininen H, Rikkert MO, Verbeek MM, Spiru L, Blennow K. Prevalence and prognostic value of CSF markers of Alzheimer's disease pathology in patients with subjective cognitive impairment or mild cognitive impairment in the DESCRIPA study: a prospective cohort study. Lancet Neurol. 2009;8(7):619–27. https://doi.org/10.1016/S1474-4422(09)70139-5. Epub 2009 June 10. PubMed PMID: 19523877

35. van Rossum IA, Vos SJ, Burns L, Knol DL, Scheltens P, Soininen H, Wahlund LO, Hampel H, Tsolaki M, Minthon L, L'italien G, van der Flier WM, Teunissen CE, Blennow K, Barkhof F, Rueckert D, Wolz R, Verhey F, Visser PJ. Injury markers predict time to dementia in subjects with MCI and amyloid pathology. Neurology. 2012;79(17):1809–16. https://doi.org/10.1212/WNL.0b013e3182704056. Epub 2012 Sep 26. PubMed PMID: 23019259; PubMed Central PMCID: PMC3475623
36. Stomrud E, Minthon L, Zetterberg H, Blennow K, Hansson O. Longitudinal cerebrospinal fluid biomarker measurements in preclinical sporadic Alzheimer's disease: a prospective 9-year study. Alzheimers Dement (Amst). 2015;1(4):403–11. https://doi.org/10.1016/j.dadm.2015.09.002. eCollection 2015 DecPubMed PMID: 27239521; PubMed Central PMCID: PMC4879483
37. Sutphen CL, Jasielec MS, Shah AR, Macy EM, Xiong C, Vlassenko AG, Benzinger TL, Stoops EE, Vanderstichele HM, Brix B, Darby HD, Vandijck ML, Ladenson JH, Morris JC, Holtzman DM, Fagan AM. Longitudinal cerebrospinal fluid biomarker changes in preclinical Alzheimer disease during middle age. JAMA Neurol. 2015;72(9):1029–42. https://doi.org/10.1001/jamaneurol.2015.1285. PubMed PMID: 26147946; PubMed Central PMCID: PMC4570860
38. Xiong C, Jasielec MS, Weng H, Fagan AM, Benzinger TL, Head D, Hassenstab J, Grant E, Sutphen CL, Buckles V, Moulder KL, Morris JC. Longitudinal relationships among biomarkers for Alzheimer disease in the adult children study. Neurology. 2016;86(16):1499–506. https://doi.org/10.1212/WNL.0000000000002593. Epub 2016 Mar 23. PubMed PMID: 27009258; PubMed Central PMCID: PMC4836885
39. Roe CM, Fagan AM, Grant EA, Hassenstab J, Moulder KL, Maue Dreyfus D, Sutphen CL, Benzinger TL, Mintun MA, Holtzman DM, Morris JC. Amyloid imaging and CSF biomarkers in predicting cognitive impairment up to 7.5 years later. Neurology. 2013;80(19):1784–91. https://doi.org/10.1212/WNL.0b013e3182918ca6. Epub 2013 Apr 10. PubMed PMID: 23576620; PubMed Central PMCID: PMC3719431
40. Toledo JB, Zetterberg H, van Harten AC, Glodzik L, Martinez-Lage P, Bocchio-Chiavetto L, Rami L, Hansson O, Sperling R, Engelborghs S, Osorio RS, Vanderstichele H, Vandijck M, Hampel H, Teipl S, Moghekar A, Albert M, Hu WT, Monge Argilés JA, Gorostidi A, Teunissen CE, De Deyn PP, Hyman BT, Molinuevo JL, Frisoni GB, Linazasoro G, de Leon MJ, van der Flier WM, Scheltens P, Blennow K, Shaw LM, Trojanowski JQ; Alzheimer's Disease Neuroimaging Initiative Alzheimer's disease cerebrospinal fluid biomarker in cognitively normal subjects. Brain 2015;138(Pt 9):2701-2715. https://doi.org/10.1093/brain/awv199. Epub 2015 July 27. PubMed PMID: 26220940; PubMed Central PMCID: PMC4643624.
41. Olsson A, Vanderstichele H, Andreasen N, De Meyer G, Wallin A, Holmberg B, Rosengren L, Vanmechelen E, Blennow K. Simultaneous measurement of beta-amyloid (1-42), total tau, and phosphorylated tau (Thr181) in cerebrospinal fluid by the xMAP technology. Clin Chem. 2005;51(2):336–45. Epub 2004 Nov 24. PubMed PMID: 15563479
42. Lewczuk P, Kornhuber J, Vanderstichele H, Vanmechelen E, Esselmann H, Bibl M, Wolf S, Otto M, Reulbach U, Kölsch H, Jessen F, Schröder J, Schönknecht P, Hampel H, Peters O, Weimer E, Perneczky R, Jahn H, Luckhaus C, Lamla U, Supprian T, Maler JM, Wiltfang J. Multiplexed quantification of dementia biomarkers in the CSF of patients with early dementias and MCI: a multicenter study. Neurobiol Aging. 2008;29(6):812–8. Epub 2007 Jan 19. PubMed PMID: 17239996
43. Schindler SE, Gray JD, Gordon BA, Xiong C, Batrla-Utermann R, Quan M, Wahl S, Benzinger TLS, Holtzman DM, Morris JC, Fagan AM. Cerebrospinal fluid biomarkers measured by Elecsys assays compared to amyloid imaging. Alzheimers Dement. 2018;14(11):1460–9. https://doi.org/10.1016/j.jalz.2018.01.013. Epub 2018 Mar 2. PubMed PMID: 29501462; PubMed Central PMCID: PMC6119652
44. Hansson O, Seibyl J, Stomrud E, Zetterberg H, Trojanowski JQ, Bittner T, Lifke V, Corradini V, Eichenlaub U, Batrla R, Buck K, Zink K, Rabe C, Blennow K, Shaw LM, Swedish BioFINDER study group; Alzheimer's Disease Neuroimaging Initiative. CSF biomarkers of Alzheimer's disease concord with amyloid-β PET and predict clinical progression: a study of fully automated immunoassays in BioFINDER and ADNI cohorts. Alzheimers Dement. 2018;14(11):1470–81. https://doi.org/10.1016/j.jalz.2018.01.010. Epub 2018 Mar 1. PubMed PMID: 29499171; PubMed Central PMCID: PMC6119541
45. Mattsson N, Andreasson U, Persson S, Arai H, Batish SD, Bernardini S, Bocchio-Chiavetto L, Blankenstein MA, Carrillo MC, Chalbot S, Coart E, Chiasserini D, Cutler N, Dahlfors G, Duller S, Fagan AM, Forlenza O, Frisoni GB, Galasko D, Galimberti D, Hampel H, Handberg A, Heneka MT, Herskovits AZ, Herukka SK, Holtzman DM, Humpel C, Hyman BT, Iqbal K, Jucker M, Kaeser SA, Kaiser E, Kapaki E, Kidd D, Klivenyi P, Knudsen CS, Kummer MP, Lui J, Lladó A, Lewczuk P, Li QX, Martins R, Masters C, McAuliffe J, Mercken M, Moghekar A, Molinuevo JL, Montine TJ, Nowatzke W, O'Brien R, Otto M, Paraskevas GP, Parnetti L, Petersen RC, Prvulovic D, de Reus HP, Rissman RA, Scarpini E, Stefani A, Soininen H, Schröder J, Shaw LM, Skinningsrud A, Skrogstad B, Spreer A, Talib L, Teunissen C, Trojanowski JQ, Tumani H, Umek RM, Van Broeck B, Vanderstichele H, Vecsei L, Verbeek MM, Windisch M, Zhang J, Zetterberg H, Blennow K. The Alzheimer's Association external quality control program for cerebrospinal fluid biomarkers. Alzheimers Dement.

2011;7(4):386–395.e6. https://doi.org/10.1016/j.jalz.2011.05.2243. Erratum in: Alzheimers Dement. 2011 Sep;7(5):556. PubMed PMID: 21784349; PubMed Central PMCID: PMC3710290

46. Mattsson N, Andreasson U, Persson S, Carrillo MC, Collins S, Chalbot S, Cutler N, Dufour-Rainfray D, Fagan AM, Heegaard NH, Robin Hsiung GY, Hyman B, Iqbal K, Kaeser SA, Lachno DR, Lleó A, Lewczuk P, Molinuevo JL, Parchi P, Regeniter A, Rissman RA, Rosenmann H, Sancesario G, Schröder J, Shaw LM, Teunissen CE, Trojanowski JQ, Vanderstichele H, Vandijck M, Verbeek MM, Zetterberg H, Blennow K. Alzheimer's Association QC Program Work Group. CSF biomarker variability in the Alzheimer's Association quality control program. Alzheimers Dement. 2013;9(3):251–61. https://doi.org/10.1016/j.jalz.2013.01.010. Erratum in: Alzheimers Dement. 2015 Feb;11(2):237. Käser, Stephan A [corrected to Kaeser, Stephan A]; Rissman, Robert [corrected to Rissman, Robert A]. PubMed PMID: 23622690; PubMed Central PMCID: PMC3707386
47. Hansson O, Mikulskis A, Fagan AM, Teunissen C, Zetterberg H, Vanderstichele H, Molinuevo JL, Shaw LM, Vandijck M, Verbeek MM, Savage M, Mattsson N, Lewczuk P, Batrla R, Rutz S, Dean RA, Blennow K. The impact of preanalytical variables on measuring cerebrospinal fluid biomarkers for Alzheimer's disease diagnosis: a review. Alzheimers Dement. 2018;14(10):1313–33. https://doi.org/10.1016/j.jalz.2018.05.008. Epub 2018 Jun 23. Review. PubMed PMID: 29940161
48. Sato C, Barthélemy NR, Mawuenyega KG, Patterson BW, Gordon BA, Jockel-Balsarotti J, Sullivan M, Crisp MJ, Kasten T, Kirmess KM, Kanaan NM, Yarasheski KE, Baker-Nigh A, Benzinger TLS, Miller TM, Karch CM, Bateman RJ. Tau kinetics in neurons and the human central nervous system. Neuron. 2018;98(4):861–4. https://doi.org/10.1016/j.neuron.2018.04.035. PubMed PMID: 29772204; PubMed Central PMCID: PMC6192252
49. He Z, Guo JL, McBride JD, Narasimhan S, Kim H, Changolkar L, Zhang B, Gathagan RJ, Yue C, Dengler C, Stieber A, Nitla M, Coulter DA, Abel T, Brunden KR, Trojanowski JQ, Lee VM. Amyloid-β plaques enhance Alzheimer's brain tau-seeded pathologies by facilitating neuritic plaque tau aggregation. Nat Med. 2018;24(1):29–38. https://doi.org/10.1038/nm.4443. Epub 2017 Dec 4. PubMed PMID: 29200205; PubMed Central PMCID: PMC5760353
50. Smith R, Wibom M, Pawlik D, Englund E, Hansson O. Correlation of in vivo [18F]flortaucipir with postmortem Alzheimer disease tau pathology. JAMA Neurol. 2018;76:310. https://doi.org/10.1001/jamaneurol.2018.3692. [Epub ahead of print] PubMed PMID: 30508025
51. Mattsson N, Schöll M, Strandberg O, Smith R, Palmqvist S, Insel PS, Hägerström D, Ohlsson T, Zetterberg H, Jögi J, Blennow K, Hansson O. (18) F-AV-1451 and CSF T-tau and P-tau as biomarkers in Alzheimer's disease. EMBO Mol Med. 2017;9(9):1212–23. https://doi.org/10.15252/emmm.201707809. PubMed PMID: 28743782; PubMed Central PMCID: PMC5582410
52. Mattsson N, Smith R, Strandberg O, Palmqvist S, Schöll M, Insel PS, Hägerström D, Ohlsson T, Zetterberg H, Blennow K, Jögi J, Hansson O. Comparing (18)F-AV-1451 with CSF t-tau and p-tau for diagnosis of Alzheimer disease. Neurology. 2018;90(5):e388–95. https://doi.org/10.1212/WNL.0000000000004887. Epub 2018 Jan 10. PubMed PMID: 29321235; PubMed Central PMCID: PMC5791788
53. Ovod V, Ramsey KN, Mawuenyega KG, Bollinger JG, Hicks T, Schneider T, Sullivan M, Paumier K, Holtzman DM, Morris JC, Benzinger T, Fagan AM, Patterson BW, Bateman RJ. Amyloid β concentrations and stable isotope labeling kinetics of human plasma specific to central nervous system amyloidosis. Alzheimers Dement. 2017;13(8):841–9. https://doi.org/10.1016/j.jalz.2017.06.2266. Epub 2017 July 19. Erratum in: Alzheimers Dement. 2017 Oct;13(10):1185. PubMed PMID: 28734653; PubMed Central PMCID: PMC5567785
54. Nakamura A, Kaneko N, Villemagne VL, Kato T, Doecke J, Doré V, Fowler C, Li QX, Martins R, Rowe C, Tomita T, Matsuzaki K, Ishii K, Ishii K, Arahata Y, Iwamoto S, Ito K, Tanaka K, Masters CL, Yanagisawa K. High performance plasma amyloid-β biomarkers for Alzheimer's disease. Nature. 2018;554(7691):249–54. https://doi.org/10.1038/nature25456. Epub 2018 Jan 31. PubMed PMID: 29420472
55. Mattsson N, Zetterberg H, Janelidze S, Insel PS, Andreasson U, Stomrud E, Palmqvist S, Baker D, Tan Hehir CA, Jeromin A, Hanlon D, Song L, Shaw LM, Trojanowski JQ, Weiner MW, Hansson O, Blennow K, ADNI Investigators. Plasma tau in Alzheimer disease. Neurology. 2016;87(17):1827–35. Epub 2016 Sep 30. PubMed PMID: 27694257; PubMed Central PMCID: PMC5089525
56. Tatebe H, Kasai T, Ohmichi T, Kishi Y, Kakeya T, Waragai M, Kondo M, Allsop D, Tokuda T. Quantification of plasma phosphorylated tau to use as a biomarker for brain Alzheimer pathology: pilot case-control studies including patients with Alzheimer's disease and down syndrome. Mol Neurodegener. 2017;12(1):63. https://doi.org/10.1186/s13024-017-0206-8. PubMed PMID: 28866979; PubMed Central PMCID: PMC5582385
57. Mielke MM, Hagen CE, Xu J, Chai X, Vemuri P, Lowe VJ, Airey DC, Knopman DS, Roberts RO, Machulda MM, Jack CR Jr, Petersen RC, Dage JL. Plasma phospho-tau181 increases with Alzheimer's disease clinical severity and is associated with tau- and amyloid-positron emission tomography. Alzheimers Dement. 2018;14(8):989–97. https://doi.org/10.1016/j.jalz.2018.02.013. Epub 2018 Apr 5. PubMed PMID: 29626426; PubMed Central PMCID: PMC6097897

58. Goedert M, Spillantini MG, Crowther RA. Cloning of a big tau microtubule-associated protein characteristic of the peripheral nervous system. Proc Natl Acad Sci U S A. 1992;89(5):1983–7. PubMed PMID: 1542696; PubMed Central PMCID: PMC48578
59. Couchie D, Mavilia C, Georgieff IS, Liem RK, Shelanski ML, Nunez J. Primary structure of high molecular weight tau present in the peripheral nervous system. Proc Natl Acad Sci U S A. 1992;89(10):4378–81. PubMed PMID: 1374898; PubMed Central PMCID: PMC49085
60. Herukka SK, Simonsen AH, Andreasen N, Baldeiras I, Bjerke M, Blennow K, Engelborghs S, Frisoni GB, Gabryelewicz T, Galluzzi S, Handels R, Kramberger MG, Kulczyńska A, Molinuevo JL, Mroczko B, Nordberg A, Oliveira CR, Otto M, Rinne JO, Rot U, Saka E, Soininen H, Struyfs H, Suardi S, Visser PJ, Winblad B, Zetterberg H, Waldemar G. Recommendations for cerebrospinal fluid Alzheimer's disease biomarkers in the diagnostic evaluation of mild cognitive impairment. Alzheimers Dement. 2017;13(3):285–95. https://doi.org/10.1016/j.jalz.2016.09.009. Epub 2016 Oct 27. Review. PubMed PMID: 28341066
61. Simonsen AH, Herukka SK, Andreasen N, Baldeiras I, Bjerke M, Blennow K, Engelborghs S, Frisoni GB, Gabryelewicz T, Galluzzi S, Handels R, Kramberger MG, Kulczyńska A, Molinuevo JL, Mroczko B, Nordberg A, Oliveira CR, Otto M, Rinne JO, Rot U, Saka E, Soininen H, Struyfs H, Suardi S, Visser PJ, Winblad B, Zetterberg H, Waldemar G. Recommendations for CSF AD biomarkers in the diagnostic evaluation of dementia. Alzheimers Dement. 2017;13(3):274–84. https://doi.org/10.1016/j.jalz.2016.09.008.
62. Jack CR Jr, Bennett DA, Blennow K, Carrillo MC, Dunn B, Haeberlein SB, Holtzman DM, Jagust W, Jessen F, Karlawish J, Liu E, Molinuevo JL, Montine T, Phelps C, Rankin KP, Rowe CC, Scheltens P, Siemers E, Snyder HM, Sperling R, Contributors. NIA-AA research framework: toward a biological definition of Alzheimer's disease. Alzheimers Dement. 2018;14(4):535–62. https://doi.org/10.1016/j.jalz.2018.02.018. Review. PubMed PMID: 29653606; PubMed Central PMCID: PMC5958625

Journal of Alzheimer's Disease 70 (2019) 485–501
DOI 10.3233/JAD-190023
IOS Press

Oral Immunization with Soybean Storage Protein Containing Amyloid-β 4–10 Prevents Spatial Learning Decline

Takeshi Kawarabayashi[a,b,*], Teruhiko Terakawa[c,d], Atsushi Takahashi[c], Hisakazu Hasegawa[c], Sakiko Narita[b], Kaoru Sato[b], Takumi Nakamura[b,e], Yusuke Seino[b], Mie Hirohata[b], Nobue Baba[f], Tetsuya Ueda[f], Yasuo Harigaya[g], Fuyuki Kametani[h], Nobuyuki Maruyama[i], Masao Ishimoto[j], Peter St. George-Hyslop[k] and Mikio Shoji[a,b]

[a]*Department of Neurology, Geriatrics Research Institute Hospital, Maebashi, Aomori, Japan*
[b]*Department of Neurology, Institute of Brain Science, Hirosaki University Graduate School of Medicine, Hirosaki, Aomori, Japan*
[c]*Hokko Chemical Industry Co., Ltd, Atsugi-shi, Kanagawa, Japan*
[d]*Inplanta Innovations Inc. Yokohama, Kanagawa, Japan*
[e]*Department of Neurology, Gunma University Graduate School of Medicine, Maebashi, Gunma, Japan*
[f]*Bioanalysis Department, LSI Medience Corporation, Itabashi-ku, Tokyo, Japan*
[g]*Department of Neurology, Maebashi Red Cross Hospital, Maebashi, Japan*
[h]*Department of Dementia and Higher Brain Function, Tokyo Metropolitan Institute of Medical Science, Tokyo, Japan*
[i]*Graduate School of Agriculture, Kyoto University, Uji, Kyoto, Japan*
[j]*Institute of Crop Science, NARO, Tsukuba, Ibaraki, Japan*
[k]*Tanz Centre for Research in Neurodegenerative Diseases, and Departments of Medicine, Medical Biophysics and Laboratory Medicine and Pathobiology, University of Toronto, Toronto, Ontario, Canada*

Accepted 9 May 2019

Abstract. Amyloid-β (Aβ) plays a central role in the pathogenesis of Alzheimer's disease (AD). Because AD pathologies begin two decades before the onset of dementia, prevention of Aβ amyloidosis has been proposed as a mean to block the pathological cascade. Here, we generate a transgenic plant-based vaccine, a soybean storage protein containing Aβ4–10, named Aβ+, for oral Aβ immunization. One mg of Aβ+ or control protein (Aβ–) was administered to TgCRND8 mice once a week from 9 weeks up to 58 weeks. Aβ+ immunization raised both anti-Aβ antibodies and cellular immune responses. Spatial learning decline was prevented in the Aβ+ immunized group in an extended reference memory version of Morris water maze test from 21 to 57 weeks. In Tris-buffered saline (TBS), sodium dodecyl sulfate (SDS), and formic acid (FA) serial extractions, all sets of Aβ species from Aβ monomer, low to high molecular weight Aβ oligomers, and Aβ smears had different solubility in TgCRND8 brains. Aβ oligomers decreased in TBS fractions, corresponding to an increase in high molecular weight Aβ oligomers in SDS extracts and Aβ smears in FA fraction of the Aβ+ treated group. There was significant

*Correspondence to: Takeshi Kawarabayashi, MD, PhD, Department of Neurology, Geriatrics Research Institute Hospital, 3-26-8, Otomo-machi, Maebashi, Gunma, 371-0847, Japan. Tel.: +81 27 253 3311; E-mail: tkawara@ronenbyo.or.jp.

ISSN 1387-2877/19/$35.00

inhibition of histological Aβ burden, especially in diffuse plaques, and suppression of microglial inflammation. Processing of amyloid-β protein precursor was not different between Aβ+ and Aβ− groups. No evidence of amyloid-related inflammatory angiopathy was observed. Thus, Aβ+ oral immunization could be a promising, cheap, and long-term safe disease-modifying therapy to prevent the pathological process in AD.

Keywords: Alzheimer's disease, Alzheimer vaccines, amyloid-β oligomers, plant, prevention, soybean, spatial memory

INTRODUCTION

Based on the amyloid cascade hypothesis in Alzheimer's disease (AD) [1, 2], many disease-modifying therapies (DMTs) are now being developed. However, none have succeeded in phase III clinical trials. Although the first clinical trial with an amyloid-β (Aβ) vaccine, AN1792, was stopped because of meningoencephalitis [3], subsequent studies revealed that AN1792 induced anti-Aβ antibodies, removed Aβ accumulations, and slowed the progression rate of cognitive dysfunction [4, 5]. Since then, many trials have attempted to improve the safety of Aβ immunotherapies by avoiding T-cell autoimmune responses [6–8]. In a phase Ib randomized trial, aducanumab, an antibody against aggregated forms of Aβ, reduced Aβ burden accompanied by a slowing of cognitive impairment in prodromal and mild AD patients [9]. A phase II study of Aβ vaccine CAD106 against $Aβ_{1–6}$ evoked a strong serological response and demonstrated acceptable safety and tolerability [10]. A phase IIa trial of Aβ vaccine UB-311 against Aβ1–14 has been started based on favorable phase I trial results [11]. Case studies, the Alzheimer Disease Neuroimaging Initiative (ADNI), and the Dominantly Inherited Alzheimer's Network (DIAN) have shown that AD pathology begins more than 20 years before the onset of dementia [12–14]. For this reason, DMT trials aimed at preventing the onset of AD, such as the DIAN-Trials Unit [15] and Alzheimer's Prevention Initiative (API) [16], are now ongoing.

Mucosal vaccination is the ideal immunization for good accessibility, needle-free delivery, and protective immune responses in both mucosal and systemic immune compartments [17]. This method induces regulatory T cells, leading to a decrease in the systemic T-cell response and increased secretion of immune-inhibitory cytokines. Plants are advantageous platforms for recombinant vaccines because of their low cost, industrial scale production, and the absence of contamination from toxins and pathogens that are produced in bacterial and yeast systems [18]. Although plant-based Aβ vaccines using potatoes, tomatoes, green pepper leaves, rice, and tobacco have been reported [19–21], their effect on amyloid deposition and learning was examined only in the study with transgenic rice [21]. Booster injections of Aβ peptide were necessary in their procedure, and most transgenic plants did not produce sufficient amounts of Aβ. We have developed an approach based upon an innovative transgenic soybean that produces 870 mg/g of transgenic soybean seed storage protein containing Aβ4–10 (Aβ+), which is sufficient sequence of Th2 epitope [22] for safe oral immunization without T-cell responses and additional Aβ peptide booster injections [23]. Here, we validate the efficacy of Aβ+ oral vaccines using an AD mouse model, TgCRND8 [24, 25].

MATERIALS AND METHODS

Preparation of transgenic soybean protein Aβ+

Three tandem repeats of the Th2 epitope portion of Aβ4–10 (FRHDSGY) [22] were inserted into three portions of the flexible disordered regions II-IV of soybean glycinin A1aB1b, a carrier subunit protein of 11S globulins [26] (Fig. 1A). The seed specific glycinin promoter, cDNA for A1aB1b containing $Aβ_{4–10}$ sequences or a wild type A1aB1b cassette for controls, and glycinin 1 terminator constructs to plasmids were transformed into soybean immature embryos. A1aB1b with $Aβ_{4–10}$ and wild type A1aB1b were expressed in protein storage vacuoles [23]. Purified A1aB1b containing Aβ4–10, referred to as Aβ+, and wild type control A1aB1b, referred to as Aβ− were used.

Oral immunization

TgCRND8 expresses a mutant (K670N/M671L and V717F) human amyloid-β protein precursor (AβPP) 695 transgene under the regulation of the Syrian hamster prion promoter on a C3H/B6 strain background [24, 25]. TgCRND8 mice show spatial learning deterioration at 3 months of age that are accompanied by both increasing levels of Aβ and increasing numbers of amyloid plaques in the

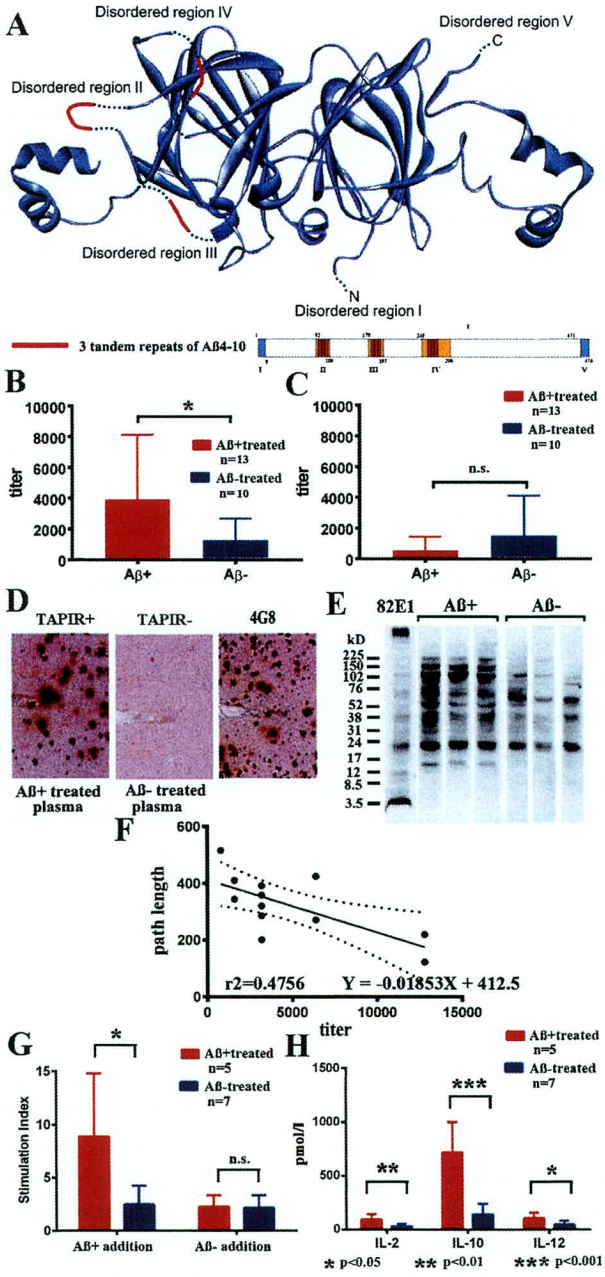

Fig. 1. Transgenic plant protein A1aB1b and immune responses. A) The structure of transgenic plant protein A1aB1b containing $A\beta_{4-10}$ (Aβ+). Three tandem repeats of $A\beta_{4-10}$ were inserted into the three disordered regions of soybean 11S globulin, A1aB1b, that are marked in red. B) IgG antibody titer against Aβ+ in plasma from Aβ+ immunized mice (red, $n=12$) significantly increased compared with Aβ– immunized mice (blue, $n=10$, $p<0.05$). C) IgG antibody titer against Aβ– in plasma was much less than that against Aβ+ and did not differ between Aβ+ (red, $n=12$) and Aβ– (blue, $n=10$) immunized mice. D) Aβ+ immunized mouse plasma diluted with blocking solution (1:2,000) labeled senile plaque Aβ amyloid in an AD brain (TAPIR+; left). Control stain of the AD brain using Aβ– treated mouse plasma (1:2,000, TAPIR-; middle) and anti-Aβ antibody (4G8; right). The figures show representative staining from Aβ+ and Aβ– treated mice. E) The SDS fraction of non-oral vaccine treated TgCRND8 mice was stained with plasma (1:400) from Aβ+ and Aβ– treated mice. Plasma from Aβ+ treated mice showed more staining compared with that from Aβ– treated mice in bands at 16, 40, 56, 102, 150, and 200 kD. F) The antibody titer against Aβ+ and average path length to reach the hidden platform during 1–10 days of the last Morris water maze test showed a significant linear regression correlation. Determination coefficients ($r^2=0.4756$) and regression equations ($Y=-0.01853X+412.5$) are shown ($n=12$; $n=6$ for 43 weeks, and $n=6$ for 59 weeks). G) Thymidine uptake by stimulation of Aβ+ was significantly increased in Aβ+ treated mouse splenocytes (red, $n=5$) compared with those in the Aβ– treated group (blue, $n=7$, $p<0.05$). No increase in thymidine uptake by stimulation of Aβ– was shown in both Aβ+ and Aβ– treated groups ($p=0.628$). H) Stimulation of Aβ+ significantly increased the amounts of released cytokines, IL–2 ($p<0.01$), IL–10 ($p<0.001$), and IL–12 ($p<0.05$) in Aβ+ treated mouse splenocytes (red, $n=5$) compared with those in Aβ– treated mice (blue, $n=7$).

brain [24]. One mg of purified Aβ+ or control Aβ– with 10 μg cholera toxin subunit B (Crucell, Leiden, Netherlands) was administered into the guts via a catheter every week from 9 weeks old until 22~58 weeks old. All animal experiments followed the ARRIVE guidelines, and were approved by the Ethics Committee of Hirosaki University (approval number M13007-1).

Morris water maze (MWM) test

Memory was evaluated by a spatial reference memory version of the MWM test every 4 weeks, as previously described [24, 25, 27]. Tests began on the first day of 13 weeks old and continued for 9 more consecutive days just 4 weeks after the first oral administration at 9 weeks old. These consecutive 10-day tests were repeated every 4 weeks until 21, 41, and 57 weeks old. The swim path of a mouse during each trial was recorded by a video camera connected to a video tracking system (Noldus EthoVision XT, Noldus Information Technology, Wageningen, Netherlands). The mouse was given 4 consecutive 60 s training trials for 10 days. The location of a hidden escape platform was in the center of one of the pool's quadrants and was left in the same position during 10 consecutive days. Probe trial was administered 24 h after the 10th day of training. During the probe trial, the escape platform was removed from the pool, and the mice were allowed to search the pool uninterrupted for 60 s [24, 27].

Brain preparation

Under anesthesia with halothane, brains and cerebrospinal fluid (CSF) were collected at 23 weeks (Aβ+ $n=9$, male 5, female 4, Aβ– $n=11$, male 4, female 7), 43 weeks (Aβ+ $n=7$, male 4, female 3, Aβ– $n=6$, male 4, female 2), and 59 weeks (Aβ+ $n=6$, male 4, female 2, Aβ– $n=7$, male 5, female 2) after the last MWM test. Brains were removed and cut into sagittal sections along the midline. One hemisphere was fixed in 4% paraformaldehyde with 0.1 M phosphate-buffered saline (PBS, pH 7.6) for 8 h, and embedded in paraffin. The other half of the brain was fractionated by three sequential extraction steps using Tris-buffered saline (TBS) with protease inhibitors (Complete®, Roche Diagnostics, Basel, Switzerland), 2% sodium dodecyl sulfate (SDS) in water with the same protease inhibitors, and then 70% formic acid (FA) in water for biochemical analysis of Aβ species [28, 29].

Immune response to oral administration of Aβ+ and Aβ-

Microplates (MICROLON, Greiner bio-one, Austria) were coated overnight at 4°C with Aβ+, Aβ–, or Aβ1–42 peptides (0.5 μg/well) with 0.01 M PBS (pH 7.4), washed with PBS, and blocked with Blocker Casein in PBS (Thermo Fisher, Waltham, MA). After incubating with plasma samples in each well for 45 min at room temperature and washing, samples were reacted with anti-mouse IgG- or IgA-conjugated horseradish peroxidase (Thermo Fisher) in Blocker Casein PBS at 37°C for 30 min, and color development using 100 μl of tetramethylbenzidine for 15 min was performed. H_2SO_4 was added to stop the reaction, and signals were measured at 450 nm using an ELISA reader.

Splenocytes from 59-week-old mice were isolated, cultured, and restimulated, as previously described [30]. Aβ+, Aβ–, or Aβ1–42 was added to splenocytes at final concentrations of 100 μg/ml in triplicated wells, and 1 μCi of [^{3}H]-thymidine was added to cells at 72 h. Cells were harvested after 18 h and thymidine incorporation was measured using a 1450 Microbeta liquid scintillation counter (Perkin Elmer, Waltham, MA). The stimulation index (SI) was calculated using the following formula: counts per minute (CPM) of the well with antigen per CPM with no antigen. An SI index >3 indicates a proliferative cellular immune response of the splenocytes. Supernatants were collected just before the addition of [^{3}H]-thymidine and stored at –80°C for cytokine assays. Released cytokines were measured using Mouse Pro-Inflammatory TH1/TH2 9-plex (MesoScale Discovery, Rockville, MD) according to the manufacturer's protocol. The Multi-Spot ELISA plates were precoated with antibodies specific for the following cytokines: interferon-γ, Interleukin (IL)-1β, IL-10, IL-12 total, IL-2, IL-4, IL-5, keratinocyte chemoattractant/human growth-regulated oncogene (KC/GRO), and tumor necrosis factor-α (TNF-α), and detected with SULFO-TAG detection antibodies. Light emitted upon electrochemical stimulation was read using a SECTOR Imager 2400A (Meso Scale Discovery).

Antibodies for western blot and immunostaining

The following antibodies to Aβ were used for western blots and immunostaining. Monoclonal antibodies: 82E1 (anti-Aβ1–16, IBL, Fujioka, Gunma, Japan), BA-27 (anti-$Aβ_{1–40}$) [31], BC-05

(anti-$A\beta_{35-43}$) [31], 4G8 (anti-$A\beta_{18-22}$, Signet Lab), and 6E10 (anti-$A\beta_{3-8}$, Covance Research Products Inc); Polyclonal antibodies: Aβ-N (anti-$A\beta_{1-5}$, IBL), Ab9204 [32], anti-$A\beta_{40}$ (Cat# 44–348, Thermo Fisher), and anti-$A\beta_{42}$ (Cat#44–344, Thermo Fisher). A monoclonal antibody against Aβ4–10, named PEP3, was newly produced. Other antibodies included Iba1 for microglial markers (Wako Cat# 019-19471), anti-GFAP (Dako Cat# N1506), anti-CD5 (Cat# 550522 Clone 53-7.3, BD Pharrmingen, Franklin Lakes, NJ), anti-AβPP antibody Saeko (anti-C-terminal 30 amino acids of AβPP [29]), anti-mouse tau antibody, TAU-5 (Thermo Fisher Cat# MA1-26600), and PHF-1 against phosphorylated tau (pTau) at serine 396/serine 404 (gift from Davies P).

ELISA for levels of $A\beta_{40}$, $A\beta_{42}$, AβOs, and sAβPP

Human β Amyloid ELISA Kits for $A\beta_{x\text{-}40}$ and $A\beta_{x\text{-}42}$ (294-64701 for $A\beta_{x\text{-}40}$; 290-62601 for $A\beta_{x\text{-}42}$; Wako), Human Amyloid β oligomers (82E1-specific) Assay Kit-IBL (#27725, IBL [33]), a Human sAPPα (highly sensitive) Assay Kit (#27734, IBL), and a Human sAPPβ-sw (highly sensitive) Assay Kit (#27733, IBL).

Western blot analysis

All prepared samples were boiled at 70°C for 10 min in SDS sample buffer, separated on a 4–12% NuPAGE Bis–Tris Gel (Cat# NP0321, Thermo Fisher), and electrotransferred to an Immobilon P (MerckMillipore, Burlington, MA) membrane at 100 V for 1.5 h. The signal intensities of proteins labeled using Supersignal (Cat#34076, Thermo Fisher) were quantified using a luminoimage analyzer (LAS 1000-mini, Fuji Film, Tokyo, Japan). $A\beta_{42}$ peptides (Cat#A9810, Sigma-Aldrich, St. Louis, MO) were used as control Aβ peptides.

Pathological analysis

Five-μm-thick sections were immersed in 0.5% periodic acid to block intrinsic peroxidase, and then treated with 99% FA for Aβ and tau staining for 3 min. After blocking with 5% normal goat or horse serum in 50 mM PBS (pH 7.4) containing 0.05% Tween 20 and 4% Block Ace (Cat# UK-B80, DS Pharma Biomedical, Suita, Osaka, Japan), sections were incubated overnight with the primary antibodies. Specific labeling was visualized using a Vectastain Elite ABC kit (Vector, Burlingame, CA). Tissue sections were counterstained with hematoxylin. Immunostaining areas of Aβ or Iba1 in 10 randomly selected ROIs (872 μm × 671 μm) in the frontal, temporal, and parietal cortex of 3 serial slides were measured in total using Image Pro Plus ver.4.5 (Media Cybernetics, Rockville, MD) after adjustment for artifact staining. The presence of hemorrhage was examined using Berlin blue staining. For the tissue amyloid plaque immunoreactivity (TAPIR) to identify antibody raised against Aβ+, paraffin sections of brains from AD patients and controls were stained with plasma from Aβ+ and Aβ– treated mice diluted with blocking solution (1:2,000). Congo red stain was used to stain core plaques.

Statistical analysis

Data were expressed as the mean ± standard deviation (SD) except for Fig. 2. Two-way analysis of variance (ANOVA), with *post hoc* tests (Bonferroni's multiple comparisons test), was used for analyzing longitudinal alteration. In Fig. 2, data are expressed as the mean ± standard error (SE), and two-way repeated ANOVA was used. Mann–Whitney *U* test was applied for comparison between two groups. Prism 7 software (GraphPad, La Jolla, CA) and IBM SPSS Statistics 25 (IBM, Armonk, NY) were used for statistical analyses. A value of $p < 0.05$ was considered to be significant for all statistical tests.

RESULTS

Oral immunization raised adapted immune responses

Significant positive rates of IgG antibodies against Aβ+ were found in the Aβ+ treated group (Fig. 1B; $p < 0.05$). IgG antibodies against Aβ– were much lower than those against Aβ+, and there was no difference between the Aβ+ and Aβ– treated groups (Fig. 1C). IgG antibodies against $A\beta_{1-42}$ peptides, and IgA antibodies against Aβ+, Aβ–, and $A\beta_{1-42}$ were not detected. Plasma (1:2,000) from 59-week-old Aβ+ immunized mice labeled Aβ amyloid plaques in the human AD brain (TAPIR+; Fig. 1D). The SDS fraction of non-oral vaccine treated TgCRND8 mice was stained with plasma (1:400) from Aβ+ and Aβ– treated mice. Plasma from Aβ+ treated mice showed more staining compared with that from Aβ– treated mice in bands at 16, 40, 56, 102, 150, and 200 kD (Fig. 1E). The

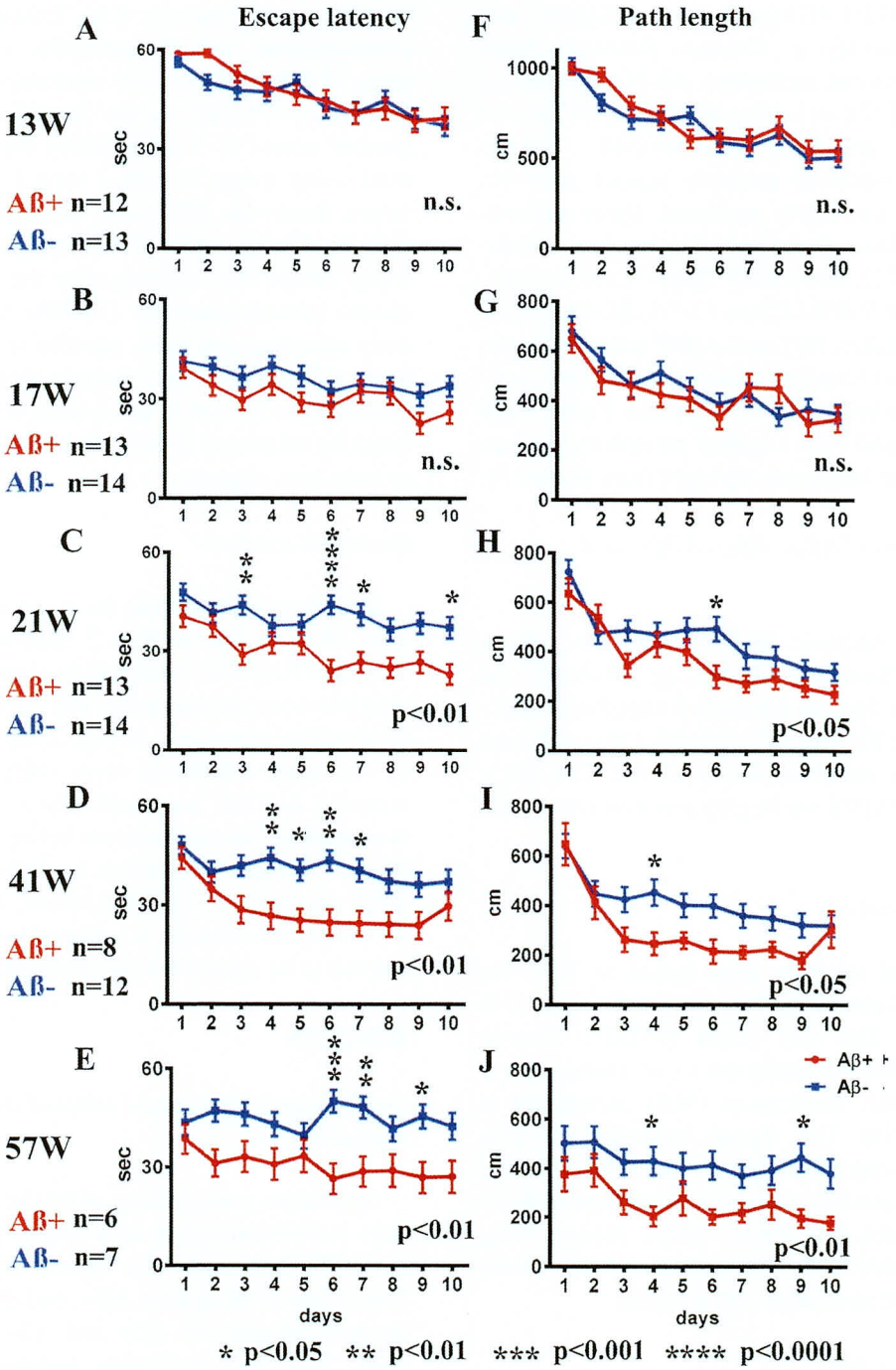

Fig. 2. Spatial reference memory version of the MWM test from 13 to 57 weeks old. A-E) escape latency, and F-J) path-length at 13, 17, 21, 41, and 57 weeks. Escape latency and path-length analyses showed significant improvement in Aβ+ treated mice (red line) from 21 weeks old (C, H) compared with Aβ– treated mice (blue line) (escape latency $p < 0.01$, path-length $p < 0.05$). Aβ+ treated mice continued to show significantly better performances in escape latency and path-length than those of Aβ– treated mice until 57 weeks old ($p < 0.05$ to 0.01; D, E, I, J). Statistical significance by two-way repeated ANOVA was shown in lower right of each line graph. The asterisk shows the result of *post hoc* analysis at each day. Mann–Whitney U test was applied for comparison between two groups. Analyzed mice numbers are $n = 12$ for Aβ+, $n = 13$ for Aβ– at 13 weeks; $n = 13$ for Aβ+, $n = 14$ for Aβ– at 17, 21 weeks; $n = 8$ for Aβ+, $n = 12$ for Aβ– at 41 weeks; and $n = 6$ for Aβ+, $n = 7$ for Aβ– at 57 weeks.

antibody titer against Aβ+and average path length to reach the hidden platform during 1–10 days of the last Morris water maze test showed a significant linear regression correlation (Fig. 1F; $p < 0.05$). This finding suggested a close correlation between evoked anti-Aβ oligomers antibody titers and preservation of special learning ability, as shown in the Fig. 2.

Splenocytes from the Aβ+ treated group showed significant proliferation against Aβ+ addition compared with those of the Aβ– treated group (Fig. 1G; $p < 0.05$). Aβ– treated splenocytes did not react with both Aβ+ and Aβ– addition. Significantly increased levels of IL-2, IL-10, and IL-12 were revealed in the media from the Aβ+ treated group compared with the Aβ– treated group ($p < 0.01$ for IL-2, $p < 0.001$ for IL-10, and $p < 0.05$ for IL-12). The levels of interferon-γ, IL-1β, IL-4, IL-5, KC/GRO, and TNF-α were not different between the groups. IL-10 levels were markedly increased compared with those of IL-12, suggesting inhibition of proinflammatory cytokines and the predominance of a Th2 response (Fig. 1H).

Aβ+ prevented spatial learning decline

In the first trial at 13 weeks, there were no differences between Aβ+ and Aβ– treated mice in escape latency or path-length to reach the hidden platform (Fig. 2A and F). For escape latency and path-length analysis, improvements due to learning effects were recognized in the second trial in both groups (Fig. 2B, G). The escape latency and path-length in Aβ+ treated mice were significant shorter than those of the Aβ– treated group at 21 weeks old (escape latency Fig. 2C; $p < 0.01$, path-length Fig. 2H; $p < 0.05$) suggesting improved learning in Aβ+ treated mice. Aβ+ treated mice continued to show significantly better performances than Aβ– treated mice until 57 weeks old (Fig. 2D, E, I, and J; $p < 0.05$–0.01). There were no significant differences in the probe trials.

Decreased soluble AβOs by ELISA

Almost all $Aβ_{40}$ and $Aβ_{42}$ monomers accumulated in the SDS and FA fractions (Fig. 3B, C, E, F). In the TBS, SDS, and FA soluble fractions, the amount of $Aβ_{40}$ and $Aβ_{42}$ did not differ between the Aβ+ and Aβ– groups at any of the ages tested (Fig. 3A, B, D–F), except for increased $Aβ_{40}$ in the FA fraction of Aβ+ group (Fig. 3C; $p < 0.05$). AβOs measured by 82E1/82E1 ELISA longitudinally showed that the amount of AβOs in the TBS fraction was significantly decreased in the Aβ+ treated group compared with the Aβ– treated group (Fig. 3G; $p < 0.0001$). AβOs ELISA showed trace amounts of soluble AβOs in both the SDS and FA extracted fractions compared with the amounts of $Aβ_{40}$ and $Aβ_{42}$ in the Aβ+ and Aβ– groups, and no difference between the Aβ+ and Aβ– treated groups (Fig. 3H, I).

Longitudinal appearance of AβOs species in TgCRND8 without oral immunization trial

Since 82E1/82E1 ELISA could only measure some AβOs species, the basic age-dependent presence of all Aβ species were directly examined by western blots in 3-step brain extracts from TgCRND8 at 13, 23, 43, and 59 weeks of age. In TBS fractions, Aβ monomers were labeled by 82E1 from 13 weeks, and the amount increased with age (Fig. 4A, D). AβOs except high molecular weight (HMW) AβOs larger than 200 kDa were difficult to detect in this fraction because of the existence of mouse IgGs, as shown in lane 59N from a non-transgenic TgCRND8 littermate at 59 weeks old (Fig. 4A, G). In SDS fractions, however, there were marked Aβ monomers, low molecular weight (LMW) AβOs (di-, tri-, tetra-, and Aβ*56 [34], and HMW AβOs larger than 200 kDa. Respective AβOs species increased with age (Fig. 4B, E, H). In FA fractions, Aβ monomers, Aβ dimers and diffuse smear patterns were observed (Fig. 4C, F, I). Many Aβ species with different solubility and aggregation properties were accumulated from the early period in TgCRND8 brains, suggesting that 82E1/82E1 ELISA detected only some of the accumulated AβOs. Aβ monomers increased with age in the TBS, SDS, and FA fractions, HMW oligomers increased with age in the TBS and SDS fractions, and Aβ smear increased in the FA fractions, although not significantly with the small sample size.

4G8, anti-$Aβ_{40}$, and anti-$Aβ_{42}$ weakly detected LMW AβOs, but HMW AβOs could not be detected (Fig. 4J–L). These findings suggest that the C-terminal site of Aβ caused conformational changes in Aβ when incorporated into HMW large assemblies, leading to C-terminal epitope blockade of Aβ species including $Aβ_{40}$ and $Aβ_{42}$. In support of this, western blots of aggregated synthetic $Aβ_{42}$ showed that N-terminus antibodies (Ab9204, Aβ-N, and PEP3) clearly detected HMW AβOs; however, antibodies against the mid portion (6E10 and 4G8) and C-terminus 42 (anti-$Aβ_{42}$ and BC-05) of Aβ could not detect HMW AβOs (Fig. 4M). Antibodies against C-terminus 40 (anti-$Aβ_{40}$, BA-27) did not detect

55

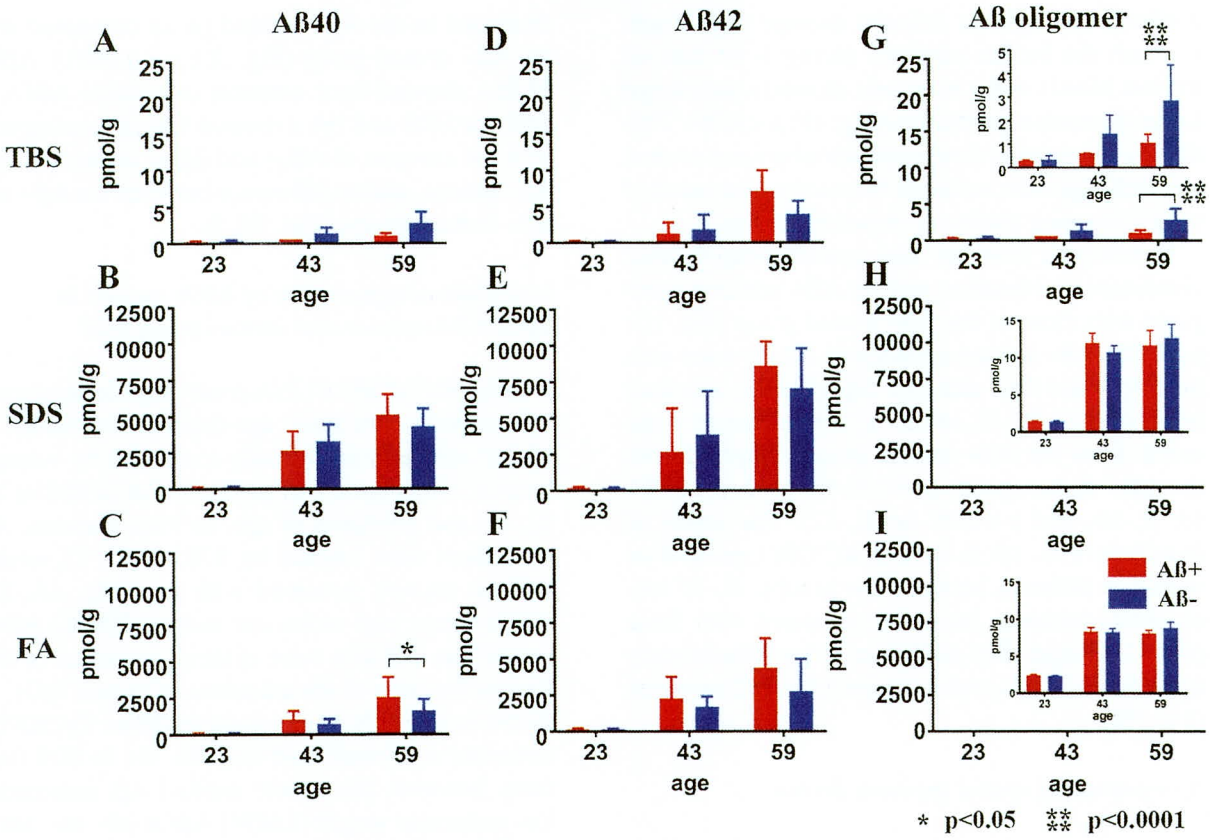

Fig. 3. Longitudinal change in $A\beta_{40}$, $A\beta_{42}$, and AβOs in TBS, SDS, and FA fractions from Aβ+ or Aβ– treated mouse brains. Amounts of $A\beta_{x\text{-}40}$ (A–C), $A\beta_{x\text{-}42}$ (D–F), and AβOs (G–I) in TBS, SDS, and FA fractions of Aβ+ (red) and Aβ– (blue) immunized mouse brains measured using ELISA at 23, 43, and 59 weeks old. There were no significant differences in the levels of $A\beta_{x\text{-}40}$ (A, B) and $A\beta_{x\text{-}42}$ (D–F) between Aβ+ and Aβ– treated groups at any time points or in any fractions, except for the $A\beta_{x\text{-}40}$ in the FA fraction at 59 weeks old (C: *p<0.05). Significant suppression of AβOs in TBS soluble fractions was revealed in Aβ+ treated mice compared with Aβ– treated mice (G and enlarged illustration, ****$p < 0.0001$). Amounts of AβOs in SDS and FA fractions were very low compared with $A\beta_{40}$ and $A\beta_{42}$ in the same fraction (H, I). Mice at 23 weeks ($n = 9$ for Aβ+, $n = 11$ for Aβ–), 43 weeks ($n = 7$ for Aβ+, $n = 6$ for Aβ–), and 59 weeks ($n = 6$ for Aβ+, $n = 7$ for Aβ–) were measured by ELISA.

synthetic $A\beta_{42}$. The C-terminal epitopes of HMW AβOs were blocked resulting no staining by C-terminus-specific antibodies. Immunostaining of TgCRND8 brains showed decreased immunostaining by anti-$A\beta_{40}$ or anti-$A\beta_{42}$ compared with that by Aβ-N (Fig. 4N). C-terminal epitope blockade of HMW AβOs is one reason for the decrease of Aβ burden labeled by anti-C terminal antibodies.

Western blotting of Aβ+ treated brains

Based on these analyses, Aβ species in three fractions of both Aβ+ and Aβ– groups were analyzed by western blots using 82E1 at 23, 43, and 59 weeks of age. In TBS fractions, soluble Aβ monomers in the Aβ+ treated group were decreased at 23, 43, and 59 weeks. Trace amounts of HMW AβOs were detected at 59 weeks; however, there was no difference between the Aβ+ and Aβ– groups (Fig. 5A–C). In SDS fractions, Aβ monomers and LMW AβOs were detected equally at 23, 43, and 59 weeks. However, accumulation of HMW AβOs was slightly increased in the Aβ+ treated group at 23, 43, and 59 weeks (Fig. 5D–F). In FA fractions, monomers and dimers of Aβ increased with age equally in both groups (Fig. 5G–I). Smear patterns of Aβ were markedly observed in the Aβ+ group at 59 weeks of age (Fig. 5I). Using quantification of the bands, TBS soluble Aβ monomer decreased significantly in Aβ+ treated groups by two-way ANOVA ($p < 0.001$, Fig. 5J). Using *post-hoc* analysis, significance was detected at 59 weeks ($p < 0.001$, Fig. 5J). SDS soluble HMW oligomers and Aβ smear in the FA fraction increased significantly in Aβ+ treated groups by two-way ANOVA (Fig. 5N, $p < 0.01$ for SDS soluble HMW oligomers, and Fig. 5O, $p < 0.0001$ for

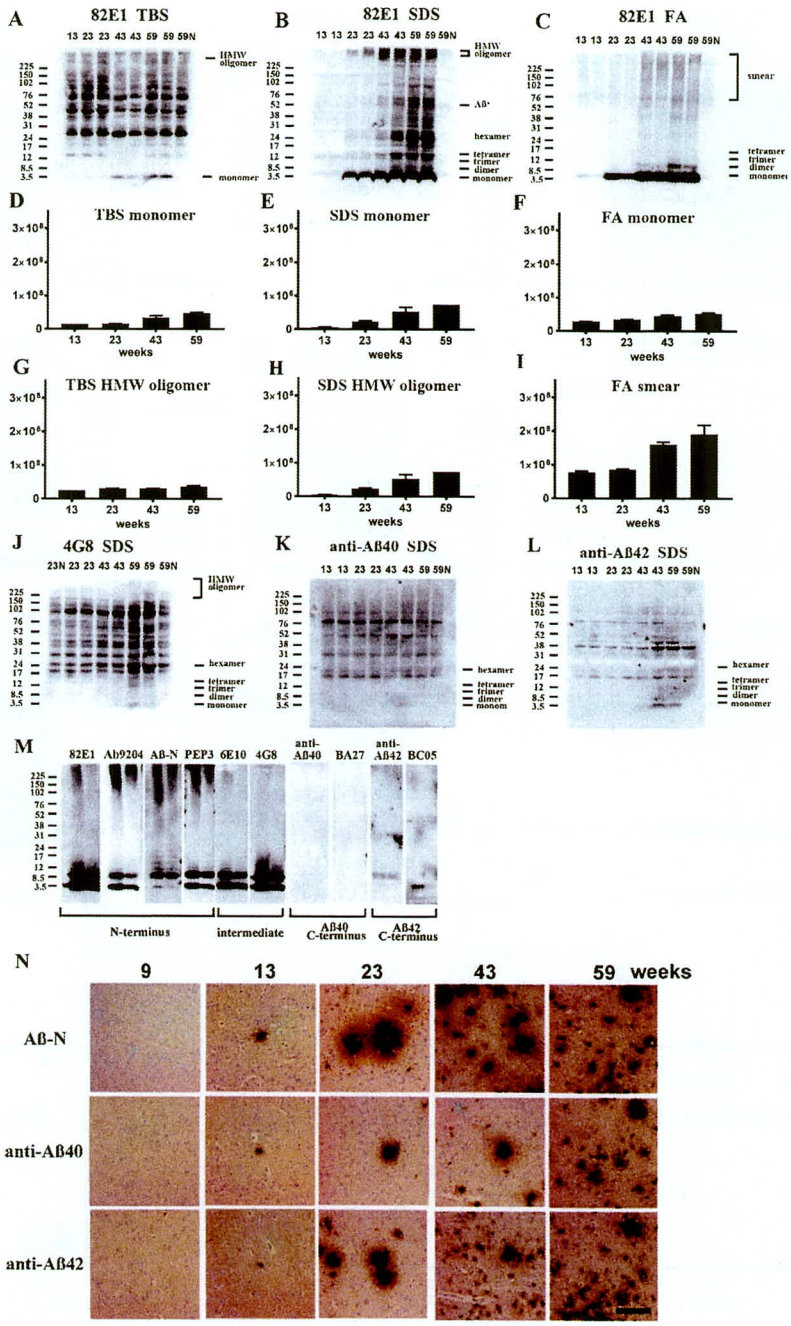

Fig. 4. Age-dependent increase of Aβ monomer and Aβ oligomers in brains of TgCRND8 without an oral immunization trial (A–L), antibody epitope mapping of aggregated synthetic $A\beta_{1-42}$ (M), and immunostaining of TgCRND8 brains without an oral immunization trial (N). D–I are quantification of Aβ monomer in each fraction (D–F), HMW oligomers in TBS and SDS fraction (G, H), and Aβ smear in the FA fraction (I). 59N indicates nontransgenic littermates at 59 weeks. A) In TBS fractions, Aβ monomers were detected by 82E1 from 13 weeks and the amount increased with age (D). Other molecular weight oligomers except HMW oligomers (G) were difficult to detect because of the existence of mouse IgGs. B) In SDS fractions, Aβ monomers and AβOs, including di-, tri-, tetra-, and Aβ*56, and HMW AβOs, were visualized from 13 weeks. Respective species increased with age (E, H). C) In FA fractions, Aβ monomers from 13 weeks, Aβ dimers from 43 weeks, and diffuse smear patterns from 43 weeks were found (F, I). J–L) 4G8, anti-$A\beta_{40}$, and anti-$A\beta_{42}$ weakly detected LMW AβOs, but could not detect HMW AβOs. M) HMW AβOs were detected by antibodies against the N-terminus (82E1, Ab9204, Aβ-N, and PEP3), and were weakly detected by antibodies against the mid portion of Aβ (6E10 and 4G8), but were not detected by anti-$A\beta_{42}$ and BC-05. Anti-C-terminus to $A\beta_{40}$ (anti-$A\beta_{40}$ and BA-27) did not detect $A\beta_{1-42}$. N) Immunostaining of TgCRND8 brains using Aβ-N (1:1000), anti-$A\beta_{40}$ (1:1000), and anti-$A\beta_{42}$ (1:400) showed age-dependent Aβ deposition. Aβ burden labeled by anti-$A\beta_{40}$ and anti-$A\beta_{42}$ were weaker than those by Aβ-N. Bar represents 100 μm. One mouse at 13 weeks, 2 mice at 23 weeks, 43 weeks, and 59 weeks were used for analysis.

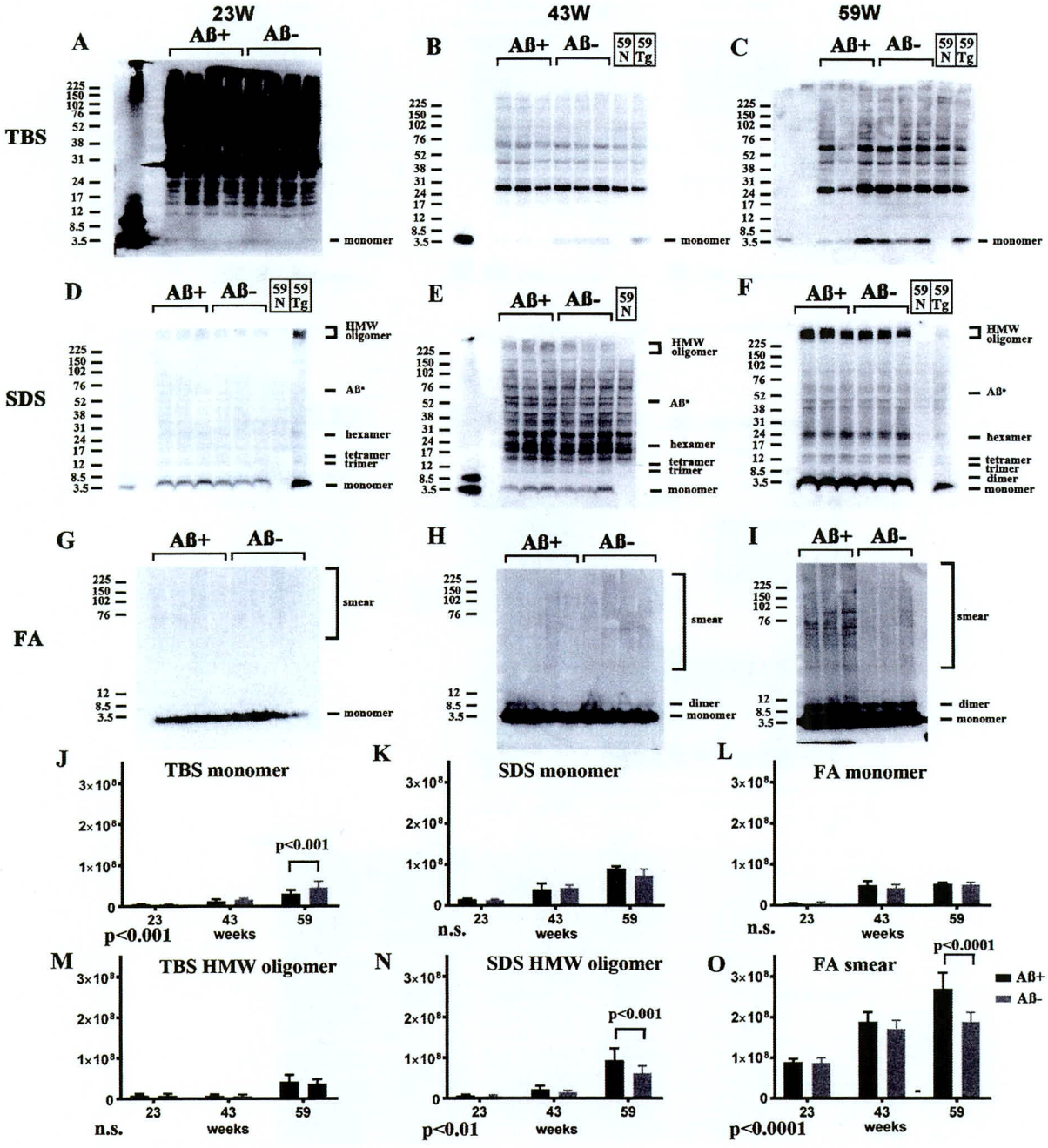

Fig. 5. Longitudinal comparison of Aβ species (23, 43, and 59 weeks) in TBS (A–C), SDS (D–F), and FA (G–I) extracts from Aβ+ and Aβ– treated mice in western blots using 82E1. For controls, a nontransgenic mouse at 59 weeks (59N) and a TgCRND8 mouse at 59 weeks without treatment (59Tg) were used. Aβ monomer in each fraction (J–L), HMW oligomers in the TBS fraction (M), and SDS fraction (N), and Aβ smear in the FA fraction (O) were quantified. The results of two-way ANOVA are shown in the lower left of each figure (J–O). In TBS fractions, soluble Aβ monomers in Aβ+ treated mice were decreased compared with those in Aβ– treated mice at 23, 43, and 59 weeks (A–C, J). To detect Aβ monomers clearly at 23 weeks, the membrane was exposed for longer than the other blots (A). Small amounts of HMW AβOs were detected only at 59 weeks, but they did not differ between the Aβ+ and Aβ– groups (A–C, M). In SDS fractions, Aβ monomers and LMW AβOs were detected equally at 23, 43, and 59 weeks (D–F, K). Accumulation of HMW AβOs was inversely increased in the Aβ+ treated group at 23, 43, and 59 weeks (D–F, N). In FA fractions, monomers and dimers of Aβ increased with age equally in both groups (G–I, L). However, smear patterns of Aβ were markedly visualized in the Aβ+ group at 59 weeks (G–I, O). Mice at 23 weeks ($n=9$ for Aβ+, $n=11$ for Aβ–), 43 weeks ($n=7$ for Aβ+, $n=6$ for Aβ–), and 59 weeks ($n=6$ for Aβ+, $n=7$ for Aβ–) were used.

Aβ smear). By *post-hoc* analysis significance was detected at 59 weeks ($p < 0.001$ for SDS soluble HMW oligomers, Fig. 5N, and $p < 0.0001$ for Aβ smear, Fig. 5O). HMW oligomers in the TBS fraction and Aβ monomer in the SDS and FA fractions did not differ between the Aβ+ and Aβ– groups (Fig. 5M,K,L). Since TBS soluble AβOs detected by 82E1/82E1 ELISA seem to be recovered as Aβ monomers in western blots using SDS sample buffer, these results correspond to AβOs ELISA result that Aβ+ immunization suppressed soluble AβOs. Furthermore, it was suggested that Aβ+ immunization accelerated the conversion of LMW AβOs to HMW AβOs in SDS fractions, and finally increased smear Aβ accumulation in most insoluble FA fractions.

Suppressed Aβ-immunoreactive load and adverse reaction

Age-related Aβ-immunoreactive load measured using the total area of Aβ-N immunostaining was significantly suppressed in the Aβ+ treated group compared with that of the Aβ– group (Fig. 6A, C; $p < 0.0001$). Congo red staining showed that most Aβ deposition was Congo red-negative diffuse plaques (Fig. 6A). Separate evaluation of core plaques (Fig. 6D; $p < 0.0001$) and diffuse plaques (Fig. 6E; $p < 0.0001$) revealed that a large part of the age-related increase in the area of amyloid burden and also decrease by immunization consisted of diffuse plaques. Immunostaining by anti-$A\beta_{40}$ or anti-$A\beta_{42}$ also showed significant suppression of amyloid burden in the Aβ+ group compared with the Aβ– group (Fig. 6F; $p < 0.001$, 6G $p < 0.0001$).

Microglial burden based on Iba1 labeling was significantly decreased in the Aβ+ treated group compared with the Aβ– treated group (Fig. 6B, H; $p < 0.0001$). Astrocytosis detected using an anti-GFAP antibody was not different between both groups of mice at any age. Both infiltration of CD5-positive lymphocytes or macrophages, and microhemorrhage by Berlin blue staining, were not detected in both Aβ+ and Aβ– treated mice in any examined brain sections (data not shown).

No alteration in AβPP processing and tau

Full length AβPP, C-terminal fragments of AβPP (CTFs) showed no differences between the Aβ+ and Aβ– groups from 23 to 59 weeks (Fig. 6I). The amount of α- and β-cleaved soluble AβPP (sAβPPα, sAβPPβ) detected by ELISA also showed no differences in both groups during 23–59 weeks (Fig. 6J, K). Levels of the total tau and pTau amount (Fig. 6L, M) did not differ between the Aβ+ and Aβ– treated groups at all ages. Additionally, there were almost no bands of pTau in western blots of FA extracts of TgCRND8 brains, corresponding with the lack of neurofibrillary tangles in TgCRND8 brains by Gallyas silver staining (data not shown).

CSF $A\beta_{40}$ and $A\beta_{42}$

$A\beta_{40}$ and $A\beta_{42}$ in CSF decreased with aging. They were decreased in Aβ+ treated mice compared with Aβ– treated mice, although there was no significant difference between Aβ+ and Aβ– mice with the small sample size (Aβ+ $n = 7$ for 23 weeks, $n = 4$ for 43 weeks and $n = 6$ for 59 weeks; Aβ– $n = 9$ for 23 weeks, $n = 2$ for 43 weeks, and $n = 4$ for 59 weeks) because of the difficulty in drawing CSF from mice (Fig. 6N,O).

DISCUSSION

To evaluate the potential utility of Aβ+ oral immunization to prevent cognitive decline in TgCRND8, we adopted an extended reference memory version of the MWM test, requiring hippocampus-dependent spatial working memory, with a longitudinal design that mimicked human clinical trials [24]. At 21 weeks, escape latencies and path-lengths became worse in the Aβ– group, whereas the Aβ+ group remained in the same levels. The performances of the Aβ+ group were significantly better during 21–59 weeks than those in the Aβ– group. Our extended MWM test study showed the preventative efficacy of Aβ+ oral immunization on Aβ-related learning impairment. As previously indicated [35], probe tests were inadequate for extended MWM test which consisted of extensive long-time and repeated behavioral evaluation. The same repeated trials in every 4 weeks in Aβ immunization trial of TgCRND8 mice also failed to show significant difference in probe trials [24]. Extensive overtraining by trials for a long duration may achieve the saturated level of memory, and may make it difficult to detect subtle changes in probe trials even among hippocampal damaged animals [36, 37]. Recent cohort observation studies have confirmed that Aβ amyloidosis caused impairment of episodic memory in the preclinical stage, and executive and global functions in the symptomatic stage before onset of dementia [38–40]. Rigorous and detailed cognitive assessments to repeatedly evaluate subtle cognitive impairments over a long duration are necessary for preclinical prevention trials such

59

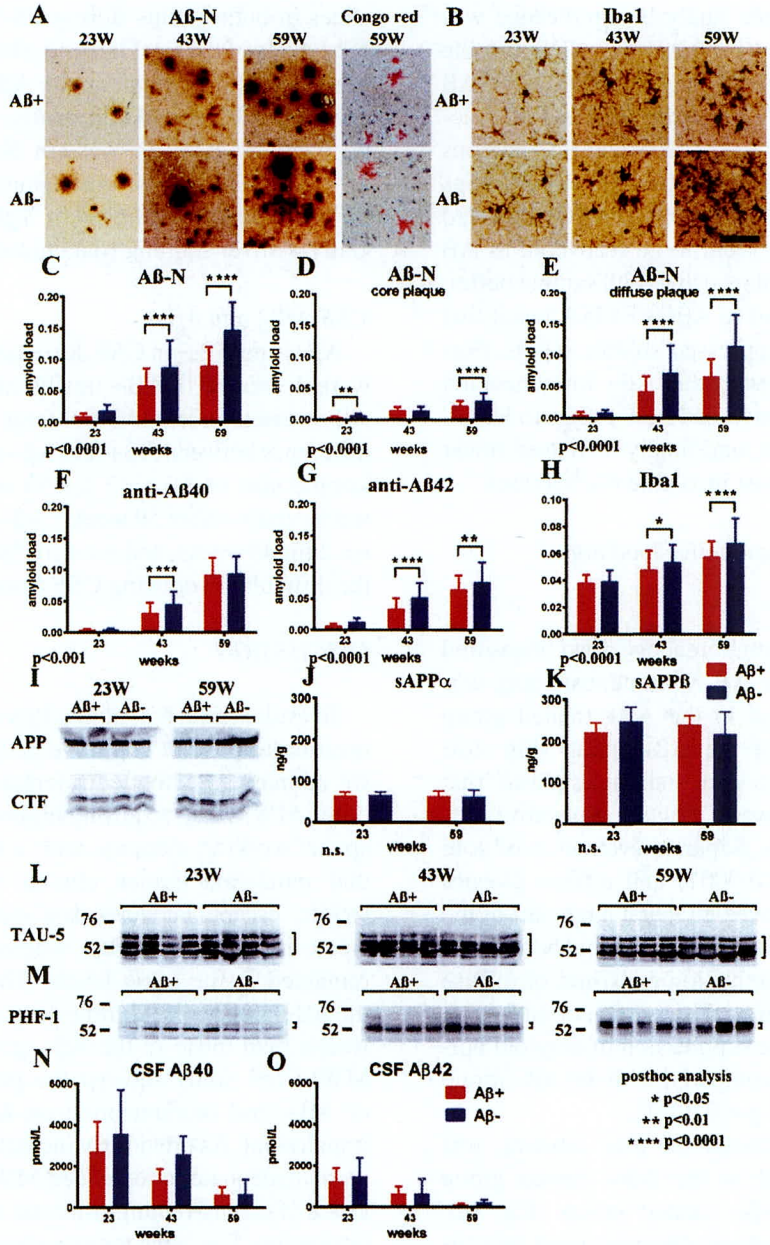

Fig. 6. Staining of Aβ+ or Aβ– treated brains with Aβ-N and Congo red (A), microglial marker Iba1 (B) in Aβ+ or Aβ– treated mouse brains, quantification of Aβ burden (C–G), Iba1 (H), western blot of AβPP and CTFs (I), ELISA of sAβPPα (J), sAβPPβ (K), western blotting of total tau (L), phosphorylated tau (M), CSF $A\beta_{40}$ (N), and $A\beta_{42}$ (O) measured by ELISA. A) Aβ-immunoreactive load using Aβ-N was suppressed in the Aβ+ treated group compared with that of the Aβ– group. Most Aβ staining showed diffuse plaques that are not stained with Congo red. B) Microgliosis was weaker in the Aβ+ treated group than that in the Aβ– treated group. Bar represents 100 μm in A and 200 μm in B. C) The area labeled by Aβ-N was significantly suppressed in the Aβ+ treated group compared with that in the Aβ– treated group ($p < 0.0001$). D, E) The area occupied by diffuse plaques was more than 3-fold of that by core plaques. Both plaques were suppressed by Aβ+ treatment (D, $p < 0.0001$; E, $p < 0.0001$). Large part of the Aβ decrease by immunization consisted of diffuse plaques. Aβ burdens detected by anti-$A\beta_{40}$ (F) and anti-$A\beta_{42}$ (G) were significantly decreased in the Aβ+ treated group (F, $p < 0.001$; G, $p < 0.0001$). H) The area of Iba1 staining in Aβ+ treated mice was smaller than that in Aβ– treated mice ($p < 0.0001$). The numbers of mice analyzed: 23 weeks ($n = 9$ for Aβ+, $n = 11$ for Aβ–), 43 weeks ($n = 7$ for Aβ+, $n = 6$ for Aβ–), and 59 weeks ($n = 6$ for Aβ+, $n = 7$ for Aβ–). I) AβPP, CTFβ, and CTFα, and other CTFs in SDS fractions did not differ between the Aβ+ and Aβ– treated groups from 23 to 59 weeks. (J, K) The amount of sAβPPα and sAβPPβ in the TBS fractions detected by ELISA did not differ between Aβ+ (Red) and Aβ– (Blue) treated groups from 23 to 59 weeks. L, M) The amount of total tau (TAU-5) and phosphorylated tau (pTau) (PHF-1) did not differ between Aβ+ and Aβ– treated mice from 23 to 59 weeks. N, O) $A\beta_{40}$ and $A\beta_{42}$ in CSF decreased with aging. They were decreased in Aβ+ treated mice compared to Aβ– treated mice, although there was no significance difference between Aβ+ and Aβ– mice (Aβ+ n–=–7 for 23 weeks, $n = 4$ for 43 weeks and $n = 6$ for 59 weeks; Aβ– $n = 9$ for 23 weeks, $n = 2$ for 43 weeks, and $n = 4$ for 59 weeks).

as DIAN, API, or A4 studies [15, 16, 41]. Based on these findings, our extended reference memory version of the MWM test is a competent way to develop preventive DMTs in basic level of model animal experiments.

A previous $A\beta_{42}$ immunization study reported a reduction in behavior impairment and plaques in TgCRND8 mice; however, Aβ amounts measured by ELISA did not decrease [24]. Administration of anti-Aβ antibody m266 to PDAPP mice and BAM-10 to Tg2576 mice rapidly reversed the memory deficits without altering brain Aβ burden [42, 43]. The same findings were observed in our experiments, which revealed reduced cognitive impairment and Aβ burden, but no differences in the total amounts of $A\beta_{40}$ and $A\beta_{42}$ measured by ELISA between Aβ+ and Aβ– groups except for increased $A\beta_{40}$ in the FA fraction. Decreased TBS-soluble AβOs were the significantly suppressed Aβ species. This observation supported the notion that these soluble AβOs species contribute to neuronal/synaptic injury and cognitive impairment.

Because the ELISA-based Aβ assay could not recover the whole amount of Aβ species, we next intensely surveyed Aβ species using western blotting of the same 3-step extracts to avoid overlooking other cardinal Aβ molecules. Analyses of untreated TgCRND8 mice revealed the age-related accumulation of all Aβ species: Aβ monomers in the TBS fraction; a large part of all sets of AβOs with LMW to HMW in the SDS fraction [28]; and age-related Aβ monomers, dimers, and smears in the FA fraction. These different LMW to HMW AβOs species were not measured by AβOs ELISA, and the C-terminus of HMW AβOs species were blocked [44]. Histological examination also confirmed increased plaque immunoreactivity by N-terminal antibodies compared to those by anti-$A\beta_{40}$ and $A\beta_{42}$. Thus, diverse Aβ species with conformational changes, modifications, and different lengths and solubilities were accumulated in the brains. For this reason, we carefully analyzed Aβ accumulation using not only ELISA, but also conventional western blots to decide which is the cardinal Aβ molecule that is toxic for the nervous system and causes cognitive dysfunction.

In a comparison study between Aβ+ and Aβ– treated groups, visualized TBS soluble Aβ monomers were decreased by Aβ+ treatment during weeks 23–59. Because AβOs in the TBS fraction were easily degraded into monomers using SDS sample buffer in western blotting experiments, these findings may partially correspond with the decreased amount of AβOs detected by ELISA in the Aβ+ treated group. Consistent with ELISA findings, almost all insoluble aggregated Aβ species in the SDS and FA fractions did not show obvious differences between the Aβ+ and Aβ– treated groups. Conversely, HMW AβOs in the SDS fraction and smear Aβ in the FA fraction were increased in the Aβ+ treated group compared with the Aβ– treated group. These findings suggested that toxic soluble AβOs in Aβ+ treated brains may be sequestered into highly insoluble and aggregated AβOs and Aβ fibrils. The same findings have been suggested previously, because the amyloid fibril is a protective structure in AD pathology [45–47]. CSF $A\beta_{40}$ and $A\beta_{42}$ levels were decreased in Aβ+ treated mice compared with Aβ– treated mice, although there was no significant difference between Aβ+ and Aβ– mice because of the small sample size. Previous immunization studies showed increased Aβ in CSF by increased clearance of Aβ [48]. Decreased amounts of CSF Aβ are thought to be due to the deposition of Aβ in the brain, because CSF Aβ decreases correlate with Aβ plaques [29, 49]. Decreased amounts of Aβ in Aβ+ treated mice suggested that the effect of immunization is not by enhanced clearance of Aβ but sequestration of Aβ in an insoluble fraction in the brain.

Histological evaluation showed that reduction of diffuse plaques was more prominent than the reduction of core plaques by Aβ+ immunization. Diffuse plaques were composed of scant Aβ amyloid fibrils. No difference of Aβ levels by ELISA may imply a lower decrease in core plaques. Together with biochemical analyses, Aβ+ immunization may facilitate the sequestration of toxic soluble AβOs into insoluble and HMW AβOs within the compact aggregated Aβ amyloid core. Liu et al. separated AβOs into neurotoxic type 1 AβOs and non-neurotoxic type 2 AβOs. Type 2 AβOs, which occupy the majority of AβOs sequestrated around dense core plaques (~95% in 21-month-old Tg2576 mice), accounted for less than 15% of the cortex [46]. Hong et al. showed that diffusible, highly bioactive oligomers represent a critical minority of soluble Aβ in AD brain [50]. It is still unclear what types of AβOs exert the main neurotoxicity [33, 42–54]. We have previously shown that accumulation of Aβ dimers in lipid rafts is the earliest event corresponding to behavioral deficits in Tg2576 mice [55]. Aβ dimers are also shown to be cardinal molecules for synaptic dysfunction in Aβ amyloid cascades in AD pathogenesis [56, 57]. Injection of LMW oligomers into the brain induced rapid and persistent impairment of memory, associated with

61

decreased hippocampal synaptophysin [58]. AβOs neurotoxicity and their induction of tauopathy are canceled by AβOs-specific monoclonal antibodies [59]. The recent success of a phase Ib randomized trial of aducanumab also showed that antibodies against aggregated forms of Aβ are clinically useful [9]. Together with these findings, our study suggested that soluble AβOs are the cardinal Aβ species responsible for neurotoxicity and are valid targets for DMTs.

Inverse increases in HMW Aβ oligomers and Aβ smear have not been reported in previous Aβ immunization studies. There are some studies on decreased Aβ neurotoxicity through the accelerated conversion of Aβ oligomers into Aβ fibrils. Using chaperone protein HspB1, Aβ oligomers were converted into large nontoxic aggregates, and their toxicity was sequestrated [60]. Peptides that enhance the formation of amorphous aggregates of Aβ attenuated the paralysis of transgenic *Caenorhabditis elegans* [61]. Meanwhile, activated microglia are shown to take up Aβ, cluster Aβ inside, and release aggregated Aβ, which contributed to plaque growth [62]. Based on these reports, we speculated the presence of sequestration mechanisms that convert toxic Aβ oligomers into HMW Aβ aggregates for reduction of Aβ toxicity.

62 Both ELISA and TAPIR showed the presence of specific IgG antibodies against $A\beta_{4-10}$ structural epitopes within A1aB1b in Aβ+ immunized mice. In western blotting, antibodies were shown to detect several Aβ oligomers. Splenocytic proliferation and cytokine release against Aβ+ stimulation also implied the presence of adaptive cellular immune responses. We found no histological meningoencephalitis or bleeding in mouse brains. Our mucosal Aβ+ immunization significantly decreased microgliosis, indicating that it suppressed glial-mediated inflammatory responses. These findings suggested that our Aβ+ oral immunization could safely raise moderate and continuous innate and humoral immune responses.

Our Aβ+ immunization did not alter basic AβPP processing or the signaling process of the AβPP intracellular C-terminal domain [63]. Accumulation of *p*Tau was only detected in dystrophic neurites associated with core plaques. Pathological conversion and spreading of aggregated tau was facilitated in the dystrophic neurites around core plaques [64]. Because numbers of core plaques were not so different, the amount of *p*Tau was not significantly different.

Preclinical initiation and long-term maintenance of DMT against Aβ amyloidosis have been proposed to halt the progression of cognitive impairment and the onset of dementia. This strategy, which will likely necessitate weekly or monthly injections of antibodies, carries two risks. First, it may enhance risks of side effects. Second, the cost of long-term treatment with antibodies is likely to be prohibitively high when applied on national scales to large numbers of people. The use of oral plant vaccines offers advantages of extremely low cost and better safety compared with synthetic compounds or antibodies. For these reasons, our plant-based soybean Aβ+ oral vaccine strategy is cheap, safe and as effective as others.

In conclusion, our results revealed that Aβ+ oral immunization suppressed soluble AβOs production and prevented cognitive impairment without obvious adverse reactions. Oral immunization by Aβ+ could be a promising DMT for prevention of the pathological processes of AD.

ACKNOWLEDGMENTS

We thank Eiki Tsushima for statistical analysis, Kaori Haga for research assistance, Takaomi C. Saido for Ab9201, and Peter Davies for PHF-1. Research reported in this publication was supported by the Longevity Science Committee of the Ministry of Health and Welfare of Japan; Scientific Research (C) (18K07385 MS and 19K07989 TK) from the Ministry of Education, Science, and Culture of Japan; Study of prevention for neurodegenerative diseases by new antiaging methods in Hirosaki University Institutional Research Grant; Development of Fundamental Technologies for the Production of High-value Materials Using Transgenic Plants by the Ministry of Economy, Trade, and Industry of Japan.

Authors' disclosures available online (https://www.j-alz.com/manuscript-disclosures/19-0023r1).

REFERENCES

[1] Hardy JA, Higgins GA (1992) Alzheimer's disease: The amyloid cascade hypothesis. *Science* **256**, 184-185.

[2] Selkoe DJ, Hardy J (2016) The amyloid hypothesis of Alzheimer's disease at 25 years. *EMBO Mol Med* **8**, 595-608.

[3] Orgogozo JM, Gilman S, Dartigues JF, Laurent B, Puel M, Kirby LC, Jouanny P, Dubois B, Eisner L, Flitman S, Michel BF, Boada M, Frank A, Hock C (2003) Subacute meningoencephalitis in a subset of patients with AD after Aβ42 immunization. *Neurology* **61**, 46-54.

[4] Gilman S, Koller M, Black RS, Jenkins L, Griffith SG, Fox NC, Eisner L, Kirby L, Rovira MB, Forette F, Orgogozo JM; AN1792(QS-21)-201 Study Team (2005) Clinical effects

of Aβ immunization (AN1792) in patients with AD in an interrupted trial. *Neurology* **64**, 1553-1562.

[5] Serrano-Pozo A, William CM, Ferrer I, Uro-Coste E, Delisle MB, Maurage CA, Hock C, Nitsch RM, Masliah E, Growdon JH, Frosch MP, Hyman BT (2010) Beneficial effect of human anti-amyloid-β active immunization on neurite morphology and tau pathology. *Brain* **133**, 1312-1327.

[6] Bard F, Barbour R, Cannon C, Carretto R, Fox M, Games D, Guido T, Hoenow K, Hu K, Johnson-Wood K, Khan K, Kholodenko D, Lee C, Lee M, Motter R, Nguyen M, Reed A, Schenk D, Tang P, Vasquez N, Seubert P, Yednock T (2003) Epitope and isotype specificities of antibodies to β-amyloid peptide for protection against Alzheimer's disease-like neuropathology. *Proc Natl Acad Sci U S A* **100**, 2023-2028. Erratum in *Proc Natl Acad Sci U S A* (2004) **101**, 11526.

[7] Lemere CA, Masliah E (2010) Can Alzheimer disease be prevented by amyloid-β immunotherapy? *Nat Rev Neurol* **6**, 108-119.

[8] Wisniewski T, Goñi F (2015) Immunotherapeutic approaches for Alzheimer's disease. *Neuron* **85**, 1162-1176.

[9] Sevigny J, Chiao P, Bussière T, Weinreb PH, Williams L, Maier M, Dunstan R, Salloway S, Chen T, Ling Y, O'Gorman J, Qian F, Arastu M, Li M, Chollate S, Brennan MS, Quintero-Monzon O, Scannevin RH, Arnold HM, Engber T, Rhodes K, Ferrero J, Hang Y, Mikulskis A, Grimm J, Hock C, Nitsch RM, Sandrock A (2016) The antibody aducanumab reduces Aβ plaques in Alzheimer's disease. *Nature* **537**, 50–56.

[10] Vandenberghe R, Riviere ME, Caputo A, Sovago J, Maguire RP, Farlow M, Marotta G, Sanchez-Valle R, Scheltens P, Ryan JM, Graf A (2016) Active Aβ immunotherapy CAD106 in Alzheimer's disease: A phase 2b study. *Alzheimers Dement (N Y)* **3**, 10–22.

[11] Wang CY, Wang PN, Chiu MJ, Finstad CL, Lin F, Lynn S, Tai YH, De Fang X, Zhao K, Hung CH, Tseng Y, Peng WJ, Wang J, Yu CC, Kuo BS, Frohna PA (2017) UB-311, a novel UBITh® amyloid β peptide vaccine for mild Alzheimer's disease. *Alzheimers Dement (N Y)* **3**, 262-272.

[12] Lippa CF, Nee LE, Mori H, St George-Hyslop P (1998) Abeta-42 deposition precedes other changes in PS-1 Alzheimer's disease. *Lancet* **352**, 1117-1118.

[13] Weiner MW, Veitch DP, Aisen PS, Beckett LA, Cairns NJ, Cedarbaum J, Green RC, Harvey D, Jack CR, Jagust W, Luthman J, Morris JC, Petersen RC, Saykin AJ, Shaw L, Shen L, Schwarz A, Toga AW, Trojanowski JQ; Alzheimer's Disease Neuroimaging Initiative (2015) 2014 Update of the Alzheimer's Disease Neuroimaging Initiative: A review of papers published since its inception. *Alzheimers Dement* **11**, e1-120.

[14] Bateman RJ, Xiong C, Benzinger TL, Fagan AM, Goate A, Fox NC, Marcus DS, Cairns NJ, Xie X, Blazey TM, Holtzman DM, Santacruz A, Buckles V, Oliver A, Moulder K, Aisen PS, Ghetti B, Klunk WE, McDade E, Martins RN, Masters CL, Mayeux R, Ringman JM, Rossor MN, Schofield PR, Sperling RA, Salloway S, Morris JC; Dominantly Inherited Alzheimer Network (2012) Clinical and biomarker changes in dominantly inherited Alzheimer's disease. *N Engl J Med* **367**, 795-804.

[15] Mills SM, Mallmann J, Santacruz AM, Fuqua A, Carril M, Aisen PS, Althage MC, Belyew S, Benzinger TL, Brooks WS, Buckles VD, Cairns NJ, Clifford D, Danek A, Fagan AM, Farlow M, Fox N, Ghetti B, Goate AM, Heinrichs D, Hornbeck R, Jack C, Jucker M, Klunk WE, Marcus DS, Martins RN, Masters CM, Mayeux R, McDade E, Morris JC, Oliver A, Ringman JM, Rossor MN, Salloway S, Schofield PR, Snider J, Snyder P, Sperling RA, Stewart C, Thomas RG, Xiong C, Bateman RJ (2013) Preclinical trials in autosomal dominant AD: Implementation of the DIAN-TU trial. *Rev Neurol (Paris)* **169**, 737-743.

[16] Reiman EM, Langbaum JB, Fleisher AS, Caselli RJ, Chen K, Ayutyanont N, Quiroz YT, Kosik KS, Lopera F, Tariot PN (2011) Alzheimer's Prevention Initiative: A plan to accelerate the evaluation of presymptomatic treatments. *J Alzheimers Dis* **26 Suppl 3**, 321-329.

[17] Shahid N, Daniell H (2016) Plant-based oral vaccines against zoonotic and non-zoonotic diseases. *Plant Biotechnol J* **14**, 2079-2099.

[18] Kwon KC, Verma D, Singh ND, Herzog R, Daniell H (2013) Oral delivery of human biopharmaceuticals, autoantigens and vaccine antigens bioencapsulated in plant cells. *Adv Drug Deliv Rev* **65**, 782-799.

[19] Rosales-Mendoza S, Rubio-Infante N, Zarazúa S, Govea-Alonso DO, Martel-Gallegos G, Moreno-Fierros L (2014) Plant-based vaccines for Alzheimer's disease: An overview. *Expert Rev Vaccines* **13**, 429-441.

[20] Gonzalez-Castro R, Acero Galindo G, García Salcedo Y, Uribe Campero L, Vazquez Perez V, Carrillo-Tripp M, Gevorkian G, Gomez Lim MA (2018) Plant-based chimeric HPV-virus-like particles bearing amyloid-β epitopes elicit antibodies able to recognize amyloid plaques in APP-tg mouse and Alzheimer's disease brains. *Inflammopharmacology* **26**, 817-827.

[21] Nojima J, Maeda A, Aoki S, Suo S, Yanagihara D, Watanabe Y, Yoshida T, Ishiura S (2011) Effect of rice-expressed amyloid β in the Tg2576 Alzheimer's disease transgenic mouse model. *Vaccine* **29**, 6252-6258.

[22] McLaurin J, Cecal R, Kierstead ME, Tian X, Phinney AL, Manea M, French JE, Lambermon MH, Darabie AA, Brown ME, Janus C, Chishti MA, Horne P, Westaway D, Fraser PE, Mount HT, Przybylski M, St George-Hyslop P (2002) Therapeutically effective antibodies against amyloid-β peptide target amyloid-β residues 4-10 and inhibit cytotoxicity and fibrillogenesis. *Nat Med* **8**, 1263-1269.

[23] Maruyama N, Fujiwara K, Yokoyama K, Cabanos C, Hasegawa H, Takagi K, Nishizawa K, Uki Y, Kawarabayashi T, Shouji M, Ishimoto M, Terakawa T (2014) Stable accumulation of seed storage proteins containing vaccine peptides in transgenic soybean seeds. *J Biosci Bioeng* **118**, 441-447.

[24] Janus C, Pearson J, McLaurin J, Mathews PM, Jiang Y, Schmidt SD, Chishti MA, Horne P, Heslin D, French J, Mount HT, Nixon RA, Mercken M, Bergeron C, Fraser PE, St George-Hyslop P, Westaway D (2000) Aβ peptide immunization reduces behavioural impairment and plaques in a model of Alzheimer's disease. *Nature* **408**, 979-982.

[25] Chishti MA, Yang DS, Janus C, Phinney AL, Horne P, Pearson J, Strome R, Zuker N, Loukides J, French J, Turner S, Lozza G, Grilli M, Kunicki S, Morissette C, Paquette J, Gervais F, Bergeron C, Fraser PE, Carlson GA, George-Hyslop PS, Westaway D (2001) Early-onset amyloid deposition and cognitive deficits in transgenic mice expressing a double mutant form of amyloid precursor protein 695. *J Biol Chem* **276**, 21562-21570.

[26] Adachi M, Takenaka Y, Gidamis AB, Mikami B, Utsumi S (2001) Crystal structure of soybean proglycinin A1aB1b homotrimer. *J Mol Biol* **305**, 291-305.

[27] Janus C (2004) Search strategies used by APP transgenic mice during spatial navigation in the Morris water maze. *Learn Mem* **11**, 337-346.

[28] Harigaya Y, Shoji M, Kawarabayashi T, Kanai M, Nakamura T, Iizuka T, Igeta Y, Saido TC, Sahara N, Mori H, Hirai S (1995) Modified amyloid β protein ending at 42 or 40 with different solubility accumulates in the brain of Alzheimer's disease. *Biochem Biophys Res Commun* **211**, 1015-1022.

[29] Kawarabayashi T, Younkin LH, Saido TC, Shoji M, Ashe KH, Younkin SG (2001) Age-dependent changes in brain, CSF, and plasma amyloid β protein in the Tg2576 transgenic mouse model of Alzheimer's disease. *J Neurosci* **21**, 372-381.

[30] Maier M, Seabrook TJ, Lemere CA (2005) Modulation of the humoral and cellular immune response in Aβ immunotherapy by the adjuvants monophosphoryl lipid A (MPL), cholera toxin B subunit (CTB) and E. coli enterotoxin LT(R192G). *Vaccine* **23**, 149-159.

[31] Suzuki N, Cheung TT, Cai XD, Odaka A, Otvos L Jr, Eckman C, Golde TE, Younkin SG (1994) An increased percentage of long amyloid β protein secreted by familial amyloid β protein precursor (βAPP717) mutants. *Science* **264**, 1336-1340.

[32] Saido TC, Iwatsubo T, Mann DM, Shimada H, Ihara Y, Kawashima S (1995) Dominant and differential deposition of distinct β-amyloid peptide species, AβN3(pE), in senile plaques. *Neuron* **14**, 457-466.

[33] Xia W, Yang T, Shankar G, Smith IM, Shen Y, Walsh DM, Selkoe DJ (2009) A specific enzyme-linked immunosorbent assay for measuring β-amyloid protein oligomers in human plasma and brain tissue of patients with Alzheimer disease. *Arch Neurol* **66**, 190-199.

[34] Lesné S, Koh MT, Kotilinek L, Kayed R, Glabe CG, Yang A, Gallagher M, Ashe KH (2006) A specific amyloid-β protein assembly in the brain impairs memory. *Nature* **440**, 352-357.

[35] Markowska AL, Long JM, Johnson CT, Olton DS (1993) Variable-interval probe test as a tool for repeated measurements of spatial memory in the water maze. *Behav Neurosci* **107**, 627-632.

[36] Morris RGM, Schenk F, Tweedie F, Jarrard LE (1990) Ibotenate lesions of hippocampus and/or subiculum: Dissociating components of allocentric spatial learning. *Eur J Neurosci* **2**,1016-1028.

[37] Boksa P, Krishnamurthy A, Brooks W (1995) Effects of a period of asphyxia during birth on spatial learning in the rat. *Pediatr Res* **37**, 489-96.

[38] Hedden T, Oh H, Younger AP, Patel TA (2013) Meta-analysis of amyloid-cognition relations in cognitively normal older adults. *Neurology* **80**, 1341-1348.

[39] Insel PS, Mattsson N, Mackin RS, Schöll M, Nosheny RL, Tosun D, Donohue MC, Aisen PS, Jagust WJ, Weiner MW; Alzheimer's Disease Neuroimaging Initiative (2016) Accelerating rates of cognitive decline and imaging markers associated with β-amyloid pathology. *Neurology* **86**, 1887-1896.

[40] Petersen RC, Wiste HJ, Weigand SD, Rocca WA, Roberts RO, Mielke MM, Lowe VJ, Knopman DS, Pankratz VS, Machulda MM, Geda YE, Jack CR Jr (2016) Association of elevated amyloid levels with cognition and biomarkers in cognitively normal people from the community. *JAMA Neurol* **73**, 85-92.

[41] Sperling RA, Rentz DM, Johnson KA, Karlawish J, Donohue M, Salmon DP, Aisen P (2014) The A4 study: Stopping AD before symptoms begin? *Sci Transl Med* **6**, 228fs13.

[42] Dodart JC, Bales KR, Gannon KS, Greene SJ, DeMattos RB, Mathis C, DeLong CA, Wu S, Wu X, Holtzman DM, Paul SM (2002) Immunization reverses memory deficits without reducing brain Abeta burden in Alzheimer's disease model. *Nat Neurosci* **5**, 452-457.

[43] Kotilinek LA, Bacskai B, Westerman M, Kawarabayashi T, Younkin L, Hyman BT, Younkin S, Ashe KH (2002) Reversible memory loss in a mouse transgenic model of Alzheimer's disease. *J Neurosci* **22**, 6331-6335.

[44] Ahmed M, Davis J, Aucoin D, Sato T, Ahuja S, Aimoto S, Elliott JI, Van Nostrand WE, Smith SO (2010) Structural conversion of neurotoxic amyloid-β(1-42) oligomers to fibrils. *Nat Struct Mol Biol* **17**, 561-567.

[45] Cheng IH, Scearce-Levie K, Legleiter J, Palop JJ, Gerstein H, Bien-Ly N, Puoliväli J, Lesné S, Ashe KH, Muchowski PJ, Mucke L (2007) Accelerating amyloid-β fibrillization reduces oligomer levels and functional deficits in Alzheimer disease mouse models. *J Biol Chem* **282**, 23818–23828.

[46] Liu P, Reed MN, Kotilinek LA, Grant MK, Forster CL, Qiang W, Shapiro SL, Reichl JH, Chiang AC, Jankowsky JL, Wilmot CM, Cleary JP, Zahs KR, Ashe KH (2015) Quaternary structure defines a large class of amyloid-β oligomers neutralized by sequestration. *Cell Rep* **11**, 1760–1771.

[47] Ryan TM, Roberts BR, McColl G, Hare DJ, Doble PA, Li QX, Lind M, Roberts AM, Mertens HD, Kirby N, Pham CL, Hinds MG, Adlard PA, Barnham KJ, Curtain CC, Masters CL (2015) Stabilization of nontoxic Aβ-oligomers: Insights into the mechanism of action of hydroxyquinolines in Alzheimer's disease. *J Neurosci* **35**, 2871-2884.

[48] Siemers ER, Sundell KL, Carlson C, Case M, Sethuraman G, Liu-Seifert H, Dowsett SA, Pontecorvo MJ, Dean RA, Demattos R (2016) Phase 3 solanezumab trials: Secondary outcomes in mild Alzheimer's disease patients. *Alzheimers Dement* **12**, 110-120.

[49] Strozyk D, Blennow K, White LR, Launer LJ (2003) CSF Aβ42 levels correlate with amyloid-neuropathology in a population-based autopsy study. *Neurology* **60**, 652-656.

[50] Hong W, Wang Z, Liu W, O'Malley TT, Jin M, Willem M, Haass C, Frosch MP, Walsh DM (2018) Diffusible, highly bioactive oligomers represent a critical minority of soluble Aβ in Alzheimer's disease brain. *Acta Neuropathol* **136**, 19-40.

[51] Walsh DM, Klyubin I, Fadeeva JV, Cullen WK, Anwyl R, Wolfe MS, Rowan MJ, Selkoe DJ (2002) Naturally secreted oligomers of amyloid β protein potently inhibit hippocampal long-term potentiation *in vivo*. *Nature* **416**, 535-539.

[52] Lacor PN, Buniel MC, Chang L, Fernandez SJ, Gong Y, Viola KL, Lambert MP, Velasco PT, Bigio EH, Finch CE, Krafft GA, Klein WL (2004) Synaptic targeting by Alzheimer's-related amyloid β oligomers. *J Neurosci* **24**, 10191-10200.

[53] Cleary JP, Walsh DM, Hofmeister JJ, Shankar GM, Kuskowski MA, Selkoe DJ, Ashe KH (2005) Natural oligomers of the amyloid-β protein specifically disrupt cognitive function. *Nat Neurosci* **8**, 79-84.

[54] Tomiyama T, Matsuyama S, Iso H, Umeda T, Takuma H, Ohnishi K, Ishibashi K, Teraoka R, Sakama N, Yamashita T, Nishitsuji K, Ito K, Shimada H, Lambert MP, Klein WL, Mori H (2010) A mouse model of amyloid β oligomers: Their contribution to synaptic alteration, abnormal tau phosphorylation, glial activation, and neuronal loss *in vivo*. *J Neurosci* **30**, 4845-4856.

[55] Kawarabayashi T, Shoji M, Younkin LH, Wen-Lang L, Dickson DW, Murakami T, Matsubara E, Abe K, Ashe

KH, Younkin SG (2004) Dimeric amyloid β protein rapidly accumulates in lipid rafts followed by apolipoprotein E and phosphorylated tau accumulation in the Tg2576 mouse model of Alzheimer's disease. *J Neurosci* **24**, 801-809.

[56] Shankar GM, Li S, Mehta TH, Garcia-Munoz A, Shepardson NE, Smith I, Brett FM, Farrell MA, Rowan MJ, Lemere CA, Regan CM, Walsh DM, Sabatini BL, Selkoe DJ (2008) Amyloid-β protein dimers isolated directly from Alzheimer's brains impair synaptic plasticity and memory. *Nat Med* **14**, 837-842.

[57] Müller-Schiffmann A, Herring A, Abdel-Hafiz L, Chepkova AN, Schäble S, Wedel D, Horn AH, Sticht H, de Souza Silva MA, Gottmann K, Sergeeva OA, Huston JP, Keyvani K, Korth C (2016) Amyloid-β dimers in the absence of plaque pathology impair learning and synaptic plasticity. *Brain* **139**, 509-525.

[58] Figueiredo CP, Clarke JR, Ledo JH, Ribeiro FC, Costa CV, Melo HM, Mota-Sales AP, Saraiva LM, Klein WL, Sebollela A, De Felice FG, Ferreira ST (2013) Memantine rescues transient cognitive impairment caused by high-molecular-weight Aβ oligomers but not the persistent impairment induced by low-molecular-weight oligomers. *J Neurosci* **33**, 9626-9634.

[59] Takamura A, Okamoto Y, Kawarabayashi T, Yokoseki T, Shibata M, Mouri A, Nabeshima T, Sun H, Abe K, Urisu T, Yamamoto N, Shoji M, Yanagisawa K, Michikawa M, Matsubara E (2011) Extracellular and intraneuronal HMW-AbetaOs represent a molecular basis of memory loss in Alzheimer's disease model mouse. *Mol Neurodegener* **6**, 20.

[60] Ojha J, Masilamoni G, Dunlap D, Udoff RA, Cashikar AG (2011) Sequestration of toxic oligomers by HspB1 as a cytoprotective mechanism. *Mol Cell Biol* **31**, 3146-3157.

[61] Yang A, Wang C, Song B, Zhang W, Guo Y, Yang R, Nie G, Yang Y, Wang C (2017) Attenuation of β-amyloid toxicity *in vitro* and *in vivo* by accelerated aggregation. *Neurosci Bull* **33**, 405-412.

[62] Baik SH, Kang S, Son SM, Mook-Jung I (2016) Microglia contributes to plaque growth by cell death due to uptake of amyloid β in the brain of Alzheimer's disease mouse model. *Glia* **64**, 2274-2290.

[63] Kimberly WT, Zheng JB, Guénette SY, Selkoe DJ (2001) The intracellular domain of the β-amyloid precursor protein is stabilized by Fe65 and translocates to the nucleus in a notch-like manner. *J Biol Chem* **276**, 40288-40292.

[64] Li T, Braunstein KE, Zhang J, Lau A, Sibener L, Deeble C, Wong PC (2016) The neuritic plaque facilitates pathological conversion of tau in an Alzheimer's disease mouse model. *Nat Commun* **7**, 12082.

Contents lists available at ScienceDirect

Journal of the Neurological Sciences

journal homepage: http://ees.elsevier.com

Letter to the Editor

An autopsy case of primary lateral sclerosis with Alzheimer's disease

Takumi Nakamura [a,*], Tomoya Kon [b], Takeshi Kawarabayashi [c], Koichi Wakabayashi [b], Yoshio Ikeda [a], Mikio Shoji [c]

[a] Department of Neurology, Gunma University Graduate School of Medicine, 3-39-22 Showa-machi, Maebashi 371-8511, Japan
[b] Department of Neuropathology, Hirosaki University Graduate School of Medicine, 5 Zaifu-cho, Hirosaki 036-8562, Japan
[c] Geriatrics Research Institute and Hospital, 3-26-8 Otomo-machi, Maebashi 371-0847, Japan

ARTICLE INFO

Keywords
Primary lateral sclerosis
Motor neuron disease
Alzheimer's disease
Autopsy
TDP-43

66

Dear Editor,

Primary lateral sclerosis (PLS) is a rare type of motor neuron disease (MND) characterized by the loss of upper motor neurons without lower motor neuron involvement [1]. In contrast, amyotrophic lateral sclerosis (ALS) is a common type of MND that is occasionally complicated by frontotemporal dementia (FTD) as the TDP-43 proteinopathy. However, there are few studies on the relationship of PLS with ALS, FTD and TDP-43 proteinopathy because of the rarity of autopsy cases. Here, we report a 68-year-old woman who exhibited typical clinical symptoms of PLS at onset, which then progressed to FTD, although her pathological diagnosis was PLS complicated by Alzheimer's disease (AD) pathology.

1. Case report

The patient had a past history of hypertension, diabetes and cholecystectomy for cholelithiasis in X-16 year, and no neurological family history. In X year, she became easily angered, and often cried or laughed. In X + 1 year, she developed dysarthria and gait disturbance, and was admitted to our hospital for neurological examination. Her general condition and vital signs were normal. She demonstrated emotional incontinence, irritability, apathy, non-fluent aphasia, dysphasia, spasticity and exaggerated deep tendon reflex in the jaw and all extremities, and snout, palmomental, Hoffmann's and Babinski reflexes were present. Spastic gait disturbance was observed. Her Mini Mental State Examination score was 26/30 with slightly disturbed orientation, calculation and delayed recall. The trail making test was severely impaired (required 92 s on part A and 297 s with 7 commission errors on part B). No muscle weakness, atrophy or involuntary movements were observed. The sensory system and cerebellar system were intact. Hematological blood tests were normal, but the hemoglobin A1c level was 7.8%. Cerebrospinal fluid examination was normal. MRI revealed mild diffuse atrophy and no abnormal intensities in the brain. On ^{123}I-iomazenil SPECT, hypoperfusion of the bilateral posterior cingulate gyrus, precuneus and prefrontal area was observed (Fig. 1A). She was clinically diagnosed as PLS. In X + 2 year, her dysphagia progressively worsened and she underwent gastrostomy. She had marked loss of motivation, mutism and emaciation. In X + 3 year, she was admitted again to our hospital for worsening of aspiration pneumonia and respiratory ventilation. She died on hospital day 3 at the age of 70. Autopsy was performed on the same day.

2. Neuropathology

The brain weighed 1184 g. Grossly, there was atrophy of the bilateral frontal lobes, especially in the precentral gyri (Fig. 1B). Marked neuronal loss with phosphorylated TDP-43-positive neuronal and glial cytoplasmic inclusions was found in the motor cortex (Fig. 1C, D); Many neuronal cytoplasmic inclusions and short dystrophic neurites were found in the motor cortex, predominantly in layer 2 (FTLD-TDP type A) [2]. Mild neuronal loss was also evident in the putamen and substantia nigra. Severe degeneration of the cortico-spinal tracts

Abbreviations: PLS, primary lateral sclerosis; MND, motor neuron disease; ALS, amyotrophic lateral sclerosis; FTD, frontotemporal dementia; AD, Alzheimer's disease; MRI, magnetic resonance imaging; SPECT, single-photon emission computed tomography.

* Corresponding author.
E-mail address: takumi.n@gunma-u.ac.jp (T. Nakamura)

https://doi.org/10.1016/j.jns.2020.116792
Received 15 January 2020; Received in revised form 12 March 2020; Accepted 19 March 2020
Available online xxx
0022-510/

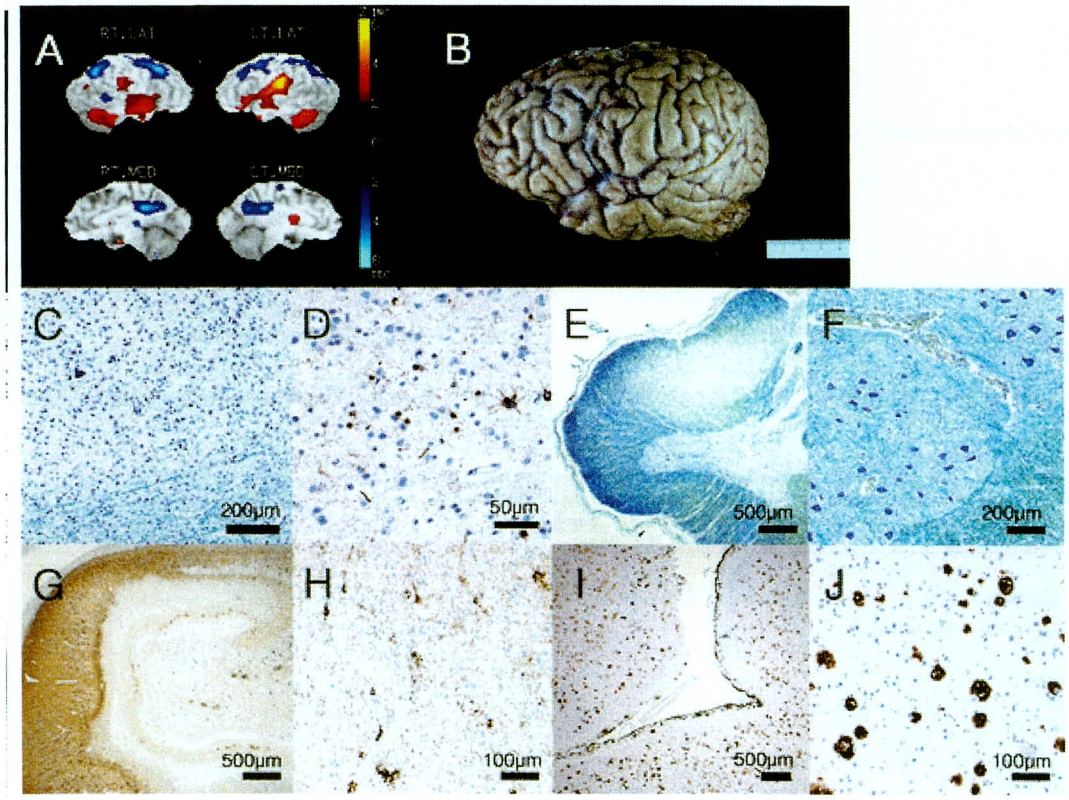

Fig. 1. The findings on ^{123}I-iomazenil SPECT with 3-dimensional stereotractic surface projection (A) and brain autopsy findings (B–J). Hypoperfusion of the bilateral posterior cingulate gyrus, precuneus and prefrontal area on cerebral perfusion scintigraphy (A). Lateral view of the brain showing atrophy of the bilateral frontal lobes, especially in the precentral gyri (B). Marked neuronal loss (Klüver-Barrera staining) (C) with TDP-43-positive neuronal and glial cytoplasmic inclusions (phosphorylated TDP-43 immunostaining) (D) in the precentral gyrus. Severe degeneration of the lateral cortico-spinal tract in the 7th cervical cord (E) and mild neuronal loss in the anterior horn in the 4th lumbar cord (F) (Klüver-Barrera staining). Phosphorylated tau immunostaining of the hippocampus (G) and insular cortex (H) showing many neurofibrillary tangles. Amyloid-β immunostaining of the olfactory (I) and parietal cortices (J) showing severe senile plaque pathology.

was found in the spinal cord (Fig. 1E). Mild to moderate neuronal loss was found in the anterior horn of the cervical cord, whereas neuronal loss was mild in the thoracic and lumbar cord (Fig. 1F). A few TDP-43-positive skein-like and round inclusions, but not glial cytoplasmic inclusions, were found in the facial and hypoglossal nuclei and spinal anterior horn. No Bunina bodies were seen in the lower motor neurons.

Immunostaining revealed widespread occurrence of neurofibrillary tangles, especially in the temporal lobe and insular cortex (Fig. 1G, H) (Braak stage IV), and severe senile plaque pathology in the cerebral (Fig. 1I, J) and cerebellar cortex (Braak stage C). Moderate number of neuritic plaques and a few neurofibrillary tangles were seen in the precentral gyrus. By National Institute on Aging–Alzheimer's Association guidelines, this case had an intermediate level of AD (A3, B2, C3) [3]. Thus, she was pathologically diagnosed as having PLS complicated with AD.

3. Discussion

Since TDP-43-positive neuronal cytoplasmic inclusions were found in the lower motor neurons, our case might be pathologically categorized as PLS: upper-motor-predominant ALS with frontotemporal lobar degeneration [4]. To our knowledge, only one case of PLS complicated by mild AD pathology (Braak stage I-A) has been reported [5]. However, the patient did not meet the PLS diagnostic criteria proposed by Pringle et al. [1] in terms of disease duration in life. The diagnosis was carried out based on autopsy findings of neuronal degeneration with TDP-43 pathology in the precentral gyrus.

In our case, the cognitive impairment was suggested to be a clinical phenotype of FTD. In a review of cognitive functions, 22% (40 out of 181) of PLS patients exhibited clinical phenotypes of FTD [6]. The origin of dementia due to PLS or ALS is caused by advanced TDP-43 pathology in the frontotemporal lobe, which causes frontotemporal degeneration, termed PLS-FTD [7]. In our case, we were unable to make a pathological diagnosis of PLS-FTD because the degeneration and TDP-43 pathology had not spread into the temporal or frontal lobe. We consider the episodes of cognitive impairment and severe emotional incontinence to have been due to MND. Emotional incontinence, whose origin was not clear but was considered to be bilateral corticobulbar tract pathology [8] and frontal cortex dysfunction [9], was characterized by the pathological crying and laughing. In our case, irritability, apathy and personality change, in addition to pathological crying and laughing, may have been emotional incontinence of MND affected by AD symptoms, thus mimicking FTD.

Globular glial tauopathies can similarly present with the clinical phenotype of PLS-FTD [10]. Although this disease concept is 4-repeat tauopathies characterized by globular glial inclusions and non-fibrillar tau in astrocytes, the autopsy findings of our case did not include these characteristics. We report a markedly rare case of PLS complicated by advanced AD pathology (Braak stage IV-C). As cases that are clinically diagnosed as ALS/PLS-FTD can include those of pathological ALS/PLS-AD, further reports are required.

Funding

None.

Declaration of Competing Interest

None.

References

[1] C E Pringle, et al., Primary lateral sclerosis: clinical features, neuropathology and diagnostic criteria, Brain 115 (2) (1992) 495–520.
[2] I R Mackenzie, et al., A harmonized classification system for FTLD-TDP pathology, Acta Neuropathol. 122 (1) (2011) 111–113.
[3] T J Montine, et al., National Institute on Aging-Alzheimer's Association guidelines for the neuropathologic assessment of Alzheimer's disease: a practical approach, Acta Neuropathol. 123 (1) (2012) 1–11.
[4] T Kosaka, et al., Primary lateral sclerosis: upper-motor-predominant amyotrophic lateral sclerosis with frontotemporal lobar degeneration--immunohistochemical and biochemical analyses of TDP-43, Neuropathology 32 (4) (2012) 373–384.
[5] P A Engel, M Grunnet, Atypical dementia and spastic paraplegia in a patient with primary lateral sclerosis and numerous neocortical beta amyloid plaques: new disorder or Alzheimer's disease variant?, J. Geriatr. Psychiatry Neurol. 13 (2) (2000) 60–64.
[6] B S de Vries, et al., A case series of PLS patients with frontotemporal dementia and overview of the literature, Amyotroph. Lateral Scler. Frontotemporal. Degener. 18 (7–8) (2017) 534–548.
[7] D W Dickson, K A Josephs, C Amador-Ortiz, TDP-43 in differential diagnosis of motor neuron disorders, Acta Neuropathol. 114 (1) (2007) 71–79.
[8] H Oppenheim, Text-book of Nervous Diseases for Physicians and Students, Vol. 1, O. Schulze & Company, 1911.
[9] A Hübers, et al., Pathological laughing and crying in amyotrophic lateral sclerosis is related to frontal cortex function, J. Neurol. 263 (9) (2016) 1788–1795.
[10] Z Ahmed, et al., Globular glial tauopathies (GGT) presenting with motor neuron disease or frontotemporal dementia: an emerging group of 4-repeat tauopathies, Acta Neuropathol. 122 (4) (2011) 415–428.

Geriatrics Gerontology International

DOI: 10.1111/ggi.13847

ORIGINAL ARTICLE
BIOLOGY

CogEvo, a cognitive function balancer, is a sensitive and easy psychiatric test battery for age-related cognitive decline

Sadanobu Ichii,[1] Takumi Nakamura,[1,2] Takeshi Kawarabayashi,[1,2,3] Masamitsu Takatama,[3] Tetsuya Ohgami,[4] Kazushige Ihara[1] and Mikio Shoji[1,3,5]

[1]Department of Social Medicine, Hirosaki University Graduate School of Medicine, Hirosaki, Japan
[2]Department of Neurology, Gunma University Hospital, Maebashi, Japan
[3]Department of Neurology, Dementia Research Center, Geriatrics Research Institute and Hospital, Maebashi, Japan
[4]Department of Pharmacology, Aomori University, Aomori, Japan
[5]Department of Neurobiology and Behavior, Gunma University Graduate School of Medicine, Maebashi, Japan

Correspondence
Director Mikio Shoji MD PhD, Department of Neurology, Dementia Research Center, Geriatrics Research Institute and Hospital, 3-26-8 Ootomo-machi, Maebashi 371-0847 Japan.
Email: m-shoji@ronenbyo.or.jp

Received: 7 August 2019
Revised: 26 October 2019
Accepted: 26 November 2019

Aim: We examined whether a newly developed computer-aided neuropsychiatric series of test, CogEvo, is necessary and sufficient for the evaluation of cognitive function in older people.

Methods: A total of 272 participants in worthwhile life activity for the prevention of decline in mobility and cognitive function were administered tests every week at 33 locations in Fukaura-machi, Japan. Basic profile information, a Mini-Mental State Examination (MMSE), a CogEvo and a clock drawing test were used in the present study.

Results: Our results are summarized as: (i) the total score of the CogEvo and MMSE tests decreased significantly according to age and in age group analysis; (ii) scores from the CogEvo and MMSE tests showed a significant correlation; (iii) MMSE scores showed marked ceiling effects; (iv) analysis of cognitive domains, such as orientation, attention, memory and executive function, and spatial cognition using CogEvo showed significant age-dependent impairment; (v) CogEvo discriminated three score groups of MMSE results with sensitivity and specificity of 70% and 60% in the <23 score group, 78% and 54% in the 24–26 score group, and 85% and 70% in the >27 score group, respectively; (vi) CogEvo memory tests reflected more detailed recall function than registration function; and (vii) CogEvo spatial cognition test results were correlated with test items of the MMSE and clock drawing tests.

Conclusions: CogEvo is an easy and potentially useful computer-aided test battery that can be used to evaluate age-related or pathological decline in cognitive function from middle age and in preclinical stages of dementia. **Geriatr Gerontol Int 2020; 20: 248–255.**

Keywords: age-related cognitive decline, cognitive function balancer, computer-aided psychiatric test battery.

Introduction

The number of dementia patients is rapidly increasing with the increasing older adult population in Japan. Cognitive impairment decreases life independence and impairs the quality of life in older adult populations. For dementia patients, medical therapy and home and social care intervention are necessary as well. These burdens are stressful for the family and caregivers, and are major factors in increasing national costs of medical care. Recent advances in dementia research have suggested that early detection of cognitive impairment and intervention are beneficial for dementia prevention, possible disease-modifying therapy and development of social care systems for dementia patients. Pharmacists instruct patients to maintain adequate use of prescribed drugs from the pharmacy and home based on Japanese law. However, common prescriptions that are 90-days long and polypharmacy of >6 drugs for elderly and dementia patients cause dropout from compliance, leading to low efficacy or adverse effects. Pharmacists should understand the cognitive function of people who are prescribed drugs easily and properly. To improve these situations, we hold educational campaigns about worthwhile life activity, including recollection, for the prevention of a decline in mobility and cognitive function in a salon for middle-aged to elderly people at 33 locations in the Fukaura-machi area, Aomori, Japan. Based on this activity, we examined whether a newly developed computer-aided neuropsychiatric battery, "CogEvo, a cognitive function balancer", is necessary and sufficient for the evaluation of cognitive function in older people.

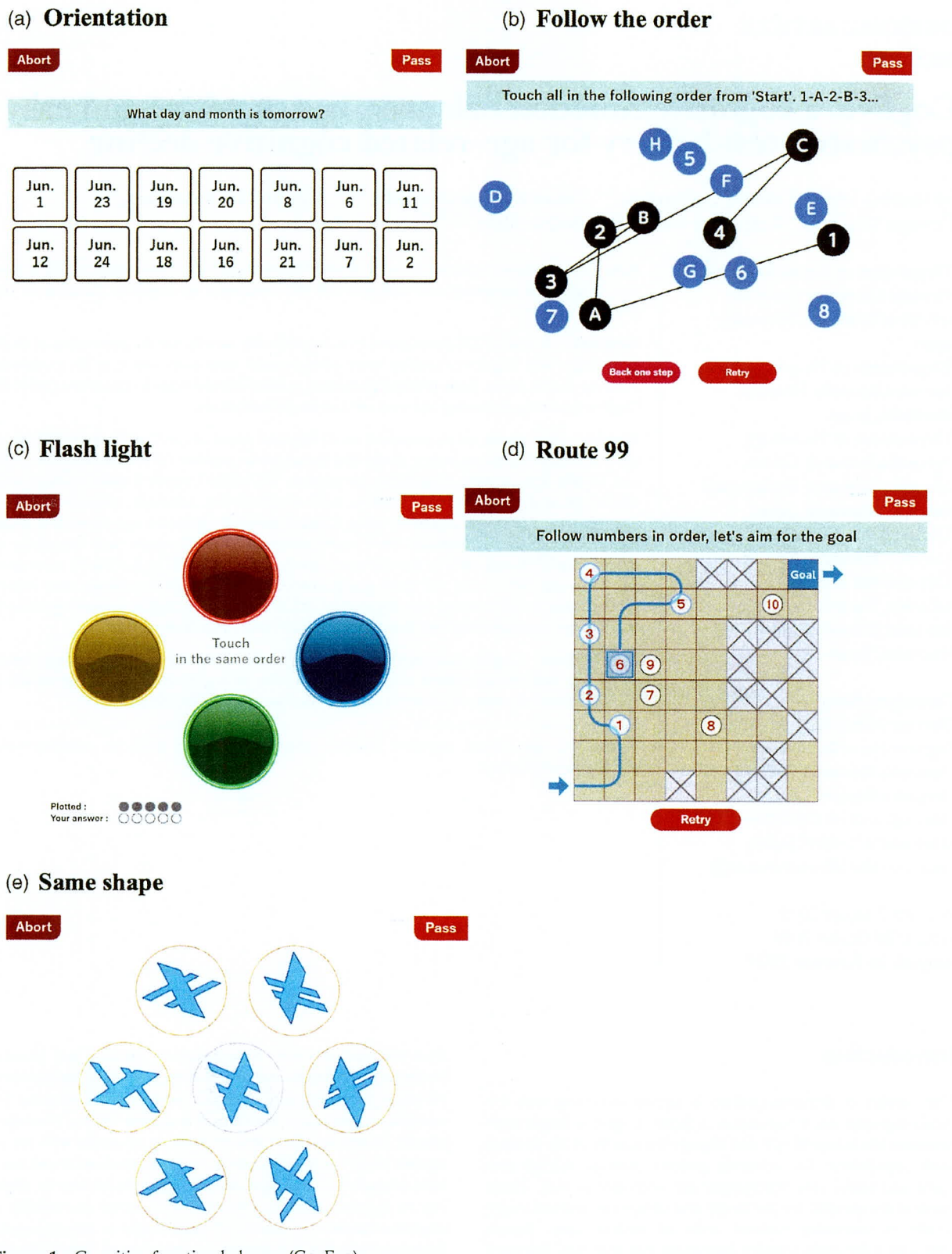

Figure 1 Cognitive function balancer (CogEvo).

Methods

Participants

A total of 272 participants were enrolled in this study. They consisted of 242 women and 27 men. The mean age was 79.5 ± 7 years, and the age range was from 40–97 years. They participated in worthwhile life activity for the prevention of decline in mobility and cognitive function in a salon for middle-aged to elderly people. These activities took place every week at 33 locations in Fukaura-machi, Japan. Approximately two to 20 people who participated in the activity were interviewed and examined after brief instruction on dementia and related disorders. The examination items were basic profile information on the participants, a Mini-Mental State Examination (MMSE),[1–3] a cognitive function balancer (CogEvo; Total Brain Care, Kobe, Japan) and a clock drawing test (CDT).[4–7] The mean examination times were 10 min in for the MMSE, 10 min for the CogEvo and 1 min for the CDT. This study was approved by the ethics committee of Hirosaki University (2017–1039). All participants provided written informed consent.

CogEvo, a cognitive function balancer

CogEvo is a computer-aided cognitive function test battery that uses a touch panel consisting of five basic tasks to evaluate orientation, attention, memory, executive function and spatial cognition. After audiovisual usage instruction, the participant pushes the start icon. If the answer is correct, 1 point is added. Incorrect answers are worth 0 points in five domain tasks. The scores for response time include four domain tasks, except the flashing light task. Each point is calculated according to the following formula: response time points = (standardized time limit – actual response time by tested participants) / standardized time limit × 100 points. The standardized time limit is the mean plus three standard deviations (3SD) of the time required for each task procedure based on preliminary trial data of CogEvo balancer for 50 000 participants. Total scores are the sum of both scoring systems.

Orientation
The task of selecting the correct day, week and time of the examination day was included. Questions were randomly presented as 14 choices of days, seven choices of the week and 14 choices of time on a touch panel (Fig. 1a).

Visual attention: Follow the order
The purpose of the test was to touch numbers, Japanese hiragana or alphabet characters, and then touch both characters alternatively, on the panel according to their order. For example, the participant touched 1, 2, 3..., A, B, C, D... and 1, A, 2, B, 3, C, ... Each question consisted of following six digits, 12 characters and alternate combinations of eight digits with eight characters (Fig. 1b).

Memory task: Flashing light
After memorization of the random order of flashing red, blue, green and yellow lights, the participant touched the lights in the same order. Each light flashed for 1 s. In some cases, the same color light flashed in series. The task started with two lights flashing, and then the light number increased up to 16 flashing trials in the case of correct answers. Result points were calculated only as they related to accurate answering rates (Fig. 1c).

Executive function: Route 99
Participants traced squares on the panel from the start to the goal in sequence following randomly displayed digits in order from

Table 1 Baseline characteristics of participants

Participants	Total population	40–69 years	70–79 years	80–89 years	90–99 years	MMSE >27	MMSE 24–26	MMSE <23
No. participants	272	21	105	134	12	121	103	48
Mean age (years)	79.5 ± 7.0	64.6 ± 6.3	75.7 ± 2.5	83.7 ± 2.8	92.8 ± 2.3	77.4 ± 7.2	80.52 ± 6.1	82.94 ± 6.4
Female	246	20	96	118	12	107	95	44
Total score of CogEvo	1001.1 ± 281.8	1344.9 ± 216.9	1097.8 ± 231.4	893.4 ± 251.9	755.1 ± 246.5	1128.1 ± 248.4	954.6 ± 252.5	780.4 ± 252.2
Orientation	245.8 ± 86.2	315.7 ± 59.3	266.0 ± 77.1	223.2 ± 85.6	200.3 ± 92.8	277.4 ± 70.7	240 ± 80.8	178.8 ± 91.9
Follow the order	155.1 ± 50.1	212.1 ± 50.7	170.7 ± 43.6	137.9 ± 43.7	111.3 ± 38.4	176.5 ± 42.9	148.1 ± 47.8	116 ± 43.7
Flashing light	245.2 ± 122.8	338.6 ± 105.2	268.0 ± 110.7	218.4 ± 123.9	181.7 ± 103.1	283.3 ± 123.2	230 ± 111	181.7 ± 111.7
Route 99	130.9 ± 46.3	175.2 ± 38.2	138.3 ± 41.5	120.5 ± 45.6	105.0 ± 43.8	144.8 ± 46.1	122.9 ± 42.2	111 ± 45.1
Same shape	224 ± 90.7	303.3 ± 84.6	254.9 ± 78.1	193.4 ± 84.9	156.9 ± 76.0	246 ± 85.7	213.6 ± 87.2	190.8 ± 95.9
MMSE score	25.8 ± 3.3	27.7 ± 2.3	26.7 ± 2.6	25.3 ± 3.7	24.1 ± 2.9	28.5 ± 1.1	25.1 ± 0.8	20.6 ± 3.4
CDT	7.7 ± 2.4	9.1 ± 0.9	8.0 ± 2.2	7.4 ± 2.7	7.4 ± 3.0	8.5 ± 1.8	7.8 ± 2.3	5.8 ± 3.3

CDT, clock drawing test; MMSE, Mini-Mental State Examination.

1 to 10. Oblique passage or a route using the same square was prohibited. The task consisted of 16 squares (4 × 4), 36 squares (6 × 6) and 64 squares (8 × 8; Fig. 1d).

Spatial cognition: Same shape

The participants selected the same figure displayed on the center of the panel from six other figures around the center. A total of four questions consisted of randomly selecting seven figures from the total of 34 figures. The center figure and answer figure were in different locations, and at different rotation angles every time (Fig. 1e).

CDT

The person was given a blank piece of paper and told to draw a clock that showed the time.[4] Scoring was carried out based on 10 points by Rouleau[5] except for prescribing the time as 10 min after 10 o'clock instead of 10 min after 11 o'clock.

Statistical analysis

Statistical analysis was carried out using linear regression analysis for correlation analyses, one-way ANOVA with Turkey's multiple comparison tests for ordinal analyses, the Kruskal–Wallis test with Dunn's multiple comparison tests, an unpaired *t*-test and a Mann–Whitney test after normality testing using GraphPad Prism, version 8 (GraphPad Software, San Diego, CA, USA). Receiver operating characteristic analyses were carried out using R Commander version 2.4.0 for windows (The Institute of Statistical Mathematics, Tokyo: https://cran.ism.ac.jp). Statistical significance was set at $P < 0.05$.

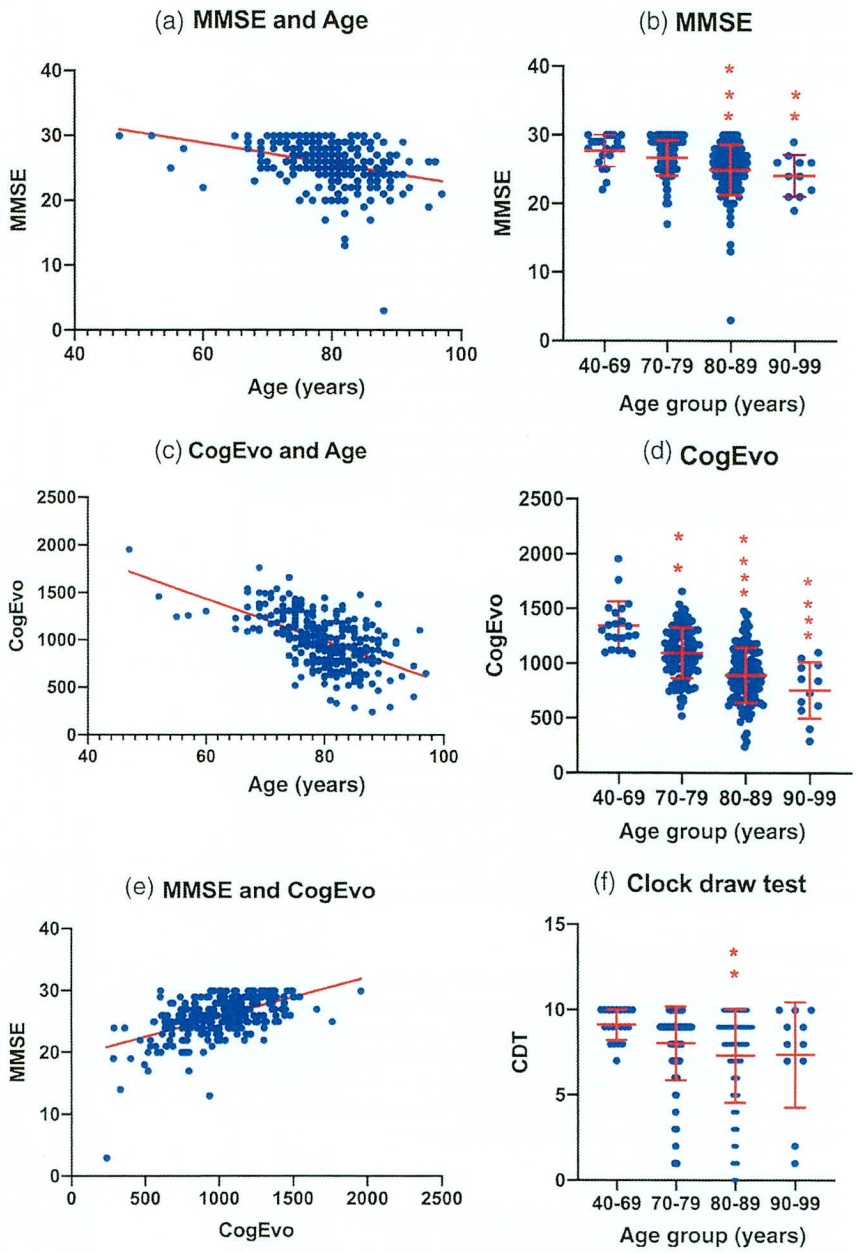

Figure 2 Association studies among the Mini-Mental State Examination (MMSE), CogEvo, clock drawing test and age. $^{**}P < 0.005$; $^{***}P < 0.0005$; $^{****}P < 0.0001$.

Results

Basic profiles of participants are summarized in Table 1. We divided the total 272 participants into four groups according to age to analyze the age-related natural course of cognitive function. The first group with participants aged 40–69 years included 21 participants (group 1), the next group had people who were aged 70–79 years and there were 105 in the group (group 2), the third group had people who were aged 80–89 year and there were 134 in the group (group 3), and the eldest group was aged 90–99 years and there were 12 people in the group (group 4). Groups 2 and 3 had enough participants for statistical analyses, but female-dominant differences were observed in all groups. Total scores and subclassification domain items of the CogEvo,

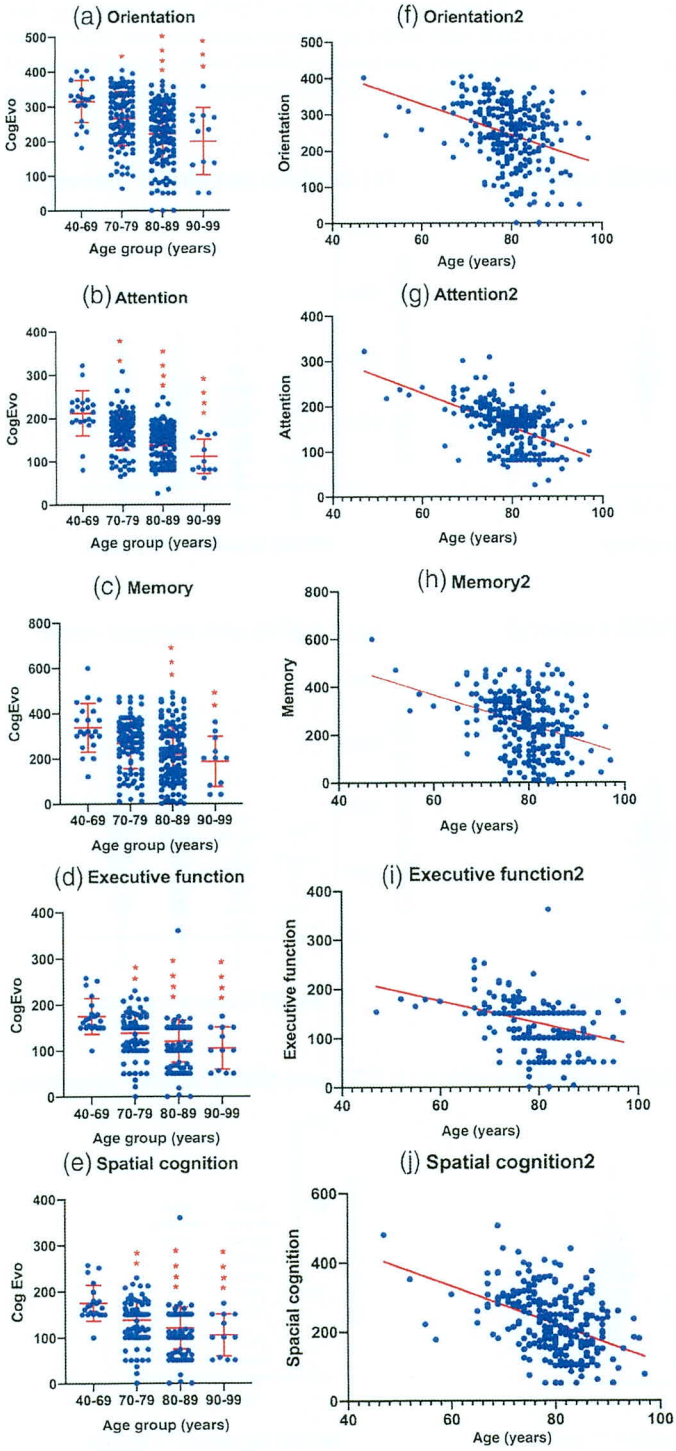

Figure 3 Age-related decline of scores in CogEvo. $^{*}P < 0.05$; $^{**}P < 0.005$; $^{***}P < 0.0005$; $^{****}P < 0.0001$.

MMSE tests and the CDT are presented in Table 1. The mean scores for the total participants were 1001.1 ± 281.8 in the CogEvo tests, 25.8 ± 3.3 in the MMSE test and 7.7 ± 2.4 in the CDT, respectively. These scores declined with age.

We also divided the total participants into three groups according to cut-off scores for the MMSE; that is, 24 and 26 points, which are commonly used to discriminate dementia from normal individuals,[2] and for registration criteria of the cognitively unimpaired (CU),[8,9] mild cognitive impairment (MCI)[10] and dementia (D)[11] in recent cohort studies, such as the Alzheimer's Disease Neuroimaging Initiative[12–14] and the Dominantly Inherited Alzheimer Network.[15] The numbers of participants, mean age, sex, and total and subclassified domain scores of CogEvo, MMSE scores and CDT scores are described in Table 1. Each score of the CogEvo, MMSE and CDT was also assessed according to the cut-off score groups of the MMSE.

Then, we analyzed the association of total CogEvo scores and MMSE scores, with age. Both MMSE scores against age ($y = -0.1602*X + 38.53$, $r^2 = 0.1115$, $P < 0.0001$; Fig. 2a) and total CogEvo scores against age ($Y = -22.19*X + 2766$, $r^2 = 0.3011$, $P < 0.0001$; Fig. 2c) showed significant negative correlations. MMSE scores and total CogEvo scores showed a significant positive correlation ($Y = 0.006471*X + 19.30$, $r^2 = 0.2973$, $P < 0.0001$; Fig. 2e). Ceiling effects were noted in the association between MMSE and total CogEvo scores, and between MMSE scores and age because of the upper 30 points in the MMSE. However, these limitations were

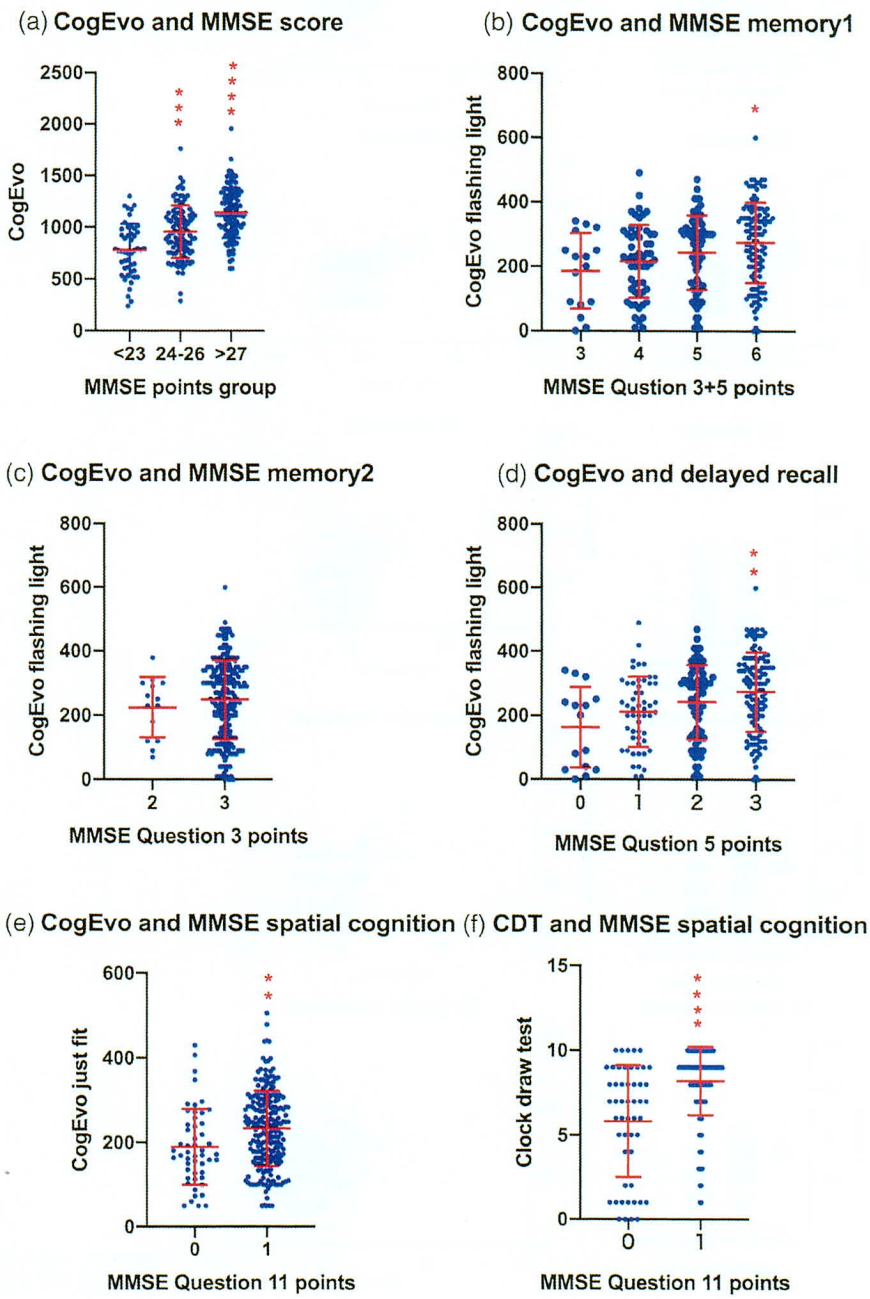

Figure 4 Association study of memory and spatial cognition in the CogEvo test and clock drawing test (CDT). *$P < 0.05$; **$P < 0.005$; ***$P < 0.0005$; ****$P < 0.0001$. MMSE, Mini-Mental State Examination.

not observed in the linear regression curve between CogEvo scores against age (Fig. 2c).

We also compared the MMSE scores, total CogEvo scores and five subscore items of the CogEvo, such as orientation, attention, memory, executive function and spatial cognition, and CDT scores in the four age-dependent groups. Total scores of the MMSE showed significant decreases in group 3 ($P = 0.0003$) and group 4 ($P = 0.0028$; Fig. 2b) compared with those of group 1. Total scores of the CogEvo test were significantly decreased in the corresponding age groups (group 2: $P = 0.0029$; group 3: $P < 0.0001$; and group 4: $P < 0.0001$; Fig. 2d). However, the CDT only showed significance in group 3 ($P = 0.0025$; Fig. 2f) compared with group 1.

In the orientation item of the CogEvo test, a significant decline in scores was observed in group 2 ($P = 0.0297$), group 3 ($P < 0.0001$) and group 4 ($P = 0.0009$) compared with group 1 (Fig. 3a). In the attention items, a significant decline was shown in group 2 ($P = 0.0033$), group 3 ($P < 0.0001$) and group 4 ($P < 0.0001$; Fig. 3b). In the memory domain, significance was recognized in group 3 ($P = 0.0002$) and group 4 ($P = 0.0031$; Fig. 3c). Scores of executive functions also showed a significant decrease between group 2 ($P = 0.0011$), group 3 ($P < 0.0001$) and group 4 ($P < 0.0001$) (Fig. 3d). In spatial cognition items, a significant decline was observed in group 2 ($P = 0.0011$), group 3 ($P < 0.0001$) and group 4 ($P < 0.0001$; Fig. 3e). We also carried out a simple linear regression analysis between age and five subscore items of the CogEvo test. All subscore items also showed a significant linear correlation with age. Respective regression coefficients were −4.276 in orientation, −3.805 in attention, −6.259 in memory, −2.308 in executive function and −5.539 in spatial cognition. The coefficient of determinations (r^2) were 0.1194 in orientation, 0.2799 in attention, 0.1262 in memory, 0.1208 in executive function and 0.1812 in spatial cognition. These findings suggested that all five subscore items decreased according with age; however, attention subscores were more affected by the effect of age compared with the other four subscore items (Fig. 3f–j).

Then, we compared the subscale scores of the subclassification groups and domains of the CogEvo and MMSE tests. Total CogEvo scores were significantly increased in the 24–26 points group ($P = 0.0002$) and the >27 points group ($P < 0.0001$) compared with the <23 points group. Significance was observed in the 27 points group compared with the between 24 and 26 points group ($P < 0.0001$; Fig. 4a). To further study the memory domains, scores of the CogEvo flashing light and scores for questions 3 + 5 in the MMSE were analyzed, showing a significant increase in CogEvo scores between MMSE scores of 3 points and 6 points ($P = 0.0441$), and between 4 points and 6 points ($P = 0.0131$; Fig. 4b). A separate analysis showed no significant differences between 2 and 3 points for the MMSE question 3 (Fig 4c). However, significances were recognized between 0 and 3 points ($P = 0.0091$) and 1 and 3 points ($P = 0.007$) for MMSE question 5 (Fig. 4d), suggesting the CogEvo flashing light test reflected more delayed recall function memory items than those of the registration function. To analyze spatial cognition items, associations between MMSE question 11, CogEvo same shape and CDT were examined. Both item scores showed a significant relationship with MMSE question 11 for CogEvo same shape (0–1 point: $P = 0.0002$; Fig. 4e) and in the CDT (0–1 point: $P < 0.0001$; Fig. 4f).

Finally, we examined the sensitivity and specificity of the CogEvo total scores using receiver operating characteristic analysis for discriminate CU, MCI and D cut-offs defined by MMSE scores. Setting 809 points of the total scores of the CogEvo test, the D and MCI groups were discriminated at a sensitivity of 70% and specificity of 60%. At 995 points of the CogEvo test, sensitivity of 78% and specificity of 54% were observed between the MCI and CU groups. A sensitivity of 85% and specificity of 70% at 1018 points were obtained for comparisons between the D and CU groups.

Discussion

MMSE is the worldwide established screening neuropsychiatry test that consists of orientation of time and place, memory registration and recall, attention and calculation, language, and executive and visuospatial proficiency assessment.[1] Testing took 5–10 min, and the cut-off value of 23 out of 24 discriminated moderate-to-severe cognitive impairment.[2,3] However, scores were highly dependent on age and education level.[16] Population-based norms have been reported from the age of 6 years to >85 years,[17,18] and the natural decline of MMSE scores is 3–4 points per year in Alzheimer's disease.[16,19] MMSE is a basic variable for observational study, such as Alzheimer's Disease Neuroimaging Initiative[12–14] and Dominantly Inherited Alzheimer Network,[15] and is one of the end-points of intervention study of disease-modifying drugs. For this reason, a comparison between the MMSE and CogEvo is meaningful.

The total examination time for the MMSE and CogEvo test is almost the same; however, the machinery instructions for the task and automatic score calculation seem to be easier and more consistent compared with the MMSE. Both total scores of MMSE and CogEvo test showed age-dependent cognitive decline (Fig. 2). Ceiling effects at 30 points in the MMSE decreased the usefulness for detecting slight age-related cognitive impairment (Fig. 2a,e). As MMSE was developed to discriminate dementia from normal behavior,[1,2] it suggests difficulty in recognizing slight cognitive impairment. In contrast, the CogEvo test was shown to detect these slight age-related cognitive impairments clearly (Fig. 2c,d), suggesting that CogEvo is feasible for evaluating age-related or preclinical cognitive decline from 65 years onwards in cohort studies or preclinical intervention trials. Further analysis in the subclassified domain of cognition showed that CogEvo also showed significant age-related cognitive decline in orientation, attention, memory, executive function and spatial cognition (Fig. 3). However, the CDT did not show a clear significance and ceiling effects. The CDT is considered to be a test for discrimination between normal behavior and dementia, similar to the MMSE. Thus, CogEvo seems to be a sensitive test battery for age-related cognitive decline.

These findings suggest that the CogEvo test might also be feasible for preclinical observation studies or clinical trials for the prevention of dementia. In the MMSE, the range for the CU participants and participants with MCI was 24–30, and for mild Alzheimer's disease dementia the range was 20–26.[12,13] The CDR score and education duration-dependent delayed recall score of the logical Memory II subscale for Wechsler Memory Scale-Revised were additional criteria for discernment of CU, MCI and mild Alzheimer's disease dementia.[10] For this reason, we validated whether the CogEvo test could separate cut-off points of 24 and 26 in MMSE scores. As shown in Figure 4a, CogEvo significantly discriminated these groups with cut-offs at 780.4 points, and a sensitivity of 78% and specificity of 54%, and at 1128.1 points with a sensitivity 70% and specificity of 60%, suggesting that these cut-offs also exist in the CogEvo total points range 0–2500 points.

Then, we further validated memory and the spatial cognition domain of CogEvo in detail. In comparisons between registration and recall functions of memory domain, CogEvo results were correlated with delayed recall more than registration (Fig. 4b–d). Both CogEvo and CDT significantly responded to MMSE question 11; however, a wide range of scores for the CogEvo test without

ceiling effects is considered more feasible for examining the spatial cognition domain.

As Alzheimer's disease and neurodegenerative dementia diseases develop cognitive impairment after a very long preclinical period, discriminating physical age-dependent declines in cognitive functions is very difficult, and therefore there is meaning in inventing a neuropsychiatry battery of the tests for evaluating age-related cognitive decline. Clinical trials on disease-modifying therapy are also changing ideas on the prevention in preclinical states. For this purpose, many computer-aided or iPad-based test batteries, such as Cogstate[20,21] and CANTAB,[22–25] are emerging in this field. These batteries have been applied in cohort studies, such as the Dominantly Inherited Alzheimer Network. The present study used CogEvo, which is one of the recently introduced tests. A limitation of CogEvo is there have been few validation cohort studies and comparison studies with other kinds of PC-based batteries. This is the first validation study. We therefore are planning validation of CogEvo in other international cohort studies and comparison studies with Montreal Cognitive Assessment, Cogstat, CANTAB and other tests.

Acknowledgements

We thank the research assistants. This study was supported by Scientific Research (C) (18 K07385 MS, 19 K07989 TK) from the Ministry of Education, Science and Culture of Japan.

Disclosure statement

The authors declare no conflict of interest.

References

1 Folstein MF, Folstein SE, McHugh PR. "Mini-mental state". A practical method for grading the cognitive state of patients for the clinician. *J Psychiatr Res* 1975; **12**: 189–198.
2 Tombaugh TN, McIntyre NJ. The mini-mental state examination: a comprehensive review. *J Am Geriatr Soc* 1992; **40**: 922–935.
3 Norris D, Clark MS, Shipley S. The mental status examination. *Am Fam Physician* 2016; **94**: 635–641.
4 Critchley M. *The Parietal Lobes*. Baltimore: The Williams and Wilkins Company, 1953; 1–430.
5 Rouleau I, Salmon DP, Butters N, Kennedy C, McGuire K. Quantitative and qualitative analyses of clock drawings in Alzheimer's and Huntington's disease. *Brain Cogn* 1992; **18**: 70–87.
6 Sunderland T, Hill JL, Mellow AM *et al.* Clock drawing in Alzheimer's disease. A novel measure of dementia severity. *J Am Geriatr Soc* 1989; **37**: 725–729.
7 Kim S, Jahng S, Yu KH, Lee BC, Kang Y. Usefulness of the clock drawing test as a cognitive screening instrument for mild cognitive impairment and mild dementia: an evaluation using three scoring systems. *Dement Neurocogn Disord* 2018; **17**: 100–109.
8 Knopman DS, Haeberlein SB, Carrillo MC *et al.* The National Institute on Aging and the Alzheimer's Association research framework for Alzheimer's disease: perspectives from the research roundtable. *Alzheimers Dement* 2018; **14**: 563–575.
9 Jack CR Jr, Bennett DA, Blennow K *et al.* NIA-AA research framework: toward a biological definition of Alzheimer's disease. *Alzheimers Dement* 2018; **14**: 535–562.
10 Morris JC, Storandt M, Miller JP *et al.* Mild cognitive impairment represents early-stage Alzheimer disease. *Arch Neurol* 2001; **58**: 397–405.
11 McKhann GM, Knopman DS, Chertkow H *et al.* The diagnosis of dementia due to Alzheimer's disease: recommendations from the National Institute on Aging-Alzheimer's Association workgroups on diagnostic guidelines for Alzheimer's disease. *Alzheimers Dement* 2011; **7**: 263–269.
12 Petersen RC, Aisen PS, Beckett LA *et al.* Alzheimer's Disease Neuroimaging Initiative (ADNI): clinical characterization. *Neurology* 2010; **74**: 201–209.
13 Iwatsubo T, Iwata A, Suzuki K *et al.* Japanese and North American Alzheimer's Disease Neuroimaging Initiative studies: harmonization for international trials. *Alzheimers Dement* 2018; **14**: 1077–1087.
14 Veitch DP, Weiner MW, Aisen PS *et al.* Understanding disease progression and improving Alzheimer's disease clinical trials: recent highlights from the Alzheimer's Disease Neuroimaging Initiative. *Alzheimers Dement* 2019; **15**: 106–152.
15 Bateman RJ, Xiong C, Benzinger TL *et al.* Clinical and biomarker changes in dominantly inherited Alzheimer's disease. *N Engl J Med* 2012; **367**: 795–804.
16 Knopman D, Selens O. 17 neuropsychatry of dementia. In: Heilman KM, Valenstein E, eds. *Clinical Neuropsyclogy*, 5th edn. New York: Oxford University Press, 2012; 582–636.
17 Crum RM, Anthony JC, Bassett SS, Folstein MF. Population-based norms for the mini-mental state examination by age and educational level. *JAMA* 1993; **269**: 2386–2391.
18 Shoji M, Fukushima K, Wakayama M *et al.* Intellectual faculties in patients with Alzheimer's disease regress to the level of a 4–5-year-old child. *Geriatr Gerontol Int* 2002; **02**: 143–147.
19 Han L, Cole M, Bellavance F, McCusker J, Primeau F. "Tracking cognitive decline in Alzheimer's disease using the mini-mental state examination": a meta-analysis. *Int Psychogeriatr* 2000; **12**: 231–247.
20 Mielke MM, Machulda MM, Hagen CE *et al.* Performance of the CogState computerized battery in the Mayo Clinic Study on Aging. *Alzheimers Dement* 2015; **11**: 1367–1376.
21 Stricker NH, Lundt ES, Edwards KK *et al.* Comparison of PC and iPad administrations of the Cogstate Brief Battery in the Mayo Clinic Study of Aging: assessing cross-modality equivalence of computerized neuropsychological tests. *Clin Neuropsychol* 2018; **10**: 1–25.
22 Robbins TW, James M, Owen AM, Sahakian BJ, McInnes L, Rabbitt P. Cambridge Neuropsychological Test Automated Battery (CANTAB): a factor analytic study of a large sample of normal elderly volunteers. *Dementia* 1994; **5**: 266–281.
23 Lenehan ME, Summers MJ, Saunders NL, Summers JJ, Vickers JC. Does the Cambridge Automated Neuropsychological Test Battery (CANTAB) distinguish between cognitive domains in healthy older adults? *Assessment* 2016; **23**: 163–172.
24 Koo BM, Vizer LM. Mobile Technology for cognitive assessment of older adults: a scoping review. *Innov Aging* 2019; **3**: igy038.
25 Ciesielska N, Sokołowski R, Mazur E, Podhorecka M, Polak-Szabela A, Kędziora-Kornatowska K. Is the Montreal cognitive assessment (MoCA) test better suited than the mini-mental state examination (MMSE) in mild cognitive impairment (MCI) detection among people aged over 60? Meta-analysis. *Psychiatr Pol* 2016; **50**: 1039–1052.

How to cite this article: Ichii S, Nakamura T, Kawarabayashi T, et al. CogEvo, a cognitive function balancer, is a sensitive and easy psychiatric test battery for age-related cognitive decline. Geriatr. Gerontol. Int. 2020;20:248–255. https://doi.org/10.1111/ggi.13847

Contents lists available at ScienceDirect

Neuroscience Letters

journal homepage: www.elsevier.com/locate/neulet

Research article

Novel ELISAs to measure total and phosphorylated tau in cerebrospinal fluid

Takeshi Kawarabayashi[a,b,c,*], Takumi Nakamura[b,c], Kazuya Miyashita[d], Isamu Fukamachi[d], Yusuke Seino[e], Mikio Shoji[a,c,f]

[a] Department of Neurology, Dementia Research Center, Geriatrics Research Institute and Hospital, 3-26-8 Otomo-machi, Maebashi, 371-0847, Japan
[b] Department of Neurology, Gunma University Hospital, 3-39-15 Showamachi, Maebashi, 371-8511, Japan
[c] Department of Social Medicine, Hirosaki University Graduate School of Medicine, 5 Zaifu-cho, Hirosaki, 036-8216, Japan
[d] Immuno-Biological Laboratories Co., Ltd, 1091-1 Naka Aza-Higashida, Fujioka, 375-0005, Japan
[e] Department of Neurology, Hirosaki National Hospital, 1 Tominocho, Hirosaki, 036-8545, Japan
[f] Department of Neurobiology and Behavior, Gunma University Graduate School of Medicine 3-39-22 Showamachi, Maebashi, 371-8511, Japan

ARTICLE INFO

Keywords:
Alzheimer's disease
Tau
Phosphorylated tau
ELISA
Cerebrospinal fluid

ABSTRACT

Cerebrospinal fluid (CSF) total tau (t-tau) and tau protein phosphorylated at threonine 181 (p181tau) are established biomarkers for Alzheimer's disease (AD). Herein, we measured t-tau and p181tau to evaluate novel enzyme-linked immunosorbent assays (ELISAs) using 72 CSF samples including from patients with AD with dementia (ADD) and various neurodegenerative diseases. Our assay system showed good correlations with widely used ELISA systems for t-tau and p181tau and showed that serum and hemoglobin contamination in CSF samples did not decrease sensitivity. Significant increases in both t-tau and p181tau levels were observed in ADD. These findings suggested that our ELISAs were reliable assays for CSF t-tau and p181tau similar to commonly used ELISAs.

1. Introduction

Many large cohort studies, including the Alzheimer's Disease Neuroimaging Initiative (ADNI) [1,2] and the Dominantly Inherited Alzheimer's Network (DIAN) [3,4], have confirmed the efficacy of neuropsychiatric tests, cerebrospinal fluid CSF biomarkers, and neuroimaging including magnetic resonance imaging, fluorodeoxyglucose positron emission tomography PET, and amyloid and tau PET, for diagnosis of the natural course of Alzheimer's disease (AD). These markers have provided strong evidence of the signatures of AD pathology in the brain. Approximately 4500 research articles including meta-analysis have already been published on the CSF biomarkers of AD, confirming the usefulness of CSF Aß, t-tau, and phosphorylated tau as diagnostic and predictive markers for AD and its preclinical states [5]. Based on these findings, low CSF Aß42 or cortical amyloid PET ligand binding have been adopted as biomarkers for Aß amyloidosis (labeled "A") in the A/T/N classification system of the novel National Institute on Aging and Alzheimer's Association (NIA-AA) research framework criteria [6]. High CSF phosphorylated-tau and positive tau PET are also biomarkers for tauopathy (labeled "T"). Biomarkers of neurodegeneration or neuronal degeneration (labeled "N") are increased CSF tau, fluorodeoxyglucose PET hypometabolism, and atrophy on brain magnetic resonance imaging. The NIA-AA research framework proposed diagnostic criteria based on the biological definition of AD for observational and interventional research.

A comparative study of tau protein phosphorylated at threonine 181 (p181tau) and that at threonine 231 showed the same specify to discriminate AD with dementia from non-AD type dementia [7]. Assays of p181tau showed better discrimination of AD and dementia with Lewy bodies. Based on these studies, CSF p181tau assays are commonly adopted for measuring CSF p-tau using an enzyme-linked immunosorbent assay (ELISA) such as the p181tau assay system produced by Fujirebio Europe, as INNOTEST® PHOSPHO-TAU(181 P) [8,9]. Recent multiple simultaneous assay systems of CSF Aß42, t-tau, and p181tau, such as INNO-BIA AlzBIo3 for Luminex® or Elecsys are essentially identical using the same antibodies for the respective assays

Abbreviations: AD, Alzheimer's disease; ADD, Alzheimer's disease with dementia; ADNI, Alzheimer's Disease Neuroimaging Initiative; CSF, cerebrospinal fluid; CU, cognitively unimpaired normal controls; DIAN, dominantly inherited Alzheimer's network; ENC, encephalitis; ELISA, enzyme-linked immunosorbent assay; MCI, mild cognitive impairment; NIA-AA, National Institute on Aging and Alzheimer's Association; NADD, Non-Alzheimer type dementia; OND, other neurological diseases; PET, positron emission tomography; p181tau, Tau protein phosphorylated at threonine 181; t-tau, total tau

* Corresponding author at: Department of Neurology, Dementia Research Center, Geriatrics Research Institute and Hospital, 3-26-8 Otomo-machi, Maebashi, 371-0847, Japan.
E-mail address: tkawara@ronenbyo.or.jp (T. Kawarabayashi).

https://doi.org/10.1016/j.neulet.2020.134826
Received 18 July 2019; Received in revised form 21 November 2019; Accepted 5 February 2020

[10–13]. However, these ELISA assays are expensive for routine work and can be affected by blood contamination. Because CSF is obtained by lumbar puncture procedures, blood contamination occurs frequently. For this reason, we herein evaluated novel ELISA systems for t-tau and p181tau by comparison with INNOTEST®hTAU Ag and INNOTEST PHOSPHO-TAU (181 P) assays.

2. Materials and methods

2.1. Subjects

A total of 72 CSF samples were examined from 12 patients with ADD, 6 with encephalitis (ENC), 22 with non-AD dementia (NADD), and 27 with other neurological diseases (OND), and 5 cognitively unimpaired control subjects (CU). Among the 6 ENC samples, 2 samples lacked sufficient volumes for p181tau assay and these were excluded for both p181tau assays. ADD was diagnosed based on NIA-AA criteria defined by positive A + T+N + biomarker changes [6]. The NADD group consisted of 3 patients with frontotemporal dementia [14,15], 3 with corticobasal degeneration [16], 3 with normal pressure hydrocephalus, and 12 with progressive supranuclear palsy [17]. The clinically diagnosed OND group using respective recent criteria included 4 patients with amyotrophic lateral sclerosis [18], 1 with cerebral amyloid angiopathy, 2 with polyneuropathy, 2 with multiple sclerosis and related disorders, 9 with multiple system atrophy [19], 6 with Parkinson's disease [20], and 3 with spinocerebellar degeneration. Additionally, 3 CSF samples from 2 patients with severe ENC and 1 CU were used for dilution and recovery tests. The basic profile is summarized in Table 1, and no statistical differences were observed in age distribution between the NADD and OND groups. Lumber puncture for CSF examination was performed in the morning in accordance with a standard protocol. CSF samples were immediately centrifuged at 3000 rpm for 10 min, and stored in polypropylene vials at −80 °C until analysis.

2.2. ELISA

CSF t-tau and p181tau were measured using a Human Total Tau Assay kit (ELISA #27811) and a Human Phospho Tau 181 P Assay kit (ELISA #27812), respectively, provided by Immuno-Biological Laboratories Co., Ltd., Japan IBL. The captured antibody was Anti-hTau441-E22A3 Rat IgG monoclonal antibody for both assays. The detection antibodies were HRP-conjugated anti-Tau441-E21A5A1 Rat IgG monoclonal antibody Fab' for t-tau and HRP-conjugated anti-hTau p181-Rk27A6 Rat monoclonal IgG Fab' for p181tau. For comparison, CSF t-tau and p181tau from the same sample were measured using Phinoscholar®•hTAU and Phinoscholar®•pTAU ELISA kits (Nipro Corp. Osaka, Japan), respectively, which were from a Japanese provider and completely identical to INNOTEST®hTAU Ag and PHOSPHO-TAU (181 P) supplied by Fujirebio Inc., Tokyo, Japan. The captured antibodies were AT120 for t-tau and HT7 for p181tau, and the detection antibodies were BT2 and HT7 for t-tau and AT270 for p181tau, respectively. The assays were carried out in accordance with the manufacturers' protocols.

Table 1
Subject profile.

	Number	Male	Female	Mean age (Y)	Age range (Y)
ADD	12	4	8	64	41–77
CU	5	5	0	68	56–76
ENC	6	3	3	48	26–74
NADD	22	12	10	74	50–83
OND	27	12	15	61	22–82

ADD: Alzheimer's disease with dementia; CU: cognitively unimpaired normal controls; ENC: encephalitis, NADD: non-Alzheimer type dementia; OND; other neurological diseases.

2.3. Recovery test using serum- and hemoglobin-contaminated samples

Serum from a normal control was 2-fold serially diluted using assay buffer from 2- to 16-fold. Standard tau at 550 pg/ml and standard phosphorylated p181tau at 114 pg/ml were added to the samples, assayed, and compared with control samples without serum. Control CSF with 490 mg/dl hemoglobin added was 2-fold serially diluted from 490 mg/dl to 3.8 mg/dl and separated into tubes. Then, 137.5 pg/ml of standard t-tau and 28.8 pg/ml of standard p181tau were added to each tube and assayed to evaluate recovery.

2.4. Dilution test of CSF samples from encephalitis subjects

CSF samples from 2 patients with severe ENC and one CU were serially diluted from 2- to 512-fold and assayed (n = 2) using t-tau and p181tau ELISAs. First-order regression analyses were performed using the respective values.

2.5. Statistical analyses

Statistical analyses was carried out using linear regression analysis for correlation analyses, assay values among the respective groups were analyzed using the Kruskal–Wallis test with multiple comparison tests for non-parametric data using GraphPad Prism, version 8 (GraphPad Software, San Diego, CA). No significant differences were observed in the mean age distribution of the ADD, CU, NDD, and OND groups. Statistical significance was set at $p < 0.05$.

3. Results

Simple regression analysis of t-tau measured using the Human Total Tau Assay kit (ELISA #27811) and Phinoscholar®•hTAU ELISA kit showed a significant relationship as $Y = 0.9641*X+78.93$ ($r^2 = 0.9229$, $p < 0.0001$ from 72 CSF samples. The values of p181tau measured using the Human Phospho Tau181 P Assay kit (ELISA #27812) and Phinoscholar®•pTAU ELISA kit also showed a close correlation as $Y = 0.9687*X-9.799$ ($r^2 = 0.9601$. $p < 0.0001$) from 70 CSF samples (Fig. 1).

Recovery tests using serum-contaminated samples showed mean recovery rates for t-tau and p181tau of 82.3–91.3 % and 99.0–104.0 %, respectively. The mean recovery rates using hemoglobin-contaminated samples for t-tau and p181tau were 92–115.9 % and 92.8–110.5 %, respectively.

Dilution tests of CSF samples from 2 patients (cases 1 and 2) with severe ENC and one CU showed linear correlations of measured tau values in cases with meningitis, case 1 ($Y = 1078*X + 3.969$; $r^2 = 0.9995$, < 0.0001) and case 2 ($Y = 342.1*X + 0.4972$; $r^2 = 0.9994$, < 0.0001), and CU ($Y = 146.0*X - 1.974$; $r^2 = 0.9952$, < 0.0001). The assay values of p181tau also showed a linear relationship in case 1 ($Y = 24.27*X + 0.3213$; $r^2 = 0.9989$, < 0.0001), case 2 ($Y = 68.22*X + 0.6485$; $R^2 = 0.9998$, < 0.0001), CU ($Y = 57.85*X - 0.06096$; $R^2 = 1.000$, < 0.0001) (Fig. 2).

Assay values of mean and standard deviations of t-tau using a Human Total Tau Assay kit (ELISA #27811) were 852.3 ± 317.5 pg/ml in patients with ADD, 372.0 ± 114.2 pg.ml in CU, 1054 ± 1076 pg/ml with ENC, 402.0 ± 136.1 pg/ml with NADD, and 419.0 ± 240.1 pg/ml with OND. Significant increases in t-tau levels was recognized in patients with ADD compared with those with NADD ($p < 0.0040$) and OND ($p < 0.0012$) (Fig. 3a). T-tau levels measured using Phinoscholar®•hTAU were 848.5 ± 399.5 pg/ml in patients with ADD, 295.5 ± 90.01 pg/ml in CU, 1001 ± 981.6 pg/ml with ENC, 309.5 ± 102.7 pg/ml with NADD, and 354.1 ± 199.7 pg/ml with OND. The same significant elevation of t-tau measured using

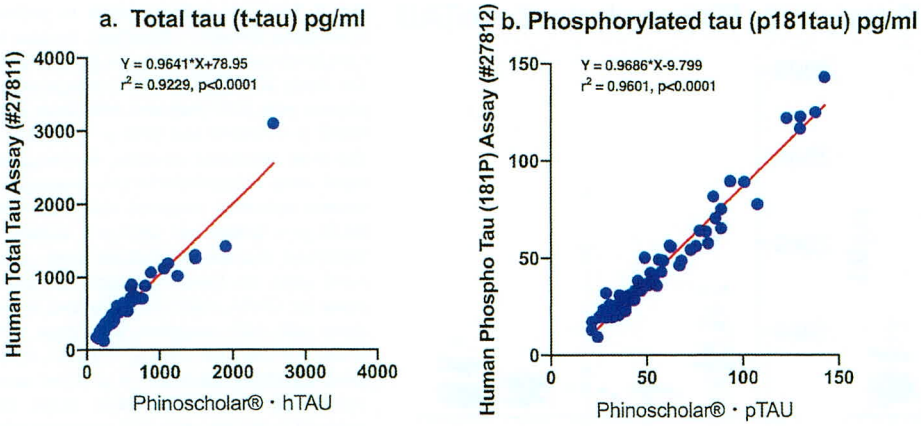

Fig. 1. Correlation study of t-tau and p181tau using both ELISAs. (a)Simple regression analysis from 72 CSF samples showing a significant relationship, $Y = 0.9641*X + 78.93$ ($r^2 = 0.9229$, $p < 0.0001$, between t-tau value measured using the Human Total Tau Assay kit (ELISA #27811) and Phinoscholar®•hTAU. b Measured values of p181tau from 70 CSF samples using the Human Phospho Tau 181 P Assay kit (ELISA #27812) and Phinoscholar®•pTAU ELISA kit show a close correlation, $Y = 0.9687*X-9.799$ ($r^2 = 0.9601$. $p < 0.0001$).

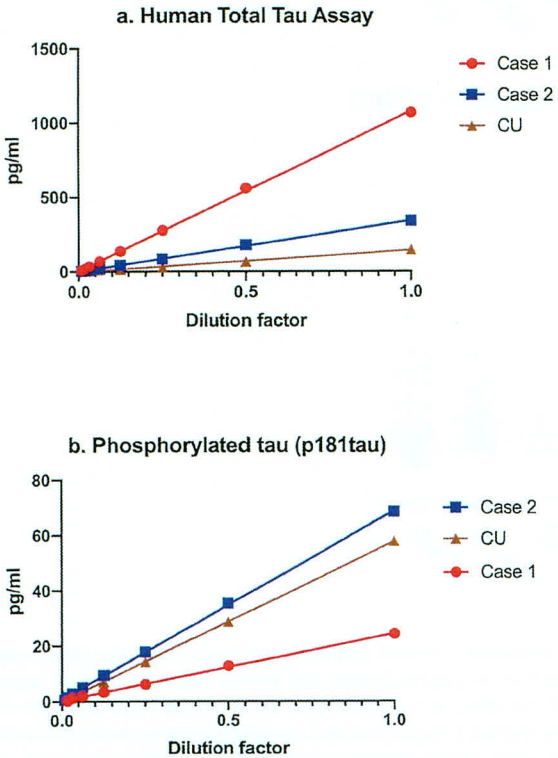

Fig. 2. Dilution tests of CSF samples with encephalitis (ENC) and a cognitively unimpaired normal control (CU). (a) Dilution tests of CSF samples from 2 patients with ENC (cases 1 and 2) and one CU show a linear correlation of measured tau values in cases with meningitis case 1 (red: $Y = 1078*X + 3.969$; $r^2 = 0.9995$, < 0.0001) and case 2 (blue: $Y = 342.1*X + 0.4972$; $r^2 = 0.9994$, < 0.0001), and CU (brown: $Y = 146.0*X - 1.974$; $r^2 = 0.9952$, < 0.0001) using the Human Total Tau Assay kit (ELISA #27811). (b) The assay values of p181tau also show a linear relationship in case 1 ($Y = 24.27*X + 0.3213$; $r^2 = 0.9989$, < 0.0001), case 2 ($Y = 68.22*X + 0.6485$; $R^2 = 0.9998$, < 0.0001), and CU ($Y = 57.85*X - 0.06096$; $R^2 = 1.000$, < 0.0001 using the Human Phospho Tau 181 P Assay kit (ELISA #27812).

Phinoscholar®•hTAU was observed in patients with ADD compared with NADD ($p < 0.0009$) and OND ($p < 0.0009$) (Fig. 3b).

Assay values of the mean and standard deviations of p181tau using the Human Phospho Tau (181 P) Assay kit (ELISA #27812) were 89.55 ± 34.63 pg/ml in patients with ADD, 33.48 ± 9.572 pg/ml in CU, 31.93 ± 12.49 pg/ml with ENC, 34.49 ± 12.29 pg/ml with NADD, and 33.33 ± 17.80 pg/ml with OND. Significant increases in p181tau levels were recognized in patients with ADD compared with those with NADD ($p = 0.001$) and OND ($p < 0.0001$) (Fig. 3c). p181tau levels measured using Phinoscholar®•pTAU ELISA kits were 99.78 ± 31.83 pg/ml in patients with ADD, 45.18 ± 13.45 pg.ml in CU, 37.33 ± 8.691 pg/ml with ENC, 45.20 ± 14.58 pg/ml with NADD, and 47.03 ± 21.57 pg/ml with OND. The same significant elevation of p181tau measured using Phinoscholar®•pTAU ELISA kits was observed in patients with ADD compared with those with ENC ($P = 0.0133$), NADD ($p = 0.0004$) and OND ($p = 0.0001$) (Fig. 3d).

4. Discussion

The sensitivity of Human Total Tau Assay ELISA #27811 was 4.31 pg/ml and that of Human Phospho Tau (181 P) Assay ELISA #27812 was 3.06 pg/ml. Assay ranges for t-tau and p181tau were 17.2–1,100 pg/ml and 3.6–230 pg/ml, respectively. Intra- and inter-assay coefficients of variation were 1.7–3.2 % in the t-tau assay and 2.0–4.5 % in the p181tau assay. In accordance with the manufacturers' instructions, the assay ranges of Phinoscholar®•hTAU for t-tau and Phinoscholar®•pTAU for p181tau were 75–1,200 and 25–500 pg/ml, respectively. Intra- and inter-assay coefficients of variation were also less than 10 % in both assay systems. These findings suggested that basic assay accuracy and precision of both ELISA #27811 for t-tau and ELISA #27812 for p181tau were sufficient compared with those for Phinoscholar®•hTAU and pTAU. The assay range of ELISA #27812 is narrower than Phinoscholar®•pTAU. However, our previous study in a separate group of subjects [21] showed CSF p181tau levels were 41.7 ± 19 pg/ml in control subjects and significantly increased to 88.62 ± 29.69 pg/ml in patients with AD and mild cognitive impairment (MCI) in the Phinoscholar®•pTAU assay. In the present results, p181tau levels measured using Phinoscholar®•pTAU were 99.78 ± 31.83 pg/ml in patients with ADD, 45.18 ± 13.45 pg/ml in CU. Both p181tau assay results implied that ELISA #27812 can evaluate a wide range of CSF p181tau values in patients with AD and MCI within the assay rage of ELISA #27812.

Then, we evaluated the associations between two different assay systems for CSF t-tau and p181tau. Simple regression analysis was carried out between t-tau values measured using ELISA #27811 and those using Phinoscholar®•hTAU, and between p181tau values measured using ELISA #27812 and those using Phinoscholar®•pTAU. These analyses showed significant strong correlations for t-tau (regression coefficient = 0.9641, coefficient of determination: $r^2 = 0.9229$, $p < 0.0001$) and for p181tau (regression coefficient = 0.9686, coefficient of determination: $r^2 = 0.9601$, $p < 0.0001$). These data indicated the presence of highly similar linearities between the measured values using ELISA #27811 and Phinoscholar®•hTAU and between ELISA #27812 and Phinoscholar®•pTAU. For this reason, both assay systems functioned almost identically and it may be feasible to assay t-tau and

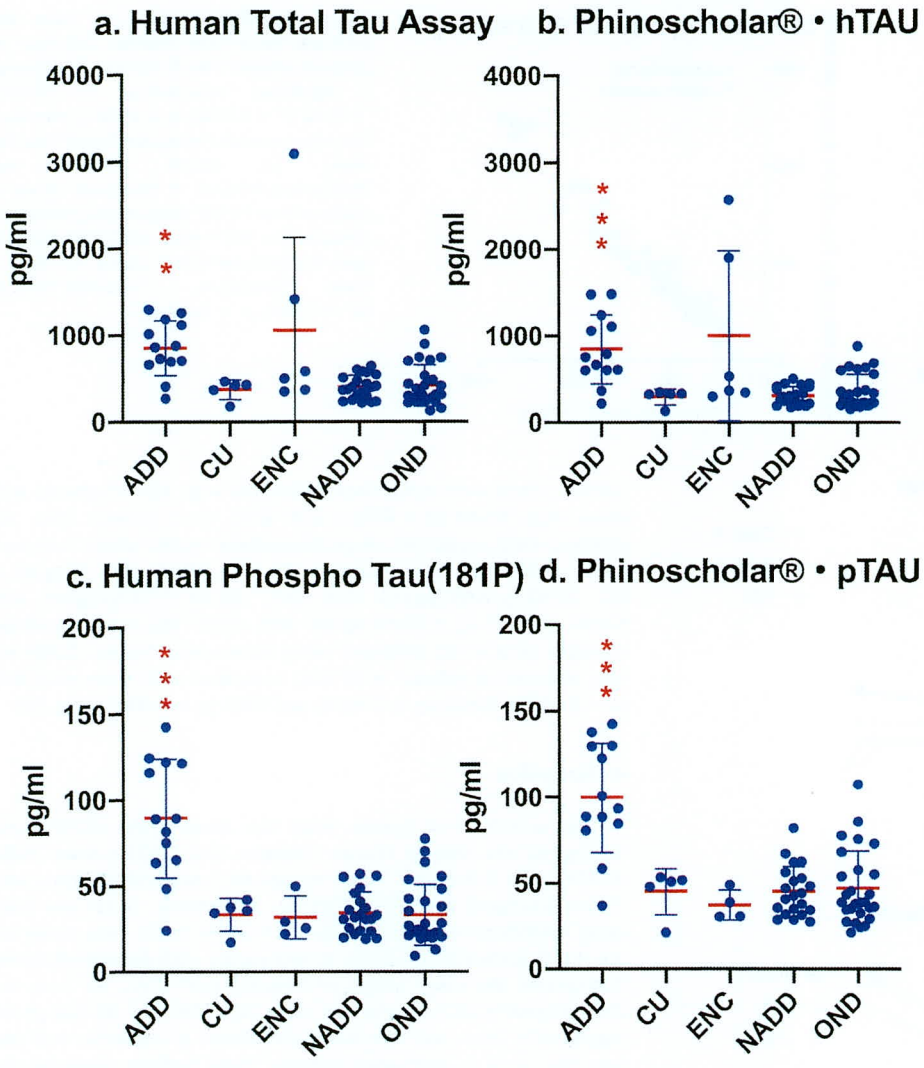

Fig. 3. T-tau and p181tau levels in various neurological diseases. a Significant increase of t-tau levels measured using the Human Total Tau Assay kit (ELISA #27811) recognized in patients with ADD compared with those with NADD $p < 0.0040$ and OND $p < 0.0012$. b The same significant elevation of t-tau measured using Phinoscholar®•hTAU observed in patients with ADD compared with those with NADD $p < 0.0009$ and OND $p < 0.0009$. c Significant increase of p181tau levels measured using the Human Phospho Tau 181 P Assay kit (ELISA #27812) recognized in patients with ADD compared with those with NADD $p = 0.001$ and OND $p < 0.0001$. d The same significant elevation of p181tau measured using Phinoscholar®•pTAU ELISA kits observed in patients with ADD compared with those with ENC $P = 0.0133$, NADD $p = 0.0004$ and OND $p = 0.0001$.

p181tau although the number of neurological disorders was small.

Then, we evaluated ELISAs #27811 and #27812 for whether the measured t-tau and p181tau values actually detected brain neurodegeneration processes in as "N" and tauopathy as "T", which are newly adopted research diagnostic criteria for AD. As shown in Fig. 3, assay values using ELISA #27811 significantly detected neurodegeneration in patients with ADD and ENC (Fig. 3a). ELISA #27812 specifically detected tauopathy in patients with ADD (Fig. 3c). These findings were essentially identical to those obtained using the Phinoscholar®•hTAU and pTAU assay systems. Thus, ELISAs #27811 and #27812 were able to evaluate the presence of neurodegeneration and tauopathy as well as conventical Phinoscholar® systems.

Accidental contamination with blood is a frequent occurrence in lumber puncture procedures and routine in cerebrovascular disease and central nervous system infection [22,23]. In these diseases, CSF protein levels and white and red blood cell counts are prominently increased. Previously, we and others indicated that markedly increased CSF t-tau in cerebrovascular diseases and meningoencephalitis in Phinoscholar® hTAU assay in spite of Phinoscholar®•pTAU [21,24]. Tau and other proteins may likewise be affected by binding proteins or degradation by proteases present in plasma [25,26]. If CSF samples were spiked with 5,000 erythrocytes/μL, small but significant increases in p181tau concentration of 11 % [27] or 14 % [28] were recorded using Phinoscholar®•pTAU. For this reason, CSF samples with apparent blood contamination or with hemolysis are usually excluded before assaying. However, our study showed that small amount of serum or hemoglobin did not affect the #27811 and #27812 ELISA systems. Our dilution tests using 2 ENC patients and normal subjects showed clear linearity in the assay values. Recovery tests with the addition of serum and hemoglobin in normal control CSF samples showed 84–103 % recovery rates. These findings also suggested that the #27811 and #27812 ELISAs assay are safe and effective even with low levels of blood contamination.

Recent progress in biomarker studies has clarified trace amount of plasma t-tau and p181tau can be measured using newly developed devices, and it is feasible to predict and diagnose the onset of MCI and AD [28,29]. If CSF t-tau and p181tau assays can be translated into blood biomarker assays, as reported, these will provide substantial progress in biomarker studies for AD. Although usage of our assay system was limited within a CSF study, such basic studies are useful for application to blood assay systems. We are planning to expand our assay system for further application to plasma assay systems.

5. Conclusions

The #27811 and #27812 ELISAs described here are reliable assay systems for CSF t-tau and p181tau similar to commonly used commercial ELISAs, Phinoscholar®•hTAU and Phinoscholar®•pTAU.

Funding

This study was supported by the Amyloidosis Research Committee Surveys and Research on Special Diseases, the Longevity Science Committee of the Ministry of Health and Welfare of Japan; Scientific Research (C) (18K07385 MS, 19K07989 TK) from the Ministry of Education, Science, and Culture of Japan.

CRediT authorship contribution statement

Takeshi Kawarabayashi: Conceptualization, Methodology, Investigation, Writing - original draft, Funding acquisition. **Takumi Nakamura:** Investigation. **Kazuya Miyashita:** Investigation, Formal analysis. **Isamu Fukamachi:** Investigation, Visualization. **Yusuke Seino:** Investigation. **Mikio Shoji:** Project administration, Software, Validation, Writing - review & editing, Supervision, Funding acquisition.

Declaration of Competing Interest

The authors have no conflict of interest to report.

Acknowledgments

We thank Naoko Nakahata for research assistance. This study was approved by the Ethics Committee of Hirosaki University (2017-112). All participants provided written informed consent. I. F., and M. S. conceptualized and designed the study. T. K, T. N., Y. S., K. M. acquired and analyzed the data. T. K., I. F., and M.S. drafted the text and prepared the figures.

References

[1] L.M. Shaw, H. Vanderstichele, M. Knapik-Czajka, C.M. Clark, P.S. Aisen, R.C. Petersen, K. Blennow, H. Soares, A. Simon, P. Lewczuk, R. Dean, E. Siemers, W. Potter, V.M. Lee, J.Q. Trojanowski, Cerebrospinal fluid biomarker signature in Alzheimer's disease neuroimaging initiative subjects, Ann. Neurol. 65 (2009) 403–413, https://doi.org/10.1002/ana.21610 PMID: 19296504; PubMed Central PMCID: PMC2696350.

[2] S.E. Schindler, J.D. Gray, B.A. Gordon, C. Xiong, R. Batrla-Utermann, M. Quan, S. Wahl, T.L.S. Benzinger, D.M. Holtzman, J.C. Morris, A.M. Fagan, Cerebrospinal fluid biomarkers measured by Elecsys assays compared to amyloid imaging, Alzheimers Dement. 14 (2018) 1460–1469, https://doi.org/10.1016/j.jalz.2018.01.012 PMID:29580670; PubMed Central PMCID: PMC6110083.

[3] R.J. Bateman, C. Xiong, T.L. Benzinger, A.M. Fagan, A. Goate, N.C. Fox, D.S. Marcus, N.J. Cairns, X. Xie, T.M. Blazey, D.M. Holtzman, A. Santacruz, V. Buckles, A. Oliver, K. Moulder, P.S. Aisen, B. Ghetti, W.E. Klunk, E. McDade, R.N. Martins, C.L. Masters, R. Mayeux, J.M. Ringman, M.N. Rossor, P.R. Schofield, R.A. Sperling, S. Salloway, J.C. Morris, Clinical and biomarker changes in dominantly inherited Alzheimer's disease, N. Engl. J. Med. 367 (2012) 795–804, https://doi.org/10.1056/NEJMoa1202753 Erratum in: N Engl J Med. 367(8) (2012) 780. PubMed PMID: 22784036; PubMed Central PMCID: PMC3474597.

[4] A.M. Fagan, C. Xiong, M.S. Jasielec, R.J. Bateman, A.M. Goate, T.L. Benzinger, B. Ghetti, R.N. Martins, C.L. Masters, R. Mayeux, J.M. Ringman, M.N. Rossor, S. Salloway, P.R. Schofield, R.A. Sperling, D. Marcus, N.J. Cairns, V.D. Buckles, J.H. Ladenson, J.C. Morris, D.M. Holtzman, Longitudinal change in CSF biomarkers in autosomal-dominant Alzheimer's disease, Sci. Transl. Med. 6 (2014) 226ra230, , https://doi.org/10.1126/scitranslmed.3007901 PubMed PMID: 24598588; PubMed Central PMCID: PMC4038930.

[5] B. Olsson, R. Lautner, U. Andreasson, A. Ohrfelt, E. Portelius, M. Bjerke, M. Holtta, C. Rosen, C. Olsson, G. Strobel, E. Wu, K. Dakin, M. Petzold, K. Blennow, H. Zetterberg, CSF and blood biomarkers for the diagnosis of Alzheimer's disease: a systematic review and meta-analysis, Lancet Neurol. 15 (2016) 673–684, https://doi.org/10.1016/S1474-4422(16)00070-3 Review. PubMed PMID: 27068280.

[6] C.R. Jack Jr., D.A. Bennett, K. Blennow, M.C. Carrillo, B. Dunn, S.B. Haeberlein, D.M. Holtzman, W. Jagust, F. Jessen, J. Karlawish, E. Liu, J.L. Molinuevo, T. Montine, C. Phelps, K.P. Rankin, C.C. Rowe, P. Scheltens, E. Siemers, H.M. Snyder, R. Sperling, NIA-AA Research Framework: toward a biological definition of alzheimer's disease, Alzheimers Dement. 14 (2018) 535–562, https://doi.org/10.1016/j.jalz.2018.02.018 Review. PubMed PMID: 29653606; PubMed Central PMCID: PMC5958625.

[7] H. Hampel, K. Buerger, R. Zinkowski, S.J. Teipel, A. Goernitz, N. Andreasen, M. Sjoegren, J. DeBernardis, D. Kerkman, K. Ishiguro, H. Ohno, E. Vanmechelen, H. Vanderstichele, C. McCulloch, H.J. Moller, P. Davies, K. Blennow, Measurement of phosphorylated tau epitopes in the differential diagnosis of Alzheimer disease: a comparative cerebrospinal fluid study, Arch. Gen. Psychiatry 61 (2004) 95–102, https://doi.org/10.1001/archpsyc.61.1.95 PubMed PMID: 14706948.

[8] E. Vanmechelen, H. Vanderstichele, P. Davidsson, E. Van Kerschaver, B. Van Der Perre, M. Sjogren, N. Andreasen, K. Blennow, Quantification of tau phosphorylated at threonine 181 in human cerebrospinal fluid: a sandwich ELISA with a synthetic phosphopeptide for standardization, Neurosci. Lett. 285 (2000) 49–52, https://doi.org/10.1016/s0304-3940(00)01036-3 PubMed PMID: 10788705.

[9] H. Arai, M. Terajima, M. Miura, S. Higuchi, T. Muramatsu, N. Machida, H. Seiki, S. Takase, C.M. Clark, V.M. Lee, et al., Tau in cerebrospinal fluid: a potential diagnostic marker in Alzheimer's disease, Ann. Neurol. 38 (1995) 649–652, https://doi.org/10.1002/ana.410380414 PubMed PMID: 7574462.

[10] A. Olsson, H. Vanderstichele, N. Andreasen, G. De Meyer, A. Wallin, B. Holmberg, L. Rosengren, E. Vanmechelen, K. Blennow, Simultaneous measurement of beta-amyloid(1-42), total tau, and phosphorylated tau (Thr181) in cerebrospinal fluid by the xMAP technology, Clin. Chem. 51 (2005) 336–345, https://doi.org/10.1373/clinchem.2004.039347 PubMed PMID: 15563479.

[11] P. Lewczuk, J. Kornhuber, H. Vanderstichele, E. Vanmechelen, H. Esselmann, M. Bibl, S. Wolf, M. Otto, U. Reulbach, H. Kolsch, F. Jessen, J. Schroder, P. Schonknecht, H. Hampel, O. Peters, E. Weimer, R. Perneczky, H. Jahn, C. Luckhaus, U. Lamla, T. Supprian, J.M. Maler, J. Wiltfang, Multiplexed quantification of dementia biomarkers in the CSF of patients with early dementias and MCI: a multicenter study, Neurobiol. Aging 29 (2008) 812–818, https://doi.org/10.1016/j.neurobiolaging.2006.12.010 PubMed PMID: 17239996.

[12] S.E. Schindler, J.D. Gray, B.A. Gordon, C. Xiong, R. Batrla-Utermann, M. Quan, S. Wahl, T.L.S. Benzinger, D.M. Holtzman, J.C. Morris, A.M. Fagan, Cerebrospinal fluid biomarkers measured by Elecsys assays compared to amyloid imaging, Alzheimers Dement. 14 (2018) 1460–1469, https://doi.org/10.1016/j.jalz.2018.01.013 PubMed PMID: 29501462; PubMed Central PMCID: PMC6119652.

[13] O. Hansson, J. Seibyl, E. Stomrud, H. Zetterberg, J.Q. Trojanowski, T. Bittner, V. Lifke, V. Corradini, U. Eichenlaub, R. Batrla, K. Buck, K. Zink, C. Rabe, K. Blennow, L.M. Shaw, CSF biomarkers of Alzheimer's disease concord with amyloid-beta PET and predict clinical progression: a study of fully automated immunoassays in BioFINDER and ADNI cohorts, Alzheimers Dement. 14 (2018) 1470–1481, https://doi.org/10.1016/j.jalz.2018.01.010 PubMed PMID: 29499171; PubMed Central PMCID: PMC6119541.

[14] K. Rascovsky, J.R. Hodges, D. Knopman, M.F. Mendez, J.H. Kramer, J. Neuhaus, J.C. van Swieten, H. Seelaar, E.G. Dopper, C.U. Onyike, A.E. Hillis, K.A. Josephs, B.F. Boeve, A. Kertesz, W.W. Seeley, K.P. Rankin, J.K. Johnson, M.L. Gorno-Tempini, H. Rosen, C.E. Prioleau-Latham, A. Lee, C.M. Kipps, P. Lillo, O. Piguet, J.D. Rohrer, M.N. Rossor, J.D. Warren, N.C. Fox, D. Galasko, D.P. Salmon, S.E. Black, M. Mesulam, S. Weintraub, B.C. Dickerson, J. Diehl-Schmid, F. Pasquier, V. Deramecourt, F. Lebert, Y. Pijnenburg, T.W. Chow, F. Manes, J. Grafman, S.F. Cappa, M. Freedman, M. Grossman, B.L. Miller, Sensitivity of revised diagnostic criteria for the behavioural variant of frontotemporal dementia, Brain 134 (2011) 2456–2477, https://doi.org/10.1093/brain/awr179 PubMed PMID: 21810890; PubMed Central PMCID: PMC3170532.

[15] L. Chare, J.R. Hodges, C.E. Leyton, C. McGinley, R.H. Tan, J.J. Kril, G.M. Halliday, New criteria for frontotemporal dementia syndromes: clinical and pathological diagnostic implications, Journal of neurology, neurosurgery, Psychiatry 85 (2014) 865–870, https://doi.org/10.1136/jnnp-2013-306948 PubMed PMID: 24421286.

[16] M.J. Armstrong, I. Litvan, A.E. Lang, T.H. Bak, K.P. Bhatia, B. Borroni, A.L. Boxer, D.W. Dickson, M. Grossman, M. Hallett, K.A. Josephs, A. Kertesz, S.E. Lee, B.L. Miller, S.G. Reich, D.E. Riley, E. Tolosa, A.I. Troster, M. Vidailhet, W.J. Weiner, Criteria for the diagnosis of corticobasal degeneration, Neurology 80 (2013) 496–503, https://doi.org/10.1212/WNL.0b013e31827f0fd1 PubMed PMID: 3359374; PubMed Central PMCID: PMC3590050.

[17] G.U. Hoglinger, G. Respondek, M. Stamelou, C. Kurz, K.A. Josephs, A.E. Lang, B. Mollenhauer, U. Muller, C. Nilsson, J.L. Whitwell, T. Arzberger, E. Englund, E. Gelpi, A. Giese, D.J. Irwin, W.G. Meissner, A. Pantelyat, A. Rajput, J.C. van Swieten, C. Troakes, A. Antonini, K.P. Bhatia, Y. Bordelon, Y. Compta, J.C. Corvol, C. Colosimo, D.W. Dickson, R. Dodel, L. Ferguson, M. Grossman, J. Kassubek, F. Krismer, J. Levin, S. Lorenzl, H.R. Morris, P. Nestor, W.H. Oertel, W. Poewe, G. Rabinovici, J.B. Rowe, G.D. Schellenberg, K. Seppi, T. van Eimeren, G.K. Wenning, A.L. Boxer, L.I. Golbe, I. Litvan, Clinical diagnosis of progressive supranuclear palsy: the movement disorder society criteria, Mov. Disord. 32 (2017) 853–864, https://doi.org/10.1002/mds.26987 PubMed PMID:28467028; PubMed Central PMCID: PMC5516529.

[18] M. de Carvalho, R. Dengler, A. Eisen, J.D. England, R. Kaji, J. Kimura, K. Mills, H. Mitsumoto, H. Nodera, J. Shefner, M. Swash, Electrodiagnostic criteria for diagnosis of ALS, Clin. Neurophysiol. 119 (2008) 497–503, https://doi.org/10.1016/j.clinph.2007.09.143 Review. PubMed PMID: 18164242.

[19] S. Gilman, G.K. Wenning, P.A. Low, D.J. Brooks, C.J. Mathias, J.Q. Trojanowski, N.W. Wood, C. Colosimo, A. Durr, C.J. Fowler, H. Kaufmann, T. Klockgether, A. Lees, W. Poewe, N. Quinn, T. Revesz, D. Robertson, P. Sandroni, K. Seppi, M. Vidailhet, Second consensus statement on the diagnosis of multiple system atrophy, Neurology 71 (2008) 670–676, https://doi.org/10.1212/01.wnl.0000324625.00404.15 PubMed PMID: 18725592; PubMed Central PMCID: PMC2676993.

[20] R.B. Postuma, D. Berg, M. Stern, W. Poewe, C.W. Olanow, W. Oertel, J. Obeso, K. Marek, I. Litvan, A.E. Lang, G. Halliday, C.G. Goetz, T. Gasser, B. Dubois, P. Chan, B.R. Bloem, C.H. Adler, G. Deuschl, MDS clinical diagnostic criteria for Parkinson's disease, Mov. Disord. 30 (2015) 1591–1601, https://doi.org/10.1002/mds.26431 Review. PubMed PMID: 26474317.

[21] Y. Seino, T. Nakamura, T. Kawarabayashi, M. Hirohata, S. Narita, Y. Wakasaya, K. Kaito, T. Ueda, Y. Harigaya, M. Shoji, Cerebrospinal Fluid and Plasma Biomarkers in Neurodegenerative Diseases, J. Alzheimers Dis. 68 (2019) 395–404,

https://doi.org/10.3233/JAD-181152 PubMed PMID: 30814356.
[22] K.H. Shah, K.M. Richard, S. Nicholas, J.A. Edlow, Incidence of traumatic lumbar puncture, Academic emergency medicine: official journal of the Society for Academic Emergency Medicine 10 (2003) 151–154 PubMed PMID: 12574013.
[23] O. Hansson, A. Mikulskis, A.M. Fagan, C. Teunissen, H. Zetterberg, H. Vanderstichele, J.L. Molinuevo, L.M. Shaw, M. Vandijck, M.M. Verbeek, M. Savage, N. Mattsson, P. Lewczuk, R. Batrla, S. Rutz, R.A. Dean, K. Blennow, The impact of preanalytical variables on measuring cerebrospinal fluid biomarkers for Alzheimer's disease diagnosis: a review, Alzheimers Dement. 14 (2018) 1313–1333, https://doi.org/10.1016/j.jalz.2018.05.008 PubMed PMID: 29940161.
[24] M. Shoji, E. Matsubara, T. Murakami, Y. Manabe, K. Abe, M. Kanai, M. Ikeda, Y. Tomidokoro, M. Shizuka, M. Watanabe, M. Amari, K. Ishiguro, T. Kawarabayashi, Y. Harigaya, K. Okamoto, T. Nishimura, Y. Nakamura, M. Takeda, K. Urakami, Y. Adachi, K. Nakashima, H. Arai, H. Sasaki, K. Kanemaru, H. Yamanouchi, Y. Yoshida, K. Ichise, K. Tanaka, M. Hamamoto, H. Yamamoto, T. Matsubayashi, H. Yoshida, H. Toji, S. Nakamura, S. Hirai, Cerebrospinal fluid tau in dementia disorders: a large scale multicenter study by a Japanese study group, Neurobiol. Aging 23 (2002) 363–370 PubMed PMID: 11959397.
[25] P. Lewczuk, P. Riederer, S.E. O'Bryant, M.M. Verbeek, B. Dubois, P.J. Visser, K.A. Jellinger, S. Engelborghs, A. Ramirez, L. Parnetti, C.R. Jack Jr., C.E. Teunissen, H. Hampel, A. Lleo, F. Jessen, L. Glodzik, M.J. de Leon, A.M. Fagan, J.L. Molinuevo, W.J. Jansen, B. Winblad, L.M. Shaw, U. Andreasson, M. Otto, B. Mollenhauer, J. Wiltfang, M.R. Turner, I. Zerr, R. Handels, A.G. Thompson, G. Johansson, N. Ermann, J.Q. Trojanowski, I. Karaca, H. Wagner, P. Oeckl, L. van Waalwijk van Doorn, M. Bjerke, D. Kapogiannis, H.B. Kuiperij, L. Farotti, Y. Li, B.A. Gordon, S. Epelbaum, S.J.B. Vos, C.J.M. Klijn, W.E. Van Nostrand, C. Minguillon, M. Schmitz, C. Gallo, A. Lopez Mato, F. Thibaut, S. Lista, D. Alcolea, H. Zetterberg, K. Blennow, J. Kornhuber, Cerebrospinal fluid and blood biomarkers for neurodegenerative dementias: an update of the consensus of the task force on biological markers in psychiatry of the world federation of societies of biological psychiatry, World J. Biol. Psychiatry 19 (2018) 244–328, https://doi.org/10.1080/15622975.2017.1375556 PubMed PMID: 29076399; PubMed Central PMCID: PMC5916324.
[26] S.A. Park, J.H. Kang, E.S. Kang, C.S. Ki, J.H. Roh, Y.C. Youn, S.Y. Kim, S.Y. Kim, A consensus in Korea regarding a protocol to reduce preanalytical sources of variability in the measurement of the cerebrospinal fluid biomarkers of Alzheimer's disease, J. Clin. Neurol. 11 (2015) 132–141, https://doi.org/10.3988/jcn.2015.11.2.132 PubMed PMID: 25851891; PubMed Central PMCID: PMC4387478.
[27] M.J. Leitao, I. Baldeiras, S.K. Herukka, M. Pikkarainen, V. Leinonen, A.H. Simonsen, A. Perret-Liaudet, A. Fourier, I. Quadrio, P.M. Veiga, C.R. de Oliveira, Chasing the effects of pre-analytical confounders - a multicenter study on CSF-AD biomarkers, Front. Neurol. 6 (2015) 153, https://doi.org/10.3389/fneur.2015.00153 PubMed PMID: 26217300; PubMed Central PMCID: PMC4495343.
[28] H. Tatebe, T. Kasai, T. Ohmichi, Y. Kishi, T. Kakeya, M. Waragai, M. Kondo, D. Allsop, T. Tokuda, Quantification of plasma phosphorylated tau to use as a biomarker for brain Alzheimer pathology: pilot case-control studies including patients with Alzheimer's disease and down syndrome, Mol. Neurodegener. 12 (2017) 63, https://doi.org/10.1186/s13024-017-0206-8 PubMed PMID: 28866979; PubMed Central PMCID: PMC5582385.
[29] M.M. Mielke, C.E. Hagen, J. Xu, X. Chai, P. Vemuri, V.J. Lowe, D.C. Airey, D.S. Knopman, R.O. Roberts, M.M. Machulda, C.R. Jack Jr., R.C. Petersen, J.L. Dage, Plasma phospho-tau181 increases with Alzheimer's disease clinical severity and is associated with tau- and amyloid-positron emission tomography, Alzheimers Dement. 14 (2018) 989–997, https://doi.org/10.1016/j.jalz.2018.02.013 PubMed PMID: 29626426; PubMed Central PMCID: PMC6097897.

ORIGINAL ARTICLE

Nationwide survey on cerebral amyloid angiopathy in Japan

K. Sakai[a], M. Ueda[b], W. Fukushima[c], A. Tamaoka[d], M. Shoji[e], Y. Ando[b] and M. Yamada[a]

[a]*Department of Neurology and Neurobiology of Aging, Kanazawa University Graduate School of Medical Sciences, Kanazawa;* [b]*Department of Neurology, Graduate School of Medical Sciences, Kumamoto University, Kumamoto;* [c]*Department of Public Health, Osaka City University Graduate School of Medicine, Osaka;* [d]*Department of Neurology, Faculty of Medicine, University of Tsukuba, Tsukuba; and* [e]*Department of Neurology, Hirosaki University Graduate School of Medicine, Hirosaki, Japan*

Keywords:
cerebral amyloid angiopathy, hemorrhage, inflammation, nationwide survey, vasculitis

Received 28 December 2018
Accepted 18 June 2019

European Journal of Neurology 2019, **0:** 1–7

doi:10.1111/ene.14031

Background and purpose: A nationwide survey was conducted to understand the epidemiology of cerebral amyloid angiopathy-related intracerebral hemorrhage (CAA-related ICH) and cerebral amyloid angiopathy-related inflammation/vasculitis (CAA-ri) in Japan.

Methods: To estimate the total number and clinical features of patients with CAA-related ICH and CAA-ri between January 2012 and December 2014 and to analyze their clinical features, questionnaires were sent to randomly selected hospitals in Japan.

Results: In the first survey, 2348 of 4657 departments responded to the questionnaire (response rate 50.4%). The total numbers of reported patients with CAA-related ICH and CAA-ri were 1338 and 61, respectively, and their total numbers in Japan were estimated to be 5900 [95% confidence interval (CI) 4800–7100] and 170 (95% CI 110–220), respectively. The crude prevalence rates were 4.64 and 0.13 per 100 000 population, respectively. The clinical information of 474 patients with CAA-related ICH obtained in the second survey was as follows: (i) the average age of onset was 78.4 years; (ii) the prevalence increased with age; (iii) the disease was common in women; and (iv) hematoma most frequently occurred in the frontal lobe. Sixteen patients with CAA-ri for whom data were collected in the second survey had the following characteristics: (i) median age of onset was 75 years; (ii) cognitive impairment and headache were the most frequent initial manifestations; and (iii) focal neurological signs, such as motor paresis and visual disturbance, were frequently observed during the clinical course.

Conclusions: The numbers of patients with CAA-related ICH and CAA-ri in Japan were estimated.

Introduction

Cerebral amyloid angiopathy (CAA) is characterized by amyloid deposition in the blood vessel walls of the brain and leptomeninges and causes several neurological conditions, such as intracerebral hemorrhages (ICHs) and inflammation with and without granulomatous vasculitis [1,2]. Sporadic amyloid β-protein (Aβ) type CAA is the most common form of CAA [3].

Correspondence: Masahito Yamada, Department of Neurology and Neurobiology of Aging, Kanazawa University Graduate School of Medical Sciences, 13-1 Takara-machi, Kanazawa 920-8640, Japan (tel.: +81 76 265 2290, fax: +81 76 234 4253; e-mail: m-yamada@med.kanazawa-u.ac.jp).

A previous nationwide survey of patients with CAA in Japan revealed the clinical features of CAA-related ICH, including its parietal predilection, significant female predominance, and prognosis [4]. In this study, the crude number, prevalence and clinical features of patients with not only CAA-related ICH but also CAA-related inflammation/vasculitis (CAA-ri) were examined using a nationwide survey in Japan.

Methods

A nationwide survey of CAA-related ICH and CAA-ri was conducted by the Amyloidosis Research

Committee. The survey comprised two stages. The first stage of the survey was conducted to estimate the number of CAA-related ICH and CAA-ri patients. The total numbers of patients with suspected or confirmed CAA-related ICH and CAA-ri who visited hospitals in Japan between January 2012 and December 2014 were collected. The second survey aimed to clarify the clinicoepidemiological characteristics of CAA-related ICH and CAA-ri.

Clinical diagnostic criteria for CAA-related ICH based on the Boston criteria [5] (Table S1) and CAA-ri based on previously proposed criteria [6] (Table S2) were used to recognize appropriate patients. The original criteria had a specific age restriction; however, age was removed from the criteria for cases without a pathological diagnosis to collect more information about patients.

First-stage survey

The departments of neurology, gastroenterology, cardiology, neurosurgery, urology, rheumatology, hematology and nephrology from all hospitals in Japan were listed. These hospitals were categorized according to the institution type and the number of hospital beds. Hospitals were then randomly selected from each category. The sampling rates were 2.5% for general hospitals with 99 or fewer beds, 5% for hospitals with 100–199 beds, 10% for hospitals with 200–299 beds, 20% for hospitals with 300–399 beds, 40% for hospitals with 400–499 beds and 100% for hospitals with 500 or more beds. University hospitals and special departments where patients with CAA-related ICH and CAA-ri were likely to visit were also included, with the additional restriction that at least one department should be sampled in one prefecture. To ensure the feasibility of the study, the sampling rates that were used in previous nationwide epidemiological surveys were modified [7–9]. The number of surveyed departments, the actual sampling rate and the response rate are shown in Table S3. Some hospitals that were expected to treat many patients were also selected and were included in the 'selected hospitals' category.

The questionnaire, which simply enquired about the number of patients with CAA-related ICH and CAA-ri who visited the hospital between January 2012 and December 2014, was mailed out to the hospital. The estimated number with a 95% confidence interval (CI) was calculated using the method reported in previous studies [9]. The population of Japan in 2015 (n = 127 094 745) was used to calculate the prevalence rate.

Second-stage survey

A second questionnaire on the detailed clinical features of each patient, including clinical features, brain imaging, laboratory tests and pathological examinations (Tables S4 and S5), was sent to 842 hospitals, which answered that there were the appropriate patients in the first-stage survey. Those patients who did not meet the clinical diagnostic criteria were excluded. Duplicate cases were also excluded. The clinical and pathological features of the patients with CAA-related ICH and CAA-ri were analyzed.

Statistical analysis

Fisher's exact probability test irrespective of the number of patients in each cell was used to analyze female-to-male ratio and site distribution of hematoma in the cerebral cortex. The estimated cortical volumes (%) were used to assess the relationship between cortical volumes and the site distribution of the hematoma: 41.0% frontal lobe, 19.3% parietal lobe, 22.3% temporal lobe and 18.3% occipital lobe [10]. Statistical significance was defined as $P < 0.05$. Statistical analysis was performed using SPSS version 22 (IBM, Armonk, NY, USA).

The paper was prepared based on the Standards of Reporting of Neurological Disorders guidelines [11].

Ethical approval

This study was approved by the institutional review board of the Graduate School of Medical Sciences, Kumamoto University, and the medical ethics committee of Kanazawa University. As this survey used anonymized pre-existing medical data, informed consent from each patient was waived.

Results

Estimated number and prevalence of patients with CAA-related ICH and CAA-ri in Japan

In the first-stage survey, 2348 out of 4657 departments responded to the questionnaire (response rate 50.4%). The reported numbers of patients with CAA-related ICH and CAA-ri were 1338 and 61, respectively (Table S3). The total numbers of patients with CAA-related ICH and CAA-ri were estimated to be 5900 (95% CI 4800–7100) and 170 (95% CI 110–220), respectively. The crude prevalence rates of CAA-related ICH and CAA-ri were 4.64 and 0.13 per 100 000 population, respectively.

Analysis of patients with CAA-related ICH identified by the second-stage survey

In the second-stage survey, 369 of 842 departments responded to the questionnaire (response rate 43.8%). A total of 474 cases with CAA-related ICH were examined. Some patients received a diagnosis of ICH by computed tomography study only. Regarding magnetic resonance imaging (MRI), detailed methods of MRI scans in each case were unavailable. The results are summarized in Table 1. Eleven cases (2.3%) were less than 55 years of age at disease onset. All patients had no apparent family history of CAA. Eighty-six of 439 (19.7%) patients also received a diagnosis of Alzheimer's disease. The clinical manifestations are summarized in Table 2.

With regard to age distribution (Fig. 1a, b), the prevalence increased with age. CAA commonly occurred in individuals aged between 75 and 84 years. Regarding the prevalence of CAA-related ICH calculated according to the population in 2015, the most frequently affected individuals were those aged between 85 and 94 years (Fig. 1b). Significant female predominance was observed. The calculated female-to-male ratio was 1.48, whereas the female-to-male ratio for the population over 35 years old in Japan in 2015 was 1.11 ($P = 0.001$, for differences in proportions between men and women).

The sites of hematoma at the first episode of hemorrhage were described in 462 patients. Hemorrhage frequently occurred in the frontal lobe (32.3%), followed by the parietal lobe (21.9%), temporal lobe (15.6%), occipital lobe (8.9%) and cerebellum (0.4%). More than two cerebral lobes were involved in 89 (19.3%) cases. There were insufficient data regarding the area of the cerebral hematoma in eight (1.7%) cases. In cases with ICH showing hematoma confined to one cerebral lobe (363 patients), the parietal lobe was a more probable site of ICH based on the estimated cortical volume ($P = 0.047$), whereas the occipital lobe was a less probable site of ICH based on the estimated cortical volume ($P = 0.057$). The hematoma was uniformly distributed as per the cortical volume in frontal ($P = 0.544$) and temporal ($P = 0.363$) lobes.

Neuropathological examinations were carried out in 40 out of 474 (8.4%) cases, including three cases with autopsy and 37 cases with biopsy. In the autopsied

Table 1 Characteristics of the CAA-related ICH cases analyzed

	Total	Definite	Probable CAA with supporting pathology	Probable	Possible
Number of patients	474	15	25	157	277
Male/female	191/283	3/12	12/13	53/104	123/154
Age at onset (years)[a]	78.4 ± 10.0 (37–99)	76.5 ± 6.1 (57–83)	76.4 ± 5.7 (59–85)	78.1 ± 9.2 (53–97)	78.4 ± 10.9 (37–99)
Follow-up periods (months)[a]	9.0 ± 19.3 (0–157)	8.0 ± 18.2 (0–69)	8.3 ± 17.3 (0–78)	15.5 ± 27.8 (0–157)	5.7 ± 11.4 (0–95)
Use of antithrombotic treatments					
Antiplatelet drugs	67 (14.3%)	3 (20%)	4 (16%)	18 (11.5%)	42 (15.2%)
Anticoagulant drugs	27 (5.7%)	0 (0%)	4 (16%)	5 (3.2%)	18 (6.5%)
Both	8 (1.7%)	0 (0%)	1 (4%)	0 (0%)	7 (2.5%)
Occurrence of the hemorrhage					
Single	311 (65.6%)	10 (66.7%)	20 (80%)	0 (0%)	271 (97.8%)
Recurrent	80 (16.9%)	4 (26.7%)	3 (12%)	82 (52.2%)	0 (0%)
Simultaneous multiple	62 (13.1%)	0 (0%)	2 (8%)	60 (38.2%)	0 (0%)
Recurrence of the hemorrhage					
Once	35 (7.4%)	2 (13%)	0 (0%)	33 (20.4%)	0 (0%)
Twice	26 (5.5%)	2 (13%)	2 (8%)	22 (14.0%)	0 (0%)
Three times	10 (2.1%)	0 (0%)	0 (0%)	10 (5.7%)	0 (0%)
Four times	3 (0.6%)	1 (6.7%)	0 (0%)	2 (1.3%)	0 (0%)
Five times	0 (0%)	0 (0%)	0 (0%)	0 (0%)	0 (0%)
Six times	1 (0.2%)	0 (0%)	0 (0%)	1 (0.6%)	0 (0%)
Treatment					
Conservative	399 (83.8%)	1 (6.7%)	1 (4%)	144 (91.7%)	252 (91.0%)
Operation	60 (12.7%)	12 (80%)	23 (92%)	9 (5.7%)	16 (5.8%)
Hematoma suction	5 (1.1%)	0 (0%)	1 (4%)	1 (0.6%)	3 (1.1%)
Small vessel disease markers					
Cerebral cortical microbleeds	186 (39.2%)	7 (46.7%)	10 (40%)	60 (38.2%)	109 (39.4%)
Cortical microinfarcts	134 (28.3%)	5 (33.3%)	9 (36%)	39 (24.8%)	81 (29.2%)
Cerebral white matter lesions	161 (34.0%)	3 (20%)	5 (20%)	57 (36.3%)	96 (34.7%)

CAA, cerebral amyloid angiopathy; ICH, intracerebral hemorrhage. [a]Mean ± SD (range).

Table 2 Manifestations of CAA-related ICH

	First episode	Second episode	Third episode	Fourth episode	Fifth episode
Number of patients	442	77	24	9	2
Period from the previous episode (months)[a]		29.7 ± 34.8 (0–184)	14.7 ± 15.1 (0–52)	10.1 ± 21.4 (0–66)	10 ± 14.1 (0–20)
sBP[a] (mmHg)	157.4 ± 30.8 (92–260)	139.9 ± 24.0 (100–203)	146.9 ± 21.7 (118–198)	124.4 ± 22.6 (103–155)	160 ± 17.0 (148–172)
dBP[a] (mmHg)	83.8 ± 20.9 (30–221)	80.8 ± 16.6 (54–125)	78.6 ± 12.4 (58–102)	77.8 ± 19.6 (51–98)	87 ± 8.5 (81–93)
Manifestations					
Disturbance of consciousness	304 (68.8%)	41 (53.2%)	17 (70.8%)	6 (66.7%)	0 (0%)
Hemiparesis	274 (62.0%)	43 (55.8%)	13 (54.2%)	5 (55.6%)	1 (50%)
Cognitive impairment	208 (47.1%)	41 (53.2%)	15 (62.5%)	5 (55.6%)	2 (100%)
Blindness	115 (26.0%)	14 (18.2%)	7 (29.2%)	1 (11.1%)	0 (0%)
Seizure	30 (6.8%)	6 (7.8%)	5 (21%)	1 (11.1%)	0 (0%)
Meningeal signs	29 (6.6%)	4 (5.2%)	1 (4.2%)	0 (0%)	0 (0%)

CAA, cerebral amyloid angiopathy; dBP, diastolic blood pressure; ICH, intracerebral hemorrhage; sBP, systolic blood pressure. [a]Mean ± SD (range).

cases, two patients demonstrated CAA only in the frontal cortical vessels; another patient showed widespread leptomeningeal and cortical CAA in the cerebrum and cerebellum. Aβ deposition on the vessel walls of two patients was confirmed using an immunolabeling method. One patient with severe CAA also received a pathological diagnosis of AD. In the biopsied cases, 26 out of 37 patients demonstrated leptomeningeal CAA, cortical CAA or both. Immunohistochemistry in 10 patients showed that the vessel walls were positive for Aβ deposition.

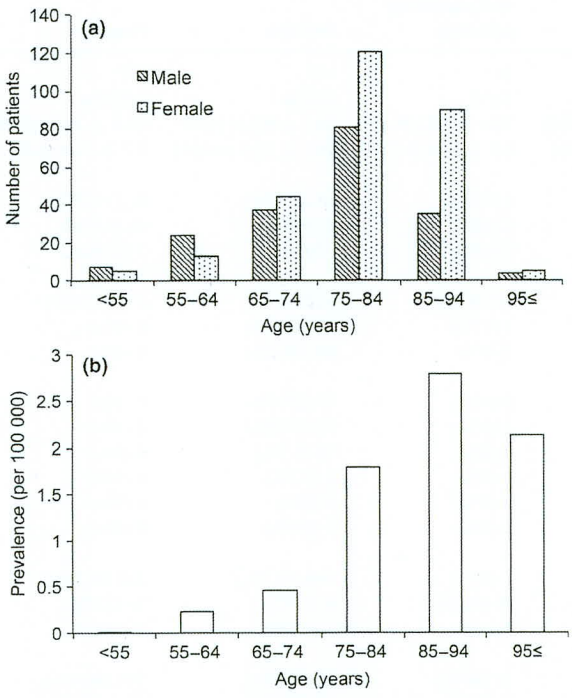

Figure 1 Distribution (a) and prevalence (b) of the age of onset of cerebral amyloid angiopathy-related intracerebral hemorrhage.

Analysis of the patients with CAA-ri identified by the second-stage survey

In all, 16 patients with CAA-ri were analyzed. The clinical manifestations and the laboratory findings are summarized in Table 3. Cognitive impairment and headache were the most frequent initial manifestations, followed by visual disturbance and motor paresis. Dizziness, sensory impairment, psychiatric features and seizure were also observed in each case.

Only one patient underwent cerebrospinal fluid (CSF) screening for the presence of anti-Aβ antibody, and elevated antibody levels were observed. Brain MRI was performed in all cases (Table 3). Angiography was performed only in one patient and demonstrated no apparent abnormal findings.

Neuropathological examinations were carried out in nine out of 16 patients (56.3%), including two patients with autopsy and seven patients with biopsy. Two patients who underwent biopsy had no apparent CAA in the tissues examined. CAA was revealed in the other seven patients; transmural and/or intramural inflammation, fibrinoid necrosis, perivascular inflammation and multinucleated cells were demonstrated in

Table 3 Characteristics of CAA-ri

Number of patients	16
Male/female	9/7
Age at onset[a] (years)	75 (53–83)
Diagnosis	
Pathological/clinical data only	7/9
Mode of onset	
Acute/subacute	7/9
Follow-up periods[a] (months)	31 (2–94)
Manifestations	
Focal neurological signs	12 (75%)
Disturbance of consciousness	10 (62.5%)
Headache	9 (56.3%)
Psychiatric symptoms	9 (56.3%)
Seizure	7 (43.8%)
Fever	1 (6.3%)
Cerebrospinal fluid (n = 11)	
Pleocytosis[a] (cells/μl)	4/11 (36.4%) (2; 0–25)
Protein[a] (mg/l)	5.9 (3.4–14.8)
MRI (n = 16)	
Tumor-like findings	6/16 (37.5%)
Cortical microbleeds	4/16 (25%)
Lobar macrohemorrhage	1/16 (6.3%)
Meningeal enhancement	3/10 (30%)

CAA-ri, cerebral amyloid angiopathy-related inflammation/vasculitis; MRI, magnetic resonance imaging. [a]Median with range.

six, four, six and two cases, respectively. Five patients showed a positive Aβ immunostaining.

Thirteen patients were treated with corticosteroid. Cyclophosphamide was added to the treatment of two patients. Ten patients improved after the therapy; however, three patients demonstrated no apparent improvement after the treatment.

Discussion

Estimated total number and prevalence of patients with CAA-related ICH and CAA-ri

The total number and prevalence of patients with CAA-related ICH and CAA-ri were estimated for the first time. CAA presents with several phenotypes, including CAA-related memory impairment and asymptomatic imaging abnormalities [12]; however, the focus was on CAA-related ICH and CAA-ri in this study. A population-based cohort study investigating age-related brain changes on MRI showed that 3.0% of neurologically healthy adults demonstrated strictly lobar cerebral microbleeds [13]. Furthermore, the western population showed more frequent strictly lobar cerebral microbleeds than the eastern population (western 4.5% vs. eastern 2.0%) [14].

It has been well demonstrated that the number of CAA-related ICH cases increases with age [3,4,15]. The results of our study were similar to those reported in previous studies. Many patients in the eldest age group could be underdiagnosed in this clinical survey.

With regard to the female-to-male ratio amongst patients with CAA, our previous nationwide survey of non-hypertensive CAA-related lobar ICH demonstrated a female predominance (corrected female-to-male ratio 2.2) [4]. This survey showed the same female predominance (female-to-male ratio 1.48).

No study had estimated the total number or crude prevalence of patients with CAA-ri. Since clinical diagnosis without pathological examinations is difficult to achieve [6,16], a large number of patients with CAA-ri could be underdiagnosed. Validated clinical diagnostic criteria were proposed, showing a specificity of 97% and a sensitivity of 82% for the probable criteria, and a specificity of 68% and a sensitivity of 82% for the possible criteria [16]. Well-documented clinical diagnostic criteria are essential to recognize the exact number and prevalence of patients with CAA-ri. Furthermore, enlightening activity about CAA-ri is crucial to accurately diagnose patients with CAA-ri.

Clinical features of CAA-related ICH

With regard to the recurrence of ICH, 16.9% of the CAA-related ICH patients experienced recurrent hemorrhage in a mean follow-up of 9.0 months (Table 1). In a single-center study on CAA, 56 out of 229 (19.2%) cases demonstrated recurrent ICH in a median follow-up of 2.8 years [17].

According to the results of neuropathological studies, CAA appears more frequently in the occipital lobe, followed by the frontal and temporal lobes [3]. However, some studies demonstrated that the frontal lobe is the most frequently affected area in patients with CAA [15,18]. In contrast, probable CAA-related ICH lesions, including macrohemorrhages and microhemorrhages, show a predilection for posterior brain regions, particularly the occipital and temporal lobes [19,20]. Our previous nationwide survey demonstrated that the actual frequency of ICH was higher in the frontal and parietal lobes and that ICH was found to be predominant in the parietal lobe after adjustment using estimated cortical volume [4]. In this study, the frontal lobe was the common site of hematoma; however, after correcting for lobar volume, the parietal lobe was found to be the most frequent site of ICH. A difference of frequent bleeding site between current and previous studies could be related to the number of patients examined. The predilection of CAA-related ICH, especially symptomatic macrohemorrhage, could not be explained by the distribution of CAA, whereas cortical microhemorrhages are compatible with the severity of CAA, suggesting that CAA-related

microhemorrhages and macrohemorrhages have distinct pathomechanisms.

Clinical features of CAA-ri

The average age of disease onset indicated in our study was similar to that reported in previous studies [21]. The most common features were cognitive decline, seizure and headache [6,21]. In this study, cognitive impairment and headache were the most frequent initial manifestations. As CAA is observed more frequently in the occipital lobe [3,19], visual disturbance could be a clinical clue to suspect CAA-ri.

With regard to the CSF findings of patients with CAA-ri, the anti-Aβ antibody could be a useful marker for the diagnosis [22]. Only one patient in this study was examined for anti-Aβ antibody in the CSF. This test is not widely available in Japan. Although patients with CAA-ri had no specific findings in imaging studies, leptomeningeal lesions alone or accompanied by white matter abnormalities were frequent in patients with CAA-ri [23]. Several patients showed tumor-like findings and meningeal enhancement, which were consistent with those reported in previous studies [24,25].

Limitations of the study

Since patients with CAA-related ICH and CAA-ri were identified via a nationwide survey, the patient population might be biased by the survey method and responses from the institutions. Identification of the patients with CAA-related ICH and CAA-ri were entrusted to doctors in charge in the department who responded to the enquiry. It is unclear whether hospital records were searched systematically. As most of the patients in this study had a clinically probable or possible CAA-related ICH, other causes of brain hemorrhage could not be completely excluded. This study was performed as a cross-sectional study. It is impossible to analyze recurrence rate using survival curves. Moreover, it was not possible to assess exact risk factors of recurrent hemorrhage.

In this study, clinical data of patients with CAA-related ICH and CAA-ri were collected. Since patients with CAA could show various clinical presentations other than lobar hemorrhage and inflammation, further surveys targeting more clinical features of CAA are essential to elucidate the epidemiological details of CAA.

Conclusions

The numbers of patients with CAA-related ICH and CAA-ri in Japan were estimated. Since a large number of patients could be underdiagnosed, the clinical diagnostic criteria must be improved to recognize the epidemiological details of CAA-related ICH and CAA-ri.

Acknowledgements

The assistance of the doctors at the various institutions throughout Japan who participated in this study is gratefully acknowledged. The study was supported by a grant from the Amyloidosis Research Committee, Intractable Disease Division of the Japanese Ministry of Health and Welfare.

Disclosure of conflicts of interest

The authors declare no financial or other conflicts of interest.

Supporting Information

Additional Supporting Information may be found in the online version of this article:

Table S1. Criteria for diagnosis of cerebral amyloid angiopathy (CAA)-related intracerebral hemorrhage

Table S2. Diagnostic criteria for cerebral amyloid angiopathy (CAA)-related inflammation/vasculitis

Table S3. Number of total, surveyed, responding departments and number of reported patients with cerebral amyloid angiopathy-related intracerebral hemorrhage (CAA-related ICH) and cerebral amyloid angiopathy-related inflammation/vasculitis (CAA-ri)

Table S4. The questionnaire regarding cerebral amyloid angiopathy-related intracerebral hemorrhage sent to the hospitals

Table S5. The questionnaire regarding cerebral amyloid angiopathy-related inflammation/vasculitis sent to the hospitals

References

1. Yamada M. Cerebral amyloid angiopathy: emerging concepts. *J Stroke* 2015; **17:** 17–30.
2. Charidimou A, Boulouis G, Gurol ME, *et al.* Emerging concepts in sporadic cerebral amyloid angiopathy. *Brain* 2017; **140:** 1829–1850.
3. Yamada M, Tsukagoshi H, Otomo E, Hayakawa M. Cerebral amyloid angiopathy in the aged. *J Neurol* 1987; **234:** 371–376.
4. Hirohata M, Yoshita M, Ishida C, *et al.* Clinical features of non-hypertensive lobar intracerebral hemorrhage related to cerebral amyloid angiopathy. *Eur J Neurol* 2010; **17:** 823–829.

5. Knudsen KA, Rosand J, Karluk D, Greenberg SM. Clinical diagnosis of cerebral amyloid angiopathy: validation of the Boston criteria. *Neurology* 2001; **56:** 537–539.
6. Chung KK, Anderson NE, Hutchinson D, Synek B, Barber PA. Cerebral amyloid angiopathy related inflammation: three case reports and a review. *J Neurol Neurosurg Psychiatry* 2011; **82:** 20–26.
7. Hashimoto S, Fukutomi K, Nagai M, *et al.* Response bias in the nationwide epidemiological survey of an intractable disease in Japan. *J Epidemiol* 1991; **1:** 27–30.
8. Hashimoto S, Fukutomi K, Shimizu H, *et al.* A study on methodological issues in nationwide epidemiological surveys of intractable diseases. *Bull Inst Public Health* 1993; **42:** 219–228. (in Japanese with English abstract).
9. Kuriyama S, Kusaka Y, Fujimura M, *et al.* Prevalence and clinicoepidemiological features of moyamoya disease in Japan: findings from a nationwide epidemiological survey. *Stroke* 2008; **39:** 42–47.
10. Kennedy DN, Lange N, Makris N, *et al.* Gyri of the human neocortex: an MRI-based analysis of volume and variance. *Cereb Cortex* 1998; **8:** 372–384.
11. Bennett DA, Brayne C, Feigin VL, *et al.* Development of the Standards of Reporting of Neurological Disorders (STROND) checklist: a guideline for the reporting of incidence and prevalence studied in neuroepidemiology. *Neurology* 2015; **85:** 821–828.
12. Greenberg SM, Al-Shahi Salman R, Biessels GJ, *et al.* Outcome markers for clinical trials in cerebral amyloid angiopathy. *Lancet Neurol* 2014; **13:** 419–428.
13. Yakushiji Y, Charidimou A, Noguchi T, *et al.* Total small vessel disease score in neurologically healthy Japanese adults in the Kashima Scan Study. *Intern Med* 2018; **57:** 189–196.
14. Yakushiji Y, Wilson D, Ambler G, *et al.* Distribution of cerebral microbleeds in the East and West: individual participant meta-analysis. *Neurology* 2019; **92:** e1086–e1097.
15. Masuda J, Tanaka K, Ueda K, Omae T. Autopsy study of incidence and distribution of cerebral amyloid angiopathy in Hisayama, Japan. *Stroke* 1988; **19:** 205–210.
16. Auriel E, Charidimou A, Gurol ME, *et al.* Validation of clinicoradiological criteria for the diagnosis of cerebral amyloid angiopathy-related inflammation. *JAMA Neurol* 2016; **73:** 197–202.
17. Boulouis G, Charidimou A, Pasi M, *et al.* Hemorrhage recurrence risk factors in cerebral amyloid angiopathy: comparative analysis of the overall small vessel disease severity score versus individual neuroimaging markers. *J Neurol Sci* 2017; **380:** 64–67.
18. Vinters HV, Gilbert JJ. Cerebral amyloid angiopathy: incidence and complications in the aging brain II. The distribution of amyloid vascular changes. *Stroke* 1983; **14:** 924–928.
19. Greenberg SM, Eng JA, Ning M, Smith EE, Rosand J. Hemorrhage burden predicts recurrent intracerebral hemorrhage after lobar hemorrhage. *Stroke* 2004; **35:** 1415–1420.
20. Rosand J, Muzikansky A, Kumar A, *et al.* Spatial clustering of hemorrhages in probable cerebral amyloid angiopathy. *Ann Neurol* 2005; **58:** 459–462.
21. Corovic A, Kelly S, Markus HS. Cerebral amyloid angiopathy associated with inflammation: a systemic review of clinical and imaging features and outcome. *Int J Stroke* 2018; **13:** 257–267.
22. Piazza F, Greenberg SM, Savoiardo M, *et al.* Anti-amyloid β autoantibodies in cerebral amyloid angiopathy-related inflammation: implications for amyloid-modifying therapies. *Ann Neurol* 2013; **73:** 449–458.
23. Salvarani C, Morris JM, Giannini C, *et al.* Imaging findings of cerebral amyloid angiopathy, Aβ-related angiitis (ABRA), and cerebral amyloid angiopathy-related inflammation: a single-institution 25-year experience. *Medicine (Baltimore)* 2016; **95:** e3613.
24. Scolding NJ, Joseph F, Kirby PA, *et al.* Abeta-related angiitis: primary angiitis of the central nervous system associated with cerebral amyloid angiopathy. *Brain* 2005; **128:** 500–515.
25. Sakai K, Hayashi S, Sanpei K, Yamada M, Takahashi H. Multiple cerebral infarcts with a few vasculitic lesions in the chronic stage of cerebral amyloid angiopathy-related inflammation. *Neuropathology* 2012; **32:** 551–556.

Contents lists available at ScienceDirect

Neuroscience Letters

journal homepage: www.elsevier.com/locate/neulet

Research article

MicroRNA expression profiles of neuron-derived extracellular vesicles in plasma from patients with amyotrophic lateral sclerosis

Masataka Katsu[a], Yuka Hama[b], Jun Utsumi[b], Ken Takashina[a], Hiroshi Yasumatsu[a], Fumiaki Mori[c], Koichi Wakabayashi[c], Mikio Shoji[d], Hidenao Sasaki[b,*]

[a] Research Unit/Neuroscience Sohyaku, Innovative Research Division, Mitsubishi Tanabe Pharma Corporation, 1000, Kamoshida-cho, Aoba-ku, Yokohama, 227-0033, Japan
[b] Department of Neurology, Faculty of Medicine and Graduate School of Medicine, Hokkaido University, Kita-15 Nishi-7, Kita-ku, Sapporo, 060-8638, Japan
[c] Department of Neuropathology, Institute of Brain Science, Hirosaki University Graduate School of Medicine, 5 Zaifu-cho, Hirosaki, 036-8562, Japan
[d] Department of Neurology, Hirosaki University Graduate School of Medicine, 5 Zaifucho, Hirosaki, 036-8216, Japan

ARTICLE INFO

Keywords:
Bioinformatics
MicroRNA
ALS
Extracellular vesicles

ABSTRACT

Circulating microRNAs (miRNAs) in peripheral blood have been extensively investigated as biomarkers for early diagnosis and monitoring of disease progression. However, their cellular origin as well as their link to the pathophysiology, especially neurodegenerative disease, remains largely unknown. In the present study, we isolated neuron-derived extracellular vesicles (EVs) in plasma by immunoaffinity purification and comprehensively analyzed their miRNA expression profiles using microarray. A total of 30 miRNAs were differentially regulated in amyotrophic lateral sclerosis (ALS) plasma relative to healthy control plasma. Gene ontology analysis revealed that biological processes implicated in both up-regulated and down-regulated miRNAs were involved in synaptic vesicle-related pathways. Especially, 4 miRNAs in plasma neuro-derived EVs seemed to be regulated in the similar manner as those in formalin-fixed paraffin-embedded motor cortex samples from ALS patients. The target genes for the 4 miRNAs partly overlapped in *STX1B*, *RAB3B*, and *UNC13A* genes. *UNC13A* has been reported to be associated with increased odds of sporadic ALS in multiple genome-wide association studies. Our data suggest that miRNAs extracted from neuron-derived EVs in plasma reflect miRNA alterations in the brain as potential biomarkers of ALS.

1. Introduction

MicroRNAs (miRNAs) are small, single-stranded, non-coding RNAs that play important roles in gene-regulation by targeting mRNAs for cleavage or translational repression [1]. A single miRNA can directly repress translation of hundreds of genes [2] and each mRNA transcript may be regulated by multiple miRNAs [3]. Therefore, dysregulation of miRNAs is implicated in a wide variety of biological processes and various disease including neurological disease such as amyotrophic lateral sclerosis [4,5]. The miRNA expression profiles of frozen tissues [6] and formalin-fixed paraffin-embedded (FFPE) samples [5] from postmortem cases with neurological disease can be valuable sources for analyzing pathological processes.

Importantly, miRNAs are found in biological fluids such as urine, blood, and cerebrospinal fluid. Stably circulating miRNAs are known to bind either to RNA binding proteins [7], or high-density lipoproteins [8], or to be encapsulated in extracellular vesicles (EVs) like exosomes and microvesicles, where miRNAs are presumed to be protected from RNase in body fluids [9]. EVs are released by most cell types and carry a cargo of proteins and nucleic acids including miRNAs. Their contents reflect the physiological state of the cells of origin and alterations during disease. EVs can be enriched for their cellular origin with an immunocapture method as they express cell-specific markers on the membrane [10,11]. Accumulating evidence suggests that EVs released by neurons are detected in the blood stream and expression levels of pathogenic, synaptic, and lysosomal proteins in neuron-derived EVs in plasma are altered in neurological disorders [12–20]. Therefore, extracts from neuron-derived EVs in plasma are potential biomarkers for diagnosis and monitoring of neurological disease. However, an analysis of miRNAs in neuron-derived EVs in plasma has not yet been reported

* Corresponding author.
E-mail addresses: katsu.masataka@me.mt-pharma.co.jp (M. Katsu), hama@pop.med.hokudai.ac.jp (Y. Hama), jutsumi@pop.med.hokudai.ac.jp (J. Utsumi), takashina.ken@mh.mt-pharma.co.jp (K. Takashina), yasumatsu.hiroshi@mp.mt-pharma.co.jp (H. Yasumatsu), neuropal@hirosaki-u.ac.jp (F. Mori), koichi@hirosaki-u.ac.jp (K. Wakabayashi), mshoji@hirosaki-u.ac.jp (M. Shoji), h-isasak@med.hokudai.ac.jp, h_isasak@pop.med.hokudai.ac.jp (H. Sasaki).

https://doi.org/10.1016/j.neulet.2019.03.048
Received 30 January 2019; Received in revised form 5 March 2019; Accepted 26 March 2019

so far.

Amyotrophic lateral sclerosis (ALS) is a fatal, adult-onset neurodegenerative disease characterized clinically by the progressive loss of upper and lower motor neurons, leading rapidly to atrophy of bulbar, limb, or respiratory muscles. There is no effective medical treatment [21]. In the present study, we used a microarray method to comprehensively analyze miRNA expression profiles of neuron-derived EVs in plasma from patients with ALS and healthy donors. A subsequent comparison of our results with our previous data enabled us to provide an overview of the miRNA expression profiles related to ALS pathology.

2. Materials and methods

2.1. Subjects and sample collection

Patients with ALS (n = 5) and age-matched healthy control subjects (n = 5) enrolled in this study which was approved by the Institutional Ethics Committee of Hokkaido University Faculty of Medicine and Graduate School of Medicine. The age and gender of donors are shown in Table S1. ALS patients were clinically diagnosed by board-certified neurologists at the Department of Neurology, Hokkaido University Hospital, and at participating research institutes. All of the ALS patients were considered sporadic cases because of no evidence of a family history of the disease. No genetic testing for ALS was performed. Blood was collected in disodium ethylene diaminotetraacetate tubes and centrifuged immediately, after which the plasma was separated from and frozen at −80°C until further processing.

2.2. Isolation of neuron-derived EVs in plasma

Neuron-derived EVs in plasma were prepared by the methods described previously with slight modifications [13]. Briefly, 2 mL plasma was incubated with polyethylene glycol with a molecular weight of 8000 Da for 1 h at 4 °C, and crude EV fraction was precipitated by centrifugation at 1500 × *g* for 30 min. Each EV pellet was resuspended in PBS containing 1% BSA, protease inhibitor cocktail, and phosphatase inhibitor cocktail. The mixture was incubated with biotinylated mouse anti-human CD171 (L1CAM) antibody (clone5G3, eBioscience) overnight at 4 °C, followed by incubation with streptavidin agarose resin (Thermo Scientific) for 1 h at room temperature. The monoclonal antibody eBio5G3 recognizes CD171, also known as neural cell adhesion molecule L1. L1CAM/CD171 (Gene ID: 3897) is a neuronal glycoprotein belonging to the immunoglobulin supergene family. CD171 has been shown to function as a cell adhesion molecule mediating homotypic and heterotypic cell-cell interactions in neuronal myelination, neurite outgrowth, and regeneration. After centrifugation at 800 × *g* for 4 min at 4 °C, pellets were washed with PBS, resuspended with 0.1 mol/L glycine-HCl (pH 3.0), and vigorously mixed for 2 min at room temperature to dissociate captured EVs from anti-CD171 antibody-resin conjugates. Each EV suspension was neutralized using 0.5 mol/L Tris HCL (pH 8.5). The median diameter of isolated EVs was measured by using DelsaMax Core Particle Size Analyzer (Beckman Colter). To confirm neuron-specific properties of isolated EVs, the expression of neuron-specific markers (SNAP25 and synaptophysin), and EV-specific markers (CD63 and CD81) was evaluated by flow cytometry using Exosome-Human Isolation/Detection Reagent (Thermo Fisher Scientific). Isolated EVs were cryopreserved at -80 °C until further processing.

2.3. Total RNA extraction and miRNA expression analysis

Total RNA in neuron-derived EVs was extracted using 3D-gene RNA extraction reagent from liquid sample kit (TORAY Industries) according to the manufacturer's protocol. RNA concentration was measured using a 2100 Bioanalyzer with an Agilent RNA 6000 pico kit (Agilent Technologies). The extracted total RNA was concentrated and labeled using 3D-Gene miRNA labeling kit, and the labeled RNAs were hybridized on to a 3D-Gene chip (TORAY Industries). The 3D-Gene Human miRNA Oligo Chip (Ver. 21) was designed to detect miRNA sequences registered in the miRBase Release 21 (http://microrna.mirbase.org/). After carefully washing the chips, the fluorescence signals were obtained with a 3D-Gene Scanner and analyzed with 3D-Gene Extraction software as reported previously [5]. To compare miRNA profiles of neuron-derived EVs in plasma with those of FFPE brain samples (control n = 4, ALS n = 6) [5], the common global normalization was conducted after the number of miRNA probes for Ver. 21 chip was adjusted to that for Ver. 17 chip by which FFPE samples were analyzed. The FFPE specimens employed were from the motor cortex of patients with sporadic ALS and from normal subjects, and all the diagnoses were confirmed by neuropathological examination using immunohistochemistry for TDP-43 and ubiquitin [5]. No genetic testing for ALS was performed. In case a miRNA was upregulated in neuron-derived EVs of patients with ALS relative to control, the miRNA detected in all control subjects and ALS patients was included in further analysis, while in case a miRNA was down-regulated, the miRNA detected in all control subjects was included in further analysis. MiRNA and subjects were clustered by Manhattan (city-block) distance using Cluster 3.0 software [22] and viewed in a heatmap using Java TreeView 1.1.6r4 software [23].

2.4. miRNA target prediction and pathway enrichment analysis

Bioinformatics prediction of target genes and miRNA binding sites was performed using the miRmap software (http://mirmap.ezlab.org/) [24]. Gene Ontology (GO) enrichment analyses for candidate miRNA targets were performed by PANTHER classification system (http://www.pantherdb.org/) [25]. The PANTHER Overrepresentation Test (release 20181003) was used to evaluate the data against the GO database (released 2018-09-06).

Additionally, to estimate the biological relationship of similarly behaved miRNAs from neuron-derived EVs and FFPE samples, target genes of those miRNAs were predicted and used in enrichment analysis by MetaCore™ software (version 6.37 build 69500, Clarivate Analytics, https://portal.genego.com/cgi/data_manager.cgi).

2.5. Statistical analysis

All data are presented as mean ± standard error of the mean. Statistical analyses were determined by unpaired Student's t-test. Data were analyzed with GraphPad Prism, version 7 (GraphPad Software Inc., CA, USA) and p-values less than 0.05 were considered statistically significant.

3. Results

3.1. Characterization of neuron-derived EVs

We isolated neuron-derived EVs using polymer-based precipitation, followed by immunoaffinity purification with anti-CD-171 antibody. The median diameter of neuron-derived EVs from healthy control as measured by dynamic light scattering was approximately 150 nm, similar to that described in previous reports (Fig. S1A) [16,20,26]. Flow cytometry data of EVs isolated from healthy control plasma by anti-CD-171 showed expression of neuron-specific markers, SNAP25 and synaptophysin, and of EV specific markers, CD81 and CD63 (Fig. S1B). These results suggest that the isolated EVs were of neuronal origin.

3.2. miRNA analysis and candidate target genes in ALS

We did a comprehensive analysis of miRNA expression profiles of neuron-derived EVs from plasma using a microarray method. An average number of 623 ± 47 and 476 ± 103 miRNAs were detected in neuron-derived EVs from healthy control subjects and patients with

Table 1
MicroRNAs significantly up- and down-regulated in neuron-derived EVs from patients with ALS.

	miRNA name	Ratio		miRNA name	Ratio
Up-regulated	hsa-miR-4736	1.59	Down-regulated	hsa-miR-1268a	0.91
	hsa-miR-4700-5p	1.44		hsa-miR-2861	0.90
	hsa-miR-1207-5p	1.24		hsa-miR-4508	0.89
	hsa-miR-4739	1.22		hsa-miR-4507	0.88
	hsa-miR-4505	1.21		hsa-miR-3176	0.82
	hsa-miR-24-3p	1.15		hsa-miR-4745-5p	0.79
	hsa-miR-149-3p	1.15		hsa-miR-3911	0.74
	hsa-miR-4484	1.15		hsa-miR-3605-5p	0.73
	hsa-miR-4688	1.14		hsa-miR-150-3p	0.71
	hsa-miR-4298	1.13		hsa-miR-3940-3p	0.68
	hsa-miR-939-5p	1.13		hsa-miR-4646-5p	0.66
	hsa-miR-371a-5p	1.09		hsa-miR-4687-5p	0.65
	hsa-miR-3619-3p	1.09		hsa-miR-4788	0.65
				hsa-miR-4674	0.65
				hsa-miR-1913	0.61
				hsa-miR-634	0.61
				hsa-miR-3177-3p	0.60

Data are shown as fold-change relative to control group (set as 1.0).

ALS, respectively. No significant difference in the detectable number of miRNAs was found between the two groups. In ALS, 13 miRNAs were significantly up-regulated and 17 miRNAs were significantly down-regulated compared to controls (Table 1). A hierarchical clustering analysis of the 30 miRNAs differentially regulated in ALS is depicted in Fig. 1, where a cluster composed only of ALS patients is seen. Although several proteins in neuron-derived EVs from plasma have been analyzed in previous studies [12–20], this is the first report describing a comprehensive miRNAs analysis of neuron-derived EVs isolated from peripheral blood samples.

3.3. GO analysis of predicted target genes for altered miRNA in ALS

92

To examine the biological functions of differentially regulated miRNAs in neuron-derived EVs, the candidate target gene of 13 up-regulated and 17 down-regulated miRNAs were identified using the miRmap software. The top 50 candidate target genes for each of the 13 up-regulated and 17 down-regulated miRNAs were selected in order of the miRmap score. A total of 650 candidate genes for the 13 up-regulated miRNAs (Table S2A) and 850 candidate genes for the 17 down-regulated miRNAs (Table S2B) in ALS were subjected to GO enrichment analysis to predict their properties. The genes altered by up-regulated miRNAs (Table 2A) and down-regulated miRNAs (Table 2B) in ALS were both involved in synaptic vesicle-related pathway, such as synaptic vesicle docking and exocytosis, regulation of neurotransmitter secretion, and synaptic vesicle cycle. These results suggest that synaptic vesicle-mediated transport may be affected in ALS.

3.4. Comparison of miRNAs in neuron-derived EVs with those in FFPE samples from motor cortex of patients with ALS

To investigate miRNA expression profiles in the brain, we first compared miRNA expression profiles of neuron-derived EVs in healthy control plasma with those in FFPE samples from the motor cortex of healthy controls, as previously reported [5]. The total number of miRNA species, 322 for neuron-derived EVs and 829 for FFPE, were detected in all control subjects from each source. Of the 322 miRNAs detected in neuron-derived EVs, 299 (92.9%) miRNAs were found to be expressed in FFPE samples as indicated in Fig. 2. These results suggest that most of miRNAs species isolated from neuron-derived EVs were composed of a subpopulation of miRNAs expressed in the brain tissue. These observations indicate that miRNA profiling of neuron-derived EVs offer a big advantage in the clinical investigation neurodegenerative diseases since neuron-derived EVs can be more easily collected from blood than those from cerebrospinal fluid and brain tissue.

We further compared the differentially expressed miRNAs in our two categories. An analysis of the microarray data showed that a total of 96 miRNAs were differentially regulated in FFPE samples from patients with ALS relative to control subjects. Ten of these samples were also significantly up- or down-regulated in neuron-derived EVs (Table 3), where miR-24-3p was up-regulated, and miR-1268a, miR-3911 and miR-4646-5p were down-regulated in the similar manner as those in neuron-derived EVs (Fig. 3). Furthermore, miR-24-3p and miR-1268a were also detected and regulated in the similar manner in spinal cord of ALS patients under the accession number GSE52670 (http://www.ncbi.nlm.nih.gov/geo/). Additionally, we compared data of miRNAs with top 5 high and low signal ratios in FFPE samples with data in neuron-derived EVs analysis (Table S3). Although signal ratios in ND-EVs samples were relatively less than those in FFPE samples, the results in FFPE samples were considered to reflect alterations in neuron-derived EVs samples to some extent.

These 4 miRNA target genes seem to work together in pathogenetic relations of ALS, so we further performed MetaCore enrichment analysis to evaluate the biological network and processes involved. A total of 200 target genes of 4 miRNA species (each top 50 genes for miR-24-3p, miR-1268a, miR-3911, and miR-4646-5, respectively, listed in Tables S2A and S2B) suggested a synaptic vesicle exocytosis network and neuronal synaptic vesicle processes as shown in Table 4 ($p < 0.05$, FDR < 0.05).

4. Discussion

Circulating miRNAs in the peripheral blood have been extensively investigated as biomarkers for early diagnosis and monitoring of disease progression. However, the link between miRNAs and pathogenic regions remains largely unknown to date. In the present study, we report the first overview of the miRNA expression profiles of neuron-derived EVs in plasma from patients with ALS and healthy control subjects using a microarray analysis. The isolated neuron-derived EVs expressed synaptic marker proteins such as surface antigen, synaptophysin and SNAP25. Furthermore, miR-3911 specifically expressed in the brain, according to the Genome-Tissue Expression (GTEx) database [27], was detected in these neuron-derived EVs. In addition, more than 90% of miRNAs species in isolated EV components from healthy controls were also present in a subpopulation of miRNAs expressed in brain FFPE samples from healthy controls [5]. Taken together, these results suggest that our extracted EVs in plasma reflect miRNA alterations in brain and hold promise as potential biomarkers in ALS.

The semi-quantitative microarray analysis identified a total of 30 miRNAs in the neuron-derived EVs that were differentially regulated in

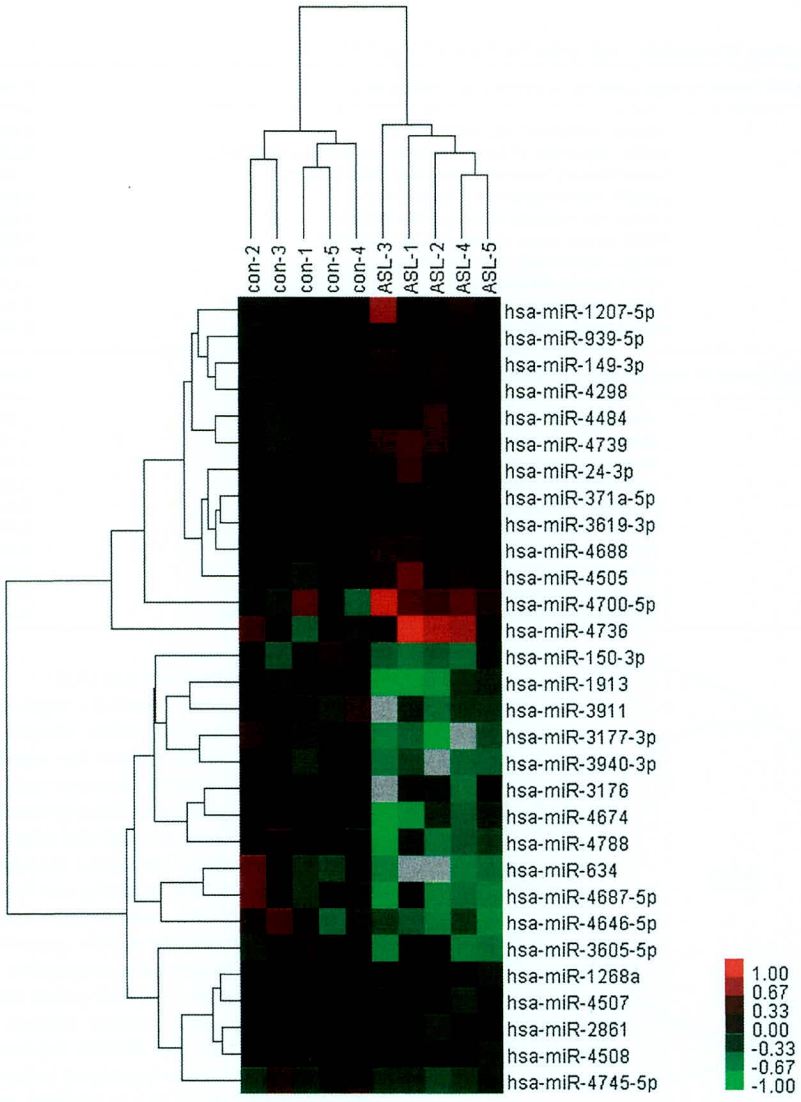

Fig. 1. Heat Map of differentially regulated miRNA from plasma samples of ALS patients (n = 5) and controls (n = 5) as identified by microarray. MiRNAs and subjects are hierarchically clustered by Manhattan distance on the y and x axis, respectively. The relative mRNA expression is depicted according to the color scale shown on the right. Green, black, red, and gray indicate fold changes relative to controls as low, mean, high, and missing data, respectively. Thirty miRNAs were significantly up-regulated or down-regulated in ALS patients compared with controls.

ALS relative to controls. Gene ontology analysis revealed that significantly enriched biological processes implicated in up- and down-regulated in ALS were both specifically related to synaptic vesicle-related pathways including synaptic vesicle docking and exocytosis, regulation of neurotransmitter secretion, and synaptic vesicle cycle. After comparing miRNA expression profiles of neuron-derived EVs with those of FFPE samples from the motor cortex in ALS, miR-24-3p, miR-1268a, miR-3911 and miR-4646-5p were seen to be differentially regulated in the similar manner. These 4 species of miRNAs were potentially involved in synaptic vesicle-related pathway and network.

Although the roles of each of miRNAs detected in this study have not been examined, we can hypothesize the potential roles of each of miRNAs as predicted from web-based bioinformatics analysis and published literature. A precursor of miR-3911 is located across the last exon-intron boundary of *STXBP1*, which encodes Syntaxin binding protein 1 (also known as Munc18-1). Intriguingly, miR-3911 putatively binds to the last exon of *STXBP1* according to at least two target-prediction tools, miRmap [24] and TargetScan [3], although *STXBP1* does not rank in the top 50. Munc18-1 is a critical protein for synaptic vesicle release since deletion of Munc18-1 leads to a complete loss of neurotransmitter secretion [28]. Munc18-1 binds to Syntaxin-1 and forms Synataxin-1/Munc18-1 complex, rendering soluble N-ethylmaleimide-sensitive factor attachment protein receptor (SNARE) complex incompetent. SNARE complex is composed of Syntaxin-1, Synaptobrevin-2 and SNAP25, which are essential for vesicle fusion and Ca^{2+}-dependent neurotransmitter release. Furthermore, the target genes potentially modulated by miR-3911 include *RAB3B* and *UNC13A* (also known as Munc13-1) (Table S2B). Rab3 is highly enriched in synaptic vesicles in brain and plays important roles in synaptic vesicle docking and Ca^{2+}-dependent neurotransmitter release through Rab3-effector protein, Rab3 interacting molecules (RIM)s [29]. RIMs recruit both Ca^{2+}-channels on plasma membrane and Rab3 on synaptic vesicles in the active zone [30]. Munc13-1 is essential for vesicle priming, which enables synaptic vesicles to fuse rapidly in response to a calcium influx by binding the SNARE complex [31]. More importantly, *UNC13A* is associated with increased odds of sporadic ALS in multiple genome-wide association studies (GWAS) [32–34], and is also related to frontotemporal cortical atrophy leading to an impaired cognitive

Table 2
Top 10 enriched biological processes of candidate target genes for ALS-specific miRNAs.

(A)	GO Bilogical Process of target genes for 13 up-regulated miRNAs in ALS	P-value	FDR
1	synaptic vesicle docking (GO:0016081)	2.56E-04	2.89E-02
2	positive regulation of neurotransmitter transport (GO:0051590)	3.21E-05	7.31E-03
3	vesicle docking involved in exocytosis (GO:0006904)	1.16E-04	1.71E-02
4	synaptic vesicle exocytosis (GO:0016079)	4.72E-06	1.86E-03
5	calcium ion regulated exocytosis (GO:0017156)	1.66E-05	4.58E-03
6	SMAD protein signal transduction (GO:0060395)	1.29E-04	1.86E-02
7	synaptic vesicle cycle (GO:0099504)	3.13E-07	2.73E-04
8	vesicle docking (GO:0048278)	2.12E-04	2.58E-02
9	synaptic vesicle transport (GO:0048489)	1.46E-05	4.27E-03
10	establishment of synaptic vesicle localization (GO:0097480)	1.46E-05	4.19E-03

(B)	GO Bilogical Process of target genes for 17 down-regulated miRNAs in ALS	P-value	FDR
1	vesicle docking involved in exocytosis (GO:0006904)	1.03E-05	7.70E-03
2	synaptic vesicle exocytosis (GO:0016079)	1.69E-04	4.03E-02
3	vesicle docking (GO:0048278)	2.12E-04	4.56E-02
4	regulation of neurotransmitter secretion (GO:0046928)	9.39E-05	2.64E-02
5	regulation of synaptic vesicle cycle (GO:0098693)	5.80E-05	1.86E-02
6	synaptic vesicle cycle (GO:0099504)	5.08E-05	1.74E-02
7	regulation of neurotransmitter transport (GO:0051588)	4.01E-05	1.50E-02
8	protein localization to plasma membrane (GO:0072659)	1.44E-04	3.54E-02
9	regulation of exocytosis (GO:0017157)	4.92E-05	1.72E-02
10	modulation of chemical synaptic transmission (GO:0050804)	2.61E-05	1.47E-02

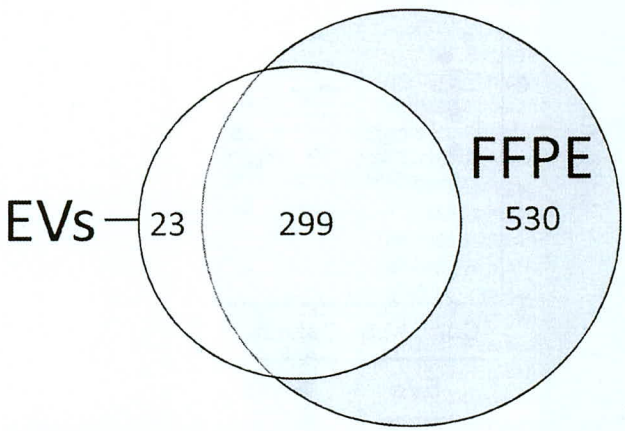

Fig. 2. Differentially expressed miRNAs detected in EVs and FFPE samples from control subjects. The Venn diagram demonstrates the number of detected miRNA species.

Table 3
Differentially expressed miRNAs in both neuron-derived EVs and FFPE samples from patients with ALS.

miRNA name	Neuron-derived EVs		FFPE	
	Ratio	P-value	Ratio	P-value
similar alteration				
hsa-miR-24-3p	1.15	0.049	3.1	0.012
hsa-miR-1268a	0.91	0.031	0.76	0.044
hsa-miR-3911	0.74	0.024	0.53	0.001
hsa-miR-4646-5p	0.66	0.023	0.67	0.046
different alteration				
hsa-miR-939-5p	1.13	0.037	0.61	0.013
hsa-miR-3619-3p	1.09	0.036	0.34	0.014
hsa-miR-4298	1.13	0.043	0.71	0.034
hsa-miR-4700-5p	1.44	0.032	0.74	0.043
hsa-miR-4736	1.59	0.035	0.59	0.028
hsa-miR-4739	1.22	0.022	0.65	0.046

Data are shown as fold-change relative to control group (set as 1.0).

performance in sporadic ALS [35].

The target genes putatively regulated by miR-24-3p were *RAB3B* and *ISTN1* (Table S2A). *ISTN1* encodes Intersectin-1 that involves synaptic vesicle replenishment by regulated complex formation with Synapsin I [36]. Another important target gene regulated by miR-24-3p is the vacuolar protein sorting-associated protein 53 homolog (*VPS53*), which interacts with the ALS-like target gene, *VPS54*. Vps53 is a component of the Golgi-associated retrograde protein (GARP) complex, which is required for tethering and fusion of endosome-derived transport vesicles to the trans-Golgi network by binding to the SNARE complex on the vesicles. A point mutation of Vps54 consisting of GARP complex is known to cause progressive motor neuron degeneration of the wobbler mouse [37]. MiR-1268a may regulate synaptic vesicle-related pathway more potently because it potentially targets *STX1B*, *STXBP1*, *UNC13A*, and *RAB3D*. Interestingly, miR-1268a also targets *KIAA0513*, which was implicated in increased odds of sporadic ALS in GWAS studies [32,33,38]. In addition, putative target genes in synaptic vesicle release machinery modulated by miR-4646-5p included *RAB3B* and *ITSN1*. These results suggest that key genes for synaptic function may be dysregulated in ALS. Indeed, recent evidence indicates that a set of 15 synaptic function genes including *STX1B*, *STXBP1* and *UNC13A* has been down-regulated in the spinal cord from patients with ALS using RNA sequencing technology [6].

To examine the candidate miRNAs that potentially regulate SNARE complex and its modulators like Munc13-1 and Munc18-1, the top 50 candidate miRNAs for each of representative genes of synaptic vesicle-related proteins were selected from the miRmap score (Table S4). Surprisingly, 4 miRNAs differentially regulated in neuron-derived EVs appeared in the top 10 miRNAs that putatively target *STXBP1*. Moreover, *STX1A*, *STX1B*, *RAB3A* *UNC13A*, and *VAMP2*/Synaptobrevin-2, *CPLX1*/Complexin-1 were believed to be regulated by at least 2 miRNAs differentially regulated in neuron-derived EVs. Interestingly, a recent, report indicating that TDP-43 depletion in microglia not only promotes amyloid clearance but also induce synapse loss, provided insight into the mechanism of ALS [39]. Our findings of synapse-related miRNAs support this report and implicate neuron-derived EVs containing miRNAs as potential biomarkers for ALS.

These results may reflect the limitations imposed by the common mechanisms of the transport and function of EVs such as exosomes, although the hierarchical clustering analysis showed a cluster composed only of ALS patients. Therefore, these findings suggest that

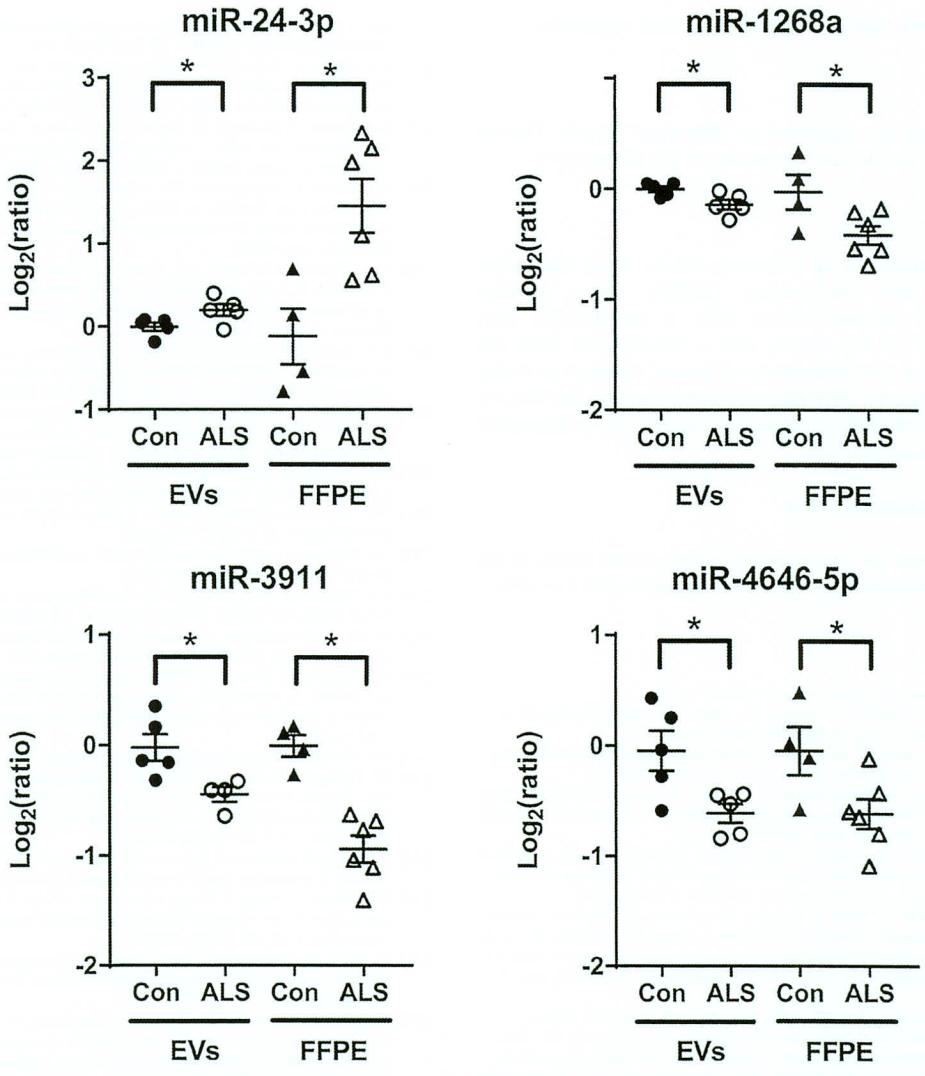

Fig. 3. miRNAs significantly regulated in the same direction in both neuron-derived EVs and FFPE samples from patients with ALS. Scatterplots along with error bars for mean ± standard error of the mean show relative expression levels of miR-3911, miR4646-5p, miR-24-3p, and miR1268a. * $p < 0.05$ vs. the control using Student's t-test.

Table 4
Four miRNAs (miR-24-3p, miR-1268a, miR-3911, miR-4646-5) target enrichment analysis by MetaCore.

(A)	Enrichment by Process Networks	P-value	FDR
1	transport synaptic vesicle exocytosis	1.93E-04	1.78E-02

(B)	Enrichment by GO Processes	P-value	FDR
1	regulation of short-term neuronal synaptic plasticity	1.48E-09	5.66E-06
2	nervous system development	9.61E-09	1.84E-05
3	regulation of synaptic vesicle priming	1.94E-08	2.48E-05
4	vesicle docking involved in exocytosis	5.94E-08	5.69E-05
5	positive regulation of synaptic transmission	8.96E-08	6.87E-05

(A) Network (p-value < 0.05, FDR < 0.05) are shown. (B) Top 5 GO processes (p-value < 0.05, FDR < 0.05) are shown.

differentially regulated miRNAs in ALS are at least partially reflective of the pathophysiological processes in ALS. MiRNAs in neuron-derived EVs can be very useful diagnostic biomarkers; however, these miRNAs should be validated by RT-PCR and a larger patient cohort is needed to evaluate whether there is a correlation between altered miRNAs in ALS and clinical characteristics including age of onset, disease duration, symptom severity, and disease type.

5. Conclusions

In conclusion, we isolated neuron-derived EVs in plasma from patients with ALS and healthy control subjects, and provided an overview of the miRNA expression profile of neuron-derived EVs. These miRNAs overlapped with the miRNAs expressed in the FFPE samples from the motor cortex of ALS patients. Although further validation with a larger sample size is needed, the identification of dysregulated miRNAs in neuron-derived EVs from ALS patient plasma present themselves as diagnostic tools to help in early detection and monitoring of the disease.

Author contributions

MK carried out the experiments, analyzed the data, and wrote the manuscript. YH performed experimental work. HS, MS, FM, and WK performed clinical diagnoses, obtained completed informed consent forms, and collected samples. JU provided advice regarding data analysis and the manuscript. HY and TK supervised the study. HS designed and supervised this work and provided critical revisions of the

manuscript. All authors read and approved the final manuscript.

Conflict of interest

This study was partly supported by Mitsubishi Tanabe Pharma Corporation. MK, HY and KT are employees of this Corporation.

Funding

This study was supported by a Grant-in-Aid by Japan Agency for Medical Research and Development (AMED), grant numbers JP17ek0109110 and JP16ek0109048 (HS), a Grand-in-Aid from Research Committee of the Ataxia, and a Grant-in-Aid from the Research Committee of CNS Degenerative Diseases, Research on Policy Planning and Evaluation for Rare and Intractable Diseases, the Ministry of Health, Labour and Welfare of Japan (HS), and in part by Mitsubishi Tanabe Pharma Corporation (HS).

Appendix A. Supplementary data

Supplementary material related to this article can be found, in the online version, at doi:https://doi.org/10.1016/j.neulet.2019.03.048.

References

[1] D.P. Bartel, Metazoan MicroRNAs, Cell 173 (2018) 20–51.
[2] D. Baek, J. Villen, C. Shin, F.D. Camargo, S.P. Gygi, D.P. Bartel, The impact of microRNAs on protein output, Nature 455 (2008) 64–71.
[3] R.C. Friedman, K.K. Farh, C.B. Burge, D.P. Bartel, Most mammalian mRNAs are conserved targets of microRNAs, Genome Res. 19 (2009) 92–105.
[4] I. Takahashi, Y. Hama, M. Matsushima, M. Hirotani, T. Kano, H. Hohzen, I. Yabe, J. Utsumi, H. Sasaki, Identification of plasma microRNAs as a biomarker of sporadic Amyotrophic Lateral Sclerosis, Mol. Brain 8 (2015) 67.
[5] K. Wakabayashi, F. Mori, A. Kakita, H. Takahashi, J. Utsumi, H. Sasaki, Analysis of microRNA from archived formalin-fixed paraffin-embedded specimens of amyotrophic lateral sclerosis, Acta Neuropathol. Commun. 2 (2014) 173.
[6] A.M. D'Erchia, A. Gallo, C. Manzari, S. Raho, D.S. Horner, M. Chiara, A. Valletti, I. Aiello, F. Mastropasqua, L. Ciaccia, F. Locatelli, F. Pisani, G.P. Nicchia, M. Svelto, G. Pesole, E. Picardi, Massive transcriptome sequencing of human spinal cord tissues provides new insights into motor neuron degeneration in ALS, Sci. Rep. 7 (2017) 10046.
[7] J.D. Arroyo, J.R. Chevillet, E.M. Kroh, I.K. Ruf, C.C. Pritchard, D.F. Gibson, P.S. Mitchell, C.F. Bennett, E.L. Pogosova-Agadjanyan, D.L. Stirewalt, J.F. Tait, M. Tewari, Argonaute2 complexes carry a population of circulating microRNAs independent of vesicles in human plasma, Proc. Natl. Acad. Sci. U. S. A. 108 (2011) 5003–5008.
[8] K.C. Vickers, B.T. Palmisano, B.M. Shoucri, R.D. Shamburek, A.T. Remaley, MicroRNAs are transported in plasma and delivered to recipient cells by high-density lipoproteins, Nat. Cell Biol. 13 (2011) 423–433.
[9] H. Valadi, K. Ekstrom, A. Bossios, M. Sjostrand, J.J. Lee, J.O. Lotvall, Exosome-mediated transfer of mRNAs and microRNAs is a novel mechanism of genetic exchange between cells, Nat. Cell Biol. 9 (2007) 654–659.
[10] K.M. Kanninen, N. Bister, J. Koistinaho, T. Malm, Exosomes as new diagnostic tools in CNS diseases, Biochim. Biophys. Acta 1862 (2016) 403–410.
[11] A.G. Thompson, E. Gray, S.M. Heman-Ackah, I. Mager, K. Talbot, S.E. Andaloussi, M.J. Wood, M.R. Turner, Extracellular vesicles in neurodegenerative disease – pathogenesis to biomarkers, Nat. Rev. Neurol. 12 (2016) 346–357.
[12] M. Shi, C. Liu, T.J. Cook, K.M. Bullock, Y. Zhao, C. Ginghina, Y. Li, P. Aro, R. Dator, C. He, M.J. Hipp, C.P. Zabetian, E.R. Peskind, S.C. Hu, J.F. Quinn, D.R. Galasko, W.A. Banks, J. Zhang, Plasma exosomal alpha-synuclein is likely CNS-derived and increased in Parkinson's disease, Acta Neuropathol. 128 (2014) 639–650.
[13] M.S. Fiandaca, D. Kapogiannis, M. Mapstone, A. Boxer, E. Eitan, J.B. Schwartz, E.L. Abner, R.C. Petersen, H.J. Federoff, B.L. Miller, E.J. Goetzl, Identification of preclinical Alzheimer's disease by a profile of pathogenic proteins in neurally derived blood exosomes: a case-control study, Alzheimers Dement. 11 (2015) 600–607 e601.
[14] D. Kapogiannis, A. Boxer, J.B. Schwartz, E.L. Abner, A. Biragyn, U. Masharani, L. Frassetto, R.C. Petersen, B.L. Miller, E.J. Goetzl, Dysfunctionally phosphorylated type 1 insulin receptor substrate in neural-derived blood exosomes of preclinical Alzheimer's disease, FASEB J. 29 (2015) 589–596.
[15] E.J. Goetzl, A. Boxer, J.B. Schwartz, E.L. Abner, R.C. Petersen, B.L. Miller, D. Kapogiannis, Altered lysosomal proteins in neural-derived plasma exosomes in preclinical Alzheimer disease, Neurology 85 (2015) 40–47.
[16] E.J. Goetzl, M. Mustapic, D. Kapogiannis, E. Eitan, I.V. Lobach, L. Goetzl, J.B. Schwartz, B.L. Miller, Cargo proteins of plasma astrocyte-derived exosomes in Alzheimer's disease, FASEB J. 30 (2016) 3853–3859.
[17] E.J. Goetzl, D. Kapogiannis, J.B. Schwartz, I.V. Lobach, L. Goetzl, E.L. Abner, G.A. Jicha, A.M. Karydas, A. Boxer, B.L. Miller, Decreased synaptic proteins in neuronal exosomes of frontotemporal dementia and Alzheimer's disease, FASEB J. 30 (2016) 4141–4148.
[18] C.N. Winston, E.J. Goetzl, J.C. Akers, B.S. Carter, E.M. Rockenstein, D. Galasko, E. Masliah, R.A. Rissman, Prediction of conversion from mild cognitive impairment to dementia with neuronally derived blood exosome protein profile, Alzheimers Dement. (Amst.) 3 (2016) 63–72.
[19] E.J. Goetzl, E.L. Abner, G.A. Jicha, D. Kapogiannis, J.B. Schwartz, Declining levels of functionally specialized synaptic proteins in plasma neuronal exosomes with progression of Alzheimer's disease, FASEB J. 32 (2018) 888–893.
[20] L. Goetzl, N. Merabova, N. Darbinian, D. Martirosyan, E. Poletto, K. Fugarolas, O. Menkiti, Diagnostic potential of neural exosome cargo as biomarkers for acute brain injury, Ann. Clin. Transl. Neurol. 5 (2018) 4–10.
[21] M.A. van Es, O. Hardiman, A. Chio, A. Al-Chalabi, R.J. Pasterkamp, J.H. Veldink, L.H. van den Berg, Amyotrophic lateral sclerosis, Lancet 390 (2017) 2084–2098.
[22] M.J. de Hoon, S. Imoto, J. Nolan, S. Miyano, Open source clustering software, Bioinformatics 20 (2004) 1453–1454.
[23] A.J. Saldanha, Java Treeview–extensible visualization of microarray data, Bioinformatics 20 (2004) 3246–3248.
[24] C.E. Vejnar, M. Blum, E.M. Zdobnov, miRmap web: comprehensive microRNA target prediction online, Nucleic Acids Res. 41 (2013) W165–W168.
[25] H. Mi, A. Muruganujan, J.T. Casagrande, P.D. Thomas, Large-scale gene function analysis with the PANTHER classification system, Nat. Protoc. 8 (2013) 1551–1566.
[26] M. Mustapic, E. Eitan, J.K. Werner Jr., S.T. Berkowitz, M.P. Lazaropoulos, J. Tran, E.J. Goetzl, D. Kapogiannis, Plasma extracellular vesicles enriched for neuronal origin: a potential window into brain pathologic processes, Front. Neurosci. 11 (2017) 278.
[27] The Genotype-Tissue Expression (GTEx) project, Nat. Genet. 45 (2013) 580–585.
[28] M. Verhage, A.S. Maia, J.J. Plomp, A.B. Brussaard, J.H. Heeroma, H. Vermeer, R.F. Toonen, R.E. Hammer, T.K. van den Berg, M. Missler, H.J. Geuze, T.C. Sudhof, Synaptic assembly of the brain in the absence of neurotransmitter secretion, Science (New York, N.Y.) 287 (2000) 864–869.
[29] Y. Wang, M. Okamoto, F. Schmitz, K. Hofmann, T.C. Sudhof, Rim is a putative Rab3 effector in regulating synaptic-vesicle fusion, Nature 388 (1997) 593–598.
[30] P.S. Kaeser, L. Deng, Y. Wang, I. Dulubova, X. Liu, J. Rizo, T.C. Sudhof, RIM proteins tether Ca2+ channels to presynaptic active zones via a direct PDZ-domain interaction, Cell 144 (2011) 282–295.
[31] C. Ma, L. Su, A.B. Seven, Y. Xu, J. Rizo, Reconstitution of the vital functions of Munc18 and Munc13 in neurotransmitter release, Science (New York, N.Y.) 339 (2013) 421–425.
[32] F.P. Diekstra, V.M. Van Deerlin, J.C. van Swieten, A. Al-Chalabi, A.C. Ludolph, J.H. Weishaupt, et al., C9orf72 and UNC13A are shared risk loci for amyotrophic lateral sclerosis and frontotemporal dementia: a genome-wide meta-analysis, Ann. Neurol. 76 (2014) 120–133.
[33] K.B. Ahmeti, S. Ajroud-Driss, A. Al-Chalabi, P.M. Andersen, J. Armstrong, A. Birve, H.M. Blauw, et al., A. Consortium, Age of onset of amyotrophic lateral sclerosis is modulated by a locus on 1p34.1, Neurobiol Aging 34 357 (2013) e357–319.
[34] M.A. van Es, J.H. Veldink, C.G. Saris, H.M. Blauw, P.W. van Vught, A. Birve, R. Lemmens, et al., Genome-wide association study identifies 19p13.3 (UNC13A) and 9p21.2 as susceptibility loci for sporadic amyotrophic lateral sclerosis, Nat. Genet. 41 (2009) 1083–1087.
[35] K. Placek, G.M. Baer, L. Elman, L. McCluskey, L. Hennessy, P.M. Ferraro, E.B. Lee, V.M.Y. Lee, J.Q. Trojanowski, V.M. Van Deerlin, M. Grossman, D.J. Irwin, C.T. McMillan, UNC13A polymorphism contributes to frontotemporal disease in sporadic amyotrophic lateral sclerosis, Neurobiol. Aging 73 (2019) 190–199.
[36] Correction for Gerth, et al., Intersectin associates with synapsin and regulates its nanoscale localization and function, Proc. Natl. Acad. Sci. U. S. A. 114 (2017) E11060.
[37] T. Schmitt-John, VPS54 and the wobbler mouse, Front. Neurosci. 9 (2015) 381.
[38] F.P. Diekstra, C.G. Saris, W. van Rheenen, L. Franke, R.C. Jansen, M.A. van Es, P.W. van Vught, et al., Mapping of gene expression reveals CYP27A1 as a susceptibility gene for sporadic ALS, PLoS One 7 (2012) e35333.
[39] R.C. Paolicelli, A. Jawaid, C.M. Henstridge, A. Valeri, M. Merlini, J.L. Robinson, E.B. Lee, J. Rose, S. Appel, V.M. Lee, J.Q. Trojanowski, T. Spires-Jones, P.E. Schulz, L. Rajendran, TDP-43 depletion in microglia promotes amyloid clearance but also induces synapse loss, Neuron 95 (2017) 297–308 e6.

ARTICLES
https://doi.org/10.1038/s41591-020-0781-z

nature medicine

A soluble phosphorylated tau signature links tau, amyloid and the evolution of stages of dominantly inherited Alzheimer's disease

Nicolas R. Barthélemy[1], Yan Li[1,2], Nelly Joseph-Mathurin[3], Brian A. Gordon[3], Jason Hassenstab[1], Tammie. L. S. Benzinger[3], Virginia Buckles[1], Anne M. Fagan[1], Richard J. Perrin[4], Alison M. Goate[5], John C. Morris[1], Celeste M. Karch[6], Chengjie Xiong[2], Ricardo Allegri[7], Patricio Chrem Mendez[7], Sarah B. Berman[8], Takeshi Ikeuchi[9], Hiroshi Mori[10], Hiroyuki Shimada[10], Mikio Shoji[11], Kazushi Suzuki[12], James Noble[13], Martin Farlow[14], Jasmeer Chhatwal[15], Neill R. Graff-Radford[16], Stephen Salloway[17,18], Peter R. Schofield[19,20], Colin L. Masters[21,22], Ralph N. Martins[23], Antoinette O'Connor[24], Nick C. Fox[24], Johannes Levin[25,26,27], Mathias Jucker[28,29], Audrey Gabelle[30], Sylvain Lehmann[30], Chihiro Sato[1], Randall J. Bateman[1]✉, Eric McDade[1]✉ and the Dominantly Inherited Alzheimer Network*

Development of tau-based therapies for Alzheimer's disease requires an understanding of the timing of disease-related changes in tau. We quantified the phosphorylation state at multiple sites of the tau protein in cerebrospinal fluid markers across four decades of disease progression in dominantly inherited Alzheimer's disease. We identified a pattern of tau staging where site-specific phosphorylation changes occur at different periods of disease progression and follow distinct trajectories over time. These tau phosphorylation state changes are uniquely associated with structural, metabolic, neurodegenerative and clinical markers of disease, and some (p-tau217 and p-tau181) begin with the initial increases in aggregate amyloid-β as early as two decades before the development of aggregated tau pathology. Others (p-tau205 and t-tau) increase with atrophy and hypometabolism closer to symptom onset. These findings provide insights into the pathways linking tau, amyloid-β and neurodegeneration, and may facilitate clinical trials of tau-based treatments.

The microtubule-associated protein tau (MAPT or τ) plays an essential role in the morphology and physiology of neurons[1,2]. Phosphorylation is an important post-translational modification for regulating the normal function of tau in axonal stabilization, and can occur at over 80 different positions[3]. However, excessive phosphorylation of tau (p-tau) appears to increase the probability of tau aggregating into intracellular insoluble paired helical filaments and neurofibrillary tangles (NFTs)[4,5], which are primarily composed of hyperphosphorylated tau. Intracellular NFTs in the cerebral cortex are a defining pathological feature of Alzheimer's disease (AD) and correlate with the onset of clinical symptoms long after the appearance of extracellular aggregated amyloid-β (Aβ) 'plaques'[6,7], which begin to develop up to two decades before symptom onset[8,9]. In AD, soluble p-tau181 (pT181) and t-tau are elevated in the cerebrospinal fluid (CSF)[10–12] and begin to increase before symptom onset in both dominantly inherited AD (DIAD) and sporadic AD (sAD)[13,14]. It has been proposed that these changes reflect the effects of neuronal death (neurodegeneration) passively

[1]Department of Neurology, Washington University School of Medicine, Saint Louis, MO, USA. [2]Division of Biostatistics, Washington University School of Medicine, Saint Louis, MO, USA. [3]Department of Radiology, Washington University School of Medicine, Saint Louis, MO, USA. [4]Department of Pathology, Washington University School of Medicine, Saint Louis, MO, USA. [5]Department of Neuroscience, Icahn School of Medicine at Mount Sinai, New York, NY, USA. [6]Department of Psychiatry, Washington University School of Medicine, Saint Louis, MO, USA. [7]Fundación para la Lucha contra las Enfermedades Neurológicas de la Infancia (FLENI) Instituto de Investigaciones Neurológicas Raúl Correa, Buenos Aires, Argentina. [8]University of Pittsburgh School of Medicine, Pittsburgh, PA, USA. [9]Niigata University, Niigata, Japan. [10]Osaka City University, Osaka, Japan. [11]Hirosaki University, Hirosaki, Japan. [12]Tokyo University, Tokyo, Japan. [13]Columbia University, College of Physicians and Surgeons, New York, NY, USA. [14]Department of Neurology, Indiana University, Indianapolis, IN, USA. [15]Massachusetts General Hospital, Harvard Medical School, Boston, MA, USA. [16]Department of Neurology, Mayo Clinic Jacksonville, Jacksonville, FL, USA. [17]Butler Hospital, Providence, RI, USA. [18]Brown University, Providence, RI, USA. [19]Neuroscience Research Australia, Sydney, New South Wales, Australia. [20]School of Medical Sciences, University of New South Wales, Sydney, New South Wales, Australia. [21]The Florey Institute of Neuroscience and Mental Health, Melbourne, Victoria, Australia. [22]University of Melbourne, Melbourne, Victoria, Australia. [23]Edith Cowan University, Perth, Western Australia, Australia. [24]Dementia Research Centre, Institute of Neurology, University College London, London, UK. [25]German Center for Neurodegenerative Diseases (DZNE) Munich, Munich, Germany. [26]Department of Neurology, Ludwig-Maximilians Universität München, Munich, Germany. [27]Munich Cluster for Systems Neurology (SyNergy), Munich, Germany. [28]German Center for Neurodegenerative Diseases (DZNE), Tübingen, Germany. [29]Hertie-Institute for Clinical Brain Research, University of Tübingen, Tübingen, Germany. [30]Laboratoire de Biochimie et Protéomique Clinique and CRB, INSERM-UM, CHU Montpellier, Montpellier, France, Montpellier, France. *A list of members and affiliations appears at the end of the paper. ✉e-mail: batemanr@wustl.edu; ericmcdade@wustl.edu

releasing tau and NFTs[15,16] into the CSF. However, in other tauopathies with significant NFT pathology and neurodegeneration (for example, progressive supranuclear palsy and frontotemporal lobar degeneration-tau), CSF levels of soluble pT181 and t-tau do not increase[17,18], and in AD, NFTs measured by tau positron emission tomography (tau-PET) only modestly correlate with CSF t-tau and p-tau[19,20]. Moreover, recent work in DIAD and sAD has suggested that NFTs, as measured by tau-PET, primarily increase at symptom onset 10–15 years after[21–25] soluble tau increase[9,26,27]. Furthermore, the rate of the increase of p-tau and tau levels may actually slow as neurodegeneration increases[8,13,28]. These observations suggest that the tauopathy of AD is a more dynamic process than is currently conceptualized[15], that soluble and aggregated tau probably have important differences, and that cerebral Aβ may trigger a process that leads to the unique tauopathy of AD[22,29–37]. This concept is further supported by an increase in the active production of soluble tau in the presence of aggregated amyloid in humans[33]. ^{11}C-Pittsburgh compound B (PiB)-PET imaging of cortical aggregated Aβ has detected Aβ pathology two decades before the appearance of symptoms in DIAD[8,38], but has not consistently been linked with a rise in CSF tau and pT181 (ref. [8]). However, unresolved questions include: 'what is the relationship of tau to aggregated Aβ?' and 'what are the different tau pathophysiological changes that occur during the preclinical and clinical stages of AD?'. The answers to these questions will help identify the tau pathophysiological processes that are related to AD and neurodegeneration, which is a critical step needed to advance therapeutic and diagnostic targets for the disease.

An important limitation to understanding the tauopathy of AD has been the lack of methods that can simultaneously quantify phosphorylation at multiple positions of the tau protein in a population representing the full clinicopathological spectrum of AD (that is, from 'at risk' to dementia). To further explore these questions and limitations, we developed a mass spectrometry method to measure the phosphorylation occupancy (phosphorylated to unphosphorylated) at multiple tau phosphorylation sites in the proline-rich protein domain ranging from 150–220 residues[33] in CSF, independent of variation in t-tau levels. We measured CSF from a large cohort of comprehensively studied participants with DIAD ($n=370$), as well as a cohort of adult participants either with sAD or with unaffected cognition but a risk of disease (based on the presence of abnormal Aβ pathology) ($n=104$) (Table 1 and Supplementary Table 1). We quantified multiple positions throughout tau and the associated phosphorylation occupancy to determine disease stage-specific changes in soluble p-tau isoforms. The relatively predictable age of disease onset in DIAD families[39] enables us to infer the pattern of change across decades of AD progression. This cohort was recruited and evaluated by the Dominantly Inherited Alzheimer Network (DIAN)—a global, multi-site, observational study of adults with, and at risk of carrying, causative mutations for early-onset AD. Participants undergo a comprehensive, standardized assessment of biofluids and brain imaging, with cognitive and clinical assessments.

The results of our investigation show that hyperphosphorylation at specific sites of the tau protein is a dynamic process that changes first based on the pathological state (that is, the presence and amount of aggregated Aß) and then based on the stage of disease and clinical stage (cognitively normal or cognitively impaired) of AD in both DIAD and sAD. Furthermore, in DIAD, we demonstrate that these phosphorylation sites have opposite trajectories of change at different stages over the 30 years of the DIAD process and have different associations with brain hypometabolism, atrophy and cognitive decline (Fig. 1). These findings suggest a predictable progression of changes in tau phosphorylation (an AD–tau staging system) and support recent tau kinetic studies demonstrating aggregated Aß-related active release of phosphorylated tau[33]. Moreover, this AD–tau staging suggests potential tau targets for the development of tau-specific therapeutics and provides downstream measures for therapies targeting early amyloid pathology.

Results

Disease stage and progression are associated with site-specific differences in tau hyperphosphorylation and longitudinal rates of change in DIAD and sAD. The certainty of disease and predictability of symptom onset of DIAD enables the staging of individuals based on the estimated years to symptom onset (EYO)[8,9,26] (that is, the age of an individual at the time of assessment relative to the age of onset of others with the mutation). Therefore, we determined whether there were temporal differences in the pattern of phosphorylation of CSF tau as it relates to the EYO. This was done by estimating the differences in the amount and rate of change in phosphorylation over time between mutation carriers and non-carriers based on the EYO. There were two important findings. First, there was evidence that increases in t-tau and phosphorylation at specific sites occurred in a relative order: phosphorylation of tau at threonine 217 (pT217/T217) (which occurred at around −21 EYO) was followed by that of threonine 181 (pT181/T181) (−19 EYO), then t-tau increase (−17 EYO), then phosphorylation of tau at threonine 205 (pT205/T205) (−13 EYO) (Fig. 2, Extended Data Fig. 1a–e and Supplementary Table 2). The initial increase of pT217/T217, and to a lesser extent in pT181/T181, occurred at a similar time to when PiB-PET SUVR began to increase (−19 EYO) (see below).

Second, pT217/T217 and pT181/T181 began to decline significantly near the time of symptom onset, while phosphorylation at pT205/T205 slowed and t-tau levels continued to increase. Of note, the concentrations of all of the corresponding unphosphorylated isoforms (T181, S202/T205 and T217) increased with disease progression, suggesting that the decrease in the phosphorylation ratio for pT217/T217 and pT181/T181 was not a result of a disproportionate rise in unphosphorylated peptides specifically related to these two sites, nor a decrease in total levels of tau protein (Extended Data Fig. 2). At the 202 position of serine (pS202/S202), there was no significant change in phosphorylation over the course of the disease (Fig. 2 and Extended Data Fig. 2c).

Next, we assessed whether the above findings were also seen in an elderly group of patients with sAD and non-carriers who were at risk for AD, based on the presence of abnormal Aβ biomarkers (preclinical AD ($n=63$)) or normal Aβ biomarkers ($n=39$). This group of participants underwent the following clinical assessments: the Clinical Dementia Rating (CDR) scale, CSF collection and Aβ measures cross-sectionally. Because sAD is associated with a later age and additional pathologies (for example, higher vascular disease burden and greater TAR DNA-binding protein 43 inclusions) compared with a more 'pure' form of AD in DIAD, it is possible that there could be important differences in tau phosphorylation between the two types of AD. However, the preclinical sAD population lacked a predictor of disease onset similar to EYO in DIAD, and longitudinal CSF data were not available; therefore, we compared the two groups based on: (1) the absence or presence of amyloid pathology (to define a similar AD risk state); and (2) the stage of dementia symptoms, using the CDR (where CDR 0 = no dementia, CDR 0.5 = very mild dementia and CDR ≥ 1 = mild to moderate dementia)[10] (Fig. 3c).

Overall, there was a similar pattern of phosphorylation changes at each site for both cohorts. In both DIAD and sAD, pT217/T217 and pT181/T181 ratios increase significantly with the presence of amyloid pathology and then less so with more advanced stages of symptoms. However, the rate of phosphorylation of T205 and levels of t-tau increase at later stages and continue increasing as clinical disease progresses. Similarly, in both DIAD and sAD, the phosphorylation of pS202 remains relatively stable with amyloid pathology and disease progression. Notably, there was evidence that in DIAD there is a greater magnitude of phosphorylation and higher levels of t-tau for each category compared with sAD.

Table 1 | Demographic, CSF, neuroimaging and cognition measures for mutation carriers versus non-carriers and the cohort of non-familial at-risk and symptomatic participants

Cohort with DIAN		Mutation carriers		Mutation non-carriers	*P* value
	n[a]	Asymptomatic (*n* = 152)	Symptomatic (*n* = 77)	(*n* = 141)	
Age (years)	370	34.4 ± 8.9	46.2 ± 9.2	38.5 ± 12.2	<0.0001
Female (*n* (%))	370	84 (55.3)	39 (50.7)	88 (62.4)	0.15
Apolipoprotein-E ε4 (*n* (%))	370	48 (31.6)	23 (29.9)	51 (36.2)	0.67
EYO (years)	370	−13.4 ± 8.7	3.42 ± 3.47	−9.2 ± 12.5	<0.0001
Cortical PiB-PET SUVR	304 (133, 50, 121)	1.76 ± 0.89	2.82 ± 1.27	1.06 ± 0.17	<0.0001
PiB+ (*n* (%))[b]	304 (133, 50, 121)	81 (60.9)	48 (96.0)	2 (1.65)	<0.0001
CSF pT181/T181	370	26.5 ± 7.2	34.2 ± 7.7	21.7 ± 2.3	<0.0001
CSF pT181 level (ng ml^{-1})	370	0.14 ± 0.09	0.30 ± 0.19	0.088 ± 0.034	<0.0001
CSF pT205/T205	370	0.44 ± 0.24	0.93 ± 0.36	0.34 ± 0.13	<0.0001
CSF pT205 level (ng ml^{-1})	370	0.003 ± 0.003	0.011 ± 0.008	0.002 ± 0.001	<0.0001
CSF pT217/T217	370	3.49 ± 3.08	8.42 ± 4.05	1.25 ± 0.66	<0.0001
CSF pT217 level (ng ml^{-1})	370	0.015 ± 0.018	0.054 ± 0.047	0.004 ± 0.004	<0.0001
CSF pS202/S202	370	2.77 ± 0.80	2.52 ± 0.68	3.10 ± 0.72	<0.0001
CSF pS202 level (ng ml^{-1})	370	0.016 ± 0.006	0.025 ± 0.011	0.014 ± 0.005	<0.0001
CSF tau level (ng ml^{-1})	370	0.51 ± 0.21	0.82 ± 0.41	0.40 ± 0.14	<0.0001
Precuneus (mm)	344 (146, 64, 134)	2.37 ± 0.15	2.10 ± 0.24	2.38 ± 0.14	<0.0001
Cortical FDG-PET SUVR	318 (137, 59, 122)	1.73 ± 0.14	1.57 ± 0.18	1.71 ± 0.14	<0.0001
Hippocampal volume (mm^3)	344 (146, 64, 134)	8,863 ± 970	7,290 ± 1214	8,787 ± 775	<0.0001
Cognitive composite (*z* score)	356 (151, 66, 139)	−0.096 ± 0.640	−1.67 ± 0.85	−0.03 ± 0.59	<0.0001

At-risk and sAD cohort					
	n[c]	Amyloid negative (*n* = 39)	Amyloid positive		
			Asymptomatic (*n* = 18)	Symptomatic (*n* = 45)	*F* value[d]
Age (years)	102	73.3 ± 8.6	71.6 ± 6.4	72.6 ± 6.2	0.41
Female (*n* (%))	102	17 (44)	8 (44)	31 (69)	0.041 (*P* value)
MMSE score	102	28.7 ± 1.6	29.4 ± 0.5	23.6 ± 3.9	45.44***
CSF pT181/T181	102	13.8 ± 1.3	16.6 ± 2.9	18.8 ± 2.5	53.55***
CSF pT205/T205	102	0.14 ± 0.06	0.2 ± 0.08	0.33 ± 0.11	50.6***
CSF pT217/T217	102	3.3 ± 1.4	8.2 ± 4.8	10 ± 4.1	39.18***
CSF pS202/S202	102	1.4 ± 0.48	1.2 ± 0.33	1.38 ± 0.45	1.042
CSF tau level (ng ml^{-1})	102	0.76 ± 0.31	0.89 ± 0.32	1.1 ± 0.41	7.14**

Continuous measures are presented as means ± s.d. For mutation carriers and non-carriers, the significance of the difference among asymptomatic mutation carriers, symptomatic mutation carriers and non-carriers was calculated using a *t*-test based on an LME model (for continuous outcomes) and a generalized LME model with a logistic link (for categorical outcomes). All of the mixed models included a random family effect to account for the correlations on the outcome measures between participants within the same family. For the non-familial at-risk and symptomatic cohort, the *P* values were calculated by one-way analysis of variance (for continuous outcomes) and chi-squared test (for categorical outcomes). [a]Total number of participants, with numbers of asymptomatic mutation carriers, symptomatic mutation carriers and non-carriers, respectively, in parentheses). [b]PiB+ = standard uptake value ratio (SUVR) > 1.25. [c]Total number of amyloid-negative and amyloid-positive (asymptomatic and symptomatic) participants. [d]**$P = 0.01$; ***$P = 0.001$. All other *F* values had a *P* value > 0.05. MMSE, mini-mental state examination; p, phosphorylated; S, serine; T, threonine.

Next, we evaluated the proportion of participants in both cohorts who exceeded the values considered abnormal for t-tau and each p-tau isoform for each category of PiB-PET (positive or negative) and clinical progression (CDR = 0, 0.5 or ≥1). Extended Data Fig. 3 and Supplementary Table 3 show very similar patterns for DIAD and sAD as they relate to the sequential increases in phosphorylation at pT217/T217 and pT181/T181 first, coinciding with the presence of PiB-PET amyloid, followed by increases in pT205/T205 and t-tau with the development and progression of clinical symptoms.

These results indicate that phosphorylation of tau changes at specific sites by disease stage. In DIAN in particular, this suggests a cascade of changes in soluble tau that is more dynamic than was previously realized, and that tau does not monotonically increase in phosphorylation states or rates. The emergence of PiB-PET Aβ and the onset of clinical decline, separated by nearly two decades, mark two important stages of soluble tau phosphorylation changes in DIAD and sAD and suggest that the two different pathways to AD have a similar pattern of evolution in the abnormal processing of tau and expression in the CSF.

Cerebral amyloid pathology is associated with site-specific differences in tau hyperphosphorylation in presymptomatic DIAD. Given the temporal sequence of changes in tau species identified using disease predictability (EYO), we then sought to determine whether changes in other biomarkers across the disease could reveal important associations with the different sites of phosphorylation in DIAD. To explore the relationship of aggregated Aβ and

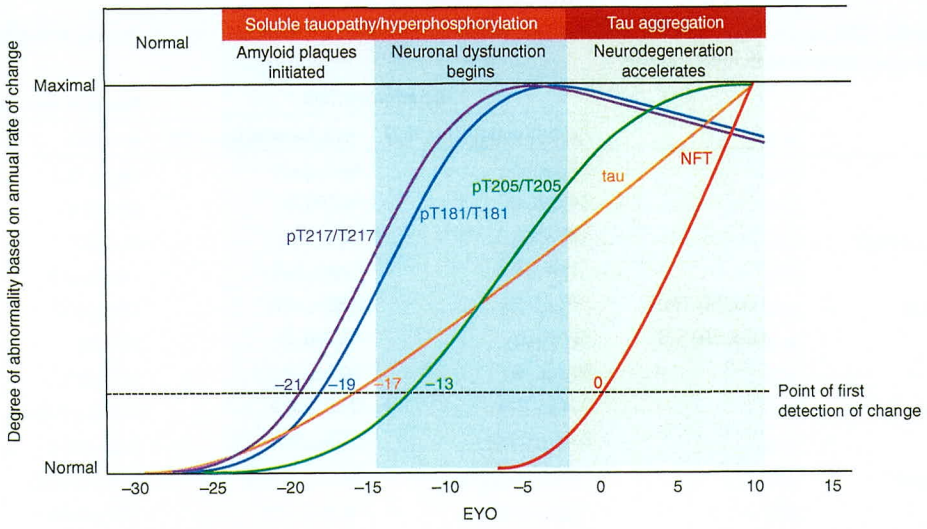

Fig. 1 | Stages of tau pathology. Tau pathophysiology evolves through distinct phases in DIAD. Measures of four different soluble tau species and aggregated tau in DIAD show, over the course of 35 years, that tau sequentially changes by stage of disease related to amyloid plaques, cortical atrophy and metabolism. Starting with the development of fibrillar amyloid pathology, levels of pT217 (purple) and pT181 (blue) begin to increase. Then, with the increase in neuronal dysfunction (decreased cortical metabolism), levels of pT205 (green) begin to increase, along with soluble t-tau (orange). Lastly, with the onset of neurodegeneration (based on cortical atrophy and clinical decline), tau-PET tangles (red) begin to develop, while pT217 and pT181 decrease. Together, the dynamic and diverging patterns of soluble and aggregated tau begin in close relationship with amyloid pathology and change over the course of the disease.

soluble tau phosphorylation, we compared the SUVR value of cortical PiB-PET, which reliably identifies significant brain-aggregated Aß (SUVR > 1.25), with the p-tau isoforms, to determine concordance with aggregated Aß (amyloid-positive SUVR ≥ 1.25; amyloid-negative SUVR < 1.25) (Fig. 3a). pT217/T217 had a 97.2% area under the curve (AUC) (95% confidence interval (CI) = 0.94–0.99); pT181/T181 had an 89.1% AUC (95% CI = 0.83–0.94); pT205/T205 had a 74.5% AUC (95% CI = 0.69–0.82); t-tau had a 72% AUC (95% CI = 0.65–0.79); and pS202/S202 had a 69% AUC (95% CI = 0.62–0.77) to classify asymptomatic participants as having PiB-PET SUVR levels consistent with aggregated Aβ. This indicates that at the early stages of significant fibrillar Aβ plaques, an increase of phosphorylation has already begun at specific positions linking these two processes in time, and also demonstrates that an increase in the phosphorylation occupancy on T217 could serve as a sensitive diagnostic marker for aggregated Aβ plaque pathology measured by PiB-PET, identifying a potentially unique signature of Aβ-related tau processing in DIAD. When using CSF-soluble Aβ in DIAD to determine abnormal amyloid levels, we found the same order for the soluble tau measures in classifying participants as amyloid positive (Aβ 42/40 ≥ 0.0776) or amyloid negative (Aβ 42/40 < 0.0776), but lower AUC values for each (Supplementary Table 4). Additionally, we compared this mass spectrometry-based method with one of the most advanced immunoassays (the Roche Elecsys pT181 and t-tau CSF electrochemiluminescence method) and found the mass spectrometry method to be superior, indicating a greater sensitivity to detecting early AD pathology in DIAD (Supplementary Table 5).

We then compared the ratios (standardized to a *z* score across all mutation carriers) at four phosphorylation sites and t-tau levels by PiB-PET SUVR quartiles to explore the cross-sectional relationship between total aggregated Aβ load and phosphorylation (Fig. 3b). All phosphorylation sites except S202 demonstrated increased levels of phosphorylation with greater PiB-PET SUVR; in contrast, pS202/S202 had a decrease in phosphorylation with increasing PiB-PET SUVRs. These results suggest that the events initially leading to increased tau phosphorylation in AD are probably related to aggregated Aβ pathology, potentially through regulation by distinct kinases and phosphatases that are phosphorylation-site specific[11]. Yet, as aggregated Aβ burden continues to increase, there are differences between the amount of phosphorylation that continues to occur among different p-tau isoforms. Importantly, among mutation non-carriers, the only participants who showed an increase in pT217/T217 were those who were amyloid positive (SUVR > 1.25; $n = 4$).

Next, we assessed whether phosphorylation of tau was associated with the anatomical distribution of cerebral aggregated Aβ pathology by exploring the cross-sectional correlations between the baseline p-tau phosphorylation sites and cortical and subcortical regions of amyloid plaque deposition as measured by PiB-PET SUVR in the asymptomatic mutation carriers (Fig. 3d and Supplementary Table 6). pT217/T217, pT181/T181 and pT205/T205 phosphorylation was positively correlated with PiB-PET SUVR throughout the brain, but pS202/S202 was negatively correlated. In the precuneus—a region of early amyloid plaque deposition[38]—correlations with tau phosphorylation were compared based on the strength of bivariate regression, controlling for age, gender and EYO and adjusted for multiple comparisons. We found an order of correlations from greatest to least of pT217/T217 ($r = 0.53$; s.e.m. = 0.06; $P < 10^{-30}$) > pT205/T205 ($r = 0.37$; s.e.m. = 0.075; $P < 10^{-5}$) > pT181/T181 ($r = 0.35$; s.e.m. = 0.075; $P < 10^{-6}$), with positive correlations with PiB-PET SUVR. In contrast, pS202/S202 had an inverse correlation ($r = -0.46$; s.e.m. = 0.067; $P < 10^{-7}$), suggesting that phosphorylation at this site is reduced with increasing aggregated Aβ pathology. We found a similar rank ordering for nearly all regions of PiB-PET and p-tau isoform correlations and statistically significant differences between the different p-tau measure correlations, most commonly for pT217/T217 having the greatest associations.

Neuroimaging markers of disease progression are associated with site-specific differences in tau hyperphosphorylation in pre-

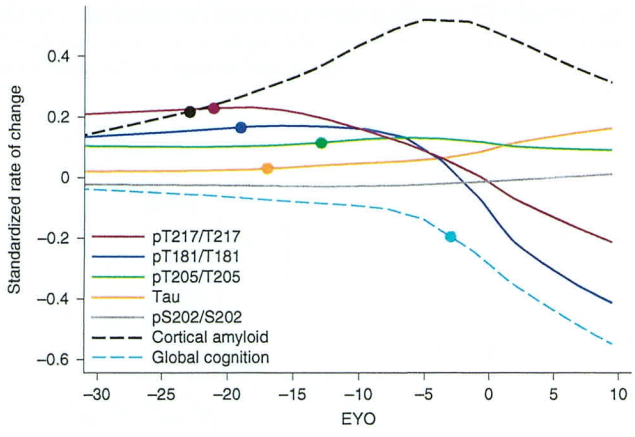

Fig. 2 | Longitudinal changes of different p-tau sites are specific to disease stage and change in opposite directions as AD progresses in dominantly inherited mutation carriers. LME model-estimated annual rates of change for each site of phosphorylation, based on the standardized mutation carrier data ($n=370$), plotted by EYO along with PiB-PET (black dashed line; $n=304$) and cognitive decline (aqua dashed line; $n=356$). The solid circles represent the points at which the rate of change for each variable first become different for mutation carriers compared with non-carriers. This highlights the pattern of change for p-tau isoforms over the course of the AD spectrum and the close association between amyloid plaque growth and the increase in pT217/T217, with plaques beginning to increase at −21 EYO and hyperphosphorylation of T217 (purple) also beginning at −21 EYO, followed by an increase in hyperphosphorylation of T181 (blue) at −19 EYO and a decrease in the phosphorylation rate at these two sites associated with a decline in cognition. In contrast, phosphorylation of T205 (green) continues increasing throughout disease progression and t-tau levels (orange) increase at an increased rate near the time of symptom onset. Levels of pS202 do not increase throughout the disease course.

symptomatic DIAD. In addition to using EYO, disease advancement in DIAD can be estimated using neuroimaging measures that track various components of disease progression (for example, brain atrophy and metabolic decline). These measures have been shown to change at different periods of time before symptom onset in DIAD, with declining cerebral metabolism (measured by ^{18}F fluorodeoxyglucose [FDG]-PET) occurring up to 18 years before symptom onset and brain atrophy (determined by magnetic resonance imaging (MRI)) occurring up to 13 years before symptom onset[38,42–44]. This raises the question of whether these biomarkers are likewise correlated with tau phosphorylation at specific sites. To examine this, we performed bivariate cross-sectional correlations between the phosphorylation sites and t-tau and imaging measurements from 34 cortical and six subcortical brain regions, controlling for sex, age and EYO. We focused the analyses on asymptomatic mutation carriers in order to identify any associations at the earliest stages of disease progression, before severe neurodegeneration. The phosphorylation state of pS202/S202 was not included in these analyses given its relative lack of change over disease progression.

MRI. Hyperphosphorylation was inversely associated with cortical thickness in asymptomatic mutation carriers: pT205/T205, and to a lesser extent pT217/T217, was most strongly associated with a decrease in cortical and subcortical thickness throughout the brain (Fig. 4a and Supplementary Table 7), while t-tau levels showed fewer regional associations and weaker correlations. Hyperphosphorylation at pT181/T181 had the lowest overall correlation with cortical atrophy and was restricted to the medial and lateral parietal lobes and medial dorsomedial frontal lobes. This suggests that the initial rise in pT205/T205 at −13 EYO may be related to the underlying process of cortical atrophy, which we have previously shown to begin at approximately −13 EYO in the precuneus[38]. Previous work in DIAN and other DIAD cohorts has shown that significant atrophy, as measured by MRI, does not occur until closer to disease onset, which would indicate that although an increase in CSF tau and phosphorylated tau may in part be related to a passive release in neurodegeneration, their initial rise is probably the consequence of other processes.

FDG-PET. In addition to cortical atrophy, a decline in glucose metabolism in neurons and glia is associated with disease progression in AD. Therefore, we tested whether there were distinct associations between cortical or subcortical metabolic impairment and tau phosphorylation. In the asymptomatic mutation carriers, phosphorylation at pT205/T205 was correlated with glucose hypometabolism throughout the cortex and subcortical regions, as measured by FDG-PET (Fig. 4b and Supplementary Table 8). There were minimal associations identified for the other p-tau sites and t-tau levels in asymptomatic mutation carriers.

Together, these results indicate that the underlying processes leading to neuronal impairment and neurodegeneration during asymptomatic disease progression, as measured by neuroimaging, have different associations with tau phosphorylation, with pT205/T205 most strongly correlated with both.

Fig. 3 | Specific soluble tau phosphorylation sites are differentially associated with amyloid plaques in DIAD and sAD. a, Receiver operating characteristics of tau phosphorylation with Aß pathology based on Aβ PiB-PET (SUVR cutoff of 1.25) in DIAD ($n=252$). There is a near-perfect association with Aβ pathology for pT217/T217 (purple; AUC = 0.97). AUC values for the other phosphorylation ratios were: 0.89 (pT181/T181; blue); 0.74 (pT205/T205; green); 0.72 (t-tau; orange) and 0.69 (pS202/S202; gray). b, Standardized (*z* score) phosphorylation ratios (pT217/T217, pT181/T181, pS202/S202 and pT205/T205) and t-tau levels by Aβ PiB-PET quartile ($n=47$ for Q1; $n=48$ for Q2; $n=48$ for Q3; $n=48$ for Q4) for mutation carriers suggest site-specific differences in phosphorylation with increasing Aβ PiB-PET levels. pT217, pT181, pT205 and t-tau increase as Aβ PiB-PET increases. There was a significant decrease in the phosphorylation of S202 at the highest Aβ PiB-PET quartiles relative to the lowest (Wilcoxon rank-sum test). **c**, Change in phosphorylation rates and t-tau levels for DIAD ($n=209$) and sAD ($n=86$) across the spectrum of clinical progression (blue = cognitively normal/amyloid negative). For DIAD, there is evidence of a higher ratio of phosphorylation, and in both DIAD and sAD, the phosphorylation of T217 and T181 increases once amyloid pathology begins, followed by a plateau. In contrast, pT205 and t-tau levels increase at later stages of disease progression. For S202 in both DIAD and sAD, there is minimal change in the phosphorylation rate across the disease spectrum (Mann–Whitney *U*-test). For the box plots in **b** and **c**, the middle line represents the median; the upper and lower notches show the median ± 1.58× the interquartile range/square root(number of observations); and the upper (and lower) whiskers represent the largest observation greater (or less than or equal to) the upper (or lower) hinge + 1.58× the IQR. **d**, Cross-sectional, bivariate correlations between cortical and subcortical Aβ PiB-PET SUVR and site-specific phosphorylation for asymptomatic mutation carriers ($n=152$). Colors represent correlations, with positive correlations in yellow/red and negative correlations in blue. *P* values for the correlations were derived from a *z*-test using the covariance matrix of the bivariate LME models. All correlations represent statistically significant values surviving a false discovery rate ($P<0.05$) with Benjamini–Hochberg correction. They are arranged by correlation strength from top to bottom. CN, cognitively normal; MS, mass spectrometry.

Cognitive decline and brain atrophy are associated with site-specific differences in tau hyperphosphorylation in DIAD. Previous studies have shown that AD dementia is more closely related to neocortical NFT pathology than neocortical Aβ pathology[15], yet the relationship between soluble tau and cognition remains uncertain[16]. Therefore, we assessed the longitudinal change in the soluble tau

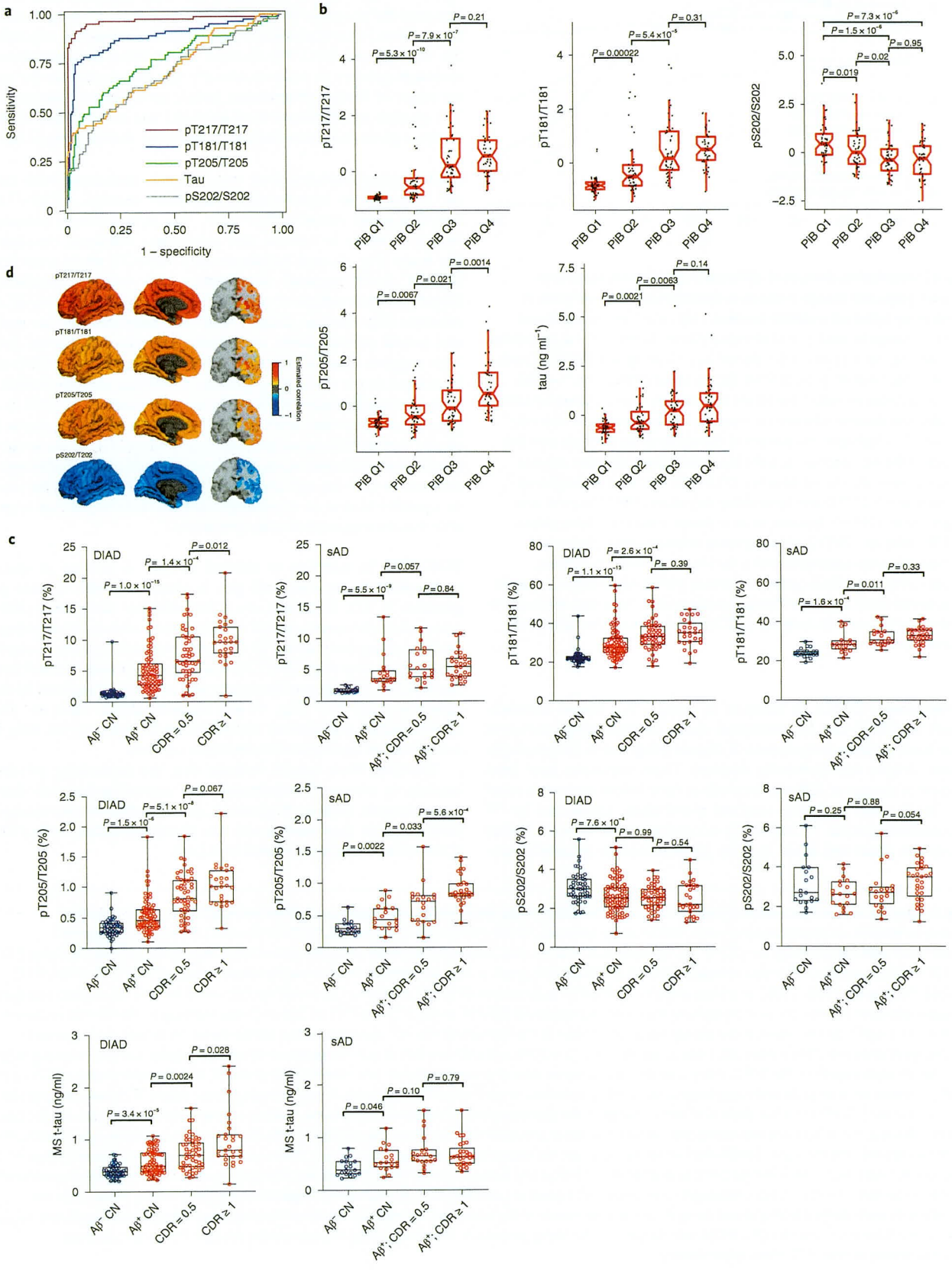

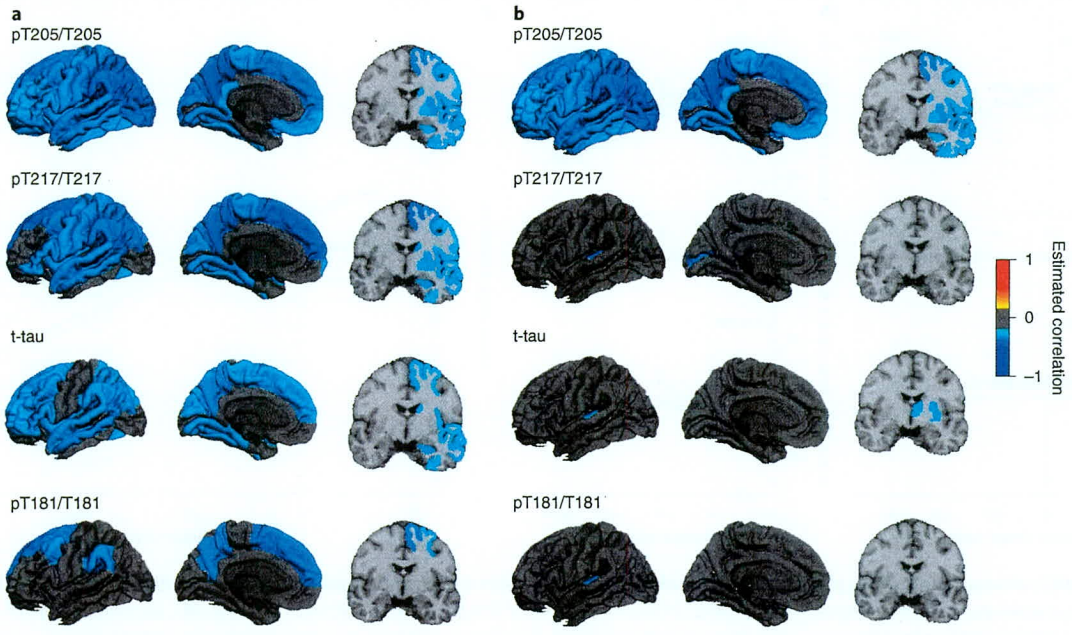

Fig. 4 | Tau phosphorylation positions are differentially related to brain atrophy and hypometabolism in DIAD. a, Bivariate correlations between cortical and subcortical atrophy and site-specific phosphorylation ratios in asymptomatic mutation carriers ($n=152$) demonstrate an increases in pT205/T205 and pT217/T217, followed by t-tau, and less for pT181/T181. **b**, Bivariate correlations between cortical and subcortical brain metabolism, as measured by FDG-PET, and site-specific phosphorylation ratios in asymptomatic mutation carriers ($n=152$) demonstrate an increase in pT205/T205 associated with a decrease in most cortical and subcortical regions, but not for the other p-tau sites or t-tau. *P* values for the correlations were calculated using chi-squared tests based on the bivariate LME models, with Benjamini–Hochberg correction for multiple comparisons.

phosphorylation ratio and t-tau levels over time compared with clinical outcomes[47]. We performed a mixed-effects model with longitudinal cognitive performance on the neuropsychological composite as the outcome and annual change in CSF tau measures (derived from individual linear mixed-effects (LME) models), time and their interactions as the predictors, adjusting for age, sex, education and familial relation (participants of the same family). We tested all mutation carriers (symptomatic and asymptomatic) for this analysis, in order to include a stage of the disease with significant cognitive decline, and found differential effects between phosphorylation site and cognitive decline. t-tau monotonically increased with worsening cognition and pT217/T217 and pT181/T181 decreased with worsening cognition, while pT205/T205 demonstrated less change relative to cognitive decline and pS202/S202 had no association with cognitive change. As pT217/T217 and pT181/T181 decreased, cognitive decline accelerated (t-value$=2.35$, $P = 0.02$ and 2.11, $P=0.04$ (Fig. 5 and Supplementary Table 9). For asymptomatic participants (CDR$=0$), there was evidence that an increase in pT181/T181, pT205/T205 and t-tau levels was associated with the initial decline in cognition. This suggests that decreased phosphorylation of T217 and T181, as much as increased soluble t-tau, presents an important marker of cognitive decline. We also evaluated the longitudinal change in the soluble tau phosphorylation ratio and t-tau levels over time compared with longitudinal MRI measures of neurodegeneration (atrophy of the hippocampus and precuneus cortex) and found very similar results to those for cognition (Extended Data Figs. 4 and 5). This further supports the finding that a decrease in the rate of phosphorylation of certain sites of tau represents an important marker of neurodegeneration and symptomatic disease progression.

These findings provide a modification to the current theory that a continuous rise in CSF tau phosphorylation is associated with cognitive dysfunction. We identified two general patterns: for some sites, phosphorylation decreased significantly as cognitive decline began, whereas other sites showed a continuous increase or no change with disease progression (see the increasing versus decreasing rates in Fig. 5).

Increasing levels of t-tau are correlated with baseline cortical NFTs, as measured by tau-PET in DIAD. Recent tau-PET (^{18}F-flortaucipir (AV-1451)) studies with DIAD participants have suggested that an aggregated tau increase occurs following the onset of clinical symptoms[21,25]. We tested the hypothesis that soluble p-tau is a marker of NFT pathology. We explored the relationship between longitudinal changes in CSF t-tau and p-tau isoforms leading up to the time when tau-PET was performed to assess whether faster changes of phosphorylation ratios are associated with higher tau-PET SUVR (greater aggregated tau). In a limited number of participants (ten mutation carriers and four non-carriers), a single tau-PET scan was performed within 72 h of the CSF sample being obtained. For these individuals, CSF samples had also been obtained on previous visits (within 1–3 years).

First, we confirmed that tau-PET SUVR in mutation carriers only increased near the time of symptom onset (Extended Data Fig. 6), suggesting that in DIAD mutation carriers, clinical decline begins when the tau-PET signal starts to increase. Second, we found that a longitudinal increase in CSF t-tau leading up to the time of tau-PET was associated with an elevated global cortical tau-PET composite ($P=0.05$) value (Supplementary Table 10) and that this association was related to multiple posterior and limbic cortical regions. Similarly, when exploring the Spearman correlation for the rate of change of soluble tau measures and baseline tau-PET SUVR, we found evidence that increasing levels of t-tau ($r=0.58$; $P=0.08$) but also pT205/T205 ($r=0.74$; $P=0.02$) were associated with higher tau-PET levels, whereas there was a suggestion of decreases in pT217/T217 ($r=-0.2$; $P=0.58$) and pT181/T181 ($r=-0.27$; $P=0.46$) with higher tau-PET levels (Extended Data Fig. 7 and Supplementary Table 11). Given the small number of participants

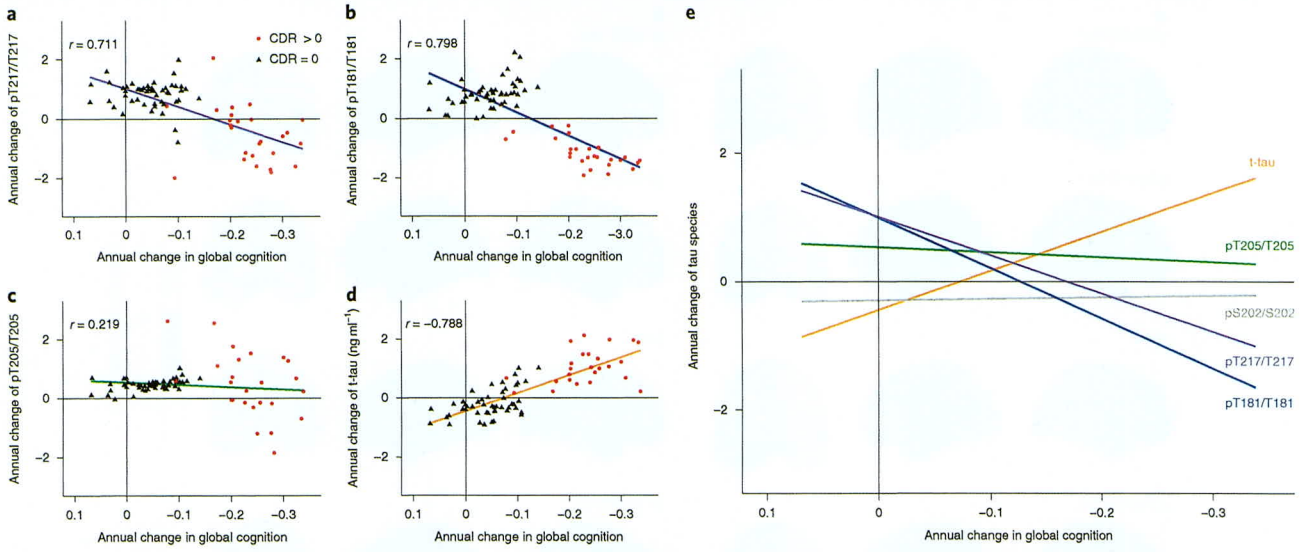

Fig. 5 | In DIAD, elevated levels of tau phosphorylation decline in some sites with the onset of dementia, in contrast with a continued rise in t-tau. **a**–**d**, Individual estimated annualized rates of change of pT217/T217 (**a**), pT181/T181 (**b**), pT205/T205 (**c**) and t-tau (**d**), standardized for all mutation carriers, correlated with the annualized change in global cognitive function. The lines represent simple linear regression and the shaded areas represent 95% CIs. Each point is an individual-level correlation between measures, with Pearson's *r* shown for all data. The linear regression was fit to those with no dementia (CDR = 0; black triangles; $n = 49$) and those with dementia (CDR > 0; red circles; $n = 27$). Declines in pT217/T217 ($r = 0.711$; $P < 0.0001$), pT181/T181 ($r = 0.798$; $P < 0.0001$) and pT205/T205 ($r = 0.219$; $P = 0.06$) were associated with cognitive decline after symptom onset (red). For t-tau, there was an inverse correlation with cognition ($r = -0.788$; $P < 0.0001$). **e**, A linear fit for all mutation carriers demonstrates that there are distinct associations between declining cognition and changes in the different p-tau isoforms and t-tau: with decreases in pT217/T217 and pT181/T181, there is an increase in t-tau associated with cognitive decline, but no associations with pT205/T205 or pS202/S202. This suggests that soluble tau species are not equivalent in AD (pS202/S202 is shown here to demonstrate the lack of association with cognition ($r = -0.09$; $P = 0.39$). Statistical significance for all of the correlations was based on two-sided *t*-test.

104

available for this analysis, there are limits to the interpretation of these results. However, by measuring multiple sites of phosphorylation simultaneously, these preliminary findings illustrate that the increases in soluble phosphorylated tau identified in DIAD, and presumably in sAD, are not necessarily a reflection of increases in aggregated tau as measured by tau-PET. In contrast, these results might suggest that a reduction in the phosphorylation rate of some sites (for example, pT181 and pT217) when aggregated tau is increasing could represent a process of sequestration by hyperphosphorylated aggregates[18].

Discussion

Although aggregated tau is a hallmark of AD pathology, important gaps remain in our understanding of how phosphorylation leads to the development of NFTs[2] and neurodegeneration in humans. Here, we demonstrate how patterns of tau phosphorylation in the CSF of DIAD mutation carriers vary over the course of AD progression. We add to the existing clinical literature the demonstration that in DIAD the process of tau phosphorylation and release into the CSF is a dynamic process that: (1) begins once aggregated Aβ pathology (as measured by PiB-PET) is established decades before symptoms, and subsequently unfolds over a period of nearly two decades; (2) occurs in a pattern such that phosphorylation of different tau sites closely follows disease progression, as revealed by levels of other biomarkers; and (3) decreases significantly in a site-dependent manner near the onset of cognitive decline and the rise in aggregated tau (as measured by tau-PET). Together, these results indicate that this method of quantifying soluble tau phosphorylation occupancy can track the AD process across its preclinical to symptomatic stages, providing a signature of p-tau pathology for this disease (Supplementary Table 12). Moreover, they challenge the purported roles of tau/p-tau in DIAD, and possibly AD in general, and recapitulate in humans those findings from animal studies that link Aβ pathology to tau hyperphosphorylation[32,34,36,49] and active cellular release, rather than release of dying neurons.

Although causality needs to be addressed in future studies, the contemporaneous increases in pT217/T217, pT181/T181 and PiB-PET SUVR suggest that the phosphorylation of tau in AD is closely linked to Aβ pathology. This is consistent with recent work in AD transgenic mice[31,32,34,50,51] and in humans, which demonstrates that tau and hyperphosphorylated tau are released from cells in an active process that is increased in the presence of aggregated Aβ[33]. Our results link Aβ pathology to a distinct change in soluble tau levels and phosphorylation patterns, shedding light on the phenomenon in which significant elevation of p-tau occurs in AD but not in other neurodegenerative tauopathies[17,18].

Recent work has shown that an increase and spread of neuritic tau aggregates (paired helical filaments in dystrophic neurites) in Aβ transgenic mice is enhanced by the presence of aggregated Aβ, occurring before established somatic NFTs[31]. It is possible that the very early increase we find in pT217/T217 and pT181/T181 may reflect this 'early' tau response to aggregated Aβ and might explain the global association of PiB-PET SUVR with these isoforms that we identified. Additionally, the lack of clinical symptoms seen during this early elevation in phosphorylation of tau suggests it occurs years before the onset of significant neurodegeneration. Our findings of an increase in pT205/T205 being associated with a decline in synaptic homeostasis could represent a protective process resulting in increased phosphorylation at T205 with synaptic distress from chronic Aß exposure, at least in DIAD[31]. Importantly, we have shown that t-tau levels appear to rise to similar levels with disease progression (Supplementary Fig. 2). This would indicate that the differences we have detected in the phosphorylation occupancy in DIAD are less likely to just reflect a difference in the amount of

intraneuronal tau protein produced and released into the CSF compartment. Rather, it might suggest that with different stages of the disease (Fig. 1), there are unique activations of the different kinases responsible for phosphorylating the tau protein preferentially at specific sites[41].

These data call into question some common assumptions about the role of soluble tau and p-tau in AD. Specifically, the current diagnostic framework in AD emphasizes the presence of biomarkers representing AD-specific and non-specific pathologies (for example, Aβ, p-tau and tau)[15]. Within this diagnostic framework, soluble p-tau and t-tau are often presumed to be passively released from degenerating neurons, with p-tau associated with aggregated NFTs and t-tau associated with axonal degeneration. Cross-sectional associations between phosphorylation levels and tau-PET measures in previous studies and our own data (Extended Data Fig. 8 and Supplementary Table 13) suggest that soluble p-tau and aggregated tau by tau-PET are correlated. In contrast, the more appropriate longitudinal measures indicate that soluble tau phosphorylation occupancy decreases during the time of tau increase[25], at least in DIAD, demonstrating an inverse correlation. One possible explanation for this is similar to what has been observed with soluble/aggregated Aβ[52]: that the dramatic increase of aggregated tau sequesters phosphorylated tau[53] in the brain, decreasing CSF levels. In addition, early phosphorylation modifications suggest that hyperphosphorylation, although a marker of pathophysiology, is not necessarily a marker of tau-related NFTs.

A reduction of tau through proteostatic mechanisms cannot be excluded[54] as a cause for the decrease in phosphorylation, but the continued increase of t-tau (Supplementary Fig. 3) would suggest that this is probably not the cause for the decreasing rate of phosphorylation for some sites. Similarly, a recent study has shown that the new production of tau and levels in the CSF do not appear to change in the presence of elevated tau (tau-PET)[33]. In either case, our findings of the negative correlation between the phosphorylation ratios of pT217/T271 or pT181/T181 and longitudinal cognitive decline and MRI measures of neurodegeneration highlight the importance of the reversal in phosphorylation rate of some tau sites in disease progression. Elucidating the cause for this decline could lead to a better understanding of the links between soluble tau and neuronal dysfunction and the use of CSF p-tau/tau in AD prognostication.

In summary, we have demonstrated that in AD associated with autosomal dominant mutations, CSF tau hyperphosphorylation occurs very early and exhibits pattern of site-specific changes at different stages of the disease. The underlying mechanisms behind these findings will have important implications for the understanding of the disease and for tau-directed therapies for AD.

Online content

Any methods, additional references, Nature Research reporting summaries, source data, extended data, supplementary information, acknowledgements, peer review information; details of author contributions and competing interests; and statements of data and code availability are available at https://doi.org/10.1038/s41591-020-0781-z.

Received: 11 May 2019; Accepted: 30 January 2020;
Published online: 11 March 2020

References

1. Goedert, M., Spillantini, M. G., Jakes, R., Rutherford, D. & Crowther, R. A. Multiple isoforms of human microtubule-associated protein tau: sequences and localization in neurofibrillary tangles of Alzheimer's disease. *Neuron* **3**, 519–526 (1989).
2. Grundke-Iqbal, I. et al. Abnormal phosphorylation of the microtubule-associated protein τ (tau) in Alzheimer cytoskeletal pathology. *Proc. Natl Acad. Sci. USA* **83**, 4913–4917 (1986).
3. Kimura, T., Sharma, G., Ishiguro, K. & Hisanaga, S. Phospho-tau bar code: analysis of phosphoisotypes of tau and its application to tauopathy. *Front. Neurosci.* **12**, 44 (2018).
4. Crowther, R. A. Straight and paired helical filaments in Alzheimer disease have a common structural unit. *Proc. Natl Acad. Sci. USA* **88**, 2288–2292 (1991).
5. Fitzpatrick, A. W. P. et al. Cryo-EM structures of tau filaments from Alzheimer's disease. *Nature* **547**, 185–190 (2017).
6. Price, J. L., Davis, P. B., Morris, J. C. & White, D. L. The distribution of tangles, plaques and related immunohistochemical markers in healthy aging and Alzheimer's disease. *Neurobiol. Aging* **12**, 295–312 (1991).
7. Qian, J., Hyman, B. T. & Betensky, R. A. Neurofibrillary tangle stage and the rate of progression of Alzheimer symptoms: modeling using an autopsy cohort and application to clinical trial design. *JAMA Neurol.* **74**, 540–548 (2017).
8. McDade, E. et al. Longitudinal cognitive and biomarker changes in dominantly inherited Alzheimer disease. *Neurology* **91**, e1295–e1306 (2018).
9. Bateman, R. J. et al. Clinical and biomarker changes in dominantly inherited Alzheimer's disease. *N. Engl. J. Med.* **367**, 795–804 (2012).
10. Fagan, A. M. et al. Cerebrospinal fluid tau/β-amyloid$_{42}$ ratio as a prediction of cognitive decline in nondemented older adults. *Arch. Neurol.* **64**, 343–349 (2007).
11. Vandermeeren, M. et al. Detection of tau proteins in normal and Alzheimer's disease cerebrospinal fluid with a sensitive sandwich enzyme-linked immunosorbent assay. *J. Neurochem.* **61**, 1828–1834 (1993).
12. Mori, H. et al. Tau in cerebrospinal fluids: establishment of the sandwich ELISA with antibody specific to the repeat sequence in tau. *Neurosci. Lett.* **186**, 181–183 (1995).
13. Schindler, S. E. et al. Emerging cerebrospinal fluid biomarkers in autosomal dominant Alzheimer's disease. *Alzheimers Dement.* **15**, 655–665 (2019).
14. Toledo, J. B., Xie, S. X., Trojanowski, J. Q. & Shaw, L. M. Longitudinal change in CSF Tau and Aβ biomarkers for up to 48 months in ADNI. *Acta Neuropathol.* **126**, 659–670 (2013).
15. Jack, C. R. Jr. et al. NIA-AA research framework: toward a biological definition of Alzheimer's disease. *Alzheimers Dement.* **14**, 535–562 (2018).
16. Jack, C. R. Jr. et al. A/T/N: an unbiased descriptive classification scheme for Alzheimer disease biomarkers. *Neurology* **87**, 539–547 (2016).
17. Hu, W. T. et al. Reduced CSF p-Tau181 to Tau ratio is a biomarker for FTLD-TDP. *Neurology* **81**, 1945–1952 (2013).
18. Hampel, H. et al. Measurement of phosphorylated tau epitopes in the differential diagnosis of Alzheimer disease: a comparative cerebrospinal fluid study. *Arch. Gen. Psychiatry* **61**, 95–102 (2004).
19. La Joie, R. et al. Associations between AV1451 tau PET and CSF measures of tau pathology in a clinical sample. *Neurology* **90**, e282–e290 (2018).
20. Mattsson, N. et al. ^{18}F-AV-1451 and CSF T-tau and P-tau as biomarkers in Alzheimer's disease. *EMBO Mol. Med.* **9**, 1212–1223 (2017).
21. Gordon, B. A. et al. Tau PET in autosomal dominant Alzheimer's disease: relationship with cognition, dementia and other biomarkers. *Brain* **142**, 1063–1076 (2019).
22. Jack, C. R. Jr. et al. The bivariate distribution of amyloid-β and tau: relationship with established neurocognitive clinical syndromes. *Brain* **142**, 3230–3242 (2019).
23. Johnson, K. A. et al. Tau positron emission tomographic imaging in aging and early Alzheimer disease. *Ann. Neurol.* **79**, 110–119 (2016).
24. Mattsson, N. et al. Predicting diagnosis and cognition with ^{18}F-AV-1451 tau PET and structural MRI in Alzheimer's disease. *Alzheimers Dement.* **15**, 570–580 (2019).
25. Quiroz, Y. T. et al. Association between amyloid and Tau accumulation in young adults with autosomal dominant Alzheimer disease. *JAMA Neurol.* **75**, 548–556 (2018).
26. Fleisher, A. S. et al. Associations between biomarkers and age in the presenilin 1 E280A autosomal dominant Alzheimer disease kindred: a cross-sectional study. *JAMA Neurol.* **72**, 316–324 (2015).
27. Toledo, J. B., Xie, S. X., Trojanowski, J. Q. & Shaw, L. M. Longitudinal change in CSF Tau and Aβ biomarkers for up to 48 months in ADNI. *Acta Neuropathol.* **126**, 659–670 (2013).
28. Fagan, A. M. et al. Longitudinal change in CSF biomarkers in autosomal-dominant Alzheimer's disease. *Sci. Transl. Med.* **6**, 226ra230 (2014).
29. Price, J. L. & Morris, J. C. Tangles and plaques in nondemented aging and "preclinical" Alzheimer's disease. *Ann. Neurol.* **45**, 358–368 (1999).
30. Ittner, L. M. et al. Dendritic function of Tau mediates amyloid-β toxicity in Alzheimer's disease mouse models. *Cell* **142**, 387–397 (2010).
31. Cohen, A. D. et al. Early striatal amyloid deposition distinguishes Down syndrome and autosomal dominant Alzheimer's disease from late-onset amyloid deposition. *Alzheimers Dement.* **14**, 743–750 (2018).
32. Maia, L. F. et al. Changes in amyloid-β and Tau in the cerebrospinal fluid of transgenic mice overexpressing amyloid precursor protein. *Sci. Transl. Med.* **5**, 194re192 (2013).

105

33. Sato, C. et al. Tau kinetics in neurons and the human central nervous system. *Neuron* **98**, 861–864 (2018).
34. Schelle, J. et al. Prevention of tau increase in cerebrospinal fluid of APP transgenic mice suggests downstream effect of BACE1 inhibition. *Alzheimers Dement.* **13**, 701–709 (2017).
35. Zempel, H., Thies, E., Mandelkow, E. & Mandelkow, E. M. Aβ oligomers cause localized Ca^{2+} elevation, missorting of endogenous Tau into dendrites, Tau phosphorylation, and destruction of microtubules and spines. *J. Neurosci.* **30**, 11938–11950 (2010).
36. Saman, S. et al. Exosome-associated Tau is secreted in tauopathy models and is selectively phosphorylated in cerebrospinal fluid in early Alzheimer disease. *J. Biol. Chem.* **287**, 3842–3849 (2012).
37. Jin, M. et al. Soluble amyloid β-protein dimers isolated from Alzheimer cortex directly induce Tau hyperphosphorylation and neuritic degeneration. *Proc. Natl Acad. Sci. USA* **108**, 5819–5824 (2011).
38. Gordon, B. A. et al. Spatial patterns of neuroimaging biomarker change in individuals from families with autosomal dominant Alzheimer's disease: a longitudinal study. *Lancet Neurol.* **17**, 241–250 (2018).
39. Ryman, D. C. et al. Symptom onset in autosomal dominant Alzheimer disease: a systematic review and meta-analysis. *Neurology* **83**, 253–260 (2014).
40. Morris, J. C. The Clinical Dementia Rating (CDR): current version and scoring rules. *Neurology* **43**, 2412–2414 (1993).
41. Medina, M. & Avila, J. Further understanding of tau phosphorylation: implications for therapy. *Expert Rev. Neurother.* **15**, 115–122 (2015).
42. Benzinger, T. L. et al. Regional variability of imaging biomarkers in autosomal dominant Alzheimer's disease. *Proc. Natl Acad. Sci. USA* **110**, E4502–E4509 (2013).
43. Quiroz, Y. T. et al. Cortical atrophy in presymptomatic Alzheimer's disease presenilin 1 mutation carriers. *J. Neurol. Neurosurg. Psychiatry* **84**, 556–561 (2013).
44. Ridha, B. H. et al. Tracking atrophy progression in familial Alzheimer's disease: a serial MRI study. *Lancet Neurol.* **5**, 828–834 (2006).
45. Arriagada, P. V., Growdon, J. H., Hedley-Whyte, E. T. & Hyman, B. T. Neurofibrillary tangles but not senile plaques parallel duration and severity of Alzheimer's disease. *Neurology* **42**, 631–639 (1992).
46. Okonkwo, O. C. et al. Cerebrospinal fluid profiles and prospective course and outcome in patients with amnestic mild cognitive impairment. *Arch. Neurol.* **68**, 113–119 (2011).
47. Bateman, R. J. et al. The DIAN-TU Next Generation Alzheimer's prevention trial: adaptive design and disease progression model. *Alzheimers Dement.* **13**, 8–19 (2017).
48. Yanamandra, K. et al. Anti-tau antibody administration increases plasma tau in transgenic mice and patients with tauopathy. *Sci. Transl. Med.* **9**, eaal2029 (2017).
49. He, Z. et al. Amyloid-β plaques enhance Alzheimer's brain tau-seeded pathologies by facilitating neuritic plaque tau aggregation. *Nat. Med.* **24**, 29–38 (2018).
50. Buerger, K. et al. CSF phosphorylated tau protein correlates with neocortical neurofibrillary pathology in Alzheimer's disease. *Brain* **129**, 3035–3041 (2006).
51. Ittner, A. et al. Site-specific phosphorylation of tau inhibits amyloid-β toxicity in Alzheimer's mice. *Science* **354**, 904–908 (2016).
52. Potter, R. et al. Increased in vivo amyloid-β42 production, exchange, and loss in presenilin mutation carriers. *Sci. Transl. Med.* **5**, 189ra177 (2013).
53. Yamada, K. et al. In vivo microdialysis reveals age-dependent decrease of brain interstitial fluid tau levels in P301S human tau transgenic mice. *J. Neurosci.* **31**, 13110–13117 (2011).
54. Van der Kant, R. et al. Cholesterol metabolism is a druggable axis that independently regulates tau and amyloid-β in iPSC-derived Alzheimer's disease neurons. *Cell Stem Cell* **24**, 363–375.e9 (2019).

the Dominantly Inherited Alzheimer Network

106

Ricardo Allegri[7], Randy Bateman[31], Jacob Bechara[19], Tammie Benzinger[31], Sarah Berman[32], Courtney Bodge[33], Susan Brandon[31], William (Bill) Brooks[19], Jill Buck[34], Virginia Buckles[31], Sochenda Chea[35], Jasmeer Chhatwal[36,37], Patricio Chrem Mendez[7], Helena Chui[38], Jake Cinco[39], Jack Clifford[35], Carlos Cruchaga[31], Tamara Donahue[31], Jane Douglas[39], Noelia Edigo[7], Nilufer Erekin-Taner[35], Anne Fagan[31], Martin Farlow[34], Colleen Fitzpatrick[36], Gigi Flynn[31], Nick Fox[39], Erin Franklin[31], Hisako Fujii[10], Cortaiga Gant[31], Samantha Gardener[23], Bernardino Ghetti[34], Alison Goate[40], Jill Goldman[41], Brian Gordon[31], Neill Graff-Radford[35], Julia Gray[31], Alexander Groves[31], Jason Hassenstab[31], Laura Hoechst-Swisher[31], David Holtzman[31], Russ Hornbeck[31], Siri Houeland DiBari[25], Takeshi Ikeuchi[9], Snezana Ikonomovic[32], Gina Jerome[31], Mathias Jucker[28], Celeste Karch[31], Kensaku Kasuga[9], Takeshi Kawarabayashi[11], William (Bill) Klunk[32], Robert Koeppe[42], Elke Kuder-Buletta[28], Christoph Laske[28], Jae-Hong Lee[43], Johannes Levin[25], Ralph Martins[23], Neal Scott Mason[44], Colin Masters[22], Denise Maue-Dreyfus[31], Eric McDade[31], Hiroshi Mori[10], John Morris[31], Akem Nagamatsu[11], Katie Neimeyer[41], James Noble[41], Joanne Norton[31], Richard Perrin[31], Marc Raichle[31], Alan Renton[40], John Ringman[38], Jee Hoon Roh[43], Stephen Salloway[33], Peter Schofield[19], Hiroyuki Shimada[10], Wendy Sigurdson[31], Hamid Sohrabi[23], Paige Sparks[36], Kazushi Suzuki[11], Kevin Taddei[23], Peter Wang[31], Chengjie Xiong[31] and Xiong Xu[31]

[31]St. Louis School of Medicine, Washington University, St. Louis, MO, USA. [32]University of Pittsburgh, Pittsburgh, PA, USA. [33]Butler Hospital, Brown University, Providence, RI, USA. [34]Indiana University, Bloomington, IN, USA. [35]Mayo Clinic Jacksonville, Jacksonville, FL, USA. [36]Brigham and Women's Hospital, Boston, MA, USA. [37]Massachusetts General Hospital, Boston, MA, USA. [38]University of Southern California, Los Angeles, CA, USA. [39]University College London, London, UK. [40]Icahn School of Medicine at Mount Sinai, New York, NY, USA. [41]Columbia University, New York, NY, USA. [42]University of Michigan, Ann Arbor, MI, USA. [43]Asan Medical Center, Seoul, Republic of Korea. [44]University of Pittsburgh Medical Center, Pittsburgh, PA, USA.

Methods

Study design. Participants with at least a 50% risk of inheriting a DIAD mutation from families with a confirmed genetic mutation in *PSEN1*, *PSEN2* or *APP* were enrolled in the DIAN study (National Institute on Aging U19 Clinical Trial; AG032438) (dian.wustl.edu; clinicaltrials.gov number NCT00869817)[55]. All procedures were approved by the Institutional Review Board (IRB) of Washington University and conformed to local IRB and ethics committee guidelines. The presence or absence of a DIAD mutation was determined using PCR-based amplification of the appropriate exon, followed by Sanger sequencing. At each study visit, participants underwent comprehensive clinical assessments, cognitive testing, neuroimaging and CSF studies; however, at each visit, each participant may not have completed all of these study procedures. The details of study structure and assessments can be found in previous publications[9,55]. Follow-up intervals were determined by the clinical status (normal or impaired) of each participant and by their EYO, and ranged from annual to every 3 years. Data were obtained from quality-controlled data (annual quality assessments for irregular results and missing data from 26 January 2009 to 30 June 2017) and included 370 participants ($n=150$ with longitudinal CSF evaluations, with a median time between visits of 2.8 years).

The non-familial population represented two cohorts recruited at the Knight Alzheimer Disease Research Center at Washington University and the Centres Mémoire Resources et de Recherche, Centre Hospitalier Universitaire (CHU) de Montpellier. All participants underwent detailed clinical cognitive assessments, CSF assessments and a diagnosis of preclinical AD or AD confirmed with abnormal amyloid biomarkers. All procedures were approved by the IRB of Washington University and ethics committees at CHU de Montpellier.

EYO. In DIAD, there is almost 100% penetrance, with age at symptom onset in mutation carriers being relatively consistent for each mutation and within each family. This allows for the designation of EYO. EYO was defined as follows. A parental age at earliest symptom onset was established for each participant by semi-structured interview. The parental age at onset for each mutation was then entered into a database consisting of the combined symptom onset values from DIAN and those from previous publications on DIAD cohorts. These were used to compute an average age of onset specific to each mutation[39]. The mutation-specific age of onset was subtracted from each participant's age at the time of clinical assessment to define the individual's EYO. When a specific mutation's average age of onset was unknown, the parental or proxy age of onset was used to define the EYO[39]. For participants who were symptomatic at baseline, as assessed by a CDR > 0, the reported age of actual symptom onset was subtracted from the age at each clinical assessment to define EYO.

Clinical assessments. Standardized clinical evaluations, including the use of a study partner, were performed for each DIAD participant. The CDR was used to indicate dementia stage. Participants were rated as cognitively normal (CDR = 0) or having very mild dementia (CDR = 0.5), mild dementia (CDR = 1) or moderate dementia (CDR = 2)[40]. Evaluating clinicians were blind to genetic status. A comprehensive neuropsychological battery assessing general cognitive function, memory, attention, executive function, visuospatial function and language was performed at each visit[56]. From these tests, we developed a cognitive composite that reliably detects decline across the range of EYO and CDR values[57]. The composite represents the average of the *z* scores from tests including episodic memory, complex attention and processing speed and a general cognitive screen (mini-mental state examination).

For the non-familial cohorts, all participants underwent a standardized, detailed clinical assessment specific to each of the two centers. A diagnosis of AD was based on the National Institute of Neurological and Communicative Disorders and Stroke–Alzheimer Disease and Related Disorders Association[58] criteria, and was confirmed with abnormal amyloid biomarkers. Dementia severity was based on the CDR. Additional details of the cohort can be found in previous publications[59].

CSF tau analyses. CSF was collected, via standard lumbar puncture procedures using an atraumatic Sprotte spinal needle (22 Ga), into two 13-ml polypropylene tubes. CSF was flash-frozen upright on dry ice. Samples collected in the United States were shipped overnight on dry ice to the DIAN Biomarker Core laboratory at Washington University (St. Louis, Missouri, United States), whereas samples collected at international sites were stored at −80 °C and shipped quarterly on dry ice. Upon arrival, each sample was subsequently thawed, combined into a single polypropylene tube and aliquoted (500 µl each) into polypropylene microcentrifuge tubes (05-538-69C; Corning Life Science), after which they were re-flash-frozen on dry ice and stored at −80 °C.

Each thawed CSF sample was mixed with 25 µl of a solution containing ^{15}N-441 tau internal standard (2.5 ng per sample), 50 mM guanidine, 10% NP-40 and 10× protease inhibitor cocktail (Roche). Tau was extracted by immune capture using incubation under rotation at room temperature for 2 h with 20 µl of sepharose beads cross-linked to Tau-1 (tau epitope 192–199) and HJ8.5 (tau epitope 27–35) antibodies. Beads were spun by centrifugation, then rinsed three times with 1 ml of 25 mM triethylammonium bicarbonate. Samples were digested overnight at 37 °C with 400 ng of trypsin Gold (Promega). AQUA peptides (Life Technologies) were spiked to obtain an amount of 5 fmol per labeled phosphorylated peptide and 50 fmol per labeled unmodified peptide in each sample. The peptide mixture was loaded on TopTip C18 tips, washed with 0.1% formic acid solution and eluted with 60% acetonitrile/0.1% formic acid solution. Eluates were dried using a Speedvac and dried samples were stored at −80 °C before analysis. Samples were resuspended in 25 µl of 2% acetonitrile/0.1% formic acid. Extracts were analyzed by nano liquid chromatography coupled to high-resolution tandem mass spectrometry (HRMS/MS) using parallel reaction monitoring using HCD fragmentation. Nano liquid chromatography–HRMS/MS experiments were performed using a nanoAcquity UPLC system (Waters) coupled to a Fusion Tribrid mass spectrometer (Thermo Fisher Scientific). For each sample, 5 µl was injected. Peptide separation was achieved at 60 °C in 24 min on a Waters HSS T3 column (75 µm × 100 mm; 1.8 µm). Mobile phases were: (A) 0.1% formic acid in water; and (B) 0.1% formic acid in acetonitrile. The gradient used was 0.5% B at 0 min, 5% B at 7.5 min and 18% B at 22 min, then the column was rinsed for 2 min with 95% B. The flow rate was set at 700 nl min^{-1} for 7.5 min, then 400 nl min^{-1} for the rest of the analysis. Data were acquired in the positive ion mode at a spray voltage of 2,200 V (Nanospray Flex ion source; Thermo Fisher Scientific) and the ion transfer tube was set at 270 °C. The S-lens radio frequency voltage was set at 60 V. HRMS/MS transitions (Supplementary Table 14) were extracted using Skyline software (MacCoss laboratory). CSF tau phosphorylation levels were calculated using measured ratios between HRMS/MS transitions of endogenous unphosphorylated peptides and ^{15}N-labeled peptides from the protein internal standard. Ratios of phosphorylation on T181, S202, T205 and T217 were measured using the ratio of the HRMS/MS transitions from phosphorylated peptides and the corresponding unphosphorylated peptides. Each phosphorylated/unphosphorylated peptide endogenous ratio was normalized using the ratio measured on the HRMS/MS transitions of the corresponding AQUA phosphorylated/unphosphorylated peptide internal standards.

All samples from the DIAN longitudinal and the cross-sectional studies were run together with waste CSF (longitudinal and cross-sectional study) and CSF pool (cross-sectional study) quality controls to monitor inter-assay variability for each variable at low CSF tau (normal level) and high CSF tau levels (AD typical level). The corresponding values and inter-assay coefficient of variation are incorporated in Supplementary Tables 1–5. In both studies, the inter-assay coefficient of variation was typically below 20%. A low percentage of the investigated samples had CSF pT205 and pT217 levels below the lowest limit of quantitation (4.7 and 4.5%, respectively), defined as levels providing liquid chromatography–mass spectrometry signals leading to a coefficient of variation of more than 20%.

CSF samples from sAD at Washington University were collected as described previously[59]. Aliquots from the collection performed at hour 32 were used for the analysis. CSF samples from sAD at Montpellier were collected in polypropylene tubes using lumbar puncture methods (Starstedt; 10 ml; 62.610.201) in line with standard operating procedures[60], transferred at a temperature of 4 °C within less than 4 h to the laboratory and centrifuged at 1,000*g* at 4 °C for 10 min. Aliquots of CSF supernatant (0.5 ml) were subsequently collected in 1.5-ml Eppendorf microtubes (Eppendorf Protein LoBind; ref0030108.116) and stored at −80 °C before shipping on dry ice, additional storage at −80 °C and analysis. These samples were used and tested without performing an additional freeze–thaw cycle. The methods used for the handling and traceability of the samples were in keeping with the procedures recommended in the biobank quality standard NFS 96–900, for which the laboratory is certified. Additional details were described previously[61].

Brain imaging. Amyloid deposition, glucose metabolism, tau (NFT)-PET and cortical thickness/subcortical volumes were assessed using ^{11}C-PiB-PET, ^{18}F-FDG-PET, ^{18}F-AV-1451 and volumetric T1-weighted MRI scans, respectively. Standard procedures were used to ensure consistency in the data collection of all DIAN sites[58]. The ^{11}C-PiB-PET scan consisted of 70 min of dynamic scanning after a bolus injection of ~13 mCi of PiB with regional standard uptake ratios (SUVRs) determined from the 40- to 70-min timeframe. The ^{18}F-FDG-PET scan started 30 min after a bolus injection of ~5 mCi and lasted 30 min. The ^{18}F-AV-1451 data were acquired from the 80- to 100-min window after bolus injection and were converted to SUVRs. The T1 magnetic resonance sequence was an accelerated magnetization-prepared rapid acquisition with gradient echo acquired on 3T scanners (parameters: repetition time = 23,000; echo time = 2.95; 1.0 × 1.0 × 1.2 mm^3 resolution). All tau and PiB-PET data have been reported in previous publications[9,21].

The PiB and FDG SUVRs from 34 cortical and six subcortical regions of interest (ROIs) were obtained using FreeSurfer software (http://surfer.nmr.mgh.harvard.edu/). The SUVRs were processed with total cerebellum gray matter as reference regions and ROI data were corrected for partial volume effects using a regional point spread function[62] in a geometric transfer matrix framework.

Statistical analysis. Baseline characteristics of the participants were summarized as means ± s.d. for continuous variables and *n* (column percentage) for categorical variables. *P* values for comparing the differences among asymptomatic mutation carriers, symptomatic mutation carriers and non-carriers, as defined at baseline, were obtained using LME models for continuous variables and generalized LMEs

with a logistic link for categorical variables. All of the models incorporated a random family effect to account for the correlations on the outcome measures between participants within the same family. The cut point for baseline cortical PiB-PET SUVR was chosen such that the difference in the longitudinal rate of change of cortical PiB-PET between mutation carriers and non-carriers first starts to differ significantly from 0.

The cross-sectional relationships of the different tau phosphorylation sites with PiB, FDG and cortical thickness/subcortical volume were evaluated in all asymptomatic mutation carriers (CDR = 0; $n = 152$) using multivariate LME models on each ROI. The models included fixed effects of EYO and random intercepts at the family level. Compared with the simple correlation estimation method (Pearson or Spearman correlation), the multivariate LME model can adjust for covariates such as EYO, as well as accounting for the correlation within the family cluster[63,64]. *P* values for testing the correlations were corrected using the Benjamini–Hochberg method[65], to control the false discovery rate due to multiple testing.

For the within-individual annual rate of change over the longitudinal follow-up, the best linear unbiased predictors for each biomarker were estimated using LME models, which were then plotted against the baseline EYO to examine biomarker trajectories. LME or linear spline mixed-effects models, where appropriate, were then used to determine the baseline EYO point from which mutation carriers became significantly different from non-carriers in the baseline level and the rate of change for each biomarker. The details of the linear spline mixed-effects models can be found in a recent publication[8]. The LME or linear spline mixed-effects models included the fixed effects of mutation group (mutation carrier or non-carrier), baseline EYO, time since baseline and all possible two- or three-way interactions among them. Sex, years of education and apolipoprotein-E $\varepsilon 4$ status were considered as covariates, but only those effects that were significant were retained in the models. The random effects included in the models were the random intercepts for family clusters, individual random intercept and random slope with unstructured covariance matrix, to account for the within-subject correlation due to repeated measures. The adjusted difference in the mean level at baseline and difference in the rates of change between mutation carriers and non-carriers were then tested using the approximate *t*-test derived from the models to determine the first EYO point at which the difference became significant.

To visualize the differences in the rates of change among t-tau, tau phosphorylation site, cortical PiB and global cognition across the range of EYO values, measures of mutation carriers were first standardized using the mean and standard deviation of non-carriers. The rate of change of each measure for each mutation carrier was then calculated using LME modeling, and LOESS curves were fitted to visually represent the trajectories of the standardized rates of change over the EYO.

The utility of the baseline and annual rate of change of t-tau and p-tau in predicting longitudinal cognitive decline among mutation carriers was evaluated using LME modeling, controlling for the effect of baseline age, sex and apolipoprotein-E $\varepsilon 4$ status. Random effects in the models included the random intercepts for family clusters, individual random intercept and random slope with unstructured covariance matrix.

Linear regressions were used to examine whether the annual rate of change of tau and p-tau position for mutation carriers and non-carriers, leading up to and including the point when the tau-PET was performed, could predict tau-PET SUVR, controlling for the effect of age. Due to the limited number of participants, a family cluster was not included.

All analyses were conducted using SAS 9.4 (SAS Institute) and RStudio (version 3.4.3). $P < 0.05$ was considered to be statistically significant and all statistical tests were two sided.

Reporting Summary. Further information on research design is available in the Nature Research Reporting Summary linked to this article.

Data availability

The data that support the findings of this study can be requested from DIAN at https://dian.wustl.edu/our-research/observational-study/dian-observational-study-investigator-resources/.

Code availability

All codes used for data analyses are available upon request from the corresponding authors.

References

55. Morris, J. C. et al. Developing an international network for Alzheimer research: the Dominantly Inherited Alzheimer Network. *Clin. Investig. (Lond.)* **2**, 975–984 (2012).
56. Storandt, M., Balota, D. A., Aschenbrenner, A. J. & Morris, J. C. Clinical and psychological characteristics of the initial cohort of the Dominantly Inherited Alzheimer Network (DIAN). *Neuropsychology* **28**, 19–29 (2014).
57. Lim, Y. Y. et al. BDNF Val66Met moderates memory impairment, hippocampal function and tau in preclinical autosomal dominant Alzheimer's disease. *Brain* **139**, 2766–2777 (2016).
58. McKhann, G. et al. Clinical diagnosis of Alzheimer's disease: report of the NINCDS-ADRDA Work Group under the auspices of Department of Health and Human Services Task Force on Alzheimer's Disease. *Neurology* **34**, 939–944 (1984).
59. Patterson, B. W. et al. Age and amyloid effects on human central nervous system amyloid-beta kinetics. *Ann. Neurol.* **78**, 439–453 (2015).
60. Del Campo, M. et al. Recommendations to standardize preanalytical confounding factors in Alzheimer's and Parkinson's disease cerebrospinal fluid biomarkers: an update. *Biomark. Med.* **6**, 419–430 (2012).
61. Barthelemy, N. R. et al. Tau protein quantification in human cerebrospinal fluid by targeted mass spectrometry at high sequence coverage provides insights into its primary structure heterogeneity. *J. Proteome Res.* **15**, 667–676 (2016).
62. Su, Y. et al. Partial volume correction in quantitative amyloid imaging. *Neuroimage* **107**, 55–64 (2015).
63. Luo, J., D'Angelo, G., Gao, F., Ding, J. & Xiong, C. Bivariate correlation coefficients in family-type clustered studies. *Biom. J.* **57**, 1084–1109 (2015).
64. Xiong, C. et al. Longitudinal relationships among biomarkers for Alzheimer disease in the Adult Children Study. *Neurology* **86**, 1499–1506 (2016).
65. Benjamini, Y. & Hochberg, Y. Controlling the false discovery rate: a practical and powerful approach to multiple testing. *J. R. Stat. Soc. B* **57**, 289–300 (1995).

Acknowledgements

Data collection and sharing for this project was supported by the DIAN (UF1AG032438), funded by the National Institute on Aging, German Center for Neurodegenerative Diseases and Raul Carrea Institute for Neurological Research (FLENI), with partial support via research and development grants for dementia from the Japan Agency for Medical Research and Development and the Korea Health Technology R&D Project, through the Korea Health Industry Development Institute, MRC Dementias Platform UK (MR/L023784/1 and MR/009076/1) and AOI Lady Biobank CHU. The development and performance of the mass spectrometry analyses was supported by the Alzheimer's Association Research Fellowship (AARF-16-443265 to N.R.B.), Fondation Plan Alzheimer (to A.G. and S.L.), BrightFocus (A20143845 to R.J.B.), the National Institute of Neurological Disorders and Stroke (R01NS095773 to R.J.B.) and the National Institute on Aging (K23 AG046363 to E.M.). This manuscript has been reviewed by DIAN Study investigators for scientific content and consistency of data interpretation with previous DIAN Study publications. We acknowledge the altruism of the participants and their families and contributions of the DIAN research and support staff at each of the participating sites for their contributions to this study. We thank J. Ringman and B. Ghetti for reviewing the manuscript and making suggestions.

Author contributions

N.R.B. and C.S. performed the mass spectrometry analyses. Y.L., C.X., N.J.-M. and B.A.G. performed the statistical and imaging analyses. N.R.B., Y.L., R.J.B. and E.M. designed the study and wrote the initial draft of the manuscript. All authors collected samples and data, helped to interpret the results and reviewed drafts of the manuscript.

Competing interests

R.J.B. has equity ownership interest in C2N Diagnostics and receives royalty income based on technology (stable isotope labeling kinetics and blood plasma assay) licensed by Washington University to C2N Diagnostics. R.J.B. receives income from C2N Diagnostics for serving on the scientific advisory board. Washington University, with R.J.B., E.M. and N.R.B. as co-inventors, has submitted the US nonprovisional patent application 'Cerebrospinal fluid (CSF) tau rate of phosphorylation measurement to define stages of Alzheimer's disease and monitor brain kinases/phosphatases activity'. R.J.B. has received honoraria from Janssen and Pfizer as a speaker, and from Merck and Pfizer as an advisory board member. E.M. has received royalty payments for an educational program supported by Eli Lilly and as a member of a scientific advisory board for Eli Lilly.

Additional information

Extended data is available for this paper at https://doi.org/10.1038/s41591-020-0781-z.

Supplementary information is available for this paper at https://doi.org/10.1038/s41591-020-0781-z.

Correspondence and requests for materials should be addressed to R.J.B. or E.M.

Peer review information Brett Benedetti and Kate Gao were the primary editors on this article and managed its editorial process and peer review in collaboration with the rest of the editorial team.

Reprints and permissions information is available at www.nature.com/reprints.

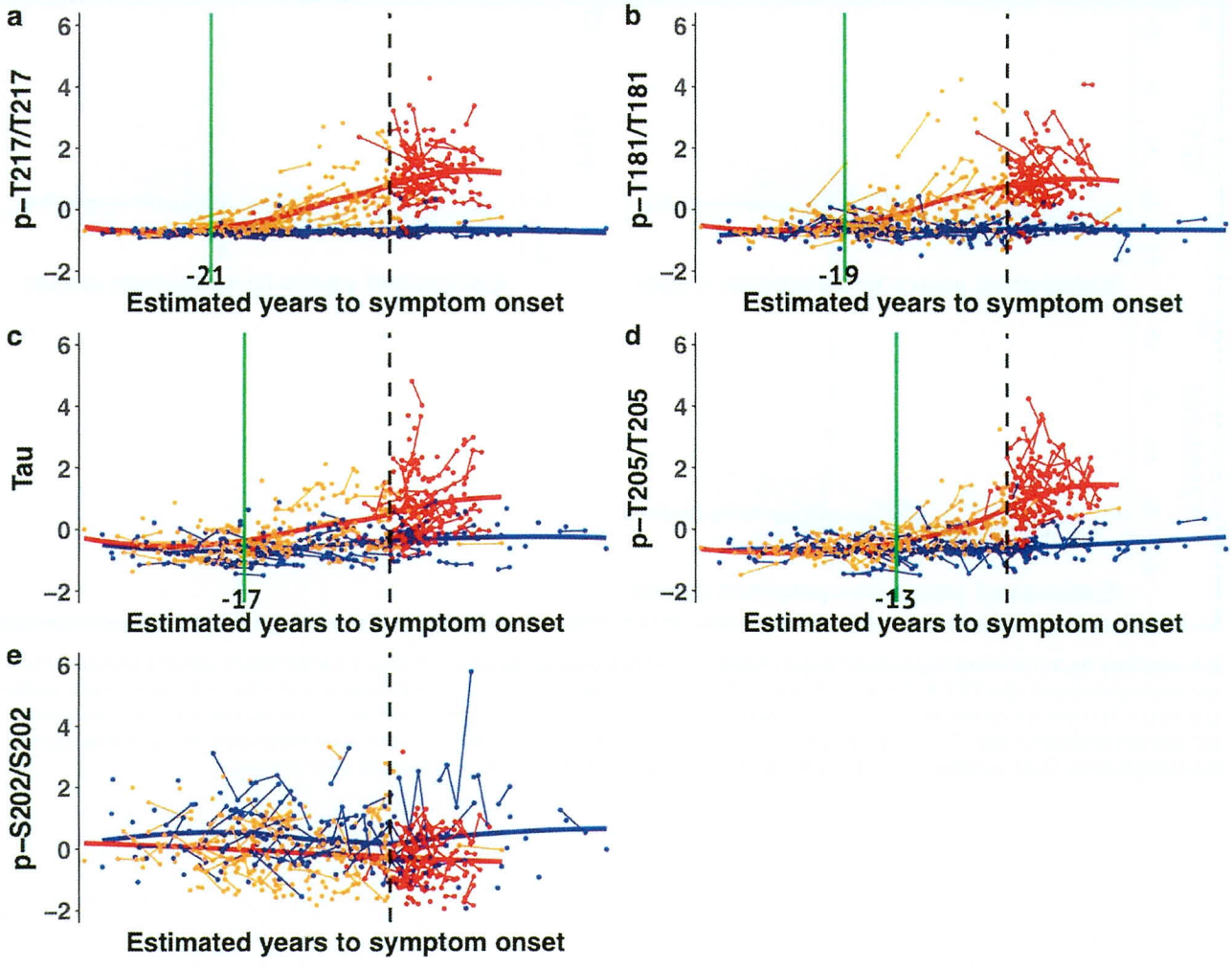

Extended Data Fig. 1 | Individual longitudinal changes of different phosphorylated-tau sites and total tau highlights differences in the time of increase relative to disease onset. Individual, z-transformed, longitudinal changes in the ratio of phosphorylation of **a**, pT217/T217, **b**, pT181/T181 **c**, total tau, **d**, pT205/T205, and **e**, pS202/S202 for mutation carriers (orange = asymptomatic mutation carriers, (n = 152), red = symptomatic mutation carriers (n = 77)) and non-carriers (blue, (n = 141)) across the estimated years to symptom onset (EYO). The vertical dashed line is the point of expected symptom onset, the vertical green line represents the model estimated time when the rate of change for each p-tau isoform becomes greater for mutation carriers compared to non-carriers.

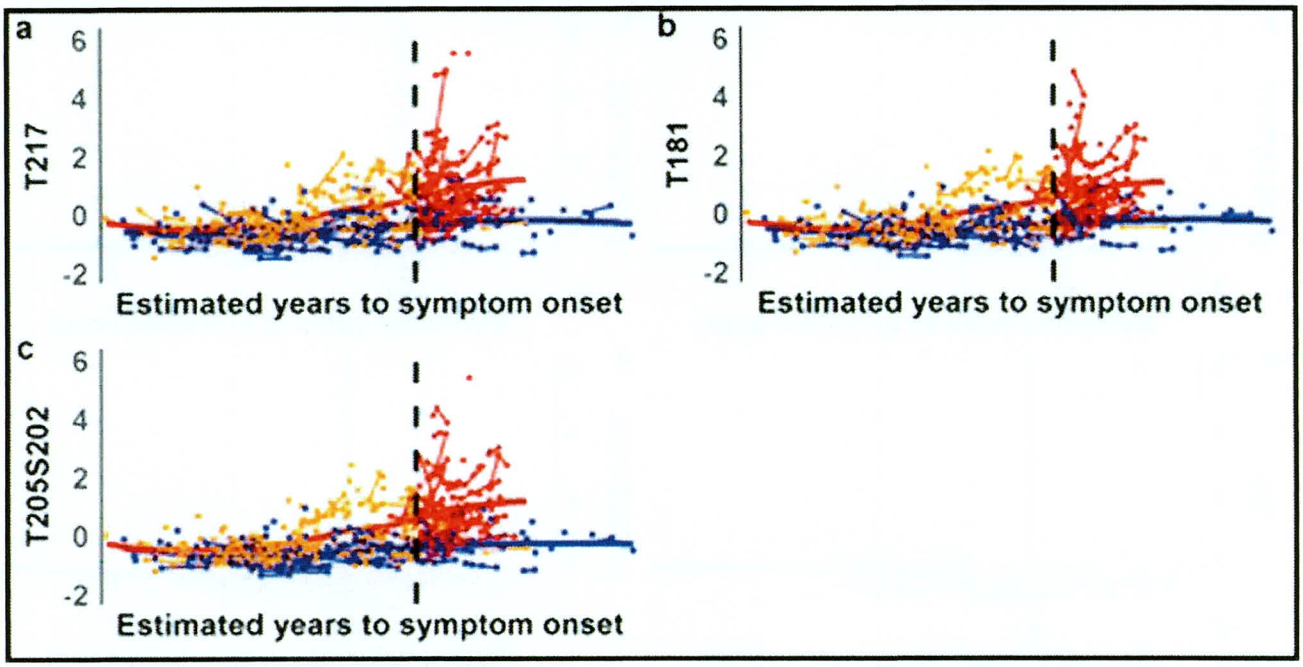

Extended Data Fig. 2 | Individual longitudinal changes of different unphosphorylated-tau sites. Individual, z-transformed, longitudinal changes in the unphosphorylated levels of **a**, T217, **b**, T181 **c**, T205 for mutation carriers (orange = asymptomatic mutation carriers, (n = 152), red = symptomatic mutation carriers (n = 77)) and non-carriers (blue, (n = 141)) across the estimated years to symptom onset (EYO). The solid line represents a LOESS fit to cross-sectional and longitudinal data. The vertical dashed line is the point of expected symptom onset. Compared to the phosphorylation ratios of each site (Extended Data Fig. 1), the increase in the unphosphorylated levels appears to be more similar over the progression of disease.

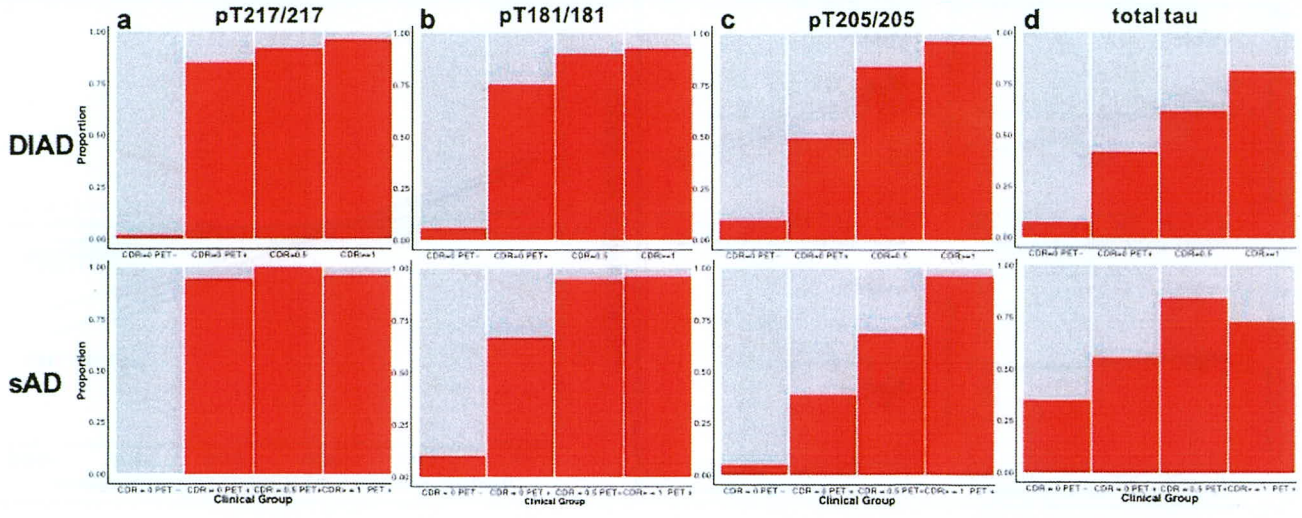

Extended Data Fig. 3 | Change in tau phosphorylation state is site dependent and related to amyloid PET and disease stage in DIAD and sAD. Bar charts illustrating the proportion of participants that have p-tau ratios and total tau levels that exceed the normal values (biomarker + (red)) (a- d) as the stage of disease progresses from cognitively normal/PiB-PET normal to cognitively normal/PiB-PET positive then to mild dementia (CDR 0.5) and greater (CDR > 0.5). The top row is DIAD (n = 210) and the bottom row sAD (n = 83). The figure demonstrates very similar patterns for each phosphorylation ratio and total tau levels across the progression of disease and indicate a similar ordering in DIAD and SAD, generalizing these findings to AD.

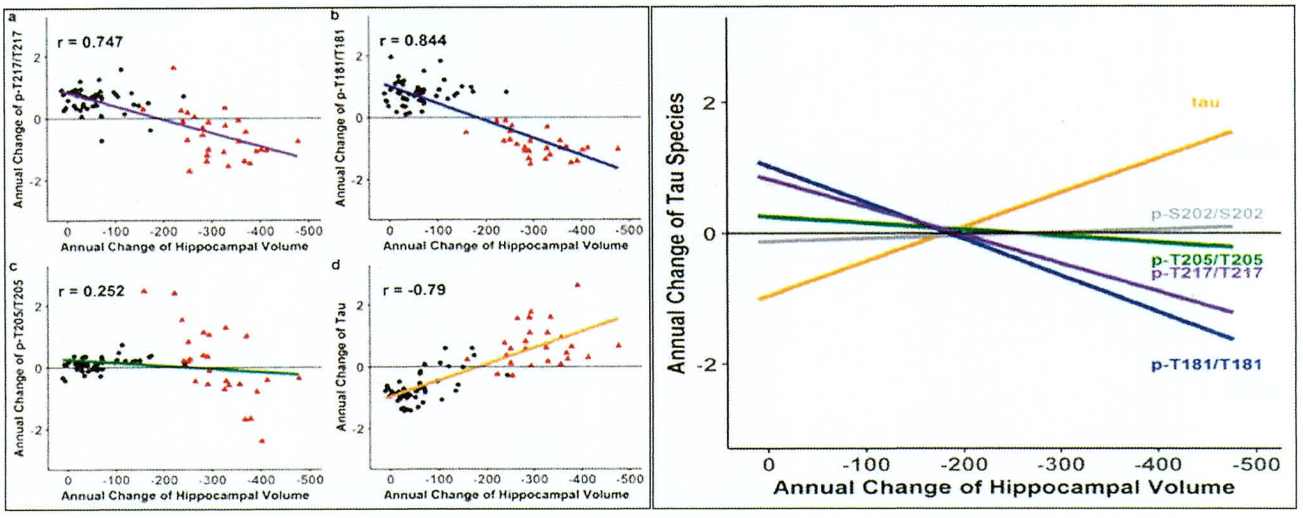

Extended Data Fig. 4 | Elevated levels of tau phosphorylation decline in some sites with atrophy of hippocampal volumes in contrast to a continued rise in total tau. Estimated individual annual rates of change of p-tau isoforms and total tau, standardized by the mean and standard deviation of the estimated rate of change for all mutation carriers, (y-axis) for mutation carriers were correlated with the annual change in hippocampal volumes (**a-d**). The linear regression was fit to those with no dementia (CDR 0, black circle, n = 48) and dementia (CDR > 0, red triangle, n = 27). A decline in pT217/T217 (a), r = 0.74($p < 0.0001$), pT181/T181 (b), r = 0.84 ($p < 0.0001$) and pT205/T205, r = 0.25 ($p = 0.03$) phosphorylation rate was associated with hippocampal volume decline. For total tau there was an inverse correlation with atrophy (d), r = −0.79($p < 0.0001$). (e) A linear fit for all mutation carriers demonstrates there are distinct associations between declining cognition and changes in the different p-tau isoforms and total tau: with decreases in pT217/T217 and pT181/T181 and an increase in total tau associated with cognitive decline; and no associations with pT205/T205 or pS202/S202. This suggests that soluble tau species are not equivalent in AD (pS202/S202) is shown here to demonstrate the lack of association with cognition, r = -0.07 ($p = 0.57$). Statistical significance of the correlations was calculated using z test.

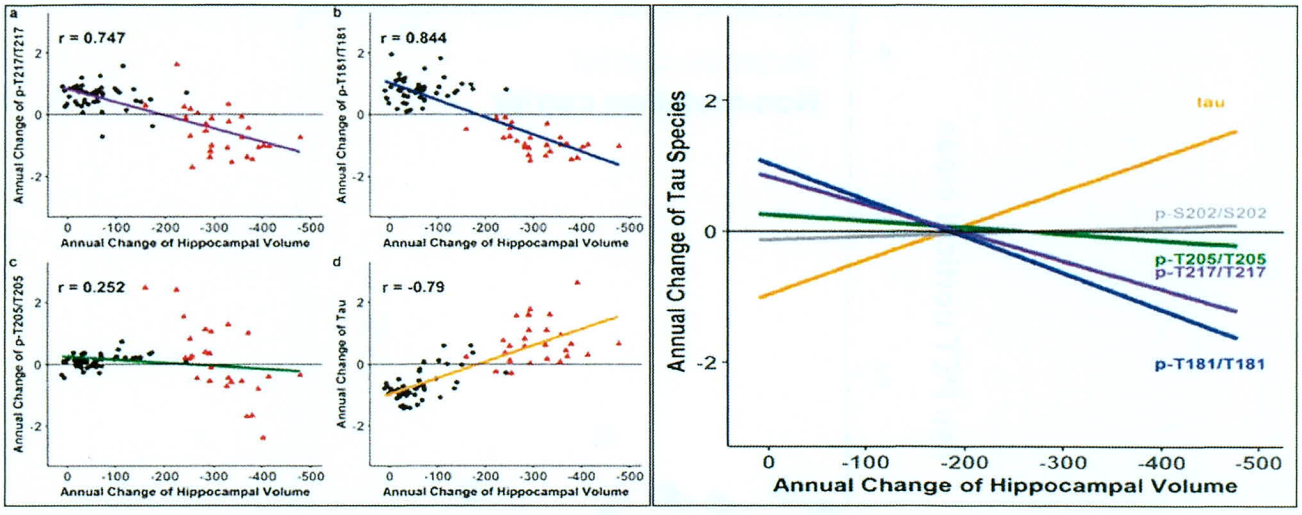

Extended Data Fig. 5 | Elevated levels of tau phosphorylation decline in some sites with atrophy of precuneus cortex in contrast to a continued rise in total tau. Estimated individual annual rates of change of p-tau isoforms and total tau, standardized by the mean and standard deviation of the estimated rate of change for all mutation carriers, (y-axis) for mutation carriers were correlated with the annual change in hippocampal volumes (**a-d**). The linear regression was fit to those with no dementia (CDR 0, black circle, n = 48) and dementia (CDR > 0, red triangle, n = 27). A decline in pT217/T217 (a), r = 0.75 ($p < 0.0001$), pT181/T181 (b), r = 0.83 ($p < 0.0001$) and pT205/T205, r = 0.19 ($p = 0.09$) phosphorylation rate was associated with precuneus cortical decline. For total tau there was an inverse correlation with atrophy (d), r = -0.77($p < 0.0001$). (e) A linear fit for all mutation carriers demonstrates there are distinct associations between declining cognition and changes in the different p-tau isoforms and total tau: with decreases in p-T217 and p-T181 and an increase in total tau associated with cognitive decline; and no associations with pT205/T205 or pS202/S202. This suggests that soluble tau species are not equivalent in AD (pS202/S202 is shown here to demonstrate the lack of association with cognition, r = -0.04 ($p = 0.72$). Statistical significance of the correlations was calculated using two-sided *t* tests.

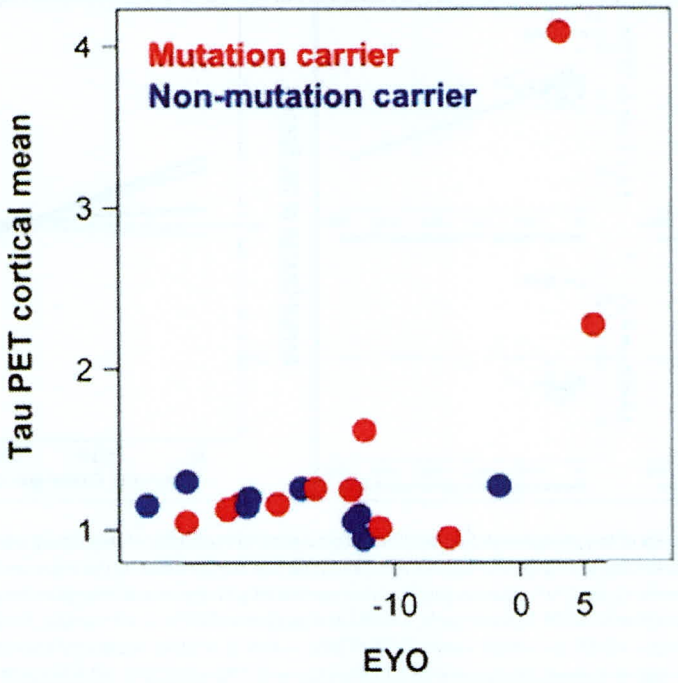

Extended Data Fig. 6 | Tau PET increases near symptom onset in DIAD mutation carriers. The mean cortical standardized unit value ratio (SUVR), y-axis, for mutation carriers (red, n = 12) and non-carriers (blue, n = 9) over estimated years to symptom onset (EYO), x-axis, for those participants with a longitudinal CSF evaluation preceding the time of tau-PET. The plot shows that for mutation carriers there is little elevation in tau-PET until the point of estimated symptom onset (EYO=0). This figure shows that the neurofibrillary tangle (NFT) pathology detected by AV-1451 occurs much later than the increase in multiple soluble phosphotau sites suggesting that these soluble markers of tau are likely a marker of NFT pathology, but rather might predispose to the development of the hyperphosphorylated, insoluble tau deposits characteristic of AD pathology.

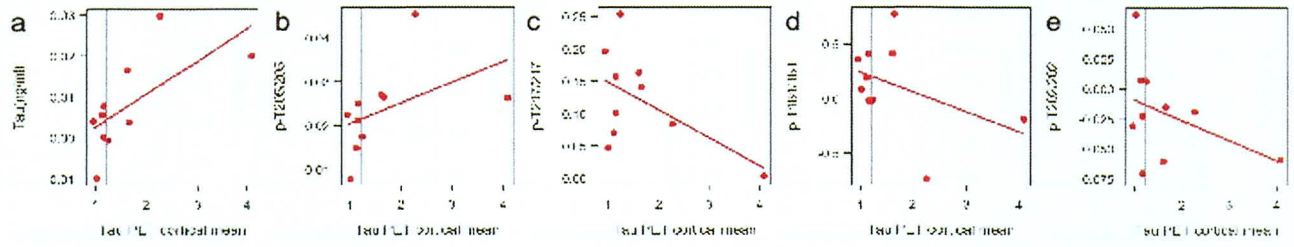

Extended Data Fig. 7 | Longitudinal change in tau and tau phosphorylation sites are differentially related to neurofibrillary tau (tau-PET) in dominantly inherited AD. Individual, rates of change of phosphorylation and total tau (y-axis) in mutation carriers only leading up to the time of tau-PET scan (x-axis) (n = 12). The vertical line is an SUVR of 1.22 and represents a conservative estimate of the point when cortical tau-PET is considered elevated for tau aggregates compared to non-carriers. The plots suggest that increases in soluble tau and p-T205 are associated with higher levels of aggregated tau, whereas the rate of phosphorylation at p-T217 and p-T181 decrease as levels of aggregated tau increase. These findings suggest that there are differences between increasing levels of tau and phosphorylation at different sites and may indicate that, in some instances, soluble p-tau maybe sequestered as the burden of hyperphosphorylated aggregates increase with the spreading of tau pathology. They also suggest that with the increase in aggregated tau there is a rise in soluble tau levels which could represent either passive or active release with greater burden of aggregated tau pathology.

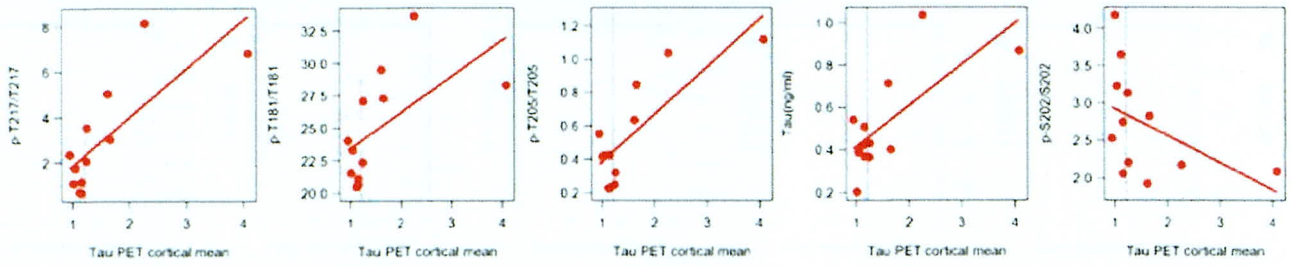

Extended Data Fig. 8 | Spearman correlation of the cross-sectional association of p-tau phosphorylation, total tau (y-axis) and tau PET (x-axis) for mutation carriers (n = 12). The vertical line is an SUVR of 1.22 and represents a conservative estimate of the point when cortical tau-PET is considered elevated for tau aggregates compared to non-carriers.

Clinical & Experimental
Neuroimmunology

Clinical and Experimental Neuroimmunology **10** (2019) 138–141

CASE REPORT

Hypereosinophilic syndrome presenting with inflammation in the retroparotid space and showing Villaret's syndrome

Yusuke Seino, Takumi Nakamura, Mie Hirohata, Takeshi Kawarabayashi and Mikio Shoji

Department of Neurology, Hirosaki University Graduate School of Medicine, Hirosaki, Japan

Keywords
denervated tongue; hypereosinophilia; retroparotid space; reversible change; Villaret's syndrome

Correspondence
Yusuke Seino, MD, PhD, Department of Neurology, Hirosaki University Graduate School of Medicine, 5-Zaifu-cho, Hirosaki, Aomori 036-8216, Japan.
Tel: 81-172-39-5142
Fax: 81-172-39-5143
Email: seino@hirosaki-u.ac.jp

Received: 27 November 2018; revised: 17 December 2018; accepted: 21 December 2018.

Abstract

Background Hypereosinophilia syndrome (HES) is a rare disease characterized by the association between hypereosinophilia and eosinophil-mediated organ infiltration and damage or dysfunction. The cause of hypereosinophilia is classified as neoplastic, reactive and idiopathic. However, hypereosinophilia causes tissue and organ damage, regardless of the underlying etiology. The common manifestations are pulmonary, skin and gastrointestinal. Rarely, neurological lesions are manifested. As neurological lesions of HES, mononeuritis multiplex, radiculopathy, optic neuritis, meningitis and cerebral infarction have been reported.

Case presentation A 43-year-old woman suffered from dysphagia and hoarseness, after symptoms of fever and sore throat 1 month earlier. On admission, her physical examination was unremarkable, except for neck pain on the right side. The neurological examination showed "Villaret's syndrome": Horner's sign on the right side, and paralysis of the right glossopharyngeal nerve, vagus nerve, accessory nerve and hypoglossal nerve. Laboratory tests showed marked eosinophilia and it gradually worsened. The maximum eosinophil count increased to 3474/mm^3. Magnetic resonance imaging showed a high-intensity area with contrast effect spreading in the retroparotid space in the short T1 inversion recovery image, and a high-intensity area spreading in the deep gray matter of the cerebrum in the fluid-attenuated inversion recovery image. Treatment started with steroid pulse therapy. After therapy, eosinophils normalized on the next day, and multiple cranial nerve palsy improved gradually and normalized. Six months later, the abnormal signal of the retroparotid space had disappeared on magnetic resonance imaging.

Conclusions HES is a multisystem dysfunction secondary to eosinophilic infiltration. In rare cases, HES causes inflammation in the retroparotid space and causes Villaret's syndrome.

Introduction

Hypereosinophilia syndrome (HES) is a rare disease characterized by the association between hypereosinophilia and eosinophil-mediated organ infiltration and damage or dysfunction. Clinical presentation of patients might be very heterogeneous, as it is strictly correlated to organ damage mediated by eosinophils. Hypereosinophilia might intrinsically cause tissue and organ damage, regardless of the underlying etiology. Organ damage might be observed when the number of eosinophils exceeds 2000/mm^3.[1]

The common manifestations are pulmonary, skin and gastrointestinal. Rarely, cardiac difficulties and neurological lesions are manifested. As neurological lesions of HES, mononeuritis multiplex, radiculopathy, optic neuritis, meningitis and cerebral infarction have been reported.[2–6] The present patient a showed high-intensity area with contrast effect spreading in the retroparotid space in the short T1 inversion

117

recovery image of the magnetic resonance imaging (MRI; Fig. 1a,b), and a high-intensity area spreading in the deep gray matter of the cerebrum on the fluid-attenuated inversion recovery image (Fig. 1e). No similar case with neurological symptoms of HES has ever been reported.

Case report

We present a 43-year-old woman who suffered from dysphagia and hoarseness, after symptoms of fever and sore throat 1 month earlier. She was admitted to a local clinic because of fever and sore throat. She was diagnosed as tonsillitis and treated with antibiotics. After therapy, her symptoms improved. However, the sore throat recurred, and dysphagia and hoarseness also appeared after 1 month. She was admitted to a local clinic again. At that time, she was had paralysis of the hypoglossal nerve and right side vocal cord. For this reason, she was admitted to the Department of Neurology, Hirosaki University Hospital, Hirosaki, Japan. Her past medical, drug allergy, travel, contact with animals and family history were not significant.

On admission, the patient's vital signs and physical examination were unremarkable, except for neck pain on the right side. No clinical findings of parasitic infection were observed. The neurological examination showed "Villaret's syndrome": Horner's sign on the right side, and paralysis of the right glossopharyngeal nerve, vagus nerve, accessory nerve and hypoglossal nerve (Fig. 2a–c).[7] Laboratory tests showed marked eosinophilia of 1826/mm^3 (23% of white blood cell count) with normal other blood counts and peripheral smear. After admission, her eosinophilia gradually worsened. The maximum eosinophil count increased to 3474/mm^3 (43% of white blood cell count). The immunoglobulin E level and erythrocyte sedimentation rate were normal. Antiphospholipid antibodies, perinuclear antineutrophil cytoplasmic antibodies, cytoplasmic antineutrophil cytoplasmic antibodies and *Aspergillus* antigen were negative. Cerebrospinal fluid examination was normal. Blood cultures and throat culture were negative. The antistreptolysin O titers, and the antibody titer of Epstein–Barr virus and mycoplasma showed no significant change. MRI showed a high-intensity area with contrast effect spreading in the retroparotid space (around the right carotid artery and internal jugular vein), and a high-intensity area was also confirmed in the right tongue on the short T1 inversion recovery image (Fig. 1a,b). A needle biopsy was carried out from the retroparotid space showing a high-intensity area on MRI. In the specimen, only lymphocytes were detected. Eosinophils and heteromorphic cells were not observed. Biopsy was carried out from the right palatine tonsil. In the specimen, only lymphocytes were detected.

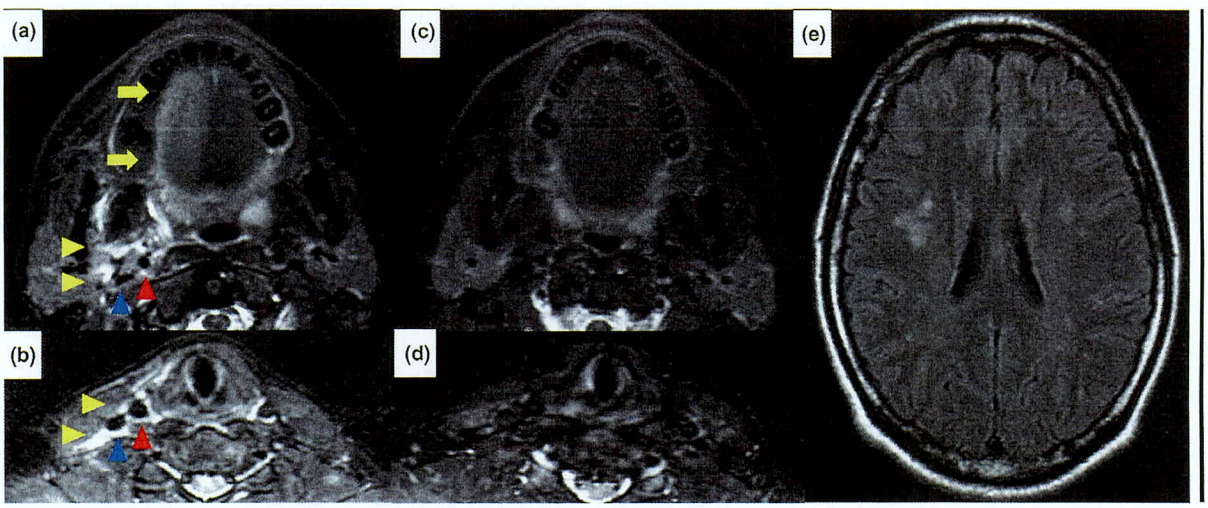

Figure 1 (a,b) Magnetic resonance imaging showed a high-intensity area with contrast effect spreading in the retroparotid space (yellow arrowhead) around the right carotid artery (red arrowhead) and internal jugular vein (blue arrowhead), and a high-intensity area was also confirmed in the right tongue (arrow) in the short T1 inversion recovery image. (c,d) The abnormal signal area of the magnetic resonance image in the right side of the tongue and retroparotid space disappeared 6 months after treatment. (e) A high-intensity area spreading in the deep gray matter of the cerebrum on the fluid-attenuated inversion recovery image.

Eosinophils and heteromorphic cells were not observed.

After hospitalization, eosinophils increased further and numbness in the distal part of left leg appeared. A nerve conduction study showed the decrease in sensory nerve action potentials of the left sural nerve. Nerve biopsy was carried out from the left sural nerve. Nerve biopsy showed axonal degeneration and regenerative changes. Muscle biopsy was carried out from the left biceps brachii. Muscle biopsy showed neither vasculitis nor myositis.

Treatment started with steroid pulse therapy. After therapy, eosinophils decreased to 4/mm^3 (0.1% of white blood cell count) on the next day. The neck pain and numbness in the distal part of the left leg improved immediately. Hypoglossal nerve palsy improved gradually and normalized. Six months later, the patient had made a complete recovery. The abnormal signal area on the MRI in the retroparotid space and right side of the tongue disappeared (Fig. 1c,d). However, the abnormal signal area in the deep gray matter of cerebrum did not change significantly.

After steroid pulse therapy, the patient took oral prednisolone at a dose of 50 mg/day (1 mg/kg/day), and then gradually stopped in 6 months. She has had no relapses or other neurological symptoms for 10 years.

Discussion

Neurological manifestations associated with HES are reported as encephalopathy, cerebral embolic disease, peripheral neuropathy and eosinophilic meningitis.[2–6] However, the present patient did not fit any case of HES reported in the past.

As the pathology of HES, Yoshikawa suggested three potential mechanisms: direct eosinophilic infiltration, the remote or local effects of secreted eosinophil products and embolic infarction.[8] The exact mechanism of eosinophil-induced tissue damage is not known, but eosinophils transit through the blood before migrating into tissues. Specific selectins, adhesion molecules, chemokines and cytokines (interleukin-5) successively and collectively contribute to eosinophil homing. Eosinophils are directly cytotoxic and can affect a local release of toxic substances, such as enzymes, reactive oxygen species, pro-inflammatory cytokines and arachidonic acid-derived factors.[9]

In the present case, biopsy was carried out from the abnormal signal site of the retroparotid space on the MRI, but only lymphocytes were detected. After treatment with a steroid, the abnormal signal disappeared and normalized. Therefore, it was suspected that secreted eosinophil products induce local inflammation around the blood vessel, and ischemic changes as a result of inflammatory cell infiltration into nutrient vessel walls in cranial nerves cause cranial neuropathy. Local inflammation of the retroparotid space around the right carotid artery and internal jugular vein causes multiple cranial neuropathy, "Villaret's syndrome." The retroparotid space is the only area where the lower four cranial nerves (IX, X, XI, and XII) and sympathetic fibers to the eye lie in close proximity and show "Villaret's syndrome."[7]

High-intensity change in the right side of the tongue is considered as a result of hypoglossal nerve denervation. There is a similar image change report in the skeletal muscle that caused denervation. Edema of the neurogenic muscle is considered to be the cause.[10]

The high-intensity change of MRI in the deep gray matter of the cerebrum was suspected to be a result of HES. This lesion did not change after steroid therapy. Lee reported the pathology of central nervous system involvement in HES.[11] In that report, eosinophils were found in just four of 11 cases. Eosinophils infiltrated into the brain parenchyma in two cases, eosinophils were limited to inside the lumen of the vessels in one case and eosinophils were limited in the cerebrospinal fluid in another case. Eosinophil infiltration was not found in the patients with

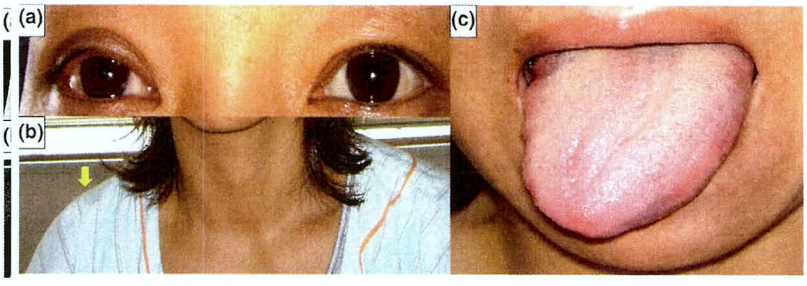

Figure 2 Villaret's syndrome (right hypoglossal nerve, vagus nerve, accessory nerve, hypoglossal nerve palsies and right Horner's sign). (a) Right Horner's sign. (b) Accessory nerve palsy. (c) Hypoglossal nerve palsy.

infarctions. As eosinophil infiltration was not found in pathological studies of patients with HES, they concluded that the lesions in the brain likely did not result from direct invasion by eosinophils. Another study has emphasized that the cytotoxic effect of proteins released by circulating eosinophils, subsequent endothelial damage and thrombus formation are responsible for brain infarction of HES.[12]

HES sometimes causes extravascular inflammation. As a result of extravascular inflammation of the right carotid artery and internal jugular vein, there is a possibility of causing the lower cranial neuropathy, "Villaret's syndrome."

Disclosure of ethical statement

Informed consent was obtained from the patient.

Conflict of interest

None declared.

References

1. Roufosse F, Weller P. Practical approach to the patient with hypereosinophilia. *J Allergy Clin Immunol.* 2010; **26**: 39–44.
2. Dorfman LJ, Ransom BR, Forno LS, et al. Neuropathy in the hypereosinophilic syndrome. *Muscle Nerve.* 1983; **6**: 291–8.
3. Nascimento O, De FM, Chimelli L, et al. Peripheral neuropathy in hypereosinophilic syndrome with vasculitis. *Arq Neuropsiquiatr.* 1991; **49**: 450–5.
4. Lincoff NS, Schlesinger DJ. Recurrent optic neuritis as the presenting manifestation of primary hypereosinophilic syndrome: a report of two cases. *J Neuroophthalmol.* 2005; **25**: 116–12.
5. Weingarten JS, O'Sheal SF, Margolis WS. Eosinophilic meningitis and the hypereosinophilic syndrome. Case report and review of the literature. *Am J Med.* 1985; **78**: 674–6.
6. Kwon SU, Kim JC, Kim JS. Sequential magnetic resonance imaging findings in hypereosinophilia-induced encephalopathy. *J Neurol.* 2001; **248**: 279–84.
7. Le Villaret M. syndrome nerveux de l'espace rétro-parotidien postérieur. *Rev Neurol.* 1916; **29**: 188–90.
8. Yoshikawa H. Neuropathological findings in hypereosinophilic syndrome. *Intern Med.* 2003; **42**: 381–2.
9. Blanchard C, Rothenberg ME. Biology of the eosinophil. *Adv Immunol.* 2009; **101**: 81–121.
10. Kim SJ, Hong SH, Jun WS, et al. MR imaging mapping of skeletal muscle denervation in entrapment and compressive neuropathies. *Radiographics.* 2011; **31**: 319–32.
11. Lee D, Ahn TB. Central nervous system involvement of hypereosinophilic syndrome: a report of 10 cases and a literature review. *J Neurol Sci.* 2014; **347**: 281–7.
12. Prick JJ, Gabreëls-Festen AA, Korten JJ, van der Wiel TW. Neurological manifestations of the hypereosinophic syndrome (HES). *Clin Neurol Neurosurg.* 1988; **90**: 269–73.

Journal of Alzheimer's Disease 68 (2019) 395–404
DOI 10.3233/JAD-181152
IOS Press

Cerebrospinal Fluid and Plasma Biomarkers in Neurodegenerative Diseases

Yusuke Seino[a,*], Takumi Nakamura[a], Takeshi Kawarabayashi[a], Mie Hirohata[a], Sakiko Narita[a], Yasuhito Wakasaya[a], Kozue Kaito[b], Tetsuya Ueda[b], Yasuo Harigaya[c] and Mikio Shoji[a]
[a]*Department of Neurology, Hirosaki University Graduate School of Medicine, Hirosaki, Japan*
[b]*Bioanalysis Department, LSI Medience Corporation, Itabashi-ku, Tokyo, Japan*
[c]*Department of Neurology, Maebashi Red Cross Hospital, Maebashi, Japan*

Handling Associate Editor: Akihiko Nunomura

Accepted 31 December 2018

Abstract. Cerebrospinal fluid (CSF) amyloid-β ($A\beta_{42}$) and tau are biomarkers for Alzheimer's disease (AD); however, the effects of other neurodegenerative processes on these biomarkers remain unclear. We measured $A\beta_{40}$, $A\beta_{42}$, total tau, phosphorylated-tau, and α-synuclein in CSF and plasma using matched samples from various neurodegenerative diseases to expand our basic knowledge on these biomarkers and their practical applications. A total of 213 CSF and 183 plasma samples were analyzed from cognitively unimpaired subjects, and patients with Alzheimer's disease dementia (ADD), mild cognitive impairment (MCI), non-AD dementias, and other neurological diseases. The CSF/plasma ratios of $A\beta_{40}$ and $A\beta_{42}$ were approximately 25:1. $A\beta_{40/42}$ ratios in CSF and plasma were both 10:1. The CSF total tau/P181tau ratio was 6:1. The CSF/plasma α-synuclein ratio was 1:65. Significantly decreased $A\beta_{42}$ levels and an increased $A\beta_{40/42}$ ratio in CSF in ADD/MCI suggested that these relationships were specifically altered in AD. Increased total tau levels in ADD/MCI, encephalopathy, and multiple system atrophy, and increased P181tau in ADD/MCI indicated that these biomarkers corresponded to neurodegeneration and tauopathy, respectively. Although CSF α-synuclein levels were increased in ADD/MCI, there was no merit in measuring α-synuclein in CSF or plasma as a biomarker. The combination of biomarkers by the $A\beta_{40/42}$ ratio × p181tau reflected specific changes due to the AD pathology in ADD/MCI. Thus, CSF $A\beta_{40}$, $A\beta_{42}$, p181tau, and tau were identified as biomarkers for aggregated Aβ associated state (A), aggregated tau associated state (T), and neurodegeneration state (N) pathologies in AD based on the NIA-AA criteria. Overlaps in these biomarkers need to be considered in clinical practice for differential diagnoses of neurodegenerative diseases.

Keywords: $A\beta_{40}$, $A\beta_{42}$, α-synuclein, cerebrospinal fluid, neurodegenerative diseases, phosphorylated-tau, plasma, total-tau

INTRODUCTION

Many large cohort studies, including the Alzheimer's Disease Neuroimaging Initiative [1] and Dominantly Inherited Alzheimer Network [2], have confirmed the efficacy of neuropsychiatric tests, cerebrospinal fluid (CSF) biomarkers, and neuroimaging, including MRI, FDG PET, and amyloid and tau PET, for the diagnosis of Alzheimer's disease (AD). These markers have provided strong evidence for the signatures of the AD pathology in the brain. About 4,500 research (including meta-analysis) articles have already been published on the CSF biomarkers of AD, confirming the usefulness of CSF amyloid-β (Aβ), tau, and phosphorylated tau as diagnostic and predictive markers for AD and its pre-disease states.

Sensitivities and specificities for the diagnosis of mild cognitive impairment (MCI) due to AD and AD dementia (ADD) were revised due to advances in

*Correspondence to: Yusuke Seino, MD, PhD, Department of Neurology, Hirosaki University Graduate School of Medicine, 5 Zaifu-cho, Hirosaki, 036-8216, Japan. Tel.: +81 172 39 5142; Fax: +81 0172 39 5143; E-mail: seino@hirosaki-u.ac.jp.

ISSN 1387-2877/19/$35.00

neuroimaging by amyloid and tau PET as well as rigorous clinical assessments in definite cohorts. Plasma $A\beta_{42}$ levels were recently shown to be closely associated with Aβ amyloidosis in the brain [5]. Plasma phosphorylated-tau has also emerged as a promising novel biomarker for AD [6]. Based on these findings, low CSF $A\beta_{42}$ or cortical amyloid PET ligand binding has been adopted as biomarkers for Aβ plaques (labeled "A") in the ATN classification system of the NIA-AA research framework. High CSF phosphorylated-tau and positive tau PET were also biomarkers for tauopathy (labeled "T"). The NIA-AA research framework proposed diagnostic criteria based on the biological definition of AD for observational and interventional research [7].

In most of the articles, the above usefulness as a diagnostic marker for AD was examined by comparison with only normal controls. In only a few studies, changes in many other neurodegenerative diseases were examined in a similar manner to the present study [8–11]. Differential diagnosis from neurodegenerative diseases, such as dementia and MCI, with different causes in clinical settings, is important. In addition, potential changes in such various diseases should be clarified in clinical settings [8–11]. Thus, many of which were small-scale studies on individual biomarkers. We herein examined CSF and matched plasma samples to analyze CSF and plasma $A\beta_{40}$ and $A\beta_{42}$, CSF total tau and phosphorylated-tau at serine 181 (p181tau), and CSF and plasma α-synuclein in various neurogenerative diseases in order to expand our basic knowledge on these biomarkers and their practical clinical applications.

MATERIALS AND METHODS

Subjects

A total of 213 CSF and 183 plasma samples were examined from neurological disease patients admitted to our department and cognitively unimpaired volunteer subjects (CU). These CSF and plasma samples were collected at the same time as lumber puncture and a routine blood examination. The diagnoses of probable ADD and MCI were based on the core clinical criteria of NIA-AA [12, 13]. Clinically diagnosed neurological diseases by recent respective criteria included 3 cases of frontotemporal dementia cases (FTD) [14, 15], 22 of Parkinson's disease (PD) [16], 15 of multiple system atrophy (MSA) [17], 9 of corticobasal degeneration (CBD) [18], 16 of progressive supranuclear palsy (PSP) [19], and 30 of amyotrophic lateral sclerosis (ALS) [20]. Other neurological diseases included 10 cases of encephalitis and encephalopathy (ENC). Thirty-two CU subjects were also examined. The subject profiles are shown in Table 1. This study was approved by the Ethics Committee of Hirosaki

122

Table 1
Baseline characteristics of participants

Disease	CSF					Plasma				
	Number	Male	Female	Mean age (range)		Number	Male	Female	Mean age (range)	
ADD/MCI	17	8	9	70	(51–83)	12	5	7	67	(51–77)
(AD)	12	5	7	67	(51–75)	10	4	6	65	(51–74)
(MCI)	5	3	2	77	(70–83)	2	1	1	76	(75–77)
FTD	3	3	0	68	(58–75)	3	3	0	68	(58–75)
NPH	4	1	3	80	(76–83)	4	1	3	80	(76–83)
ENC	10	4	6	51	(26–74)	7	2	5	52	(38–66)
MS	10	3	7	37	(19–62)	8	1	7	35	(19–57)
NMO	10	3	7	48	(21–75)	7	2	5	49	(21–75)
PD	22	9	13	68	(49–80)	22	9	13	68	(49–80)
MSA	15	7	8	67	(58–81)	15	7	8	67	(54–81)
CBD	9	4	5	72	(67–78)	8	3	5	72	(67–78)
PSP	16	9	7	72	(63–82)	14	7	7	72	(63–80)
SCD	21	9	12	62	(35–80)	21	9	12	62	(35–80)
ALS	30	22	8	66	(49–83)	25	17	8	67	(49–83)
PN	12	8	4	72	(63–82)	7	4	3	50	(27–62)
CU	32	17	15	57	(17–85)	28	14	14	58	(22–85)
other	2	1	1	57, 70		2	1	1	57, 70	
total	213	108	105	62	(17–85)	183	85	98	62	(19–85)

ADD, Alzheimer dementia; MCI, mild cognitive impairment; FTD, frontotemporal dementia; NPH, normal pressure hydrocephalus; ENC, meningoencephalitis, MS, multiple sclerosis, NMO, neuromyelitis optica; PD, Parkinson's disease; MSA, multiple system atrophy; CBD, corticobasal degeneration; PSP, progressive supranuclear palsy; SCD, spinocerebellar degeneration; ALS, amyotrophic lateral sclerosis; PN, polyneuropathy; CU, cognitively unimpaired control subjects.

University (2017-112). All participants provided written informed consent.

Assay

After the sampling of CSF by lumber puncture and blood in an EDTA-2Na tubes, samples were immediately centrifuged at 3,000 rpm for 10 min, separated, stored in a polypropylene tube, and frozen at –80°C until used. Sandwich ELISA was used to quantify $A\beta_{1-40}$ and $A\beta_{1-42}$ levels in CSF using Human β Amyloid (1–40) ELISA Kit Wako II and a Human/Rat β Amyloid (1–42) ELISA Kit Wako High-Sensitive. Plasma $A\beta_{x-40}$ and $A\beta_{x-42}$ levels were measured using Human/Rat β Amyloid (40) ELISA Kit Wako II and a Human/Rat β Amyloid (42) ELISA Kit Wako High-Sensitive according to the manufacturer's instructions (Wako Pure Chemical Industries, Ltd., Osaka, Japan). Microplates were pre-coated with monoclonal BAN-50 (IgG, anti-$A\beta_{1-16}$) or BNT77 (IgA, anti-$A\beta_{11-28}$, specific for $A\beta_{11-16}$) and sequentially incubated with 25 μl of samples followed by horseradish peroxidase-conjugated BA27 (anti-$A\beta_{1-40}$ $(Fab')^2$, specific for $A\beta_{40}$,) or BC05 (anti-$A\beta_{35-43}$ $(Fab')^2$, specific for $A\beta_{42/43}$). CSF total tau and phosphorylated-tau (ptau181) were measured by INNOTEST®hTAU Ag and PHOSPHO-TAU (181P) (FUJIREBIO Inc., Tokyo, Japan). Captured antibodies were AT120 for total tau and HT7 for ptau181, and detection antibodies were BT2 and HT7 for total tau and AT270 for ptau181, respectively. Sensitivities were 0.019 and 0.049 pmol/L (assay range, 1.0–100 pmol/L) in the $A\beta_{1-40}$ and $A\beta_{x-40}$ assay, and 0.06 and 0.024 pmol/L (assay range, 0.01–20.0 pmol/L) in the $A\beta_{1-42}$ and $A\beta_{x-42}$ assay, respectively. Assay ranges for total tau and ptau181 were 75~1,200 and 25~500 pg/ml, respectively. CSF and plasma α-synuclein were measured by the human α-synuclein ELISA kit consisting of a captured rabbit monoclonal antibody to α-synuclein 118–123 and a detection biotinylated mouse monoclonal antibody to α-synuclein 103–107 (SIG-38974, Covance Inc., NJ, USA). The assay range was 6.1~1,500 pg/ml. Intra- and inter-assay coefficients of variation were less than 10% in all assay systems.

Statistical analysis

Assay values among the respective groups were analyzed using the Kruskal-Wallis test with multiple comparison tests for non-parametric data using GraphPad Prism, version 7 (GraphPad Software, San Diego, CA). Since the number of MCI cases was small, ADD and MCI cases were statistically analyzed as one group, ADD/MCI. In the CSF analysis, mean age was significantly higher in the PSP and normal pressure hydrocephalus (NPH) groups than in the CU group ($p = 0.0057$ and $p = 0.0095$, respectively). In the plasma analysis, mean age was higher in the NPH group and lower in the MS group than in the CU group ($p = 0.0191$ and $p = 0.0326$, respectively). No significant differences were observed in the mean age distribution of other groups.

RESULTS

CSF and plasma $A\beta_{40}$ levels in CU were $1{,}829 \pm 645$ and 73.9 ± 9.2 pmol/ml, respectively. CSF $A\beta_{40}$ levels were higher in ADD/MCI than in CU. However, no significant differences were observed in CSF and plasma $A\beta_{40}$ levels among the respective diseases (Fig. 1a, d). The CSF/plasma $A\beta_{40}$ ratio was 25.1 ± 10.2 in CU. This ratio did not significantly differ among disease groups (Fig. 1g).

CSF and plasma levels of $A\beta_{42}$ in CU were 173.8 ± 66.4 and 7.8 ± 2.0 pmol/ml, respectively. CSF $A\beta_{42}$ levels were 101.2 ± 29.93 pmol/ml in ADD/MCI, and significantly lower than those in CU (Fig. 1b, $p = 0.0005$). No significant differences were observed in plasma $A\beta_{42}$ levels among the diseases (Fig. 1e). The CSF/plasma $A\beta_{42}$ ratio was 23.0 ± 11.3 in CU. This ratio was significantly lower in ADD/MCI than in CU ($p = 0.181$, Fig. 1h).

CSF $A\beta_{40/42}$ ratios were 10.8 ± 1.9 in CU and 22.69 ± 6.0 in ADD/MCI. A significantly increased ratio was observed in ADD/MCI ($p < 0.0001$), while no significant differences were observed among the other diseases (Fig. 1g). The plasma $A\beta_{40/42}$ ratio was 10.0 ± 2.4 in CU. No significant changes were observed among groups (Fig. 1f). The CSF/plasma $A\beta_{40/42}$ ratio was significantly higher in ADD/MCI (2.10 ± 0.41) than in CU (1.16 ± 0.38) (Fig. 1i, $p < 0.0001$). The higher CSF $A\beta_{40/42}$ ratio resulted in a significant increased CSF/plasma $A\beta_{40/42}$ ratio in ADD/MCI (Fig. 1h).

These results suggested a relationship between the CSF/plasma ratio in $A\beta_{40}$ and $A\beta_{42}$ levels and between the $A\beta_{40/42}$ ratio in CSF and plasma. CSF $A\beta_{40}$ and $A\beta_{42}$ were cleared into plasma at approximately 25~23:1. $A\beta_{40/42}$ ratios were 10.8 in CSF and 10 in plasma, suggesting that the $A\beta_{40/42}$ ratio remained constant in CSF and plasma. These

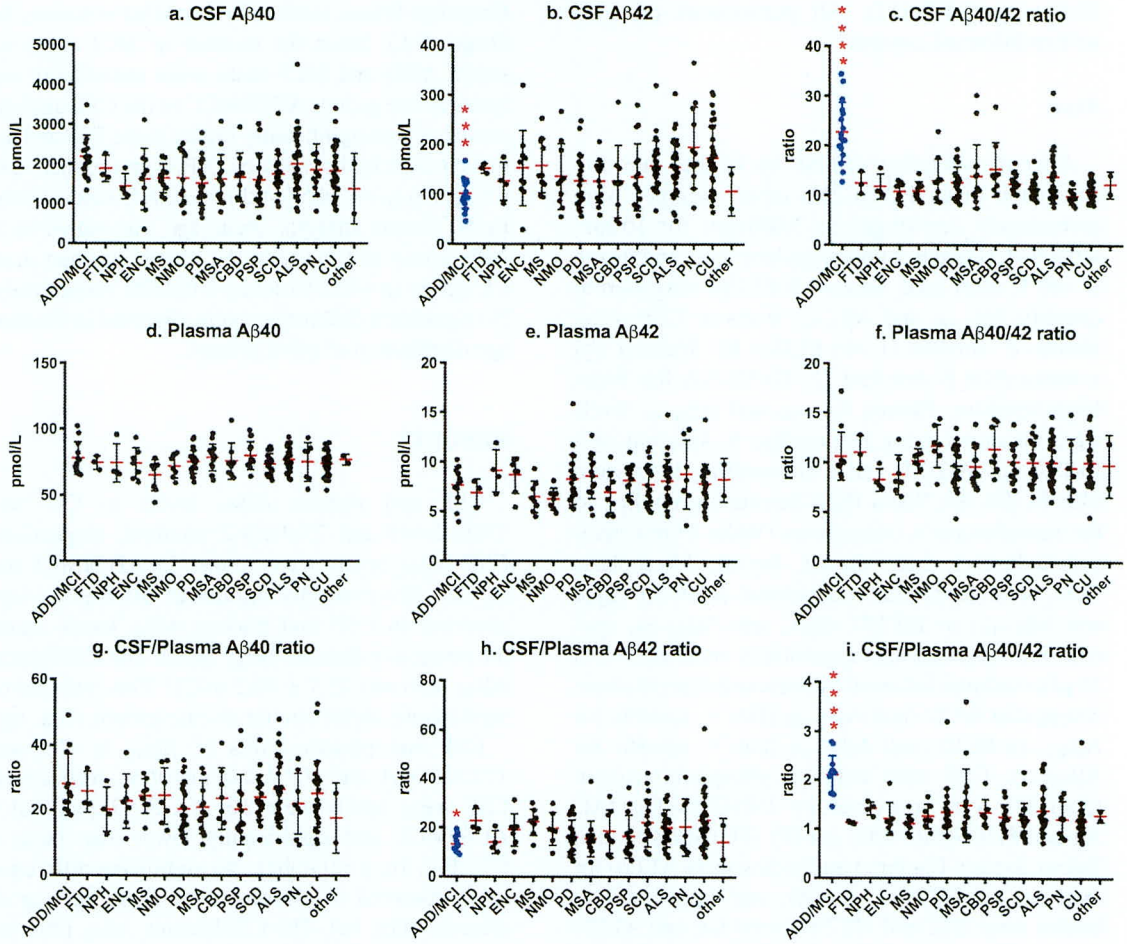

Fig. 1. CSF and plasma $A\beta_{40}$ and $A\beta_{42}$ in neurological diseases. *$p < 0.05$; ***$p < 0.0005$; ****$p < 0.0001$.

relationships resulted in a CSF/plasma $A\beta_{40/42}$ ratio that was close to 1 in CU. Thus, the relationship between $A\beta_{40}$ and $A\beta_{42}$ and its ratio were specifically altered in AD.

CSF total tau levels were 259.3 ± 162.8 pg/ml in CU, and were significantly higher at 738.4 ± 290.6 pg/ml in ADD/MCI ($p < 0.0001$), 1,337 ± 1554 pg/ml in ENC ($p = 0.036$), and 415.7 ± 158.2 pg/ml in MSA ($p = 0.0164$) than in CU. One patient with Creutzfeldt-Jacob disease (CJD) had a CSF tau level of 1,554 pg/ml (Fig. 2a). P181tau levels were 41.69 pg/ml in CU and significantly increased to 88.62 ± 29.69 pg/ml in ADD/MCI ($p < 0.0001$). No significant changes were observed in other diseases (Fig. 1b). The CSF total tau/p181 tau ratio was 6.0 ± 1.8 in CU, and increased to 8.2 ± 1.2 in ADD/MCI ($p = 0.0038$), 38.8 ± 55.6 in ENC ($p = 0.013$), and 10.2 ± 3.1 in MSA ($p < 0.0001$). In CJD, this ratio was 25.9 (Fig. 2c). Specific changes due to AD processes were recognized in P181tau levels.

The CSF and plasma α-synuclein levels in CU were 1.7 ± 0.8 and 90.2 ± 54.2 ng/ml, respectively. The CFS α-synuclein level was significantly higher in ADD/MCI than in CU and other neurological diseases ($p = 0.006$; Fig. 2d). The plasma α-synuclein levels showed no significant intergroup difference. The measured values significantly overlapped among all groups (Fig. 2e). The ratio of plasma/CSF α-synuclein in CU was 65.3 ± 57.8, showing an inverse correlation, i.e., high in the plasma and low in the CSF, unlike other biomarkers such as Aβ and tau (Fig. 2f). CSF total tau/α-synuclein ratio was 4.1 ± 1.8 in CU and increased to 7.22 ± 3.41 in MSA ($p = 0.009$), but was not significant in PD (Fig. 2g). The CSF p181 tau/α-synuclein ratio was 25.8 in

124

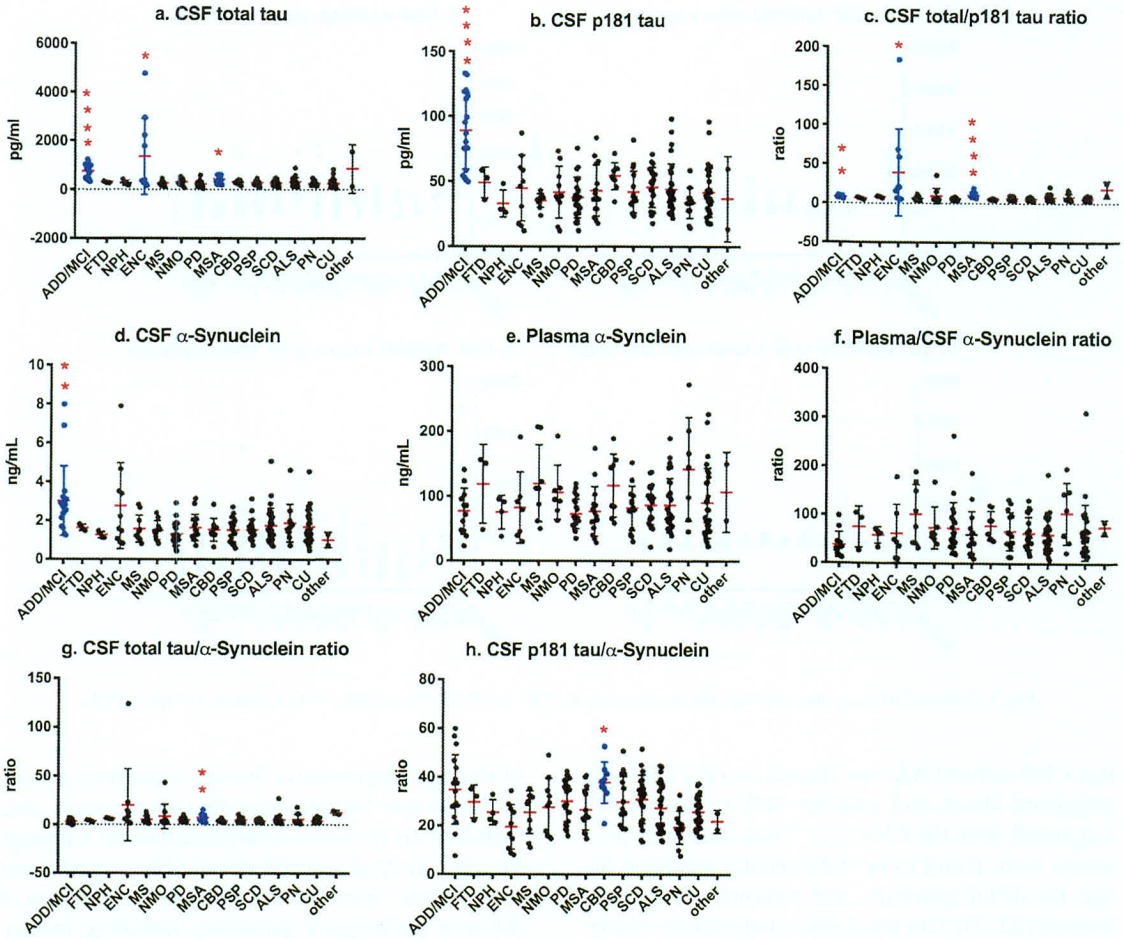

Fig. 2. Total tau, phosphorylated-tau in CSF, and α-synuclein in CSF and plasma. *$p < 0.05$; **$p < 0.005$; ***$p < 0.0001$.

CU and increased to 37.9 ± 8.4 in CBD ($p = 0.021$) (Fig. 2h).

The combination of biomarkers by the CSF $A\beta_{40/42}$ ratio × total tau (the AD index [3]) was significantly higher in ADD/MCI (17,409 ± 8859; $p < 0.0001$) and MSA (6,223 ± 4,658; $p = 0.0286$) than in CU (Fig. 3a). The CSF $A\beta_{40/42}$ ratio × p181tau was 2,088 ± 999 in ADD/MCI (Fig. 3b; $p < 0.0001$). The CSF $A\beta_{40/42}$ ratio × p181tau combination reflected specific changes due to the AD pathology in AD and MCI. Further combinations of the $A\beta_{40/42}$ ratio × total tau/α-synuclein ratio showed increased levels in ADD/MCI (74.46 ± 34.79; $p = 0.0097$), ENC (226.4 ± 452.7; $p = 0.0312$), and MSA (90.5 ± 39.8; $p = 0.0002$) (Fig. 3c). The combination of the $A\beta_{40/42}$ ratio × p181 tau/α-synuclein was significantly increased in ADD/MCI (801.4 ± 396.3; $p < 0.0001$) and CBD (604.5 ± 317.9; $p = 0.01$) (Fig. 3d).

DISCUSSION

Despite marked overlaps among a small number of individual groups, the present study on CSF $A\beta_{40}$ and $A\beta_{42}$ in various neurological diseases due to different pathological processes showed specific changes in $A\beta_{42}$ and in the $A\beta_{40/42}$ ratio, which is consistent with previous findings [3, 8–11]. $A\beta_{42}$ levels and their ratios to $A\beta_{40}$ as an internal control were considered to reflect the specific processes of brain Aβ amyloidosis [1, 2], but not those of tauopathy, synucleinopathies, or other pathological cascades. Plasma Aβ levels and their ratios have not provided definitive findings due to prominent overlaps among the disease groups studied [21, 22]. Recent studies revealed

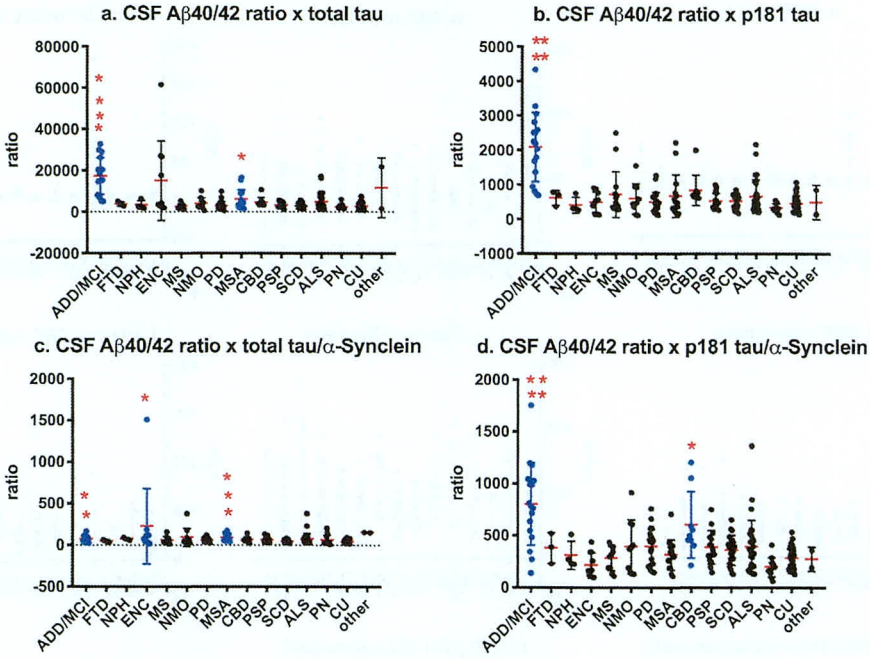

Fig. 3. Index of $A\beta_{40/42}$, tau, p181tau, and α-synuclein in CSF. $*p<0.05$; $**p<0.005$; $***p<0.0005$; $****p<0.0001$.

that CNS-derived Aβ was cleared into the CSF and peripheral blood, and only 30~50% of plasma Aβ originated from the CNS [22]. These clearance processes were found to be differentially regulated by age, the *APOE* genotype, and presence of Aβ amyloidosis [22, 33]. Our small-scale study did not clearly show slight differences in Aβ levels due to brain Aβ amyloidosis; however, the results obtained demonstrated that the CSF/plasma ratio of $A\beta_{40}$ and $A\beta_{42}$ remained mostly constant at approximately 25 to 1 and also that the ratio between $A\beta_{40}$ and $A\beta_{42}$ was also constant at 10 to 1 in CSF and plasma. Even though this was a small-scale study, the present results also showed that the relationships between $A\beta_{40}$ and $A\beta_{42}$ in CSF and plasma were specifically altered in AD pathological processes, suggesting that overlaps among other neurodegenerative processes need to be considered in clinical practice.

Since we did not complete plasma tau and ptau181 assays, we herein only analyzed CSF total tau and ptau181 in subjects. Similarly, our multicenter study in which CSF total tau was measured in 1,031 subjects showed overlapping values in the tauopathy and other neurological disease groups, with moderate measurement sensitivity and specificity as a biomarker using mean ± 2 SD as a cutoff value, instead of ROC analysis [8]. The diagnostic criteria of the neurodegenerative diseases have been revised based on new findings over the past 16 years, and, therefore, are reviewed in the present study. Although the same overlaps were observed in the present study, total tau was increased in some diseases because of different pathological processes, including tauopathy due to AD, acute brain injury by ENC and CJD, and axonal degeneration in MSA [24]. No significant changes were detected in total tau, p181tau, or their ratio in CBD, PSP, or FTD, as previously reported [11, 25–29]. These findings were consistent with the present results on total tau, thereby confirming it as a definitive biomarker for AD and brain injury, as recommended in the novel framework diagnostic criteria "N+" as a biomarker for neurodegeneration [7]. CSF p181tau was previously identified as a specific biomarker for tauopathy, "T+" in AD [7]. The present results on the CSF total tau/p181tau ratio suggest that it was 6:1 and that the phosphorylated-tau tangle pathology increased p181tau and secondarily induced brain injury due to increased total tau levels (8:1), even in AD.

In contrast to AD biomarkers, significant changes in CSF α-synuclein levels were not observed, as previously reported for PD [30–34] and MSA [35]. In previous studies, blood contamination was strictly excluded [30–35]. However, as recently reported,

Table 2
Assay results and mean values and standard deviations (SD) in respective groups

Disease	mean CSF level ± SD					mean plasma level ± SD		
	$A\beta_{40}$	$A\beta_{42}$	Total tau	P181tau	α-synuclein	$A\beta_{40}$	$A\beta_{42}$	α-synuclein
ADD/MCI	2183 ± 538	101 ± 30	738 ± 291	88.6 ± 30	3.02 ± 1.8	77.7 ± 12.4	7.63 ± 1.85	76.6 ± 35.5
(AD)	2184 ± 637	94 ± 27	824 ± 288	98 ± 28	2.79 ± 1.8	74.1 ± 9.7	7.22 ± 1.74	77.7 ± 37.5
(MCI)	2180 ± 200	119 ± 32	532 ± 187	66.1 ± 21	3.55 ± 1.93	95.4 ± 9.5	9.65 ± 0.78	71.4 ± 34.2
FTD	1883 ± 333	152 ± 10	302 ± 35	48.9 ± 12	1.64 ± 0.16	74.2 ± 5.2	6.9 ± 1.4	118.5 ± 60.7
NPH	1433 ± 320	126 ± 39	269 ± 102	32.9 ± 10	1.27 ± 0.16	74.1 ± 14.5	9.10 ± 2.12	75.2 ± 26.2
ENC	1612 ± 779	153 ± 76	1337 ± 1554	44.8 ± 25	2.76 ± 2.22	73.8 ± 11.9	8.68 ± 1.80	82.4 ± 55.0
MS	1638 ± 366	158 ± 55	240 ± 102	35.4 ± 5	1.58 ± 0.70	65.0 ± 11.7	6.51 ± 1.57	120.0 ± 59.1
NMO	1638 ± 666	136 ± 67	301 ± 136	41.7 ± 20	1.5 ± 0.50	71.5 ± 8.9	6.27 ± 1.10	106.2 ± 42.0
PD	1516 ± 565	126 ± 42	217 ± 119	37.8 ± 16	1.31 ± 0.59	75.0 ± 8.7	8.24 ± 2.50	73.1 ± 22.6
MSA	1619 ± 613	126 ± 53	416 ± 158	42.9 ± 20	1.64 ± 0.68	78.5 ± 10.1	8.56 ± 2.22	76.9 ± 38.2
CBD	1665 ± 612	126 ± 73	312 ± 76	54.2 ± 10	1.54 ± 0.59	75.7 ± 13.9	6.98 ± 2.06	116.8 ± 48.7
PSP	1593 ± 680	135 ± 67	270 ± 90.4	42.0 ± 16	1.52 ± 0.63	79.8 ± 10.6	8.14 ± 1.52	81.8 ± 34.2
SCD	1745 ± 494	158 ± 55	261 ± 106	45.6 ± 15	1.54 ± 0.54	73.5 ± 7.9	7.72 ± 2.06	86.3 ± 30.1
ALS	2017 ± 814	155 ± 61	344 ± 169	44.8 ± 20	1.72 ± 0.9	77.4 ± 8.9	8.13 ± 2.33	80.6 ± 36.3
PN	1851 ± 660	195 ± 82	249 ± 94	33.6 ± 12	1.89 ± 0.97	75.2 ± 14.6	8.79 ± 3.45	142.3 ± 79.9
CU	1829 ± 645	174 ± 66	259 ± 163	41.7 ± 19	1.7 ± 0.84	73.9 ± 9.2	7.80 ± 2.02	90.2 ± 54.2
other	742, 2007	72, 142	147, 1554	13.7, 60.0	0.74, 2.36	73.9, 79.7	9.80, 9.68	63.4, 150.6
total	1764 ± 642	146 ± 62	375 ± 440	45.7 ± 22	1.77 ± 1.05	75.2 ± 10.2	7.90 ± 2.13	89.6 ± 45.1

Measurement units of CSF and plasma $A\beta_{40}$ and $A\beta_{42}$ were presented as pmol/L. Units of CSF total tau and phosphorylated-tau were pg/mL. Measurement units of CSF and plasma α-synuclein were ng/mL.

it is irrelevant, and, instead, special antibodies are used [36]. Our ELISA system demonstrated no changes in CSF and plasma α-synuclein levels due to hemolysis (α-synuclein is abundant in erythrocytes), suggesting that hemolysis examination is not necessary [37]. α-Synuclein levels were 65-fold higher in plasma than in CSF, suggesting an inverse relationship between CSF and plasma than those for other AD biomarkers. The presence of α-synuclein is considered to be one of the reasons responsible for elevated CSF α-synuclein levels in patients with severe traumatic brain injury [38]. Peripheral appearances, such as Lewy bodies in ganglion neurons, nerves, and skin, were another difference observed in synucleinopathies. Significant increases in CSF α-synuclein in ADD and MCI may be caused by efflux due to a blood-brain barrier disturbance in AD brains. As described above, Aβ and tau levels are lower in blood than in the CSF, whereas α-synuclein level are 65-fold higher in plasma than in the CSF. A recent study suggested that CSF total tau/α-synuclein or p181tau/α-synuclein serve as biomarkers for the diagnose of PD and the monitoring of its severity [39]. However, the present results do not support this finding. The ratios of tau and p181tau adjusted by α-synuclein levels suggested slightly increased tau due to axonal degeneration in MSA and slightly increased p181tau due to intraneuronal p181tau accumulation in CBD (Fig. 2g, h).

We previously proposed a combination of biomarkers, the CSF $A\beta^{40/42}$ ratio × total tau (AD index [3]), to enhance the discriminating power for AD pathology (Fig. 3a). In the present study, using p181 levels instead of those of total tau as the AD ptau index, the CSF $A\beta_{40/42}$ ratio × p181tau, achieved greater sensitivity for the AD pathology and reduced interference caused by increases in total tau levels due to non-specific brain injuries (Fig. 3b). The clinical and practical aspects of this AD ptau index need to be examined in more detail. The addition of the α-synuclein factor to the AD ptau index was not useful (Fig. 3c, d). Thus, CSF $A\beta_{40}$, $A\beta_{42}$, p181tau, and tau are considered to be specific biomarkers for the A, T, and N classifications of the NIA-AA criteria framework. However, overlaps in these markers need to be considered in differential diagnoses of other neurodegenerative diseases with coincident AD pathologies. It is necessary to further confirm our results by large prospective studies.

ACKNOWLEDGMENTS

We thank Naoko Nakahata for research assistance. This study was supported by the Amyloidosis Research Committee Surveys and Research on Special Diseases, the Longevity Science Committee of the Ministry of Health and Welfare of Japan; Scientific Research (C) (18K07385 MS) from the Ministry of Education, Science, and Culture of Japan; the Hirosaki University Institutional Research Grant, and the Center of Innovation

Science and Technology-based Radical Innovation and Entrepreneurship Program from the Japan Science and Technology Agency.

Authors' disclosures available online (https://www.j-alz.com/manuscript-disclosures/18-1152r1).

REFERENCES

[1] Shaw LM, Vanderstichele H, Knapik-Czajka M, Clark CM, Aisen PS, Petersen RC, Blennow K, Soares H, Simon A, Lewczuk P, Dean R, Siemers E, Potter W, Lee VM, Trojanowski JQ; Alzheimer's Disease Neuroimaging Initiative (2009) Cerebrospinal fluid biomarker signature in Alzheimer's disease neuroimaging initiative subjects. *Ann Neurol* **65**, 403-413.

[2] Bateman RJ, Xiong C, Benzinger TL, Fagan AM, Goate A, Fox NC, Marcus DS,Cairns NJ, Xie X, Blazey TM, Holtzman DM, Santacruz A, Buckles V, Oliver A,Moulder K, Aisen PS, Ghetti B, Klunk WE, McDade E, Martins RN, Masters CL, Mayeux R, Ringman JM, Rossor MN, Schofield PR, Sperling RA, Salloway S, Morris JC; Dominantly Inherited Alzheimer Network (2012) Clinical and biomarker changes in dominantly inherited Alzheimer's disease. *N Engl J Med* **367**, 795-804.

[3] Kanai M, Matsubara E, Isoe K, Urakami K, Nakashima K, Arai H, Sasaki H, Abe K, Iwatsubo T, Kosaka T, Watanabe M, Tomidokoro Y, Shizuka M, Mizushima K, Nakamura T, Igeta Y, Ikeda Y, Amari M, Kawarabayashi T, Ishiguro K, Harigaya Y, Wakabayashi K, Okamoto K, Hirai S, Shoji M (1998) Longitudinal study of cerebrospinal fluid levels of tau, A beta1-40, and A beta1-42(43) in Alzheimer's disease: A study in Japan. *Ann Neurol* **44**, 17-26.

[4] Olsson B, Lautner R, Andreasson U, Öhrfelt A, Portelius E, Bjerke M, Hölttä M, Rosén C, Olsson C, Strobel G, Wu E, Dakin K, Petzold M, Blennow K, Zetterberg H (2016) CSF and blood biomarkers for the diagnosis of Alzheimer's disease: A systematic review and meta-analysis. *Lancet Neurol* **15**, 673-684.

[5] Nakamura A, Kaneko N, Villemagne VL, Kato T, Doecke J, Doré V, Fowler C, Li QX, Martins R, Rowe C, Tomita T, Matsuzaki K, Ishii K, Ishii K, Arahata Y, Iwamoto S, Ito K, Tanaka K, Masters CL, Yanagisawa K (2018) High performance plasma amyloid-β biomarkers for Alzheimer's disease. *Nature* **554**, 249-254.

[6] Tatebe H, Kasai T, Ohmichi T, Kishi Y, Kakeya T, Waragai M, Kondo M, Allsop D, Tokuda T (2017) Quantification of plasma phosphorylated tau to use as a biomarker for brain Alzheimer pathology: Pilot case-control studies including patients with Alzheimer's disease and down syndrome. *Mol Neurodegener* **12**, 63.

[7] Jack CR Jr, Bennett DA, Blennow K, Carrillo MC, Dunn B, Haeberlein SB, Holtzman DM, Jagust W, Jessen F, Karlawish J, Liu E, Molinuevo JL, Montine T, Phelps C, Rankin KP, Rowe CC, Scheltens P, Siemers E, Snyder HM, Sperling R; Contributors (2018) NIA-AA Research Framework: Toward a biological definition of Alzheimer's disease. *Alzheimers Dement* **14**, 535-562.

[8] Shoji M, Matsubara E, Murakami T, Manabe Y, Abe K, Kanai M, Ikeda M, Tomidokoro Y, Shizuka M, Watanabe M, Amari M, Ishiguro K, Kawarabayashi T, Harigaya Y, Okamoto K, Nishimura T, Nakamura Y, Takeda M, Urakami K, Adachi Y, Nakashima K, Arai H, Sasaki H, Kanemaru K, Yamanouchi H, Yoshida Y, Ichise K, Tanaka K, Hamamoto M, Yamamoto H, Matsubayashi T, Yoshida H, Toji H, Nakamura S, Hirai S (2002) Cerebrospinal fluid tau in dementia disorders: A large scale multicenter study by a Japanese study group. *Neurobiol Aging* **23**, 363-370.

[9] Clark CM, Xie S, Chittams J, Ewbank D, Peskind E, Galasko D, Morris JC, McKeel DW Jr, Farlow M, Weitlauf SL, Quinn J, Kaye J, Knopman D, Arai H, Doody RS,DeCarli C, Leight S, Lee VM, Trojanowski JQ (2003) Cerebrospinal fluid tau and beta-amyloid: How well do these biomarkers reflect autopsy-confirmed dementia diagnoses? *Arch Neurol* **60**, 1696-1702.

[10] Ewers M, Mattsson N, Minthon L, Molinuevo JL, Antonell A, Popp J, Jessen F,Herukka SK, Soininen H, Maetzler W, Leyhe T, Bürger K, Taniguchi M, Urakami K,Lista S, Dubois B, Blennow K, Hampel H (2015) CSF biomarkers for the differential diagnosis of Alzheimer's disease: A large-scale international multicenter study. *Alzheimers Dement* **11**, 1306-1315.

[11] Paterson RW, Slattery CF, Poole T, Nicholas JM, Magdalinou NK, Toombs J, Chapman MD, Lunn MP, Heslegrave AJ, Foiani MS, Weston PSJ, Keshavan A, Rohrer JD, Rossor MN, Warren JD, Mummery CJ, Blennow K, Fox NC, Zetterberg H, Schott JM (2018) Cerebrospinal fluid in the differential diagnosis of Alzheimer's disease: Clinical utility of an extended panel of biomarkers in a specialist cognitive clinic. *Alzheimers Res Ther* **10**, 32.

[12] McKhann GM, Knopman DS, Chertkow H, Hyman BT, Jack CR Jr, Kawas CH, Klunk WE, Koroshetz WJ, Manly JJ, Mayeux R, Mohs RC, Morris JC, Rossor MN, Scheltens P,Carrillo MC, Thies B, Weintraub S, Phelps CH (2011) The diagnosis of dementia due to Alzheimer's disease: Recommendations from the National Institute on Aging-Alzheimer's Association workgroups on diagnostic guidelines for Alzheimer's disease. *Alzheimers Dement* **7**, 263-269.

[13] Albert MS, DeKosky ST, Dickson D, Dubois B, Feldman HH, Fox NC, Gamst A, Holtzman DM, Jagust WJ, Petersen RC, Snyder PJ, Carrillo MC, Thies B, Phelps CH (2011) The diagnosis of mild cognitive impairment due to Alzheimer's disease: Recommendations from the National Institute on Aging-Alzheimer's Association workgroups on diagnostic guidelines for Alzheimer's disease. *Alzheimers Dement* **7**, 270-279.

[14] Rascovsky K, Hodges JR, Knopman D, Mendez MF, Kramer JH, Neuhaus J, van Swieten JC, Seelaar H, Dopper EG, Onyike CU, Hillis AE, Josephs KA, Boeve BF, Kertesz A, Seeley WW, Rankin KP, Johnson JK, Gorno-Tempini ML, Rosen H, Prioleau-Latham CE, Lee A, Kipps CM, Lillo P, Piguet O, Rohrer JD, Rossor MN, Warren JD, Fox NC, Galasko D, Salmon DP, Black SE, Mesulam M, Weintraub S, Dickerson BC, Diehl-Schmid J, Pasquier F, Deramecourt V, Lebert F, Pijnenburg Y, Chow TW, Manes F, Grafman J, Cappa SF, Freedman M, Grossman M, Miller BL (2011) Sensitivity of revised diagnostic criteria for the behavioural variant of frontotemporal dementia. *Brain* **134**, 2456-2477.

[15] Chare L, Hodges JR, Leyton CE, McGinley C, Tan RH, Kril JJ, Halliday GM (2014) New criteria for frontotemporal dementia syndromes: Clinical and pathological diagnostic implications. *J Neurol Neurosurg Psychiatry* **85**, 865-870.

[16] Postuma RB, Berg D, Stern M, Poewe W, Olanow CW, Oertel W, Obeso J, Marek K, Litvan I, Lang AE, Halliday G, Goetz CG, Gasser T, Dubois B, Chan P, Bloem BR, Adler CH, Deuschl G (2015) MDS clinical diagnostic criteria for Parkinson's disease. *Mov Disord* **30**, 1591-1601.

128

[17] Gilman S, Wenning GK, Low PA, Brooks DJ, Mathias CJ, Trojanowski JQ, Wood NW, Colosimo C, Dürr A, Fowler CJ, Kaufmann H, Klockgether T, Lees A, Poewe W, Quinn N, Revesz T, Robertson D, Sandroni P, Seppi K, Vidailhet M (2008) Second consensus statement on the diagnosis of multiple system atrophy. *Neurology* **71**, 670-676.

[18] Armstrong MJ, Litvan I, Lang AE, Bak TH, Bhatia KP, Borroni B, Boxer AL, Dickson DW, Grossman M, Hallett M, Josephs KA, Kertesz A, Lee SE, Miller BL, Reich SG, Riley DE, Tolosa E, Tröster AI, Vidailhet M, Weiner WJ (2013) Criteria for the diagnosis of corticobasal degeneration. *Neurology* **80**, 496-503.

[19] Höglinger GU, Respondek G, Stamelou M, Kurz C, Josephs KA, Lang AE Mollenhauer B, Müller U, Nilsson C, Whitwell JL, Arzberger T, Englund E, Gelpi E, Giese A, Irwin DJ, Meissner WG, Pantelyat A, Rajput A, van Swieten JC, Troakes C, Antonini A, Bhatia KP, Bordelon Y, Compta Y, Corvol JC, Colosimo C, Dickson DW, Dodel R, Ferguson L, Grossman M, Kassubek J, Krismer F, Levin J, Lorenzl S, Morris HR, Nestor P, Oertel WH, Poewe W, Rabinovici G, Rowe JB, Schellenberg GD, Seppi K, van Eimeren T, Wenning GK, Boxer AL, Golbe LI, Litvan I; Movement Disorder Society-endorsed PSP Study Group (2017) Clinical diagnosis of progressive supranuclear palsy: The movement disorder society criteria. *Mov Disord* **32**, 853-864.

[20] de Carvalho M, Dengler R, Eisen A, England JD, Kaji R, Kimura J, Mills K, Mitsumoto H, Nodera H, Shefner J, Swash M (2008) Electrodiagnostic criteria for diagnosis of ALS. *Clin Neurophysiol* **119**, 497-503.

[21] Xu W, Kawarabayashi T, Matsubara E, Deguchi K, Murakami T, Harigaya Y, Ikeda M, Amari M, Kuwano R, Abe K, Shoji M (2008) Plasma antibodies to Abeta40 and Abeta42 in patients with Alzheimer's disease and normal controls. *Brain Res* **1219**, 169-179.

[22] Ovod V, Ramsey KN, Mawuenyega KG, Bollinger JG, Hicks T, Schneider T, Sullivan M, Paumier K, Holtzman DM, Morris JC, Benzinger T, Fagan AM, Patterson BW, Bateman RJ (2017) Amyloid β concentrations and stable isotope labeling kinetics of human plasma specific to central nervous system amyloidosis. *Alzheimers Dement* **13**, 841-849.

[23] Nakamura T, Kawarabayashi T, Seino Y, Hirohata M, Nakahata N, Narita S, Itoh K, Nakaji S, Shoji M (2018) Aging and APOE-e4 are determinative factors of plasma Aβ42 levels. *Ann Clin Transl Neurol* **5**, 1184-1191.

[24] Laurens B, Constantinescu R, Freeman R, Gerhard A, Jellinger K, Jeromin A, Krismer F, Mollenhauer B, Schlossmacher MG, Shaw LM, Verbeek MM, Wenning GK, Winge K, Zhang J, Meissner WG (2015) Fluid biomarkers in multiple system atrophy: A review of the MSA Biomarker Initiative. *Neurobiol Dis* **80**, 29-41.

[25] Hall S, Öhrfelt A, Constantinescu R, Andreasson U, Surova Y, Bostrom F, Nilsson C, Håkan W, Decraemer H, Någga K, Minthon L, Londos E, Vanmechelen E, Holmberg B, Zetterberg H, Blennow K, Hansson O (2012) Accuracy of a panel of 5 cerebrospinal fluid biomarkers in the differential diagnosis of patients with dementia and/or parkinsonian disorders. *Arch Neurol* **69**, 1445-1452.

[26] Scherling CS, Hall T, Berisha F, Klepac K, Karydas A, Coppola G, Kramer JH, Rabinovici G, Ahlijanian M, Miller BL, Seeley W, Grinberg LT, Rosen H, Meredith J Jr, Boxer AL (2014) Cerebrospinal fluid neurofilament concentration reflects disease severity in frontotemporal degeneration. *Ann Neurol* **75**, 116-126.

[27] Wagshal D, Sankaranarayanan S, Guss V, Hall T, Berisha F, Lobach I, Karydas A, Voltarelli L, Scherling C, Heuer H, Tartaglia MC, Miller Z, Coppola G, Ahlijanian M, Soares H, Kramer JH, Rabinovici GD, Rosen HJ, Miller BL, Meredith J, Boxer AL (2015) Divergent CSF τ alterations in two common tauopathies: Alzheimer's disease and progressive supranuclear palsy. *J Neurol Neurosurg Psychiatry* **86**, 244-250.

[28] Hansson O, Janelidze S, Hall S, Magdalinou N, Lees AJ, Andreasson U, Norgren N, Linder J, Forsgren L, Constantinescu R, Zetterberg H, Blennow K; Swedish BioFINDER study (2017) Blood-based NfL: A biomarker for differential diagnosis of parkinsonian disorder. *Neurology* **88**, 930-937.

[29] Hampel H, Toschi N, Baldacci F, Zetterberg H, Blennow K, Kilimann I, Teipel SJ, Cavedo E, Melo Dos Santos A, Epelbaum S, Lamari F, Genthon R, Dubois B, Floris R, Garaci F, Lista S; Alzheimer Precision Medicine Initiative (APMI) (2018) Alzheimer's disease biomarker-guided diagnostic workflow using the added value of six combined cerebrospinal fluid candidates: Aβ(1-42), total-tau, phosphorylated-tau, NFL, neurogranin, and YKL-40. *Alzheimers Dement* **14**, 492-501.

[30] Hong Z, Shi M, Chung KA, Quinn JF, Peskind ER, Galasko D, Jankovic J, Zabetian CP, Leverenz JB, Baird G, Montine TJ, Hancock AM, Hwang H, Pan C, Bradner J, Kang UJ, Jensen PH, Zhang J (2010) DJ-1 and alpha-synuclein in human cerebrospinal fluid as biomarkers of Parkinson's disease. *Brain* **133**, 713-726.

[31] Mollenhauer B, Trautmann E, Taylor P, Manninger P, Sixel-Döring F, Ebentheuer J, Trenkwalder C, Schlossmacher MG (2013) Total CSF α-synuclein is lower in de novo Parkinson patients than in healthy subjects. *Neurosci Lett* **532**, 44-48.

[32] Kang JH, Irwin DJ, Chen-Plotkin AS, Siderowf A, Caspell C, Coffey CS, Waligórska T, Taylor P, Pan S, Frasier M, Marek K, Kieburtz K, Jennings D, Simuni T, Tanner CM, Singleton A, Toga AW, Chowdhury S, Mollenhauer B, Trojanowski JQ, Shaw LM; Parkinson's Progression Markers Initiative (2013) Association of cerebrospinal fluid β-amyloid 1-42, T-tau, P-tau181, and α-synuclein levels with clinical features of drug-naive patients with early Parkinson disease. *JAMA Neurol* **70**, 1277-1287.

[33] Kang JH, Mollenhauer B, Coffey CS, Toledo JB, Weintraub D, Galasko DR, Irwin DJ, Van Deerlin V, Chen-Plotkin AS, Caspell-Garcia C, Waligórska T, Taylor P, Shah N, Pan S, Zero P, Frasier M, Marek K, Kieburtz K, Jennings D, Tanner CM, Simuni T, Singleton A, Toga AW, Chowdhury S, Trojanowski JQ, Shaw LM; Parkinson's Progression Marker Initiative (2016) CSF biomarkers associated with disease heterogeneity in early Parkinson's disease: The Parkinson's Progression Markers Initiative study. *Acta Neuropathol* **131**, 935-949.

[34] Shi M, Tang L, Toledo JB, Ginghina C, Wang H, Aro P, Jensen PH, Weintraub D, Chen-Plotkin AS, Irwin DJ, Grossman M, McCluskey L, Elman LB, Wolk DA, Lee EB, Shaw LM, Trojanowski JQ, Zhang J (2018) Cerebrospinal fluid α-synuclein contributes to the differential diagnosis of Alzheimer's disease. *Alzheimers Dement* **14**, 1052-1062.

[35] Shi M, Bradner J, Hancock AM, Chung KA, Quinn JF, Peskind ER, Galasko D, Jankovic J, Zabetian CP, Kim HM, Leverenz JB, Montine TJ, Ginghina C, Kang UJ, Cain KC, Wang Y, Aasly J, Goldstein D, Zhang J (2011) Cerebrospinal fluid biomarkers for Parkinson disease diagnosis and progression. *Ann Neurol* **69**, 570-580.

[36] Ishii R, Tokuda T, Tatebe H, Ohmichi T, Kasai T, Nakagawa M, Mizuno T, El-Agnaf OM (2015) Decrease in plasma

levels of α-synuclein is evident in patients with Parkinson's disease after elimination of heterophilic antibody interference. *PLoS One* **10**, e0123162.

[37] Goldman JG, Andrews H, Amara A, Naito A, Alcalay RN, Shaw LM, Taylor P, Xie T, Tuite P, Henchcliffe C, Hogarth P, Frank S, Saint-Hilaire MH, Frasier M, Arnedo V, Reimer AN, Sutherland M, Swanson-Fischer C, Gwinn K; Fox Investigation of New Biomarker Discovery, Kang UJ (2018) Cerebrospinal fluid, plasma, and saliva in the BioFIND study: Relationships among biomarkers and Parkinson's disease Features. *Mov Disord* **33**, 282-288.

[38] Mondello S, Buki A, Italiano D, Jeromin A (2013) α-Synuclein in CSF of patients with severe traumatic brain injury. *Neurology* **80**, 1662-1668.

[39] Delgado-Alvarado M, Gago B, Gorostidi A, Jiménez-Urbieta H, Dacosta-Aguayo R, Navalpotro-Gómez I, Ruiz-Martínez J, Bergareche A, Martí-Massó JF, Martínez-Lage P, Izagirre A, Rodríguez-Oroz MC (2017) Tau/α-synuclein ratio and inflammatory proteins in Parkinson's disease: An exploratory study. *Mov Disord* **32**, 1066-1073.

Internal Medicine
The Japanese Society of Internal Medicine

doi: 10.2169/internalmedicine.2638-19
Intern Med Advance Publication
http://internmed.jp

[CASE REPORT]

A Case of Perineuritis Successfully Treated with Early Aggressive Immunotherapy

Takumi Nakamura[1], Takeshi Kawarabayashi[1], Yusuke Seino[1], Mie Hirohata[1], Koichi Wakabayashi[2] and Mikio Shoji[1]

Abstract:

Perineuritis is a rare type of peripheral neuropathy defined by swelling and cellular infiltration in the perineurium. We herein report a 52-year-old man who presented with subacute onset pain from the back to the lower limbs, muscle weakness and hypoesthesia. A sural nerve biopsy revealed perineuritis, consisting of inflammatory cell infiltration and swelling of the perineurium. Oral prednisolone, plasma exchange and intravenous immunoglobulin treatment were all effective, leading to significant improvement of the symptoms.

Key words: perineuritis, immunotherapy, painful neuropathy, diabetes, rare neuropathy

(Intern Med Advance Publication)
(DOI: 10.2169/internalmedicine.2638-19)

Introduction

Perineuritis was first reported in 1972 is as a rare type of peripheral neuropathy characterized by specific pathological findings. Swelling and cellular infiltration in the perineurium, with deposits of immunoglobulin (Ig) G and IgM are the typical pathological findings (1). Comorbidity of diabetes mellitus, leprosy (2), cryoglobulinemia (3), malignancies (including non-Hodgkin's lymphoma) (4-7), ulcerative colitis (8), infection or collagen disease suggests an immune-mediated mechanism (9). Clinical symptoms of perineuritis also vary. The first reported cases were both characterized by an onset with predominantly distal painful sensory neuropathy (1), but cases of onset with mononeuritis multiplex, sensory motor neuropathy or polyradiculopathy have since been reported (8). Therefore, immunosuppressive therapies have historically been employed, and Eric et al. reported that immunosuppressive therapy was effective in 7 out of 12 cases (58%) of perineuritis (7).

We herein report a case of perineuritis characterized by severe pain in a middle-aged man with well-controlled diabetes that responded well to immunosuppressive therapy.

Case Report

A 52-year-old man developed back pain 4 months ago and the prick-like pain spread to the entire back. One month later, left foot numbness and foot drop appeared. The same symptoms extended to the right foot, and constipation and nocturia additionally developed. Twenty days before admission to the hospital, right hand numbness and pain in the back and both feet worsened, causing sleeplessness. The administration of analgesics (clonazepam: 2 mg, tramadol: 250 mg, amitriptyline: 10 mg, alprazolam: 0.4 mg, pentazocine injection at 15 mg per day) and a rescue dose of morphine did not improve his pain. He had a few years' history of diabetes mellitus, which was well controlled by dietary therapy, and had drunk approximately 55 g of alcohol per day over the past 30 years; he stopped drinking at the onset of symptoms.

A neurological examination at admittance revealed distal dominant muscle weakness of both lower extremities, especially of the tibialis anterior (0 in MMT), hypoesthesia below both knees, allodynia in both planta, and loss of lower limb reflexes. He was unable to stand or walk due to painful paraplegia. His blood count was normal. Blood chemistry revealed mild liver damage. Hemoglobin A1c was 6.5% (ref-

[1]Department of Neurology, Hirosaki University Graduate School of Medicine, Japan and [2]Department of Neuropathology, Hirosaki University Graduate School of Medicine, Japan
Received: January 8, 2019; Accepted: April 9, 2019; Advance Publication by J-STAGE: June 27, 2019
Correspondence to Dr. Takumi Nakamura, takumi.n@hirosaki-u.ac.jp

Table. **The Results of Nerve Conduction Studies.**

MOTOR NERVE	CMAP(mV) Distal	Proximal	Latency(msec) Distal	Proximal	MCV(m/sec)	F-latency (msec)
rt. Median	5.4 (>5.0)	4.4	3.9 (<4.0)	7.7	58.7 (>55.0)	27.2
rt. Ulnar	9.0 (>5.0)	3.2	2.6 (<3.2)	7.6	49.5 (>55.0)	26.5
rt. Tibial	not evoked					
lt. Median	8.1 (>5.0)	7.6	3.5 (<4.0)	7.3	55.3 (>55.0)	27.4
lt. Ulnar	8.9 (>5.0)	6.1	2.7 (<3.2)	6.9	55.4 (>55.0)	26.1
lt. Tibial	0.06 (>7.0)	0.05	8.4 (<5.7)	17.9	40.6 (>40.0)	not evoked

SENSORY NERVE	SNAP(μV) Distal	Proximal	Latency(msec) Distal	Proximal	SCV(m/sec) Distal	Proximal
rt. Median	10.4 (>14.0)	5.5	2.9 (<2.9)	6.7	52.4 (>55.0)	60.5
rt. Ulnar	12.3 (>10.0)	6.5	2.5 (<2.4)	6.4	55.6 (>55.0)	59.3
rt. Sural	8.1 (>8.0)		1.9 (<3.6)		53.8 (>40.0)	
lt. Median	5.5 (>14.0)	2.3	2.9 (<2.9)	6.5	55.4 (>55.0)	54.9
lt. Ulnar	24.1 (>10.0)	8.7	2.1 (<2.4)	5.9	65.4 (>55.0)	61.2
lt. Sural	4.7 (>14.0)		2.6 (<3.6)		46.9 (>40.0)	

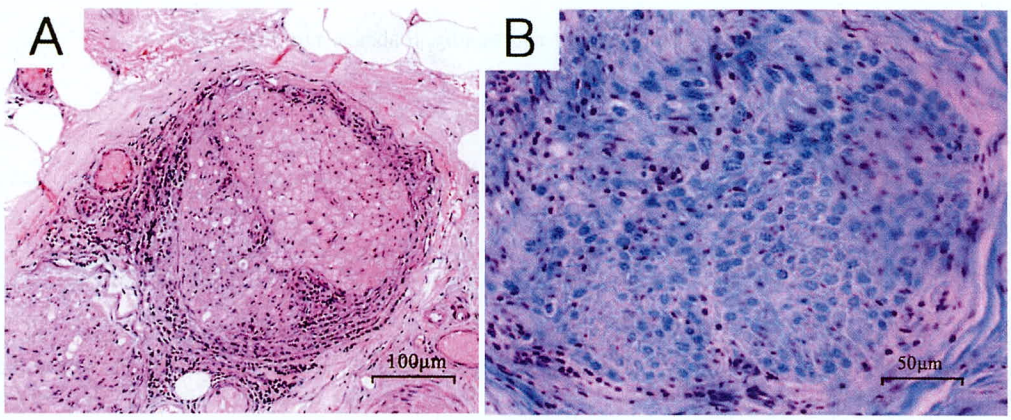

Figure 1. **Hematoxylin and Eosin staining (A) and Klüver-Barrera stained (B) images of the sural nerve. Inflammatory cells were distributed in the circumference of the nerve bundle with swelling of the perineurium. Inflammatory cell infiltration in the nerve bundle and loss of myelinated nerve fibers were mild.**

erence value: less than 6.2%), and the fasting blood sugar level was 115 g/dl. Ferritin was high at 467 ng/ml, but iron and total iron binding capacity were normal. The renal function, thyroid hormone, vitamin B group and blood sedimentation rate were normal. Antinuclear antibody, cryoglobulin and uroporphyrin were negative. A cerebrospinal fluid analysis demonstrated albuminocytologic dissociation with a cell count of 2/μl, protein level of 80.1 mg/dl, immunoglobulin G index of 0.94, normal myelin basic protein and negative oligoclonal band. Brain and lumbar magnetic resonance imaging findings were normal. Whole-body computed tomography revealed no evidence of malignant tumor. An electromyogram demonstrated denervation and neurogenic changes in the lower limb muscles. Nerve conduction studies indicated decreased compound muscle action potential and sensory nerve action potential with severe motor axon damage to the tibial nerve and mild sensory axon damage to the sural nerve (Table). A sural nerve biopsy revealed inflammatory cell infiltration and swelling of the perineurium (Fig. 1). No findings suggestive of vasculitis or abnormal deposits were noted.

Although single oral prednisolone (initial dose of 60 mg per day) therapy slightly improved his pain, the combination of plasma exchange and intravenous immunoglobulin therapy with oral prednisolone markedly improved his muscle weakness and sensory disturbance (Fig. 2). Nearly complete recovery of painful paraplegia, constipation, nocturia and sleeplessness was observed. His condition did not deteriorate following tapering of steroids.

Discussion

Perineuritis was first reported by Asbury in 1972 as distally dominant recurrent painful neuropathy characterized by

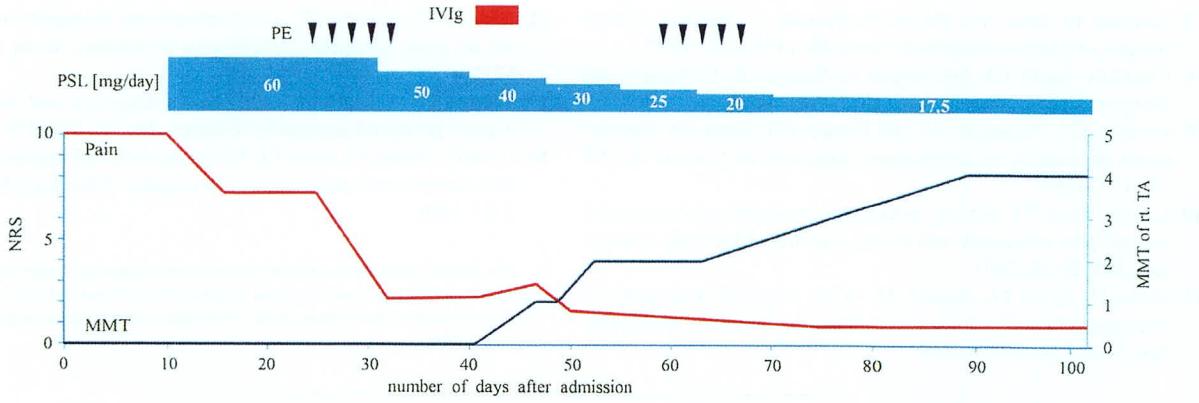

Figure 2. Clinical course after hospital admission. The clinical condition was evaluated based on the degree of pain with the numerical rating scale (NRS) and strength of the tibialis anterior (TA) muscle, which were the most characteristic findings in the present case. Both symptoms improved with treatment. The NRS improved to 1, and the MMT score for the TA muscle improved to 4. Prednisone was gradually tapered to 17.5 mg/day at discharge.

inflammation in the perineurium (1). Other clinical symptoms and comorbid diseases were also reported (1-8, 10). As our patient did not have any other malignancy or autoimmune disease, this case was diagnosed as perineuritis complicated with diabetes mellitus (7).

In this case, the most important differential diagnosis was diabetic neuropathy. Although alcoholic neuropathy was also considered as a differential diagnosis of his painful neuropathy (11), it was excluded because the symptoms were aggravated after temperance in our patient. Some cases of diabetic neuropathy can lead to the subacute onset of painful neuropathy, such as treatment-induced neuropathy of diabetes due to the rapid correction of hyperglycemia (12), acute painful diabetic neuropathy due to the continuation of hyperglycemia (13) or radiculoplexus neuropathy caused by microvasculitis (14) mimicking perineuritis symptoms. Perineuritis is difficult to diagnose by electrophysiological examinations because both axonopathy and demyelination may be observed (7). High levels of protein in the cerebrospinal fluid are not specific among these diseases (7). Perineuritis complicated by diabetes mellitus develops irrespective of blood sugar control (7). Although perineuritis was suggested to be related to diabetes mellitus in previous reports (7), its pathogenesis due to diabetes complications has not been clarified because of the lack of pathologically specific findings. Therefore, a nerve biopsy examination should be performed for diabetes mellitus patients who develop painful neuropathy with no history of rapid correction of hyperglycemia or continuation of hyperglycemia because the treatment approach for perineuritis with diabetes mellitus differs from that for diabetic neuropathy.

Although there is no standard treatment, Asbury first empirically reported on the efficacy of immunosuppressive therapy for the treatment of perineuritis. Eric reported that 7 out of 12 (58 percent) patients with perineuritis saw their condition improved by immunosuppressive therapy including oral or intravenous prednisolone, intravenous immunoglobulin, plasmapheresis, immunosuppressant and total lymphoid irradiation (7). In our case, single oral prednisolone administration was not sufficient for relief. Although there was no exacerbation of blood glucose control, no improvement was observed. Therefore, we conducted plasmapheresis and intravenous immunoglobulin administration simultaneously with oral prednisolone. These combined treatments were effective, and the patient had almost no pain or muscle weakness when low doses of analgesics were administered (pregabalin: 150 mg per day and clonazepam: 1 mg per day).

At present, the patient is receiving oral prednisolone according to the standard treatment for vasculitis syndrome. We intend to taper oral prednisolone as much as possible. If recurrence or side effects of prednisolone appear, we will consider the addition of an immunosuppressant. A trial for combined immunotherapy may be useful for establishing a standard therapy for perineuritis with diabetic mellitus.

The authors state that they have no Conflict of Interest (COI).

References

1. Asbury AK, Picard EH, Baringer JR. Sensory perineuritis. Arch. Neurol **26**: 302-312, 1972.
2. Koike H, Hashimoto R, Tomita M, et al. The wide range of clinical manifestations in leprous neuropathy. Intern Med **50**: 2223-2226, 2011.
3. Konishi T, Saida K, Ohnishi A, Nishitani H. Perineuritis in mononeuritis multiplex with cryoglobulinemia. Muscle Nerve **5**: 173-177, 1982.
4. Tomita M, Koike H, Kawagashira Y, et al. Clinicopathological features of neuropathy associated with lymphoma. Brain **136**: 2563-2578, 2013.
5. Yamada M, Owada K, Eishi Y, Kato A, Yokota T, Furukawa T. Sensory perineuritis and non-Hodgkin's T-cell lymphoma. Eur Neurol **34**: 298-289, 1994.
6. Furusho K, Watanabe M, Ohkoshi N, Tamaoka A, Shoji S. A case of sensory perineuritis with Bowen disease. Rinsho Shinkeigaku **42**: 527-529, 2002.

7. Sorenson EJ, Sima AA, Blaivas M, Sawchuk K, Wald JJ. Clinical features of perineuritis. Muscle Nerve **20**: 1153-1157, 1997.
8. Chad DA, Smith TW, DeGirolami U, Hammer K. Perineuritis and ulcerative colitis. Neurology **36**: 1377-1379, 1986.
9. Bourque CN, Anderson BA, del Campo CM, Sima AA. Sensorimotor perineuritis--an autoimmune disease? Can J Neurol Sci **12**: 129-133, 1985.
10. Lee SS, Yoon TY. Sensory perineuritis presented as a mononeuritis multiplex associated with livedo vasculitis. Clin Neurol Neurosurg **103**: 56-58, 2001.
11. Koike H, Iijima M, Sugiura M, et al. Alcoholic neuropathy is clinicopathologically distinct from thiamine-deficiency neuropathy. Ann Neurol **54**: 19-29, 2003.
12. Gibbons CH, Freeman R. Treatment-induced neuropathy of diabetes: an acute, iatrogenic complication of diabetes. Brain **138**: 43-52, 2015.
13. Thomas PK. Classification, differential diagnosis, and staging of diabetic peripheral neuropathy. Diabetes **46**: S54-S57, 1997.
14. Dyck PJ, Norell JE, Dyck PJ. Microvasculitis and ischemia in diabetic lumbosacral radiculoplexus neuropathy. Neurology **53**: 2113-2121, 1999.

134

意識障害・介護拒否・食事拒否などの臨床症状を示した嗜銀顆粒性認知症の１剖検例

公益財団法人老年病研究所附属病院　内科
高　玉　真　光　　長　嶺　士　郎

公益財団法人老年病研究所附属病院　病理診断科
鈴　木　慶　二　　福　田　利　夫

公益財団法人老年病研究所附属病院　脳神経内科
岡　本　幸　市

はじめに

嗜銀顆粒性認知症（argyrophilic grain dementia）はアルツハイマー型病変を伴わない認知症患者でBraakらにより初めて1987年に記載された．特徴的な嗜銀性顆粒が大脳辺縁系皮質や扁桃核に多数みられて認知症を来す疾患である[1]．今回，認知症，介護拒否，食事拒否などの臨床症状を示し，剖検により嗜銀顆粒性認知症と診断した症例を報告する．

症　　例

患　者：85歳　女性．

主　訴：食事を摂取しない．

家族歴：80歳の時，夫と死別，子供なし．

既往歴：70歳頃より高血圧．76歳で大腿骨頸部骨折のため観血的治療．

臨床経過：80歳の時，一人暮らしとなってから訪問販売員と知り合い，さまざまな家具やふとん，不必要な土地などを購入するようになった．その頃から記憶力や認知機能の低下がみられ，金銭管理も出来なくなり，A婦人に銀行預金の通帳を預かってもらい，生活費を受け取るようになった．

82歳の時著しいめまいと意識障害があり，救急車で来院．会話は出来たが，日時は不明，起立も困難で軽度の運動失調が認められたが，病的反射は出現していない．病状が回復してから通院に際して介護保険を申請し，主治医，介護支援専門員，民生委員，介護者のA婦人らとケアカンファレンスを開催したが，本人には介護については拒否するなど「頑固」に反対してしまうなどの行動があった．その後，地域包括支援センターの保健師と知り合い，親しく会話するようになり小規模多機能施設に入所出来るための日常生活の介護を受けていた．

85歳となった年の１月17日，施設内で意識を失って救急搬送されて来院した．介護士からの話では，７日前から食事を摂取しなくなり，２日前から水も飲まなくなっていた．

入院後，輸液を行い意識は徐々に回復した．頭部CT所見では前頭葉，側頭葉の萎縮があり，両側の海馬回周囲に萎縮がみられた（図１，図２）．

入院後も食欲がなく，食事を拒否，リハビリテーションも希望せず，服薬もしなかった．

２月12日，突然の腹痛と発熱があり，意識が消失した．急性腹膜炎の診断の下に治療を行ったが，血圧が低下して死亡．

検査所見では脱水と低蛋白血症が認められ

ていた.

検査成績：T-CHO 103mg/dl, HDL-C 54mg/dl, TG 54mg/dl, AST 13mg/dl, ALT 6mg/dl, LD 169mg/dl, ALP 179mg/dl, γ-GTP 9mg/dl, TP 4.0g/dl, ALB 1.6g/dl, UA 3.5mg/dl, BUN 18.1mg/dl, CRE 1.32mg/dl, eGFR 29.6

病理解剖学的診断：（図3～5）

主病名

1．胃潰瘍窄孔，化膿性腹膜炎

2．直腸癌

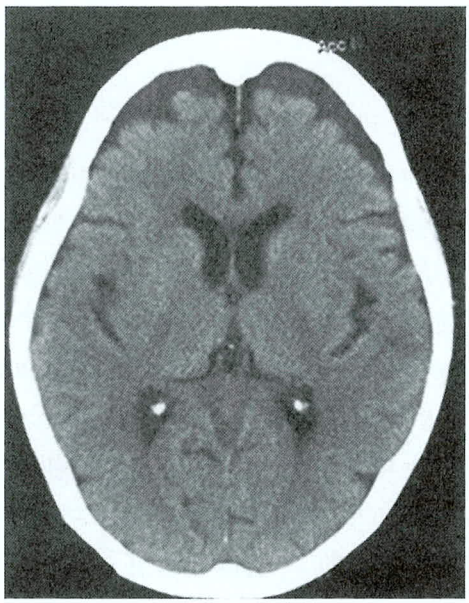

図1　両側前頭葉に萎縮がみられる

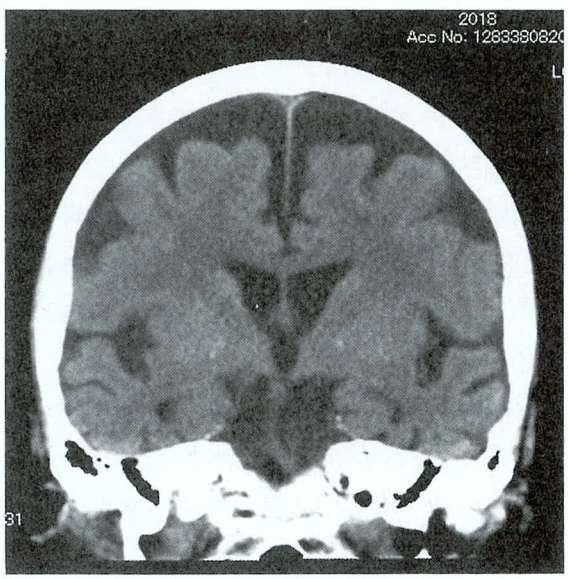

図2　両側側頭葉

頭頂葉に萎縮がみられる

副病変

1．嗜銀顆粒性認知症

(1) 脳萎縮1,045g，(2) 神経原線維性変化

2．脳内小動脈硬化

3．心萎縮　240g

4．肺水腫，うっ血　165g　180g

5．肺萎縮　600g

6．左右腎動脈硬化症　65：75g

7．脾萎縮　45g

8．下垂体，甲状腺，副腎萎縮

剖検所見：アルツハイマー型認知症として治療中に腹膜炎と敗血症で死亡した症例であり，剖検により胃潰瘍穿孔による腹膜炎，腹水貯留が確認された．諸蔵器には萎縮がみられたが，気管支炎，敗血症性変化はみられなかった．

脳の老人性変化は海馬回に限局した神経原線維性変化であり，老人斑はみられず，海馬

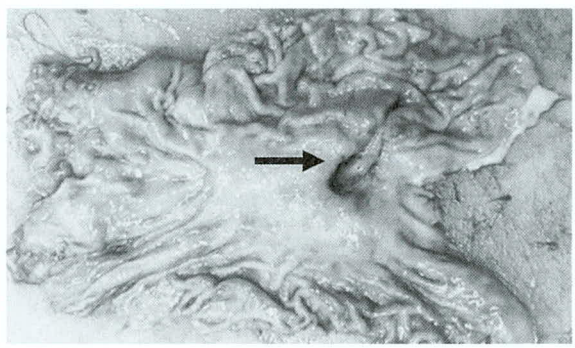

図3　胃潰瘍穿孔

胃体部前壁，約9mm（矢印）

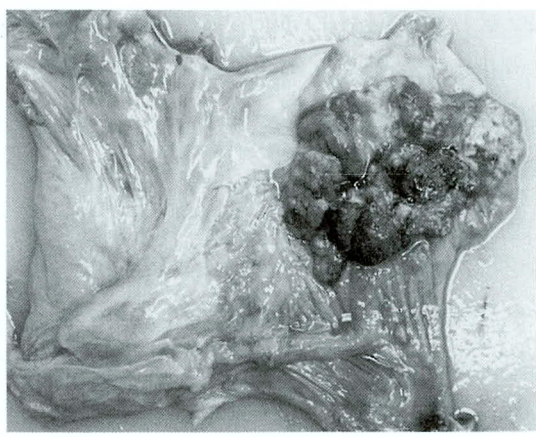

図4　直腸癌

3型，鶏卵大，高分化型腺癌漿膜下まで浸潤

回の神経原線維変化とともに，タウ染色陽性，Gallyas-Braak 染色陽性の多数の嗜銀顆粒の沈着がみられ，嗜銀顆粒性認知症と診断された（図６～９）．

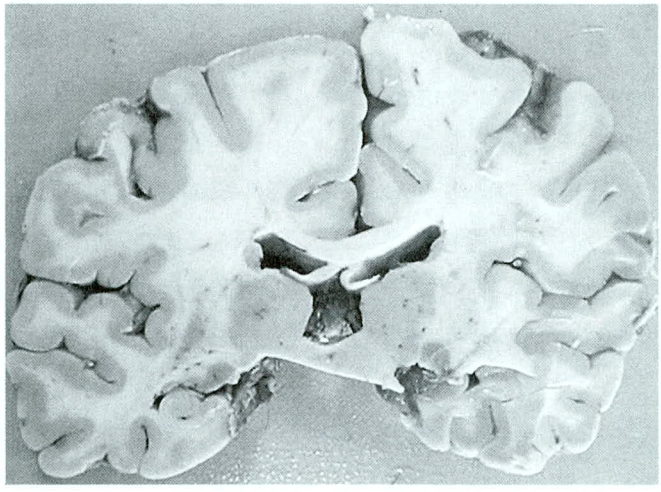

図５　大脳前額断面
限局性病変なし，基底核・視床・
海馬回にも明らかな萎縮はない

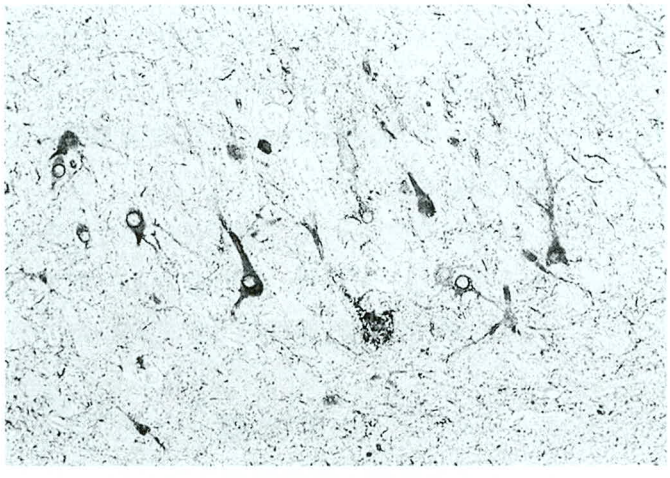

図６　海馬回の神経原線維変化
（AT8 免疫染色）

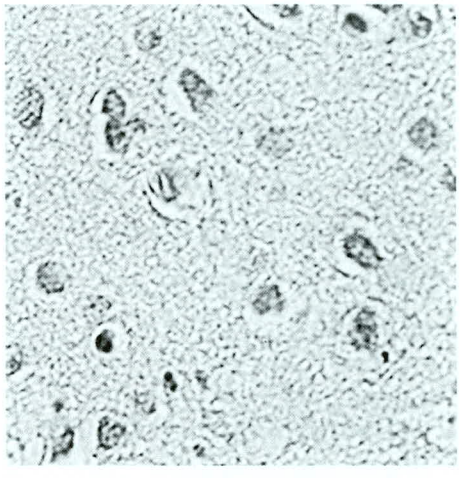

図７　老人斑はない
（4G8 免疫染色）

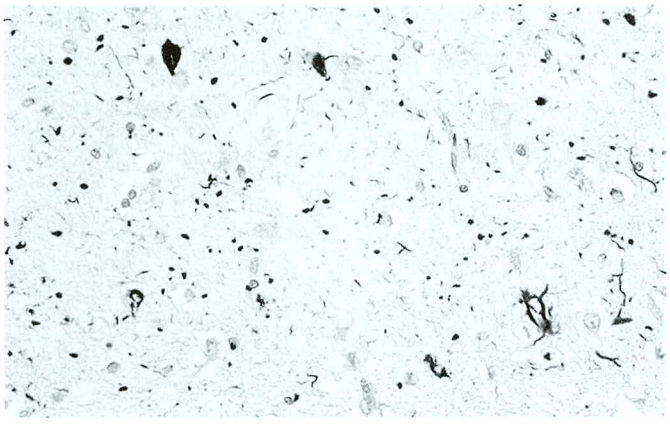

図８　海馬傍回
神経原線維変化と多数の嗜銀顆粒がみられる
（Gallyas-Braak 染色）

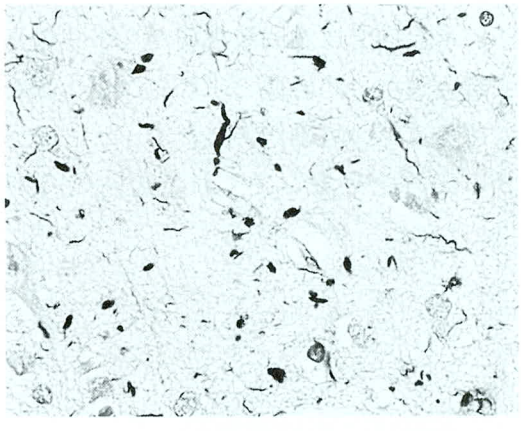

図９　神経原線維性変化と嗜銀顆粒
（強拡大，Gallyas-Braak 染色）

「非アルツハイマー型変性性認知症」

初老期，老年期に認知症としての症状を示す疾患には，アルツハイマー型認知症と脳血管性認知症が代表的である．非アルツハイマー型変性性認知症（non-Alzheimer dementias: NAD）はアルツハイマー型認知症以外の変性性認知症の総称である．この中には1）レビー小体型認知症，2）タウ蛋白の蓄積を特徴とする疾患（ピック病，進行性核上性麻痺，皮質基底核変性症，嗜銀顆粒性認知症など）がある[1]．

嗜銀顆粒性認知症は嗜銀性顆粒が大脳辺縁系皮質や扁桃核に多数みられ認知症を示す疾患である．またこの嗜銀性顆粒はアルツハイマー型認知症やタウオパチーを示す変性疾患にも加齢に伴って迂回回・扁桃核から出現し，側頭葉内側面から海馬に及び，さらに島回・前帯状回へと広がり種々の認知症と併存する[3]．症状は認知症が中心症状で，軽度アルツハイマー型認知症の症状を示すことが多いが，一部行動・性格の変化などの前頭葉症状が出現し，前頭側頭型認知症と診断されることもある[2]．

「この症例の臨床所見から学んだこと」

1）認知症の進行は緩徐で，軽度の認知障害を示したが4～5年間近隣の人には気付かれることはなかった．

2）本症例では訪問販売員から多くの品物を購入したり，必要と思われない土地を購入するなどの行動があった．

3）これを注意してくれた近隣のA婦人を深く信頼し，銀行預金通帳を預けて，生活費として現金を下ろしてもらっていたことを聴き，金銭管理が不能となったことを知った．

4）性格変化があり，易怒性が明らかになり，MMSEなどの検査は拒否された．

5）初期には見当識は保たれており，記憶障害も認められなかったが，徐々に認知障害が進行した．地域包括支援センターの保健師と交際が出来るようになった頃から，金銭管理が出来ず，日常生活に介護が必要となり，小規模多機能施設に入所することが出来た．しかし自己中心的な行動が著しく，自分が好む物だけ食べるようになり，入浴や介護を拒否していた．

6）2-3週間後には全く食事をしなくなり脱水症状を生じて救急車で搬送された．自己中心的な行動と命令的な話し方からアルツハイマー型認知症よりも前頭側頭型変性症が疑われた．

7）76歳の時に左大腿骨頸部骨折のため医療を受けたことがあり，認知症がみられてから死亡までの全経過は約5年であった．

引用文献

1）平井俊策編：痴呆症のすべて(2)，317～324，2005

2）山口晴保：認知症の正しい理解と包括的医療・ケアのポイント(3)，323～324，2016

3）齊藤祐子：嗜銀顆粒性認知症と神経線維変化型老年期認知症：日本医師会雑誌147(2)，「認知症トータルケア」113～115，2018

本人・家族の希望に沿った生活を支える認知症初期集中支援チームの活動と地域連携の事例

【前橋市認知症初期支援チーム】

群馬県立県民健康科学大学
上　山　真　美

群馬医療福祉大学
山　口　智　晴

公益財団法人老年病研究所附属病院
高　玉　真　光

認知症介護研究・研修東京センター
山　口　晴　保

はじめに

わが国の65歳以上の認知症高齢者数を見ると，2025年には約５人に１人になると推計[1]されている．このように増加する認知症高齢者への対策として厚生労働省は，認知症施策推進総合戦略（以下，新オレンジプラン）を2015年に策定した．新オレンジプランは７つの柱で構成され，その一つが「認知症の容態に応じた適時・適切な医療・介護等の提供」[2]である．そして，その柱の主な政策の一つが認知症初期集中支援チーム（以下，支援チーム）の設置となる．前橋市では2018年度末までの全国の市町村に設置する目標に先駆け，2013年度のモデル事業より支援チームを設置し，医療・介護に結びついていない事例や介護困難な事例などに対する支援を行っている．

今回，本人・家族の希望に沿った在宅での生活の継続を支えた支援チームの活動事例について報告する．なお，症例が特定されないように，内容を損なわない範囲で一部改変した．

症　例

対　象：80代の男性
既往歴：脳梗塞（再発あり）
家族構成：妻・娘と同居
定期受診：脳梗塞発症後，家族が付き添い病院の外来受診継続
主症状（家族より）：物忘れが著しい，寝てばかりいる
介護保険：認定切れ
サービス利用：なし
支援チーム依頼経路：娘が地域包括支援センターへ相談後，支援チームへ依頼

問題の見極めとアセスメント

支援チームの主担当者が，地域包括支援センターの担当者等と対象の自宅を訪問して初

期評価を行い，月に2回開催している多職種（認知症専門医，作業療法士，看護師，社会福祉士，等）によるチーム員会議（市の地域包括支援センター担当保健師と本事業受託地域包括支援センター主任介護支援専門員も参加）にて詳細を検討した．初期評価と検討した内容を以下に記す．

1．生活上に生じている問題

対象は自力でむせなく食事摂取でき，杖を使用してトイレは一人で使用できる一方，ほとんどの時間をベッド上に臥床して過ごしていた．活気がなくアパシーの状態であると考えられた．四肢の筋力は低下しフレイルの状態であり，今後歩行困難や嚥下機能の低下が予測された．起居動作時には痛みを口にしており，痛みが活動を低下させる一因であると考えられた．山口キツネ・ハト模倣テストでは，キツネは模倣できハトは模倣できなかったことから，認知症があると推測された．脳梗塞を繰り返しており，幻視やパーキンソニズム，常同行動は見られない等から，血管性認知症が疑われ，更なる認知機能の低下及び虚血性疾患再発のリスクが考えられた．なお，対象にテストをされているというストレスを与えないように，山口キツネ・ハト模倣テストを行ったが，HDS-Rのような認知テストは行わなかった．

対象の入浴は娘が介助をしていた．娘は対象が入浴をしたがらないことに負担感を抱いていた．ADLや認知機能の低下により，入浴介助は更に介助量の増加が予測された．

2．評価票による初期評価

評価は，Dementia Assessment Sheet in Community-based Integrated Care System（以下，DASC-21），Dementia Behavior Distrbance Scale短縮版（以下，DBD-13），Zarit介護負担尺度日本語短縮版（以下，J-ZBI-8）により行った．DASC-21は，認知機能と生活機能を総合的に評価する指標で21項目からなる．満点は84点，31点以上で認知症の可能性があり，得点が高いほうが認知機能の低いことを表す．DBD-13は認知症の行動心理症状を評価する指標で13項目からなる．満点は52点で得点が高いほうが症状の悪化を示す．J-ZBI-8は家族の介護負担を評価する指標で8項目からなる．満点は32点で，得点が高いほうが介護負担感の強いことを表す．

家族による対象の初期評価得点は，DASC-21 65点（この点数は中等度以上の認知症を示す），DBD-13 11点，J-ZBI-8 10点であった．

3．生活上の困りごとと希望

対象が生活で困っていることは無いと発言していた．しかし，対象の言動から痛みによる苦痛，物忘れによる不安があると判断した．また，通所系サービスの利用は希望せず，家での生活を希望していた．介護している妻は，自身の腰痛のため対象への身体的介護はできないが，生活のほとんどを臥床して過ごしていることを心配していた．娘はADLと認知症症状の悪化を心配し，入浴に対する介護負担軽減と，対象が望む家での生活の継続を希望していた．

実際の支援内容と結果

支援はチーム員会議での検討を重ねながら，支援チームと地域（地域包括担当者，主治医，ケアマネジャ，往診医，訪問リハビリ等）との多職種の協働により実施した．その内容は，①介護保険の申請，②訪問リハビリの導入と経過観察，③家族への心理・社会的サポート，④体調不良時の緊急対応，⑤体調不良時に往診を受けられる体制作り，であった．

上記支援を実施した結果，訪問リハビリは週1回を継続でき，ADL能力の低下を予防し入浴介助時の負担を軽減することにつな

がった．また，他者と会話をする機会となった．妻と娘には，各職種が連携したうえで，適宜連絡を入れサポートを行うことで疑問点や不安の改善につながった．また，ケアマネジャと支援チーム員が状況確認をした際，対象の体調不良を察知して緊急対応を支援したことにより，重症に至らず，在宅生活を継続できていた．

支援チームが介入した期間は約6か月であった．介入初期評価と最終評価の各指標の得点は，DASC-21が65点から68点，DBD-13が11点から17点，J-ZBI-8が10点から9点に変化した．つまり，認知機能や行動心理症状はやや悪化したにもかかわらず，家族の介護負担感はわずかに軽減していた．

考　　察

新オレンジプランでは，認知症の人が住み慣れた地域の良い環境で自分らしく暮らし続けるために，必要としていることに的確に応えていくことを旨としつつ，7つの柱に沿って，施策を総合的に推進していくこと[2]としている．これらの施策の一つに支援チームが位置づけられている[2]．支援チームは，複数の専門職が家族の訴え等により認知症が疑われる人や認知症の人及びその家族を訪問し，アセスメント，家族支援などの初期支援を包括的，集中的に行い，自立生活のサポートを行うチームと定義[3]されている．

「初期集中支援」の「初期」とは，認知症の「初期」にとどまらず，初めて触れる「初動（First Touch）」としての意味合いも含まれる[4]．「集中」には，本人・家族・支援者・専門職者がアセスメントからプランの立案・実施・家族支援等に至るまで，人的・資源的にも集中してサポートを行い，従来の介護支援システムや医療システムへ引き継いでいくといった意味合いを含む[4]．

本症例は，「初動」の意味合いが強く，要介護認定は受けていたが適切なサービスの利用には至らず，認定期限切れになっていた．また，医療は外来受診により継続されていたが，急な体調不良時の往診が可能な体制は整備されていなかった．認知症高齢者の家族介護者は，疑念解消に向けた模索を行い，抱えきれない困惑と焦燥感等を抱くとされる[5]．本症例でも家族は既往疾患や認知機能の低下に伴う症状に困惑し，対象の生活支援に困難と不安を抱えていると考えられた．

支援チームの本質は，認知症の総合アセスメントを行い，診断へのアクセスを確保し，診断後の支援として，本人・家族の視点を尊重しながらステージに応じた統合ケアの導入を調整することにある[6]．認知症は，認知機能が障害されることにより生活に支障をきたし，これらが進行することによって本人及び家族は生活上の困難が増大していく．本症例では，認知機能や行動・心理症状はやや悪化したにもかかわらず，家族の介護負担感をわずかながら軽減できた．これは支援チームがその機能を発揮し，多職種との協働により，症例にあった地域医療やサービスにつなげられたことにより，介護をする家族が現状を認識し生活上の困難を軽減できたためであると示唆された．

支援チームでは，今後も対象と家族の望む生活を重視したオーダーメイドの医療及び生活支援を多職種との連携協働により実践していく必要がある．

文　　献

1）内閣府，平成29年度版高齢社会白書，https://www8.cao.go.jp/kourei/whitepaper/w-2017/html/gaiyou/s1_2_3.html

2）厚生労働省，認知症施策推進総合戦略（新オレンジプラン）https://www.mhlw.go.jp/stf/seisakunitsuite/bunya/0000064084.html

3）厚生労働省，認知症初期集中支援チームについて，https://www.mhlw.go.jp/file/06-seisakujouhou-12600000-seisakutoukatsukan/0000035310.pdf
4）石川智久：認知症医療の問題点．日本早期認知症学会誌10(2)：64–65，2017.
5）秋吉知子，中島洋子，草場知子：認知症診断初期にある認知症高齢者の家族介護者の心理．日本認知症ケア学会誌15(2)：470–476，2016.
6）粟田主一：認知症初期集中支援チームの実践テキストブック，中央法規，東京，2015.

たこつぼ型心筋症を発症した多発肺転移を伴う大腸癌の剖検例

公益財団法人老年病研究所附属病院　内科
長嶺士郎　高玉真光

公益財団法人老年病研究所附属病院　循環器科
天野晶夫

公益財団法人老年病研究所附属病院　病理診断科
福田利夫

公益財団法人老年病研究所附属病院　循環器内科
池田士郎　中野明彦

症　例

79歳女性，X月初旬より食欲低下．X月Y日，呼吸困難にて救急搬送．胸写にて両側肺に円形結節影多発，心電図にてⅡ，Ⅲ，aVf，V3～V6にてST上昇，心エコー上心尖部収縮低下を認めた．緊急心臓カテーテル検査冠動脈収縮有意狭窄なし，左室造影で心尖部の収縮低下，基部の運動良好．たこつぼ型心筋症と診断．胸腹部CTにて両側肺野に複数の腫瘤影，S状結腸壁全周性肥厚を認め，S状結腸癌，多発肺転移の診断で，best supportive careとなった．17病日後死亡された．病理解剖を行い，S状結腸癌，多発肺転移の診断．心筋では心尖部に心筋障害を認めた．転移性肺腫瘍に併発したたこつぼ型心筋症の病理解剖例を報告した．

当院における腰椎術後に腰椎の再手術を施行した症例の検討

公益財団法人老年病研究所附属病院　整形外科
島田晴彦　館野勝彦　加藤良衛
佐藤圭司

はじめに

以前に腰椎の手術を受け，一旦症状が軽快したものの再び症状が出現あるいは悪化して，再手術が必要となる症例が存在する．当科においても，完治を目指して手術を施行しても再手術が必要となる症例に遭遇する．今回，以前腰椎の手術を受け，再手術が必要となり，当科にて最近再手術を施行した腰椎疾患の6症例を検討した．

結　果

男性2例，女性4例で，再手術時年齢37～75歳，平均60歳であった．3例は初回手術を他院にて受け，このうち1例は3回の手術を受けていた．再手術時診断は腰椎椎間板ヘルニア4例，腰椎変性すべり症2例であった．再手術の術式はヘルニア摘出術2例，TLIF（経椎間孔椎体間固定術）4例であった（表1）．

症　例

症例1：37歳（再手術時）　男性
主　訴：腰痛・左下肢痛・しびれ
現病歴：10年前に腰椎椎間板ヘルニアの診断にて他医にてL4/5の椎間板摘出術を受けた．術後経過は順調であったが，9ヶ月前から腰痛・左下肢のしびれが出現し，7ヶ月前に椎間板ヘルニアの診断にてL5/S1の椎間

表1　症例（6例）

症　例	1	2	3	4	5	6
性　別	M	F	F	M	F	F
年　齢	37	71	70	75	44	63
再手術診断	腰椎椎間板ヘルニア（再発）	腰椎椎間板ヘルニア（他椎間）	腰椎変性すべり症	腰椎椎間板ヘルニア（再発）	腰椎椎間板ヘルニア（再発）	腰椎変性すべり症（再発）
病巣椎間	L5/S1	L2/3	(L3/4)L4/5	L4/5	L5/S1	L4/5
再手術術式	椎間板摘出（3回目/2回目と同椎間）	椎弓再建＋椎間板摘出（他椎間）	開窓＋TLIF	TLIF	TLIF	TLIF
再術後経過	復職	復職	ADL自立	ADL自立	復職	ADL自立
以前の手術時診断	腰椎椎間板ヘルニア	腰部脊柱管狭窄症	腰部脊柱管狭窄症・RA	腰椎椎間板ヘルニア	腰椎椎間板ヘルニア	腰椎変性すべり症
以前の手術	椎間板摘出術（1回目L4/5 2回目L5/S1）	開窓術（L3/4　L4/5）	開窓術	椎間板摘出術	椎間板摘出術	開窓術

板摘出術を受けた．術後症状は消失し，仕事に復帰していたが，１ヶ月前から再発し，症状が増強してきたため，L5/S1の同側同椎間の椎間板摘出術を施行した．症状は消失し，３回目の術後２ヶ月以降，以前の職場に復帰している．また，以前から１日約20本の喫煙者であった（図１）．

症例２：71歳女性

主　訴：腰痛・両下肢痛

現病歴：15年前に腰部脊柱管狭窄症の診断にてL3/4・L4/5の開窓術を受けた．症状は消失していたが，半年前から腰痛・両下肢痛が出現し，軽減しないため椎間板ヘルニアの診断でL2/3の椎間板摘出・椎弓再建術を施行した．術直後下肢しびれ・疼痛が増強したが，徐々に軽減し，職場復帰をしている（図２）．

症例６：63歳　女性

主　訴：腰痛・下肢痛・しびれ

現病歴：６年前，腰痛・両下肢痛・しびれがあり，すべりをともなう脊柱管狭窄部L4/5に開窓術を行った．その１年後から左膝付近にしびれが出現し，疹痛・筋力低下を生じてきた．投薬・リハビリ等の保存的治療にて軽快せず，４年前（初回術後２年）に変性すべり症の診断でL4/5のTLIFを施行した．術後症状は軽減していたが，再手術後２年半後に車の乗車中に左下肢痛が出現した．その後症

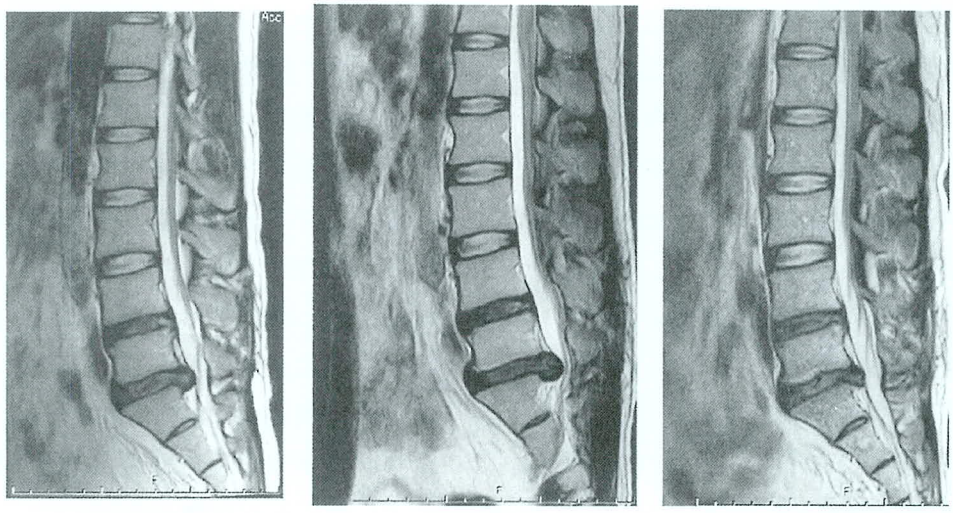

２回目の術前　　３回目術前　　３回目術後

図１　症例１

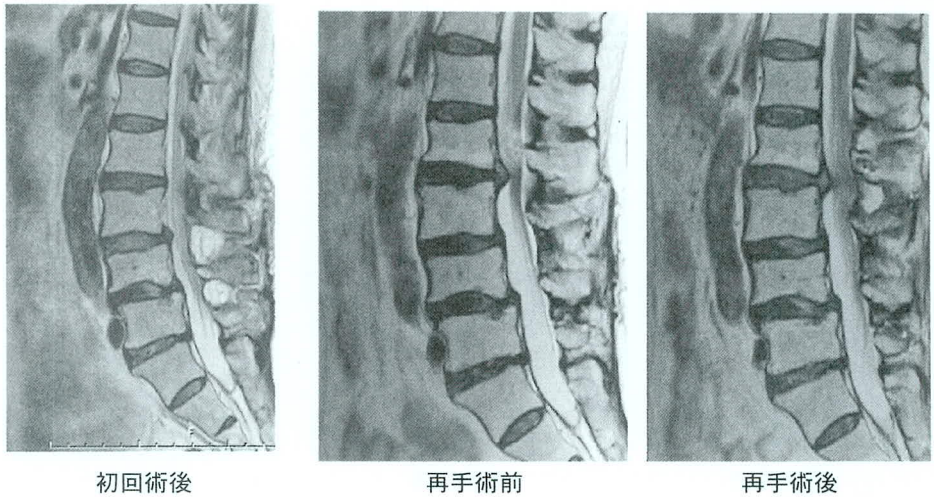

初回術後　　再手術前　　再手術後

図２　症例２

状が増強したため，当科再診し，L3/4・L5/S1の椎間板ヘルニアを認めた．症状が強く，体動困難であったため入院安静とした．2週間の入院安静にて軽快し，退院となった．しかし，その約1ヶ月半後に左下肢につれ感が出現し，さらに左下肢痛・しびれが増強したため，退院約2ヶ月半後に再入院となった．約3週間の入院にて，症状は軽減し，退院となった．現在ADLは自立しているが，時々腰痛・下肢痛が増強し，外来通院中である（図3）．

考　　察

腰椎変性疾患の手術に対する再手術の頻度は，腰椎椎間板ヘルニアはWeinsteinら[1]の報告にて術後4年で約10%と報告され，腰部脊柱管狭窄症は野地ら[2]の報告では約7.3%と報告されている．当科では直近3年間でみて76例中5例，約6.6%であった．報告とほぼ同頻度と思われる．Failed back surgeryの原因として高橋ら[3]は

1）初回手術時の局所病態診断の誤り
2）全身的疾患の見落とし
3）不適切な手術手技
4）手術合併症
5）病態の再発進行
6）心理社会的要因
7）医師—患者—家族関係の破綻

などをあげている．症例1では1回目と2・3回目の手術は椎間が異なり，直接の関連は薄いと思われるが，2回目と3回目は同側・同椎間であった．また，椎間板高は比較的高く，長期間の喫煙者であり，これらは危険因子[4]であったと思われる．症例2は2回目の手術は最初の手術とは椎間が離れており，直接の関連はないと思われる．症例3はRAがあり，徐々に椎間が破壊され，滑りが発生，進行したものと思われる．RAのコントロール・経過が危険因子と思われる．症例4・5は同椎間・同側の椎間板ヘルニアの再発であり，術後経過からみれば最初から固定術といえる．しかし最初の手術後，しばらくは通常生活ができていたことを考えると難しい判断といえる．再発した危険因子は不明である．症例6は初回手術時に変性すべりがあったが，腰痛は軽度で，動態X-Pにて椎間不安定性は軽度であったため，開窓術を行った．しかし，後日固定術となった．はじめから固定術がよかったのかもしれないが，固定術後に上下椎間に，椎間板ヘルニアを生じており，固定術の限界なのかもしれない．

今回の症例から，再手術の危険因子として

1）椎間不安定性
2）椎間板高が高い

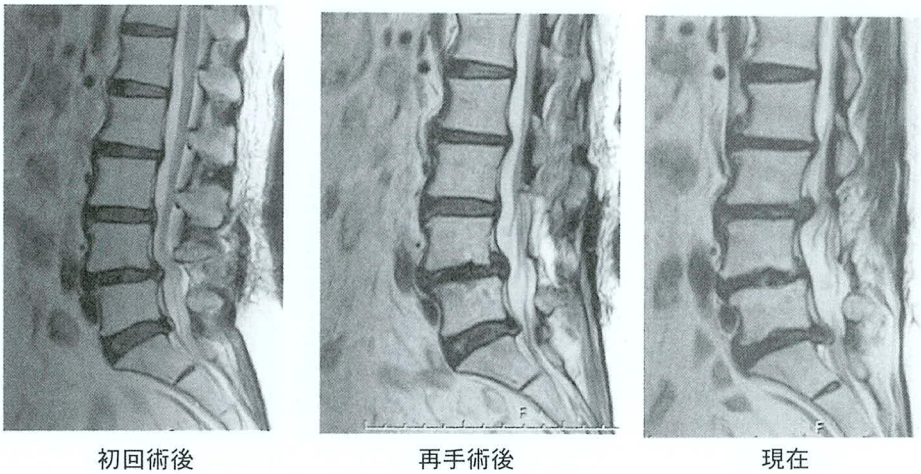

初回術後　　再手術後　　現在

図3　症例6

3）RA

4）喫煙

があげられる．再手術に関しては，開窓術・椎間板摘出術は隣接椎間への影響が少ないが，固定術に関しては可能であれば椎間の制動の手術がのぞましいと思われた．

結　　語

1）経過より，最初から，固定術が望ましかったと思われる症例があったが，その危険因子ははっきりしなかった．

2）喫煙が危険因子として疑われる症例を１例経験した．

3）椎体間固定術後，上下椎間に椎間板ヘルニアを生じた症例が１例存在した．

文　　献

1）Weinstein JN, Lurie JD, Tosteson TD, et al: Surgical versus nonoperativetreatment for lumbar disc herniation: four-year results for the Spine Patient Outcomes Research Trial (SPORT). Spine 2008; 33(25): 2789–2800

2）野地雅人，遠藤　聡：当院における腰部脊柱管狭窄症に対する再手術例の分析：日本脊髄障害医学会誌　2015；28(1)：118–119

3）高橋和久：Failed back surgery の原因．脊椎脊髄ジャーナル　2009；22(7)：822–825

4）土方保和，高橋雄一，隈元真志他：椎間板摘出後予後不良因子の検討：日本脊髄障害医学会誌　2014；27(1)：122–123

当院における禁煙指導の現状

公益財団法人老年病研究所附属病院　内科
勝山　彰　高玉真光

公益財団法人老年病研究所附属病院　薬剤部
境野智子

オリンピック委員会と世界保健機構は，オリンピック開催国に対して，強制力のある受動喫煙防止対策を取ることを進めてきた．このため，日本でも2020年までに国内ばかりではなく，東京都の条例でも対策をとることとしている．

先進諸国の中でも，日本は喫煙問題については遅れているほうではあるが，近年では発癌リスクの低減を目指して，ガン対策基本法が施行され，禁煙支援が健康保険の適応となった．

当院においても，6年前より禁煙外来を開設し，高血圧症や糖尿病，脳卒中の既往歴のある人々に対して，希望者には禁煙治療を，そうでない人についても出来る範囲での情報提供を行ってきた．

今回は，過去5年間に約40名ほど行ってきた禁煙治療についての分析を報告する．

認知症ケアサポートチームの活動実績

公益財団法人老年病研究所附属病院
松本美江　須永瑞紀　堀口布美子
飯塚由香　池田陽子　重倉麻子
金井さやか　田代明美　茂木美和
高玉真光

はじめに

高齢化の進行と共に，高齢の入院患者が増加している．認知症患者においては，身体疾患や手術，治療の過程で不安や混乱を起こしやすくなっている．また，入院による環境の変化の影響を受けやすく，認知症症状が悪化したようにみえる患者も多い．

当院では認知症ケアの質の向上を目的に平成28年８月より認知症ケアサポートチーム（Dementia support team：以下DST）を立ち上げ活動している．DST介入依頼時に患者への対応で問題となっている点，相談したい内容を病棟より提出してもらっている．今回，介入依頼内容をまとめ，DST回診・介入の状況について報告する．

DSTの役割

平成28年度診療報酬改定で，「認知症施策推進総合戦略（新オレンジプラン）」を踏まえた認知症患者への適切な医療を評価して，認知症ケア加算が新設された．当院では平成28年８月より認知症ケア加算１を算定している．

DSTは病棟における入院患者への対応力とケアの質の向上，支援のための活動をしている．チームは医師・認知症看護認定看護師・社会福祉士で構成されている．また各病棟には２～３名のリンクナースを配置しDSTと病棟をつなぐ役割を担っている．他にリハビリテーションスタッフ，薬剤師の協力を得て活動を行っている．

DSTの主な活動内容は次の通りである．

①　回診とカンファレンスの開催

週に１回全病棟を回診．回診にはDSTメンバー，各病棟のリンクナース，リハビリテーションスタッフ，薬剤師が参加．

DST介入依頼の出ている患者について状態を把握．その後，回診した患者のカンファレンスを病棟毎に行う．新たに介入依頼が出た患者と対応が困難になっている患者を中心に話し合い，ケアの方法や内服について意見交換を行う．

②　DST委員会の開催

月１回委員会を開催，参加者はDSTメンバー，各病棟のリンクナース，看護部，薬剤師，リハビリテーションスタッフ，事務職員．認知症ケアに関する情報伝達・勉強会，研修会に関する連絡調整，等について話し合っている．

③　認知症ケアに関する研修会の開催

全職員対象とした研修会と看護師対象とした研修会の２種類の研修会を毎年開催している．それぞれの研修会は全員が参加できるよう10～12回開催している．

④　認知症ケアに関するマニュアル作成

毎年内容の見直しを行い，漸次改定を行う．

DST 回診・介入の現状

対象と方法：平成28年８月から平成30年７月までのDST介入者469名についてDST介入依頼内容の集計を行った．

結　果：図１は１か月毎の回診件数，図２は病棟別の介入依頼件数である．

介入患者469名　男性200名，女性269名，平均年齢84.51歳．

病棟別の介入人数は，３号病棟（整形外科）116名，４号病棟（内科）88名，５号病棟（神経内科）102名，６号病棟（脳神経外科）55名，西棟回復期リハビリ病棟71名，新館回復期リハビリ病棟37名．

介入依頼内容：図３は介入依頼内容別の人数である．図４～９は病棟別の依頼内容別人数である．

「転倒・転落のリスク」が最も多くなっている．次いで「落ち着きがない」，「大声」，「せん妄・せん妄予防」の順になっている．

回診を行ったところ，落ち着きがない，大声，安静が守れず転倒・転落してしまうなどの行動はせん妄が関係しているケースが多く

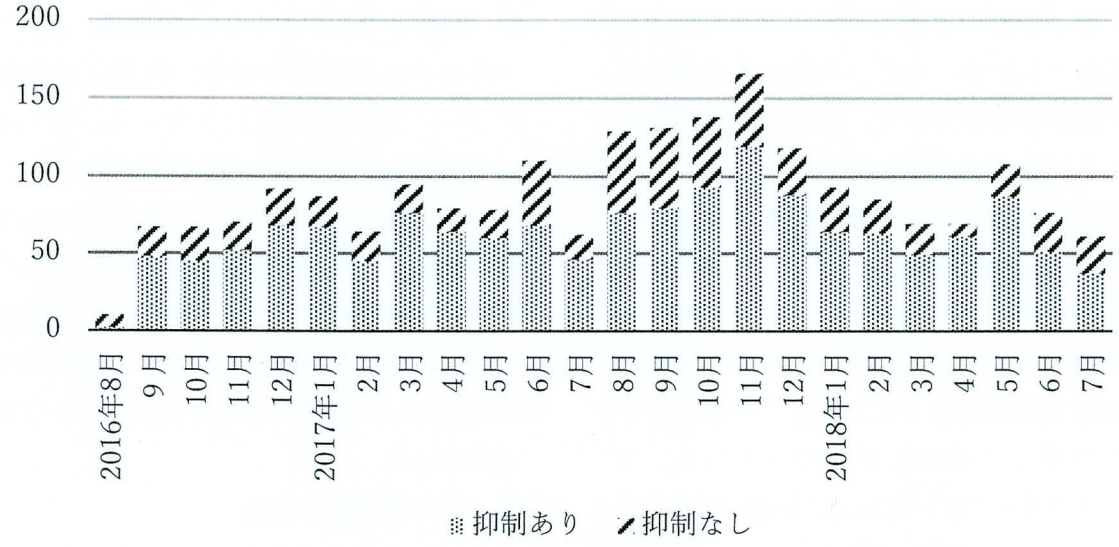

図１　１か月毎の回診件数

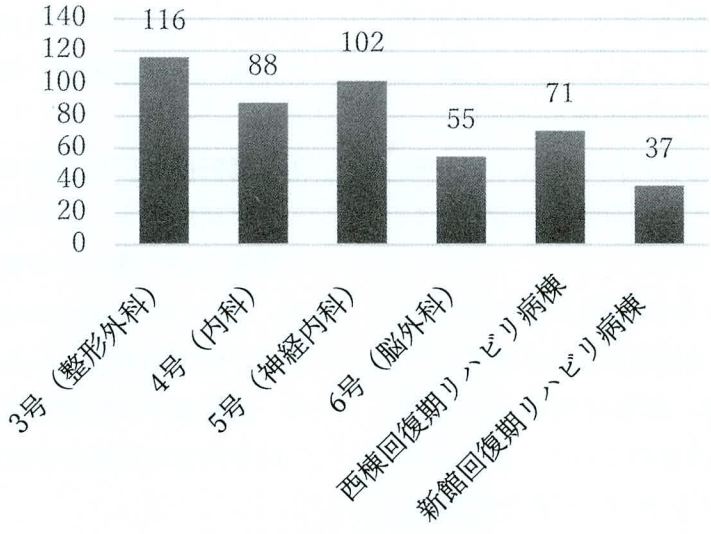

図２　病棟別の介入依頼件数

みられていた．身体疾患により入院となり，環境の変化，身体的苦痛等により脳の脆弱性がある患者はせん妄を発症し，DSTの介入が必要となっている．

急性期病棟（4号病棟・5号病棟・6号病棟）では点滴の自己抜去などルートトラブルも多くみられていた．急性期病棟では安全に治療が継続できるための対応が必要になっている．

回診回数：図10は患者毎の介入終了までの回診回数である．

一人当たりの平均回診回数は5.4回であったが，2～4回の回診を行った患者が全体の55%となっている．371名が退院まで回診を

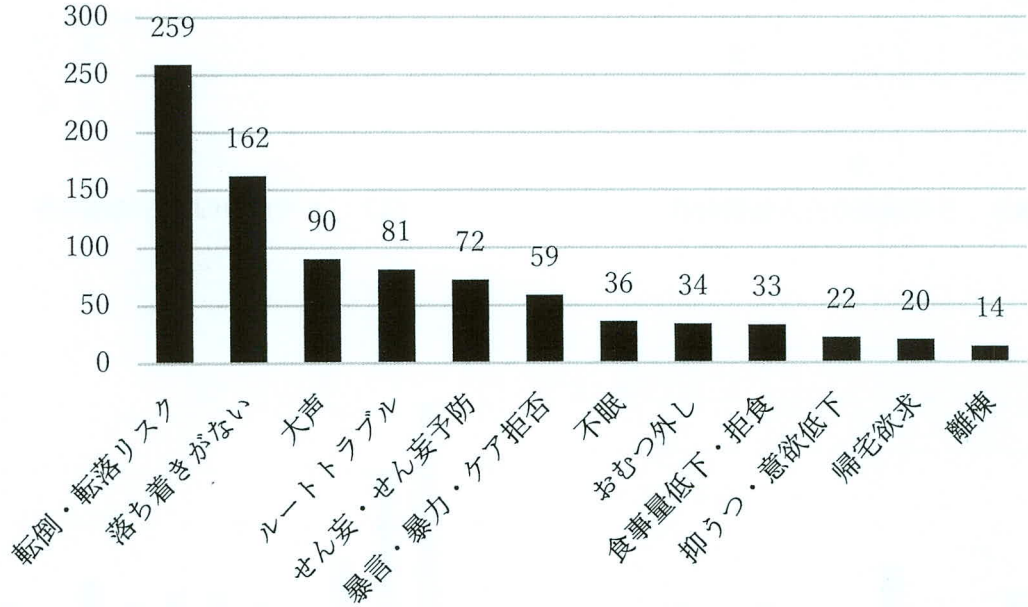

図3　介入依頼内容（全病棟）

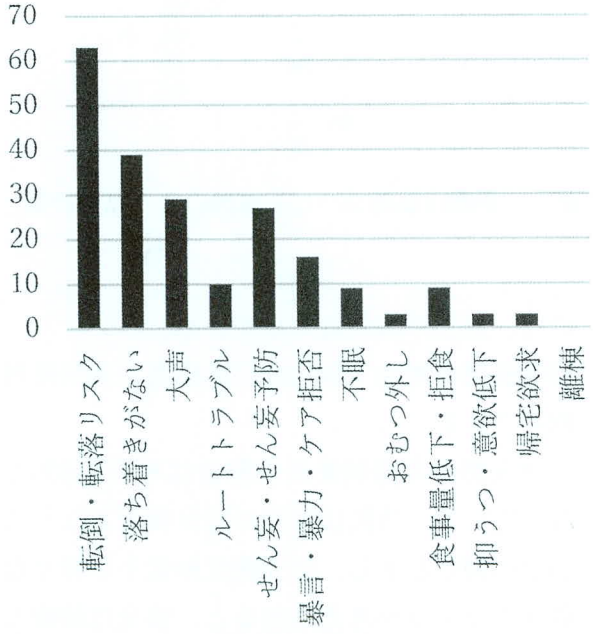

図4　3号病棟の介入依頼内容

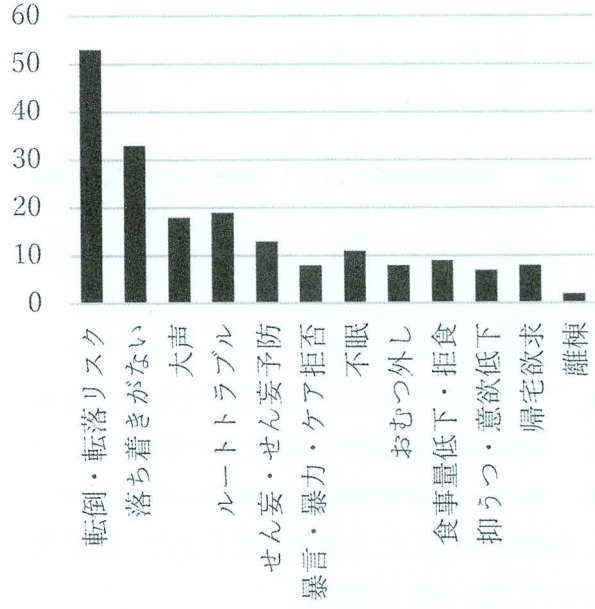

図5　4号病棟の介入依頼内容

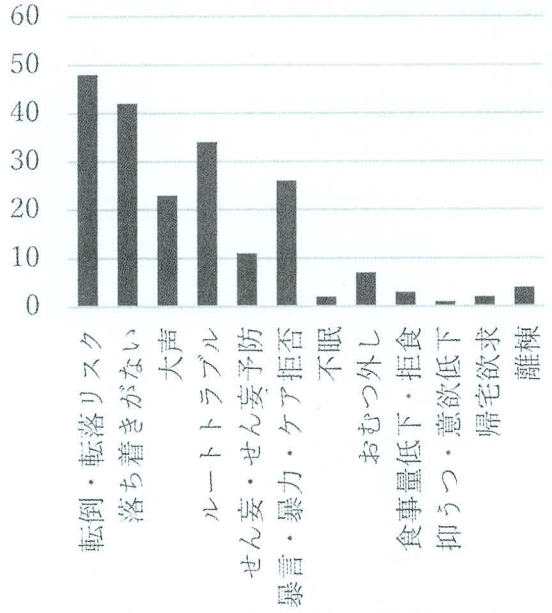

図６　５号病棟の介入依頼内容

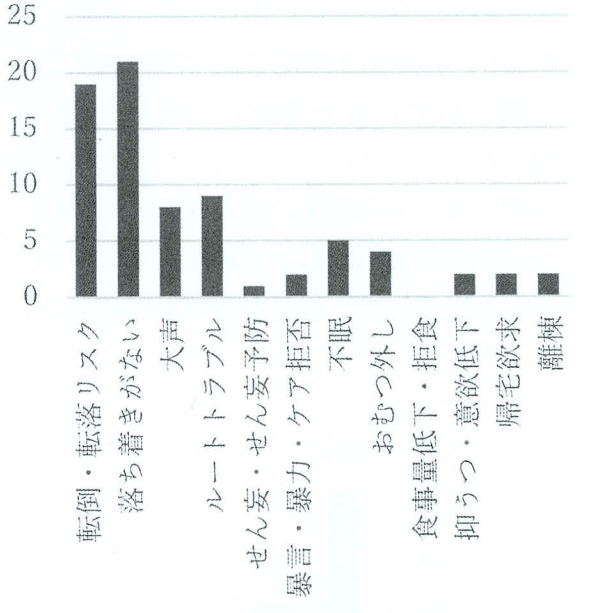

図７　６号病棟の介入依頼内容

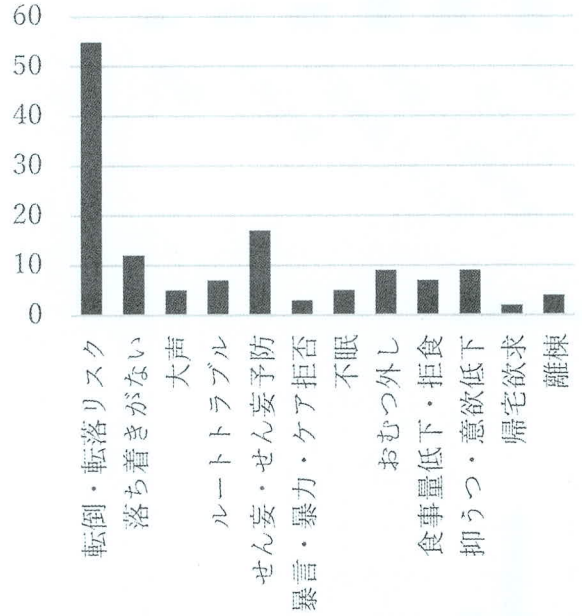

図８　西棟回復期リハビリ病棟の介入依頼内容

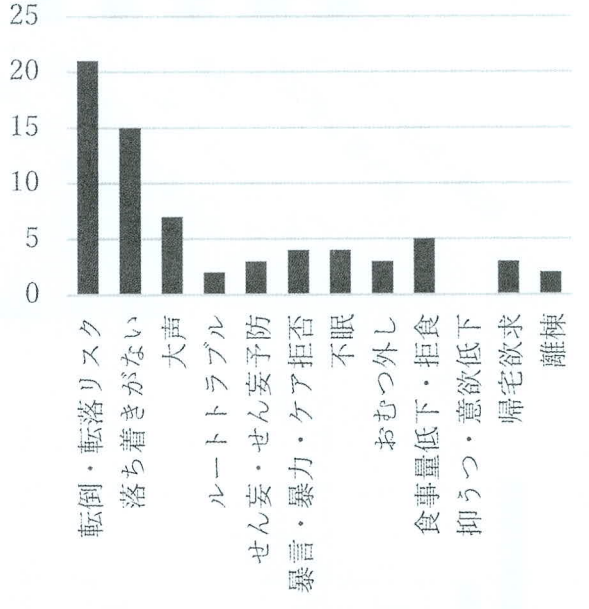

図９　新館回復期リハビリ病棟の介入依頼内容

行っていた．

入院中に介入終了となったのは98名であった．うち75名が介入依頼となった症状が改善し，穏やかな療養が可能となり終了している．また，全身状態悪化，意識レベルが低下し意識障害などにより介入終了となった患者が18名であった（図11）．

DSTによる回診は多くの場合は退院まで続け，状態の改善に努めている．

抑制使用の割合：図12は回診患者の抑制使用割合である．

介入患者の抑制使用の割合は平均70.9％となっている．当院は抑制の完全廃止となっていない現状がある．認知機能が低下し様々な危険のリスクが考えられると，安全に治療を行うために抑制の使用につながっている．

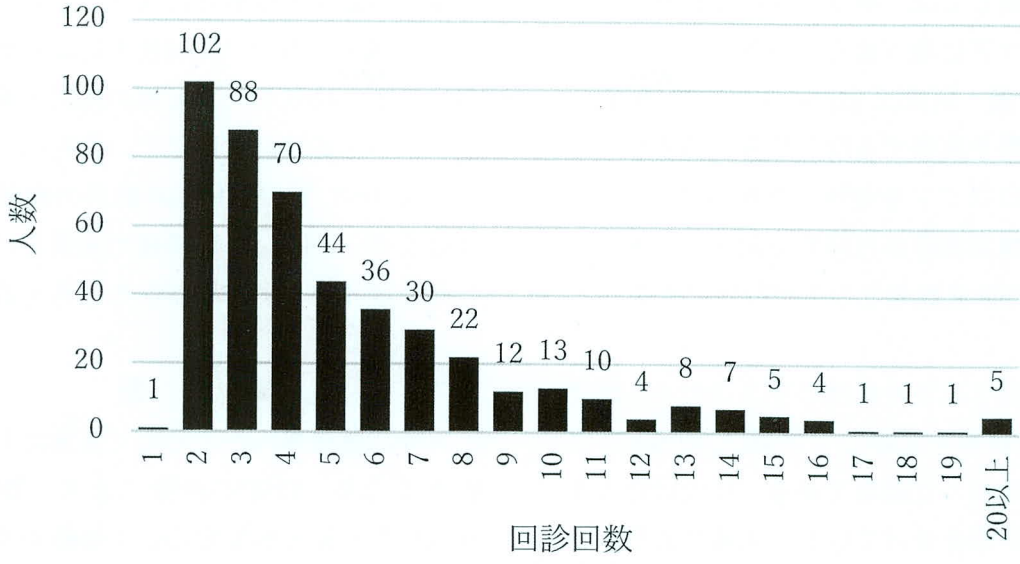

図10　患者毎の介入終了までの回診回数

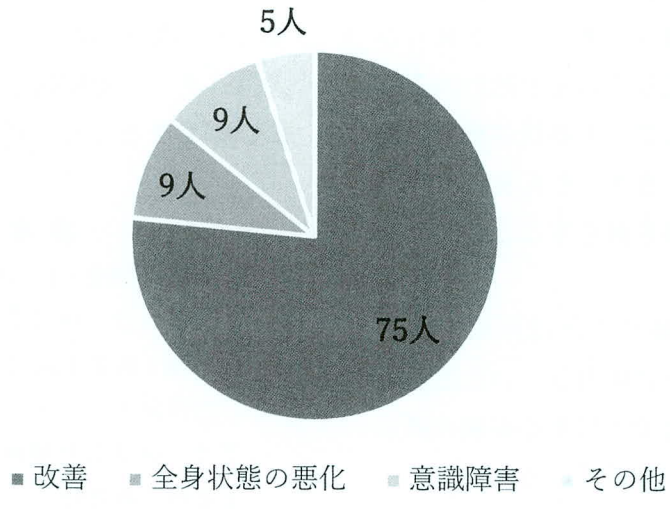

図11　入院途中に介入終了したケース

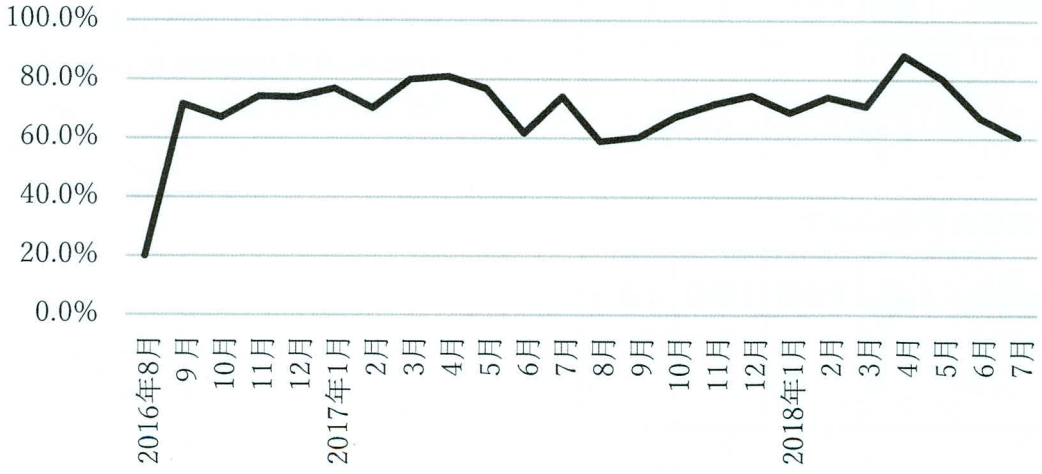

図12　回診患者の抑制使用割合

抑制に対しては，解除に向けて看護計画を立案してケアに取り組んでいる．

介入の評価：阿部式 BPSD スコアを使用して介入効果を評価する取り組みを始めた．阿部式 BPSD スコアを使用した理由は，

① 病棟看護師が短時間で記入できる．

② BPSD を数値化して可視化できる．

である．

表1，表2は3号病棟のリンクナースが介入患者の状態を観察して阿部式 BPSD スコア表記載を行った結果である．B氏は介入後1週目に手術を受けている．手術によりスコアが上がっているが，介入経過に伴い BPSD は改善している．

回診後のカンファレンスで病棟看護師から以前より抑制の数が減ってきていると報告があった．せん妄を発症していると思われる患者に内服薬を調整することで症状の緩和，夜間の入眠につながってきた．せん妄の症状が早期に落ち着き，抑制を減らすことができている．

抑制を完全に取り除くことは困難であるが，多種の抑制を同時に使用していた患者が適切に評価を行うことで使用する抑制を減らせるケースが多くなってきている．

表1　阿部式 BPSD スコア

A氏	介入開始時	介入1週目	2週目	3週目	4週目
合計点数	22	13	8	8	3

表2　阿部式 BPSD スコア

B氏	介入開始時	介入1週目	2週目	3週目	4週目
合計点数	10	6	13	7	5

今後の課題：抑制解除に向けてさらなる取り組みが必要である．抑制使用による弊害の理解を深め，抑制の代替え策の検討・実践をリンクナースを中心に進めていきたい．

今後 DST では認知症高齢者の療養環境の課題を明らかにし，多職種で連携を行い課題に取り組んでいく必要があると考える．

結　　語

入院は患者本人だけでなく家族にも心配事が多くなる．DST の活動により，認知症患者はもちろん家族も安心して治療を受けられる病院にしていきたいと考えている．群馬県高齢者福祉計画の基本目標に「高齢者の誰もが住み慣れた地域で安心して暮らせる地域づくり」が掲げられている．高齢者が在宅から入院，そして退院後も安心して暮らせるお手伝いができるよう，活動をしていきたい．

参 考 文 献

1）公益社団法人日本看護協会　認知症ケアガイドブック　株式会社照林社　2016年6月8日　第1版第1刷発行

2）内田陽子　できる！認知症ケア加算マニュアル　株式会社照林社　2016年11月23日　第1版第1刷発行

3）Abe K, Yamashita T, Hishikawa N, Ohta Y, Deguchi K, Sato K, Matsuzono K, Nakano Y, Ikeda Y, Wakutani Y, Takao Y. A new simple score (ABE) for assessing behavioral and psychological symptom of dementia. J Neurol Sci. (2015) 350: 14–17

Original Article

Ann Rehabil Med 2019;43(5):562-569
pISSN: 2234-0645 • eISSN: 2234-0653
https://doi.org/10.5535/arm.2019.43.5.562

Annals of Rehabilitation Medicine

Relationship Between Performance Improvement in Activities of Daily Living and Energy Intake in Older Patients With Hip Fracture Undergoing Rehabilitation

Hiroki Umezawa, BS[1], Yoji Kokura, BS[2], Satoko Abe, PhD[3], Chieko Suzuki, MD, PhD[4], Akiko Nishida, BS[5], Yoshie Uchiyama, BS[6], Keisuke Maeda, MD, PhD[7], Hidetaka Wakabayashi, MD, PhD[8], Ryo Momosaki, MD, PhD[9]

[1]Department of Physical Therapy, Geriatrics Research Institute and Hospital, Gunma; [2]Department of Clinical Nutrition, Keiju Medical Center, Ishikawa; [3]Department of Nursing, Showa University of Nursing and Rehabilitation Sciences, Kanagawa; [4]Department of Internal Medicine, Ajisu Kyoritsu Hospital, Yamaguchi; [5]Department of Nutrition, Gotanda Rehabilitation Hospital, Tokyo; [6]Department of Nursing, Shirakawa Kosei General Hospital, Fukushima; [7]Department of Palliative and Supportive Medicine, Graduate School of Medicine, Aichi Medical University, Aichi; [8]Department of Rehabilitation Medicine, Yokohama City University Medical Center, Kanagawa; [9]Department of Rehabilitation Medicine, Teikyo University School of Medicine University Hospital, Mizonokuchi, Kanagawa, Japan

Objective To analyze whether sufficient energy intake (EI) improves performance of activities of daily living (ADL) in patients with hip fracture admitted to rehabilitation hospitals. The adequate amount of EI for improving performance of ADL in patients with hip fracture remains unknown.

Methods This retrospective cohort study included all patients with hip fracture (n=234) admitted to rehabilitation hospitals in Japan. The inclusion criteria for this study were age >65 years and body mass index <30.0 kg/m^2. Patients who were transferred to an acute hospital and those with missing case data were excluded. According to the amount of EI, the patients were classified into energy sufficiency and shortage groups (EI/total energy expenditure ≥1.0 and <1.0, respectively). The Functional Independence Measure (FIM) and FIM gain were used to evaluate the patient disability level and change in patient status in response to rehabilitation. Finally, FIM gain was calculated as the discharge FIM score minus the admission FIM score.

Results The final analysis targeted 202 patients—53 (26.2%) were in the energy shortage group and 149 (73.8%) were in the energy sufficiency group. The energy sufficiency group had a greater FIM gain than the energy shortage group (mean, 25.1±14.2 vs. 19.7±16.4; p=0.024). Furthermore, sufficient EI in the first week since admission (β=0.165; 95% confidence interval, 0.392–5.230; p=0.023) was an independent factor of FIM gain.

Conclusion Among elderly patients with hip fracture admitted to rehabilitation hospitals in Japan, the amount of EI during the first week after admission was an independent factor of FIM gain.

Keywords Femoral fractures, Hospitals, Rehabilitation, Nutritional support, Recovery of function

Received January 29, 2019; Accepted March 20, 2019
Corresponding author: Hiroki Umezawa
Department of Physical Therapy, Geriatrics Research Institute and Hospital, 3-26-8, Ootomo-machi, Japan. Tel: +81-27-253-3311, Fax: +81-27-252-7575, E-mail: umezawa1192@gmail.com
ORCID: Hiroki Umezawa (http://orcid.org/0000-0002-6396-4718); Yoji Kokura (http://orcid.org/0000-0003-3261-8721); Satoko Abe (http://orcid.org/0000-0001-7925-0114); Chieko Suzuki (http://orcid.org/0000-0002-1362-9348); Akiko Nishida (http://orcid.org/0000-0001-6543-5062); Yoshie Uchiyama (http://orcid.org/0000-0002-5494-0837); Keisuke Maeda (http://orcid.org/0000-0001-7132-7818); Hidetaka Wakabayashi (http://orcid.org/0000-0002-0364-0818); Ryo Momosaki (http://orcid.org/0000-0003-3274-3952).

INTRODUCTION

Fundamentally speaking, malnutrition in patients with a hip fracture is a major problem that traditionally leads to poor patient outcomes. In a recent systematic literature review [1], the prevalence of malnutrition in patients with hip fracture was reported as 18.7% when assessed using the Mini Nutritional Assessment (MNA) test. Also, when accounting for body mass index (BMI) and weight loss, the percentage of malnutrition was noted at 45.7% in those patients reviewed. For this reason, malnutrition leads to many problems for the patient, including postoperative complications [2,3], poor functional improvement [4,5], longer hospital stays [2], high readmission rate [2], and the incidence of a high mortality rate [2,6]. Recently, it has been suggested that improving the nutritional status of this patient population can independently and significantly improve their physical function [7]. This is an important revelation, considering that 18.7%–45.7% of patients with fractured hip suffer from malnutrition, improving the nutritional status of these individuals will greatly improve their overall health and well-being.

Previous reports from rehabilitation hospitals in Japan suggest that in patients with hip fracture, the incidence of an improvement of the status of malnutrition in the patient is an independent factor that leads to an improved ability to perform activities of daily living (ADL). However, it remains unknown whether this effect also applies to elderly patients who have an experience with hip fracture at rehabilitation hospitals. The study of Goisser et al. [4] reported that dietary intake during the 4 days following the operation affected the improvement of ADL at 6 months after the surgery. Furthermore, Inoue et al. [5] reported that when evaluating the improvement of ADL according to the efficiency of motor Functional Independence Measure (FIM) gain, energy intakes (EIs) during the first week postoperatively were an independent factor that impacted the patient's health. It is noted that the rehabilitation hospital in Japan performs intensive rehabilitation after acute treatment and rehabilitation is provided for 2–3 hours daily [8]. It is noted that at rehabilitation hospitals, the activity of patients with hip fracture is higher when compared to the acute treatment ward. Therefore, the measured energy consumption of patients with hip fracture is higher, and has a greater caloric requirement than those in the acute phase. Nii et al. [9] reported that higher EI significantly improved the ADL in patients with stroke in rehabilitation hospitals. However, the evaluated adequate amount of EI for improving their ADL in patients with hip fracture remains unknown.

We aimed to retrospectively analyze whether sufficient EI improves ADL in patients with hip fracture in rehabilitation hospitals.

MATERIALS AND METHODS

Study design

This retrospective cohort study utilized the Japanese Rehabilitation Nutrition Database (JRND). In effect, the JRND is a large-scale database open for clinical research on rehabilitated nutrition [10]. The participants of the present study were all hip fracture patients admitted to the rehabilitation hospital in Japan who are registered in JRND. As a note, a rehabilitation hospital is a hospital where patients undertake rehabilitation for approximately 1–3 hours every day for a period ranging from 1 to 4 months, with the purpose of improving their functional capacity and returning home. The inclusion criteria in this study were age over 65 years old and a BMI less than 30.0 kg/m^2. We excluded the subjects who were transferred to an acute hospital and those with any missing case data. In this case, all subjects were followed up on until they were discharged. Informed consent was waived because of the anonymous nature of the data. The present study was approved by the Ethics Committee at the Jikei University School of Medicine (No. 27-150-[8035]).

The patient basic information, such as the age, sex, BMI, type of fracture, and surgical procedure was obtained from the database. The type of fracture was also therefore classified into femoral neck and trochanteric. The surgical procedures were classified into osteosynthesis, femoral head replacement, and other orthopedic surgery. Chiefly, the Charlson Comorbidity Index (CCI) [11] and certification for public long-term care insurance (LTCI) before hip fracture were used for analysis. Furthermore, intervals between the onset and admission, FIM score at both admission and discharge point, and the average amount of rehabilitation per day were obtained. Additionally, the Mini Nutritional Assessment (MNA) Short-Form [12], total energy expenditure (TEE), and EI on admission were acquired.

The LTCI is a public social security service in Japan, and

all users are certificated into seven levels of care after a dedicated assessment.

EI and energy sufficiency

In this study, the EI was calculated by averaging the energy provided from oral, intravenous, and enteral nutrition for 7 days after admission. Additionally, the oral EI was evaluated by a nurse or registered dietitian at each ward. Whereas an evaluation of the amount of dietary intake and the method used to calculate EI were not standardized, the visual assessment method is common in Japan, and nurses or registered nutritionists routinely evaluate the proportion of meals after each meal. These professionals also routinely calculate EIs from the leftovers and the amount of energy offered. Hence, the EI was calculated three times a day. Notably, the EI by intravenous and enteral nutrition used as per the doctor's directions was also recorded.

In this case, each patient's basal energy expenditure (BEE) was calculated using the Harris-Benedict formula [13]. In the calculation, we used the ideal body weight for patients. Going further, we estimated the TEE by multiplying BEE with a stress factor of 1.1 and an activity factor of 1.2. Incidentally, the setting of these TEEs was selected according to suggestions made by Inoue et al. [5]. The subjects were classified into an energy sufficiency group and an energy shortage group based on the amount of EI. Here, we defined the 'energy sufficiency group' with an EI/TEE of ≥1.0 and 'energy shortage group' <1.0.

Outcome measurement

In this analysis, we used FIM to evaluate patient disability level as well as a change in patient status in response to rehabilitation. FIM is composed of 13 motor scales and 5 cognitive scales [14]. This system works and sorts the functional status of a person based on the level of assistance from 1 (total assistance) to 7 (complete independence). Accordingly, the total FIM scores ranged from 18 to 126. FIM gain was calculated as the patient's discharge FIM score minus the admission FIM score. In this case, the FIM gain shows improvement in ADL during hospitalization. To some degree with a larger score, we can determine that the progression of ADL has largely improved.

Statistical analysis

In this study, all statistical analyzes were performed using IBM SPSS version 23.0 for Windows (IBM Corporation, Armonk, NY, USA). Notably, the continuous data are presented as mean±standard deviation and nonparametric data as the median (interquartile range [IQR] 25–75 percentile). In this context, the differences were analyzed using the Student t-test and Mann-Whitney U-test after confirming the normal distribution. The categorical data were expressed as incidences and percentages, with comparisons carried out using the chi-square test. The correlation analyses were carried out using Spearman rank correlation coefficients for age, CCI, number of days between onset and admission, a period of rehabilitation (min/day), FIM score at admission, and FIM gain. Also, the explanatory variable used in the multiple regression analysis was selected with reference to that reported previously [5,7]. In this case, the selected factors were based on the following eight items: age, sex, CCI, number of days from onset to the admission, the presence of surgical procedure, period of rehabilitation, FIM score at admission, and presence of certification for LTCI before hip fracture. Namely, the multicollinearity was assessed using the variance inflation factor (VIF) coefficient. Additionally, the multicollinearity was judged when the VIF was ≥2. Throughout, p-values of <0.05 were considered statistically significant.

RESULTS

In this case, there were 234 patients with hip fracture were registered with the database from November 2015 to March 2018. Notably, there were 226 patients who were included in the final analysis. Thus, out of 24 patients, 7 transferred to the acute hospital, while 17 with insufficient data were excluded. The final analysis targeted 202 patients.

To begin with, Table 1 shows the baseline characteristics of the study participants. Accordingly, of the 202 patients, 43 were males and 159 females. The mean age was 84.9±7.4 years. In this study, there were 108 patients with femoral neck fracture (53.5%) and 94 patients with trochanteric fracture (46.5%). The surgical procedure with 111 patients (55.0%) included osteosynthesis, and 74 patients (36.6%) underwent femoral head replacement. Ultimately, the median number of days (IQR 25–75

Table 1. Patient characteristics

Characteristic	All (n=202)	Energy shortage group (n=53)	Energy sufficiency group (n=149)	p-value
Age (yr)	84.9±7.4	82.1±7.6	85.9±7.0	0.001[a]
Sex, female	159 (78.7)	38 (71.7)	121 (81.2)	0.146[b]
Type of fracture				
Femoral neck	108 (53.5)	31 (58.5)	77 (51.7)	0.393[b]
Trochanteric	94 (46.5)	22 (41.5)	72 (48.3)	
Surgical procedure				
Osteosynthesis	111 (55.0)	25 (47.2)	88 (57.7)	0.604[b]
Femoral head replacement	74 (36.6)	23 (43.4)	53 (34.2)	
Others	6 (3.0)	2 (3.8)	4 (2.7)	
Nonsurgical treatment	11 (5.4)	3 (5.7)	8 (5.4)	
Charlson comorbidity index	1 (0-2)	1 (0-2)	1 (0-2)	0.550[c]
Certification for LTCI before hip fracture	93 (45.1)	30 (56.6)	63 (42.3)	0.072[b]
Days between onset and admission	22 (18.0-30.0)	21 (16.0-33.5)	22 (18.0-30.0)	0.493[c]
FIM score				
Admission	70.3±25.4	66.6±29.4	71.7±23.7	0.209[a]
Discharge	94.1±26.9	86.3±31.0	96.8±24.7	0.014[a]
FIM gain	23.8±15.0	19.7±16.4	25.1±14.2	0.024[a]
Period of rehabilitation (min/day)	104.3±29.5	104.4±25.6	104.3±30.8	0.996[a]
BMI (kg/m^2)	20.1±3.1	19.5±3.0	20.3±3.1	0.096[a]
MNA Short-Form	6.0±2.2	5.6±2.2	6.1±2.2	0.124[a]
TEE (kcal/IBW/day)	1,212±208	1,301±222	1,180±195	<0.001[a]
Energy intake	1,304±274	1,024±290	1,404±186	<0.001[a]
Energy intake (kcal/kg/day)	29.9±7.7	22.8±6.5	32.4±6.3	<0.001[a]

Values are presented as mean±standard deviation or number (%) or median (interquartile range).
LTCI, public long-term care insurance; FIM, Functional Independence Measure; BMI, body mass index; MNA, Mini Nutritional Assessment; TEE, total energy expenditure.
[a]Student t-test.
[b]Chi-square test.
[c]Mann-Whitney U-test.

percentile) from the onset of an injury to entering a rehabilitation hospital was 22 (18.0-30.0). Chiefly, 53 patients (26.2%) were in the energy shortage group, and 149 (73.8%) were in the energy sufficiency group. In comparison to the energy shortage group, the sufficiency group was significantly older (p=0.001) but also had a higher FIM score at discharge (p=0.014), and EI (p<0.001). For this reason, the TEE was significantly higher in the shortage group (p<0.001).

Next, Table 2 shows the results of the univariate analysis for FIM gain. Hence, as compared to the energy sufficiency group, the shortage group (p=0.024) were more impaired in FIM gain.

In short, Table 3 shows correlation analysis results of age, CCI, number of days from onset to admission, period of rehabilitation (min/day), FIM score at admission, and FIM gain. There was a significant correlation between FIM gain and FIM score at admission (ρ=−0.185, p<0.001).

Finally, Table 4 shows the results of multiple regression analysis for the FIM gain. Collinearity was not observed in all items in the multiploidization test using VIF. As a result, the energy sufficiency group in the first week since admission (β=0.165; 95% confidence interval [CI], 0.392 to 5.230; p=0.023) and the FIM score at admission (β=−0.304; 95% CI, −0.279 to −0.080; p=0.001) were inde-

pendent factors for FIM gain.

DISCUSSION

It is important to realize that the primary original finding of this investigation was two-fold. First, in elderly patients with hip fracture in rehabilitation hospitals, the amount of EI during the first week after admission was revealed to be an independent factor for FIM gain. Secondly, 26.2% of these patients were found to be caloric deficient.

Table 2. Univariate analysis of FIM gain

Characteristic	FIM gain	p-value
Sex		
Male	23.1±13.4	0.747[a]
Female	23.9±13.9	
Type of fracture		
Femoral neck	23.2±13.9	0.597[a]
Trochanteric	24.3±16.1	
Surgery		
Presence	23 (12-32)	0.601[b]
Absence	23 (14-36)	
Certification for LTCI before hip fracture		
Presence	23.3±14.7	0.688[a]
Absence	24.1±15.2	
Energy sufficiency		
Presence	25.1±14.2	0.024[a]
Absence	19.7±16.4	

Values are presented as mean±standard deviation or median (interquartile range).
FIM, Functional Independence Measure; LTCI, public long-term care insurance.
[a]Student t-test.
[b]Mann-Whitney U-test.

The most notable finding of this investigation was that the amount of EI during the first week after admission was an independent factor for FIM gain. The study of Inoue et al. [5] reported that EIs during the first week after the operation was an independent factor for improving motor FIM gain efficiency. Furthermore, Goisser et al. [4] reported that the number of dietary intakes during 4 days after operation affected the improvement of ADL at 6 months after surgery. Although the study design used herein is quite different from previous reports, the results are similar in spite of where the amount of EI affected the improvement of ADL. Then again, there were several investigations that have also reported that concomitant use of dietary supplements in addition to a healthy diet improves muscle mass, grip strength, and ADL [15-17]. In a review of the previous studies, it has been recognized that the muscular strength (grip strength) is strong when the intake energy is high [18,19]. Furthermore, an RCT at the rehabilitation hospitals showed that increased EI with oral nutritional supplements ingestion improved the patient grip strength [17,20]. Therefore, we did not measure muscle strength to investigate the relation between EI satisfaction and grip strength in our study. Also, it is significant to note that the shortage of EI caused a poor improvement in nutritional status, which resulted in an insufficient ADL improvement. Based on the results of the present study, to improve ADL in patients with hip fracture, it is essential for the medical staff to evaluate whether the EI of the patient is adequate. Nonetheless, while the optimal amount of EI remains unknown, the amount of daily activity and patient's condition will affect their EI, even if we assume IE/TEE >1.0 as a standard figure.

Equally important, it is also worth mentioning that 26.2% of the elderly patients with hip fracture in reha-

Table 3. Spearman rank correlation coefficients among the factors

	Charlson comorbidity index	Days from onset to admission	Period of rehabilitation (min/day)	FIM score at admission	FIM gain
Age	0.070	-0.083	-0.084	-0.351*	0.113
Charlson comorbidity index		0.095	0.051	-0.225*	-0.037
Days from onset to admission			-0.028	-0.022	-0.016
Period of rehabilitation (min/day)				0.060	0.048
FIM score at admission					-0.185*

FIM, Functional Independence Measure.
*p<0.005.

Table 4. Multivariate analysis of FIM gain

	p-value	β	95% CI		VIF
			Lower	Upper	
Age	0.960	-0.004	-0.325	0.309	1.329
Sex	0.934	0.006	-2.532	2.756	1.145
Charlson comorbidity index	0.812	-0.018	-2.217	1.739	1.192
Days from onset to admission	0.245	-0.082	-0.270	0.069	1.041
Surgical procedure, presence	0.546	-0.043	-6.025	3.199	1.070
Period of rehabilitation	0.361	0.064	-0.038	0.103	1.039
FIM score at admission	0.001	-0.304	-0.279	-0.080	1.556
Certification for LTCI before hip fracture, presence	0.066	-0.152	-4.717	0.156	1.441
Energy sufficiency, presence	0.023	0.165	0.392	5.230	1.106

FIM, Functional Independence Measure; LTCI, long-term care insurance; CI, confidence interval.

bilitation hospitals were in the energy shortage state, as compared to 82.5% in the acute phase hospital during the first week after the operation, with an average EI amount of 933.0 kcal (quartile 806.9-1,120.1) [5]. Also, for one thing 71.5% of the patients took less than 50% of their offered meal during the 4 days after the operation [4]. Furthermore, in patients in rehabilitation for cerebrovascular disorders, the average EI amount during 3 days after admission was 33.2 kcal/kg/day (quartile 29.2-39.75) [9].

Even though the fraction or percentage of the EI shortage in our study was 26.2%, it is less than that reported in acute phase hospitals. However, the EI amount of 29.9±7.7 kcal/kg/day was less than that of patients with cerebrovascular disease disorders. Whereas in the present investigation, the cause of short EI remains unknown. While in previous studies, factors of the EI shortage of hip fracture patients include changes in sensory organs, loss of a tooth, lack of primary caregivers, and in some cases, adverse effects of certain drugs [1]. These factors may have also contributed to the lower dietary intake observed in the present investigation. Despite the notation that as 1 in 4 elderly patients with hip fracture in rehabilitation hospitals may have fallen into energy shortage, it is vital to evaluate EI during the first week since admission and provide nutritional support to promote the best patient outcomes in this case.

In particular, sufficient EI and appropriate rehabilitation are essential for ADL improvement in patients with hip fracture in rehabilitation hospitals. In these cases, the combination of rehabilitation and nutrition care is called rehabilitation nutrition. In this concept, both rehabilitation and nutrition management is performed together with the International Classification Guidelines on Dysfunction and Health (ICF) to evaluate the subject's nutritional status and maximize the function of the elderly and disabled [21-23]. Moreover, as nutritional evaluation, intervention, and rehabilitation are performed concurrently; it has been surmised that rehabilitation nutrition is useful for ADL improvement in patients with hip fracture in rehabilitation hospitals.

With this in mind, we considered that the mean gain in FIM (FIM score at discharge – FIM score on admission) is greatest in patients with moderate assistance, whereas patients with low FIM scores on admission show little improvement. Because of its ceiling effects, those with high FIM scores on admission, who require minimal assistance, will subsequently have little gain in FIM [24].

Notwithstanding, there are several limitations to the present research. First, the energy ingestion methods (oral, intravenous, tube proportion) used in the included subjects were noted as unknown. Second, EI was evaluated only during the first week after the admission of the patient. In addition, the hospitalization period at the rehabilitation hospitals tends to become longer than that observed in the experience of using acute phase care facilities. Third, we did not measure the patient muscular strength in the present study. Therefore, it may be necessary to consider the length and stage of the investigation when determining results of the data.

Nevertheless, in this investigation, the EI of elderly patients with hip fracture in rehabilitation hospitals was an independent factor for FIM gain, and 26.2% of them were considered to be in an EI shortage state. Even so the present study showed that ADL could be improved more

effectively by improving the nutritional status of the patients (IE/TEE >1.0).

CONFLICT OF INTEREST

No potential conflict of interest relevant to this article was reported.

ACKNOWLEDGMENTS

We thank the staff of the following hospitals for providing the patient's data for the Japanese Rehabilitation Nutrition Database (JRND): Atagawa Hospital, Nagasaki Rehabilitation Hospital, Miharu Hospital, Tsurumaki Onsen Hospital, Haradoi Hospital, Nanko Hospital, Nishi-Hiroshima Rehabilitation Hospital, Yasuoka Hospital, Kanazawa Nishi Hospital, Sakurakai Medical Corporation Sakurakai Hospital, Sapporo Nishi-maruyama Hospital, Mihono Hospital, Tamana Regional Health Medical Center, Jikei University Daisan Hospital, Nakanoshima Iwaki Hospital, Nishinomiya Kyoritsu Neurosurgical Hospital, and Minamisoma Municipal General Hospital.

AUTHOR CONTRIBUTION

Conceptualization: all authors. Methodology: all authors. Formal analysis: Umezawa H, Kokura Y, Abe S, Suzuki C, Nishida A, Uchiyama Y. Funding acquisition: Momosaki R. Project administration: Maeda K, Wakabayashi H, Momosaki R. Visualization: Kokura Y, Abe S. Writing - original draft: Umezawa H, Kokura Y, Abe S, Suzuki C. Writing - review and editing: Umezawa H, Maeda K, Wakabayashi H, Momosaki R. Approval of final manuscript: all authors.

REFERENCES

1. Malafarina V, Reginster JY, Cabrerizo S, Bruyere O, Kanis JA, Martinez JA, et al. Nutritional status and nutritional treatment are related to outcomes and mortality in older adults with hip fracture. Nutrients 2018; 10:E555.
2. Bohl DD, Shen MR, Hannon CP, Fillingham YA, Darrith B, Della Valle CJ. Serum albumin predicts survival and postoperative course following surgery for geriatric hip fracture. J Bone Joint Surg Am 2017;99:2110-8.
3. Mazzola P, Ward L, Zazzetta S, Broggini V, Anzuini A, Valcarcel B, et al. Association between preoperative malnutrition and postoperative delirium after hip fracture surgery in older adults. J Am Geriatr Soc 2017; 65:1222-8.
4. Goisser S, Schrader E, Singler K, Bertsch T, Gefeller O, Biber R, et al. Low postoperative dietary intake is associated with worse functional course in geriatric patients up to 6 months after hip fracture. Br J Nutr 2015; 113:1940-50.
5. Inoue T, Misu S, Tanaka T, Sakamoto H, Iwata K, Chuman Y, et al. Inadequate postoperative energy intake relative to total energy requirements diminishes acute phase functional recovery from hip fracture. Arch Phys Med Rehabil 2019;100:32-8.
6. Miyanishi K, Jingushi S, Torisu T. Mortality after hip fracture in Japan: the role of nutritional status. J Orthop Surg (Hong Kong) 2010;18:265-70.
7. Nishioka S, Wakabayashi H, Momosaki R. Nutritional status changes and activities of daily living after hip fracture in convalescent rehabilitation units: a retrospective observational cohort study from the japan rehabilitation nutrition database. J Acad Nutr Diet 2018; 118:1270-6.
8. Miyai I, Sonoda S, Nagai S, Takayama Y, Inoue Y, Kakehi A, et al. Results of new policies for inpatient rehabilitation coverage in Japan. Neurorehabil Neural Repair 2011;25:540-7.
9. Nii M, Maeda K, Wakabayashi H, Nishioka S, Tanaka A. Nutritional improvement and energy intake are associated with functional recovery in patients after cerebrovascular disorders. J Stroke Cerebrovasc Dis 2016;25:57-62.
10. Takasaki M, Momosaki R, Wakabayashi H, Nishioka S. Construction and quality evaluation of the Japanese rehabilitation nutrition database. J Nutr Sci Vitaminol (Tokyo) 2018;64:251-7.
11. Charlson ME, Pompei P, Ales KL, MacKenzie CR. A new method of classifying prognostic comorbidity in longitudinal studies: development and validation. J Chronic Dis 1987;40:373-83.
12. Guigoz Y, Lauque S, Vellas BJ. Identifying the elderly at risk for malnutrition. The Mini Nutritional Assessment. Clin Geriatr Med 2002;18:737-57.
13. Long CL, Schaffel N, Geiger JW, Schiller WR, Blakemore WS. Metabolic response to injury and illness:

estimation of energy and protein needs from indirect calorimetry and nitrogen balance. JPEN J Parenter Enteral Nutr 1979;3:452-6.
14. Ottenbacher KJ, Hsu Y, Granger CV, Fiedler RC. The reliability of the functional independence measure: a quantitative review. Arch Phys Med Rehabil 1996;77:1226-32.
15. Flodin L, Cederholm T, Saaf M, Samnegard E, Ekstrom W, Al-Ani AN, et al. Effects of protein-rich nutritional supplementation and bisphosphonates on body composition, handgrip strength and health-related quality of life after hip fracture: a 12-month randomized controlled study. BMC Geriatr 2015;15:149.
16. Yoshimura Y, Bise T, Shimazu S, Tanoue M, Tomioka Y, Araki M, et al. Effects of a leucine-enriched amino acid supplement on muscle mass, muscle strength, and physical function in post-stroke patients with sarcopenia: a randomized controlled trial. Nutrition 2019;58:1-6.
17. Yoshimura Y, Uchida K, Jeong S, Yamaga M. Effects of nutritional supplements on muscle mass and activities of daily living in elderly rehabilitation patients with decreased muscle mass: a randomized controlled trial. J Nutr Health Aging 2016;20:185-91.
18. Mishra S, Goldman JD, Sahyoun NR, Moshfegh AJ. Association between dietary protein intake and grip strength among adults aged 51 years and over: What We Eat in America, National Health and Nutrition Examination Survey 2011-2014. PLoS One 2018;13: e0191368.
19. Collins PF, Stratton RJ, Elia M. Nutritional support in chronic obstructive pulmonary disease: a systematic review and meta-analysis. Am J Clin Nutr 2012;95: 1385-95.
20. Takeuchi I, Yoshimura Y, Shimazu S, Jeong S, Yamaga M, Koga H. Effects of branched-chain amino acids and vitamin D supplementation on physical function, muscle mass and strength, and nutritional status in sarcopenic older adults undergoing hospital-based rehabilitation: a multicenter randomized controlled trial. Geriatr Gerontol Int 2019;19:12-7.
21. Wakabayashi H, Sakuma K. Rehabilitation nutrition for sarcopenia with disability: a combination of both rehabilitation and nutrition care management. J Cachexia Sarcopenia Muscle 2014;5:269-77.
22. Kokura Y, Wakabayashi H, Maeda K, Nishioka S, Nakahara S. Impact of a multidisciplinary rehabilitation nutrition team on evaluating sarcopenia, cachexia and practice of rehabilitation nutrition. J Med Invest 2017;64:140-5.
23. Nagano A, Nishioka S, Wakabayashi H. Rehabilitation nutrition for iatrogenic sarcopenia and sarcopenic dysphagia. J Nutr Health Aging 2019;23:256-65.
24. Tokunaga M, Mita S, Tashiro K, Yamaga M, Hashimoto Y, Nakanishi R, et al. Methods for comparing functional independence measure improvement degree for stroke patients between rehabilitation hospitals. Int J Phys Med Rehabil 2017;5:1000394.

2．(公財)老年病研究所病理部:剖検例収載(H29)

日本病理剖検輯報第60輯　日本病理学会編 P 317～318、2018

425	87歳　F	脳梗塞後遺症 慢性心不全 [内科]	**脳アミロイドアンギオパチー**　1. 心褐色萎縮、左心室肥大　②肺うっ血･水腫、癒着性胸膜炎　3. 肝萎縮、胆嚢結石（大豆大、多数）　4. 動脈硬化性萎縮腎
426	68歳　M	運動ニューロン疾患 [神内]	**球脊髄性筋萎縮症**　1. 左心遠心性肥大　②. 肺水腫・肺うっ血・気管支肺炎　3. 肝うっ血、嚢胞（左様被膜下. クルミ大）　4. 動脈硬化性萎縮腎、腎嚢胞（拇指頭大）　5. 脾萎縮
427	95歳　F	肺炎、乳癌、痴呆 [内科]	**乳癌**（腺癌、術後再発）転：あり　1. 進行性核上麻痺（PSP）、アルツハイマー型変化群（ADC）　2. 心褐色萎縮　③. 肺うっ血･水腫（高度）、硝子膜症　4. 肝萎縮・うっ血（にくずく肝）　6. 動脈硬化性萎縮腎
428	84歳　M	心筋梗塞（新・旧）、 糖原病、急性腎不全 [神内]	**腎癌**（明細胞癌、不顕性癌・潜在癌）転：なし　1. 菌血症　2. 脳萎縮2　3. 嚥下性肺炎　4. 肝萎縮　5. 心褐色萎縮　6. 動脈硬化性萎縮腎　7. 前立腺肥大
429	93歳　F	アルツハイマー病、 脳梗塞 [内科]	**アルツハイマー病**　1. 心褐色萎縮　②. 左右肺うっ血、水腫　3. 肝萎縮　4. 腎萎縮　5. 脾萎縮（高度）　6. 膵萎縮（高度）、ラ氏島過形成　7. 甲状腺腫（右、拇指頭大）･嚢胞（左、大豆大）
430	71歳　M	くも膜下出血 [脳外]	**くも膜下出血、脳腫脹**　1. 肺水腫・肺うっ血　2. 心肥大　3. 脂肪肝　4. 前立腺肥大　5. 腎の混濁腫脹　6. 脾うっ血
431	104歳　F	胆嚢炎、腸閉塞 [内科]	**アルツハイマー型認知症**　1. 左室求心性肥大、心褐色萎縮　②. 肺水腫・肺うっ血　3. 胆嚢腫脹、胆嚢壁蜂窩織炎、線維素性胆嚢周囲炎　4. 肝萎縮・うっ血　5. 動脈硬化性萎縮腎　6. 脾萎縮（高度）
432	81歳　F	脳底動脈閉塞症 [脳外]	**脳底動脈ステント治療後、脳幹梗塞**　1. 左心室肥大　2. 気管支肺炎　3. 肝萎縮・うっ血　4. 腎動脈硬化性萎縮・うっ血　5. 脾萎縮・うっ血
433	84歳　M	急性心不全 [神内]	**アルツハイマー病**　1. 左心室肥大、冠状動脈硬化と狭窄　②. 肺水腫･肺うっ血、気管支肺炎、左癒着性胸膜炎　3. 肝萎縮　4. 腎動脈硬化性萎縮腎　5. 前立腺肥大（超クルミ大）　6. 脾うっ血
434	84歳　M	肝膿瘍、嚥下性肺炎、 脊柱障害 [内科]	**アルツハイマー病**　1. 冠状動脈バイパス術後、心外膜癒着、心筋梗塞（左室側後壁、旧）　②. 肺水腫・肺うっ血、癒着性胸膜炎　3. 肝混濁　肝周囲癒着、肝嚢胞（小指頭大）　4. 慢性胆嚢炎、胆嚢結石　5. 腎混濁腫脹　6. 感染脾　7. 回盲部ポリープ（小指頭大、脂肪腫）
435	85歳　F	嚥下性肺炎、 パーキンソン病 [循環器]	**パーキンソン病**　1. 心褐色萎縮　②. 嚥下性肺炎、気管支肺炎、右胸膜癒着　3. 肝萎縮､胆嚢腫脹　4. 左右腎動脈硬化性萎縮　5. 脾萎縮（高度）　6. 下垂体（微小腺腫、嫌色素性）　7. 甲状腺嚢胞　8. 大腸憩室
436	79歳　F	肺癌、心筋症 [内科]	**S 状結腸癌**（3 型、中分化管状腺癌）転：あり　1. 心褐色萎縮　②. 肺水腫・肺うっ血　3. 肝混濁　4. 子宮筋腫、右卵巣摘出後　5. 脾萎縮、貧血性梗塞（被膜下、小指頭大 1 個）　6. 腎動脈硬化性萎縮　7. 脳萎縮

3．研究成果の発表の事業（学会発表等）

1）第９回動脈硬化と血栓症研究会

平成31年４月19日（前橋）

アテローム血栓性脳梗塞に対する急性期血行再建術における血栓性合併症と抗血栓療法の検討

宮本直子、内藤　功

老年病研究所附属病院脳神経外科

2）World Confederation for Physical Therapy 2019

令和１年５月10日～13日（ジュネーブ）

(1) Comparison of Physical Activity Intensity Estimated by Measuring Heart Rate during Rehabilitation among Inpatients with Subacute Stroke（回復期病棟入院中の脳卒中患者における理学療法中の身体活動強度の比較～心拍数モニターによる検証～）

Kazuya Fujii[1)], Masaki Kobayashi[1)], Toru Saito[1)], Shiori Kasahara[1)], Takafumi Shimura[1)], Chihiro Tajima[1)], Yasujiro Sakai[1)], Kohei Kurokawa[1)], Tomoyuki Shinohara[2)], Shigeru Usuda[3)]

Geriatrics Research Institute and Hospital[1)]

Takasaki University of Health and Welfare[2)]

Gunma University Graduate School of Health Sciences[3)]

(2) Accuracy of a wrist-worn heart rate monitor compared with a chest strap heart rate monitor in patients with stroke（入院中の脳卒中患者における手首装着型心拍計の胸部心拍数と比較した正確性の検討）

Masaki Kobayashi[1)], Kazuya Fujii[1)], Toru Saito[1)], Shiori Kasahara[1)], Takafumi Shimura[1)], Chihiro Tajima[1)], Yasujiro Sakai[1)], Kohei Kurokawa[1)], Tomoyuki Shinohara[2)], Shigeru Usuda[3)]

Geriatrics Research Institute and Hospital[1)]

Takasaki University of Health and Welfare[2)]

Gunma University Graduate School of Health Sciences[3)]

3）第64回北関東頭頸部血管内手術懇話会

令和１年５月11日（前橋）

(1) 最近のステント併用コイル塞栓術の症例

宮本直子、内藤　功、高玉　真、岩井丈幸

老年病研究所附属病院脳神経外科

(2) 母血管温存が困難なPICA限局性動脈瘤に対し、ステント併用コイル塞栓術を施行した1例

山根庸弘[1)]、長野拓郎[1)]、斉藤　太[1)]、矢尾板裕之[1)]、宮本直子[2)]、内藤　功[2)]

太田記念病院脳神経外科[1)]、老年病研究所附属病院脳神経外科[2)]

4）第60回日本神経学会学術大会

令和1年5月22日～25日（大阪）

(1) Macrophage galectin-3 in spinal white matter is a key molecule for motor neuron degeneration in ALS（脊髄白質内のマクロファージガレクチン-3は筋萎縮性側索硬化症における運動神経細胞変性の鍵となる分子である）

林　信太郎[1,2)]、山崎　亮[1)]、岡本幸市[3)]、吉良潤一[1)]

九州大学大学院医学研究院神経内科学[1)]、群馬リハビリテーション病院脳神経内科[2)]、老年病研究所附属病院神経内科[3)]

(2) Downregulation of Cx36-made electrical synapses without glutamatergic axon terminals in ALS（筋萎縮性側索硬化症におけるグルタミン作動性軸索終末なしでコキネシン36による電気的シナプスの応答能の低下）

Yuko Kobayakawa[1)], Katsuhisa Masaki[1)], Ryo Yamasaki[1)], Wataru Shiraishi[1)], Shotaro Hayashida[1)], Shintaro Hayashi[1)], Koichi Okamoto[2)], Takuya Matsushita[1)], Jun-ichi Kira[1)]

九州大学神経内科[1)]、老年病研究所附属病院神経内科[2)]

(3) Oral immunization with soybean storage protein containing Abeta4-10 in Alzheimer's model mice.（アルツハイマー病モデルマウスにおけるAbeta4-10を含むダイズ貯蔵蛋白による経口免疫療法）

Takeshi Kawarabayashi[1,2)], Takumi Nakamura[1,2,3)], Yusuke Seino[2)], Mie Hirohata[2)], Mikio Shoji[1)]

Geriatrics Research Institute Hospital[1)], Department of Neurology, Hirosaki University Graduate School of Medicine[2)], Department of Neurology, Gunma University Graduate School of Medicine[3)]

(4) CAA-related intracerebral hemorrhage in younger patients: nationwide study in Japan（日本における若年性CAA関連脳出血）

Kenji Sakai[1)], Mitsuharu Ueda[2)], Wakaba Fukushima[3)], Akira Tamaoka[4)], Mikio Shoji[5)], Yukio Ando[2)], Masahito Yamada[1)]

Department of Neurology and Neurobiology of Aging, Kanazawa University Graduate School of Medical Sciences[1], Department of Neurology, Graduate School of Medical Sciences, Kumamoto University[2], Department of Public Health, Osaka City University Graduate School of Medicine[3], Department of Neurology, Faculty of Medicine, University of Tsukuba[4], Department of Neurology, Hirosaki University Graduate School of Medicine (Geriatrics Research Institute Hospital)[5]

5）第31回日本老年医学会総会シンポジウム

令和１年６月６日（仙台）

老年医学における認知症研究の最前線　認知症のバイオマーカー～自然経過と臨床応用～

東海林幹夫

老年病研究所附属病院

6）第56回日本リハビリテーション医学会学術集会

令和１年６月12日～16日（神戸）

(1)　早期離床の実施に対するバリア分析－リハビリテーション医療スタッフは何を離床のバリアと考えるか－

宮澤佳之、梅澤浩輝、小林将生、佐藤みゆき

老年病研究所附属病院リハビリテーション部

(2)　回復期リハビリテーションにおける歩行自己効力感の経時的変化の検討

齋藤拓之[1,2]、佐藤みゆき[1]、齋藤　徹[1]、藤井一弥[1]、臼田　滋[2]

老年病研究所附属病院リハビリテーション部[1]

群馬大学大学院保健学研究科[2]

7）第16回日本脳神経血管内治療学会関東地方会

令和１年６月15日（東京）

破裂紡錘形内頸動脈瘤の一例

宮本直子、高玉　真、岩井丈幸、内藤　功

老年病研究所附属病院脳神経外科

8）第10回日本脳血管・認知症学会総会

令和１年８月３日（東京）

(1)　血漿Aβ値は腎機能により強い影響を受け、MMSEと相関する

中村琢洋[1]、瓦林　毅[2]、清野祐輔[3]、笠原浩生[1]、池田将樹[1]、池田佳生[1]、東海林幹夫[2]

群馬大学大学院医学系研究科神経内科[1]、老年病研究所附属病院脳神経内科[2]

国立病院機構弘前病院[3]

(2) 組み換えダイズ蛋白によるアルツハイマー病発症予防療法の開発

瓦林　毅[1)]、中村巧洋[2)]、甘利雅邦[1)]、高玉真光[1)]、東海林幹夫[1)]

老年病研究所附属病院脳神経内科[1)]、群馬大学大学院脳神経内科学講座[2)]

9）第９回富山ホタルイカカンファレンス

令和１年８月17日～18日（富山）

開頭手術所見から見たbridging vein dural AVFのシャント部位、シャント形態の検討

宮本直子、内藤　功

老年病研究所附属病院脳神経外科

10）9th Shonan Vascular Conference

令和１年８月24日～25日（鎌倉）

髄膜腫術前塞栓術を行った１例

宮本直子、内藤　功

老年病研究所附属病院脳神経外科

11）第53回日本作業療法学会

令和１年９月６日～８日（福岡）

脳卒中患者における二十課題干渉下での把持力制御と注意配分の関係

手島稜登[1)]、李　範爽[2)]

老年病研究所附属病院リハビリテーション部[1)]、群馬大学大学院保健学研究科[2)]

12）第230回日本神経学会関東・甲信越地方会

令和１年９月７日（東京）

経過中にMSAとの鑑別が問題となったPSAの73歳男性剖検例

清水千聖[1)]、漆田優樹[1)]、菊池雄太郎[1)]、甘利雅邦[1)]、岡本幸市[1)]、東海林幹夫[1)]、高玉真光[2)]、池田佳生[3)]

老年病研究所附属病院脳神経内科[1)]・同内科[2)]、群馬大学医学部附属病院脳神経内科[3)]

13）THE 14th ANNUAL MEETING OF MONNGOLIAN SOCIETY OF PHYSICAL AND REHABILITATION MEDICINE

令和１年９月18日～21日（ウランバートル）

Perioperative Rehabilitation and Nutritional Rehabilitation（周術期リハビリテーションとリハビリテーション栄養）

佐藤圭司

老年病研究所附属病院

14）第31回日本神経免疫学会学術集会

令和１年９月26日～27日（千葉）

(1) ALS脊髄白質に出現するgalectin-3陽性ミクログリアはTDP-43病理と正相関する

林　信太郎[1,2]、山﨑　亮[1]、岡本幸市[3]、吉良潤一[1]

九州大学大学院医学研究院神経内科学[1]、群馬リハビリテーション病院神経内科[2]、老年病研究所附属病院脳神経内科[3]

(2) 表現型不一致の一卵性品胎における多発性硬化症関連T細胞受容体レパトア解析

磯部紀子[1]、林　吏恵[2]、渡邊　充[2]、松下拓也[2]、岡本幸市[3]、吉良潤一[2]

九州大学神経治療学[1]、九州大学神経内科[2]、老年病研究所附属病院脳神経内科[3]

15）第７回日本静脈経腸栄養学会関東甲信越支部学術集会

令和１年９月29日（新潟）

フレイル・サルコペニア予防

橋場弘武

老年病研究所附属病院NST・薬剤部

16）49th Annual meeting of the Society for Neuroscience

令和１年10月19日～23日（シカゴ）

Oral immunization with soybean storage protein containing Aβ4-10（Aβ4-10を含むダイズ貯蔵蛋白による経口免疫療法）

Takeshi Kawarabayashi, Masakuni Amari, Masamitsu Takatama, Mikio Shoji

Geriatrics Research Institute and Hospital

17）第38回関東甲信越ブロック理学療法学会

令和１年10月26日～27日（前橋）

回復期リハビリテーションにおける自己効力感と歩行自立度、身体運動機能の関連性

齋藤拓之[1,2]、佐藤みゆき[1]、齋藤　徹[1]、藤井一弥[1]、臼田　滋[2]

老年病研究所附属病院リハビリテーション部[1]、群馬大学大学院保健学研究科[2]

18）第29回日本医療薬学会年会

令和１年11月２日～４日（福岡）

転倒・転落防止における薬剤師の役割

橋場弘武[1]、金古成美[1]、茂木秀敏[1]、酒井秀二[2]、高玉真光[3]

老年病研究所附属病院薬剤部[1]・同医療安全管理室[2]・同内科[3]

19）第38回日本認知症学会学術集会

令和１年11月７日～９日（東京）

(1) 組み替え大豆蛋白によるアルツハイマー病経口免疫の作用機序の検討

瓦林　毅[1,2,3]、中村琢洋[2]、清野祐輔[4]、亀谷富由樹[5]、池田佳生[2]、高玉真光[1]、東海

林幹夫[1,3]

老年病研究所附属病院[1]、群馬大学大学院医学系研究科脳神経内科学[2]、弘前大学医学部社会医学[3]、国立病院機構弘前病院[4]、東京都医学総合研究所認知症・高次脳機能研究分野[5]

⑵「DIAN研究／家族会議」

東海林幹夫

老年病研究所附属病院

20）第38回群馬IVR 研究会

令和１年11月８日（前橋）

脳底動脈瘤塞栓術後再破裂の１例

宮本直子、内藤　功、高玉　真、岩井丈幸

老年病研究所附属病院脳神経外科

21）第65回北関東頭頸部血管内手術懇話会

令和１年11月９日（前橋）

⑴　脳底動脈瘤塞栓術２年後、neck部の再発が再破裂した１例

宮本直子[1]、内藤　功[1]、高玉　真[1]、岩井丈幸[1]、富澤真一郎[2]、桑野　淳[3]、林　悟[4]

老年病研究所附属病院脳神経外科[1]、前橋脳神経外科クリニック[2]、伊勢崎佐波医師会病院脳神経外科[3]、近森病院脳神経外科[4]

⑵　頭皮AVFに対し、Onyxを用いて塞栓術を行った１例

桑野　淳[1]、荒井孝司[1]、宮本直子[2]、内藤　功[2]

伊勢崎佐波医師会病院脳神経外科[1]、老年病研究所附属病院脳神経外科[2]

22）一般社団法人群馬県言語聴覚士会第４回学術研究発表会

令和１年11月10日（前橋）

重度嚥下障害を呈したWallenberg症候群に対するアプローチ経鼻経管栄養から３食経口摂取にて自宅退院を目指した介入

早川あゆ美

老年病研究所附属病院リハビリテーション部

23）第23回群馬県看護学会

令和１年11月13日（前橋）

⑴　回復期リハビリ病棟で実施するミールラウンドのメリットと課題

鈴木　巌[1]、田代明美[1]、小林　忍[1]、早川あゆ美[2]、高橋千秋[3]

老年病研究所附属病院看護部[1]、同リハビリテーション部[2]、同栄養課[3]

⑵　眼科点眼薬管理シートの作成と活用による看護の効率化

田畑静紗、小澤恵子

老年病研究所附属病院看護部

⑶　外来のエキスパートを目指したチームの立ち上げ

反町綾乃、古嶋さゆり、平田恵子

老年病研究所附属病院看護部

24）第13回埼玉ブレインセミナー

令和１年11月15日（深谷）

コイル塞栓術ができず、クリッピングを行った脳底動脈瘤の１例

宮本直子、内藤　功

老年病研究所附属病院脳神経外科

25）日本放射線技術学会第66回関東支部研究発表大会

令和１年11月16日～17日（千葉）

X線CT検査におけるWAZA-ARIと換算係数を使用した被ばく線量の比較

藤井雅典

老年病研究所附属病院画像診断部

26）第30回全国介護老人保健施設大会

令和１年11月20日～22日（大分）

⑴　陽光苑　健口プロジェクト

戸谷麻衣子

群馬老人保健センター陽光苑

⑵　残された機能を活かした排泄支援

下藤初代

群馬老人保健センター陽光苑

⑶　低栄養改善に向けて、高玉元気ごはんの取り組み

野田末紗希

群馬老人保健センター陽光苑

27）第35回日本脳神経血管内治療学会学術集会

令和１年11月21日～23日（福岡）

⑴　Tentorial dAVFにおけるpial feederとshunt部位の検討

宮本直子、高玉　真、岩井丈幸、内藤　功

老年病研究所附属病院脳神経外科

⑵　破裂内頚動脈血豆状動脈瘤に対するLVIS STENTを用いた血管内治療成績

藍原正憲[1)]、清水立矢[1)]、山口　玲[1)]、相島　薫[1)]、好本裕平[1)]、宮本直子[2)]、内藤　功[2)]、佐藤晃之[3)]、矢島　翼[4)]、神徳亮介[4)]、大谷敏行[4)]

群馬大学脳神経外科[1)]、老年病研究所附属病院脳神経外科[2)]、高崎総合医療センター

脳神経外科[3]、深谷赤十字病院脳神経外科[4]

(3) Solitary fibrous tumorに対するNBCAによる栄養血管塞栓術の際に見られたcastの膨張所見

橋場康弘[1]、石原淳治[1]、曲澤　聡[1]、宮本直子[2]、内藤　功[2]

桐生厚生総合病院脳神経外科[1]、老年病研究所附属病院脳神経外科[2]

(4) 血管撮影室における患者抑制方法の再考

高橋康之[1]、赤岩　優[1]、佐藤高章[1]、矢嶋正範[1]、飯塚裕也[1]、藤井雅典[1]、高橋清彦[1]、宮本直子[2]、高玉　真[2]、内藤　功[2]

老年病研究所附属病院画像診断部[1]、同脳神経外科[2]

28) 30th International symposium on ALS/MND

令和１年12月４日～６日（パース）

Microglial galectin-3 in the spinal white matter is a key molecule for motor neuron degeneration in ALS（脊髄白質内のマクロファージガレクチン３は筋萎縮性側索硬化症における運動神経細胞変性の鍵となる分子である）

Shintao Hayashi[1,2], Ryo Yamasaki[1], Koichi Okamoto[3], Jun-ichi Kira[1]

Department of Neurology, Neurological Institute, Graduate School of Medical Sciences, Kyushu University[1], Department of Neurology, Gunma Rehabilitation Hospital[2], Department of Neurology, Geriatrics Research Institute and Hospital[3]

29) 令和１年度秋季群馬県医学会

令和１年12月７日（前橋）

(1) 非定型抗精神病薬（リスペリドン）が有効であった心因性多飲症の一例

中村保子[1]、島田晴彦[2]、菊池雄太郎[3]、高玉真光[1]

老年病研究所附属病院内科[1]、同整形外科[2]、同脳神経内科[3]

(2)「優性遺伝性アルツハイマー病ネットワーク（DIAN）」

東海林幹夫[1]、瓦林　毅[1]、高玉真光[2]

老年病研究所附属病院脳神経内科[1]・同内科[2]

(3) 進行性核上性麻痺の１剖検例における４リピートタウ沈着の解析

福田利夫[1]、鈴木慶二[1]、甘利雅邦[2]、岡本幸市[2]、高玉真光[3]

老年病研究所附属病院病理診断科[1]、同脳神経内科[2]、同内科[3]

(4) 遺伝子組換えダイズ蛋白によるアルツハイマー病予防法の開発

瓦林　毅[1]、高玉真光[2]、東海林幹夫[1]

老年病研究所附属病院脳神経内科[1]、同内科[2]

(5) 頸椎後縦靱帯骨化症に対して手術を施行した強直性脊椎炎の１例

島田晴彦[1]、館野勝彦[1]、加藤良衛[1]、佐藤圭司[1]、清水千聖[2]、高玉真光[3]

老年病研究所附属病院整形外科[1)]、同脳神経内科[2)]、同内科[3)]

⑹　心脳卒中との鑑別が問題となった、たこつぼ心筋症が疑われた一例

小南彩織[1)]、天野晶夫[2)]、甘利雅邦[3)]、高玉真光[4)]

老年病研究所附属病院初期臨床研修医[1)]、同循環器科[2)]、同脳神経内科[3)]、同内科[4)]

⑺　もの盗られ妄想のある症例と家族の橋渡し－前橋市認知症初期集中支援チームの連携－

【前橋市認知症初期集中支援チーム】

黒沢一美[1)]、山口智晴[2)]、高玉真光[3)]、山口晴保[4)]

訪問看護ステーション結の樹[1)]、群馬医療福祉大学[2)]、老年病研究所附属病院[3)]、認知症介護研究・研修東京センター[4)]

⑻　季節外れのインフルエンザアウトブレイクの経験

甘利雅邦[1)]、高玉　篤[2)]、天野晶夫[3)]、高玉真光[4)]

老年病研究所附属病院脳神経内科[1)]、同眼科[2)]、同循環器科[3)]、同内科[4)]

⑼　当院における回復期リハビリテーション病棟の現状

田畑直人[1)]、佐藤みゆき[1)]、堀口布美子[1)]、平野　哲[1)]、黒川公平[2)]

老年病研究所附属病院リハビリテーション部[1)]、同リハビリテーション科[2)]

30）第４回日本安全運転・医療研究会

令和１年12月13日～14日（福井）

⑴　ドライビングシューズを用いた実車評価への移行基準の検討

栗原純一、伊藤紗佑里、小柳慶起、北澤一樹

老年病研究所附属病院リハビリテーション部

⑵　当院の自動車運転再開の流れについて

小柳慶起、北澤一樹、伊藤紗佑里、栗原純一

老年病研究所附属病院リハビリテーション部

⑶　当院におけるドライビングシミュレータの使用実績について

北澤一樹、小柳慶起、伊藤紗佑里、栗原純一

老年病研究所附属病院リハビリテーション部

⑷　継続的な実車教習が運転免許停止後の機能改善につながった症例

伊藤紗佑里、小柳慶起、北澤一樹、栗原純一

老年病研究所附属病院リハビリテーション部

31）第656回日本内科学会関東地方会

令和１年12月14日（東京）

対麻痺・膀胱直腸障害とMRI上脊髄に長大病変を認めた血管内大細胞性B細胞リンパ腫の１例

菊池雄太郎[1)]、漆田優樹[1)]、清水千聖[1)]、瓦林　毅[1)]、甘利雅邦[1)]、東海林幹夫[1)]、岡本幸市[1)]、渋沢弥生[2)]

老年病研究所附属病院脳神経内科[1)]、同皮膚科[2)]

32）第29回群馬県老人保健施設大会

令和１年12月26日（前橋）

(1)　iPadを用いた多職種協働と在宅支援

小林尚貴

群馬老人保健センター陽光苑

(2)　お寿司バイキングをもっと楽しく！美味しく！

木賊菜月

群馬老人保健センター陽光苑

33）新潟脳血管内治療セミナー

令和２年１月31日～２月２日（苗場）

二期的に塞栓術を行ったCS-dAVFの２例

宮本直子、高玉　真、岩井丈幸、内藤　功

老年病研究所附属病院脳神経外科

34）The 8th International Symposium of Gunma University Initiative for Advanced Research（GIAR）

令和２年２月３日～４日（前橋）

Alzheimer's Disease: Natural Course and Therapy（アルツハイマー病の自然経過と治療）

Mikio Shoji

Geriatrics Research Institute and Hospital

35）第17回日本脳神経血管内治療学会関東地方会

令和２年２月15日（東京）

二期的に塞栓術を行った海綿静脈洞部硬膜動静脈瘻の２症例

宮本直子、高玉　真、岩井丈幸、内藤　功

老年病研究所附属病院脳神経外科

36）Neurosurgery Update Seminar 前橋

令和２年２月21日（前橋）

当院の脳動脈瘤治療（2009-2019年）－初回治療を断念した症例の検討－

内藤　功、宮本直子

老年病研究所附属病院脳神経外科

4．研究に関する事業報告

1．脳血管障害（脳卒中）の病理学的研究

1）高血圧性脳内出血の病因に関する研究

2）動脈壊死の病因に関する研究

3）脳梗塞の病因に関する研究

4）動脈硬化の発生に関する研究

5）くも膜下出血の際の脳血管れん縮に関する研究

6）脳動脈瘤の発生に関する研究

7）病理解剖の実施

No.	執刀者	年月日	年齢・性別	臨床診断
444	鈴木慶二	R 1・10・28	85歳・男性	パーキンソン病・アルツハイマー型認知症・誤嚥性肺炎
445	福田利夫	R 2・1・30	85歳・男性	多発性脳梗塞・急性冠症候群

8）動脈壁の代謝と形態に関する研究

9）動脈病変の電顕的研究

10）脳内動脈病変の電顕的研究

11）脳内小梗塞に関する研究

12）高血圧性動脈病変に関する研究

2．脳卒中（脳血管障害）の臨床的ならびに臨床病理学的研究

1）脳卒中の診断に関する研究

2）脳卒中の薬物療法に関する調査研究

3）脳血管障害と24時間血圧値の関係に関する研究

4）脳卒中の予防に関する研究

5）動脈硬化の進展と血清リポ蛋白についての研究

6）脳血管障害患者の胃腸病変に関する研究

7）脳動脈狭窄症に対する血管内手術に関する研究

8）脳動脈瘤に対する血管内手術に関する研究

3．群馬県における高齢者の健康対策に関する研究

1）高齢者の脂質代謝に関する研究

2）群馬県における長寿地区の特性に関する研究

3）生活習慣病と県勢との関連に関する研究

4）群馬県における肥満とヤセの実態に関する研究

5）群馬県における血清総コレステロール異常者の実態に関する研究

6）老年期の認知症に関する研究

7）超高齢者率の検討に関する研究

8）群馬県民の身長に関する研究

9）自殺死亡率と県勢との関係に関する研究

10）群馬県民の血色素量に関する研究

11）群馬県民の血清総コレステロールに関する研究 〜近年の動向〜

4．脊椎、脊髄病変の原因と治療に関する研究

1）高度頚椎前角障害を合併した圧迫性頚髄症における手術法に関する研究

2）頚椎症性筋萎縮症の診断と治療に関する研究

3）頚椎後方除圧後に生じる一過性上肢麻痺の原因と対策

4）上位頚椎病変の神経症候学、臨床的高位診断学の確立に関する研究

5）上位頚椎不安定性病変に対する確実な後方固定術の開発

6）破壊性頚椎病変を持つ重度慢性関節リウマチ例における、体幹支持性再獲得のための後頭骨胸椎間固定術の開発

7）後頭骨胸椎間固定術に使用するspinal instrumentationの開発

8）頚椎、腰椎、双方に狭窄因子をもつ高齢者歩行障害例の外科的治療手順に関する研究

9）骨粗鬆症に起因する重度脊柱後彎に対する矯正固定術の開発

10）麻痺性脊柱変形例における座位バランスの獲得と変形矯正に関する研究

11）高齢者の無腐性骨壊死による下肢麻痺の外科的治療法の研究

12）spinal instrumentation手術における術中、術後合併症回避のための臨床的研究

13）脊椎手術中の脊髄機能モニタリングに関する電気生理学的研究

14）骨傷の明らかでない頚髄損傷例に対する手術的治療の是非に関する研究

15）重労働者腰椎椎間板障害に対する手術治療における早期離床、退院、職場復帰確立のための臨床的研究

16）上位胸椎の生理学的動域のＸ線学的検討

17）脊椎疾患患者の長期フォローアップにおけるコンピュータ活用法の検討

5．慢性関節リウマチ治療に関する研究

1）重度慢性関節リウマチ患者の呼吸障害、嚥下困難の原因究明と治療法の研究

2）寝たきり重度慢性関節リウマチ患者の受療状況の実態解明

3）急速破壊性頚椎病変によって死に至る重度慢性関節リウマチ患者の救命手段についての研究

4）座位のみ可能なリウマチ患者における、排便動作自立のための足関節固定術の検討

5）外来通院リウマチ患者の薬物療法の副作用チェックと有効な患者指導法の研究

6．骨粗鬆症の臨床的研究

1）脳卒中患者と健常者との比較及び患側と健側の骨密度の比較研究

2）人工物挿入部（荷重部）の骨密度の変化研究

3）移植骨部の骨密度の変化研究

4）リハビリにおける脳卒中患者の骨密度の研究

5）ギプスなど固定をした場合の骨密度の変化研究

7．変形性膝関節症に関する臨床的研究

1）人工膝関節置換術に関する研究

2）大腿四頭筋筋力強化による荷重関節部の臨床変化の研究

3）側方動揺及び内反変形防止の装具開発

8．老人スポーツに関する臨床的研究

1）ゲートボールにおける腰痛に関する研究

2）高齢者のゴルフにおける臨床的研究

9．認知症に関する臨床的研究

1）認知症治療についての研究

2）認知症の発症予防に関する研究

3）認知症のバイオマーカーに関する研究

4）高次機能障害の治療に関する研究

10．神経難病の治療に関する研究

1）筋萎縮性側索硬化症の治療に関する研究

2）パーキンソン病の治療に関する研究

3）多発性硬化症の治療に関する研究

5．病理カンファレンス及び研究会の開催

(1) 病理カンファレンス

1) 平成31年４月９日

第300回病理カンファレンス　　参加者25名

剖検番号	年齢・性	臨　床　診　断	示　説　者
442	78・M	第一腰椎圧迫骨折・糖尿病 糖尿病性腎症・右慢性硬膜下血腫	福田利夫

2) 令和１年６月25日

第301回病理カンファレンス　　参加者23名

剖検番号	年齢・性	臨　床　診　断	示　説　者
443	73・M	進行性核上皮性麻痺・誤嚥性肺炎 糖尿病	福田利夫

3) 令和２年２月18日

第302回病理カンファレンス　　参加者33名

剖検番号	年齢・性	臨　床　診　断	示　説　者
444	85・M	パーキンソン病・誤嚥性肺炎 アルツハイマー型認知症前立腺癌治療後	福田利夫

(2) 老年病研究会

1）平成31年４月16日

第223回老年病研究所研究会　参加者72名

「認知症と生活習慣病治療について」　甘利雅邦（老年病研究所附属病院 脳神経内科　副院長）

「パーキンソン病は“振るえる”病気だと思っていませんか？
～パーキンソン病の早期発見と早期治療について～」　藤本健一先生（自治医大ステーション・ブレインクリニック）

2）令和１年６月４日

第224回老年病研究所研究会　参加者34名

「当院における不眠症治療薬の適正化への取り組み」　橋場弘武（老年病研究所附属病院 薬剤部長）

「循環器専門医の立場から生活習慣病の治療」　庭野野菊先生（前橋赤十字病院 心臓血管内科）

3）令和１年７月10日

第225回老年病研究所研究会　参加者187名

「認知症ポジティブ
～脳科学でひもとく笑顔の暮らしのケアのコツ～」　山口晴保先生（群馬大学　名誉教授）

4）令和１年９月４日

第226回老年病研究所研究会　参加者36名

「運動器疾患における神経障害性疼痛の治療」　竹下克志先生（自治医科大学 整形外科　教授）

5）令和１年10月31日

第227回老年病研究所研究会　参加者28名

「当院におけるトレリーフの使用経験」　甘利雅邦（老年病研究所附属病院 脳神経内科　副院長）

「パーキンソン病治療のUp to date」　西川典子先生（国立研究開発法人国立精神・神経医療研究センター病院　PDMセンター長）

6）令和２年１月30日

第228回老年病研究所研究会　参加者41名

「腎臓内科医から見たミネラルコルチコイド受容体拮抗薬の可能性」

廣村桂樹先生（群馬大学大学院医学系研究科腎臓・リウマチ内科学　教授）

「最新の心房細動アブレーションと周術期抗凝固療法」　内藤滋人先生（群馬県立心臓血管センター　病院長）

6．講演会等の開催

1）平成31年４月２日

「看護部の理念、目標及び機能並びに役割について」

福田　紫

「介護老人保健施設の理念と役割及び陽光苑の概要並びに高齢者との接し方について」

浅野裕江

新入職員院内研修会

院内新館講堂

2）平成31年４月３日

「３号病棟のスタッフ構成及び病棟の特徴・疾患並びに業務の流れについて」

狩野悦子

「４号病棟のスタッフ構成及び病棟の特徴・疾患並びに業務の流れについて」

福田　紫

「５号病棟のスタッフ構成及び病棟の特徴・疾患並びに業務の流れについて」

関根真奈美

「６号病棟のスタッフ構成及び病棟の特徴・疾患並びに業務の流れについて」

石川房江

「回復期病棟の特徴、入院の対象となる疾患、入院期間等について」

飯塚敦美

「外来のスタッフ構成、特徴及び１日の業務の流れについて」

福田　紫

「手術室のスタッフ構成、特徴、業務の流れ及び手術件数について」

西川千代乃

新入職員院内研修会

院内新館講堂

3）平成31年４月５日

「当院における脳血管障害の治療と予防の歴史」

高玉真光

新入職員院内研修会

ロイヤルチェスター前橋

4）平成31年４月８日

「検査課の業務内容、院内感染対策と手洗い方法等について」

常見佳克

「当院の画像診断装置と安全管理について」

高橋清彦

新入職員院内研修会

院内新館講堂

5）平成31年４月10日
「病院薬剤師の業務内容について」
橋場弘武
「地域医療福祉連携室・相談室の紹介」
狩野寛子
新入職員院内研修会
院内新館講堂
6）平成31年４月11日
「リハビリテーションの概念と職種等について」
中條浩樹
「医事課の業務内容等について」
經廣真人
新入職員院内研修会
院内新館講堂
7）平成31年４月12日
「病院における栄養課の役割と栄養サポートチーム（NST）について」
吉澤亜希子・澤田諒子
「病院、福祉施設の防災について」ビデオによる研修
新入職員院内研修会
院内新館講堂
8）平成31年４月13日
「これからの陽光苑に期待すること」
高玉真光
陽光苑介護長等研修会
陽光苑
9）平成31年４月15日
「患者満足度と病院の質を向上させるために～ISO9001の取り組みについて」
岩井丈幸
新入職員院内研修会
院内新館講堂
10）平成31年４月16日
「認知症と生活習慣病治療について」
甘利雅邦
Eldery Care Seminer
老年病研究所附属病院

11）平成31年４月17日
「医療安全対策及び倫理の定義・方針並びに個人情報保護等について」
酒井秀二
新入職員院内研修会
院内新館講堂

12）平成31年４月23日
「高齢者、認知症、せん妄に対する睡眠薬の使い方」
甘利雅邦
2019年度第１回地域連携学術講演会
済生会前橋病院

13）令和１年５月５日
「筋弛緩モニターについて」
増田裕一
泉工医科工業㈱社内講演会
大宮ソニックシティ

14）令和１年５月24日
「自立支援型ケア会議の意義について」
山田圭子
桐生市自立支援型ケア会議説明会
桐生市民文化会館

15）令和１年６月５日
「最新の認知症の診断と治療について」
甘利雅邦
上三川認知症セミナー
上三川いきいきプラザ

16）令和１年６月12日
「サルコペニアに対するリハビリテーション栄養の考え方」
佐藤圭司
老年病NST勉強会
院内新館講堂

17）令和１年６月18日
「高齢者、認知症、せん妄に対する睡眠薬の使い方」
甘利雅邦
渋川地区医師会地域医療連携セミナー～不眠症診療セミナー～
渋川医療センター

18）令和１年７月７日
「医療ソーシャルワーカーの記録と報告」
狩野寛子
群馬県医療ソーシャルワーカー協会新人研修
高崎健康福祉大学
19）令和１年７月17日
「認知症と高齢者てんかん」
甘利雅邦
てんかん診療を考える会
～てんかん診療ガイドライン2018 改訂をふまえて～
エテルナ高崎
20）令和１年７月18日
「骨粗鬆症治療～ロモソズマブ使用例の途中経過を含めて～」
佐藤圭司
新しい骨粗鬆症治療を考える会in群馬
ザ・リーヴスプレミアムテラス
21）令和１年７月26日
「認知症の治療と予防～アルツハイマー病は予防できるか？～」
瓦林　毅
老研病院・陽光苑夏祭り健康づくり講演会
院内新館講堂
22）令和１年７月30日
「老人保健施設の機能と役割」
高玉真光
全国老人保健施設協会実地研修
陽光苑
23）令和１年７月31日
「アルツハイマー病の診断と治療の今後の展望」
東海林幹夫
第44回もの忘れ相談医フォローアップ研修
高崎市総合保健センター
24）令和１年８月２日
「レビー小体型認知症・アルツハイマー型認知症」
岡本幸市
エーザイ㈱社内研修会
エーザイ高崎コミュニケーションオフィス

25）令和１年８月２日
「糖尿病患者に認知症が多い!?」
甘利雅邦
第４回糖尿病トータルケア研究会
ホテル1-2-3前橋マーキュリー

26）令和１年８月５日
記者発表「大豆由来ワクチンでアルツハイマー病抑制」
東海林幹夫、瓦林　毅、高玉真光
群馬県庁刀水クラブ

27）令和１年８月26日
「センター職員に必要な知識・技術等や
センター長等管理職に求められる役割等について」
山田圭子
山口県地域包括支援センター職員管理職研修会
山口県庁

28）令和１年８月29日
「もの忘れを防ぐ方法」
東海林幹夫、高玉真光
元総社ベテラン学習講座
元総社公民館ホール

29）令和１年９月６日
「骨粗鬆症リエゾンサービス（OLS）について」
佐藤圭司
老年病食事指導勉強会
院内新館講堂

30）令和１年９月７日
「新骨形成促進剤について」
佐藤圭司
テリボン研究会、テリボンアドバイザー会議
旭化成ファーマ㈱本社

31）令和１年９月15日
「認知症研究・診断治療本人点家族への支援を考える」
東海林幹夫
2019年世界アルツハイマーデー記念講演
群馬県社会福祉総合センター

32）令和１年９月25日
「高齢者、認知症、せん妄に対する睡眠薬の使い方」
甘利雅邦
不眠症診療セミナーin高崎
黒沢病院
33）令和１年９月28日
「認知症を防ごう！要介護にならないために」
東海林幹夫
「セミナー疑問・質問に答えるQ&A」
高玉真光、東海林幹夫
第26回心と体の健康セミナー
上毛新聞社上毛ホール
34）令和１年９月28日
「みんなで骨ケア！」健康相談医師として参加
佐藤圭司
第４回骨粗鬆症市民公開講座
スマーク伊勢崎
35）令和１年10月５日
「ロコモ予防～いつでも自分の足で歩き続けるために～」
佐藤圭司
TANITA FITS ME
フォレストモール新前橋
36）令和１年10月５日
「認知症の理解」
東海林幹夫
2019年青森支部結成10周年記念　世界アルツハイマーデー
記念講演会in青森　認知症の理解と家族への支援について
アピオ青森
37）令和１年10月10日
「フレイルとその類縁概念　筋力が落ちたなと感じることはありませんか」
牧　雄介
多職種事例検討会
前橋市総社公民館
38）令和１年10月29日
「老人保健施設の機能と役割」
高玉真光
全国老人保健施設協会実地研修
陽光苑

39）令和１年10月31日
「当院におけるトレリーフの使用経験」
甘利雅邦
ハッピーフェイスセミナーin前橋
群馬ロイヤルホテル

40）令和１年11月15日
「パーキンソン病の病診連携における早期診断と治療」
甘利雅邦
Takeda Parkinson's Disease Web Symposium
WEB/各サテライト会場

41）令和１年11月20日
「パーキンソン病の診療」
岡本幸市
協和キリン㈱社内講演会
協和キリン㈱群馬第１営業所

42）令和１年11月21日
「リハビリ職に期待すること　～地域づくりの視点から～」
山田圭子
吾妻セラピスト交流会
群馬リハビリテーション病院

43）令和１年11月23日
「認知症と鑑別すべき疾患とその対応」
東海林幹夫
第16回ケアマネージメント群馬フォーラムin西毛
ホテル磯部ガーデン

44）令和１年11月24日
「第７回（2019年度）難病医療相談会」
岡本幸市
群馬県難病団体連絡協議会
群馬県社会福祉総合センター

45）令和１年11月28日
「わが国における薬薬連携の現状～群馬県における更なる連携を目指して～」
橋場弘武
ニプロ㈱高崎営業所社内研修会
ニプロ㈱高崎営業所

46）令和１年12月４日
「骨粗鬆症治療薬の使用経験～骨形成促進剤を中心に～」
佐藤圭司
持田製薬㈱社内講演会
前橋テルサ

47）令和１年12月10日
「認知症の予防と生活習慣」
東海林幹夫
第11回第一病院地域認知症ケアセミナー
高崎市総合福祉センター

48）令和１年12月10日
「高齢者に対する睡眠薬の使い方」
甘利雅邦
桐生市医師会学術講演会
桐生メディカルセンター

49）令和１年12月25日
「ケアマネジメントに必要な医療との連携及び多職種協働の意義」
狩野寛子
介護支援専門員実務研修会
昌賢学園まえばしホール

50）令和２年１月３日
認知症について聞く「早期発見で元気に長生き」
高玉真光、東海林幹夫
上毛新聞掲載－新春インタビュー
院内（取材）

51）令和２年２月５日
「認知症に潜む高齢者のてんかん」
甘利雅邦
第267回前橋市薬剤師会定期研修会
群馬県生涯学習センター

52）令和２年２月12日
「骨粗鬆症治療に対する最近の考え方」
佐藤圭司
アステラス製薬㈱社内講演会
アステラス製薬㈱高崎支店

53）令和２年２月22日
「よくわかる認知症！最新の話題」
東海林幹夫
前橋地域リハビリテーション広域支援センター健康教室・介護予防教室
院内新館講堂

54）令和２年２月26日
「早期および進行期のパーキンソン病の薬物療法」
甘利雅邦
エクフィナ錠新発売記念セミナーin上越
上越アートホテル

55）令和２年３月４日
「最近の骨粗鬆症治療の考え方～リエゾンサービス～」
佐藤圭司
中外製薬㈱社内研修会
前橋テルサ

56）令和２年３月26日
「研究所就業規則及び社会保険関係法等の基礎知識について」
川端純司
令和２年度新入職員研修会
院内新館講堂

7．特殊外来教室

1）2019年４月５日（金）

第419回　春の松花堂弁当

～春野菜の栄養について～

講演　「ミトコンドリアについて」

講師　高玉真光

講演　「二次性糖尿病について」

講師　中村保子　　出席者　51名

2）2019年５月10日（金）

第420回　麺の単位を知ろう

～洋食編～

講演　「薬について」　さかえ５月号より

講師　高玉真光　　出席者　51名

3）2019年６月７日（金）

第421回　400kcalで楽しむ韓国料理

～身近な食材で作れるレシピをご紹介します～

講演　「患者さんのための食事を考える」DVD上映　　出席者　45名

4）2019年７月５日（金）

第422回　食事で脳の健康を保ちましょう

～認知症予防のあるマインド食をご紹介します～

講演　「認知症エクササイズ」　さかえ７月号より

講師　高玉真光　　出席者　47名

5）2019年８月２日（金）

第423回　風味でおいしい減塩食

～減塩のコツをご紹介します～

講演　「遺伝子組み換え大豆によるアルツハイマー予防」

講師　瓦林　毅　　出席者　50名

6）2019年９月６日（金）

第424回　骨が喜ぶ食事

～骨粗鬆症予防の食事を紹介します～

講演　「リエゾンサービス（OLS）について」

講師　佐藤圭司　　出席者　52名

7）2019年10月４日（金）

第425回　400kcalで楽しむパン献立

～パンの単位を知ろう～

講演　「眼は心の窓」

講師　高玉　篤　　出席者　49名

8）2019年11月１日（金）

第426回　秋の味覚で中華料理

～糖質の多い芋・果物の適量を知ろう～

講演　陽光苑での栄養士の活動

講師　木賊菜月

講演　「足について」さかえ11月号より

講師　野田未紗希　　出席者　54名

9）2019年12月６日（金）

第427回　油を減らしてヘルシーに

～高カロリーになりがちな冬料理のコツ～

講演　「コンビニ・スーパーの活用法」　さかえ12月号より

講師　合田　聖　　出席者　49名

10）2020年１月９日（木）

第428回　腸内環境を整えて免疫力UP！

～発酵食品を使用した料理を紹介します～

講演　「中性脂肪と減塩について」　さかえ１月号より

講師　高玉真光　　出席者　45名

11）2020年２月７日（金）

第429回　食事でアンチエイジング

～抗酸化パワーで若さを保ちましょう～

講演　「インフルエンザの予防」

「グリコアルブミンについて」

講師　高玉真光　　出席者　53名

8．糖尿病患者等食事指導教室

1）2019年４月５日（金）

『春の松花堂弁当』～春野菜の栄養について～

たけのこご飯・菜の花のかきたま汁・豚ロースの春キャベツソース

蕗と海老の炊き合わせ・ウドとワカメの酢の物・フルーツ

合計単位　5.1単位、熱量　408kcal、蛋白質　18.8g、塩分　2.1g、食物繊維　3.8g

出席者　65名

2）2019年５月10日（金）

『麺類の単位を知ろう』～洋食編～

豆乳のクリームスパゲティー・コンソメスープ・ゴボウサラダ・マリネ

おからヨーグルト

合計単位　5.1単位、熱量　408kcal、蛋白質　28.0g、塩分　2.0g、食物繊維　4.3g

出席者　63名

3）2019年６月７日（金）

『400kcalで楽しむ韓国料理』～身近な食材で作れるレシピをご紹介します～

ビビンバ丼・わかめスープ・たまごチヂミ・韓国海苔サラダ・フルーツ

合計単位　5.1単位、熱量　408kcal、蛋白質　23.3g、塩分　2.1g、食物繊維　8.4g

出席者　53名

4）2019年７月５日（金）

『食事で脳の健康を保ちましょう』～認知症予防のあるマインド食を紹介します～

さっぱりもち麦ご飯・味噌汁・豆腐とツナの照り焼き・胡瓜と長芋のもずく和え

ブドウゼリー

合計単位　5.1単位、熱量　408kcal、蛋白質　18.6g、塩分　2.5g、食物繊維　3.7g

出席者　58名

5）2019年８月２日（金）

『風味でおいしい減塩食』～減塩のコツをご紹介します～

ひじきご飯．冷や汁・鶏肉のソテー（フレッシュトマトソース）

冬瓜のカニあんかけ・ヨーグルトゼリー

合計単位　5.1単位、熱量　408kcal、蛋白質　22.5g、塩分　2.0g、食物繊維　5.0g

出席者　60名

6）2019年９月６日（金）

『骨が喜ぶ食事』～骨粗鬆症予防の食事を紹介します～

ごはん・豆乳味噌汁・鮭のきのこあんかけ・小松菜の納豆和え・きくらげのナムル

フルーツ

合計単位　5.1単位、熱量　408kcal、蛋白質　29.3g、塩分　2.3g、食物繊維　9.4g

出席者　61名

7）2019年10月４日（金）

『400kcalで楽しむパン献立』～パンの単位を知ろう～

食パンとたまごサラダ（自分で作るサンドイッチ）・きのこスープ・野菜のピクルス

ヨーグルト

合計単位　5.1単位、熱量　408kcal、蛋白質　17.9g、塩分　2.4g、食物繊維　5.2g

出席者　58名

8）2019年11月１日（金）

『秋の味覚で中華料理』～糖質の多い芋・果物の適量を知ろう～

きのこたっぷり白麻婆豆腐丼・中華スープ・さつまいも入りエビマヨ

白菜の甘酢漬け・フルーツ

合計単位　5.1単位、熱量　408kcal、蛋白質　23.0g、塩分　2.2g、食物繊維　7.6g

出席者　54名

9）2019年12月６日（金）

『油を減らしてヘルシーに』～高カロリーになりがちな冬料理のコツ～

ごはん・カレースープ・揚げない豚ミルフィーユカツ・水菜のサラダ

豆乳プリン

合計単位　5.1単位、熱量　408kcal、蛋白質　24.lg、塩分　1.8g、食物繊維　3.6g

出席者　51名

10）2020年１月９日（木）

『腸内環境を整えて免疫力UP!！』～発酵食品を使用した料理を紹介します～

生姜ご飯・もずくとたまごのスープ・カジキの味噌チーズ焼き

切り干し大根のサラダ・甘酒ミルクゼリー

合計単位　5.1単位、熱量　408kcal、蛋白質　26.lg、塩分　1.7g、食物繊維　2.5g

出席者　46名

11）2020年２月７日（金）

『食事でアンチエイジング』～抗酸化パワーで若さを保ちましょう～

カレーピラフ・トマトスープ・鮭のマスタードソテー・アーモンドサラダ

ココアプリン

合計単位　5.1単位、熱量　408kcal、蛋白質　28.4g、塩分　2.6g、食物繊維　4.7g

出席者　60名

9．医師の教育指導研修

1）指導医　高玉理事長、岡本研究所長、佐藤附属病院長、鈴木名誉院長、酒井名誉院長、中村名誉院長、東海林名誉院長、内藤名誉院長、岩井副院長、甘利副院長、天野副院長、島田副院長、増田副院長、高玉診療部長

2）教育指導を受けた医師11名

10．刊行事業

1）老年病――脳卒中、心筋梗塞、癌、糖尿病――の予防のための12条
公益財団法人老年病研究所
高玉真光

2）脳を若がえらせる話
公益財団法人老年病研究所
高玉真光、内藤　功

3）血液、血管が若返る本
公益財団法人老年病研究所長
渡辺　孝　監修（マキノ出版）

4）血液をさらさらにする本
公益財団法人老年病研究所長
渡辺　孝　監修（㈱主婦と生活社）

5）しなやかな血管をつくる本～脳卒中、狭心症、心筋梗塞を防ぐ～
公益財団法人老年病研究所長
渡辺　孝　監修（講談社）

6）長生きする人　早死にする人
公益財団法人老年病研究所長
渡辺　孝　監修（㈱主婦と生活社）

7）痴呆症のすべて
公益財団法人老年病研究所
平井俊策　編集（永井書店）

8）新・老化学
公益財団法人老年病研究所
平井俊策　編著（㈱ワールドプランニング）

9）老年期認知症ナビゲーター
公益財団法人老年病研究所
平井俊策　監修（メディカルレビュー社）

10）コレステロールを下げる生活読本
公益財団法人老年病研究所長
渡辺　孝（㈱主婦と生活者）

11）コレステロール、中性脂肪を下げる特効法101
公益財団法人老年病研究所長
渡辺　孝　監修（㈱主婦と生活社）
12）身体的治療を受ける認知症高齢者ケアの教育プログラム開発のための基礎的研究
公益財団法人老年病研究所看護部長
下平きみ子
13）老年心理学（高齢化社会をどう生きるか）
原　千恵子・中島智子　共著（培風館）
14）ドクターズガイド
公益財団法人老年病研究所長
岡本幸市（時事通信社）
15）すべてがわかるACS・運動ニューロン疾患
公益財団法人老年病研究所長
岡本幸市　分担（中山書店）
16）神経症候群（Ⅰ）
公益財団法人老年病研究所長、同附属病院長
岡本幸市・高玉真光　分担（日本臨牀社）
17）神経症候群（Ⅱ）
公益財団法人老年病研究所長、同附属病院長
岡本幸市・高玉真光　分担（日本臨牀社）
18）神経系理学療法実践マニュアル
公益財団法人老年病研究所附属病院名誉院長
酒井保治郎　分担（文光堂）
19）アンフレッド：脳・神経リハビリテーション大事典（翻訳版）
公益財団法人老年病研究所附属病院名誉院長
酒井保治郎　分担（西村書店）
20）高次脳機能障害のすべて－運動維持困難（Motor impersistence）－
公益財団法人老年病研究所附属病院名誉院長
酒井保治郎　分担（科学評論社）
21）よくわかる脳の障害とケア
公益財団法人老年病研究所附属病院名誉院長
酒井保治郎　監修（南江堂）
22）神経内科学テキスト（改定４版）
公益財団法人老年病研究所附属病院名誉院長
酒井保治郎　分担（南江堂）
23）クリプトコッカス髄膜脳炎・神経感染症を究める
公益財団法人老年病研究所長
岡本幸市　辻　省次ら編（中山書房）

24）前頭側頭葉変性症（FTLD）概論・神経症候群（第２版）、別冊日本臨床、新領域別症候群シリーズNo.27
公益財団法人老年病研究所長、同附属病院長
岡本幸市・高玉真光　分担（日本臨床社）

25）McLeod症候群・神経症候群（第２版）、別冊日本臨床、新領域別症候群シリーズNo.27
公益財団法人老年病研究所長、同附属病院長
岡本幸市・高玉真光　分担（日本臨床社）

26）こんな時のリハ処方
公益財団法人老年病研究所附属病院名誉院長
酒井保治郎（医歯薬出版）

27）今日の診断指針（第７版）
公益財団法人老年病研究所長
岡本幸市　分担（医学書院）

28）すべてがわかる神経難病医療
公益財団法人老年病研究所長
岡本幸市　分担（中山書店）

29）EBMに基づく脳神経疾患の基本治療指針－前頭側頭型認知症－（第４版）
公益財団法人老年病研究所長
岡本幸市　分担（Medical View社）

30）認知症の本人・家族の困りごとを解決する医療・介護連携の秘訣
－初期集中支援チームの実践20事例に学ぶ－
前橋市認知症初期集中支援チーム　山口晴保・山口智晴　編集
公益財団法人老年病研究所附属病院　チーム員　分担（協同医書出版社）

31）医学大辞典
公益財団法人老年病研究所附属病院名誉院長
酒井保治郎　分担（医学書院）

32）演習で学ぶ脳画像－読影からリハ介入まで－
公益財団法人老年病研究所附属病院名誉院長
酒井保治郎　監修・著（医歯薬出版）

33）神経内科学テキスト（改訂第４版）
公益財団法人老年病研究所長
岡本幸市　分担（南江堂）

34）認知症疾患診療ガイドライン2017（日本神経学会　監修）
公益財団法人老年病研究所長
岡本幸市　評価・調整委員（医学書院）

35）高次脳機能障害用語事典（種村　純編集）
公益財団法人老年病研究所附属病院名誉院長
酒井保治郎　分担（ぱーそん書房）

36）ナースが知りたい脳のはなし
公益財団法人老年病研究所附属病院名誉院長
酒井保治郎（学研メディカル秀潤社）
37）アルツハイマー型認知症　新臨床内科学（第10版）
公益財団法人老年病研究所認知症研究センター長
東海林幹夫　分担（医学書院）
38）アルツハイマー型認知症　1336専門家による私の治療（2019-20年度版）
公益財団法人老年病研究所認知症研究センター長
東海林幹夫　分担（日本医事新報社）

11. 老年病研究所附属病院事業

1．2019年度（2019．4．1～2020．3．31）における診療実績は、次のとおりである。

月別診療延人数及び診療報酬請求金額

区分 / 月別	診療延人数		請求金額
	入院	外来	
2019年4月	6,499人	8,271人	410,108,170円
5	6,691	8,218	414,074,610
6	6,482	7,760	402,140,050
7	6,137	8,489	401,920,920
8	6,185	8,241	401,563,010
9	5,950	7,793	381,385,720
10	6,259	8,488	432,771,680
11	6,791	7,688	418,591,610
12	6,752	7,904	400,575,810
2020年1月	6,733	7,643	404,858,500
2	6,329	7,188	375,714,420
3	6,494	7,355	399,989,390
合計	77,302	95,038	4,843,693,890

2．2019年度における低額診療事業実績は、次のとおりである。

1）診療費を減額した取扱患者数（延人員）

(1) 生活保護法による医療扶助患者数　1,258人

(2) 保険診療取扱患者数　15,992人

合計　17,250人

2）減免した診療費等の合計金額　27,048,000円

12. 老年病研究所附属高玉診療所事業

1．2019年度（2019．4．1～2020．3．31）における診療実績は、次のとおりである。

月別診療延人員及び診療報酬請求金額

区分／月別	外来延人数	往診人数	請求金額
2019年4月	267人	387人	5,493,490円
5	297	417	5,820,780
6	182	405	5,545,110
7	276	404	5,545,000
8	279	385	5,407,680
9	209	386	5,131,750
10	355	451	4,906,700
11	438	398	5,597,210
12	191	388	5,839,200
2020年1月	398	394	5,940,470
2	240	389	5,745,660
3	351	396	5,740,560
合計	3,483	4,800	66,713,610

2．2019年度における低額診療事業実績は、次のとおりである。

1）診療費を減額した取扱患者数（延人員）

(1) 生活保護法による医療扶助患者数　46人

(2) 保険診療取扱患者数　950人

合計　996人

2）減免した診療費等の合計金額　1,424,250円

13. 介護老人保健施設
群馬老人保健センター陽光苑事業

2019年度（2019. 4. 1～2020. 3. 31）における入所、通所者の実績は、次のとおりである。

月別入所・通所延人員及び介護報酬等収入金額

区分 / 月別	入所・通所者延人員		収入金額
	入所者	通所者	
2019年4月	2,886人	1,203人	57,928,716円
5	2,878	1,238	60,492,596
6	2,922	1,201	59,352,084
7	3,064	1,250	60,922,303
8	3,066	1,164	59,779,608
9	2,978	1,119	57,366,697
10	2,998	1,213	60,605,196
11	2,855	1,203	58,912,561
12	3,036	1,203	59,740,107
2020年1月	3,062	1,117	59,095,851
2	2,892	1,121	57,852,619
3	3,104	1,143	62,975,314
合計	35,741	14,175	715,023,652

※通所者の延人員には訪問リハビリの利用延人員が含まれている。

14. 訪問看護ステーション
ひまわり事業

その１

2019年度（2019. 4. 1～2020. 3. 31）訪問看護療養費（医療）における訪問件数、訪問回数は、次のとおりである。

月別訪問看護回数及び療養費請求金額

区分／月別	訪問看護件数	訪問看護回数	療養費請求金額
2019年４月	20件	153回	1,597,990円
5	21	165	1,726,310
6	19	147	1,503,400
7	21	218	2,075,410
8	21	172	2,012,320
9	19	167	1,721,050
10	19	166	1,723,360
11	20	167	1,727,250
12	19	153	1,612,660
2020年１月	16	129	1,308,790
2	18	132	1,366,320
3	17	148	1,493,430
合　　計	230	1,917	19,868,290

その２

2019年度（2019. 4. 1～2020. 3. 31）訪問介護給付費（介護）における訪問件数、訪問回数は、次のとおりである。

月別訪問看護回数及び療養費請求金額

区分／月別	訪問看護件数	訪問看護回数	療養費請求金額
2019年４月	31件	148回	1,329,238円
5	27	144	1,275,342
6	28	136	1,178,224
7	26	140	1,372,199
8	27	149	1,300,579
9	28	150	1,262,804
10	30	166	1,447,970
11	28	149	1,246,588
12	33	167	1,427,046
2020年１月	35	176	1,489,807
2	32	161	1,332,604
3	34	190	1,600,943
合　　計	359	1,876	16,263,344

15. 前橋市地域包括支援センター西部事業

1．前橋市の委託事業として平成21年４月１日開設、2019年度の事業実績は、次のとおりである。

(1) 介護予防支援給付

区分／月別	件数	西部直営請求額	委託先件数	委託先請求額	総件数	総請求額
2019年４月	51件	223,890円	148件	671,161円	199件	895,051円
5	53	232,670	147	669,834	200	902,504
6	54	243,186	158	711,998	212	955,184
7	56	251,966	140	626,852	196	878,818
8	53	232,670	165	742,728	218	975,398
9	50	219,500	163	746,200	213	965,700
10	51	227,463	163	729,442	214	956,905
11	53	233,190	159	708,789	212	941,979
12	52	231,853	157	709,158	209	941,011
2020年１月	48	202,400	161	720,652	209	923,052
2	47	209,863	156	692,526	203	902,389
3	47	209,863	156	698,652	203	908,515
合　　計	615	2,718,514	1,873	8,427,992	2,488	11,146,506

(2) 介護予防マネジメント費

区分／月別	ケアマネジメントA	ケアマネジメントB	ケアマネジメントC	西部件数	委託件数	総　件　数	総請求額
2019年４月	199件	0件	2件	88件	113件	201件	914,041円
5	205	0	0	91	114	205	942,832
6	195	0	0	87	108	195	868,302
7	200	0	3	93	110	203	915,674
8	191	0	1	85	106	191	849,721
9	184	0	0	85	99	184	823,075
10	183	0	0	83	100	183	820,515
11	191	0	0	88	103	191	941,979
12	197	0	1	93	105	198	888,537
2020年１月	192	0	0	89	103	192	857,052
2	196	0	0	95	101	196	883,841
3	188	0	0	88	100	188	842,515
合　　計	2,879	0	7	1,065	1,262	2,327	10,548,084

(3) 相談件数（電話・来所・訪問等）

（件）

区分／月別	相談件数	介護相談等	地域支援事業	保健福祉サービス	ケアマネジメント	権利擁護	その他
2019年4月	11	9	0	0	2	0	0
5	9	8	0	0	1	0	0
6	9	9	0	0	0	0	0
7	9	8	0	0	1	0	0
8	10	7	0	0	0	0	3
9	10	8	0	0	1	0	1
10	10	9	0	0	1	0	0
11	10	8	0	0	1	1	0
12	9	7	0	0	2	0	0
2020年1月	9	9	0	0	0	0	0
2	9	8	0	0	1	0	0
3	10	7	0	0	1	0	2
合計	115	97	0	0	11	1	6

16. 認知症初期集中支援推進事業

この事業は認知症になっても本人の意思が尊重され、できる限り住み慣れた地域で暮らし続けるために、認知症の人やその家族に早期に関わる「認知症初期集中支援チーム」を配置し、早期診断・早期対応に向けた支援体制を構築することを目的としている。

当院では、平成26年度当初から前橋市の委託を受け、積極的に事業を展開し、実践事例など公表していることから全国各地からの視察依頼が多い。2019年度の事業実績は次のとおりである。

○事業内容

① 普及啓発推進事業（認知症の早期診断・早期対応を市民および関係者へ啓発する）

② 認知症初期集中支援の実施

ア）訪問支援対象者の把握　　イ）情報収集

ウ）アセスメント　　エ）初回家庭訪問の実施

オ）チーム員会議の開催（24回）　カ）初期集中支援の実施

キ）関係機関との連携　　ク）終了と終了後のモニタリング

ケ）記録　コ）認知症初期集中支援チーム検討委員会への出席（年２回）

○事業実績

① 支援件数（支援対象者数）39名

・性別：男19名・女20名、年齢±標準偏差：81.3±6.1歳

・対象者世帯状況：独居10名、夫婦のみ13名、その他16名

② 2019年度末支援状況　支援継続中：９名、終了：30名

③ 2019年度の訪問延べ回数：93回（令和元年度支援対象者39名のみ）

○主治医との連携

① 主治医への依頼文発送：22例（うち返信あり18例）

○事業担当職員

① チーム員（２チーム配置／医療職・福祉職が各１名で１チームを編成）

・サポート医２名、歯科医師１名

・看護師２名、作業療法士３名、言語聴覚士１名、介護福祉士３名

② 事業推進担当　地域包括支援センター西部職員　１名

○視察受け入れ

県内：市内・認知症介護指導士１名（７月30日）

群馬リハビリテーション病院・作業療法士２名（９月17日・10月29日）、

市内・作業療法士２名（１月21日・２月４日）

県外：認知症介護研究・研修東京センター（８月27日／取材）

17. 居宅介護支援事業所事業

1　2019年度（2019. 4. 1～2020. 3. 31）介護給付における件数、計画費請求額は、次のとおりである。

区分 / 月別	件　　数	計画費請求額金額
2019年4月	265件	4,287,029円
5	255	4,077,521
6	252	4,037,305
7	249	4,013,143
8	261	4,177,150
9	262	4,177,376
10	261	4,202,671
11	257	4,110,228
12	264	4,235,313
2020年1月	261	4,194,429
2	255	4,088,716
3	272	4,379,531
合　　計	3,114	49,980,412

2　2019年度（2019. 4. 1～2020. 3. 31）予防介護給付における件数、計画費請求額は、次のとおりである。

区分 / 月別	件　　数	計画費請求額金額
2019年4月	64件	280,863円
5	64	282,873
6	64	280,073
7	62	278,209
8	61	270,756
9	63	282,599
10	65	291,989
11	64	284,526
12	63	277,063
2020年1月	69	315,715
2	69	303,463
3	65	288,926
合　　計	773	3,437,055

3　2019年度（2019．4．1～2020．3．31）要介護認定訪問調査における件数、請求額は、次のとおりである。

区分／月別	件　数	請　求　額
2019年4月	20件	85,428円
5	19	80,244
6	22	93,528
7	20	84,672
8	17	71,604
9	20	84,468
10	33	142,890
11	15	64,020
12	23	99,220
2020年1月	19	80,960
2	21	90,640
3	26	112,310
合　計	255	1,089,984

18. グループホームひまわり事業

2019年度（2019. 4. 1～2020. 3. 31）における入居者の実績は次のとおりである。

月別入居者延人員及び介護報酬等収入金額

区分／月別	入居者延人員	収入金額
2019年4月	810人	11,098,003円
5	837	11,466,120
6	810	11,129,984
7	829	11,401,124
8	831	11,185,677
9	811	10,312,523
10	837	12,565,454
11	799	11,099,505
12	782	10,828,380
2020年1月	822	11,092,895
2	783	10,875,121
3	837	11,679,285
合計	9,788	134,734,071

19. 認知症疾患医療センター事業

2019年度（2019. 4. 1～2020. 3. 31）における専門医療相談件数、認知症疾患に係る受診者数及び鑑別診断件数は、次のとおりである。

1　専門医療相談件数　（件）

区別＼月別		2019年4月	5	6	7	8	9	10	11	12	2020年1月	2	3	合計
電話	病気の相談	28	22	27	35	25	19	19	18	16	21	20	21	271
	受診希望	78	91	67	91	84	64	63	60	53	70	68	57	846
	介護の相談	1	3	3	0	2	2	2	1	1	2	2	0	19
	病院・施設紹介	5	10	6	7	6	5	5	1	4	5	5	1	60
	福祉サービスの利用	5	7	3	5	6	4	4	5	3	5	4	5	56
	その他	0	0	0	0	0	0	0	0	0	0	0	0	0
計		117	133	106	138	123	94	93	85	77	103	99	84	1,252
面接	病気の相談	56	53	52	65	60	46	45	29	41	47	49	43	586
	受診希望	3	5	6	8	13	10	10	3	8	10	10	7	93
	介護の相談	0	0	0	0	1	0	0	1	0	0	1	0	3
	病院・施設紹介	3	1	6	5	2	2	2	1	1	2	2	2	29
	福祉サービスの利用	3	2	3	2	3	2	2	2	2	2	2	2	27
	その他	0	0	0	0	0	0	0	0	0	0	0	0	0
計		65	61	67	80	79	60	59	36	52	61	64	54	738
合計		182	194	173	218	202	154	152	121	129	164	163	138	1,990

2　認知症疾患に係る受診者数及び鑑別診断件数　（件）

区別＼月別		2019年4月	5	6	7	8	9	10	11	12	2020年1月	2	3	合計
受診者数		64	59	47	66	66	50	49	34	41	51	53	45	625
うちかかりつけ医からの紹介		34	29	28	38	34	26	29	21	25	38	26	20	348
うち鑑別診断件数		64	59	47	66	66	50	49	34	41	51	53	45	625
検査内容	CT	3	4	3	6	1	5	0	1	1	2	1	1	28
	MRI	53	46	37	51	60	38	46	28	35	46	46	39	525
	スペクト	1	0	0	1	0	0	0	0	0	0	0	0	2
	その他	75	63	52	71	73	54	53	37	46	50	58	50	682

20. 従事役職員（令和２年３月31日現在）

１．研　究　所

職　種	常　勤	非常勤
	人	人
医師、研究員	2	1
その他の技術者	1	1
事務員	10	－
その他	－	－
計	13	2

２．附　属　病　院

医師	25(兼２)	35(兼１)
看護師	164	19
薬剤師	9	1
臨床検査技師	9(兼１)	－
栄養士	6	－
診療放射線技師	11	－
理学療法士	37	－
作業療法士	34	1
言語聴覚士	11	2
臨床工学技士	2	－
視能訓練士	2	1
歯科衛生士	3	1
司書	1	－
看護助手	38	6
その他の医療従事者	6	2
事務員	39(兼10)	12
社会福祉士	8	－
その他	3	5
計	408(兼13)	85(兼１)

３．附属高玉診療所

医師	1	－
看護師	2	－
事務員	1	1
計	4	1

4．陽　光　苑

医師	2（兼2）	3
看護師	16	－
介護福祉士	48	－
介護員	5	3
相談指導員	5	－
理学療法士	6	－
作業療法士	4	－
言語聴覚士	1	1
介護支援専門員	15(兼15)	－
薬剤師	1（兼1）	－
栄養士	1	－
事務員	3	－
その他	－	－
計	107(兼18)	7

5．訪問看護ステーションひまわり

看護師	3	3
計	3	3

6．前橋市地域包括支援センター西部

社会福祉士	3	－
介護福祉士	1	－
保健師	1	－
看護師	1	－
計	6	－

7．グループホームひまわり

看護師	1	－
介護福祉士	17	1
介護員	1	1
事務員	1	－
計	20	2

8．ケアプランセンター老研

介護支援専門員	9	－
計	9	－

合計	570(兼31)	100(兼1)

21. 貸借対照表

貸　借　対　照　表

令和　2 年　3 月 31 日現在（決算）

法人名：公益財団法人　老年病研究所
事業名：事業全体　　（単位：　円）

科目	当年度	前年度	増減
Ⅰ 資産の部			
流動資産			
現金預金	1,044,539,573	905,910,152	138,629,421
医業未収金（窓口）	80,906,250	77,737,146	3,169,104
医業未収金（振込）	801,870,699	811,374,854	△9,504,155
未収収益	42,747,213	55,471,181	△12,723,968
前払金	316,712	86,551	230,161
仮払金	428,730	340,245	88,485
薬品	33,488,825	31,850,998	1,637,827
診療材料	24,007,318	19,667,665	4,339,653
消耗備品	2,412,823	2,649,789	△236,966
流動資産合計	2,030,718,143	1,905,088,581	125,629,562
固定資産			
基本財産			
土地	32,668,000	32,668,000	
基本財産合計	32,668,000	32,668,000	0
特定資産			
退職給付引当資産	548,131,500	548,131,363	137
減価償却引当資産	825,943,065	825,942,963	102
特定資産合計	1,374,074,565	1,374,074,326	239
その他固定資産			
建物	2,630,949,619	2,751,557,384	△120,607,765
建物附属設備	96,942,144	111,591,607	△14,649,463
構築物	13,919,999	11,764,878	2,155,121
医療器械	98,065,827	62,475,189	35,590,638
車両運搬具	7,321,221	5,476,271	1,844,950
什器備品	33,302,080	36,899,492	△3,597,412
土地	1,174,921,031	1,140,053,831	34,867,200
電話加入権	1,806,122	1,806,122	
敷金	761,000	761,000	
保証金	278,000	278,000	
投資有価証券	155,623,686	155,818,686	△195,000
その他の固定資産	5,992,070	6,718,147	△726,077
リース資産		531,360	△531,360
その他固定資産合計	4,219,882,799	4,285,731,967	△65,849,168
固定資産合計	5,626,625,364	5,692,474,293	△65,848,929
資産合計	7,657,343,507	7,597,562,874	59,780,633
Ⅱ 負債の部			
流動負債			
未払金	362,943,959	400,237,433	△37,293,474
預り金	25,843,429	23,920,354	1,923,075
短期借入金	50,000,000	50,000,000	
仮受金		78,515	△78,515
リース債務		531,360	△531,360
流動負債合計	438,787,388	474,767,662	△35,980,274
固定負債			
長期借入金	629,084,000	746,338,000	△117,254,000
退職給付引当金	1,324,903,475	1,254,343,542	70,559,933
受入保証金	4,050,000	4,050,000	
固定負債合計	1,958,037,475	2,004,731,542	△46,694,067
負債合計	2,396,824,863	2,479,499,204	△82,674,341
Ⅲ 正味財産の部			

貸　借　対　照　表

令和　2 年　3 月 31 日現在（決算）

法人名：公益財団法人　老年病研究所
事業名：事業全体　　（単位：　　円）

科　　目	当　年　度	前　年　度	増　　減
一　般　正　味　財　産	5,260,518,644	5,118,063,670	142,454,974
正　味　財　産　合　計	5,260,518,644	5,118,063,670	142,454,974
負債及び正味財産合計	7,657,343,507	7,597,562,874	59,780,633

22. (公財)老年病研究所・附属病院医師(歯科医師を含む)名簿

(令和２年３月31日現在
在職者は太字)

氏　名	研究診療科名	就任年月日	退任年月日	摘要
高玉　真光	**内　科**	**昭和55.　9. 16**	**—**	**理事長**
吉田カツ江	病理、内科	昭和56.　11.　1	平成24.　3.　31	
鈴木　慶二	**病　理**	**昭和56. 11. 10**	**—**	**陽光苑副施設長**
岡本　幸市	神経内科	昭和57.　6.　2	平成25.　3.　31	
福田　利夫	病　理	昭和58.　4.　1	平成28.　3.　31	
内藤　　功	**脳神経外科**	**昭和62.　6.　2**	**—**	
佐藤　美恵	**麻酔科**	**昭和63.　7.　1**	**—**	
佐藤　圭司	**整形外科**	**平成　1.　4.　1**	**—**	**病院長**
甘利　雅邦	**神経内科**	**平成　2.　6.　2**	**—**	**副院長**
林　　陸郎	内　科	平成　2. 10.　1	平成21.　4.　24	
古川　和美	内　科	平成　4.　4.　6	平成19.　7.　20	
渡辺　　孝	循環器科	平成　4. 10.　1	平成24.　5.　13	(研究所長)
天野　晶夫	**循環器内科**	**平成　5.　6.　1**	**—**	**副院長**
一ノ瀬義雄	**泌尿器科**	**平成　5.　6.　2**	**—**	
館野　勝彦	**整形外科**	**平成　9.　6.　1**	**—**	**整形外科主監**
赤羽　信雄	眼　科	平成11.　4.　7	平成24.　3.　15	
中村　哲也	**内　科**	**平成11. 10.　4**	**—**	
高玉　　真	**脳神経外科**	**平成12.　4.　1**	**—**	**診療部長**
高玉　　篤	**眼　科**	**平成12.　5.　1**	**—**	**医局長**
青木　　純	放射線科	平成13. 12. 26	平成29.　8.　20	
池田　将樹	**神経内科**	**平成14.　6.　1**	**—**	
田所作太郎	内　科	平成14.　6.　3	平成20.　3.　31	(陽光苑副施設長)
平井　俊策	神経内科	平成14.　7.　2	平成20. 12. 31	
石川　　治	皮膚科	平成14. 10.　1	平成30.　3.　31	
黒川　公平	泌尿器科	平成15.　2. 10	平成24.　3.　31	
増田　裕一	**麻酔科**	**平成15. 10. 14**	**—**	**副院長**
岩井　丈幸	**脳神経外科**	**平成16.　4.　1**	**—**	**副院長**
清水　立矢	脳神経外科	平成17. 10.　1	平成20.　9.　30	
田野しのぶ	神経内科	平成18.　4.　1	平成17.　3.　31	
中嶋　義明	神経内科	平成18.　4.　1	平成19.　3.　31	
八巻さやか	外　科	平成18.　4.　1	平成19.　3.　31	
荻野　隆史	救命救急	平成18.　4.　1	平成27. 11. 30	
神宮　俊哉	リハビリテーション科	平成18.　9.　1	平成22.　9.　15	
藤田　清香	神経内科	平成19.　4.　2	平成15.　5.　31	
根岸　一明	神経内科	平成19.　4.　3	平成21.　3.　31	
渋沢　弥生	皮膚科	平成20.　4.　1	平成24.　3.　31	
平柳　公利	神経内科	平成20.　4.　1	平成21.　3.　31	
二瓶　治彦	整形外科	平成20.　4.　1	平成21.　3.　31	

氏　名	研究診療科名	就任年月日	退任年月日	摘要
土屋　寛子	神経内科	平成20. 4. 1	平成21. 9. 29	
斉藤　章宏	神経内科	平成20. 4. 5	平成22. 3. 20	
荻野　彩絵	眼　科	平成20. 4. 11	平成30. 3. 31	
加藤　　實	外　科	平成20. 5. 1	平成27. 3. 31	（陽光苑副施設長）
竹内　弘久	外　科	平成20. 5. 31	平成27. 12. 12	
宮本　直子	脳神経外科	平成20. 10. 1	—	
須藤貴世子	麻酔科	平成20. 11. 1	平成27. 12. 31	
安齋　徹男	循環器外科	平成21. 1. 1	平成30. 3. 31	
新井　規之	整形外科	平成21. 4. 1	平成22. 3. 31	
古田　夏海	神経内科	平成21. 4. 1	平成22. 3. 31	
松村　智文	後期研修医	平成21. 4. 1	平成23. 9. 30	
大塚　　真	神経内科	平成21. 4. 1	平成22. 3. 31	
黒沢　幸嗣	循環器内科	平成21. 4. 1	平成31. 3. 31	
小保方　優	循環器内科	平成21. 4. 1	平成23. 3. 31	
山口　晴保	神経内科	平成21. 4. 1	—	
橋本由紀子	神経内科	平成21. 4. 1	平成24. 3. 31	
中村　保子	内　科	平成21. 6. 5	—	
山岸　美保	循環器内科	平成21. 10. 6	令和 2. 3. 31	
矢嶋　久徳	泌尿器科	平成22. 1. 4	平成28. 3. 31	
島田　晴彦	整形外科	平成22. 4. 1	—	副院長
玉山　倍碩	整形外科	平成22. 4. 1	平成23. 3. 31	
牧岡　幸樹	神経内科	平成22. 4. 1	平成23. 3. 31	
関根　彰子	神経内科	平成22. 4. 1	平成24. 3. 31	
入江　忠信	循環器科	平成22. 4. 1	平成25. 3. 31	
田村　未央	循環器科	平成22. 4. 1	平成24. 3. 31	
古田みのり	臨床研修医	平成22. 4. 1	平成24. 3. 31	
長嶺　士郎	臨床研修医	平成22. 4. 1	平成30. 12. 31	
勝山　　彰	内　科	平成22. 4. 18	—	
神宮　俊哉	リハビリテーション科	平成22. 9. 15	—	
石嶋　秀行	放射線科	平成22. 12. 1	平成28. 11. 6	
金子　哲也	消化器外科	平成23. 3. 1	平成24. 3. 31	
佐鳥　圭輔	循環器内科	平成23. 3. 25	平成24. 3. 31	
笠原　浩生	神経内科	平成23. 4. 1	平成24. 3. 31	
熊坂　創真	研修医	平成23. 4. 1	平成25. 3. 31	
濱野　哲敬	研修医	平成23. 4. 1	平成25. 3. 31	
酒井保治郎	神経内科	平成23. 4. 1	—	
加藤　良衛	整形外科	平成23. 4. 1	平成25. 3. 31	
吉田カツ江	内　科	平成24. 4. 1	—	
井上　千鶴	皮膚科	平成24. 4. 1	平成27. 3. 31	
乾　　正幸	消化器科	平成24. 4. 1	平成25. 3. 31	
塚越　設貴	神経内科	平成24. 4. 1	平成25. 3. 31	

氏　名	研究診療科名	就任年月日	退任年月日	摘要
五十嵐健祐	臨床研修医	平成24. 4. 1	平成26. 3. 31	
梶原　剛	臨床研修医	平成24. 4. 1	平成30. 9. 30	
古田みのり	神経内科	平成24. 4. 1	平成27. 3. 31	
平柳　公利	神経内科	平成24. 4. 1	平成25. 3. 31	
田村峻太郎	循環器内科	平成24. 4. 1	平成25. 3. 31	
増田くに子	循環器内科	平成24. 4. 1	平成25. 3. 31	
池内　秀和	腎臓リウマチ内科	平成24. 4. 1	平成29. 3. 31	
小保方　優	循環器内科	平成24. 4. 1	平成25. 3. 31	
岡本　幸市	**神経内科**	**平成25. 4. 1**	—	研究所長
笠原　浩生	神経内科	平成25. 4. 1	平成28. 3. 31	
米元　崇	整形外科	平成25. 4. 1	平成26. 3. 31	
片山　千佳	初期研修医	平成25. 4. 1	平成26. 3. 31	
孫　莉華	初期研修医	平成25. 4. 1	平成26. 3. 31	
野村　隆則	初期研修医	平成25. 4. 1	平成27. 3. 31	
飯島　貴史	循環器内科	平成25. 4. 1	平成28. 3. 31	
佐藤　正行	神経内科	平成25. 4. 1	平成26. 3. 31	
山口　彩	呼吸器内科	平成25. 4. 1	平成27. 3. 31	
藍原　和史	循環器内科	平成25. 4. 1	平成26. 3. 31	
友松　佑介	整形外科	平成25. 5. 16	平成27. 6. 20	
加藤　良衛	**整形外科**	**平成26. 4. 1**	—	
長谷川　寛	循環器内科	平成26. 4. 1	平成27. 3. 31	
鹿嶋　友敬	眼科	平成26. 7. 1	平成29. 3. 31	
遠藤　朝美	**眼科**	**平成26. 7. 1**	—	
大島　一真	循環器内科	平成27. 4. 1	平成28. 4. 6	
市川　啓介	循環器内科	平成27. 4. 1	平成28. 3. 31	
下田　雄輝	内科	平成27. 4. 1	平成31. 3. 31	
石澤　邦彦	神経内科	平成27. 4. 1	平成30. 3. 31	
渋沢　弥生	皮膚科	平成27. 4. 1	令和 2. 3. 31	
藤田　達士	麻酔科	平成28. 2. 18	平成30. 12. 31	
野村　隆則	内科	平成28. 4. 1	平成29. 3. 31	
清水　千聖	神経内科	平成28. 4. 1	令和 2. 3. 31	
藤沢　洋輔	神経内科	平成28. 4. 1	平成29. 6. 30	
坂井　俊英	循環器内科	平成28. 4. 1	平成29. 3. 31	
入江　忠信	循環器内科	平成28. 4. 1	平成30. 3. 31	
登丸　行雄	泌尿器科	平成28. 4. 1	平成29. 6. 20	
福田　利夫	**病理診断科**	**平成28. 4. 1**	—	
塚田　圭輔	整形外科	平成28. 4. 1	平成31. 3. 31	
角田　洋平	**整形外科**	**平成28. 4. 1**	—	
山口　彩	**循環器内科**	**平成28. 4. 22**	—	
前野　敏孝	循環器内科	平成28. 5. 6	平成31. 3. 31	
岩崎　理	神経内科	平成29. 4. 1	平成30. 3. 31	

氏　名	研究診療科名	就任年月日	退任年月日	摘要
岡　　大典	神経内科	平成29.　4.　1	平成30.　3.　31	
大澤　貴志	整形外科	平成29.　4.　1	平成30.　3.　31	
飯塚あずさ	リウマチ科	平成29.　4.　1	平成29.　8.　20	
大石　裕子	リウマチ科	平成29.　4.　1	平成31.　3.　31	
吉村　幸恵	循環器内科	平成29.　4.　1	平成30.　3.　31	
山田　拓郎	消化器科	平成29.　4.　1	—	
中田　　聡	脳神経外科	平成29.　4.　1	平成30.　3.　31	
富沢真一郎	脳神経外科	平成29.　4.　6	—	
矢嶋　久徳	泌尿器科	平成29.　6. 26	—	
黒川　公平	リハビリテーション科	平成29.　7.　1	—	
中島　崇仁	放射線科	平成29.　8. 23	—	
菊池雄太郎	神経内科	平成30.　4.　1	令和　2.　3.　31	
漆田　優樹	神経内科	平成30.　4.　1	—	
村上　文崇	循環器科	平成30.　4.　1	平成31.　3.　31	
田村峻太郎	循環器科	平成30.　4.　1	—	
根井　　雅	整形外科	平成30.　4.　1	令和　2.　3.　31	
神谷真理子	整形外科	平成30.　4.　1	—	
石井　希和	脳神経外科	平成30.　4.　1	—	
雪竹　靖衛	精神科・心療内科	平成30.　7.　1	令和　1.　6.　25	
小池　陽子	内科	平成30.　9.　4	—	
山内　洋子	リハビリテーション科	平成30. 10.　1	—	
吉田くに子	循環器内科	平成30. 10. 16	—	
大西　真弘	放射線科	平成30. 12.　3	—	
渡辺　光治	リウマチ科	平成31.　1.　1	令和　2.　3.　31	
秋山　真人	内科	平成31.　4.　1	令和　2.　3.　31	
東海林幹夫	神経内科	平成31.　4.　1	—	認知症研究センター長
菅野　幸太	循環器内科	平成31.　4.　1	—	
諏訪　絢也	リウマチ科	平成31.　4.　1	—	
常岡　明加	脳神経外科	平成31.　4.　1	—	
荒巻　彩織	初期臨床研修医	平成31.　4.　1	—	
村上　　尚	初期臨床研修医	平成31.　4.　1	—	
佐藤　寿充	整形外科	平成31.　4.　2	—	
遠藤　武尊	外科	平成31.　4.　4	—	
瓦林　　毅	神経内科	令和　1.　5.　1	—	
加地　卓万	初期臨床研修医	令和　1.　5.　1	令和　2.　3.　31	
小林　　進	放射線科	令和　1.　6.　3	—	
松村　紗音	初期臨床研修医	令和　2.　2.　1	—	

〔歯科医師〕

氏　名	研究診療科名	就任年月日	退任年月日	摘要
飯島　　克	歯科・歯科口腔外科	平成 13. 6. 1	平成 27. 3. 31	
石原　宏一		平成 13. 6. 1	平成 14. 6. 15	
土屋　政敬		平成 14. 6. 17	平成 16. 5. 31	
土屋明日香		平成 16. 6. 1	平成 19. 4. 10	
野田　俊樹		平成 19. 4. 1	平成 21. 3. 31	
高沢みさき		平成 21. 4. 1	平成 23. 3. 31	
茂木　健司		平成 20. 4. 24	—	
戸谷麻衣子		平成 23. 4. 1	—	
米村　裕樹		平成 25. 4. 1	平成 26. 3. 31	
福士　宙之		平成 26. 4. 1	—	
伊達　佑生		平成 27. 4. 1	—	

あ と が き

私達の研究所業績集第20集（2020年版）を発刊することが出来ました。これも岡本研究所長をはじめ研究所職員による努力の賜と思います。

1980年９月に財団法人の研究所として認可されてから今年で40年を経過します。この貴重な論文や研究発表業績は多くの人々の健康を保ち、医学と医療の発展に役立つものと確信しております。

2019年度は国内外において多くの研究発表が行われ、国外からもモンゴル国の研修医、中国からの看護職員等の研修と交流が行われました。

業績集第20集の中には、東海林幹夫博士と瓦林毅博士の弘前大学より続いたアルツハイマー病の成り立ちと治療法についての研究論文が加わり、一層充実した業績集となりました。

また附属病院とともに、地域の医療に役立つ老人保健施設「陽光苑」事業を始め、グループホーム「ひまわり」事業、地域包括支援センター事業、認知症疾患医療センター事業、訪問看護ステーション事業、高玉診療所事業などが相互に連携協力して研究業績を重ねております。

これからも一層充実した研究と、地域社会に役立つ診療を行う所存です。また、文部科学省、厚生労働省を始め地元の群馬県や前橋市の御指導と御支援をいただきながら、研究業績をさらに発展させるため努力して参りたいと考えております。

本業績集の収集と発刊にあたり当研究所の大谷幸也事務部長、職員及び上毎印刷の関根章裕様に心より感謝いたします。

令和２年７月

公益財団法人　老年病研究所

理事長　高　玉　真　光

業　績　集（第20集）

令和２年７月29日　印刷
令和２年７月31日　発行

発行　公益財団法人 老年病研究所
印刷　上毎印刷工業株式会社